Immune System Modulation by Advanced Glycation End Products and Their Reactive Intermediates



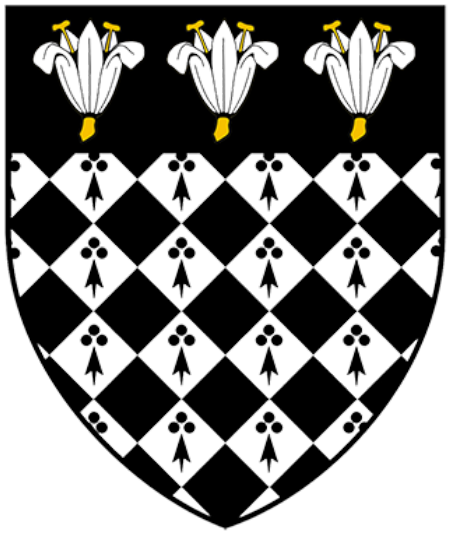

Scarlett Harris

The Sir William Dunn School of Pathology and
Magdalen College

A Thesis Submitted for the Degree of Doctor of Philosophy at the University of Oxford
Trinity Term 2020

Acknowledgements

Firstly, I would like to thank my supervisor, Professor Sattentau, who has supported me since my undergraduate degree and without whom I would not have done a DPhil. I am also very lucky to have worked with many fantastic people in the Sattentau group. I would particularly like to thank Dr Becky Moore who has been a source of both scientific and personal support throughout this DPhil. Additionally, I am very grateful to my fellow DPhil student Lu Li Jovanoska and FHS student Luis Avellano-Khan, who helped with some of this work. I'd also like to thank all of the support staff at the Dunn school and the Pathology Support Building; particularly Nicky Hamp who was also around to help. I owe particular thanks to everyone working in our flow cytometry facility, where I spent an enormous amount of time. I also need to thank my graduate advisor, Professor Paul Fairchild, who was always a very friendly source of advice.

Additionally, I would like to thank my transfer and confirmation assessors, Professor Mike Dustin, Dr Duncan Howie and Professor Jon Austyn, who I feel offered support that went beyond that required by their role. I'd like to give special thanks to Professor Siamon Gordon for his enthusiasm for the bizarre knockout mice and for introducing me to several fantastic researchers. I'm especially grateful for the help of Dr Ana Domingos and to the members of her lab for their technical advice. Similarly, thank you to the members of the Greaves group for their scientific support.

I ended up writing the bulk of this thesis in a very strange time, so I was very fortunate to be living with two fantastic people, Chloe and Ryan, who were a surrogate family throughout the lockdown, and to have many wonderful friends who supported me from a safe social distance. Finally, I would like to thank my family, who have nurtured and encouraged me for the past 25 years. I owe particular thanks to my mum, step-dad and boyfriend, Jack, who in addition to their unwavering support, were also my proof-readers.

Table of Contents

Acknowledgements……ii

Table of Contents……iii

Abstract……xi

Abbreviations……xii

Chapter 1: Introduction

1.0 Overview of the Introduction……1

1.1 Introduction to the Immune system……1

1.1.1 The Innate Immune System……2

1.1.2 The Adaptive Immune System……6

1.1.3 To Respond, or Not to Respond? That is the Question……11

1.2 Introduction to AGEs……13

1.3 AGE Formation……14

1.3.1 The Maillard Reaction……14

1.3.2 Alternative Pathways of AGE Formation……17

1.3.3 Factors Controlling AGE Formation……18

1.3.4 Modelling AGE Formation *In Vitro*……19

1.4 Specific AGE Structures……21

1.4.1 Reactive Carbonyls……21

1.4.2 Specific Adducts……22

1.4.3 Crosslinks……23

1.5 Methods for Detection……25

1.5.1 General Methods……25

1.5.2 Specific Methods……25

1.5.3 Attempts at Complete Characterisation……...26

1.6 The Problems with AGEs……26

1.6.1 AGEs and Protein Damage……..26

1.6.2 AGEs and Inflammation……..27

1.6.3 AGEs and Enhanced Immunogenicity……29

1.7 Aims of the Current Project……31

Chapter 2: Materials and Methods

2.1 General Notes……...34

2.2 AGE Modification Methods and Analysis……35

2.2.1 General Notes……35

2.2.2 Glucose Modification……36

2.2.3 GA Modification……36

2.2.4 CML Modification……..36

2.2.5 Pyrraline Modification……37

2.2.6 Carbonyl ELISAs……37

2.2.6.1 Biotin Hydrazide ELISA……37

2.2.6.2 DNPH ELISA……38

2.2.7 CML ELISA……...38

2.2.8 GA-Pyridine ELISA……...39

2.2.9 Pyrraline ELISA……39

2.2.10 TNBSA Assay……39

2.2.11 Fluorescence Measurements……40

2.2.12 SDS-PAGE……...40

2.2.13 Native PAGE……41

2.2.14 Western Blotting……...41

2.2.15 Carbonyl Western Blotting……...42

2.2.16 Fluorescent Labelling……...43

2.2.17 Biotin Labelling……43

2.2.18 C1q Binding Assay……...43

2.2.19 Complement Activation Assays……44

2.2.20 HyHEL-10 Binding ELISA……..45

2.2.21 Endotoxin Cleaning……45

2.3 Cell Culture and *In Vitro* Studies……...46

2.3.1 Cell Culture General Notes……46

2.3.2 Endotoxin Reporter Assay……..46

2.3.3 Generation of GM-CSF murine bone marrow derived DCs (BMDCs)……47

2.3.4 *In Vitro* Uptake Assays……...48

2.3.4.1 Plate-based Uptake Studies……..48

2.3.4.2 In-tube Uptake Studies……48

2.3.5 *In Vitro* Pulsing Assays……...49

2.3.6 Flow Cytometry……..49

2.3.6.1 Staining of Samples……49

2.3.6.2 Data Analysis……..52

2.3.7 RNAseq Analysis……52

2.3.8 Proteome Profiler……53

2.3.9 Luminex Assay……...53

2.3.10 PGE_2 ELISA……54

2.4 Animal Studies……54

2.4.1 Mouse Origin and Care……...54

2.4.2 Experimental Design of *In Vivo* Experiments……55

2.4.3 Subcutaneous (s.c.) Immunisation Protocols……56

2.4.4 DC Transfer Studies……57

2.4.5 Fasting Blood Glucose Measurements……57

2.4.6 Tissue Harvesting……58

2.5 Assessment of Antibody Responses……58

2.5.1 IgG, IgG1, IgG2a and IgG2c ELISAs……58

2.5.2 IgE ELISA……59

2.5.3 Examination of Natural Antibody Binding (IgM and IgG)……60

2.6 Assessment of Cellular Immune Responses……60

2.6.1 Splenocyte Harvest……60

2.6.2 Cytokine ELISAs……61

2.6.3 Thymidine Pulse……62

2.6.4 Pulsing with Naïve Splenocytes……62

2.7 Cell Isolation from Tissue Samples and Tissue Analysis……63

2.7.1 Isolation of Cells from Spleen……63

2.7.2 Isolation of Cells from Liver……63

2.7.3 Isolation of Cells from Lymph Nodes……64

2.7.4 Isolation of Cells from Fat……64

2.7.5 Measurement of Liver Triglyceride Content……64

2.7.6 Measurement of Fat Noradrenaline Content……65

2.8 Peanut Protein Manufacture and Isolation……66

2.8.1 Sourcing and Roasting of Peanuts……66

2.8.2 Production of PPE……66

2.8.3 Anion Exchange Chromatography……67

2.9 Statistical Analysis……..……..68

Chapter 3: Mechanisms of AGE-Enhanced Immunogenicity: Investigations into DC Activation and Complement Binding

3.0 Abstract……69

3.1 Introduction……..70

3.1.1 AGEs and Enhanced Immunogenicity…….……70

3.1.2 AGEs and DC Activation…….……...71

3.1.3 AGEs and Complement…….…….…73

3.2 Hypothesis and Aims…….……...75

3.3 Materials and Methods……76

3.4 Results……...77

3.4.1 Production and Characterisation of AGE-modified Proteins…….……77

3.4.2 GA-modified Samples Induce Strong Antibody Responses ……...…...…….88

3.4.3 AGE-modified Proteins Do Not Induce DC Maturation……..95

3.4.4 Establishment of an *In Vitro* Proliferation Assay to Assess B Cell Responses…….107

3.4.5 Complement and AGE-induced B cell Activation Cannot be Assessed *In Vitro* Using Mouse Serum …….……...……112

3.4.6 AGE-modified Protein Do Not Induce DC Maturation when DCs are Cultured in Mouse Serum …….....116

3.4.7 AGE-modified Proteins Induce Complement Activation……..……...122

3.4.8 AGE-modified Proteins Bind Natural Antibodies…….……127

3.5 Discussion and Conclusions…….……..130

Chapter 4: The Contribution of the Scavenger Receptors SR-A and MARCO to AGE-mediated Immunogenicity

4.0 Abstract……...138

4.1 Introduction……139

4.1.1 The Scavenger Receptor Family……...139

4.1.2 SRs Which Bind AGEs……140

4.1.3 DCs and SRs: SR-A……..141

4.1.4 DCs and SRs: MARCO……144

4.2 Hypothesis and Aims……146

4.3 Materials and Methods……..147

4.4 Results……148

4.4.1 Generation of Fluorescently-labelled AGE-modified Proteins……148

4.4.2 Glucose-modified Samples Have Enhanced DC Uptake ……...…...150

4.4.3 Uptake of Glucose-modified Samples Is Not Dependent on SR-A in In-tube Uptake Studies ……...155

4.4.4 Immunisation Studies Using SRA, MARC and SRMA Mice……..……..158

4.5 Discussion and Conclusions……..163

Chapter 5: Weight Gain Phenotype and Immunophenotyping of SR-A and MARCO KO Mice

5.0 Abstract……...167

5.1 Introduction……168

5.1.1 The Obesity Crisis……168

5.1.2 Inflammation in Obesity……...169

5.1.3 SRs and Obesity……170

5.2 Hypothesis and Aims……172

5.3 Materials and Methods……173

5.4 Results……174

5.4.1 SR KO Mice Gain Excess Body Fat……174

5.4.2 Cohousing KO and WT Mice……176

5.4.3 Immune Infiltration and Activation in Adipose Tissue……178

5.4.4 Immune Populations and Triglyceride Content of Liver Samples……181

5.4.5 Immune Populations in the Spleen and Lymph Nodes (LNs)……184

5.5 Discussion and Conclusions……191

Chapter 6: The Role of RAGE in AGE Immunogenicity

6.0 Abstract……194

6.1 Introduction……195

6.1.1 The Receptor RAGE and its Ligands……195

6.1.2 RAGE in Metabolic Disease……198

6.1.3 RAGE and Adaptive Immune Responses……199

6.2 Hypothesis and Aims……201

6.3 Materials and Methods……202

6.4 Results……203

6.4.1 Immunisation Studies Using RAGE Mice……203

6.4.2 Underweight Phenotype in the RAGE Mice……209

6.4.3 RAGE Mice have Autofluorescent Cells……211

6.5 Discussion and Conclusions……219

Chapter 7: The Impact of Dry Roasting on Immune Responses to Peanut Proteins

7.0 Abstract……...224

7.1 Introduction……225

7.1.1 The Peanut Allergy Epidemic……...225

7.1.2 Key Peanut Allergens……...226

7.1.3 Food Processing: Dry Roasting……228

7.2 Hypothesis and Aims……232

7.3 Materials and Methods……..233

7.4 Results……234

7.4.1 Optimising Conditions for Peanut Protein Extraction……..234

7.4.2 Isolating Individual Peanut Allergens……..241

7.4.3 Testing of PPE Samples for Endotoxin Contamination ……249

7.4.4 DC Uptake and Activation Studies Using Peanut Proteins……252

7.4.5 First Immunisation Studies with PPE ……255

7.4.6 Further Immunisation Studies with PPE and Isolated Ara h 1……..262

7.5 Discussion and Conclusions……..269

Chapter 8: Discussion and Conclusions

8.0 Outline of Discussion……275

8.1 Glycolaldehyde (GA) Modification: An Antibody Inducer……275

8.2 Glucose Modification: Cellular Responses……279

8.3 SRs and Adipose: Key Roles in Metabolism?……...281

Bibliography……284

Appendix.....302

Abstract

Immune System Modulation by Advanced Glycation End Products and Their Reactive Intermediates

Scarlett Harris

The Sir William Dunn School of Pathology and Magdalen College
A Thesis Submitted for the Degree of Doctor of Philosophy at the University of Oxford
Trinity Term 2020

Advanced Glycation End Products (AGEs) are a heterogenous group of protein modifications generated in a series of complex chemical reactions which begin with a non-enzymatic reaction between a reducing sugar and a free amine group. AGEs can be formed during food processing, for example, during dry roasting of peanuts. AGEs can also be formed endogenously, including during inflammation. AGE-modification can change protein recognition by the immune system. AGE-modified proteins can bind to scavenger receptors including scavenger receptor A (SR-A), a receptor expressed by macrophages and dendritic cells (DCs) which mediates internalisation of ligands. AGEs can also bind to the receptor for advanced glycation end products (RAGE), a receptor which promotes inflammation. Studies have also suggested that AGE-modified proteins can activate complement, the humoral component of the innate immune system. AGEs are reported to enhance the immunogenicity of modified proteins, that is to increase their capacity to induce adaptive immune responses. However, the mechanisms underlying this phenomenon remain unclear.

In this thesis, a variety of different AGE-modified proteins were created, the modifications characterised and the capacity to induce complement activation assessed. These were then used to immunise mice, including mice lacking SR-A, MARCO (another scavenger receptor of the same family as SR-A), or RAGE. The development of immune responses to native protein was then assessed by measuring antibody responses and performing splenocyte restimulation studies. Murine bone marrow derived DCs (BMDCs) were used to assess AGE-induced maturation of DCs and uptake of AGE-modified proteins. For the latter experiments DCs were also derived from mice lacking SR-A and/or MARCO. Lastly, proteins were also isolated from dry roasted (DR) and raw peanuts. These were characterised, assessed for DC uptake and activation and used to immune mice. The results demonstrated that glucose (GLUC)-modified hen egg lysozyme (HEL) induced significant anti-HEL splenocyte responses but no detectable IgG responses. In contrast, modification with glycolaldehyde (GA), an intermediate in AGE formation, induced significant antibody responses without significant splenocyte responses. GA-modified, but not GLUC-modified, HEL induced complement activation in ELISA-based studies. None of the tested AGE samples induced DC activation. However, GLUC-modification significantly enhanced BMDC uptake of proteins. In contrast to previous studies, this uptake was not dependent on the scavenger receptor SR-A. Indeed immunisation studies using knockout (KO) mice indicated that the receptors SR-A, MARCO and RAGE were all dispensable for the formation of GLUC-induced immune responses. However, these studies did reveal that mice lacking MARCO, particularly SR-A/MARCO double KO, gain excess body fat with age. In contrast, RAGE KO mice has lower body fat than WT controls and immune cells isolated from lymph nodes, spleen, liver and adipose tissue of RAGE KO mice were autofluorescent. The proteins isolated from DR peanuts showed low levels of AGE-modification and did not induce DC maturation or have greater DC uptake. Immunisation studies with the peanut proteins did not show that DR peanut proteins have significantly greater immunogenicity than raw peanut proteins.

To summarise, different AGE-modified proteins induce contrasting immune responses which appear to be mediated by different mechanisms. As complement deposition is known to enhance B cell responses to proteins, GA-modification may induce antibody production through complement activation. The enhanced immunogenicity of the GLUC-modified samples may be the result of increased DC uptake, however the enhanced responses do not require MARCO, SR-A or RAGE. This thesis also revealed roles for MARCO, RAGE and SR-A in regulating body adiposity, a finding which may be of significant interest with regards to obesity. However, the studies included here suggest that DR peanut proteins do not have greater immunogenicity than raw peanut proteins in murine immunisation models.

Abbreviations

2-ME – 2-Mercaptoethanol
3-DG – 3-Deoxyglucosone
25G – 25 gauge
80K-H – Protein Kinase C Substrate 80K-H
A488/647/700 – ALEXA488/647/700
AcLDL – Acetylated Low Density Lipoprotein
AGEs - Advanced Glycation End Products
ALEs – Advanced Lipoxidation End Products
ANOVA – Analysis of Variance
APC (1) – Allophycocyanin
APC (2) – Antigen Presenting Cells
ATM – Adipose Tissue Macrophage
AUC – Area Under Curve
BAFF – B-cell Activating Factor
BAT – Brown Adipose Tissue
BB – Brilliant Blue
BCA – Bicinchoninic Acid
BCR – B Cell Receptor
BG – Background
BH – Biotin Hydrazide
(m)BMDCs – (Murine) Bone Marrow Derived Dendritic Cells
(m)BMDMs – (Murine) Bone Marrow Derived Macrophages
BMI – Body Mass Index
BSA – Bovine Serum Albumin
BUV – Brilliant Ultraviolet
BV – Brilliant Violet
CCL(X) – Chemokine (C-C motif) Ligand (X)
CCR(X) – CC Chemokine Receptor Type (X)
CD – Cluster of Differentiation
Cdc42 – Cell Division Control Protein 42 Homolog
cDR – Commercial Dry Roast
CEL – (Carboxyethyl)lysine
CHI3-L1 – Chitinase-3-like protein 1
CHO – Chinese Hamster Ovary Cells
CI – Confidence Interval
CML – (Carboxymethyl)lysine
cpm – counts per minute
CRP – C-Reactive Protein
CTRL – Control
CX3CL1 – Chemokine (C-X3-C motif) Ligand 1
CXCL(X) – Chemokine (C-X-C motif) Ligand (X)
Cy7 – Cyanine-7

CTLs – Cytotoxic T Lymphocytes
DAMP – Damage Associated Molecular Pattern
DAF – Decay Accelerating Factor
DC - Dendritic Cell
DiI – 1,1'-Dioctadecyl-3,3,3',3'-Tetramethylindocarbocyanine Perchlorate
DMEM – Dulbecco's Modified Eagle Media
DMSO – Dimethyl Sulfoxide
DNA – Deoxyribonucleic Acid
DNP – Dinitrophenyl
DNPH – 2,4-Dinitrophenylhydrazine
DR – Dry Roast
EAGLEs – Either Advanced Glycation or Lipoxidation End Products
EDTA – Ethylenediaminetetraacetic Acid
EGF – Epidermal Growth Factor
Egr-1 – Early growth response 1
ELISA – Enzyme-linked Immunosorbent Assay
ERK - Extracellular Signal-regulated Kinases
FABP4 – Fatty Acid Binding Protein 4
FAD – Flavin Adenine Dinucleotide
FBS – Foetal Bovine Serum
FEEL-1/2–Fasciclin, EGF-like, laminin-type EGF-like and link domain-containing SR-1/2
FITC – Fluorescein Isothiocyanate
FMO – Fluorescence Minus One
FPLC – Fast Protein Liquid Chromatography
FSC – Forward Scatter
FVS780 – Fixable Viability Stain 780
FwB – FACS Wash Buffer
GA – Glycolaldehyde
G-CSF – Granulocyte Colony-Stimulating Factor
GLUC – Glucose
GM-CSF – Granulocyte-Macrophage Colony-Stimulating Factor
GODIC – Glyoxal-Derived Imidazoline Crosslink
GOLD – Glyoxal-Lysine Dimer
GTP – Guanosine Triphosphate
h – hour
HBSS – Hank's Balanced Salt Solution
HEK293 Cells – Human Embryonic Kidney 293 Cells
HEL- Hen Egg Lysozyme
HEPES – 4-(2-hydroxyethyl)-1-piperazineethanesulphonic acid
HFD – High Fat Diet
HGF – Hepatocyte Growth Factor
HIV – Human Immunodeficiency Virus
HMGB1 – High Mobility Group Box 1
HNE – 4-hydroxy-2-nonenal

HRP – Horseradish Peroxidase
ICR – Institute for Cancer Research
IFNγ - Interferon γ
Ig – Immunoglobulin
IL-(X) – Interleukin (X)
ILT3 - Immunoglobulin-like Transcript 3
i.p. – intraperitoneal
JAK – Janus Kinase
JNK – c-Jun N-terminal Kinase
(D)KO – (Double) Knock Out
LDL – Low Density Lipoprotein
LDS – Lithium Dodecyl Sulphate
LN – Lymph Node
LOX-1 – Lectin-like oxLDL Receptor 1
LPS – Lipopolysaccharide
Ly6C/G – Lymphocyte Antigen 6C/G
mAb – Monoclonal Antibody
MAC – Membrane Attack Complex
MARCO – Macrophage Receptor with Collagenous Structure
MAPK – Mitogen-Activated Protein Kinase
MASP – MBL Associated Serine Proteases
MBL – Mannose Binding Lectin
M-CSF – Macrophage Colony-Stimulating Factor
MD2 – Myeloid Differentiation Factor 2
MDA – Malondialdehyde
mDia1 – Diaphanous-1
MFI – Mean Fluorescence Intensity
MHC – Major Histocompatibility Complex
min – minute
MMP-(X) – Matrix Metalloproteinase (X)
MoMF – Monocyte-derived Macrophage
MOPS – 3-(N-morpholino)propanesulphonic acid
MPO – Myeloperoxidase
MS – Mass Spectrometry
NAD(P)H – Nicotinamide Adenine Dinucleotide (Phosphate) Hydrogen
NF-κB – Nuclear Factor-κB
NHS-LC-Biotin – Succinimidyl-6-(biotinamido)hexanoate – Long-Chain – Biotin
OD – Optical Density
o/n – overnight
Opti-MEM – Opti – Minimum Essential Medium
OST-48 – Oligosaccharyltransferase-48
OVA – Ovalbumin
OX40L – OX40 Ligand

oxLDL – Oxidised Low Density Lipoprotein
PAMP – Pathogen Associated Molecular Patten
PBS – Phosphate Buffered Saline
PCA – Principal Component Analysis
PE – Phycoerythrin
PGE_2 – Prostaglandin E_2
PI3K – Phosphoinositide 3-Kinase
PMA – Phorbol 12-myristate 13-acetate
PPARγ - Peroxisome Proliferator Activated Receptor γ
PPE – Peanut Protein Extract
Pref-1 – Preadipocyte Factor 1
PRR – Pattern Recognition Receptor
PYR – Pyrraline
Rac1 – Ras-related C3 Botulinum Toxin Substrate 1
RAGE – Receptor for Advanced Glycation End Products
RBC – Red Blood Cell
RBP4 – Retinol Binding Protein 4
RC – Reactive Carbonyl
Rho – Ras Homologous
RIG-I – Retinoic Acid-inducible Gene I
(ds)RNA – (double-stranded) Ribonucleic Acid
RNAseq – RNA sequencing
ROS – Reactive Oxygen Species
rpm – rotations per minute
RPMI – Roswell Park Memorial Institute Medium
RT – Room Temperature
s – Seconds
s.c. – Subcutaneous
SD – Standard Deviation
SDS – Sodium Dodecyl Sulphate
SDS-PAGE – SDS Polyacrylamide Gel Electrophoresis
SOM – Self-organising Map
SR – Scavenger Receptor
SR-A – Scavenger Receptor A
SR-B1 – Scavenger Receptor Class B Type 1
SSC – Side Scatter
STAT – Signal Transducer and Activation of Transcription
SVF – Stromal Vascular Fraction
T20 – Tween 20
TCEP – Tris(2-carboxyethyl)phosphine
TCR – T Cell Receptor
Tfh – T Follicular Helper Cells
TGFβ – Transforming Growth Factor β

Th – T helper cell
TIMP-1 – Tissue Inhibitor of Metalloproteinases 1
TLR – Toll-like Receptor
TMB – 3,3',5,5'-Tetramethylbenzidine
TNBSA – 2,4,6-Trinitrobenzene Sulphonic Acid
TNFα – Tumour Necrosis Factor α
TNF RI/II – Tumour Necrosis Factor Receptor I/II
Treg – Regulatory T Cell
Tris – Tris(hydroxymethyl)aminomethane
TWEAK - TNF-related Weak Inducer of Apoptosis
UV – Ultraviolet
VEGF – Vascular Endothelial Growth Factor
WHO – World Health Organisation
WT – Wild Type
xg – times gravity

Chapter 1: Introduction

1.0. Overview of the Introduction

This introduction starts with an overview of the immune system. It then describes the chemistry of advanced glycation end products (AGEs), their generation *in vivo* and *in vitro* and the current understanding of their immune modulatory capacity. More detailed introductions are given at the start of each chapter.

1.1 Introduction to the Immune System

The immune system consists of a variety of cell types which are located throughout the tissues of the body (Parkin and Cohen 2001). The immune system protects the body against infection, however is also has a more general role in maintaining homeostasis in an organism. Immune cells also respond to tissue damage, aid in tissue repair and are involved in embryonic development (Morimoto and Nakajima 2019; Martins et al. 2019). The immune system can be divided into the innate and adaptive immune systems. The former is evolutionarily ancient, whilst the latter is only found in jawed vertebrates (Litman, Rast, and Fugmann 2010). The innate immune system consists of cells and humoral factors which are able to respond rapidly to stimuli, albeit in a non-specific manner. In contrast, the adaptive immune system has to be instructed to respond to stimuli by the innate immune system, specifically by cells known as dendritic cells (DCs). The responses of the adaptive immune system therefore take longer to develop. However, the advantage of this system is that the response is highly specific to the original stimulus (Parkin and Cohen 2001). Moreover, the adaptive immune system has "immunological memory". That is, after a response has been developed to a stimulus (i.e. a pathogen), adaptive memory cells are formed which can recognise the stimulus and respond more rapidly on secondary encounter. This rapid secondary response provides protection against another infection with the same pathogen

and is the basis for vaccines (Charles A Janeway et al. 2001a). Stimuli which induce the development of adaptive responses against themselves are known as antigens (Sela 1998).

1.1.1 The Innate Immune System

The myeloid cells of the innate immune system are given in Table 1.1 (Parkin and Cohen 2001; MacPherson and Austyn 2012; Ross and Pawlina 2006). The major humoral component of the innate immune system is the complement system. This is a system of plasma proteins, most of which are inactive enzymes, which can be divided into three broad pathways, the classical, alternative and lectin pathways (see Figure 1.1.1) (Sarma and Ward 2011; Charles A Janeway et al. 2001b; Merle et al. 2015). The lectin and classical pathways become active when their first component binds to its ligand. This induces a conformational change allowing for activation of the subsequent components. Complement components can act as "opsonins", substances which bind to pathogens and thereby enhance phagocytosis (the process in which bacteria or other particles are engulfed and subsequently contained in intracellular vesicles called phagosomes) (Hiemstra and Daha 1998). Other complement components, namely C5a and C3a, are called anaphylatoxins and induce inflammation. The final stage in the complement pathway is the formation of the membrane attack complex. This forms a pore in target membrane (e.g. of a bacterium), resulting in lysis of the cell (Charles A Janeway et al. 2001b).

The cells which are of particular relevance to this thesis are macrophages and DCs. Macrophages are located in every tissue of the body and continually survey their environment, searching for signs of infection or tissue damage (Gordon and Plüddemann 2017). Pathogens, such as viruses and bacteria, share common motifs which are not found on host cells. These are known as pathogen associated molecular patterns (PAMPs). The classic example is lipopolysaccharide (LPS), a component of the cell wall of gram-negative

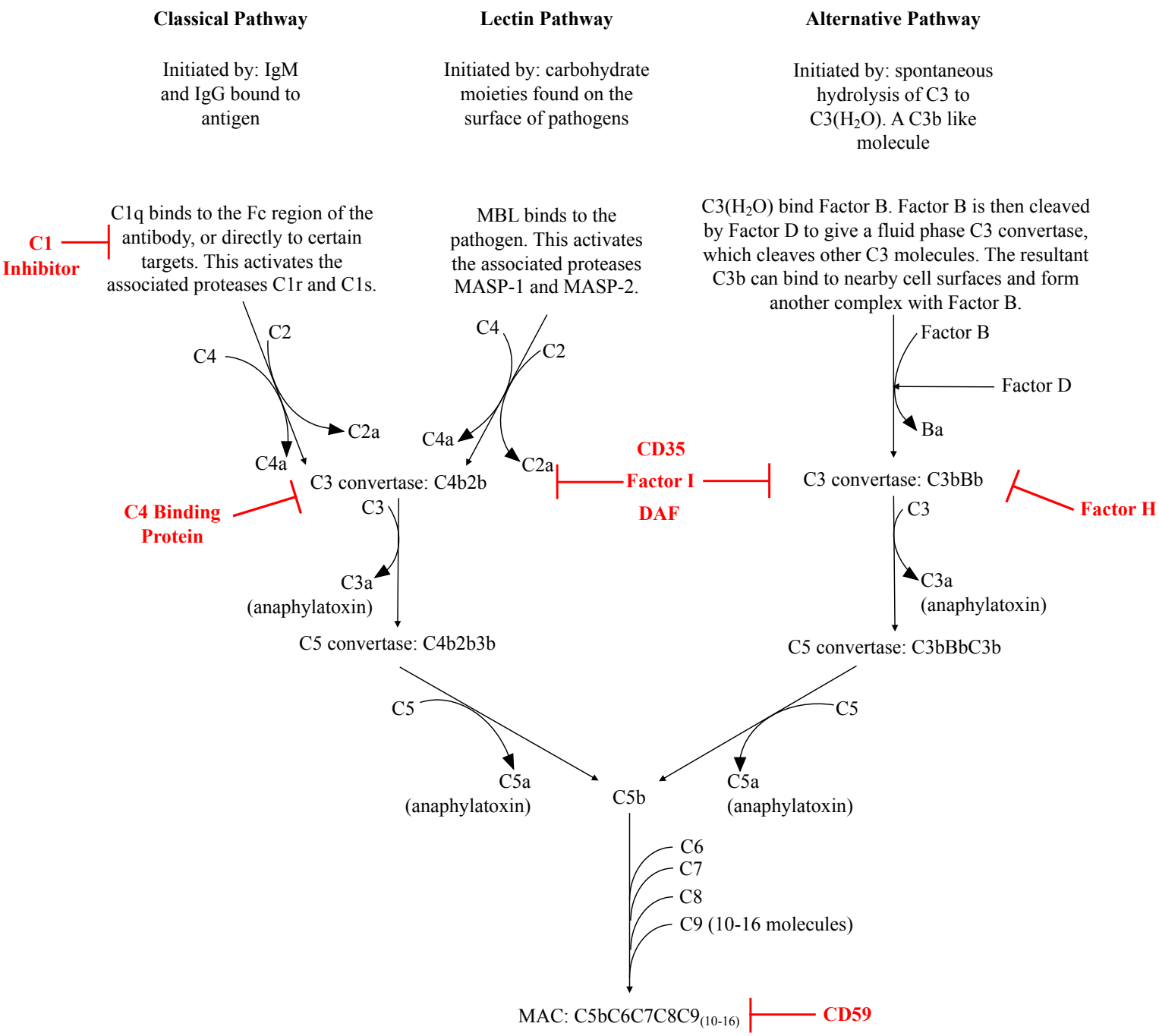

Figure 1.1.1: The pathways of the complement system. The effects of complement activation are three-fold. Firstly, complement activation induces the formation of opsonins which aid phagocytosis. The main opsonin formed is C3b, which is recognised by complement receptors on the surface of phagocytes allowing for more efficient engulfment. C3b can be further degraded into C3bi, also an opsonin, then to C3dg and C3c. C3dg can then be broken down into C3d. Secondly, complement activation results in the formation of anaphylatoxins (C5a and C3a), which are potent inducers of inflammation. Finally, the last stage of the complement pathways is the formation of the membrane attack complex. This is a pore inserted into the membrane of the target cell which results in cell lysis. Activation of the complement pathway is regulated by various inhibitors, shown here in red. For the alternative pathway, this prevents random complement activation on healthy host cells. MBL: mannose binding lectin, MASP: MBL associated serine protease, DAF: decay accelerating factor, MAC: membrane attack complex.

bacteria (Parkin and Cohen 2001). Macrophages, along with other immune cells, are able to respond to PAMPs using receptors known as pattern recognition receptors (PRRs). The first of these to be discovered was TLR4 (toll-like receptor 4), a cell surface receptor which binds to LPS (Murdock and Núñez 2016).

Other PRRs are located intracellularly, for example RIG-1 (retinoic acid inducible gene 1) is found in the cytoplasm and responds to double-stranded RNA (dsRNA) (Mogensen 2009). PRRs can also respond to host-derived molecules known as damage associated molecular patterns (DAMPs) (Vénéreau, Ceriotti, and Bianchi 2015). These are intracellular molecules which are released into the extracellular space by dying cells. Once outside the cells, DAMPs can be detected by PRRs.

Cell Type	**Function**
Macrophages	Macrophages can be divided into two broad categories. Firstly, there are tissue-resident macrophages which are present in the tissues at steady state. Secondly, monocytes can be recruited to a tissue during inflammation where they differentiate into macrophages. Tissue-resident macrophages have key roles in tissue homeostasis and continually monitor their environment using receptors which recognise tissue damage and pathogens. If a macrophage detects damage or infection, the cell releases signals which promote local inflammation. Macrophages are potent phagocytes, that is cells which internalise bacteria and other particulates into vesicles called phagosomes where bacteria can then be destroyed. The capacity of macrophages to kill internalised pathogens is enhanced by the cytokine IFNγ, a cytokine of the adaptive immune system.
Dendritic Cells (DCs)	DCs act as the bridge between the innate and adaptive immune systems. They capture antigens in their local environment and when activated, migrate to lymph nodes. Here they present antigen to and activate T cells, which are part of the adaptive immune system.
Neutrophils	Neutrophils are recruited rapidly to sites of acute inflammation. Like macrophages, they are phagocytes which phagocytose and kill bacteria. Neutrophils are short-lived cells which then die at the site of infection.
Mast Cells	Mast cells are present in mucosal tissue. They contain granules filled with pre-synthesised inflammatory mediators (e.g. histamine and inflammatory cytokines). The granules are released upon mast cell activation.
Eosinophils	Eosinophils circulate in the blood and are recruited to some sites of inflammation. They are granular and have functions which overlap with mast cells, but are not fully understood.
Basophils	Similar to mast cells, these possess granules filled with inflammatory mediators. Their roles in host defence are still not fully understood.

Table 1.1: Myeloid cells of the innate immune system. The innate immune system also includes innate cells of the lymphoid lineage, such as natural killer cells. These are not relevant to the thesis so are not included here.

Recognition of a PAMP/DAMP by innate immune cells switches the cells from a resting to active state. Ligand binding to a PRR induces intracellular signalling pathways which result in the activation of transcription factors (Mogensen 2009). One of the most famous pro-inflammatory transcription factors is NF-κB (Liu et al. 2017). This, along with other transcription factors, induces production of proteins which switch the activation state of the cell and promote inflammation. These include cytokines (signalling molecules which induce pro/anti-inflammatory signalling in cells), chemokines (signalling molecules which promote migration and recruitment of other immune cells) and adhesion molecules (Liu et al. 2017; Parkin and Cohen 2001). Collectively, these signals enhance the pathogen-killing functions of immune cells, increase vascular permeability and recruit other immune cells from the circulation (e.g. neutrophils).

However, in order to develop a full immune response activation of the adaptive immune system is required. This activation requires DCs. As with macrophages, DCs are found in tissues throughout the body and are normally in a resting "immature" state. In this state, DCs continually monitor their environment by internalising self, and non-self, proteins (Worbs, Hammerschmidt, and Förster 2017). If one of these molecules is a ligand for a PRR, the activation status of the DC changes in a process known as DC maturation (Charles A Janeway et al. 2001d). As part of this process, DCs become highly migratory and express high levels of CCR7 (Worbs, Hammerschmidt, and Förster 2017). This is a chemokine receptor which allows the DC to bind to CCL21, a chemokine expressed on lymphatic endothelial cells. Mature DCs therefore migrate through the lymphatics to lymph nodes (LNs), where they can present internalised protein to cells of the adaptive immune system. DCs therefore act as antigen presenting cells (APCs). Other cells can also act as APCs (i.e. macrophages), but DCs are particularly specialised for this task (Charles A Janeway et al. 2001d).

1.1.2 The Adaptive Immune System

The adaptive immune system consists of two main cell types, T cells and B cells (Parkin and Cohen 2001). Both contribute to immunological memory and express receptors which are highly specific to the antigen. These are called T cell receptors (TCR) and B cell receptors (BCRs) respectively (Bonilla and Oettgen 2010). The portion of the antigen which is recognised by a TCR/BCR is known as the epitope (T. C. Liang 1998). The T cells can be further divided into CD4 T cells and CD8 T cells. CD4 T cells are known as T helper cells (Th). As there name suggests, these support other immune cells to enhance the development of adaptive immune responses and increase activation of innate immune cells. CD8 T cells develop into cytotoxic T lymphocytes (CTLs) (Bonilla and Oettgen 2010). These can detect infected or damaged cells and respond by killing the cell. B cells contribute to the immune response by producing antibodies (Hoffman, Lakkis, and Chalasani 2016). These are a secreted version of the BCR which bind specifically to the recognised antigen.

When a migrating mature DC arrives at the LN, it searches for a T cell which responds to the proteins the DC has internalised. To do this, DCs process internalised proteins into small peptides. These peptides are then loaded onto molecules known as major histocompatibility complexes (MHC) and presented on the cell surface (Charles A Janeway et al. 2001d; Parkin and Cohen 2001). A T cell with the correct TCR can then recognise the peptide-MHC complex and interact with the presenting DC. There are two classes of MHC. MHC I-peptides complexes are recognised by CD8 T cells, whilst MHC II-peptide complexes are recognised by CD4 T cells (Bonilla and Oettgen 2010).

DC protein presentation alone is not sufficient to activate naïve T cells (i.e. T cells which have not encountered their antigen before). DCs must provide further instruction to the T cell in the forms of "costimulation molecules" (Charles A Janeway et al. 2001d). These are cell surface receptors which bind to their ligand expressed on T cells. Examples of

costimulatory molecules include CD80/CD86, which bind to CD28 on the T cell and provides a secondary signal for T cell activation. Additionally, DCs provide cytokine signals to T cells which provide further support to T cell activation (Luckheeram et al. 2012).

DC activation of the naïve T cell induces the T cell to produce the cytokine IL-2. T cells also express the receptor for this cytokine, which induces T cell proliferation (Charles A Janeway et al. 2001d). After 4 or 5 days of proliferation, the T cells differentiate into either effector Th cells if they are CD4 T cells, or CTLs if they are CD8 T cells. Importantly, these activated cells no longer require costimulation in order to respond to their presented antigen (Charles A Janeway et al. 2001d). The Th cells and CTLs can now leave the LN and travel to the site of infection/tissue damage where they assist in the immune response. Once the initial insult is cleared, most of the developed effector T cells will die. However, a pool of memory T cells will remain which can respond rapidly upon secondary encounter of the antigen (Charles A Janeway et al. 2001a).

The immune system will need to respond differently depending on the initiating stimulus, for example an extracellular bacteria will require a different response to a virus. Therefore there are several different types of Th cells, of which Th1/Th2 are the most famous (Zhu, Yamane, and Paul 2010). Details of these are provided in Figure 1.1.2 (Luckheeram et al. 2012). The decision to differentiate into a particular Th cell depends partly on additional costimulatory signals and cytokines provided by the DC, which are induced by the original stimulus. Whilst these are given as distinct categories, in reality these divisions are somewhat blurred. It is possible to find Th cells with a mixed phenotype which express, for example, Th1 and Th17 cytokines (Caza and Landas 2015). Likewise a Th cell of one type can transform into another type given the right signals. Moreover, the Th1/Th2 paradigm is not limited to T cells. Macrophages are also reported to be either “M1” or “M2”, activation

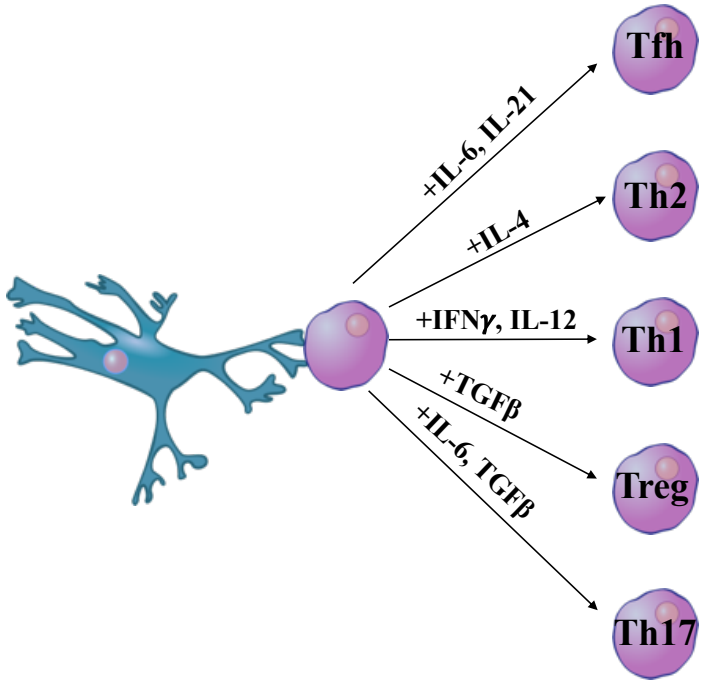

	Transcription Factor	Cytokines	Actions
Tfh	Bcl6	IL-21	Tfh cells support the activation of B cells into antibody producing plasma cells. They participate in the germinal centre reaction
Th2	GATA3	IL-4, IL-5, IL-13	Th2 cells target extracellular parasites. They promote antibody class switching, particularly to IgE. They also activate and recruit eosinophils.
Th1	T-bet	IFNγ, IL-2	Th1 cells are associated with immunity to intracellular pathogens. They enhance the capacity of macrophages to kill phagocytosed pathogens and support the development of CTLs.
Treg	FOXP3	TGFβ, IL-10	Regulates immune responses through the release of anti-inflammatory cytokines. This maintains tolerance to self and innocuous foreign antigens.
Th17	RORγt	IL-17, IL-22	Th17 cells target extracellular bacteria and fungi, they are particularly important for defence at mucosal sites.

Figure 1.1.2: This shows the development of the different CD4 T cell lineages. In addition to presenting the antigen and providing costimulatory signals, DCs secrete cytokines which direct T cell differentiation. The five main subsets of Th cells are shown, alongside the transcription factor which governs their development, the cytokines they produce and their main functions. The image of the T cells and DC were taken from the Reactome icons library. Tfh = T follicular helper cell, Treg = regulatory T cell, IL = interleukin, IFN = interferon, TGFβ = transforming growth factor β.

states which are induced by Th1 and Th2 cytokines respectively (Biswas and Mantovani 2010). However, as with the T cells, M1 vs M2 exist on a continuum rather than being completely distinct phenotypes.

The main role of Th cells is to provide support to other cells of the immune system including B cells (Bonilla and Oettgen 2010). When a B cell encounters an antigen specific for its BCR, intracellular signalling is triggered which begins to activate the B cell and the antigen is internalised (Hoffman, Lakkis, and Chalasani 2016). Antigen internalisation allows the B cell to process the protein antigen, load the resultant peptides onto MHC II, and present the resultant complex on the cell surface.

The next stage requires T cell help. Usually, T and B cells in the LN are segregated into T cells zones and B cell zones. However, upon antigen recognition the B cell migrates to the border of the B cell zone where it can interact with T cells (Hoffman, Lakkis, and Chalasani 2016). The B cell needs to encounter a T cell which recognises the same antigen, which can then provide further support to the B cell needed for full activation (Bonilla and Oettgen 2010). As with DCs, this secondary support includes costimulatory molecules (e.g. CD40 on B cells interacts with CD40 ligand on T cells) and cytokines (e.g. IL-21). Some B cells can differentiate at this stage into early memory cells or plasma cells (antibody producing cells). However, other B cells will return with T follicular helper (Tfh) cells to the B cell zone and form germinal centres (Hoffman, Lakkis, and Chalasani 2016).

Within the germinal centres, activated B cells undergo further maturation of the BCR to increase antigen affinity and "class switching", in which the antibody isotype is changed (Hoffman, Lakkis, and Chalasani 2016). There are several different classes or "isotypes" of antibodies (see Table 1.2) and each has slightly different functions (Chen and Cerutti 2011; Collins 2016; Charles A Janeway et al. 2001c). An antibody consists of two heavy chains and two light chains which each have variable regions, that participate in antigen binding,

and constant regions. The constant region of the heavy chains (the Fc region) determines the isotype of the antibody and it is this which is changed during isotype switching. Once fully mature, B cells exit the germinal centre, either as plasma cells or memory B cells. Antibodies aid the immune response by binding to and neutralising pathogens, activating complement, enhancing phagocytosis of pathogens and activating immune cells (Charles A Janeway et al. 2001c; Hoffman, Lakkis, and Chalasani 2016). Activation of immune cells is accomplished by Fc receptors present on the surface of immune cells.

Isotype	Function
IgM	This is the default isotype and is produced early in the humoral immune response. IgM antibodies tend to have low affinity, but form into pentamers which gives high avidity. IgM is a particularly good activator of complement.
IgG	IgG is the main isotype in the blood and extracellular fluid. In humans IgG is divided into four subclasses termed IgG1, IgG2, IgG3 and IgG4. In mice the subclasses are IgG1, IgG2a/c, IgG2b and IgG3. These antibodies can efficiently neutralise pathogens, and specific subclasses can act as opsonins and activators of complement. In mice, all but IgG1 can activate complement, whilst in humans it is IgG4 which cannot activate complement.
IgA	This antibody can be present as a dimer or monomer and is particularly important at mucosal sites. It can neutralise pathogens but is a weaker opsonin and complement activator than IgG.
IgE	IgE is found at very low levels in the blood and extracellular fluid as most is bound to Fc receptors present on mast cells. Binding of antigen to IgE induces release of histamine and other inflammatory mediators from mast cells.
IgD	The functions of IgD are yet to be fully understood. It is expressed along with IgM on mature B cells which have yet to encounter their antigen. It can also be secreted.
Table 1.2: Antibody Isotypes, Ig = immunoglobulin.	

The above description gives the development of T cell-dependent antibody responses. However, antibody responses can arise independently of T cells (Bonilla and Oettgen 2010). As with T cells, B cells can be divided into sub-groups. The B cells which produce antibodies with T cell help are known as follicular B cells. Additionally, there are marginal zone B cells, located in the marginal zone of the spleen, and B1 cells, located in the peritoneal and pleural cavities (Hoffman, Lakkis, and Chalasani 2016). These can produce antibodies in the absence of T cells. Typically, the antigens inducing T-independent responses are usually carbohydrates or phospholipids, which are poorly recognised by T cells. The marginal zone B cells and B1 cells can gain secondary stimuli from PRRs which they constitutively

express, allowing them to rapidly differentiate into antibody producing cells which usually produce IgM antibodies.

Additionally, B1 and marginal zone B cells can also produce antibodies in the absence of antigen-encounter, these are known as natural antibodies (Palma et al. 2018). These natural antibodies have broad specificity and bind to a range of altered self and non-self antigens (Holodick, Rodríguez-Zhurbenko, and Hernández 2017). For example, natural antibodies can recognise low density lipoprotein (LDL) which has been damaged by oxidation (oxLDL) and apoptotic cells (Palma et al. 2018). Recognition of damaged self by natural antibodies aids in the clearance of these molecules/cells. Natural antibodies can also bind to components of bacterial cells walls, thereby providing protection against infection (Holodick, Rodríguez-Zhurbenko, and Hernández 2017).

1.1.3 To Respond, or Not to Respond? That is the Question

The immune system needs to be able to tolerate innocuous stimuli (e.g. commensal bacteria, food proteins, pollen) and self molecules whilst responding sufficiently strongly to invading pathogens which could otherwise kill the host. Tolerance is not a passive process, instead self-reactive T cell and B cells are actively purged from the repertoire and there are specific cells and signals which suppress immune responses (Kretz-Rommel 2005). For example, T regulatory cells (Tregs) are a form of Th cells which act to suppress the activation of other immune cells, in part through the secretion of anti-inflammatory cytokines such as IL-10 (Luckheeram et al. 2012). Some Tregs are produced during T cell development in the thymus. However, DCs can also induce the formation of Tregs if they present antigen to naïve T cells without proper costimulation (Josefowicz, Lu, and Rudensky 2012).

Understanding the mechanisms underlying activation and tolerance in the immune system is important when there is a need to artificially induce an adaptive immune response, for

example as part of a vaccine. A variety of different vaccine types are available including subunit vaccines in which specific pathogen proteins are used for immunisation (Clem 2011). However, addition of the proteins alone in the absence of other stimuli is not enough to induce activation of the adaptive immune system. Therefore, the protein is given along with an adjuvant (Di Pasquale et al. 2015). This is a substance which can induce activation of the immune system, thereby enhancing the immune response to the vaccine.

Conversely, failure to develop tolerance can have catastrophic consequences. Autoimmune diseases occur when an individual develops an inappropriate immune response to a self-protein (Smith and Germolec 1999). Similarly, individuals develop allergies when the immune system responds to an innocuous protein such as pollen, animal fur or food. For example, in IgE-mediated food allergy, IgE antibodies are produced against antigens found in food, known as allergens (Berin 2015). These IgE antibodies result from isotype switching which is supported by Th2 cells secreting IL-4 (Luckheeram et al. 2012). IgE binds to high affinity Fc receptors found on mast cells. When antigen cross-links the IgE on these mast cells, they respond by releasing granules containing histamine and other inflammatory mediators (Yu, Freeland, and Nadeau 2016). In cases of severe allergy, the release of these factors into the bloodstream induces the smooth muscle of the respiratory system to constrict, resulting in airway obstruction, and vascular smooth muscle to relax, preventing return of blood to the heart (Reber, Hernandez, and Galli 2017). This is known as anaphylaxis and can be fatal.

Understanding the factors which govern the development of immune responses could therefore inform vaccine design and our understanding of autoimmune and allergic diseases. One factor which may alter the way a protein is recognised by the immune system is the addition of modifications known as advanced glycation end products.

1.2 Introduction to AGEs

AGEs are a large, complex group of protein modifications formed mainly during the Maillard reaction, a series of chemical reactions which begins with the non-enzymatic joining of a reducing sugar and a free amine group such as those found on lysine, arginine and the N-terminal of proteins (Luevano-Contreras and Chapman-Novakofski 2010; Ulrich 2001; Johnson et al. 2016). Following the discovery of this reaction in 1912, research mainly focused on the effect of the reaction in food (Zhang et al. 2009). The Maillard reaction is responsible for giving cooked food its brown colour and it also has an effect on the flavour and nutritive value (van Boekel 2006). It was not until the 1970s that it was recognised that this reaction could also occur in vivo (Ulrich 2001). It is now known that AGEs are formed in healthy individuals but in some diseases they are found at excessive levels where they may contribute to pathogenesis (Ulrich 2001; Ramasamy et al. 2005). For example, increased AGE formation is linked to a variety of diabetic complications including retinopathy and nephropathy (Hudson and Lippman 2018). Similarly, AGEs are found in higher levels in the plaques of Alzheimer's Disease compared to healthy brain tissue (Ramasamy et al. 2005). More recently AGE-modified proteins have been shown to have enhanced immunogenicity, that is they have a greater capacity to induce adaptive immune responses compared to unmodified proteins (Heilmann et al. 2014; Moghaddam et al. 2014). This finding has significant implications for allergy and autoimmune disease.

Given that AGEs are found both in food, particularly in western diets (Uribarri et al. 2010), and in various pathologies, it is important to understand these modifications and their effects on the body in health and disease. It is known that AGE modification changes the way a protein is recognised by cells as there are specific receptors which can recognise AGE structures. The most well characterised is the receptor for advanced glycation end products (RAGE), a member of the immunoglobulin superfamily expressed throughout the body

including on immune and endothelial cells. Binding of AGE, or any of RAGE's many other ligands, triggers proinflammatory signalling and can sustain chronic inflammation (Kierdorf and Fritz 2013). The AGE-RAGE relationship is linked to a variety of diseases including diabetes and this is discussed in more detail in Chapter 6. Other receptors include Galectin-3, OST-48 and 80K-H which together form the AGE receptor complex (Ott et al. 2014). Finally, there are a variety of scavenger receptors (SRs) which are reported to bind AGEs and control their uptake into cells, including SR-A, CD36, SR-B1, FEEL-1 and FEEL-2 (Horiuchi, Sakamoto, and Sakai 2003). These are discussed in more detail in Chapter 4. The response of a cell to AGEs is likely to depend on the exact receptors expressed by the cell and the specific modifications present. However, the extent and type of AGE modification is challenging to assess due to the diversity and complexity of AGEs, not all of which have been characterised (Schmitt et al. 2005). Moreover, many studies have only used a single modification to quantify AGE content (Van Puyvelde et al. 2014), and have not examined which specific modifications are responsible for the observed biological effect (Silván et al. 2006).

1.3 AGE Formation

1.3.1 The Maillard Reaction

The generation of AGEs is complex and incompletely understood, with multiple pathways resulting in the formation of AGE or AGE-like structures. A summary of the Maillard reaction is shown in Figure 1.3.1, but within this there are several variants (Tsekovska et al. 2016; Ott et al. 2014). In the classical, or "Hodge pathway", the process starts with a condensation reaction between a carbonyl group in a reducing sugar and a primary amine in a protein/peptide. The resultant Schiff base (a carbon-nitrogen double bond in which the nitrogen is not bonded to hydrogen), is unstable and will rearrange to form an Amadori

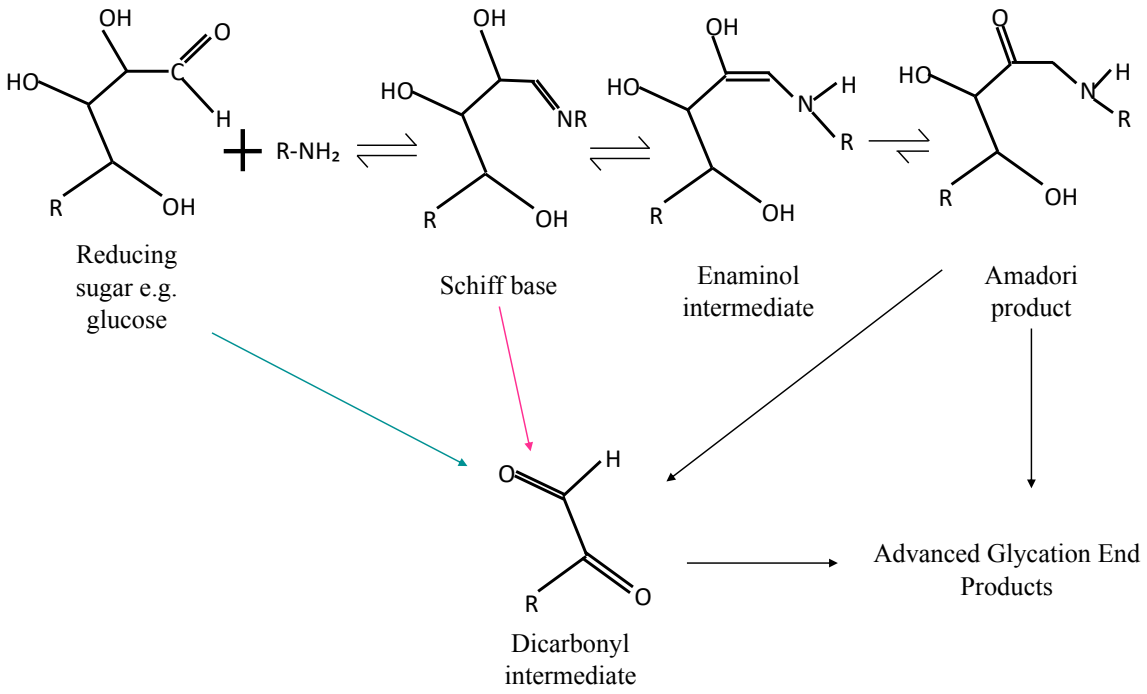

Figure 1.3.1: This is a simplified version of the Maillard reaction. This process begins with a condensation reaction between a reducing sugar and a free amine group, producing a Schiff base which can go onto form an Amadori product. In the classic Hodge pathway, AGEs are formed from this Amadori product, either by direct rearrangement or via breakdown of the product which forms highly reactive dicarbonyl intermediates. These will react with other amine groups to produce AGEs. Dicarbonyl intermediates can also be formed through fragmentation of the Schiff base (Namiki pathway, shown in pink) or autoxidation of monosaccharides (Wolff pathway, shown in teal).

product (Luevano-Contreras and Chapman-Novakofski 2010; Zhang et al. 2009). The chemical identity of this product depends on the sugar, for example reactions with glucose will produce ε-fructosyl-lysine whilst reactions with lactose produce lactulosyl-lysine (Silván et al. 2006). These Amadori products are substantially more stable than the Schiff base, however at this stage the reaction is still reversible. Progression to the next stage depends on a variety of factors including glucose concentration and presence of oxygen (Tsekovska et al. 2016). AGEs can be formed directly from rearrangement of the Amadori product. Alternatively, the Amadori product can breakdown to form highly reactive dicarbonyl intermediates such as glyoxal, methylglyoxal and 3-deoxyglucosone (3-DG). The capacity for these intermediates to react with amine groups is far greater than the original sugar, and so these can also join to proteins and undergo a variety of chemical reactions to form AGEs. Structures of these intermediates are given in Figure 1.3.2 (Vistoli

et al. 2013; Thornalley 2005). The later reactions which form AGEs are less well characterised than the initial stages and result in a huge variety of different adducts and crosslinks (Tsekovska et al. 2016).

A variant of the Maillard reaction is known as the Namiki pathway. In this the Schiff base, rather than rearranging to the Amadori product, breaks down to form the reactive dicarbonyl compounds (Thornalley 2005). Another alternative is the Wolff pathway which involves the autoxidation of monosaccharides such as glucose, fructose and glyceraldehyde to dicarbonyl intermediates. This occurs under physiological conditions and is catalysed by transition metal ions (Tsekovska et al. 2016; Ott et al. 2014). In addition to the reactive dicarbonyl compounds, AGE forming reactive aldehydes can also be formed in the Maillard reaction as a result of sugar fragmentation. These include glycolaldehyde (GA) and glyceraldehyde (Vistoli et al. 2013).

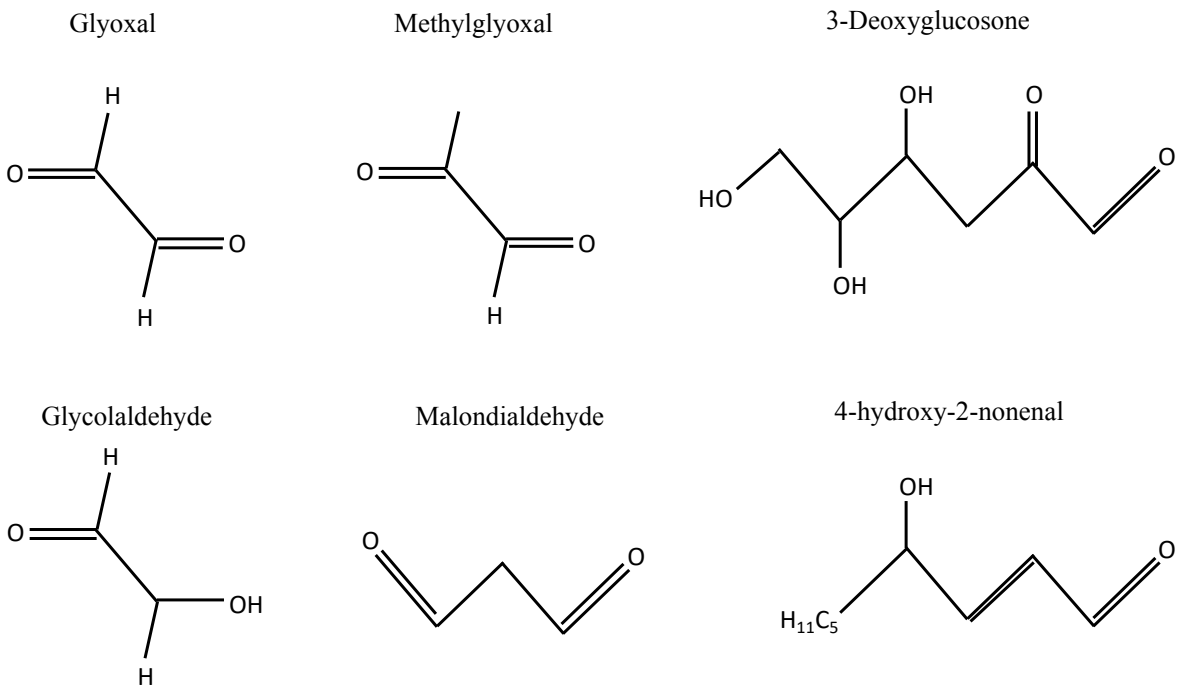

Figure 1.3.2: Structures of some reactive intermediates in AGE and ALE formation. These include dicarbonyl species (glyoxal, methylglyoxal, 3-deoxyglucosone (3-DG)), reactive aldehydes (glycolaldehyde (GA)) and lipid peroxidation products (malondialdehyde (MDA) and 4-hydroxy-2-nonenal (HNE)). ALE = advanced lipoxidation end product

1.3.2 Alternative Pathways of AGE Formation

In addition to the Maillard reaction, there are other pathways which result in AGE formation. Firstly, AGE-forming reactive products can be formed in the polyol pathway in which glucose is first converted to sorbitol and then fructose by aldose reductase and sorbitol dehydrogenase respectively. This is significant because fructose is substantially more reactive than glucose with regards to AGE formation and this pathway becomes active when intracellular levels of glucose are high (Vistoli et al. 2013; Lorenzi 2007). Additionally, the fructose can be phosphorylated to give fructose-3-phosphate. This, and its breakdown products such as 3-DG, can also react with proteins to form AGEs (Hamada et al. 1996; Ott et al. 2014).

Additionally, AGE-like structures can be formed as a results of lipid peroxidation. In this process, fatty acids in the lipid membrane bearing at least one double carbon bond, most commonly poly-unsaturated fatty acids, are attacked by free radicals. This results in the formation of lipid radicals which react with oxygen, producing lipid peroxyl radicals. These can then react to give lipid hydroperoxides which fragment to produce reactive aldehyde species (Ayala, Muñoz, and Argüelles 2014). Some of these are also found in glycation for example glyoxal and methylglyoxal, whilst others are unique. This latter group includes 4-hydroxy-2-nonenal (HNE) and malondialdehyde (MDA), see Figure 1.3.2. The reactive carbonyl (RC) species then react with nucleophilic residues in proteins such as lysine side chains to form structures known as advanced lipoxidation end products (ALEs) (Vistoli et al. 2013). Some adducts, such as (carboxymethyl)lysine (CML), can be formed either by lipid peroxidation or glycation as the reactive intermediates which generate these modifications are produced in both pathways. These common adducts are known as EAGLEs (Either Advanced Glycation or Lipoxidation End-Products)

1.3.3 Factors Controlling AGE Formation

AGE formation in food depends on the nutrient composition and conditions for cooking. The rate of the Maillard reaction is increased when using high temperature and dry heat (Uribarri et al. 2010). The formation of the Schiff base also requires an alkaline pH (Ott et al. 2014) and therefore the use of acids in cooking can prevent AGE production. Studies examining AGE content in different foods have shown levels are particularly high in animal-derived products rich in fat and protein (Uribarri et al. 2010). Processed carbohydrate-rich foods such as cookies and chips also have high levels of AGEs, whilst carbohydrate-rich, minimally-processed foods such as vegetables have generally low levels. Additionally, the reactive intermediates of AGE formation can also be found in food and other exogenous sources (e.g. cigarette smoke) and this may also contribute to AGE formation *in vivo* (Vistoli et al. 2013). The contribution of dietary AGEs to human disease is a continuing area of research and there is some controversy as to whether they have any pathological effects. Certainly, it is established that a proportion of dietary AGEs can be absorbed into the body through both passive diffusion and actively by peptide transporters, although most are rapidly excreted (Ames 2007; Delgado-Andrade 2016). Moreover, it is unclear whether these dietary AGEs have a significant biological effect once absorbed; whilst some studies have shown a positive correlation between AGE consumption, circulating AGEs and inflammatory markers, others have found no effect (Van Puyvelde et al. 2014).

In vivo the formation of AGEs is accelerated by high blood glucose. This is most noticeable in diabetes where glycation of haemoglobin is a well-established marker of long-term glucose control (Nathan, Turgeon, and Regan 2007). Time is also a significant factor determining AGE formation as *in vivo* AGE pools increase with lifespan (Delgado-Andrade 2016; Li and Yu 2018), and generally accumulate on long-lived proteins such as collagen (Tsekovska et al. 2016; Ulrich 2001). Additionally, oxidative stress also enhances EAGLE

generation. Under normal circumstances, cells have numerous enzymatic and non-enzymatic antioxidant systems to remove free radicals before they can damage proteins. However, in pro-oxidant states these protective mechanisms become overwhelmed resulting in the accumulation of reactive oxygen species (ROS) (Moldogazieva et al. 2019). These species can then initiate lipid peroxidation and oxidation of glucose, producing reactive carbonyls which react to form EAGLEs (Ellis 2007; Ryan, Nissim, and Winyard 2014).

Inflammation is also an important source of AGE-producing reactive intermediates *in vivo.* When activated, neutrophils can produce a variety of ROS through the action of a number of enzymes including myeloperoxidase (MPO). This enzyme catalyses the reaction between H_2O_2 and halide ions to produce hypohalous acids, most commonly hypochlorous acid (HOCl) (Ndrepepa 2019). These ROS are utilised for their bactericidal activity, but can also attack host molecules. With regards to AGEs, particular focus has been on the capacity of MPO-derived HOCl to attack amino acids, resulting in the formation of reactive aldehydes (Anderson et al. 1997). For example, the reaction of serine and HOCl produces GA, which can then react with proteins to produce AGEs (Anderson et al. 1999). Additionally, electrophilic arachidonic acid metabolites, either produced through cyclooxygenases or free radical attack, can also induce formation of ALEs (Vistoli et al. 2013).

1.3.4 Modelling AGE Formation *In Vitro*

As glucose is relatively unreactive (Ulrich 2001), proteins may need to be incubated with glucose for weeks or months in order to form AGE structures (Valencia, Weldon, et al. 2004; Schmitt et al. 2005). The use of reactive intermediates can substantially accelerate this process and so they are frequently used in experiments to generate AGE-modified proteins. In this thesis, GA was the most frequently used intermediate for AGE modification. Research in the early 1980s identified the capacity of this aldehyde to react with amine in

proteins, form a Schiff base and subsequently undergo the Amadori rearrangement (Acharya and Manning 1983). Later research further probed the mechanism of protein modification by GA and demonstrated that it could form AGEs under physiological conditions (Glomb and Monnier 1995). As discussed above, this intermediate is formed through the reaction between HOCl and serine, and is a breakdown product in the Maillard reaction. A scheme for known GA-mediated reactions is shown in Figure 1.3.3 (Nagai et al. 2002; Acharya and Manning 1983; Glomb and Monnier 1995). As can be seen, a single GA molecule reacting with lysine produces an Amadori product (aldoamine), which can then be oxidised to form CML or react with another amine to crosslink proteins (Glomb and Monnier 1995). Another route for CML formation from GA involves the oxidation of GA to form glyoxal. This dicarbonyl can then react with lysine to give a product which will rearrange to CML. Lastly, lysine can react with multiple molecules of GA to form the aromatic AGE GA-pyridine (Nagai et al. 2002). I have shown lysine in Figure 1.3.3 because initial studies indicated that this compound reacts predominantly with lysine rather than arginine residues (Acharya and Manning 1983).

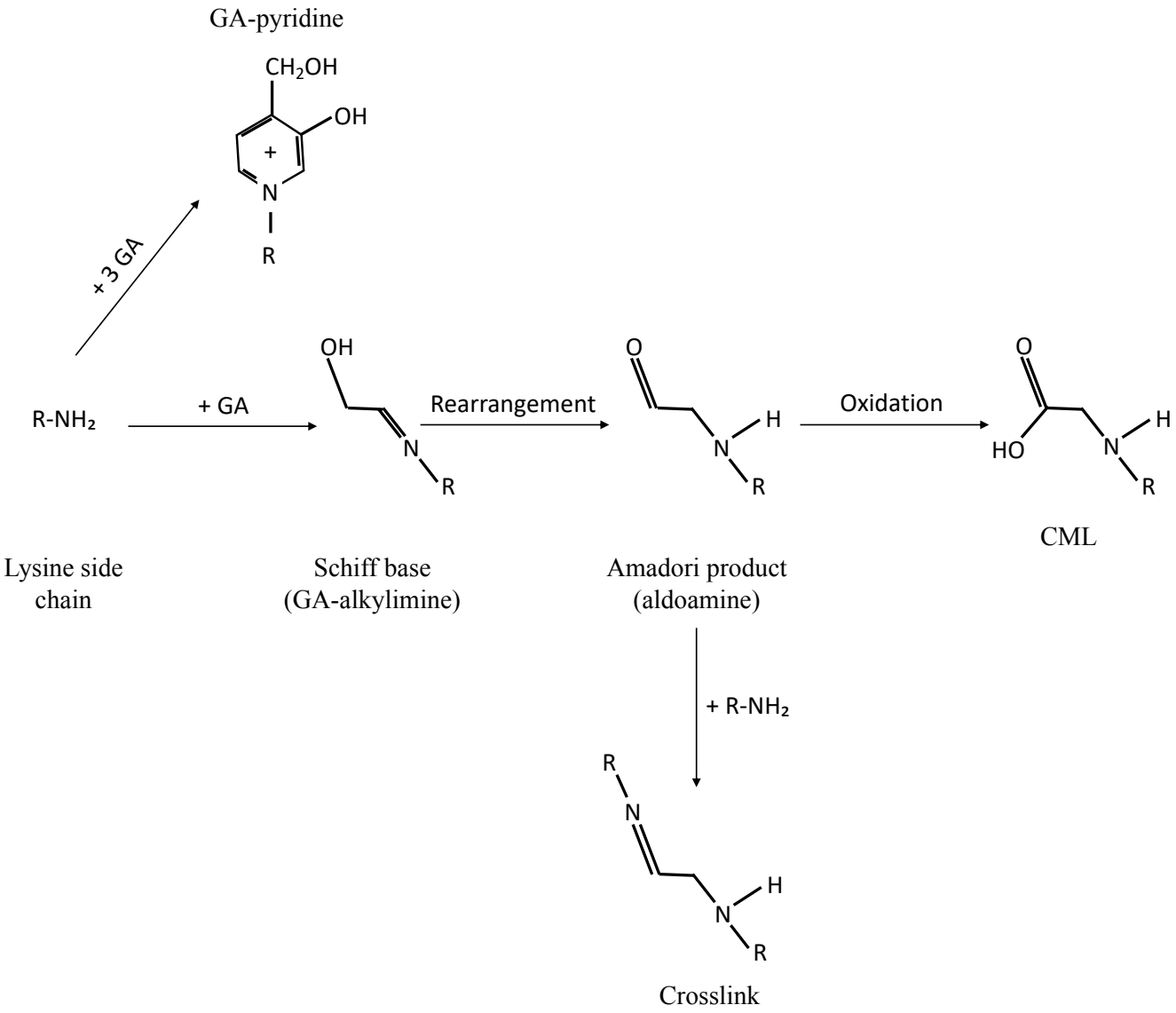

Figure 1.3.3: Reactions of GA and amine groups resulting in crosslinking of proteins, and CML and GA-pyridine formation.

1.4 Specific AGE Structures

1.4.1 Reactive Carbonyls

Given the complexity of the chemical reactions involved in their formation, it is hardly surprising that the end products are equally complex. Discussing all the variants is not possible as many have yet to be identified so this section will instead focus on a limited number of modifications. Firstly, an important general class of chemical moieties which can

be added to proteins by lipid peroxidation and glycoxidation are RCs (Fedorova, Bollineni, and Hoffmann 2014). These species can be added to proteins by a variety of pathways including through the reaction between a dicarbonyl intermediate and an amine group (Bizzozero 2009). However, a particularly important source of RC species are α,β-unsaturated aldehydes (Fedorova, Bollineni, and Hoffmann 2014). These are a group of lipid peroxidation products which have a C=C group adjacent to the aldehyde. This arrangement renders the C=C electrophilic, allowing it to react with nucleophilic amino acids in a manner which retains the aldehyde functional group (Vistoli et al. 2013; Grimsrud et al. 2008). An example of an α,β-unsaturated aldehyde is HNE which is shown in Figure 1.3.2. Another source of RCs in proteins is direct ROS attack of amino acids. The addition of RCs to proteins is called protein carbonylation and is a characteristic feature of oxidative stress (Fedorova, Bollineni, and Hoffmann 2014).

1.4.2 Specific Adducts

Figure 1.4.1 gives the structures of some key AGE adducts which are featured in the rest of this thesis (Vistoli et al. 2013; Ulrich 2001). The first of these is CML, a very common/dominant adduct often used as a marker of glycation/lipoxidation (Van Puyvelde et al. 2014). This was the first AGE to be identified and can be formed either directly from rearrangement of the Amadori product or through the reaction of the intermediate products glyoxal, GA and 3-DG with lysine (Tsekovska et al. 2016; Vistoli et al. 2013). CML is formed both in food during processing and *in vivo* and is specifically linked to many inflammatory diseases (Delgado-Andrade 2016).

The second modification shown is pyrraline, a ring structure which is also derived from 3-DG, although at a much lower rate than CML (Vistoli et al. 2013). Whilst this structure can be formed at 37°C and has been found in human serum and tissue samples (Miyata et al.

1992), its production is accelerated at higher, non-physiological temperatures. In a model *in vitro* system examining the reaction of lysine with sugars, pyrraline formation was found to peak at 140°C with a decline in production thereafter (Z. Liang et al. 2016). Pyrraline may therefore be more important as an exogenous AGE as it has been detected in a variety of food products (Li and Yu 2018). As can be seen from the structure, pyrraline has a RC group and so can react with primary amine groups to form a Schiff base. Therefore, pyrraline could form lysine-lysine crosslinks between proteins (Z. Liang et al. 2016; Ulrich 2001).

Finally, the last structure is GA-pyridine, an aromatic modification discovered more recently than CML and pyrraline. It was first identified in a study looking for GA-specific modifications. The authors immunised mice with GA modified protein and then screened for antibodies which bound to GA-modified proteins, but not the 3-DG, glyoxal, methylglyoxal, glucose or CML modified versions. The epitope of the GA-specific antibodies was then purified and the structure analysed (Nagai et al. 2002). GA-pyridine is found in human atherosclerotic plaques and seems to preferentially accumulate in foam cells.

1.4.3 Crosslinks

In addition to adducts, AGE modification can also result in both intra- and inter-molecular crosslinks in affected proteins (Tsekovska et al. 2016). Crosslinks can be formed by reactive intermediates and the identity of the crosslink depends on the amino acids involved and the reactive intermediate responsible. For example, the two dicarbonyl groups of glyoxal allow it to react with two lysine side chains or a lysine and an arginine side chain resulting in the structures GOLD (glyoxal-lysine dimer) and GODIC (glyoxal-derived imidazoline crosslink) respectively (Vistoli et al. 2013; Lederer and Klaiber 1999).

Additionally, some crosslinks are fluorescent (Ulrich 2001). This latter group includes pentosidine, an AGE which links a lysine and an arginine residue (Vistoli et al. 2013). It is unusual in that in can be derived from a large number of different sugars and reactive intermediates (Ulrich 2001). Pentosidine was also one of the first AGEs to be characterised and was first isolated from dura-mater collagen (Li and Yu 2018). Crosslinks are thought to be responsible for many of the protein/tissue damaging effects of AGEs (Ulrich 2001), and these are discussed in more detail below.

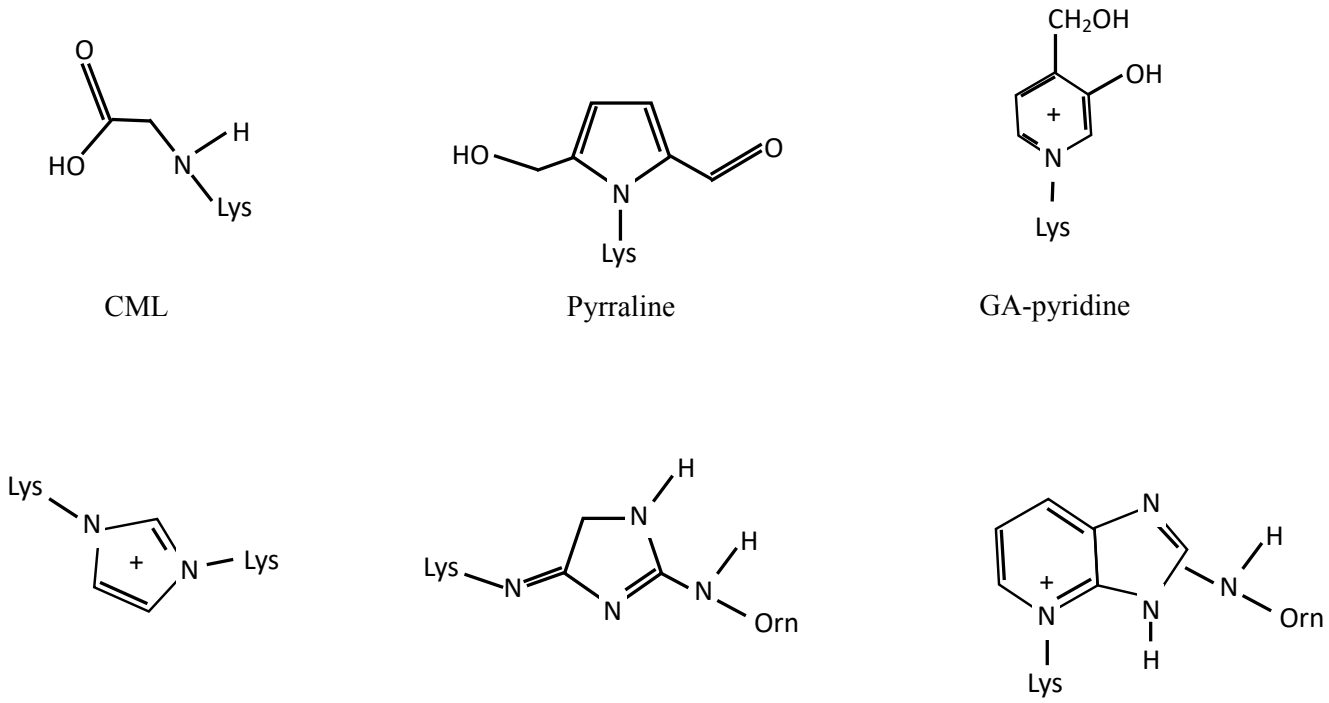

Figure 1.4.1: Structures of the adducts and crosslinks discussed in this section. CML = (carboxymethyl)lysine, GOLD = glyoxal-lysine dimer, GODIC = glyoxal-derived imidazoline crosslink

1.5 Methods for Detection

1.5.1 General Methods

A variety of different techniques have been developed to assess AGE formation in proteins. Firstly, there are methods which will give a general measure of the extent of AGE modification. For example, it is possible to determine the number of free amine groups on unreacted lysine and arginine residues meaning that the extent of modification in a protein can be evaluated (Schmitt et al. 2005). Moreover, as some AGE structures formed are fluorescent (Ulrich 2001), this property can be used to show the presence of glycation by examining excitation and emission spectra (Schmitt et al. 2005; Silván et al. 2006).

1.5.2 Specific Methods

There are also techniques for determining type and extent of specific modifications (Silván et al. 2006; Schmitt et al. 2005). For example, antibodies against specific modifications, such as CML, are available allowing content to be quantified by ELISA (Schmitt et al. 2005). As discussed above, RC groups are of particular interest and they are also a characteristic feature of protein oxidation (Fedorova, Bollineni, and Hoffmann 2014). There are several reagents which can be used to detect these, the most established being DNPH (2,4-dinitrophenylhydrazine). This has a characteristic absorbance that is maintained when it reacts with RCs and so carbonyl content can be quantified by spectrophotometry (Yan and Forster 2011; Cabiscol, Tamarit, and Ros 2014). Anti-DNP antibodies have also been developed, allowing detection with ELISA (enzyme-linked immunosorbent assay) or western blot. More recently biotin hydrazide has been used for RC detection which removes the need for secondary antibodies as tagged streptavidin is used for detection (Hensley 2015; Yan and Forster 2011).

1.5.3 Attempts at Complete Characterisation

Whilst the above methods can indicate the presence of AGEs, either generally or specifically, they can only give a limited picture of the modifications in a sample. In a perfect world, the ideal AGE analysis method would be able to identify and quantify all modifications present. Some of the more advanced biochemical techniques get closer to this goal. For example, mass spectrometry (MS) has been successfully used to identify a range of modifications in individual and complex protein samples (Renzone, Arena, and Scaloni 2015; Johnson et al. 2016; Hebling et al. 2013). However, this is a significant undertaking as MS of AGE-modified proteins can be particularly challenging (Zhang et al. 2009). The central problem is that despite more than a century of research, the chemistry of the Maillard reaction is still not well understood. As a result there are many EAGLEs which have yet to be identified and so complete characterisation is not yet possible.

1.6 The Problems with AGEs

1.6.1 AGEs and Protein Damage

The addition of AGEs to proteins can be very damaging for a number of reasons. At the most basic level, the addition of bulky adducts and crosslinks can alter the structure of proteins, rendering them non-functional (Tsekovska et al. 2016). One of the most established examples is the addition of AGEs to lens crystallin. The browning and crosslinking of the protein turns the lens opaque resulting in cataracts (Monnier and Cerami 1981; Ulrich 2001). Similarly, collagen in the extracellular matrix is also vulnerable to glucose attack. The crosslinking reduces the flexibility and elasticity of collagen which can also contribute to pathology, for example by causing blood vessels to stiffen (Delgado-Andrade 2016). These AGE modifications tend to predominantly affect long-lived proteins as extended periods of glucose exposure are required to allow Amadori products to react and accumulate

(Tsekovska et al. 2016). Therefore, this protein damage is associated with aging, and diabetes where the high sugar level accelerates AGE formation (Luevano-Contreras and Chapman-Novakofski 2010). Furthermore, as discussed above, oxidative stress also enhances EAGLE formation and rates of oxidative stress increase with age (Moldogazieva et al. 2019). Therefore, increasing AGE damage with age is a reflection both of increased time and dysregulation of metabolic functions.

An important aspect of AGE-mediated protein damage is that the modifications, particularly crosslinks, prevent proteolysis of the affected proteins (DeGroot et al. 2001), meaning the body is unable to properly dispose of them. Similarly, cells can remove damaged proteins through the proteasome system. However, the addition of AGEs to proteins makes them resistant to proteasome-mediated degradation (Ott et al. 2014). Thus, AGEs can also accumulate intracellularly where they can contribute to further cellular damage. For example, they can contribute to the formation of aggregates called lipofuscins. These also accumulate with age and are thought to be involved in the pathogenesis of a number of disorders including Alzheimer's diseases (Moreno-García et al. 2018).

1.6.2 AGEs and Inflammation

AGEs can also cause damage by inducing inflammation through RAGE. This is a PRR which binds to a variety of negatively charged ligands (Kierdorf and Fritz 2013). This interaction is reported to activate proinflammatory signalling pathways including the NF-κB pathway, resulting in the release of cytokines (e.g. IL-6) and recruitment of immune cells. Of particular interest with regard to AGEs is the capacity of this receptor to induce ROS generation and thus oxidative stress in cells. This, coupled with the capacity for RAGE to induce its own expression, is reported to produce a vicious cycle of inflammation as ROS result in AGE formation, which in turn activate RAGE to induce further RAGE expression

and ROS production, leading to further AGE generation and inflammation (Ramasamy et al. 2005; Luevano-Contreras and Chapman-Novakofski 2010; Ott et al. 2014). This receptor, its signalling pathways and links to metabolic disease are discussed in more detail in Chapter 6.

Whilst many studies have shown an inflammatory role for AGE, some have questioned this narrative. For example, in the study of Son et al, AGE-BSA (bovine serum albumin) did not induce production of proinflammatory cytokines from murine bone marrow derived macrophages (mBMDMs). Instead, their AGE-BSA sample seemed to exert anti-inflammatory effects as pre-treatment of mBMDMs with AGEs inhibited LPS-induced production of IL-6 and activation of NF-κB (Son et al. 2017). These anti-inflammatory effects seemed to be mediated by a receptor other than RAGE as inhibitors of this receptor had no effect. This results clearly contrast substantially with previous results (Ott et al. 2014). Reasons for such discrepancies between studies could include differences in cell type and species of origin. For example, in the Son et al study, AGEs could not inhibit NF-κB activation in human embryonic kidney 293 (HEK293) cells expressing TLR4, which allowed the HEK293 cells to respond to LPS. This may indicate that the mBMDMs express an additional receptor which mediates the anti-inflammatory effects of AGE and in other cell types the balance of the pro- and anti-inflammatory AGE receptors may determine outcome.

Another important factor to consider is the method used for AGE generation as differences in the extent and nature of modification could again cause differences in cellular recognition. For example, Pertynska-Marczewska et al did find an increase in the production of proinflammatory cytokines (vascular endothelial growth factor (VEGF), tumour necrosis factor α (TNFα) and IL-8) by human macrophages in response to AGE-modified proteins, but only when they used particular samples (Pertyńska-Marczewska et al. 2004).

Similarly, the presence of contaminants in the samples may also be important. Indeed, in the study of Valencia et al, the authors demonstrated binding of their AGE-modified proteins to RAGE, but their low endotoxin samples did not induce release of VEGF from endothelial cells or TNFα from peripheral blood mononuclear cells. In contrast, the RAGE ligand S100b, a member of a family of proteins which are released from cells during inflammation and act as DAMPs (Hudson and Lippman 2018), could induce release of these cytokines. The study therefore concluded the RAGE-AGE binding was not sufficient to induce cellular signalling (Valencia, Mone, et al. 2004). Whether AGE-modified proteins induce inflammation *in vivo* is still not entirely clear, but given the data we have so far it seems likely that the response will vary depending on the modifications themselves, the presence of other inflammatory factors and the cell types involved.

1.6.3 AGEs and Enhanced Immunogenicity

An additional line of investigation is how AGE-modification alters the development of adaptive immune responses to the protein. Initial work examined the capacity of Maillard reaction products to induce antibody responses *in vivo*. Witztum et al immunised guinea pigs with glucose-modified LDL and found they developed antibodies specifically to the modifications (Witztum et al. 1983). Subsequent studies have demonstrated the production of anti-AGE antibodies in animals immunised with a variety of glycated proteins. Moreover, antibodies against EAGLEs have also been isolated in patient with autoimmune/chronic inflammatory diseases (Tsekovska et al. 2016; Ryan, Nissim, and Winyard 2014). For example, Turk et al demonstrated the presence of anti-AGE autoantibodies in both diabetic and non-diabetic serum samples. However, in the diabetic subjects these antibodies formed immune complexes which the authors speculated may contribute to diabetic complications such as nephropathy (Turk et al. 2001). These results indicate that AGE modifications can

be recognised as antigens and this may contribute to the pathogenesis of immune-mediated disorders.

In most of the AGE-immunisation studies the proteins were injected in adjuvants, predominantly Freund's complete adjuvant (Akhter, Khan, and Ahmad 2015; Rasheed et al. 2009; Arif et al. 2012; Ansari et al. 2009; Mir et al. 2016; Heilmann et al. 2014). A smaller body of work has examined the immunogenicity of proteins modified with reactive intermediates such as GA, in the absence of adjuvant. These have demonstrated that the modified samples induce stronger antibody responses to the native protein compared with the unmodified samples when used to immunise mice (Moghaddam et al. 2011; Allison and Fearon 2000). These results suggest that modifications could act as natural adjuvants, enhancing the immunogenicity of the normally inert protein. Indeed, the authors of one study were able to demonstrate that GA-modification of a self-protein, cytochrome c, could induce the development of antibodies targeting the native protein (Allison and Fearon 2000). Whilst such modifications may therefore have negative consequences in terms of autoimmune responses, they could also be exploited for vaccine design. For example, Allison and Fearon demonstrated that mice could develop antibody responses to merozoite surface protein 1, an antigen of the malaria parasite which normally has low immunogenicity, when it was modified with GA.

Whilst most of these studies have focused on the development of antibody responses, some evidence is emerging which also indicates that AGEs can affect the activation of T cell responses. In a study from Han et al, treating CD4 T cells isolated from human blood with AGE-BSA before stimulation with PMA/ionomycin promoted the development of Th1 and Th17 cells (Han et al. 2014). Conversely, AGE-modified proteins inhibited Treg function. Moreover, *in vitro* activation studies using CD4 T cells derived from OT-II mice (which have a TCR specific for an ovalbumin (OVA) epitope) cultured with murine bone marrow

derived dendritic cells (mBMDCs), have demonstrated that AGE-modified OVA samples induce greater T cell proliferation and IL-2 secretion compared to native OVA (Heilmann et al. 2014). In contrast to the above study indicating AGEs induced a Th1/Th17 bias, *in vivo* immunisation studies using hen egg lysozyme (HEL) modified with GA or other aldehydes indicated that these modifications induced T cell responses against HEL with a Th2 bias (Moghaddam et al. 2011).

Overall, the possible effects of AGEs on adaptive immune response to proteins can be divided into two broad categories. Firstly, AGE modifications may be the target of the immune responses, acting as neoepitopes which are recognised by the immune system resulting in anti-AGE immune responses. Secondly, the modifications may have immunomodulatory properties, directing the immune system to respond to native epitopes preserved in the protein. Both of these mechanisms could contribute to pathology in immune-mediated disorders, for example by inducing responses to native proteins in autoimmune diseases.

1.7 Aims of the Current Project

The underlying hypothesis of this thesis is that AGE-modifications are able to activate cells of the innate and/or adaptive immune system, resulting in the formation of T and B cell responses against the native protein. Much of the literature has focused on the development of anti-AGE immune responses, thus the capacity of AGE-modifications to target immune responses to the carrier protein is relatively unexplored. However, this could be potentially useful in vaccine design, where a response to the native protein is required. Alternatively, if AGE-modifications have the capacity to break "self-tolerance" to native proteins, this could be extremely detrimental in the case of autoimmune disease.

The specific aim of this work was to uncover the mechanism(s) mediating enhanced immunogenicity of AGE-modified proteins. Studies investigating these mechanism have so far been limited and produced conflicting results. In some, AGE-modified proteins have been reported to induce maturation of DCs through RAGE (Buttari et al. 2011), whilst others have found no effect on DC maturation (Moghaddam et al. 2011). Alternatively, some studies have indicated that enhanced immunogenicity of AGE-modified proteins is the result of SR mediated uptake of modified proteins by DCs, leading to greater presentation to T cells (Heilmann et al. 2014; Ilchmann et al. 2010). To address these disparities and further clarify the mechanisms, several hypotheses were investigated:

1. AGE-modified proteins induce classical maturation of DCs, resulting in enhanced immunogenicity due to increased DC induced Th cell activation
2. AGE modification increases protein uptake by DCs in an SR-A dependent manner, leading to increased antigen-presentation and subsequently enhanced immunogenicity.
3. AGE-mediated immunogenicity is dependent on RAGE.

To probe these, model AGE-modified proteins were synthesised, their modifications characterised and *in vivo* immunogenicity examined. The capacity of the protein samples to induce maturation of mBMDCs was determined by examining expression of costimulatory molecules, changes in transcription profile and cytokine secretion. Similarly, DC uptake of modified proteins was assessed *in vitro* using flow cytometry-based uptake assays with mBMDCs and fluorescently-labelled AGE-modified proteins. These assays used BMDCs derived from SR-A, MARCO and SRA/MARCO knockout (KO) mice. MARCO, or macrophage receptor with collagenous structure, is another SR belonging to the SR-A

family. These SR KO mice, along with RAGE KO mice, were also used to test the *in vivo* immunogenicity of selected AGE modifications. During these *in vivo* studies a weight gain phenotype was observed in mice lacking MARCO and a weight loss phenotype was seen in RAGE KO mice. Further experiments were performed to further probe these phenotypes. Finally, the effects of AGE modification on clinically relevant proteins, namely peanut allergens, was examined in terms of their immunogenicity and interactions with DCs.

Chapter 2: Materials and Methods

2.1 General Notes

Below are descriptions of all the methods used in this thesis. At the start of each results chapter there is a reference list of procedures. All procedures were carried out at room temperature (RT) unless otherwise stated. Chemicals/reagents were acquired from Sigma-Aldrich, except where indicated. Plasticware was obtained from Corning, Starlab, Sarstedt, Terumo, Rainin, Generon or Greiner-Bio. For ELISAs and western blots, the wash solution was phosphate buffered saline (PBS) (ThermoFisher) with 0.05% Tween-20 (PBST20). For ELISAs, SpectraPlate-96 High Bind plates were obtained from Perkin Elmer and these were washed using a HydroSpeed Plate washer (Tecan). A list of buffers used in multiple assays is given in Table 2.1.1. Buffers used for specific experiments are given in the text. Where buffer composition is not given, this is a commercial buffer for which no composition is freely available.

Buffer	Supplier	Composition
10x PBS	ThermoFisher	1.37 M NaCl, 0.027 M KCl and 0.119 M phosphates, pH 7.4
	Gibco	1.552 M NaCl, 10.6 mM potassium phosphate monobasic and 29.7 mM sodium phosphate dibasic
PBS	Lonza	9 g/l NaCl, 144 mg/l potassium phosphate monobasic and 795 mg/l sodium phosphate dibasic
Coating buffer	Made in house	0.1 M sodium bicarbonate, pH 8.5
4x LDS sample buffer	Invitrogen	106 mM Tris-HCl, 141 mM Tris-Base, 2% LDS, 10% Glycerol, 0.51 mM EDTA, 0.22 mM SERVA Blue G250, 0.175 mM Phenol Red, pH 8.5

20x MOPS Buffer	Invitrogen	50 mM MOPS, 50 mM Tris-Base, 0.1% SDS, 1mM EDTA, pH 7.7
4x NativePage sample buffer	Invitrogen	200 mM Bis-Tris, 24 N HCl, 200 mM NaCl, 40% Glycerol, 0.004% Ponceau S, pH 7.2
20x NativePAGE running buffer	Invitrogen	1 M Bis-Tris, 1 M Tricine, pH 6.8
20x Cathode Buffer Additive	Invitrogen	0.4% Coomassie G-250
20x Transfer Buffer	Invitrogen	25 mM Bicine, 23 mM Bis-Tris, 1 mM EDTA, pH 7.2
REVERT wash solution	LiCor	6.7% Acetic Acid, 30% Methanol in water
Red Blood Cell Lying Buffer Hybri-Max	Sigma-Aldrich	8.3 g/l ammonium chloride in 0.01 M Tris-HCl buffer
Table 2.1.1: List of buffers used in the thesis.		

2.2 AGE Modification Methods and Analysis

2.2.1 General Notes

The proteins modified in this study were bovine serum albumin (BSA), ovalbumin (OVA) and hen egg lysozyme (HEL). All reactions were carried out in endotoxin-free PBS unless otherwise stated. BSA and OVA (Invivogen) were purchased as endotoxin-free samples. The HEL was not guaranteed as LPS free and so this was cleaned on an endotoxin removal column, then tested with the TLR4 reporter assay to ensure no endotoxin contamination remained (see 2.2.21 and 2.3.2). At the end of all modification procedures, the samples were passed through a 0.22 μm sterile filter and protein concentration was determined by BCA assay (ThermoFisher). Briefly, 25 μl of diluted sample or standard was pipetted into a 96-well plate and 200 μl of BCA reagent was added to each well. The samples were incubated at 37 °C for 30 mins, then absorbance read at 562 nm using a SpectraMax M5 or M3 plate reader (Molecular Devices). Samples were then stored at -80 °C.

2.2.2 Glucose Modification

1 mg/ml of native protein was incubated with 1 M Glucose for 24 weeks at 37 °C. At the end of this time period, the samples were desalted into PBS using Amicon-Ultra Centrifugal Filter Units (Millipore) of the appropriate molecular weight (10 kDa for HEL and OVA, 30 kDa for BSA). Samples which were glucose modified are referred to as GLUC modified.

2.2.3 GA Modification

Protein samples (0.25 mg/ml) were incubated with 20 mM of glycolaldehyde (GA) for 3 h or 7 days at 37 °C. Samples were then desalted as for the Glucose Modification. To reduce reactive carbonyls (RCs), 0.25 mg/ml of the GA-modified sample was incubated for 3 h at 37 °C with 20 mM of sodium borohydride. Samples were then desalted as before. Samples which are GA modified are referred to as GA 3 hr or GA 7 day. Samples which were then post-reduced are referred to as GA-PR 3 h or GA-PR 7 day. The time period refers to the length of time of the original GA modification.

2.2.4 CML Modification

There were two forms of (carboxymethyl)lysine (CML) modification used in these studies and the protocols were based on previously published results (Kislinger et al. 1999; Ikeda et al. 1996). Firstly for the intense modification, native protein at 5 mg/ml was mixed with 200 mM sodium cyanoborohydride and 100 mM glyoxylic acid for 24 h at 37 °C. This modification is referred to as CML HIGH in the text. For the mild modification, referred to as CML LOW, 5 mg/ml protein was incubated with 30 mM glyoxylic acid and 150 mM sodium cyanoborohydride for 3 h at 37 °C. At the end of the incubation, samples were desalted as before. The CML HIGH modification was so named as it involved a longer

incubation time and higher concentration of modifying reagent compared to the CML LOW condition.

2.2.5 Pyrraline Modification

3-deoxyglucosone (3-DG) (Santa Cruz Biotechnology) was dissolved in 0.1 M sodium acetate buffer (0.1 M sodium acetate mixed with 0.1 M acetic acid at a 7:3 ratio to give pH 5, acetic acid was from Scientific Laboratory Supplies). The 3-DG was mixed with 1 mg of HEL at a 4:1 molar ratio of 3-DG:lysine and the volume made up to 200 µl with the sodium acetate buffer. The samples were then lyophilised and heated to 70 °C for 1, 2 or 4 h. At the end of the incubation, samples were allowed to cool to RT, then dissolved in 1 ml of H_2O and lyophilised once more. The final sample was dissolved in PBS. The protocol was taken from previously published papers (Heilmann et al. 2014; Henle and Bachmann 1996). In the text, pyrraline modified samples are referred to as "PYR" samples.

2.2.6 Carbonyl ELISAs

2.2.6.1 Biotin Hydrazide ELISA

1 µg of protein sample in 8 µl of PBS was mixed with 2 µl of a 50 mM biotin hydrazide (BH) solution (final concentration 10 mM) or 2 µl of DMSO. These were left on a shaker for 2 h and then 290 µl of coating buffer was added. The samples were mixed and the solutions added to a 96-well ELISA plate (100 µl/well), which was left at 4 °C overnight (o/n). The plates were then washed and blocked for 1 h with 1% BSA/PBS. Next, the plates were washed again and incubated with streptavidin conjugated to horseradish peroxidase (streptavidin-HRP (GE Healthcare)) diluted 1/2000 in 1% BSA/PBS. After a final wash, plates were developed with Ultra-TMB (ThermoFisher) and stopped with 1 M H_2SO_4.

Absorbance at 450 nm and 570 nm was measured using a SpectraMax M5 or M3 plate reader.

2.2.6.2 DNPH ELISA

1 μg of protein sample was added to 10 μl of a 10 mM DNPH (2,4-dinitrophenylhydrazine) solution in 2 M HCl (VWR Chemicals) or 10 μl of 2 M HCl alone. These were left on a shaker for 2 h and then 290 μl of coating buffer was added for o/n coating onto 96-well ELISA plates (100 μl/well, plates left at 4 °C). The following day, plates were washed and then blocked with 1% BSA/PBS (200 μl/well) for 1 h. After another wash, an anti-DNP (dinitrophenyl) antibody (Invitrogen, Rabbit IgG polyclonal) was added for 1 h (1/2000 in 1% BSA/PBS, 100 μl/well), then plates were washed again and streptavidin-HRP was added for 30 mins (1/2000 in 1% BSA/PBS, 100 μl/well). Finally, plates were washed and developed as in 2.2.6.1.

2.2.7 CML ELISA

1 μg of each protein sample was diluted in coating buffer to give a total volume of 300 μl. This was then divided equally between three wells on a 96-well ELISA plate and left o/n at 4 °C. The following day the plates were washed, blocked with 200 μl of 1% BSA/PBS for 1 h, washed again and then 100 μl of a biotinylated anti-CML antibody was added per well (Abcam, diluted 1/5000 in 1% BSA/PBS, polyclonal). Alternatively, the same volume and concentration of a normal goat biotinylated polyclonal IgG was added as an isotype control (R&D). After a further wash, streptavidin-HRP was added for 30 mins (100 μl per well, 1/2000) and then wells were washed and developed as in 2.2.6.1.

2.2.8 GA-Pyridine ELISA

1 μg of protein sample was diluted in coating buffer to give a total volume of 150 μl. This solution was then pipetted into the wells of a 96-well ELISA plate (50 μl/well) and the plate left o/n at 4 °C. The next day, plates were washed, blocked with 1% BSA/PBS (100 μl/well) for 1 h, washed and then the anti-GA-Pyridine antibody (Cosmobio, diluted 1/600 in 1% BSA/PBS, 2A2) was added at 50 μl/well, for 1 h. A purified mouse IgG1 antibody (MG1-45, Biolegend) was used as an isotype control. Afterwards, the plates were washed again and a rat anti-Mouse IgG1 HRP antibody (BD Bioscience) was added for 1 h. This antibody was diluted 1/1000 and 50 μl was added per well. The ELISA plates were then washed and developed as in 2.2.6.1.

2.2.9 Pyrraline ELISA

The pyrraline ELISA was run as for the GA-Pyridine ELISA except an anti-pyrraline antibody (Cosmobio, H12) was used. The isotype control is also the same.

2.2.10 TNBSA assay

Protein samples (5 μg) in 10 μl of PBS were mixed with 40 μl of coating buffer, pH 8.5. A 5% solution of TNBSA (gift from Dr B. Lyons) was diluted 1/500 in coating buffer, 25 μl of this solution was then added to the protein samples. These were incubated for 2 h at 37 °C, then 25 μl of 10% SDS and 12.5 μl of 1 M HCl were added. The absorbance of the samples was measured at 335 nm using a quartz cuvette (Hellma Analytics). The protocol was based of standard methods available in the literature (Hermanson 2013).

2.2.11 Fluorescence Measurements

100 µl of a 1 mg/ml solution of the indicated sample was pipetted into the wells of a black, opaque bottom 96-well plate. Fluorescence was then read at 335 nm/420 nm and 370 nm/440 nm (excitation/emission) using a spectrophotometer set to read the emission from the top of the wells (SpectraMax M5 plate reader). These wavelengths were chosen as the excitation maximum for AGE-modified proteins is reported to be 335 nm with an emission maximum at 420 nm. Excitation/emission at 370 nm/440 nm is used for commercial preparations (Valencia et al. 2004; Westwood and Thornalley 1995; Schmitt et al. 2005).

2.2.12 SDS-PAGE

1 µg - 5 µg of a sample in 7.5 µl was mixed with 2.5 µl of 4x LDS sample buffer (Invitrogen) containing 10% 2-mercaptoethanol (2-ME). The samples were heated to 70 °C for 10 mins and then loaded onto 12% Bis-Tris NuPAGE gels (Invitrogen). The ladder included on each gel was the Novex sharp pre-stained protein standard (Invitrogen). Gels were run using MOPS buffer (Invitrogen) for 1 to 2 h at 150 V. Once the run was finished, gels were washed in dH_2O three times. Gels with fluorescently-labelled samples were then scanned for ALEXA488 (A488) using the Molecular Imager PharosFX system (Bio-Rad). After imaging, gels were stained using SilverQuest Silver Staining kit, performed according to the manufacturer's instructions except using half volumes (ThermoFisher). Briefly, gels were fixed in fixing solution (40% ethanol, 10% acetic acid) for 20 mins or o/n, then washed in 30% ethanol for 10 mins. Next, sensitizing solution was added for 10 mins, followed by two 10 mins washes, first in 30% ethanol and then in dH_2O. Staining solution was then added for 15 mins, before a brief (30 s) rinse in dH_2O. Developing solution was added to the gels for 4-8 mins. Once the appropriate colour development was reached, development was stopped by adding stopper solution for 10 mins. Gels were washed once more in dH_2O and

then imaged on a Gel-Doc XR+ Molecular Imager (Bio-Rad). All steps included gentle shaking. For gels with non-labelled samples, the gels were washed and either stained with silver stain as above or with SYPRO Tangerine (Invitrogen). For this latter stain, gels were incubated for 60 mins in 7.5% acetic acid containing the dye diluted 1/5000. Gels were then quickly rinsed with dH_2O and imaged on the Gel-Doc.

2.2.13 Native PAGE

2.5 µl of 4x NativePAGE sample buffer (Invitrogen) was mixed with either 1 µg (isolated proteins) or 3 µg (peanut protein extract (PPE)) of sample in 7.5 µl PBS. These samples and the ladder (NativeMark unstained protein standard, Invitrogen) were then loaded into the wells of a 3-12% NativePAGE Bis-Tris gel (Invitrogen). The anode buffer was 1x NativePAGE running buffer (Invitrogen), the cathode buffer was 1x NativePAGE running buffer supplemented with 0.1x Cathode Buffer Additive (Invitrogen) to give light blue cathode buffer. The gel was run for 90 mins at 150 V and then washed 3 times with dH_2O. For western blotting, the procedure in 2.2.14 was used with the following adjustments: the gel was soaked in 1x transfer buffer and a PVDF membrane (0.45 µm, Invitrogen) was used. The membrane was pre-wet in methanol for 30 s, rinsed in dH_2O and then equilibrated in 1x transfer buffer for several mins.

2.2.14 Western Blotting

Proteins were transferred using the semidry method. Gels were placed in 2x transfer buffer (Invitrogen) and left to equilibrate for 10 mins. In the meantime, 6 filter papers (GE Healthcare) and a nitrocellulose membrane (0.45 µm, GE Healthcare) were washed in 1x transfer buffer containing 10% methanol. The gel and the membrane were then sandwiched between six filter papers in a Bio-Rad Trans-Blot SD, semi-dry transfer cell and an 18 V

current was applied for 25 mins. For NuPAGE gels, the membrane was then briefly washed and stained using REVERT 700 Total Protein Stain (LiCor) according to the manufacturer's instructions. Briefly the membranes were incubated in 5 ml of staining solution for 5 mins and then rinsed twice with wash solution. The membrane was imaged on the LiCor Odyssey imager and next blocked in 3% BSA/PBS for 1 h. As the NativePAGE gels had been run with Coomassie stain, which makes the entire membrane fluorescent in the 700 channel, it was not possible to stain these with REVERT stain and so these were washed and placed straight in 3% BSA/PBS. After blocking, the membrane was given 3x 5 mins washes, then the primary antibodies were added (see Table 2.2.1) and the membranes left in the dark o/n at 4 °C. The next day, the membranes were washed as before and the secondary antibody was then added for 1 h at 4 °C. Finally, the membranes were washed once more and imaged on the LiCor Odyssey.

Antibody	Primary/ Secondary	Clone	Company	Dilution	Diluent
Anti-Ara h 1	Primary	MA-2F7	Indoor Biotechnologies	1/5000	3% BSA
Anti-Ara h 2	Primary	MA-1C3	Indoor Biotechnologies	1/5000	3% BSA
IRDye 800CW Goat anti-Mouse IgG	Secondary	Polyclonal	LiCor	1/10,000	3% BSA with 0.1% Tween

Table 2.2.1: Antibodies used for western blotting

2.2.15 Carbonyl Western Blotting

Protein samples (1 μg – 5 μg depending on experiment) were mixed with 10 mM BH as for the ELISA, and left on a shaker for 2 h. 3 μl of 4x LDS loading buffer containing 10% 2-ME was then added and the samples heated to 70 °C for 10 mins. Samples were then loaded onto 12% Bis-Tris NuPAGE gels and these were run as in 2.2.12. Next, the gels were transferred and stained with REVERT total protein stain as in 2.2.14. After staining,

membranes were placed into 3% BSA/PBS blocking solution and left o/n at 4 °C. The following day, membranes were washed 3x for 5 mins in PBS/T20 and then incubated with the infrared dye 800CW-streptavidin (LiCor) diluted 1/10,000 in 3% BSA/PBS with 0.1% T20 and 0.1% SDS for 1 h at 4 °C. The membrane was then washed again and imaged on the LiCor Odyssey.

2.2.16 Fluorescent Labelling

TCEP bond breaker (ThermoFisher) was added to protein samples (1 mg/ml) to give a final dilution of 1/5000, these were then left for 1 h. Next, A488 C5 Maleimide (Invitrogen) was added at a 5:1 dye to protein molar ratio, and the samples left for a further 2 h in the dark. At the end of this timepoint, the samples were desalted using Amicon-Ultra centrifugal filters then passed through 0.22 μm sterile filters.

2.2.17 Biotin Labelling

100 μl protein at 1 mg/ml was mixed with 10 μl of a freshly prepared 2 mg/ml solution of NHS-LC-Biotin (ThermoFisher) in DMSO. The solution was then left on ice o/n and desalted the following morning using the same procedure as for the protein modifications. To confirm successful labelling, labelled or control protein was coated o/n to ELISA plates (0.3 μg/well, 100 μl/well). After blocking with 1% BSA/PBS, the plates were incubated with streptavidin-HRP (1/2000, 100 μl/well), for 30 mins before developing with TMB as above.

2.2.18 C1q Binding Assay

ELISA plates were coated o/n at 4 °C with protein samples at 1 μg per well. The following day, plates were washed with PBST20, blocked for 1 h with 1% BSA/PBS (100 μl/well),

washed and then native human C1q (Abcam) was added to each well for 1 h at 50 µl/well. After a further wash, biotinylated anti-C1q (Abcam, JL-1) was then added to each well at 1 µg/ml or the indicated concentration (50 µl/well for 1 h), plates washed again and then streptavidin-HRP added for 30 mins (1/2000, 50 µl/well for 1 h). Finally, the plates were developed with TMB for 5 mins, stopped and read as for 2.2.6.1. The human anti-HIV (human immunodeficiency virus) antibody 2G12 was used a positive control in the assays as it contains an Fc domain which would be recognised by C1q. In some experiments, biotinylated C1q was used. In this case the anti-C1q step was omitted.

2.2.19 Complement Activation Assays

The complement activation assays were based on previously published protocols (Chikazawa et al. 2016). ELISA plates were coated o/n at 4 °C with 1 µg/well of protein sample. The following day plates were washed using PBST20, blocked with 1% BSA/PBS (1 h, 100 µl/well), washed and then incubated with human or mouse sera diluted in 1% BSA/PBS for 1-2 h at 37°C, 50 µl/well. Human serum was pooled from male AB donors (Sigma), whilst mouse serum was collected from naïve animals and made in house. After this incubation, the plates were washed again and anti-human C3b (Invitrogen, 6C9) or anti-mouse C3d (R&D, Goat IgG Polyclonal) was added at 0.5 µg/ml or 0.8 µg/ml respectively, 50 µl/well for 1 h. After a further wash, the HRP-conjugated secondary antibodies were added, either rat anti-mouse IgG1 (for C3b, used 1/1000, BD Bioscience) or donkey anti-goat (for C3d, used 1/5,000, Jackson ImmunoResearch), for 1 h at 50 µl/well. The plates were then washed a final time and developed as above. For the C3b activation assay, oxLDL was included as the positive control, whilst for the C3d activation assay 2G12 was used. This decision was based on pilot experiments which investigated which positive control gave the best signal for each assay. Wells which had been coated with protein but which

were not incubated with sera were used as negative controls. For experiments with heat inactivated serum, the serum was heated to 56 °C for 30 mins or the indicated period of time.

2.2.20 HyHEL-10 Binding ELISA

Plates were coated o/n at 4 °C with different modified protein samples at a concentration of 0.5 μg/ml. The following day, plates were washed, blocked with 1% BSA (100 μl/well) for 1 h and washed again. 50 μl/well HyHEL-10 (Absolute Antibody) was then added. The top concentration was 10 μg/ml and this was diluted 1/5 to give a 7 point standard curve. After a 1 h incubation, plates were washed again and HRP-conjugated rat anti-mouse IgG1, (1/2000 in 1% BSA/PBS, 50 μl/well) was added for 1 h. Finally the plates were washed and developed.

2.2.21 Endotoxin Cleaning

LPS contamination was removed from samples using an EndoTrap Red Column (Hyglos) used according to the manufacturer's instructions. Briefly, storage solution was drained from the column, which was then washed twice with 3 ml of regeneration buffer then twice with 3 ml equilibration buffer. The sample was then added, diluted in dH_2O to give 0.5x PBS, and the run through collected. A further 1 ml of 0.5x PBS was then added and collected. The column was then washed twice with 3 ml equilibration buffer, once with 3 ml regeneration buffer and finally once with 1 ml storage buffer (regeneration buffer containing 0.02% sodium azide). The bottom of the column was then closed and 1 ml of storage buffer was added before the column was then sealed. Cleaned samples were then concentrated using an Amicon-Ultra Centrifugal Filter Unit. On one occasion an EndoTrap HD column (Hyglos) was used instead. For this, the column was first washed with regeneration buffer and equilibration buffer as for the EndoTrap Red Column. However, the

EndoTrap HD column requires a minimum of 0.1 mM free Ca^{2+} and so the samples were supplemented with $CaCl_2$ (Lonza) to give 1 mM free Ca^{2+}. To ensure complete recovery of the sample, additional wash steps were included. These were two 1 ml washes with PBS supplemented with $CaCl_2$, one 1 ml dH_2O wash and one 1 ml regeneration buffer wash. The column was then washed and stored as for the EndoTrap Red.

2.3 Cell Culture and *In Vitro* Studies

2.3.1 Cell Culture General Notes

Cells were cultured in 37 °C humidified incubators with 5% CO_2. The cell lines were grown in supplemented DMEM (DMEM with 10% FBS (Gibco), 1x GlutaMAX (Gibco), 100 units/ml Penicillin, 100 μg/ml Streptomycin (Gibco) and 10 mM HEPES). Primary cells and bone marrow derived dendritic cells (BMDCs) were cultured in supplemented RPMI (RPMI with 10% FBS, 1x GlutaMAX, 100 units/ml Penicillin, 100 μg/ml Streptomycin, 10 mM HEPES, 50 μM 2-ME (Gibco)). DMEM is Dulbecco's modified eagle media and RPMI is Roswell Park Memorial Institute media. FBS is foetal bovine serum. For cell counts, a sample of a single cell suspension was mixed with trypan blue and KOVA Glasstic slides (VWR International) were used for counting. To pellet cells they were centrifuged at 400 xg for 5 mins unless otherwise stated. Flow cytometry wash buffer (FwB) was 2% FBS in PBS.

2.3.2 Endotoxin Reporter Assay

HEK293 cells transfected with TLR4-CD14-MD2 (Invivogen) were cultured according to the manufacturer's instructions. Briefly, the cells were maintained in supplemented DMEM containing 100 μg/ml Normacin (Invivogen) and selection antibiotics (10 μg/ml Blasticidin and 50 μg/ml Hygrogold (both Invivogen)) and passaged whenever the cells reached 80-90% confluency. To test samples for contamination, these cells were plated at 50,000

cells/well in a 96-well flat-bottomed plate in medium without selections antibiotics. Protein samples were then immediately added (30 μg/ml) and the plates returned to the incubator for 18 h. PBS was used as a negative control in these experiments, whilst Ultrapure-LPS (Invivogen) was used as a positive control. At the end of the incubation, supernatant was collected and IL-8 production assessed by ELISA. The ELISA kit was from Invitrogen (human IL-8), the protocol is the same as for the other cytokine ELISAs (see 2.6.2)

2.3.3 Generation of GM-CSF murine bone marrow derived DCs (BMDCs)

The femurs and tibias were collected from mice culled as in 2.4.6, and kept on ice in supplemented RPMI. Once back in the laboratory, the bones were washed in 70% ethanol for 1 min, followed by 2 washes in PBS. The head of the femur and the lower extremity of the tibia were trimmed using scissors and then a 25G needle (Terumo) was used to bore a hole in-between the condyles of each bone. Next, the bones were flushed with supplemented RPMI to remove the bone marrow. The "strings" of bone marrow were teased apart using 25G needles. The resultant cell suspension was passed through a 70 μm strainer then centrifuged. The cell pellet was resuspended in 5 ml of complete medium and the cells counted. The cells were then transferred into 6 well plates, with 4 million cells per well in 3 ml of supplemented RPMI containing 10 ng/ml granulocyte-macrophage colony-stimulating factor (GM-CSF, Biolegend). The developing DCs were cultured for 3 days before a medium change. This involved completely removing the medium, including non-adherent cells, and then replacing with medium supplemented with 10 ng/ml IL-4 (Biolegend) in addition to the 10 ng/ml GM-CSF. DCs were then left to develop for a further 3 days.

2.3.4 *In Vitro* Uptake Assays

2.3.4.1 Plate-based Uptake Studies

DCs derived according to the procedure above were harvested. The culture medium was removed and 1 ml lift buffer was added (5 mM EDTA (Amresco) and 12 mM Lidocaine in PBS). The plate was then returned to the incubator for 7-9 mins, after which a further 1 ml of supplemented RPMI was added and the cells were harvested by using a 1 ml pipette to wash the cells off the plate. The cells were then centrifuged, resuspended in 5 ml of supplemented RPMI and counted. 200,000 cells were then added per well to a 96-well flat bottomed plate and left to settle for 3 h in the incubator. At the end of this period, the RPMI medium was removed and protein samples added at 5 μg/ml in 50 μl of opti-MEM (opti-minimum essential media, Gibco). The plates were returned to the incubator for 30 mins. Cells were then harvested using lift buffer as before and moved to a U-bottomed plate. For the majority of uptake experiments, cells were then stained for CD11c and SR-A using the flow cytometry protocols.

2.3.4.2 In-tube Uptake Studies

The method for the in-tube uptake studies started the same as for the plate-based, however, instead of allowing the cells to settle in a 96-well plate the cells were transferred to 1.2ml flow cytometry tubes. Fluorescently-labelled protein samples or Dil-acLDL (Invitrogen) were then added. Again the concentration of the samples was 5 μg/ml and the total volume was 50 μl (opti-MEM). The DCs were incubated with the samples for 30 mins in the incubator as before, but the tubes were shaken every 10 mins. At the end of the incubation period, 50 μl of supplemented RPMI was added and the cells transferred to a U-bottomed plate. Cells were then stained and analysed as for the plate-based assay. AcLDL stands for acetylated LDL, a modified form of LDL which is a ligand for some scavenger receptors.

2.3.5 *In Vitro* Pulsing Assays

In the pulsing assays, DCs were incubated with different modified samples and then examined for changes in expression of cell surface molecules and cytokine secretion. For the majority of experiments, mBMDCs were lifted and plated as in 2.3.4.1. At the end of the 3 h settling period, protein samples were added to give a final concentration of 100 μg/ml. LPS, at a final concentration of 10 ng/ml, was used as a positive control whilst for the negative, PBS without protein was added. The cells were left for the time period indicated in the relevant graph, then supernatant collected and cells harvested with lift buffer for flow cytometry. For experiments examining complement activation, FBS, normal and heated mouse serum were used. BMDCs were derived in normal medium as above but then harvested and plated in RPMI without FBS. FBS or the appropriate mouse serum was then added to the wells to give a final serum concentration of 10%. The cells were then left to settle for 3 h and the same procedure followed.

As higher volumes of supernatant and a greater number of cells were required for the profiler and RNA sequencing (RNAseq) experiments, for these the BMDCs were not lifted. Instead their medium was removed and 1 ml of medium containing 100 μg/ml of protein, 10 ng/ml LPS or medium alone was added to each well. The cells were then returned to the incubator for 18 h and the following day supernatant, cells for flow cytometry or cell lysates were collected. For these experiments, when BMDCs were derived the medium was changed on day 4 and the DCs used on day 7.

2.3.6 Flow Cytometry

2.3.6.1 Staining of Samples

Samples were transferred into 96-well U-bottomed plates as outlined above. These were centrifuged, supernatants removed and the cells washed with 200 μl of PBS. Cells were

centrifuged again and 100 µl of appropriate live/dead stain was added. The plates were moved to the 37 °C incubator for 5-7 mins. After the live/dead stain, all steps were carried out at 4 °C. Cells were washed twice with 200 µl of FwB. Next, 50 µl of mouse Fc Block (BD Biosciences/Biolegend) was added to the wells for 5 mins before the addition of appropriate antibodies. The antibodies used throughout this thesis are outlined in Table 2.3.1. The optimal dilution for each antibody was determined by titration experiments. Where a range is shown, dilution varied depending on cell type and panel. Where multiple BV or BUV dyes were used, BD Brilliant Stain buffer plus was added to the antibody mix at the indicated 10 µl/test (BD Biosciences). Samples were left for 20 mins on a shaker set to 400 rotations per minute (rpm). At the end of the time point, 100 µl of FwB was added to the wells and the cells were washed twice more with 200 µl of FwB. Samples were run on a BD Fortessa X20 or BD FACS Calibur. Compensation was determined every experiment using anti-rat/hamster Ig k CompBeads (BD Bioscience). These were incubated with the appropriate amount of each dye for 20 mins at RT, before centrifugation at 200 xg for 10 mins and then resuspension in FwB. In cases where the antibody isotype could not be used with these beads, singly stained cells were used instead.

For intracellular staining of Ki67, cells were first stained for cell surface markers as above. However, on the final wash the cells were transferred to a V bottomed plate, centrifuged and wash buffer removed. The plate was then moved to a shaker and 200 µl of 70% ethanol cooled to -20 °C was added dropwise to each well. After a further 30 s on the shaker, the plate was transferred to the -20 °C freezer and left for a minimum of 2 h. After ethanol fixation all steps were carried out at RT and centrifugation time was increased to 7 mins to improve cell pelleting. For the Ki67 stain, the cells were washed 3 times with 200 µl of FwB. The cells were then mixed with Fc block as for the surface stain, and anti-Ki67 was added for 30 mins on the shaker. Cells were washed as for the surface staining and analysed

on the BD Fortessa X20.

Target	Clone	Dye	Isotype Control	Dilution
Live/Dead Cells	n/a n/a	FVS780 (BD Biosciences) Zombie Aqua (Biolegend)	n/a n/a	1/1000 – 1/4000 1/100
CCR2	SA203G11	BV421 (Biolegend)	Rat IgG2b κ BV421	1/100
CCR7	4B12	BV786 (BD Bioscience)	Rat IgG2a κ BV786	1/50
CD3	17A2	PE (Biolegend)	Rat IgG2b κ PE	1/100 – 1/200
CD4	RM4.5 GK1.5	APC (BD Biosciences) BV510 (Biolegend)	Rat IgG2a κ APC Rat IgG2b κ BV510	1/200 1/100
CD8a	53-6.7 53-6.7 53-6.7	FITC (Biolegend) BV785 (Biolegend) A700 (Biolegend)	Rat IgG2a κ FITC Rat IgG2a κ BV785 Rat IgG2a κ A700	1/200 1/100 1/200
CD11b	REA592	PE-Vio770 (Miltenyi)	REA293 PE-Vio770	1/200 – 1/250
CD11c	HL3 N418	APC (BD Bioscience) BB515 (BD Bioscience)	Armenian Hamster APC Hamster IgG2 λ BB515	1/200 1/200
CD19	6D5	BV421 (Biolegend)	Rat IgG2a κ BV421	1/100
CD25	REA568	PE-Vio770 (Miltenyi)	REA293 PE-Vio770	1/50
CD40	3/23	PE-CF594 (BD Bioscience)	Rat IgG2a κ PE-CF594	1/200
CD45	30-F11	BB700 (BD Biosciences)	Rat IgG2b κ BB700	1/450 – 1/650
CD54	3E2	BV711 (BD Bioscience)	Hamster IgG1 BV711	1/200
CD68	FA/11	BV421 (BD Biosciences)	Rat IgG2a κ BV421	1/100
CD69	REA937	APC-Vio770 (Miltenyi)	REA293 APC-Vio770	1/50
CD70	FR70	BV711 (BD Bioscience)	Rat IgG2b κ BV711	1/50
CD80	16-10A1	BUV737 (BD Bioscience)	Hamster IgG2 κ BUV737	1/200
CD86	GL1	PE (BD Bioscience)	Rat IgG2a κ PE	1/200
CD138	281-2	A647 (Biolegend)	Rat IgG2a κ A647	1/100
CD169	3D6.112	BV605 (Biolegend)	Rat IgG2a κ BV605	1/50
CD206	C068C2	BV650 (Biolegend)	Rat IgG2a κ BV650	1/50 – 1/100
CD209a	5H10	BV786 (BD Bioscience)	Rat IgG2a κ BV786	1/50
CD209b	REA125	PE (Miltenyi)	REA293 PE	1/100
CD273	TY25	BV650 (BD Bioscience)	Rat IgG2a κ BV650	1/50
CD274	MIH5	BV421 (BD Bioscience)	Rat IgG2a λ BV421	1/200
CD276	MIH32	BV786 (BD Bioscience)	Rat IgG2a κ BV786	1/50
Dectin-1	REA154	APC (Miltenyi)	REA293 APC	1/40
Galectin-3	REA1072	PE (Miltenyi)	REA293 PE	1/200
F4/80	BM8 BM8 T45-2342	PE (Biolegend) A647 (Biolegend) BUV395 (BD Biosciences)	Rat IgG2a κ PE Rat IgG2a A647 Rat IgG2a κ BUV395	1/100 1/200 1/200
Ly6C	AL-21	FITC (BD Biosciences)	Rat IgM FITC	1/100
Ly6G	1A8	APC (BD Biosciences)	Rat IgG2a κ APC	1/200
ILT3	H1.1	PE (Biolegend)	Armenian Hamster PE	1/200
Ki67	11F6	A488 (Biolegend)	Rat IgG2b κ A488	1/100
MHC II	2G9 M5/114.15.2 M5/114.15.2	FITC (BD Biosciences) BV711 (BD Biosciences) BV480 (BD Biosciences)	Rat IgG2a κ FITC Rat IgG2b κ BV711 Rat IgG2a κ BV480	1/200 1/500 1/100
OX40L	RM134L	BV421 (BD Bioscience)	Rat IgG2b κ BV421	1/50
SR-A	M204PA	PE-Cy7 (eBioscience)	Rat IgG2a κ PE-Cy7	1/160
TLR1	TR23	BV421 (BD Bioscience)	Rat IgG2a κ BV421	1/50
TLR2	6C2	A647 (BD Bioscience)	Rat IgG2b κ A647	1/200
TLR4	MTS510	BV711 (BD Bioscience)	Rat IgG2a κ BV711	1/50

Table 2.3.1: Antibodies used in this thesis. All are anti-mouse antibodies except for the Ki67 which is an anti-mouse/human antibody. FVS780 = fixable viability stain 780, BB = brilliant blue, BV = brilliant violet, BUV = brilliant ultraviolet, OX40L = OX40 ligand.

2.3.6.2 Data Analysis

Flow cytometry data was analysed using FlowJo. Unless otherwise stated all samples were processed in the following way. Firstly, the flow overtime was examined so any blockages or poor samples could be removed. The samples were then gated to remove doublets and any cellular debris. Dead cells were removed using the live/dead dyes, except for the uptake experiment where live cells were gated on scatter. Finally, specific populations were identified using fluorescence minus one (FMO) controls. An example of this gating strategy is shown in Figure 2.3.1.

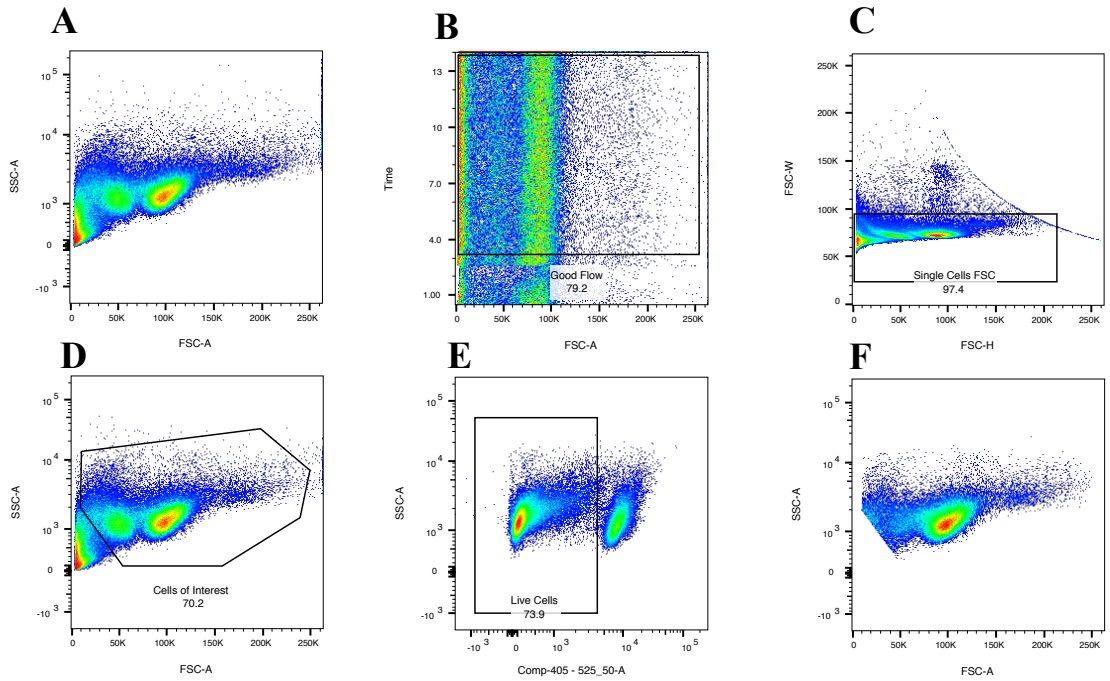

Figure 2.3.1: Standard gating strategy to clean up flow cytometry samples. The starting sample is shown in A. The flow over time is first assessed to remove any blockages and ensure good sample quality (B). Doublets are removed (C) and then any cellular debris (D). Next, dead cells are removed using a live/dead dye (E). The final result is shown in F. FSC = forward scatter, SSC = side scatter

2.3.7 RNAseq Analysis

Lysates from AGE-pulsed cells were prepared by Dr Moghaddam using an RNeasy plus micro kit (Qiagen). These were sent to the Institute of Cancer Research (ICR) for RNAseq analysis. To generate a principal component analysis (PCA) plot from the resultant data the software package Qlucore Omics Explorer was used. Pathway analysis was done using the

ConsensusPathDB database. This is a freely available meta-database which combines several pathway analysis databases and is capable of a variety of analyses including over-representation and enrichment analysis. For the former, a pre-selected list of genes was entered into the database. These were chosen by determining which genes showed significantly different expression between cells pulsed with modified or unmodified protein samples. For enrichment analysis, all genes were entered into the database along with the average expression in the AGE-pulsed and HEL-pulsed samples. Instructions for using the database are given in the published protocol (Herwig et al. 2016).

2.3.8 Proteome Profiler

Secretion of cytokines from DCs pulsed with AGE-modified proteins was assessed using Mouse XL Proteome Profiler (R&D) performed according to the manufacturer's instructions. Briefly, the membranes were blocked for 1 h in array buffer 6. In this time, 1 ml of supernatant was collected from the DCs and 0.5 ml of array buffer 4 was added. The blocking buffer was then removed from the membranes and the supernatant/array buffer 4 mixture was added. The membranes were left on a rocker o/n at 4 °C. The following day, the membranes were washed 3x for 10 mins with wash buffer and then 1.5 ml of secondary antibody was added to each membrane for 1 h on a rocker. After another wash step, the membranes were incubated for 1 h at 4 °C with IRDye 800CW streptavidin diluted 1/5000 in array buffer 6. Finally, the membranes were washed once more and imaged on the LiCor odyssey.

2.3.9 Luminex Assay

Luminex kits were purchased from R&D and used to analyse supernatant according to the manufacturer's instructions. In brief, supernatants were diluted 1:2 in RD1W buffer and the

standard curve prepared according to the instructions provided with each kit. These were then pipetted into the well of a black 96-well plate and 50 µl of magnetic-bead cocktail was added to each of the wells. After a 2 h incubation on a shaker set to 800 rpm, the supernatant was removed and the wells washed 3x with 300 µl of wash buffer using a magnetic plate washer. 50 µl of diluted secondary antibody mix was then added to the wells and the plate returned to the shaker for a further 1 h. The plates were then washed again before a 30 min incubation with streptavidin-PE. The wells were washed a final time and then the plate was read on a Luminex Bio-Plex (Bio-Rad).

2.3.10 PGE_2 ELISA

Concentrations of PGE_2 (prostaglandin E2) in supernatant samples were measured by ELISA performed according to the manufacturer's instructions (Abcam). Briefly, supernatant from pulsed DCs was diluted 1:4 in RPMI to give a total of 100 µl. This was then added to ELISA plates pre-coated with anti-mouse IgG, along with RPMI as a background and PGE_2 standards. 50 µl each of PGE_2 alkaline phosphatase conjugate and PGE_2 antibody were then added and the plate was incubated for 2 h on a shaker at 500 rpm. The plates were then washed 3x with wash buffer before adding 200 µl of Lumiphos 530 chemiluminescent immunoassay substrate to the wells and returning the plate to the shaker for 60 mins. Luminescence was then read for each well using a luminometer (SpectraMax M3).

2.4 Animal Studies

2.4.1 Mouse Origin and Care

SR-A knockout (KO) mice (SRA), MARCO KO mice (MARC) and SR-A/MARCO double KO (DKO) mice (SRMA) were kindly given to the lab by Professor S. Gordon (University

of Oxford). These were bred in the animal facility. C57BL/6J, BALB/c and CBA mice were purchased from Charles River or taken from in house stocks. RAGE KO (RAGE) mice were a gift from Professor P. Nawroth (University of Heidelberg). The C57BL/6N wildtype (WT) mice were initially bought from Charles River and then breeding pairs were established and bred in house. All mice were kept and cared for in accordance with the Home Office guidance and procedures were performed by a personal licence holder. Mice were kept in specific pathogen free conditions with regular sentinel screening. All mice used in the experiments were female.

2.4.2 Experimental Design of *In Vivo* Experiments

For the SR KO and BALB/c s.c. immunisation experiments, a randomised block design was employed with three blocks in each experiment. For the SR experiments, each block consisted of mice born at different times. Within these blocks, the mice were matched in age as closely as possible. For all experiments, mice were randomly assigned to their treatment groups using the random number function in excel. In order to avoid bias throughout the experiments, the cage order of injections, bleeds and harvests was also randomised. For all but two experiments (the DC transfer and first PPE immunisation), the solutions for immunisation were relabelled by another member of the laboratory to allow for treatments to be given blind. The experiment was unblinded after the splenocyte and antibody responses had been assessed. When pilot data was available, sample size was estimated using the power.anova.test command in Rcmdr with the significance level set to 0.05 and power set to 80%. The number of animals used in each experiment is given in the relevant figure legend. Where the sample size between groups is not equal it is because mice died between the start and end of the experiment. The exception is the DC transfer study which was limited in size by the number of BMDCs which could be reliably made from one mouse each time,

necessitating uneven group sizes groups. The age and weight of the mice at the start at each of experiment is shown in Table 2.4.1.

Experiment	Block	Age (weeks)	Average Weight (g) (Minimum-Maximum)
BALB/c s.c. immunisation	1	8	19.04 (16.4 - 21.8)
	2	10	18.83 (16.4 – 21.4)
	3	6	17.97 (16.1 – 19.6)
CBA s.c. immunisation	n/a	9	21.94 (17.8 – 26.5)
DC transfer	n/a	8	19.64 (15.9 – 20.9)
SRA/MARC/SRMA/C57BL/6J	1	20	WT-B6: 21.95 (20.4 – 24.5)
			SRA: 20.92 (19.1 – 23.4)
			MARC: 25.58 (21.2 – 30.5)
			SRMA: 31.47 (28.8 – 34.5)
	2	15	WT-B6: 22.4 (20.2 – 24.3)
			SRA: 21.2 (19.2 – 25.6)
			MARC: 24.73 (22.6 – 28.5)
			SRMA: 27.62 (22.7 -35.6)
	3	11	WT-B6: 19.47 (17.9 -21.3)
			SRA: 21.13 (17.9 – 29.2)
			MARC: 21.62 (19.7 – 22.9)
			SRMA: 21.78 (19 – 25.3)
RAGE/C57BL/6N	1	16	WT-B6N: 21.14 (18.1 – 23.3)
			RAGE: 21.7 (18.4 – 25)
	2	11	WT-B6N: 20.75 (20 – 22.7)
			RAGE: 16.83 (14.9 – 18.3)
	3	14	WT-B6N: 21.41 (20.4 – 22.6)
			RAGE: 22.08 (20 – 23.9)
PPE immunisation 1 (BALB/c)	n/a	8	Data not collected
PPE immunisation 2 (C57BL/6N)	n/a	13	20.79 (19.6 – 21.7)
Ara h 1 s.c. immunisation	n/a	8	18.34 (16 – 20.4)

Table 2.4.1: Age and weight of mice at the start of each experiment. In experiments with multiple blocks, data for each block is given. For the SR KO experiments, the weights of mice in different genotypes are shown separately.

2.4.3 Subcutaneous (s.c.) Immunisation Protocols

Mice were immunised according to the protocols outlined in Figure 2.4.1. For s.c. injections mice were immunised in the left flank with BD-microfine 8mm insulin syringes. Bloods were collected from the lateral tail veins throughout the experiment. To collect sera, bloods were allowed to clot, either for 1 h at room temperature or o/n at 4°C, and then centrifuged at 6,000 xg for 5 mins to separate the sera and blood clot. Samples were then collected and frozen until analysis. For the peanut feeding experiments, normal mouse chow was removed and 4-5 peanuts per mouse added to the cages. Remaining peanuts were then collected 16 h later and mouse chow returned. The number and weight of peanuts consumed was measured at each feed.

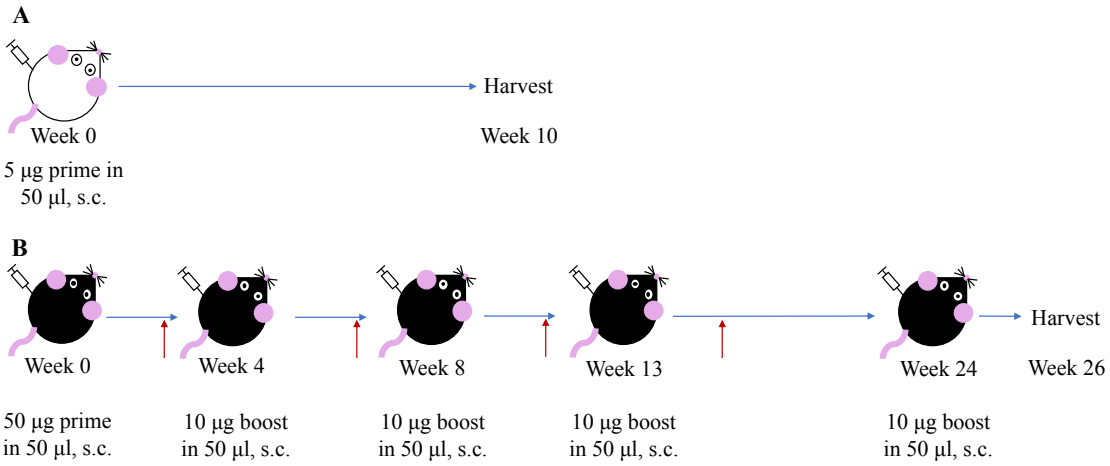

Figure 2.4.1: A shows the immunisation schedule for the BALB/c HEL and Ara h 1 s.c. experiments and the CBA s.c. experiment. B shows the immunisation protocol used for the SRA, MARC, SRMA, C57BL/6J and RAGE and C57BL/6N experiments. Sera collections are indicated by red arrows. For the Ara h 1 immunisation experiment blood was also collected at weeks 5 and 9. The immunisation schedules for the PPE immunisation experiments are given in Chapter 7. The immunisation schedule for the DC transfer experiment is shown in Chapter 3.

2.4.4 DC Transfer Studies

BMDCs were derived as in section 2.3.3. On day 6 medium was removed and replaced with 900 µl of RPMI and either 100 µl of PBS containing 100 µg of protein, 100 µl of PBS containing 100 µg of protein with 10 ng/ml LPS, or 100 µl of PBS alone. The BMDCs were incubated with these samples for 4 h. At the end of the time point, supernatant was collected and the cells washed with 3 ml of RPMI. Next, the cells were harvested in RPMI, centrifuged at 400 xg for 5 mins and then resuspended in cold HBSS (Hank's balanced salt solution, without Ca^{2+} or Mg^{2+}, Gibco) and counted. The volume of HBSS was then adjusted to give 5 million cells/ml. 100 µl of this solution was then injected i.p. (intraperitoneal) into female BALB/c mice. This process was repeated again two weeks later, and then two weeks after that the mice were culled.

2.4.5 Fasting Blood Glucose Measurements

Food was removed from the mice for 5 - 6 h. Blood was then collected from the lateral tail veins and glucose level measured using a True Metrix Blood Glucose Monitor.

2.4.6 Tissue Harvesting

At the end of the experiments, mice were culled using rising CO_2 and death was confirmed using cervical dislocation. A blood sample was then collected from the aorta or via cardiac puncture. In some experiments the mouse was then perfused with sterile PBS. A list of tissues which were collected is in Table 2.4.2. Not all tissues were collected at each harvest, the majority of experiments only required spleens.

Tissue	**Processing**
Blood Sample	Sera: see section 2.4.3
Lymph Nodes (axillary, inguinal and mesenteric)	Into RPMI with FBS for flow cytometry
s.c. Fat	Formalin fixation
	Flash frozen in liquid nitrogen
Gonadal Fat	Into PBS with 2% FBS for flow cytometry
	Formalin fixation
	Flash frozen in liquid nitrogen
Brown Adipose Tissue (BAT)	Flash frozen in liquid nitrogen
Liver	Into PBS with 2% FBS for flow cytometry
	Formalin fixation
	Flash frozen in liquid nitrogen
Spleen	Into RPMI with FBS for flow cytometry or splenocyte recall experiments
Kidney	Formalin fixation
	Flash frozen in liquid nitrogen

Table 2.4.2: List of tissues collected at harvest

2.5 Assessment of Antibody Responses

2.5.1 IgG, IgG1, IgG2a and IgG2c ELISAs

The generation of anti-HEL antibodies was assessed by ELISA using the following protocols. ELISA plates were coated o/n at 4 °C using HEL at a concentration of 10 μg/ml, 50 μl per well in coating buffer. The following day the plates were washed using PBST20, then blocked for 1 h with 100 μl of 1% BSA/PBS. Plates were then washed again and 50 μl

of sera diluted in 1% BSA/PBS was added for 1 h. At the end of this incubation, plates were washed and 50 µl of the appropriate anti-IgG antibody added (see Table 2.5.1). After a final 1 h incubation, plates were washed for a final time and then developed using Ultra-TMB. Plates were left to develop for 5 mins before the reaction was stopped with 1 M H_2SO_4. Absorbance at 450 nm and 570 nm was then read. For initial experiments, sera was diluted 1/100. For some experiments, antibody content in the sera were quantified by end point titre. The dilution for these was based on the results of the initial experiments and was typically 1/500 with a five-fold dilution series for sera sets with strong responders and 1/100 with a four-fold dilution series for lower signals. In both cases an eight-point curve was generated for each sample. The end point was determined using twice the average naïve sera signal.

2.5.2 IgE ELISA

ELISA plates were coated o/n at 4 °C with 50 µl anti-mouse IgE antibody (see Table 2.5.1) diluted 1/250 with 0.1 M coating buffer. The following day, plates were washed with PBST20, then blocked for 1 h with 1% BSA/PBS at 100 µl/well, washed again and 50 µl sera, diluted in 1% BSA/PBST20, was added to the wells. The plates were returned to 4 °C for a further o/n incubation. The following day biotin-labelled antigens (raw PPE, raw Ara h 1 or OVA, prepared in house) were added at 50 µl/well. These were at a concentration of 2 µg/ml and were diluted in 1% BSA/PBS. The plate was left for a further 2 h, washed, and then 50 µl/well streptavidin-HRP was added, diluted 1/2000 in 1% BSA/PBST20. The plates were developed for 20 mins. The dilution for initial experiments was 1/20 and for end point titres the starting dilution was 1/20 followed by 1 in 2 dilutions to give a total of 5-6 points.

2.5.3 Examination of Natural Antibody Binding (IgM and IgG)

ELISA plates were coated o/n at 4 °C with 1 μg/well of protein sample. The following day plates were washed using PBST20, blocked with 1% BSA/PBS (1 h, 100 μl/well), washed again and then incubated with naïve human or mouse sera diluted in 1% BSA/PBS for 1 h, 50 μl/well. After this incubation, the plates were washed again and anti-human IgG (1/10,000), anti-human IgM (1/1000), anti-mouse IgG (1/10,000) and anti-mouse IgM (1/1000) were added to the appropriate wells at 50 μl/well for 1 h. Details of the antibodies are given in Table 2.5.1. Both anti-IgG and the anti-mouse IgM antibodies were HRP-conjugated and so were immediately developed after this incubation. The anti-human IgM was biotinylated and so for this ELISA the plates were incubated with streptavidin-HRP for 30 mins (1/2000, 50 μl/well) and then developed.

Antibody	Clone	Manufacturer
Goat ant-mouse IgG HRP	Polyclonal (Star120p)	Bio-Rad
Rat anti-mouse IgG1 HRP	X56	BD Biosciences
Rat anti-mouse IgG2a HRP	R19-15	BD Biosciences
Goat anti-mouse IgG2c HRP	Polyclonal	Bethyl Laboratories
Rat anti-mouse IgE	R35-72	BD Biosciences
Rat anti-mouse IgM HRP	II/41	BD Biosciences
Mouse anti-human IgM Biotin	MHM-88	Biolegend
Donkey anti-human IgG HRP	Polyclonal	Jackson ImmunoResearch

Table 2.5.1: Antibodies used in ELISAs

2.6 Assessment of Cellular Immune Responses

2.6.1 Splenocyte Harvest

Before the harvest, "No Pulse" (supplemented RPMI containing an appropriate volume of PBS) or "Pulse" (supplemented RPMI containing 50 μg/ml of the relevant protein) solutions were prepared. These were then plated at 200 μl/well into 96-well U-bottomed plates. To avoid edge effects, a phenomenon in which the wells around the edge of the plate give more variable results owing to media evaporation, the wells around the edge of the plate were not

used. Spleens were then collected and crushed using a 100 μm strainer and a syringe plunger to produce a single cell suspension in supplemented RPMI. The cells were then counted and 0.5 million cells in 50 μl were then added to the wells of the prepared pulsing plate. The plates were then placed in a 37 °C incubator for a further four days. 50 μl of supernatant was collected on day 1 and IL-4 content assessed. On day 3 100 μl of supernatant was collected and 80 μl of fresh complete medium was added to the wells. IL-2, IL-5 and IFNγ secretion was measured in the day 3 sample. Thymidine pulse was started on day 3 (see below) and results gathered on day 4. This timings were part of a protocol designed in the laboratory. IL-4 was measured on day 1 as in previous experiments this cytokine was produced early during splenocyte pulsing. In contrast, IL-2, IL-5 and IFNγ secretion were found to be optimal later in the incubation and so the concentration of these cytokines were measured in the day 3 supernatant.

2.6.2 Cytokine ELISAs

Supernatant taken from the cells was assessed for IL-2, IL-5, IFNγ and IL-4 secretion using ELISA kits from Invitrogen performed according to the manufacturer's instructions. Briefly, plates were coated o/n at 4 °C using 1x capture antibody diluted in coating buffer (PBS) at 50 μl/well. The following day, plates were blocked (1x ELISA/ELISPOT diluent, 100 μl/well) and then supernatant samples (diluted 1 in 2) and the standard curve were added to the plates for 2 h (50 μl/well, diluted in 1x ELISA/ELISPOT diluent). At the end of this incubation, plates were washed and 1x detection antibody was added for 1 h, followed by 1x avidin-HRP for 30 mins, both at 50 μl/well diluted in 1x ELISA/ELISPOT diluent. Plates were then developed with TMB for 10 or 15 mins depending on the ELISA and then stopped and read as for the antibody ELISAs.

2.6.3 Thymidine Pulse

For the thymidine pulse, 20 µl of RPMI containing 1 µl (0.037 mBq) of tritiated thymidine (Perkin Elmer) was added per well. The plates were then returned to the incubator o/n. The following day, cells were lysed and radioactivity transferred to glass filter mats (Perkin Elmer) using a Micro 96 Harvester (Skatron Instruments). The activity was then measured using Betaplate Scint and a MicroBeta Trilux Scintillation counter (both Perkin Elmer).

2.6.4 Pulsing with Naïve Splenocytes

For the proliferation assay, spleens were harvested from naïve female BALB/c mice, cells isolated and plated as for 2.6.1. Cells were left unpulsed or incubated with either 0.5 µg/ml ionomycin (Invivogen) and 10 ng/ml PMA or 1 µg/ml anti-CD40 (Biolegend, HM40-3), 1 µg/ml anti-IgM (Biolegend, Goat Polyclonal) and 0.5 µg/ml LPS. There were 4 repeat plates in total and on day 1, 2 and 3 one plate was collected and cells stained for Ki67 as above. Proliferation on the final plate was assessed by thymidine incorporation. Thymidine was added to the wells on day 1 and incorporation read on day 2.

To assess direct B cell activation by AGE-modified samples, spleens from MD4 mice, transgenic for the BCR encoding HyHEL-10, were gifted to the laboratory by Dr O. Bannard. Cells were isolated and pulsed with a variety of modified proteins at a 50 µg/ml concentration for 4 days. Proliferation was assessed by thymidine incorporation and flow cytometry. For the experiment examining the contribution of complement, cells were isolated in RPMI lacking FBS. Isolated cells were added to wells containing FBS, mouse serum or heated mouse serum to give a final concentration of 10%.

2.7 Cell Isolation from Tissue Samples and Tissue Analysis

The following procedures were used for isolating cells from mouse tissues. These were based both on protocols previously established in the laboratory and on published protocols (Stagg et al. 2001; Yu et al. 2016; Stijlemans et al. 2015).

2.7.1 Isolation of Cells from Spleen

Spleens were minced into small strips using a scalpel and scissors, then digestion mix was added to give a final volume of 1 ml per 0.1 g of tissue. The digestion mix was enriched RPMI, (supplemented RPMI without 2-ME), with 0.1 mg/ml DNase I (Roche) and 1 mg/ml collagenase type IV (Worthington). Samples were left for 25 mins at 37 °C in a shaking incubator. EDTA was then added to give a final concentration of 5 mM. The samples were left at room temperature for 5 mins with gentle swirling before passing through a 100 μm strainer and adding an equal volume of enriched RPMI. Cells were spun at 400 xg for 5 mins and 1 ml of red blood cell (RBC) Lysing Buffer Hybri-Max was added for 1 min with gentle swirling. 15 ml of enriched RPMI was then added before the cells were spun again, resuspended and counted. Cells were plated at 1 million/well in a 96-well U-bottomed plate for flow cytometry.

2.7.2 Isolation of Cells from Liver

Liver samples were minced and placed in digestion mix. This was the same formula as for the spleen samples. Samples were left in a 37 °C shaking incubator for 45 mins before the addition of the same volume of enriched RPMI. Samples were passed through a 100 μm strainer and RBCs lysed as for the spleen samples. Samples were resuspended in 2 ml of enriched RPMI and 200 μl of this was added per well.

2.7.3 Isolation of Cells from Lymph Nodes

Axillary, inguinal and mesenteric lymph nodes (LNs) were collected from mice and pooled. These were then crushed using a syringe plunger and a 100 μm strainer to isolate cells into enriched RPMI. Cells were then counted and plated at 1 million/well for flow cytometry.

2.7.4 Isolation of Cells from Fat

Gonadal fat pads were minced using a scalpel/scissors and placed in digestion buffer at 1ml per 0.1 g of tissue. The digestion buffer was HBSS (with Ca^{2+}, Mg^{2+}, Gibco) containing 10 mM HEPES, 2.5 mM glucose, 2% FBS and 1 mg/ml collagenase IV. Samples were then moved to a shaking 37 °C incubator for 40 mins. An equal volume enriched RPMI was then added and the samples passed through a 100 μm strainer. Next, the tubes were spun at 100 xg for 8 mins. This separated the adipocytes which were then removed. The remaining cells were resuspended and spun at 400 xg for 5 mins. RBCs were lysed as for the spleen samples and then resuspended in 2 ml of enriched RPMI. 200 μl of this solution was added to the wells of a 96-well U bottomed plate.

2.7.5 Measurement of Liver Triglyceride Content

Liver Triglyceride content was measured according to a previously published protocol which was modified to a plate based assay to allow for high throughput experiments (Jouihan 2012). Briefly, weighed liver samples were heated at 55 °C o/n in ethanolic KOH (ethanol and 30% KOH mixed at a 2:1 ratio, KOH was from VWR International) with vortexing to break up the tissue. Once digested, 50% ethanol was added to the samples to give a final volume of 1000 μl, these were then centrifuged at 2000 xg for 10 mins. The supernatant was then collected and diluted to 1200 μl with 50% ethanol. 200 μl of this sample was then added to 215 μl of 1 M $MgCl_2$, the samples were vortexed and left on ice

for 10 mins. These were then centrifuged once more and supernatant collected. 2 µl of the final sample, glycerol standard or control (dH_2O) was then added to 160 µl of free glycerol reagent. After 15 mins on a shaker at room temperature, the absorbance was read at 540 nm.

2.7.6 Measurement of Fat Noradrenaline Content

Frozen s.c. fat samples were placed into reinforced metal hard tissue homogenising tubes (Precellys) containing 500 µl of homogenisation buffer (0.01 N HCl, 1 mM EDTA, 4 mM sodium metabisulfite). Samples were homogenized for 1 min using a Precellys 24 Tissue Homogenizer and then spun at 20,000 xg for 10 mins. Supernatants were collected and 50 µl of these were used for a noradrenaline ELISA (LDN). The ELISA was run according to manufacturer's instructions. Briefly, samples (50 µl) and standards were added to the extraction plate and made up to 100 µl using dH_2O. 25 µl of Tris-EDTA buffer was then added and the plate incubated for 60 mins on a shaker (600 rpm). The wells were then emptied and washed twice by adding 1 ml of wash buffer, shaking for 5 mins, then emptying. 150 µl of acylation buffer and 25 µl of acylation reagent were then added to each well. The plate was returned to the shaker for 20 mins, washed again and 100 µl of 0.025 M HCl added to the wells. The plate was incubated for a further 10 mins and the resultant supernatant collected. 90 µl of the supernatant was then incubated with 25 µl of enzyme solution in a microtiter plate for 2 h at 37 °C. The enzyme solution contained catechol-O-methyltransferase and the coenzyme S-adenosyl-L-methionine. 100 µl of the supernatant/enzyme mix was pipetted into the wells of a plate precoated with noradrenaline and 50 µl of an anti-noradrenaline antibody was added. The plate was incubated o/n at 4 °C. The following day, the plate was washed 4x with 300 µl wash buffer, then 100 µl enzyme conjugate (goat anti-rabbit Ig conjugated to peroxidase) was added to each well for 30 mins

with shaking at 600 rpm. After a final wash, plates were developed with TMB for 30 mins and stopped with 0.25 M sulphuric acid. Absorbance was read at 450 nm and 570 nm. Measured noradrenaline was normalised to the protein concentration in each sample. This was calculated using a BCA assay.

2.8 Peanut Protein Manufacture and Isolation

2.8.1 Sourcing and Roasting of Peanuts

Raw peanuts (Holland and Barret) were left unprocessed or roasted in house in a laboratory oven (Memmert). In initial pilot experiments the peanuts were roasted at either 160 °C or 178 °C for 5 to 20 mins. The final conditions selected for roasting were 178 °C for 20 mins. To ensure even roasting, 10 peanut kernels were spread one layer thick on tinfoil which was then wrapped to form little parcels. These parcels were roasted in small batches. Commercial dry roast (cDR) samples were purchased from supermarkets in Oxford and included KP, Tesco own-brand and M&S own-brand.

2.8.2 Production of PPE

To prevent LPS contamination all steps were carried out in a tissue culture hood and equipment was either autoclaved or cleaned with 0.5 M NaOH and ethanol. Raw, dry roast (DR) and cDR samples were ground to a paste using a pestle and mortar. The pastes were then transferred into glass vials and defatted using 4 °C acetone (Honeywell). Acetone was added to the vials which were vortexed extensively and then centrifuged at 1000 xg for 5 mins. This was repeated twice more and a minimum 20 volumes of acetone was used in total. The samples were then left to dry o/n at 4 °C. The following day the resultant powder was collected and either used immediately or frozen at -20 °C. For PPE extraction, the powder was mixed with extraction buffer (0.1 g/ml) and then left at 4 °C o/n at 300 rpm.

Details of the extraction buffers are in Table 2.8.1. The following day, the samples were centrifuged at 2000 xg for 10 mins, supernatants collected and then centrifuged again at 12,000 xg for 20 mins. For extraction in 10x PBS, the final supernatant was then concentrated using a 3 kDa Amicon-Ultra Centrifugal Filter, run through a 0.22 μm filter and then diluted with endotoxin free water (Gibco) to give a 1x PBS solution. The concentration was then assessed by BCA assay. The samples were stored at -20 °C.

Buffer	Manufacturer	pH
50 mM Sodium Carbonate	Sigma	pH 11
7 mM Sodium Borate	Sigma	pH 9.2
50 mM Tris-HCl with 0.2 M NaCl	Sigma	pH 8.2
6 M Urea	VWR Chemicals	pH 8.7
10x PBS	Gibco	pH 7.4

Table 2.8.1: Buffers used for PPE extraction

2.8.3 Anion Exchange Chromatography

Fast protein liquid chromatography (FPLC) was performed using an AKTApurifier UPC-10 (GE Healthcare) with a 1 ml MonoQ 5/5 column (GE Healthcare). Solutions for anion exchange are detailed in Table 2.8.2, all were degassed before use using bottle top 0.2 μm filtration units.

PPE samples were made up at a concentration of 1 mg/ml – 2 mg/ml and these were then loaded onto the column in start buffer. The concentration of NaCl was then increased over 40 column volumes to a final concentration of 1 M. After collection, fractions of interest were passed through a 0.22 μm filter and stored at -20°C until further use. To analyse purity, 15 μl of each sample was mixed with 5 μl of 4x LDS sample buffer containing 10% 2-ME. These were then analysed by SDS-PAGE as for 2.2.12. Samples showing a good level of purity for Ara h 1/ Ara h 2 were then concentrated using 3 kDa Amicon-Ultra Centrifugal filters sterile filtered once more and the protein concentration determined by BCA. A sample

was considered to show a good level of purity when there was a clear band of the protein of interest in the absence of other bands indicating contaminants.

Solutions	Supplier	Use
Endotoxin Free Water	Gibco	Rinse Solution
0.5 M NaOH	Sigma	Cleaning
20% Ethanol	Sigma	Storage
0.2% Sodium Cholate	Sigma	Cleaning
PBS diluted to 0.1 M NaCl, pH 7.5	Lonza	Start Buffer
PBS supplemented to 2 M NaCl, pH 7.5	Lonza/Gibco	End Buffer
Table 2.8.2: Solutions for Anion Exchange		

2.9 Statistical Analysis

The statistical analysis was performed using GraphPad Prism version 8. In graphs, the mean is usually shown and, if included, the error bars show confidence interval (CI) unless otherwise stated. Log transformations are to base 10. The statistical test is indicated in the figure legend. For most experiments, a low sample number and a non-normal distribution or inability to test normal distribution necessitated the use of non-parametric tests. The exception is the two-way ANOVA (analysis of variance) for which the author was unable to find a viable non-parametric alternative. With larger sample sizes, where it was possible to test data distribution, parametric tests were used. A result was considered statistically significant when $p \leq 0.05$.

Chapter 3: Mechanisms of AGE-Enhanced Immunogenicity: Investigations into DC Activation and Complement Binding

3.0 Abstract

The addition of AGEs to a protein is reported to enhance the protein's immunogenicity. This could have important consequences in diseases which feature AGE formation and immune activation such as autoimmune disease, atherosclerosis and allergy. However, the mechanisms underlying this phenomenon are unknown. In this report, previous findings were further investigated by examining the immunogenicity of a range of different AGE structures in the absence of extrinsic adjuvant. The capacity for these samples to induce DC, B cell and complement activation was then investigated. The results demonstrated that glycoaldehyde (GA)-modified proteins containing reactive carbonyls (RCs) were unique in their capacity to induce strong antibody responses. None of the AGE-modified proteins could induce the maturation of DCs or directly activate B cells *in vitro*. However, GA-modified proteins did bind C1q and natural antibodies, and these proteins induced complement activation. This effect was lost when RCs were removed by reduction. These results therefore suggest that enhanced complement activation seen with GA-modified proteins may explain the stronger antibody responses seen *in vivo.*

3.1 Introduction

3.1.1 AGEs and Enhanced Immunogenicity

As discussed in the introduction, the addition of AGEs to a protein has been reported to alter protein recognition by the immune system, potentially rendering a normally inert protein immunogenic. One question that needs to be answered is whether all AGE-modified proteins are equally immunogenic or whether specific structures are required. This is important because it could give insight into the underlying mechanism, based on prior knowledge of which AGEs interact with particular receptors. Understanding which AGE-structures are involved in enhanced immunogenicity could also provide potential therapeutic targets in diseases where AGEs are thought to contribute to the pathogenesis. One way to examine which structures are responsible is to specifically modify a protein. For example, Heilmann et al modified ovalbumin (OVA) to add (carboxymethyl)lysine (CML), (carboxyethyl)lysine (CEL), pyrraline or methylglyoxal-derived arginine derivatives. Incubating OVA-specific CD4 T cells with murine bone marrow derived DCs (mBMDCs) and each of these modified proteins resulted in enhanced proliferation and cytokine secretion only with pyrraline-modified OVA, suggesting this structure is responsible for enhancing immunogenicity (Heilmann et al. 2014). Moreover, both glucose-modified and pyrraline-modified OVA induced greater titres of anti-OVA antibodies compared to OVA alone in murine immunisation studies. However, other modifications were not tested for their immunogenicity *in vivo.*

An alternative approach is to remove the structure of interest and see whether the enhanced immunogenicity is also lost. For example, studies have shown that modifying a protein with GA to add RCs enhanced the development of immune responses. However, this effect is lost if RCs are removed by reduction (Moghaddam et al. 2011; Allison and Fearon 2000). As discussed in the introduction, RCs are a functional group whose addition to proteins is

characteristic of oxidative stress. They are present in the reactive intermediate species of the Maillard reaction, intermediate glycation adducts and some AGEs (Fedorova 2017; Liggins and Furth 1997). These latter studies are not necessarily incompatible with Heilman et al as pyrraline does have a RC group. However, whilst studies examining GA-mediated immunogenicity have shown that *in vivo* immune responses are enhanced the absence of adjuvant, the pyrraline study used an immunisation procedure which included an extrinsic adjuvant (alum). As such it is not yet possible to assess whether pyrraline has intrinsic immunogenicity.

3.1.2 AGEs and DC Activation

Given their role as the gatekeepers of the adaptive immune system, it is unsurprising that a number of studies have examined the effects of AGEs on DCs in an attempt to understand the enhanced immunogenicity of these proteins. DCs express a variety of receptors which can interact with AGE-modified proteins, including SR-A, Galectin-3 and RAGE (Becker et al. 2006; Breuilh et al. 2007; Hilmenyuk et al. 2010). SR-A and RAGE are both members of the SR family. The former is known to bind and internalise AGE-modified proteins (see Chapter 4), whilst the latter initiates inflammatory signalling when bound to AGEs (see Chapter 6). Lastly, Galectin-3 is an AGE-binding protein (Vlassara et al. 1995), which along with OST-48 and 80K-H, forms the AGE-receptor complex (Ott et al. 2014). This receptor has a wide variety of different roles including promoting cell proliferation, preventing apoptosis and regulating cell adhesion to the extracellular matrix and other cells (Pricci et al. 2000; Pugliese et al. 2015). Within DCs, Galectin-3 is reported to regulate migration, adhesion and T cell interactions (Vray et al. 2004; Breuilh et al. 2007). Specifically, loss of Galectin-3 in DCs increases their capacity to induce T cell responses *in vitro* and *in vivo.*

Moreover, mouse models have suggested that this receptor promotes the development of Th2 responses (Breuilh et al. 2007).

One potential mechanism for enhanced immunogenicity is increased uptake of AGE-modified by DCs, and subsequently increased presentation to T cells (discussed in more detail in Chapter 4). An alternative mechanism is that AGE-modified proteins induce the maturation of DCs, however this is controversial. In the studies of Buttari et al and Ge et al, incubation of human monocyte-derived DCs with AGE-modified proteins was found to increase expression of costimulatory molecules and release of cytokines including IL-12 and IL-10 (Buttari et al. 2011; Ge et al. 2005). It was also reported that AGE-modified proteins increased expression of RAGE on DCs and initiated the phosphorylation of p38, ERK, JNK and NF-κB (Buttari et al. 2011; Ge et al. 2005; Hilmenyuk et al. 2010). This maturation could be inhibited using anti-RAGE antibodies, and so it was concluded that DC maturation is at least partially RAGE-mediated. In contrast, studies using mBMDCs and splenic DCs found that exposure to AGE-modified proteins had no effect on the expression of costimulatory molecules or the secretion of inflammatory cytokines (Heilmann et al. 2014; Ilchmann et al. 2010; Moghaddam et al. 2011). These studies therefore provide evidence against a role for DC maturation in AGE-induced immune responses. Indeed in one study, exposure to AGEs was found to inhibit the capacity of human DCs to stimulate a mixed leukocyte reaction (Price et al. 2004).

The question of whether DCs mature in response to AGE-modified proteins therefore remains unresolved. In order to answer this we need to understand why these studies have produced different results. Obviously, there are many factors which could affect the outcome including the origin and culture conditions of the DCs, the modification protocols and the model protein studied. Another critical factor is whether there is endotoxin contamination in the samples, this may be of particular relevance in regard to AGE-modified proteins as

TLR4 and RAGE have been suggested to signal cooperatively (Ibrahim et al. 2013). As such, the majority of studies examining DC maturation referenced above measure the endotoxin levels in the samples and report minimal contamination levels (Moghaddam et al. 2011; Hilmenyuk et al. 2010; Price et al. 2004; Heilmann et al. 2014). However, Ge et al did not report whether they have tested their samples for contamination (Ge et al. 2005). Moreover, Buttari et al reported very low levels of endotoxin contamination (<0.05 EU/ml), but have added 10 μg/ml polymixin B to their cultures (Buttari et al. 2011). This is potentially problematic as polymixin has been reported to induce partial maturation of human DCs and so could have influenced the results (Valentinis et al. 2005).

3.1.3 AGEs and Complement

AGEs have also been suggested to activate the complement pathway. As discussed in the introduction, this is an evolutionary ancient part of the immune system divided into three branches, termed the classical, lectin and alternative pathways. Activation of these pathways promotes production of opsonins (e.g. C3b and iC3b), inflammation (anaphylatoxins) and cell lysis (membrane attack complex) (Sarma and Ward 2011). The effects of the complement system were originally thought to be confined to the innate immune system, however, more recent evidence has shown that the complement system can take an active role in the development of adaptive immune responses. Initial observations in the 1970s demonstrated the B cells could bind to C3 (Dunkelberger and Song 2010). Since then, complement has been shown to promote B cell activation, class switching and the formation of memory responses through complement receptors expressed on B cells and follicular DCs. More recently, complement has been shown to promote the proliferation and differentiation of T cells (Killick et al. 2018).

Recent studies suggest that recognition of AGE-modified proteins can activate the classical complement pathway. In one, C1q was shown to bind directly to various forms of AGE-modified protein (Chikazawa et al. 2016). Further *in vitro* studies demonstrated that AGE-modified BSA could induce C3b/C4b deposition when incubated with human serum and this effect was lost when C1q was removed from the serum. Alternatively, natural IgM antibodies have also been reported to bind to AGE and other oxidatively-modified proteins (Uchida 2014; Chikazawa et al. 2013). Amongst antibody subtypes, IgM is especially potent in its capacity to activate complement (Stowell et al. 2012). Thus, this is another mechanism by which AGE-modified proteins could activate complement, although this has yet to be directly demonstrated. In both cases, recognition is hypothesised to be dependent on the negative charge of the modifications. However, so far no studies have investigated whether this link contributes to AGE-induced activation of adaptive immune responses.

3.2 Hypothesis and Aims

Hypothesis: That modification of proteins with glucose or intermediates of the Maillard reaction enhances their immunogenicity via interactions with components of the innate and/or adaptive immune systems

Aims

1. To produce and characterise different modified samples representing a range of AGE structures and with low/undetectable endotoxin contamination
2. Examine *in vivo* immunogenicity of the samples to interrogate previous findings and identify structures which may enhance the development of immune responses
3. Assess the capacity of the modified proteins to induce maturation of DCs
4. Asses the capacity of the modified proteins to induce activation (i.e. proliferation) of B cells *in vitro*
5. Interrogate whether modified proteins can activate complement
6. Assess whether modified proteins are recognised by natural antibodies

3.3 Materials and Methods

A list of methods used in this chapter is shown below. For detailed protocols please refer to the indicated section in the Materials and Methods Chapter.

- Production of modified proteins (2.2.2 – 2.2.5)
- ELISAs for RCs, CML, GA-Pyridine and Pyrraline (2.2.6 – 2.2.9)
- TNBSA assay (2.2.10)
- Fluorescence Measurements (2.2.11)
- SDS-PAGE (2.2.12)
- Biotin Labelling (2.2.17)
- C1q binding and Complement Activation assays (2.2.18 – 2.2.19)
- HyHEL-10 binding ELISA (2.2.20)
- Endotoxin Reporter Assay (2.3.2)
- Generation of GM-CSF BMDCs (2.3.3)
- *In Vitro* Pulsing Assays (2.3.5)
- Flow Cytometry (2.3.6)
- RNAseq (2.3.7)
- Proteome Profiler (2.3.8)
- Luminex Assay (2.3.9)
- PGE_2 ELISA (2.3.10)
- Immunisation and Tissue Harvesting (2.4.1 – 2.4.4, 2.4.6)
- IgG, IgG1, IgG2a and IgG2c ELISAs (2.5.1)
- Examination of Natural Antibody Binding (2.5.3)
- Splenocyte Harvest, Cytokine ELISAs and Thymidine Pulse (2.6.1 – 2.6.3)
- Splenocyte Pulsing with Naïve Cells (2.6.4)
- Statistical Analysis (2.9)

3.4 Results

3.4.1 Production and Characterisation of AGE-modified Proteins

Different AGE-modified proteins were generated according to the protocols outlined in Materials and Methods section 2.2. These were designed to give a broad range of modifications (glucose modification), limited range of modifications (GA modification), or specific modifications (CML and Pyrraline modification). Long-term glucose incubation is used in variety of studies to give AGE-modified proteins, however, it takes many weeks/months to produce these samples and it is very difficult to completely characterise the changes due to the large number of adducts which can be formed (Valencia et al. 2004; Schmitt et al. 2005). In contrast GA can modify the protein within a few hours allowing for rapid production of AGE-modified proteins. Previous experiments from this laboratory had previously identified the reaction products on hen egg lysozyme (HEL) samples which had been modified with GA for 3 h (GA 3 h samples), using mass spectrometry (MS). GA modification was found to add predominantly GA-pyridine, some CML and the intermediate aldoamine which has a RC (Moghaddam et al. 2011). The RC in GA modified samples can be removed by reducing the sample with sodium borohydride (Moghaddam et al. 2011). As discussed in the introduction, GA-modified samples have been previously reported to be highly immunogenic in the absence of adjuvant and so were important to investigate. As this phenomenon is reported to be RC dependent, in these studies the reduced GA-modified sample has been used as a control. These samples are referred to as GA-PR. For specific modifications, CML and pyrraline were investigated. The latter was chosen because of the previous study which suggested this was a key mediator of AGE-mediated immunogenicity (Heilmann et al. 2014). The protocol to make this was based on that study and is more extensive than that used for other modifications, requiring the sample to be lyophilised and heated to 70 °C in the presence of 3-deoxyglucosone (3-DG). Additional controls were

therefore included for these samples, which involved the same treatment in the absence of 3-DG. Lastly, CML was selected for investigation because this is a very common AGE product which is reported to be a ligand for RAGE (Kislinger et al. 1999; Delgado-Andrade 2016).

Initial characterisation of the modified proteins was done using SDS-PAGE to evaluate shifts in molecular weight and the presence of crosslinking. Gels of the different samples are shown in Figure 3.4.1.1. The HEL gels are shown first (Figure 3.4.1.1A). This is the model protein which is used in the subsequent *in vivo* studies and the majority of the *in vitro* studies. HEL was selected as this protein had been the predominant one used in previous studies examining GA-mediated immunogenicity (Moghaddam et al. 2011; Allison and Fearon 2000). Moreover, given its small size, this protein was easier to analyse by MS and so modified versions had been well-characterised in this laboratory in previous experiments. As can be seen, the band pattern for the 3 h/7 day 37 °C, 70 °C heated control and CML modified samples appears identical. Similarly, there is only one band apparent in the glucose treated (HEL GLUC) sample but it is blurred and shifted upwards. Modification with GA induced the formation of crosslinks as indicated by the presence of a secondary band around 30 kDa. Crosslinking increased with the longer incubation and remained after reduction to remove RCs. The modification to add pyrraline (PYR) induced the largest changes with a more significant shift in the size of the primary band and the formation of many crosslinked multimers. In these studies only the HEL pyrraline modification was produced. With bovine serum albumin (BSA) (Figure 3.4.1.1.B), GA modification induced the most obvious changes, with clear smearing apparent with the 7 day sample. GLUC treatment appeared to yield a slightly higher molecular weight band. Changes with OVA induced by the modifications are less apparent on the gels, but the 7 day GA and GLUC treatments appeared to yield a slightly higher molecular weight band (Figure 3.4.1.1.C).

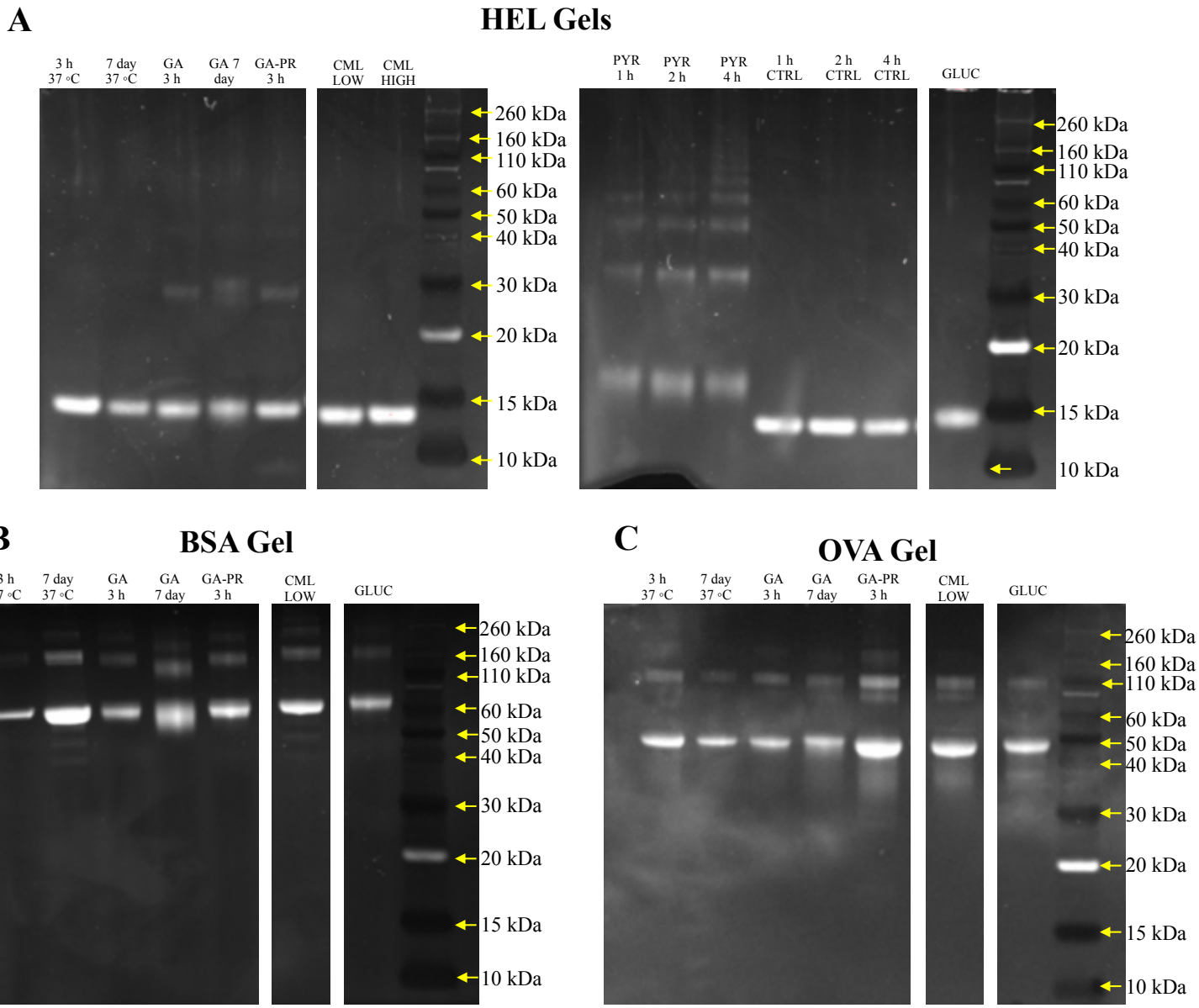

Figure 3.4.1.1: Bovine serum albumin (BSA), ovalbumin (OVA) and hen egg lysozyme (HEL) were modified using different AGE-forming protocols. Firstly, proteins were incubated with glucose at a concentration of 1 M for 24 weeks at 37 °C. Secondly, samples were incubated with 20 mM glycolaldehyde (GA) for 3 h or 7 days at 37 °C. Samples incubated without GA were used as controls. The GA 3 h sample was then reduced with sodium borohydride to remove RCs (post reduction). Additionally, proteins were modified to specifically add CML by incubating at 37 °C with glyoxylic acid and sodium cyanoborohydride, either for 24 h (CML HIGH) or 3 h (CML LOW). The CML HIGH protocol used 200 mM sodium cyanoborohydride and 100 mM glyoxylic acid, whilst the CML LOW protocol used 150 mM sodium cyanoborohydride and 30 mM glyoxylic acid. Finally, proteins were modified to add pyrraline by mixing the protein with 3-deoxyglucosone (3-DG) at a 4:1 ratio 3-DG:lysine residues. The mixed samples were then lyophilised and heated to 70 °C for 1, 2 or 4 h. Samples lyophilised and heated to 70 °C without 3-DG were used as a control. The resultant samples were run on SDS-PAGE gels which were then stained with SYPRO Tangerine stain. The molecular weight of the ladder markers is indicated. Where samples which were not used in subsequent experiments were included on the same gel, these have been removed and this is indicated by the breaks in the gels. The abbreviations used are: GLUC = glucose modified, GA 3 h/ 7 day = glycolaldehyde modified for 3 h or 7 days, 3 h/ 7 day 37 °C = sample incubated at 37°C for 3 h/ 7 day as a control, GA-PR 3 h = GA 3 h modified sample which has been post-reduced, CML HIGH = modified to add CML for 24 h, CML LOW = modified to add CML for 3 h, PYR 1/2/4 h = modified to add pyrraline for 1, 2 or 4 h, 1/2/4 h CTRL = samples lyophilised and heated to 70°C for 1, 2 or 4 h as a control for pyrraline. CTRL = control. The 3 h/ 7 day 37 °C control samples are referred to as "3 h" or "7 day" samples in subsequent figures.

Both OVA and BSA were only modified using the CML LOW protocol, this was because the more extensive protocol caused the proteins to precipitate which resulted in very low yields. For consistency with previous studies in the laboratory, HEL CML HIGH was used in all subsequent experiments.

To give a general measure of AGE formation in each of the samples, their fluorescent properties were examined. These studies examined excitation at 335 nm and 370 nm and emission at 420 nm and 440 nm respectively. The results are shown in Figure 3.4.1.2 and 3.4.1.3. As expected, controls showed no or minimal fluorescence (an additional control which involved heating the HEL for 6 months at 37 °C as a control for GLUC incubation is included in these graphs). CML modification samples were also not fluorescent, this is to be expected as this AGE does not have fluorescent properties (Tsekovska et al. 2016). In contrast, GA, GLUC or PYR modified samples all showed some degree of AGE fluorescence. This was most noticeable with the GA 7 day modification and also depended on the protein, with the BSA and OVA samples having a greater emission than the HEL. GA modification for 3 h and GLUC modification induced a similar levels of fluorescence in the samples, suggesting comparable levels of fluorescent AGE formation. As it is crosslinked species which are fluorescent (Ulrich 2001), these data fit with the SDS-PAGE results, which showed that GA modification of HEL, especially 7 days, produced crosslinks whereas GLUC modification alone did not.

Additionally, lysine usage in the modified HEL samples was also measured using a TNBSA assay. This reagent reacts with free primary amine groups to give a product which can be measured by its absorbance at 335 nm (Hermanson 2013). The results are shown in Figure 3.4.1.4. A single example of each modification type is shown in A, whilst B shows the results for multiple samples of the same type which are of particular interest in this thesis.

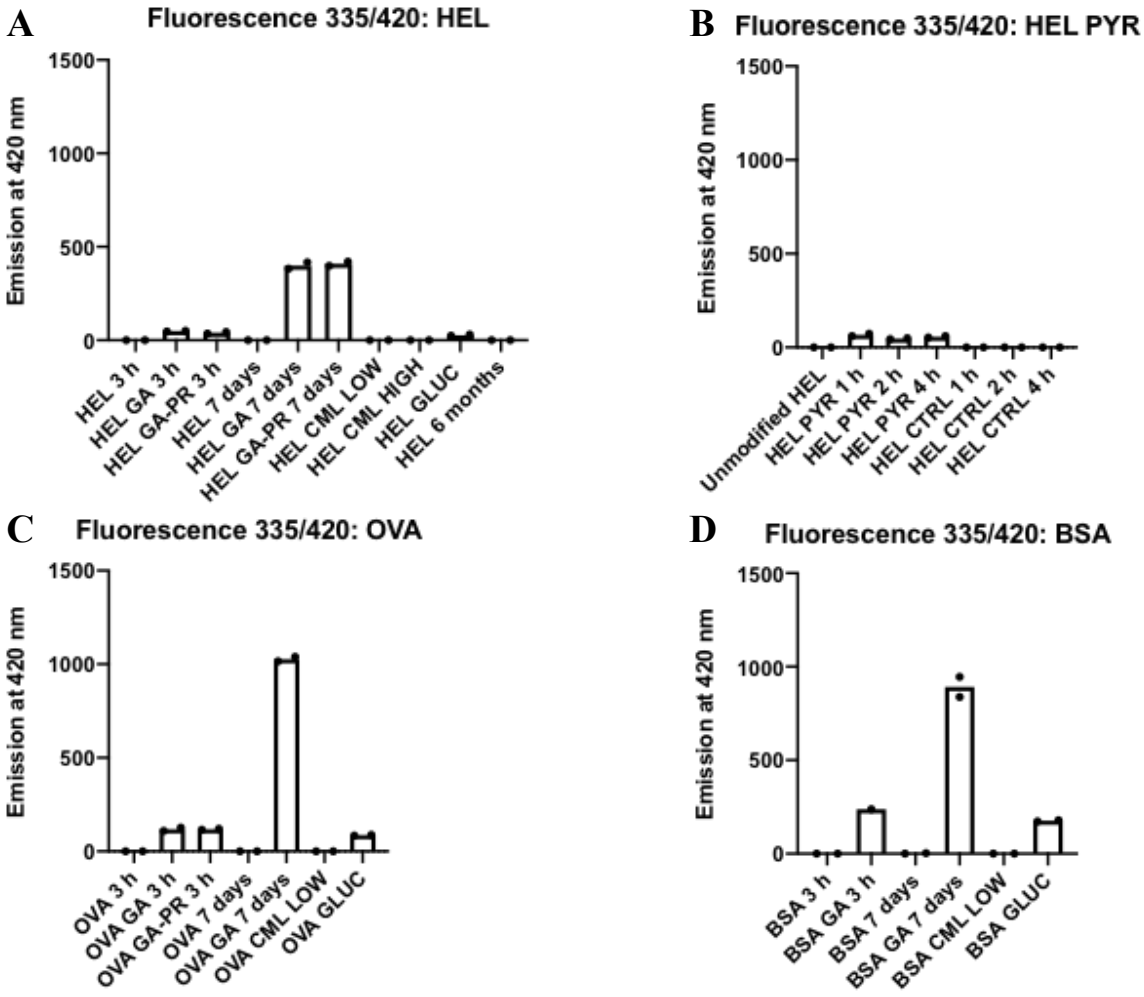

Figure 3.4.1.2: Fluorescent properties of HEL (A and B), OVA (C) and BSA (D) modified samples were assessed by measuring emission at 420 nm with excitation at 335 nm. Pilot experiments indicated that the optimal conditions for measurement required a sample of 1 mg/ml, however the low concentration of the PYR samples necessitated measurements with samples at 0.5 mg/ml, hence these samples are on a separate graph. Samples were run in technical duplicates. The bars indicate mean whilst each duplicate is shown as a dot.

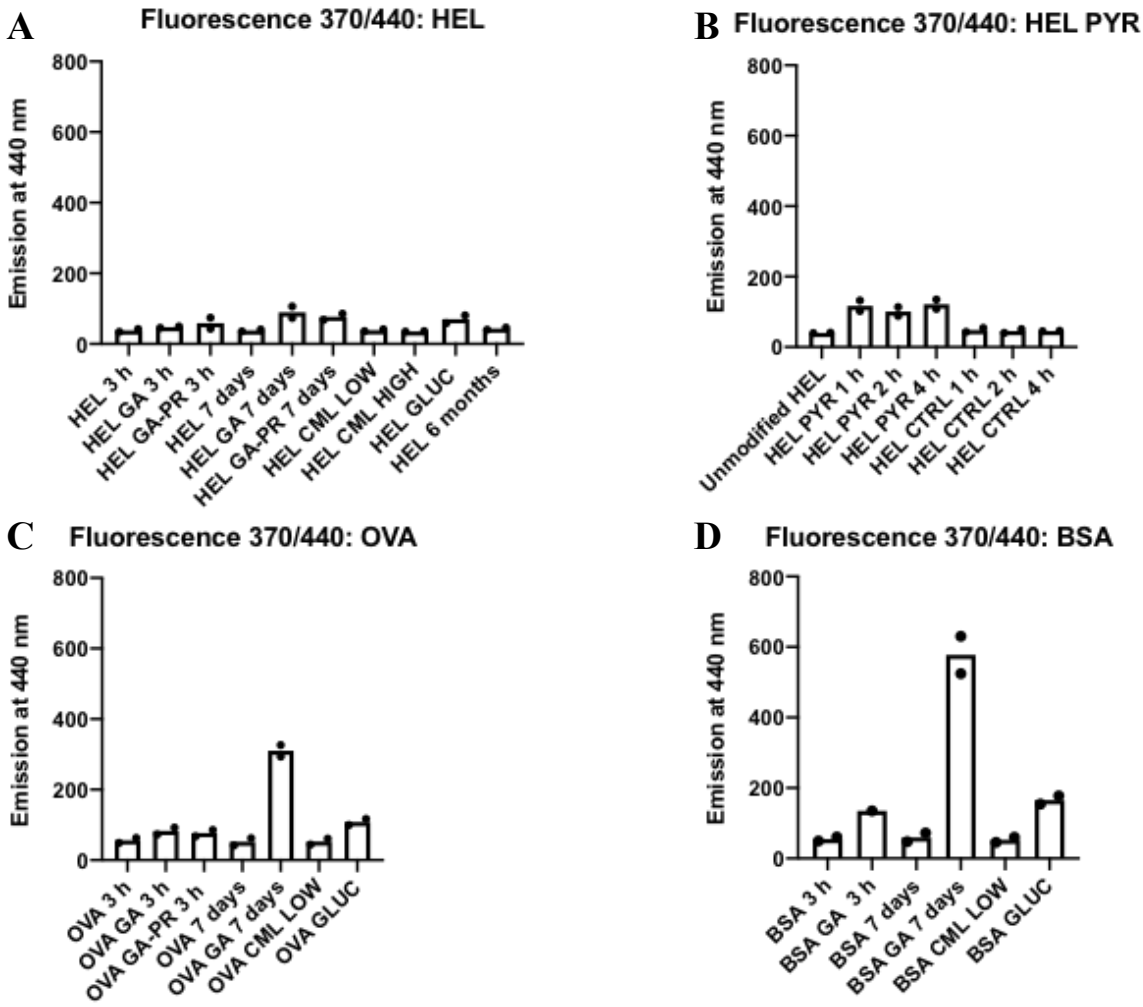

Figure 3.4.1.3: Fluorescent properties of the indicated samples were measured as in Figure 3.4.1.2, except measuring emission at 440 nm with excitation at 370 nm. Again, samples were run in technical duplicates and the bars indicate mean whilst each duplicate is shown as a dot.

In keeping with the fluorescence data, HEL GA 7 day shows the greatest level of modification, with almost complete amine usage. HEL GLUC had a greater amine usage than the GA 3 h sample despite similar fluorescence, indicating the presence of other non-fluorescent modifications.

The formation of specific modifications was then assessed using ELISAs with antibodies/reagents targeting different modifications, namely RCs, CML, GA-pyridine and pyrraline. The results are shown in Figures 3.4.1.5 to 3.4.1.8. A summary table showing the structures formed by the different protocols is given in Table 3.4.1. Only GA modification induced GA-pyridine formation, whilst only 3-DG modification induced pyrraline formation. In contrast CML was seen in a wider variety of samples including the GA and GLUC modified samples, although highest levels were seen with the CML specific modification. Likewise, RC groups were found in multiple samples, namely the GA, GLUC and PYR samples.

	RC	CML	GA-Pyridine	Pyrraline	Crosslinking
Native/heat-treated only	-	-	-	-	-
GA 3 h	++	-	+++	-	+
GA-PR 3 h	-	-	+++	-	+
GA 7 days	+	+	+++	-	++
GLUC	+	++	-	-	-
CML	-	+++	-	-	-
PYR (2 h)	+++	-	-	+++	+++

Table 3.4.1: Summary table of the different structures/features formed by the modification protocols, as measured by ELISA.

Finally, the level of endotoxin contamination in the samples was assessed. A TLR4-endotoxin reporter cell assay was used in this study and results are shown in Figure 3.4.1.9. All the samples had undetectable or extremely low contamination levels, < 0.05 ng/ml.

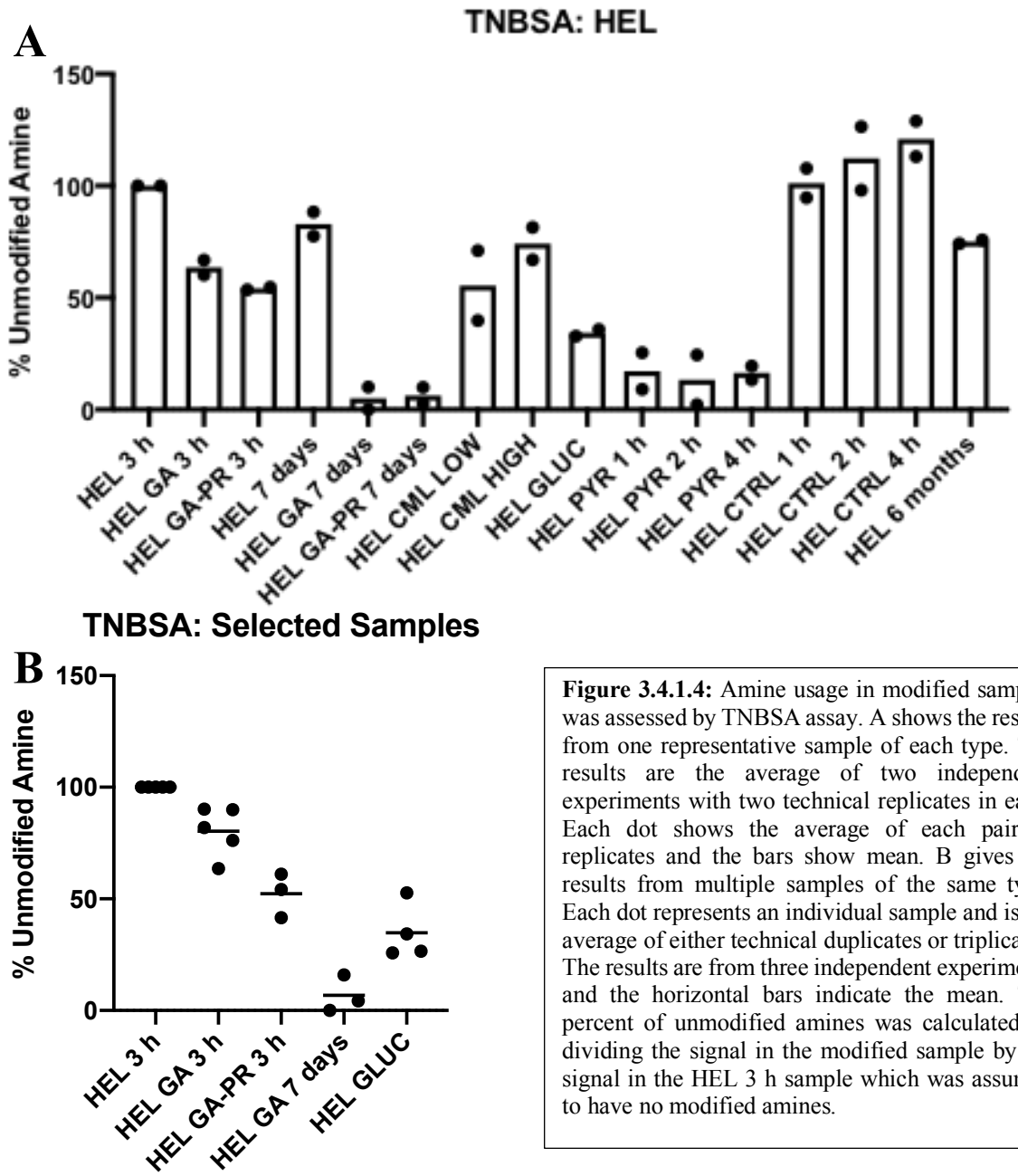

Figure 3.4.1.4: Amine usage in modified samples was assessed by TNBSA assay. A shows the results from one representative sample of each type. The results are the average of two independent experiments with two technical replicates in each. Each dot shows the average of each pair of replicates and the bars show mean. B gives the results from multiple samples of the same type. Each dot represents an individual sample and is the average of either technical duplicates or triplicates. The results are from three independent experiments and the horizontal bars indicate the mean. The percent of unmodified amines was calculated by dividing the signal in the modified sample by the signal in the HEL 3 h sample which was assumed to have no modified amines.

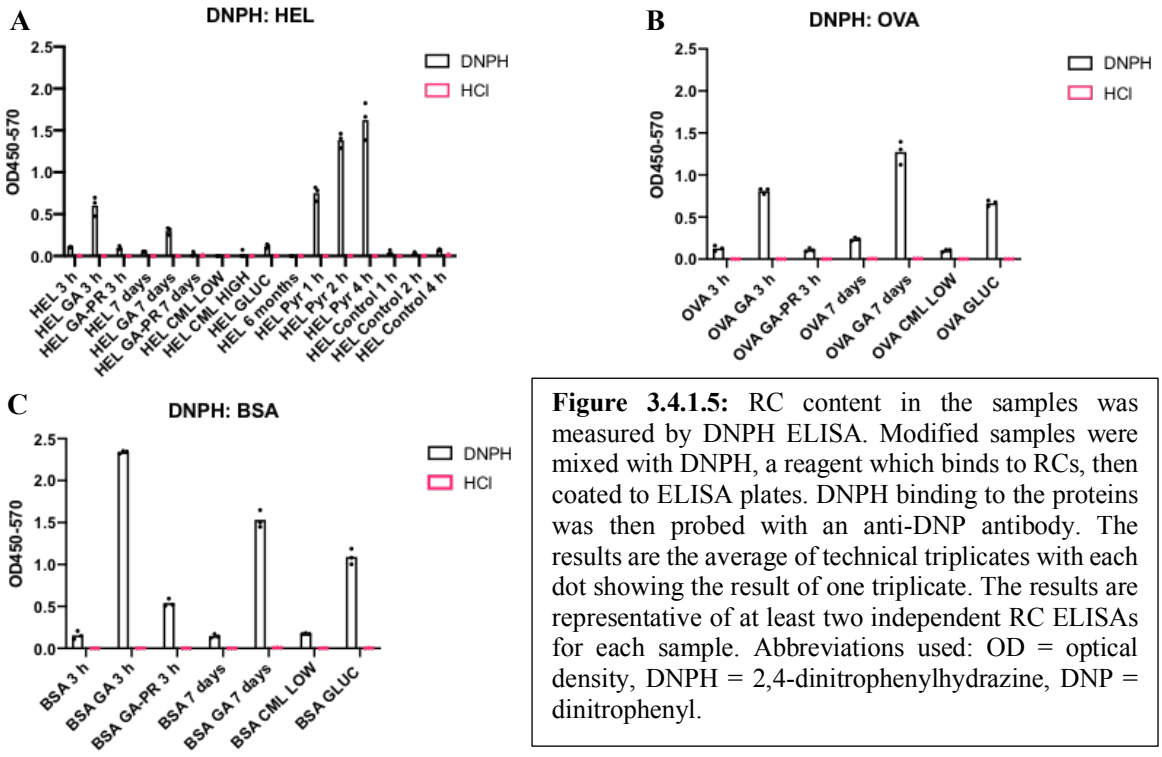

Figure 3.4.1.5: RC content in the samples was measured by DNPH ELISA. Modified samples were mixed with DNPH, a reagent which binds to RCs, then coated to ELISA plates. DNPH binding to the proteins was then probed with an anti-DNP antibody. The results are the average of technical triplicates with each dot showing the result of one triplicate. The results are representative of at least two independent RC ELISAs for each sample. Abbreviations used: OD = optical density, DNPH = 2,4-dinitrophenylhydrazine, DNP = dinitrophenyl.

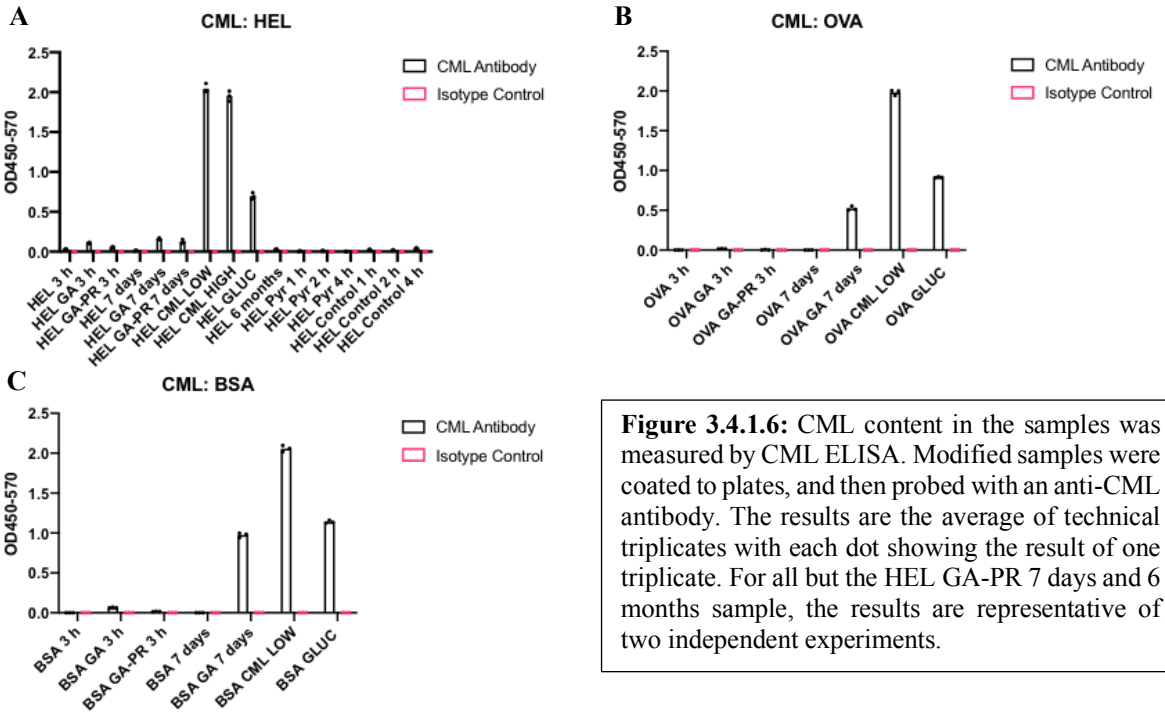

Figure 3.4.1.6: CML content in the samples was measured by CML ELISA. Modified samples were coated to plates, and then probed with an anti-CML antibody. The results are the average of technical triplicates with each dot showing the result of one triplicate. For all but the HEL GA-PR 7 days and 6 months sample, the results are representative of two independent experiments.

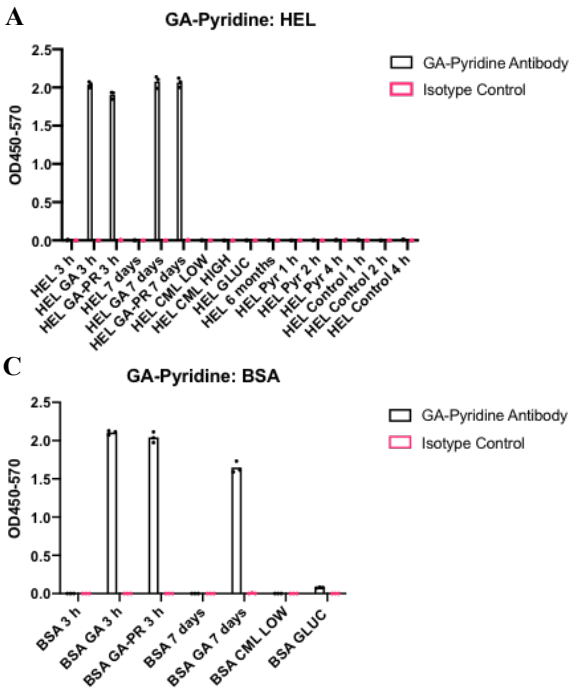

Figure 3.4.1.7: GA-Pyridine content in the samples was measured by ELISA. Modified proteins were coated to plates and GA-pyridine content assessed with an anti-GA-pyridine antibody. Each dot shows the result of a technical replicate and the bars show mean. For all but the HEL GA-PR 7 days and 6 month sample, the results are representative of two independent experiments.

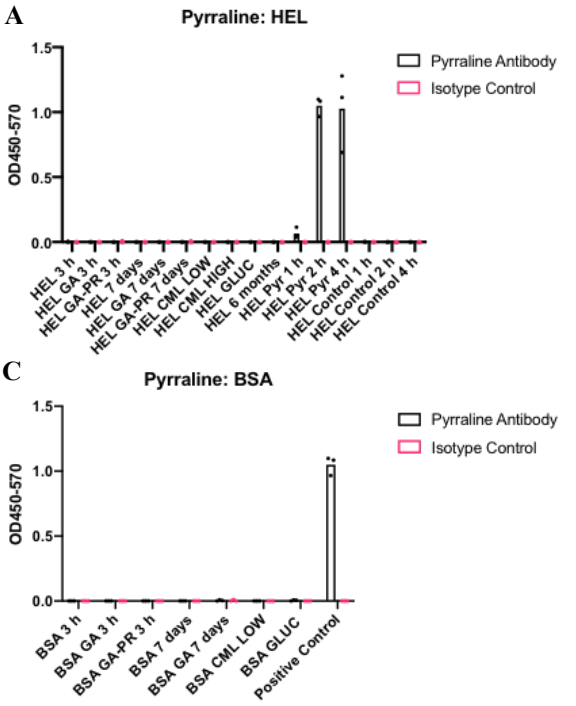

Figure 3.4.1.8: Pyrraline content in the samples was measured by ELISA. Modified samples were coated to ELISA plates and then probed with an anti-pyrraline antibody. The results are the average of technical triplicates, with each dot showing the result of one triplicate. HEL PYR 2 h is included as a positive control in B and C.

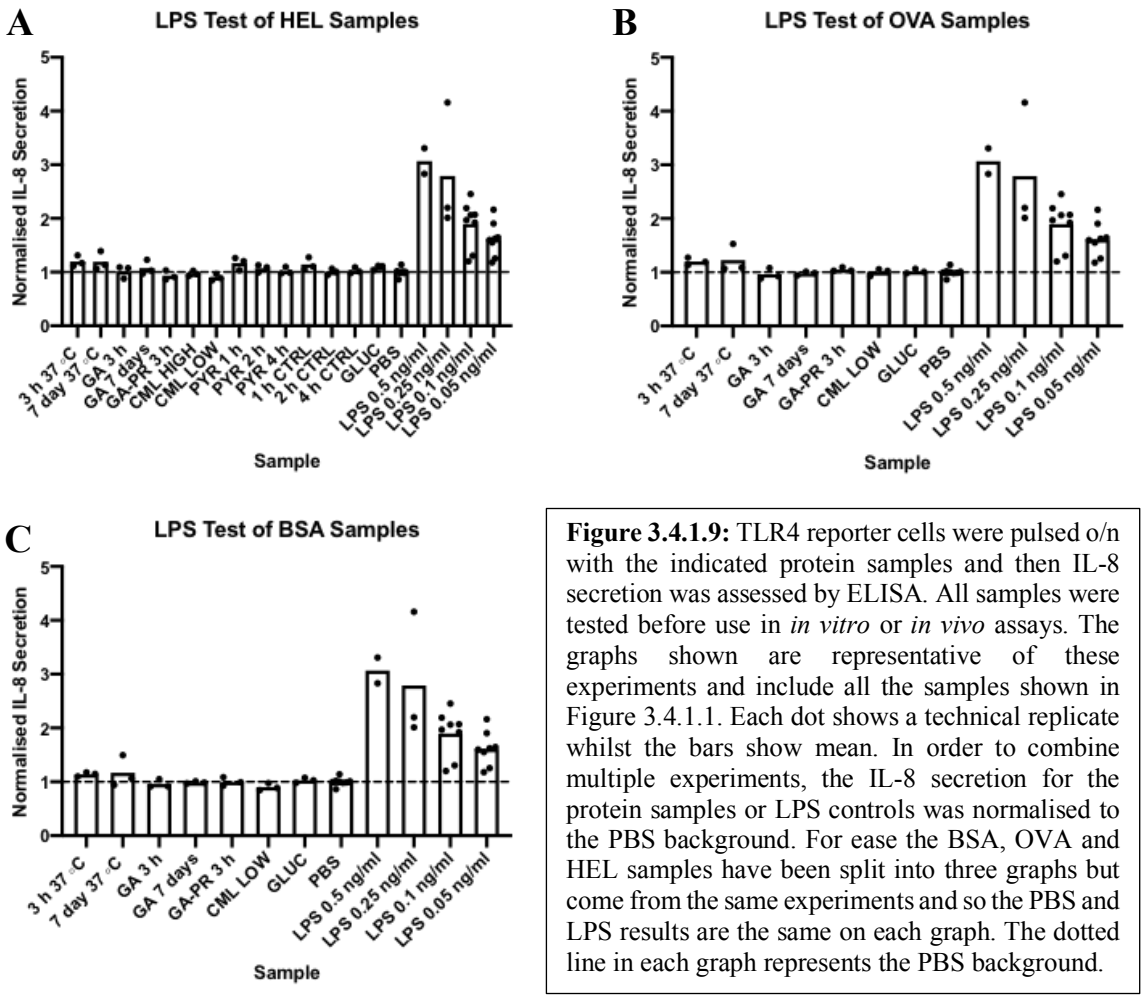

Figure 3.4.1.9: TLR4 reporter cells were pulsed o/n with the indicated protein samples and then IL-8 secretion was assessed by ELISA. All samples were tested before use in *in vitro* or *in vivo* assays. The graphs shown are representative of these experiments and include all the samples shown in Figure 3.4.1.1. Each dot shows a technical replicate whilst the bars show mean. In order to combine multiple experiments, the IL-8 secretion for the protein samples or LPS controls was normalised to the PBS background. For ease the BSA, OVA and HEL samples have been split into three graphs but come from the same experiments and so the PBS and LPS results are the same on each graph. The dotted line in each graph represents the PBS background.

3.4.2 GA-modified Samples Induce Strong Antibody Responses

Having generated and characterised different modified proteins the next stage was to examine their capacity to induce immune responses *in vivo*. To this end, female BALB/c mice were immunised with a single injection of 5 μg of the indicated protein. 10 weeks later sera were collected to measure antibody responses. These conditions were chosen based on pilot experiments in our laboratory and previously published data (Moghaddam et al. 2011), in which a single immunisation had been sufficient to induce anti-HEL IgG responses which were still detectable 8-12 weeks following immunisation. Spleens were also harvested to assess the development of cellular responses. The results are shown in Figure 3.4.2.1. As can be seen strong antibody responses were only observed in mice (4/6) immunised with the HEL GA 3 h. This response was mainly IgG1 which is characteristic of a "type 2" immune response (Mountford, Fisher, and Wilson 1994). A low IgG2a response was also noted in 2/6 HEL GA 3 h immunised mice which may indicate a mixed immune response with a Th2 bias as IgG2a is associated with Th1 responses. A detectable but weak IgG1 response was also seen in 2/6 HEL immunised mice. Although the difference in titre between HEL and HEL GA 3 h immunised mice did not reach significance with the non-parametric test, which was necessary given the small sample size and bimodal distribution, this test lacks statistical power with small sample sizes. Moreover, the difference between average end point titre in the HEL GA 3 h immunised mice was approximately 300 times greater than that seen in the HEL immunised mice (30161.4 vs 103.8). The strong antibody response seen in the HEL GA 3 h immunised mice was not accompanied by a significant splenocyte response with regard to thymidine incorporation or cytokine production. Instead, the more extensively-modified, non-antibody inducing GLUC and PYR samples seemed to induce stronger proliferation, although this did not reach significance.

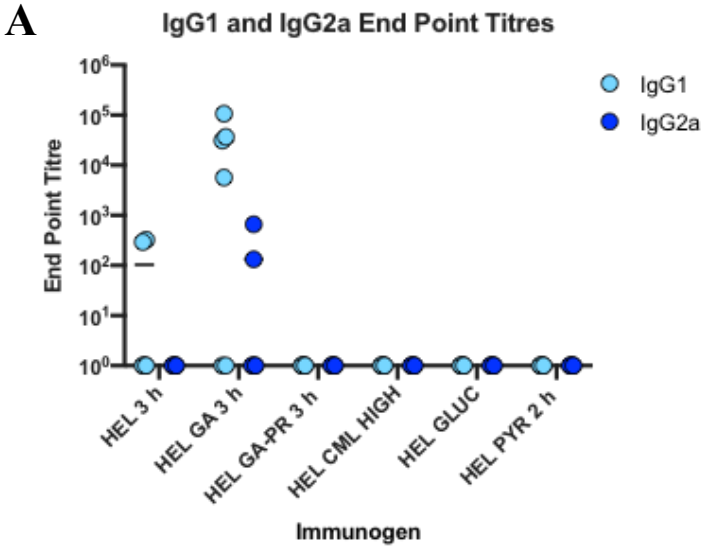

Figure 3.4.2.1: Female BALB/c mice were injected s.c. with 5 µg of the indicated protein. 10 weeks later, the mice were culled and sera taken to assess antibody responses to native HEL using ELISAs measuring IgG1 and IgG2a (A). Spleens were also collected and isolated splenocytes were pulsed with HEL or left unstimulated. On day 3, supernatant was collected and ^{3}H-thymidine was added to the wells. Proliferation was measured by thymidine incorporation the next day (B). ELISAs were used to measure cytokine release in the supernatant (C-E). For all the splenocyte assays the cytokine secretion and proliferation in the unstimulated wells was used as a background (BG) and subtracted from the pulsed value to find the specific response. The data were analysed using a Kruskal-Wallis test. There were 6 mice in each group. In all graphs, each dot shows the results from one mouse, whilst the bars indicate average. Cpm = counts per minute.

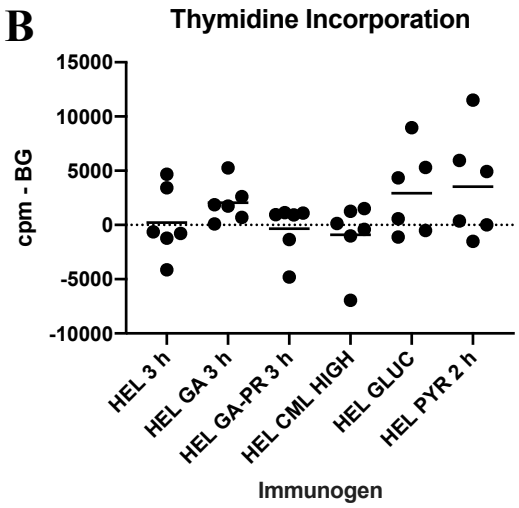

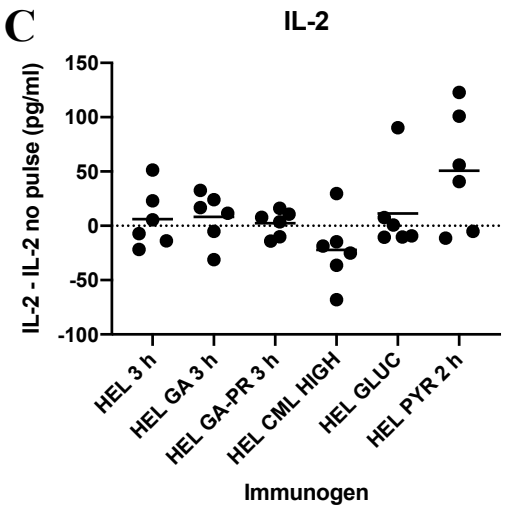

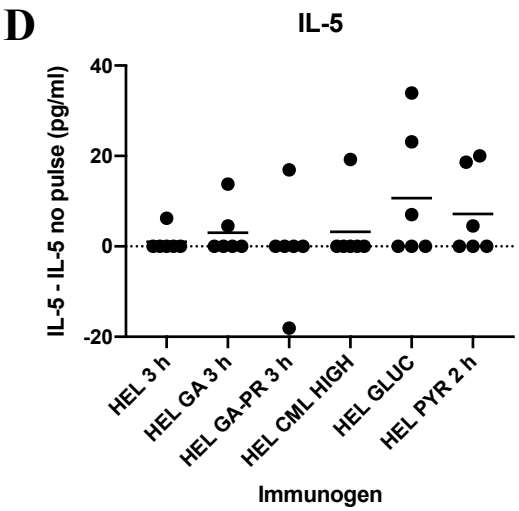

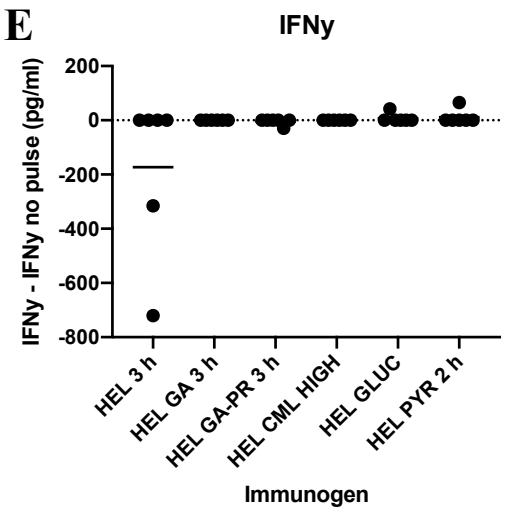

The overall results from the BALB/c studies suggested that GA-modified samples were unique in their capacity to induce antibody responses. This appeared to be RC-mediated as this antibody production was not seen in mice immunised with GA-PR samples where the RCs had been reductively eliminated. To confirm this finding another immunisation experiment was performed using GA samples and the same protocol. This experiment used CBA mice. This strain has an intrinsically Th1 biased immune system, in contrast the BALB/c stain exhibits a Th2 bias (De Vooght et al. 2010). Therefore, if the IgG1 bias remained in this experiment it would indicate that the GA samples promote the development of type 2 responses as has been previously reported (Moghaddam et al. 2011). The results for this study are shown in Figure 3.4.2.2. Examining the antibody responses we can see that again the HEL GA 3 h sample induced the strongest responses, and in this case the titres were significantly greater than the group receiving HEL alone. This is the case for both IgG1 and IgG2a, although the IgG1 titres were higher than the IgG2a titres. As with the BALB/c experiment, this indicates a mixed response with a bias towards Th2. Interestingly, mice immunised with HEL GA 7 day samples had lower antibody responses than the HEL GA 3 h group. The HEL GA 7 day sample had slightly higher CML and crosslinking, similar levels of GA-pyridine but lower RC content.

With regards to splenocyte proliferation, responses to HEL GA 3 h samples were more apparent than in the BALB/c mice study, but again these failed to reach significance. The production of cytokines indicates a more balanced response as there is clearly detectable IFNγ secretion and levels of IL-5 are comparable to those produced in the BALB/c splenocyte cultures. To summarise, the *in vivo* studies indicate that GA-modified samples,

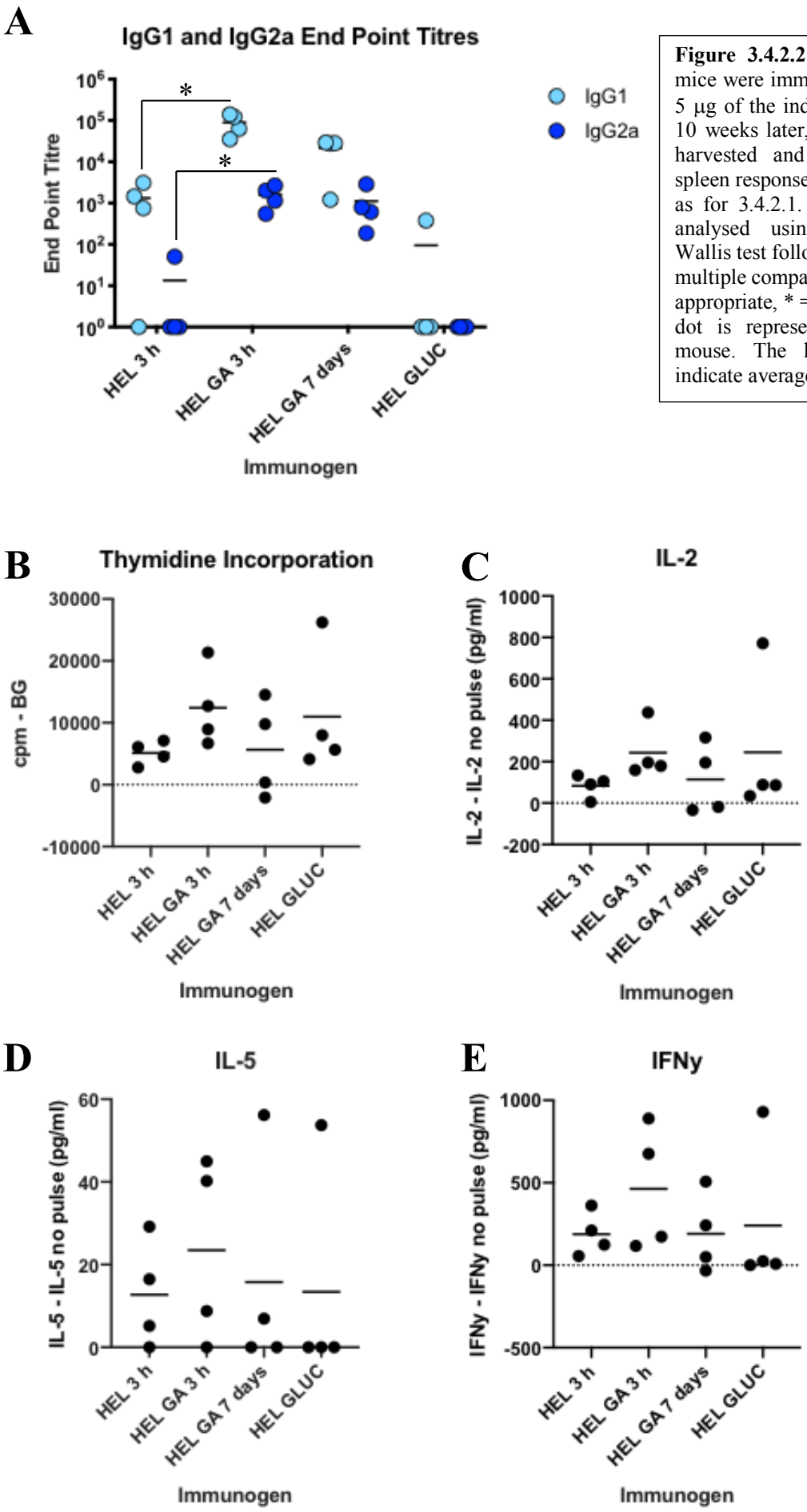

Figure 3.4.2.2: Female CBA mice were immunised s.c. with 5 μg of the indicated samples. 10 weeks later, the mice were harvested and antibody and spleen responses were assessed as for 3.4.2.1. The data were analysed using a Kruskal-Wallis test followed by Dunn's multiple comparison test where appropriate, * = $p \leq 0.05$. Each dot is representative of one mouse. The horizontal bars indicate average.

particularly the more minimally modified GA 3 h sample, induced strong antibody responses that recognised unmodified protein. This enhanced antigen-specific IgG production was not seen with other modified samples and appears to be RC-dependent. However, using this minimal immunisation protocol, corresponding T cell responses could not be confirmed.

Lastly, the capacity of modified proteins to induce immune responses in a DC transfer immunisation model was assessed in a small pilot study. The aim was to assess whether DCs alone were sufficient to carry the enhanced immunogenicity of the AGE-modified proteins. Since DCs are central to induction of adaptive immunity, this model was designed to study whether the adaptive immune activation observed was DC-dependent. DCs were pulsed for 4 h with 100 μg of AGE-modified or native protein and then 5 x 10^5 cells were injected i.p into BALB/c mice. This was done twice at weeks 0 and 2 and then mice were sacrificed at week 4 (see Figure 3.4.2.3). PBS pulsed DCs and HEL + LPS pulsed DCs were used as negative and positive controls respectively. The results are shown in Figure 3.4.2.4. As with the s.c. immunisation studies, HEL GA samples induced the strongest antibody responses with 2/3 mice developing antibody responses which were higher than those seen in the positive control. Interestingly, 2/3 of the mice immunised with DCs pulsed with HEL GLUC also developed antibody responses which contrasts with the results seen in the s.c. studies where no GLUC immunised mice developed antibodies against HEL. For the DC transfer studies, splenocytes were cultured both in goat serum and FBS. The former was necessary because as the DCs were grown in FBS, they would take up components of this and present it to lymphocytes. Thus there would be responses to FBS in the splenocyte cultures which could mask the HEL specific responses. However, previous experiments had indicated that there was lower splenocyte proliferation in cultures with goat serum which could also potentially limit the capacity of the assay to detect differences between immunisation groups. Both conditions were therefore included in the splenocyte recall experiments.

Shown in Figure 3.4.2.4 is HEL induced proliferation minus the unpulsed proliferation to determine the specific proliferation responses. Also shown are the raw data as the background proliferation was highly variable between different groups, with higher background proliferation seen in the mice immunised with DCs pulsed with HEL + LPS and with HEL GLUC (when incubated with goat serum). With regards to the specific proliferation the responses were mostly around the same level as that seen in the negative control PBS group apart from the HEL GA 3 h group when splenocytes were cultured in FBS. Overall, these results confirm that HEL GA 3 h is a strong inducer of antibody responses and that DCs pulsed with protein can induce this response. This may be through DC activation, or the DCs may transfer protein to other immune cells (e.g. B cells) which can act as antigen presenting cells (APCs) themselves (Hoffman, Lakkis, and Chalasani 2016). Given the uncertainty relating to the mechanism underlying this result the experiment was not repeated.

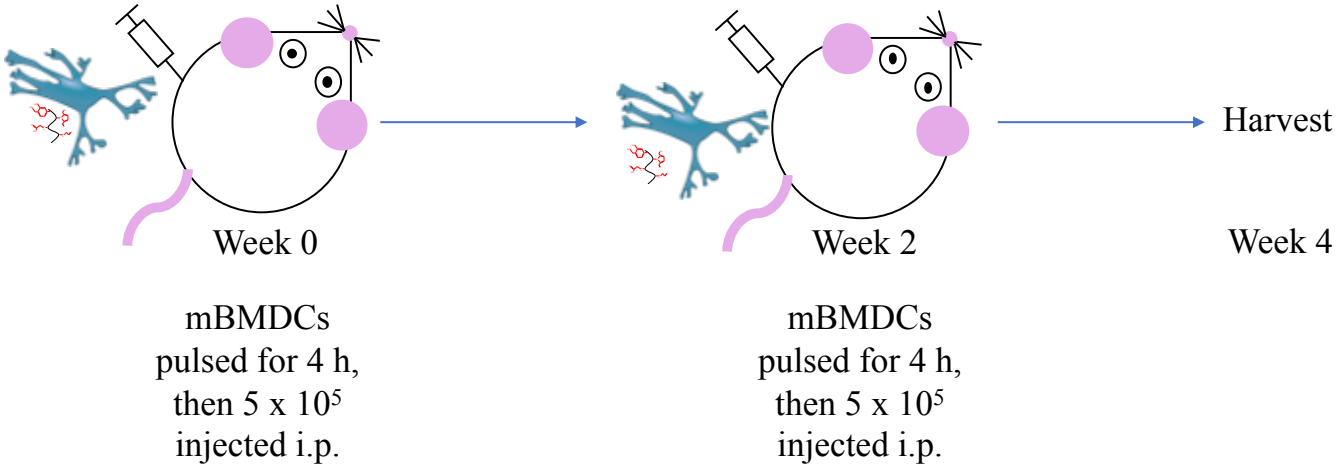

Figure 3.4.2.3: Immunisation schedule for DC transfer experiment. At both time points, the DCs were pulsed with 100 µg of modified protein, 100 µg of unmodified protein with 10 ng/ml LPS or PBS. The image of the DC is taken from the Reactome icon library.

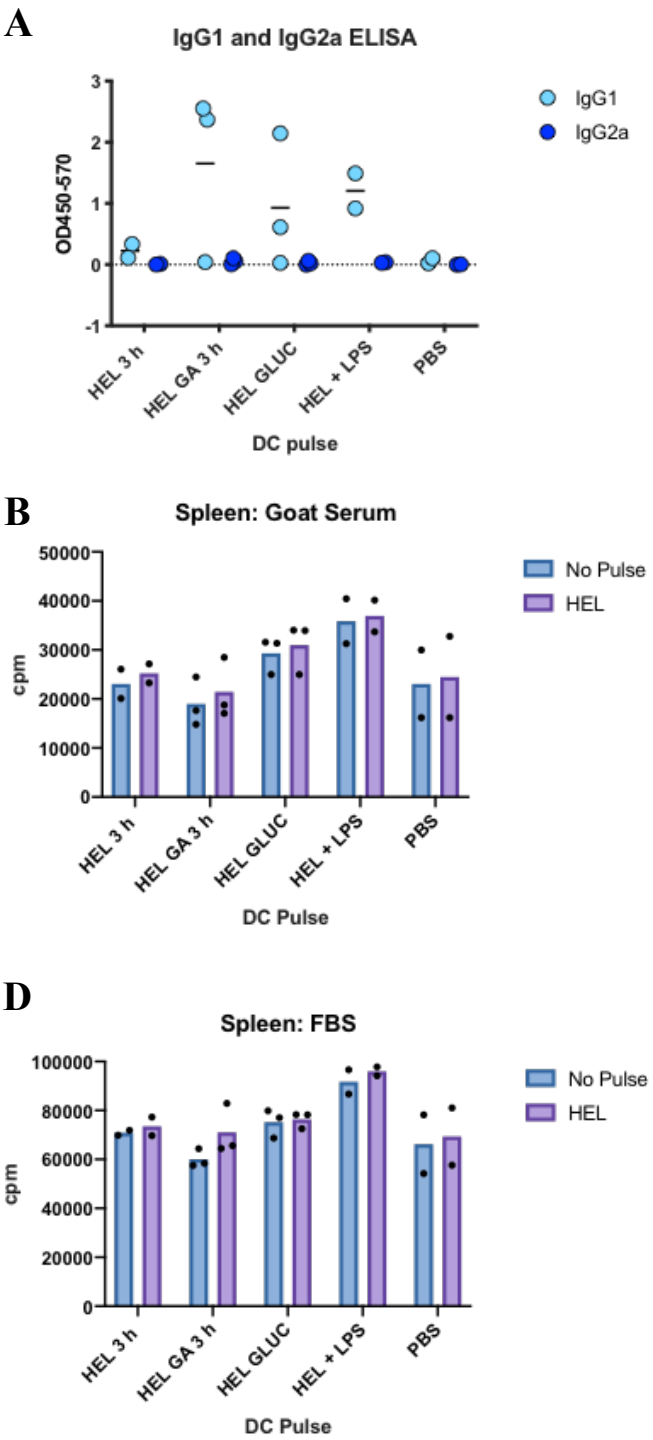

Figure 3.4.2.4: BMDCs were pulsed for 4 h with AGE-modified/unmodified HEL, PBS (negative control) or HEL + LPS (positive control). The cells were then washed and 5 x 10^5 cells were injected i.p. into female BALB/c mice. This was repeated two weeks later, then a further two weeks later the mice were culled and sera and spleens collected. As in Figure 3.4.2.1, the anti-HEL IgG1 and IgG2a responses were assessed by ELISA. The results are shown in A. The splenocytes were cultured either in goat serum or FBS and pulsed with HEL or left unpulsed. Thymidine incorporation after 3 days of culture was measured and is shown in B-E, either as raw data (B and D) or as HEL response minus unpulsed response (C and E). Each dot represents one mouse, n = 2 - 3 per group, bars show mean.

3.4.3 AGE-modified Proteins Do Not Induce DC Maturation

Having identified modifications which could enhance the development of immune responses to native protein, further experiments were performed to determine the mechanisms that underlie this phenomenon. These began by examining the effects of modified proteins on DC biology. As mentioned above, some studies have suggested that AGE-modified proteins can induce the maturation of DCs and as these cells are the gatekeepers to the adaptive immune system (Steinman 2012), this seemed like the logical place to start. The capacity of AGE-modified samples to stimulate the upregulation of selected costimulatory molecules on mBMDCs was initially examined, the results of which are shown in Figure 3.4.3.1. The selected costimulatory were CD86 (one of the key costimulatory molecules upregulated when DCs mature), CD40 (a receptor which binds to CD40 ligand on T cells to increase activation of both the DC and T cell), and OX40L (a costimulatory molecule associated with Th2 responses) (Hubo et al. 2013). As can be seen, neither the HEL GA 3 h samples nor the HEL GLUC samples induced increased expression of these molecules. In comparison, LPS caused upregulation in surface expression showing that the DCs were capable of responding. The costimulatory molecule results indicated that AGE-modified samples cannot induce classical activation of DCs, a finding in line with previous studies which had used low endotoxin AGE samples to assess effects on mBMDCs (Heilmann et al. 2014; Ilchmann et al. 2010; Moghaddam et al. 2011). However, this obviously only examines a very limited range of surface markers. To gain a complete picture of what was happening when DCs were exposed to AGEs, it was decided to use broad screens to assess changes in transcription and cytokine secretion. Firstly, RNA was collected from BMDCs pulsed o/n with HEL, HEL GA 3 h, HEL GLUC or LPS and then changes to transcription were assessed by RNAseq. This was done in collaboration with Dr Moghaddam, who prepared the lysates, and the Institute for Cancer Research (ICR), who performed the RNAseq and analysed the data.

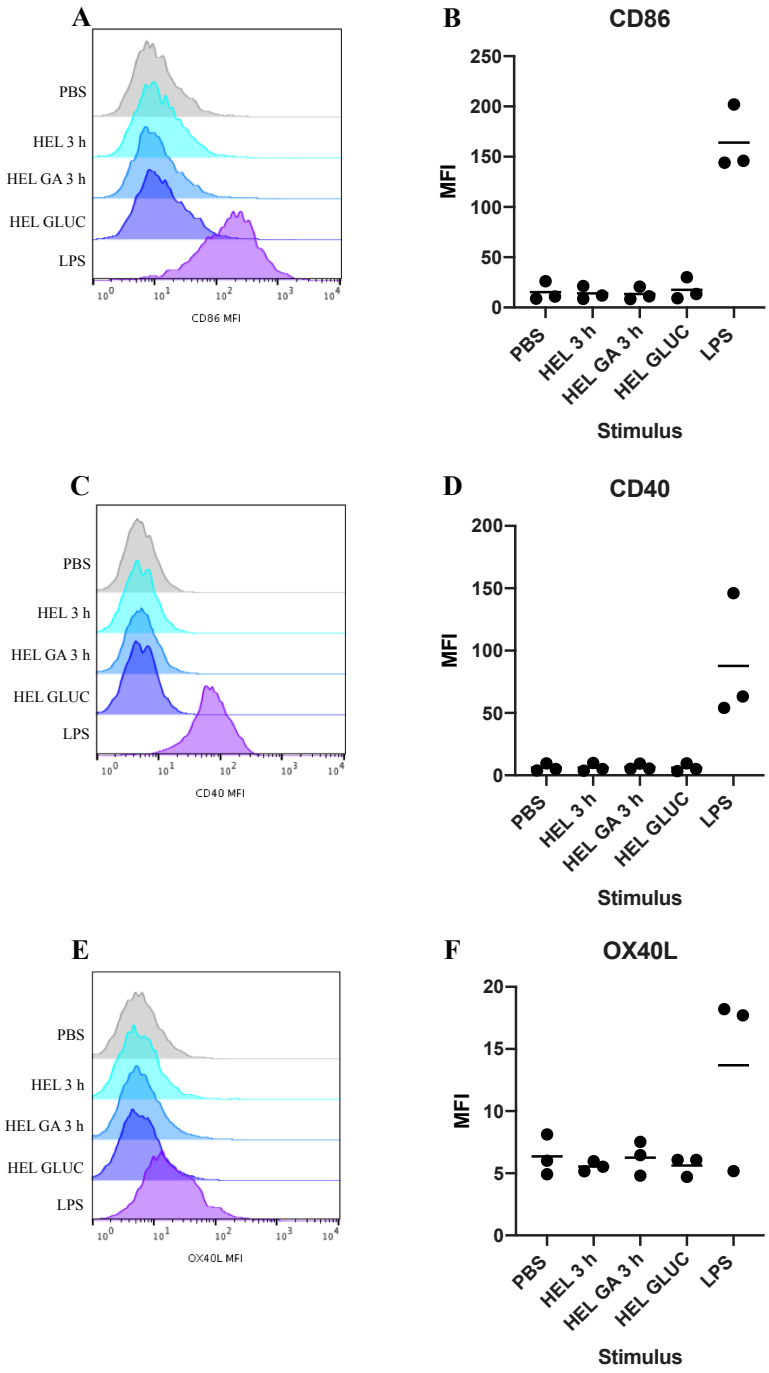

Figure 3.4.3.1: mBMDCs were pulsed with 100 µg/ml of the indicated protein samples or 10 ng/ml LPS o/n. DCs were then collected and stained for the indicated costimulation markers using fluorescently labelled antibodies. Antibody binding was then assessed by flow cytometry A, C and E show representative flow cytometry plots, whilst B, D and F show pooled data from three independent experiments. Each dot indicates the result of one experiment, the bars show mean. MFI = mean fluorescence intensity.

Figure 3.4.3.2 shows the results as a principal component analysis (PCA) plot which demonstrates that LPS treatment induced dramatic changes to the DC transcription profile. In contrast, BMDCs pulsed with AGE-modified samples showed almost no change from DCs pulsed with HEL or left unpulsed. However, a small number of genes showed

significantly different expression between HEL GLUC pulsed and HEL pulsed DCs. These are listed in the Table 3.4.2. There were no genes which showed significantly different expression between HEL and HEL GA 3 h pulsed DCs.

This dataset was then analysed using pathway analysis to identify areas of DC transcription which may have been altered by AGEs. To do this the ConsensusPathDB database was used, which combines multiple repositories (Herwig et al. 2016). Two types of analysis were done. Firstly, overrepresentation analysis, which only uses the list of genes which have significantly different expression between pulsing treatments. Secondly, enrichment analysis, which examines changes across the entire dataset, allowing for the identification of pathways in which no individual genes show significantly different expression but for which collectively there is a significant association with the pathway. The overrepresentation analysis demonstrated that the differentially expressed genes belonged to pathways which formed two clusters, one linked to the cell cycle and the other to collagen formation and cell-to-cell communication (Figure 3.4.3.2). These two sets of pathways were linked by integrin signalling. Previous studies have suggested that AGE-modified proteins can alter cell proliferation, although the exact effect is uncertain as AGE-modified proteins have been shown to both enhance and inhibit cell proliferation in different studies (C. Li et al. 2017; Yang et al. 2010; Iwamoto et al. 2008; Y. Li et al. 2017). Enrichment analysis identified many pathways altered in DCs with the most significantly affected concerning metabolism and protein production. The Venn diagram in Figure 3.4.3.2 shows the overlap between the pathways affected in HEL GLUC and HEL GA 3 h pulsed DCs compared to DCs pulsed with HEL alone, the number of pathways affected and the most significant results in each category. Overall, from the RNAseq data there were a small number of changes which indicated that the AGE-modified proteins were altering DC activation status.

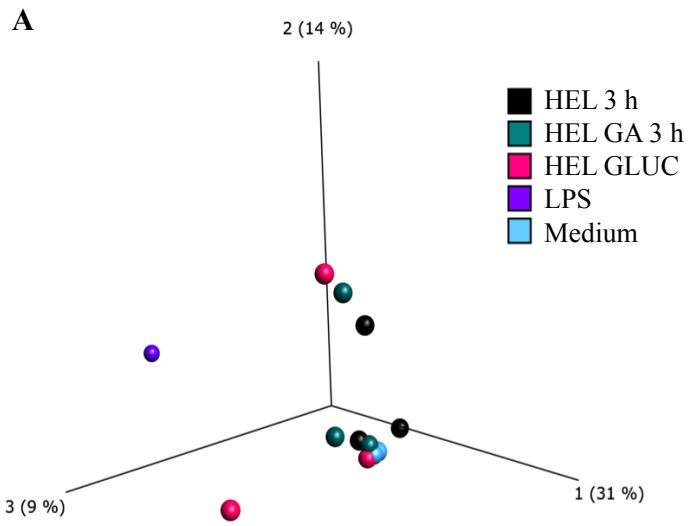

Figure 3.4.3.2: mBMDCs were pulsed o/n with 100 µg/ml of the indicated protein or 10 ng/ml of LPS. Lysates were then collected for RNA extraction. The RNAseq was performed by the ICR the data provided were used to produce the PCA plot shown in A. Each dot indicates an individual sample. The results from the RNAseq data were used for pathway analysis, either overrepresentation analysis (B) or enrichment analysis (C) using ConsensusPathDB. The former uses a pre-selected list of genes and identifies pathways which are overrepresented in that dataset. The results are represented as a map showing the significant pathways and the connections between them. The map key is given in the table. In contrast, enrichment analysis examines fold change over the entire dataset, allowing for identification of pathways where the changes may be small, but collectively the result is significant. This was used to compare gene expression in DCs pulsed with HEL GLUC or HEL GA 3 h with those pulsed with HEL 3 h. The results are shown as a Venn diagram giving the number of affected pathways, the overlap between them and the top five pathways in each category. The complete enrichment analysis results are given in the Appendix.

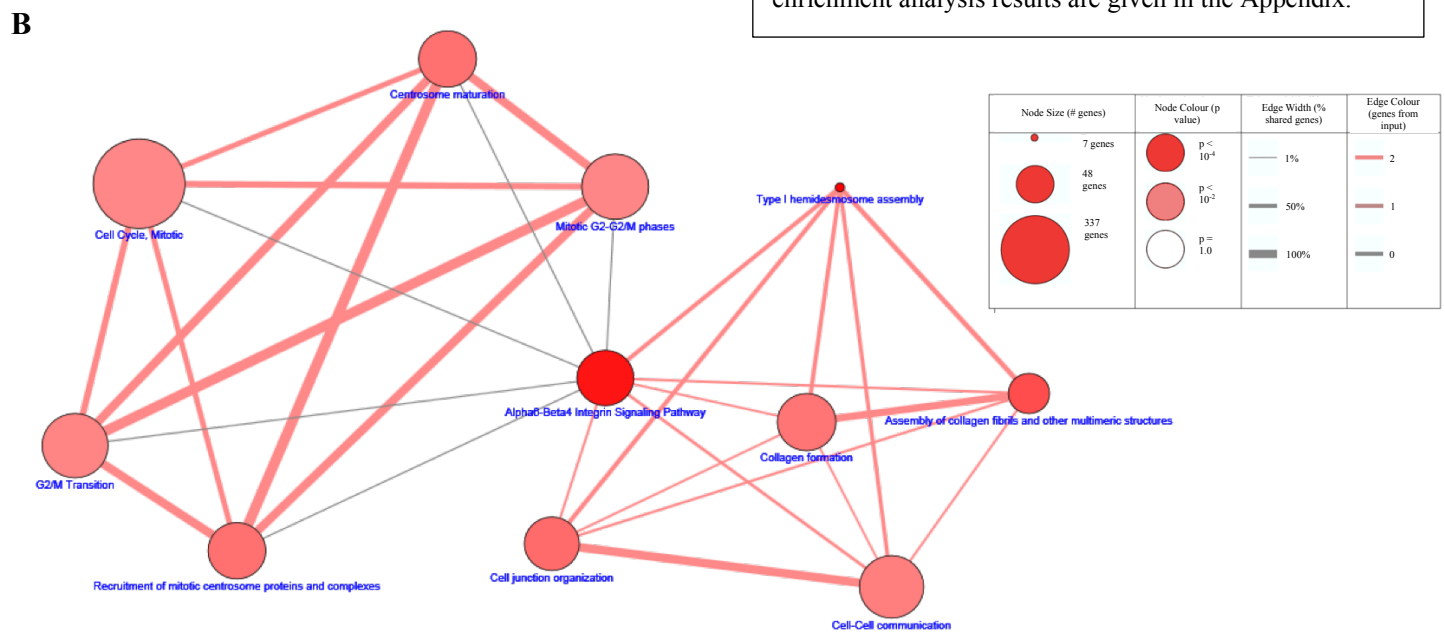

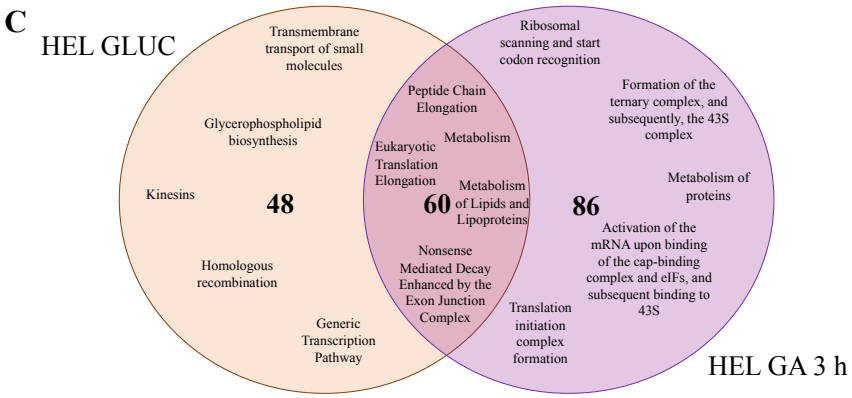

Gene	Log2 Fold Change	P value	P adj	Name of Protein	Functions
Golgb1	0.48336055	9.0232E-10	1.0557E-05	Golgin subfamily b member 1	Golgi organisation, vesicle transport, protein localisation
Macf1	0.49056049	4.0842E-09	2.3892E-05	Microtubule-actin crosslinking factor 1	Actin binding protein which is involved in a variety of processes including cell migration, focal adhesion assembly and cytoskeletal organisation
Bod1l	0.4492132	7.0518E-08	0.00027502	Biorientation of chromosomes in cell division 1-like	Part of fork protection machinery involved in DNA repair and replication fork processing
Prrc2c	0.37958739	1.761E-07	0.0005151	Proline-rich coiled-coil 2C	Involved in cell differentiation including of hematopoietic progenitor cells.
Arg1	0.47942121	2.3633E-07	0.00055302	Arginase-1	Key component of the urea cycle. Also regulator of innate and adaptive immune responses
Rrbp1	0.39734754	3.1466E-07	0.00061358	Ribosome-binding protein 1	Ribosome receptor present on the endoplasmic reticulum
Spen	0.42959899	8.9609E-07	0.00149775	Spen family transcription repressor	Negative regulator of transcription
Akap9	0.42124325	1.74E-06	0.00254478	A-kinase anchor protein 6	Regulates various signalling pathways, cell organisation and ion channels
Itga6	0.40045142	2.4956E-06	0.00324425	Integrin alpha-6	Receptor for laminin which is critical for hemidesmosome formation. Regulates cell adhesion and migration.
Ankrd11	0.39689528	3.0016E-06	0.00351189	Ankyrin repeat domain 11	Regulates histone acetylation
Tpr	0.32913802	3.3969E-06	0.00361308	Translocated promoter region	Part of the nuclear pore complex regulating mRNA export and translation. Also regulates mitotic spindle assembly.
Numa1	0.34095933	6.0307E-06	0.00587996	Nuclear mitotic apparatus protein 1	Involved in forming and maintaining the mitotic spindle. Also

					regulates chromosome segregation.
Dst	0.42550732	1.1277E-05	0.0101495	Dystonin	Organisation of the cytoskeleton, cell adhesion and intracellular transport
Slc7a8	0.35177055	1.7657E-05	0.01475638	Solute carrier family 7 (cationic amino acid transporter, y+ system), member 8	Transports small and large neutral amino acids in a sodium independent manner
Ubr4	0.30888742	1.9385E-05	0.01511995	Ubiquitin protein ligase E3 component n-recognin 4	Part of the protein ubiquitination pathway
Lpp	0.32885261	2.5889E-05	0.01840652	LIM domain containing preferred translocation partner in lipoma	Cell to cell adhesion
Myh9	0.32846783	2.6745E-05	0.01840652	Myosin-9	Cytoskeletal organisation, cell adhesion and cell shape. Also phagocytosis and monocyte differentiation
Npy	-0.3117279	6.3582E-05	0.0413285	Neuropeptide Y	Neurotransmitter which also regulate immune responses
Kmt2a	0.34889438	0.0001248	0.07160786	Lysine (K)-specific methyltransferase 2A	Histone methyltransferase with essential role in haematopoiesis
Plec	0.29536072	0.00012771	0.07160786	Plectin	Hemidesmosome assembly and cytoskeleton organisation
S100a4	-0.3710281	0.00012853	0.07160786	S100 calcium binding protein A4	Positive regulator of NF-κB signalling
Bptf	0.28215275	0.00014658	0.07795204	Bromodomain PHD finger transcription factor	Embryonic development and regulation of transcription
Slfn10-ps	0.36060067	0.00019796	0.09978691	Schlafen 10, pseudogene	Transcribed unprocessed pseudogene
Tnrc18	0.28369842	0.00020469	0.09978691	Trinucleotide repeat containing 18	Chromatin binding protein

Table 3.4.2: Genes with significantly different expression between HEL 3 h and HEL GLUC pulsed DCs. The fold change between the two conditions in shown in column two, blue indicates downregulation and red upregulation. Also shown are the p value and the p adj (p value adjusted to correct for false discovery rate). A cut off of p adj < 0.1 was used to identify significantly different expression. Function and name of protein come from the MGI and UniProt databases.

Next, changes to the secretory profile of DCs were examined using Proteome Profiler, a membrane-based sandwich immunoassay which detects qualitative changes in secretion of 121 cytokines/immunomodulators. BMDCs were pulsed with modified or control HEL samples or LPS under the same conditions as the RNAseq experiment, then supernatant was

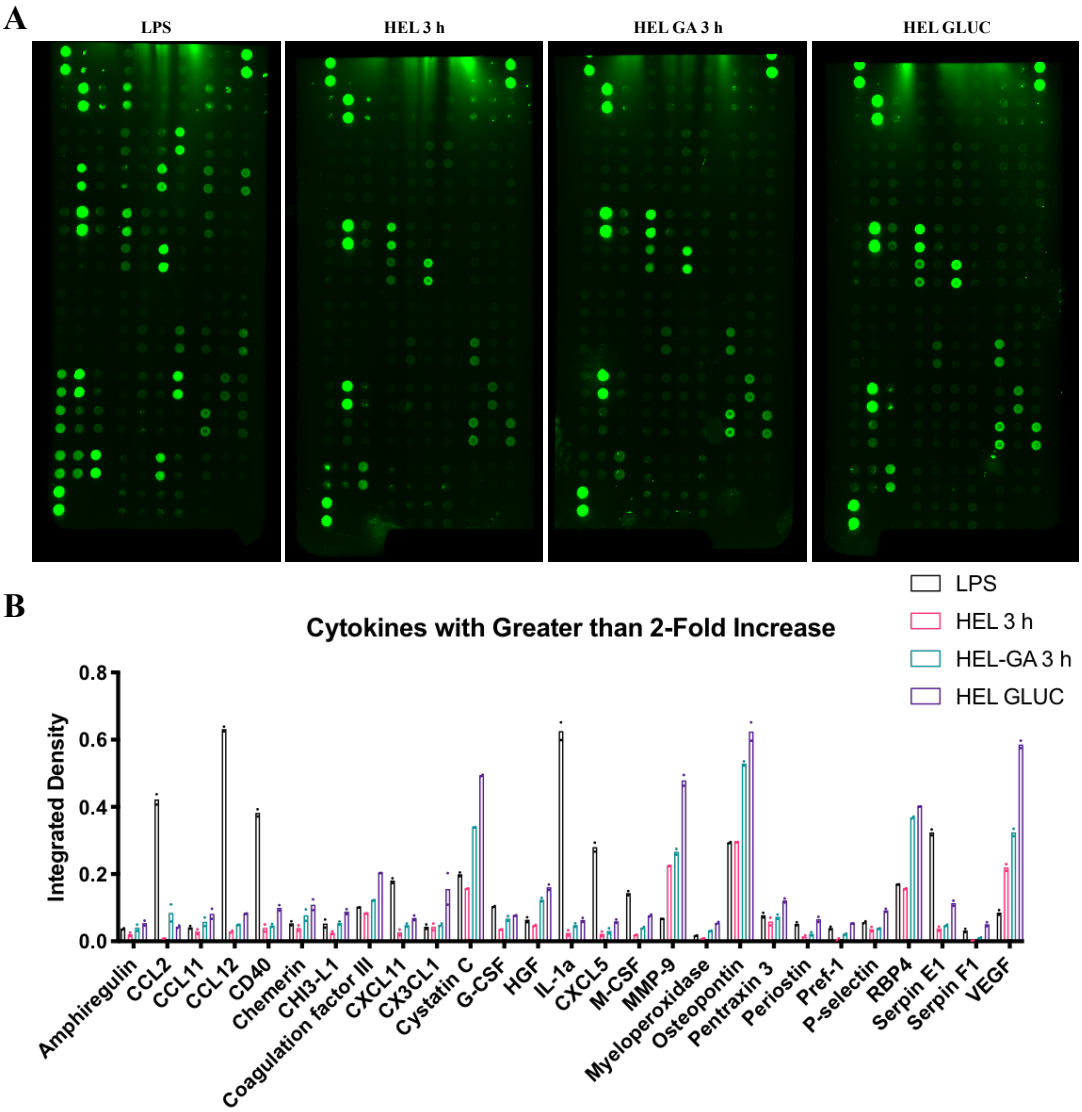

Figure 3.4.3.3: mBMDCs pulsed with 10 ng/ml LPS or different modified HEL samples at 100 µg/ml. Supernatants were collected 18 h later. Mouse XL cytokine proteome profiler was used to assess cytokine content in these supernatants. This is a membrane based assay in which antibodies specific for individual secreted proteins are bound to dots on a membrane. The membranes are incubated with the serum, allowing the antibodies to bind to proteins in the serum. Bound proteins can then be detected with streptavidin-tagged secondary antibodies. The profiler membranes are shown in A. Each protein is detected by one pair of dots. The integrated density of each pair of dots was measured using ImageJ and samples which showed at least a two-fold increase in spot intensity between HEL and HEL GA 3 h and/or HEL GLUC samples are shown in B. The bars show mean and each dot shows the integrated density of one dot on the membrane. Samples which had an integrated density of less than 0.05 were removed. HGF = hepatocyte growth factor, MMP-9 = matrix metalloproteinase-9, RBP4 = retinol binding protein 4, VEGF = vascular endothelial growth factor, Pref-1 = preadipocyte factor 1, G-CSF = granulocyte colony-stimulating factor, M-CSF = macrophage colony-stimulating factor.

collected and incubated with the membranes. These are shown in Figure 3.4.3.3. As with the RNAseq results, pulsing with modified proteins induced only very minor changes whilst LPS treatment induced the release of a large number of proteins. However, there were a few proteins which were secreted in response to HEL GA 3 h and/or HEL GLUC and these are shown in the graph beneath the profiler plots. Some of these had previously been linked to AGE-modified proteins, for example AGEs are reported to stimulate the production of both VEGF and MMP-9 (Chen et al. 2016; Zhang et al. 2011).

The results from the profiler and available literature were used to design multiplex bead arrays (Luminex^{TM} platform) to provide a more quantitative assessment of changes in cytokine secretion and extend these findings to more samples. As before, BMDCs were pulsed for 18 h with the modified samples and then supernatant was collected and analysed. The results from the first Luminex assay are in Figure 3.4.3.4. Interestingly, the LPS and HEL GA 3 h/HEL GA-PR 3 h samples seemed to induce opposing secretory profiles, for example TNFα, CXCL2, CCL3 and CCL2 production was increased by LPS but the HEL GA 3 h samples inhibited secretion of these. This may suggest that modifications in these samples induce an anti-inflammatory signal in the DCs, however, these changes were not seen with OVA GA 3 h and OVA GA-PR 3 h samples. Therefore, if the inhibition is dependent on the AGE structures then there must also be protein-dependent variation.

Moreover, many of the findings seen in the first profiler experiment were not repeated with the Luminex assay. For example, both VEGF and MMP-9 were increased in the profiler study, but their release was decreased in the Luminex assay. One of the few examples which was consistent was HGF (hepatocyte growth factor) which was increased with the modified HEL samples in both the profiler and Luminex assays. Whilst this increase was only modest (1.4-fold increase in HEL GA 3 h pulsed DCs vs HEL 3 h pulsed DCs in the Luminex assay),

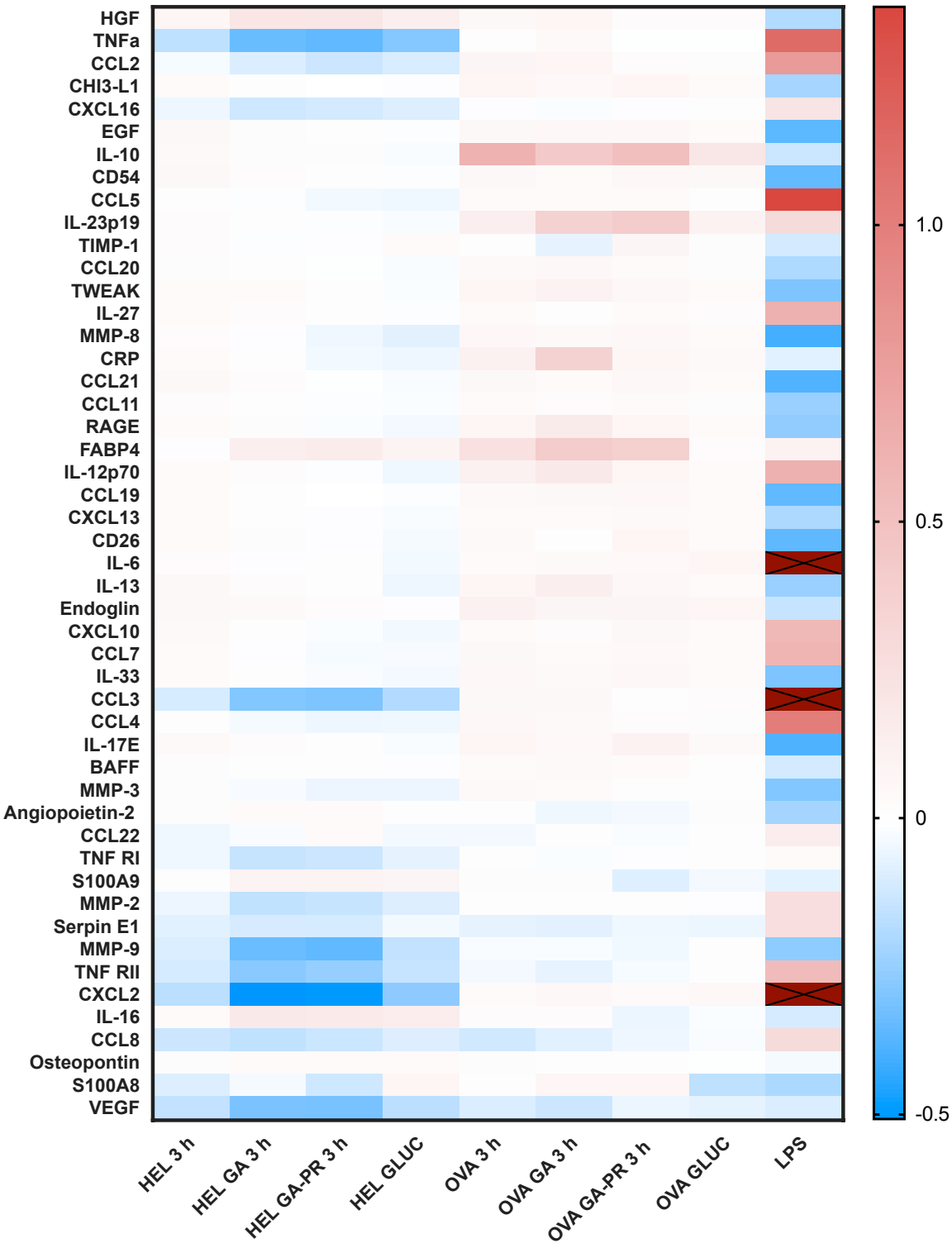

Figure 3.4.3.4: mBMDCs were pulsed with the indicated sample at a concentration of 100 µg/ml for 18 h, then supernatant was collected and cytokine content analysed by Luminex. The results are shown in the heatmap as log fold change compared to unpulsed DCs. The results are from two independent experiments using the average of two biological replicates. In the case of LPS, the concentration of three cytokines was above the limits of the standard curve, these are shown as dark red boxes with a cross through them. HGF = hepatocyte growth factor, CH13-L1 = chitinase-3-like protein 1, EGF = epidermal growth factor, TIMP-1 = tissue inhibitor of metalloproteinases 1, TWEAK = TNF-related Weak Inducer of Apoptosis, MMP = matrix metalloproteinase, CRP = c reactive protein, FABP4 = fatty acid binding protein 4, BAFF = B cell activating factor, TNF RI/II = tumour necrosis factor receptor I/II.

this cytokine is known to have immunomodulating functions. The HGF receptor cMET is reported to be essential for DC migration and although it induces tolerogenic DCs, HGF-cMET signalling in B cells is reported to enhance proliferation and antibody production (Baek et al. 2012; Ilangumaran et al. 2016). Moreover, this receptor is known to act cooperatively with the integrin signalling pathway identified in the RNAseq analysis (Chan et al. 2006). This provided a link between the two datasets and a potential mechanism by which AGE-modified proteins could alter DC responses to enhance adaptive immune responses.

The only secreted protein that seemed to be released in response to GA 3 h and GA-PR 3 h samples on both protein backgrounds was fatty acid binding protein 4 (FABP4). FABP4 is also reportedly released from human macrophages in response to GA-modified BSA binding to RAGE (Wang et al. 2011). Moreover, this protein has been suggested to play an important role in DC function, as DCs from FABP4 KO mice have reduced capacity to respond to LPS and induce T cell responses *in vitro* (Rolph et al. 2006). Therefore, this factor also seemed to be worth further investigation.

Particular cytokines of interest were selected and the secretion kinetics assessed as part of a time course. The main point of this investigation was to determine whether changes to secretion of any of these selected factors reached statistical significance and if so at what time point. Selected results are shown in Figure 3.4.3.5 and include data from the original Luminex and the time course experiments. The majority of samples showed no significant differences between the different AGE-modified samples at any time points. The example highlighted is CXCL2, whilst HEL GA 3 h and HEL GA-PR 3 h have lower production, this does not reach significance and no obvious differences are seen with the OVA samples. Also tested but not shown were CHI3-L1, TNFα, S100A9, CD26, TIMP-1, MMP-8, CCL22, VEGF, MMP-2 and MMP-9. The two factors for which there was a statistically significant

difference were HGF and FABP4. Beginning with the HGF data, at 4 h the secretion of this cytokine in response to HEL GA-PR 3 h is significantly higher than in response to unmodified HEL. This continues to rise to the 8 h time point, but then decreases again. However, this is the only modified HEL sample for which there are significant differences. Moreover, the same changes are not noted for the equivalent OVA samples where again there are no significant effects. With regards to the FABP4, again the only significant difference was noted with HEL GA-PR 3 h which had a significantly higher secretion over HEL at 18 h.

To summarise, the results clearly demonstrate that AGE-modified proteins do not induce classic maturation of DCs, consistent with previous literature. The flow cytometry, RNAseq and Luminex data all indicate that the samples induced very few significant DC responses. Moreover, whilst a small number of significant changes in the cytokine secretion of DCs pulsed could be identified with HEL GA-PR 3 h, an AGE-specific cytokine signature could not be identified as the same changes were not seen in OVA samples with the same modification. This suggests that the protein backbone can influence the DC response to AGE-modified proteins.

Nevertheless, one important question was whether the small number of DC responses seen to the HEL modified samples could explain the *in vivo* data seen in section 3.4.2. One possibility that was initially considered was that HGF-induced enhanced DC migration, thereby enhancing immune responses to AGE-modified proteins. However, this seems to be very unlikely given that the strongest DC responses were seen with HEL GA-PR 3 h which did not induce strong immune responses in the mice. Overall, these data suggest that DC activation is not a major factor contributing to the enhanced immunogenicity seen in section 3.4.2.

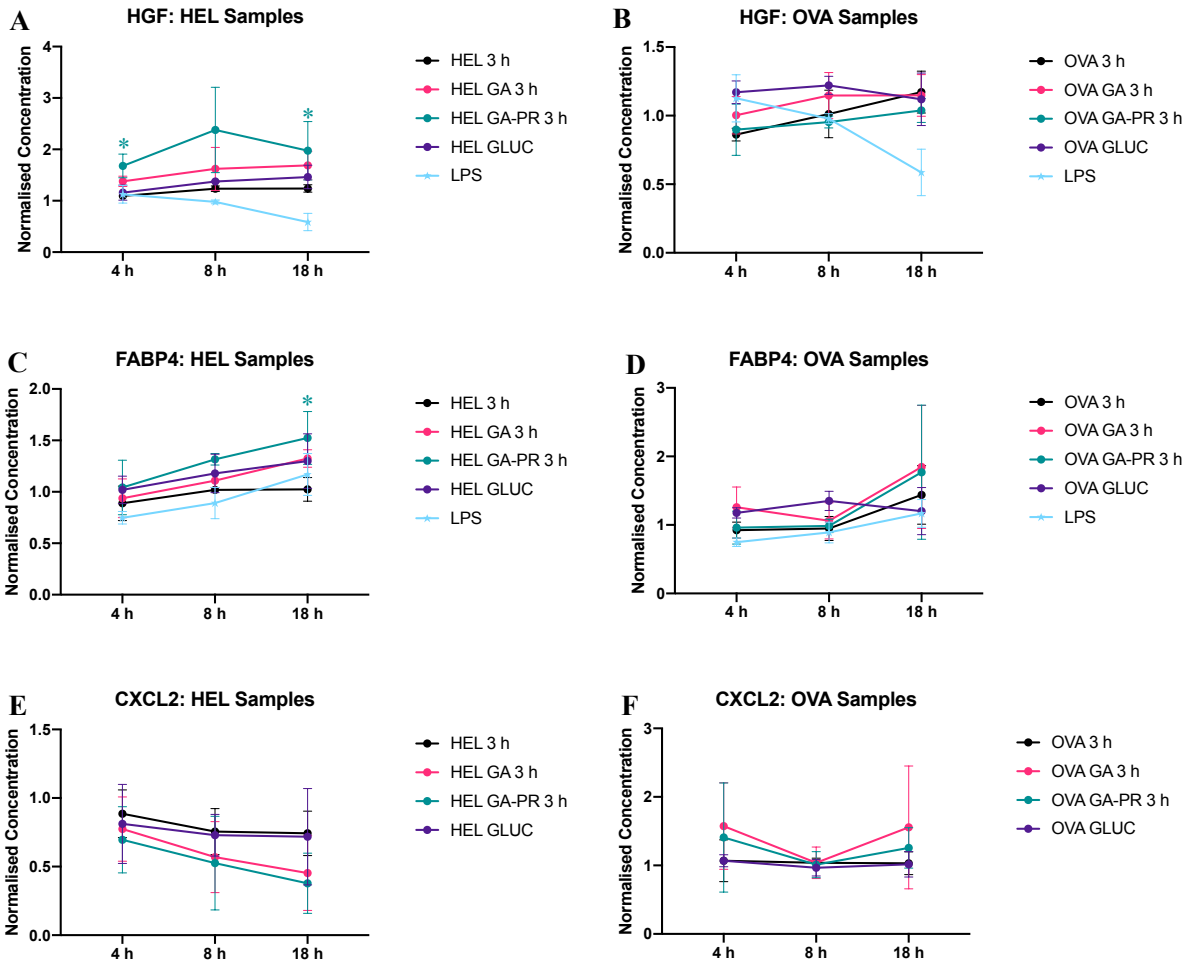

Figure 3.4.3.5: mBMDCs were pulsed with 100µg of the indicated sample and supernatant was collected at the indicated time points. Again, cytokine secretion was determined by Luminex and normalised to the concentration of cytokine in unpulsed DC samples. Selected cytokines are shown above. Data are from two independent (8 h), three independent (4 h) or four independent experiments (18 h), with two biological replicates in each. Significant differences in cytokine production between DCs pulsed with AGE-modified and control protein samples was assessed by Kruskal-Wallis with Dunn's multiple comparison test, * = $p \leq 0.05$. The dots indicate mean and the error bars show standard deviation (SD).

3.4.4 Establishment of an *In Vitro* Proliferation Assay to Assess B Cell Responses

The next possible mechanism considered was whether GA-modified samples were capable of directly activating B cells. The *in vivo* data indicated that these samples induced strong antibody responses which were not always accompanied by detectable T cell responses. As with T cells, B cell activation requires multiple signals. Crosslinking of the BCR starts B cell activation, but for the cells to survive and proliferate a second signal is required, for example signalling through TLRs or T cell help via CD40-CD40 ligand engagement (Akkaya et al. 2018). One possibility was that the RC modifications on GA-modified samples might bind to a receptor on the B cell to act as this second signal. This could then activate B cells either in the absence of Th cells, or with subsequent recruitment of T cells.

To test this hypothesis an *in vitro* proliferation assay was established in which splenocyte cultures were pulsed with different stimuli and proliferation assessed by staining for Ki67. This was done in collaboration with another DPhil student, Mrs Lu Li Jovanoska. As this was a flow cytometry assay, additional labels could be included to identify the proliferating cells (e.g. B cell or T cell). The targets selected are shown in Table 3.4.3.

Marker	Dye	Detecting
CD3	PE	T cells
CD4	BV510	Helper T cells
CD8	A700	Cytotoxic T cells
CD19	BV421	B cells
CD45	BB700	Leukocytes
CD138	A647	Plasma Cells
Ki67	A488	Proliferating Cells

Table 3.4.3: Antibodies included in the proliferation panel

The Ki67 proliferation assay is a well-established assay in the literature (Soares et al. 2010; K. H. Kim and Sederstrom 2015), but this was the first time that it had been used in our laboratory. Therefore, to begin we started by designing an assay in which splenocytes were pulsed with well-characterised stimuli and the proliferation followed over several days of culture. The stimuli selected were:

- PMA and Ionomycin: This is reported to activate B cells and T cells (Klaus et al. 1986)
- Anti-CD40, anti-IgM and LPS: This was designed to specifically activate B cells as it would provide both a BCR signal (anti-IgM) and secondary signals (anti-CD40 and LPS) (Lim, Berger, and Su 2016)

The results of the proliferation assay set-up experiment are shown in Figure 3.4.4.1. As can be seen, in the absence of stimuli splenocytes rapidly die, whereas the proportion of live cells is maintained in the pulsed cultures. Similarly, the percentage of the live cells which

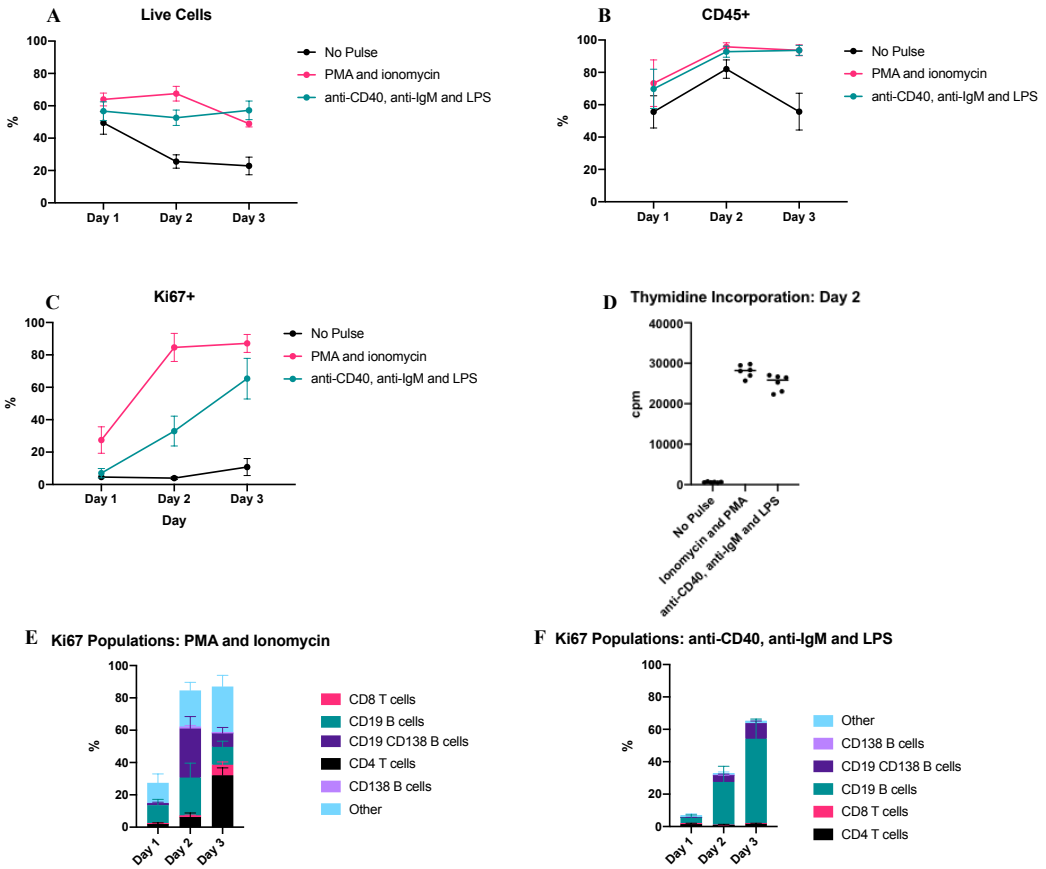

Figure 3.4.4.1: Splenocytes were isolated from 6 female BALB/c mice and pulsed with PMA and ionomycin or anti-CD40, anti-IgM and LPS. Proliferation was then measured by flow cytometry staining for the proliferation marker Ki67 on days 1, 2 and 3. A shows the percentage of live cells in the cultures whilst B shows the percentage of these which express CD45+. The percentage of CD45+ cells expressing Ki67 is shown in C. As a comparison to our established assay, thymidine incorporation was also measured on day 2 and this is shown in D. Finally, the expression of different immune markers in the CD45+ Ki67+ population was examined to determine which cells were proliferating (E and F). The population was divided into CD8 T cells (CD3+, CD8+), CD4 T cells (CD3+, CD4+), CD19 B cells (CD3-, CD19+, CD138-), CD138 B cells (CD3-, CD19- CD138+) and CD19 CD138 B cells (CD3-, CD19+, CD138+). Cells which did not fit into these categories are referred to as "other". A - C and E and F graph show mean with 95% CI, whilst D shows the results from individual mice with a bar indicating mean.

are CD45+ increases to almost 100% for splenocyte pulsed with PMA and Ionomycin/anti-CD40, anti-IgM and LPS, whereas there is a decline in the percentage which are CD45+ for unpulsed cells between day 2 and 3. The percentage of the CD45+ cells which express Ki67 is shown in Figure 3.4.4.1.C. This population increased rapidly for PMA and ionomycin with more than 80% of the CD45+ cells staining positive by day 2. The increase for cultures pulsed with anti-CD40, anti-IgM and LPS was more gradual but by day 3 more than 60% of the CD45+ cells were positive for Ki67.

The expression of the T and B cell markers amongst the proliferating cells were then analysed, these are shown in Figure 3.4.4.1.E and F. Interestingly, in the PMA and Ionomycin pulsed cultures, the first cells to respond were B cells with the T cell response becoming dominant by day 3. In comparison, the anti-CD40, anti-IgM and LPS condition was very specific in targeting B cells with the majority of Ki67+ cells being CD19+. Thus, at the end of the experiment, we had established an assay that could be used to examine B cell proliferation *in vivo.*

The next stage was to examine proliferation of B cells in response to modified samples. To guarantee that within our cultures there would be B cells capable of responding to HEL, we used splenocytes from MD4 mice. These are mice in which the genes encoding the heavy and light chains of the monoclonal (mAb) antibody HyHEL-10 have been inserted as a functional B cell receptor (BCR), thus almost all B cells are HEL BCR-specific. In the heavy chain, the γ1-constant region was replaced with a segment containing μ and δ constant regions, allowing expression of IgM and IgD BCR versions during B cell development (Goodnow et al. 1988). The HyHEL-10 antibody binding site includes AGE-modifiable residues which may be altered during GA/GLUC modification. The modified HEL versions may therefore not be recognised by this antibody (Smith-Gill, Lavoie, and Mainhart 1984). To confirm that this mAb could still recognise the modified proteins, binding was tested in

a direct ELISA. The results are shown in Figure 3.4.4.2. As can be seen, binding was not substantially affected by any of the modifications tested.

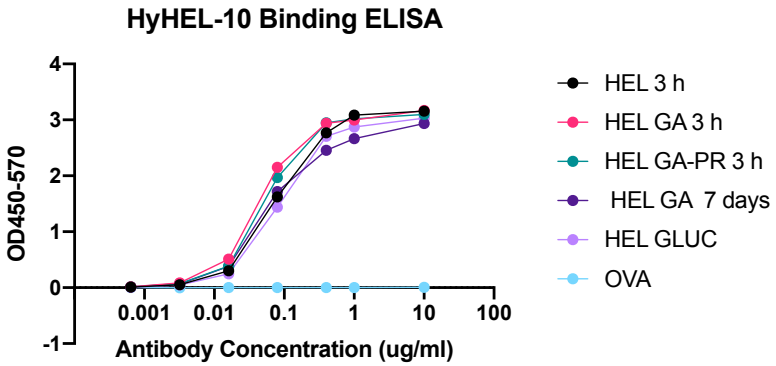

Figure 3.4.4.2: The indicated proteins were coated to ELISA plates and then probed with reducing concentrations of the anti-HEL HyHEL-10 antibody. An irrelevant protein (OVA) has been included as a negative control. In MD4 mice, the genes encoding HyHEL-10 have been inserted into the genome. As a result , the majority of the B cells express this BCR version of this antibody and recognise HEL. The purpose of the ELISA was to ensure cells from these mice could still recognise the modified proteins.

Splenocytes from the MD4 mice were then pulsed with a range of modified samples. HEL + LPS and the anti-CD40, anti-IgM and LPS combination were included as positive controls. Also included were conditions in which the cells were pulsed with HEL and OVA, or HEL and OVA GA 3 h to examine if the RC had to be on the protein recognised by the BCR. However, after 4 days in culture we failed to see responses to any of the modified proteins when measured either by thymidine proliferation (Figure 3.4.4.3) or flow cytometry (Figure 3.4.4.4). In contrast, there were good responses to the positive controls. We therefore could find no evidence for direct activation of B cells by GA-modified proteins.

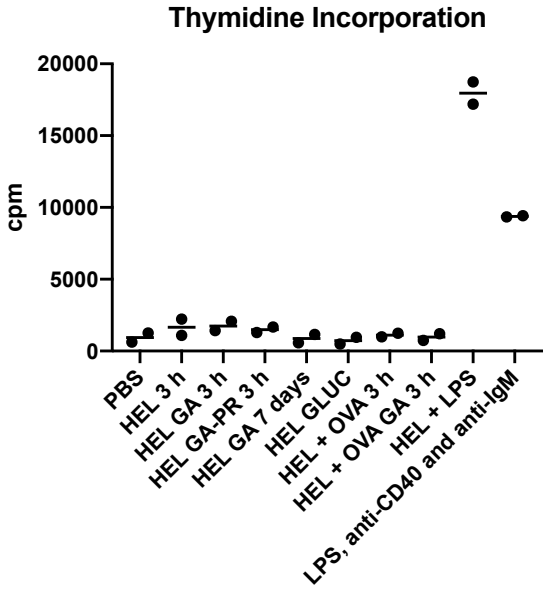

Figure 3.4.4.3: Splenocytes from MD4 mice were pulsed with various AGE-modified proteins, positive control stimuli (HEL + LPS and LPS, anti-CD40 + anti-IgM), or left unstimulated (PBS). On the third day of culture, ^{3}H-thymidine was added to the wells and 18 h later the radioactivity in the cells was measured. The counts per minute (cpm) are shown. Each point is the response of one mouse (average of triplicate cultures). The bars show the mean of the two mice.

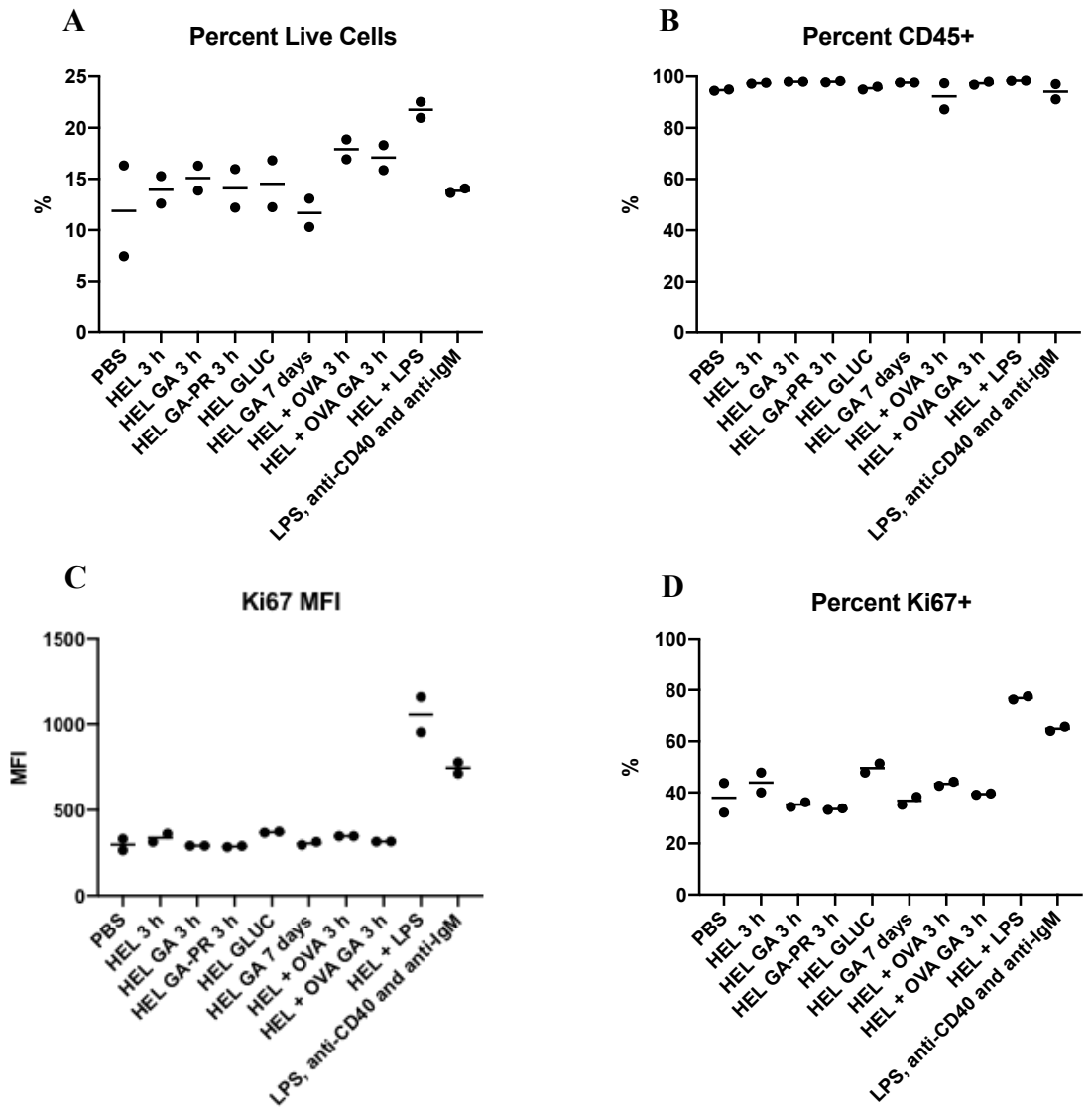

Figure 3.4.4.4: The proliferation of MD4 splenocytes pulsed with different modified proteins (see Figure 3.4.4.3) was also measured by flow cytometry using the proliferation assay established in Figure 3.4.4.1. The cells were harvested on day 4. The percentage of live cells and the percentage of these which were CD45+ is shown in A and B respectively. The Ki67 expression in the live, CD45+ cells is shown both as MFI (C) and percent positive (D). Each dot shows the response of one mouse, whilst the bar show the mean response of the two.

3.4.5 Complement and AGE-induced B cell Activation Cannot be Assessed *In Vitro* Using Mouse Serum

At the end of the first MD4 experiment, the mechanism underlying the enhanced anti-HEL IgG responses induced by GA-modified HEL was still unresolved. However, the evidence suggested the enhanced antibody responses were not due to direct RC-B cell activation or DC maturation. One factor not yet considered was the complement system. It has long been established that complement can activate B cell responses though binding of the complement component C3d to CD21 (Fearon 1998). CD21, together with CD19 and CD81, forms the B cell coreceptor complex which potentiates BCR signalling (Dunkelberger and Song 2010). In this way, C3d binding to antigen can act as a "natural adjuvant" (Dempsey et al. 1996). As discussed in this introduction, AGE-modified proteins have been suggested to activate the complement system and this is suggested to be mediated through the electronegative charge of the modifications. As the serum used in the *in vitro* cell cultures is heat treated, the above experiment would not have shown any complement mediated activation. Thus a new hypothesis for testing was that RCs in the HEL GA 3 h sample can activate the complement system, leading to deposition of C3d on the modified protein. This could then act as the secondary stimulus needed for full B cell activation.

To investigate this, the MD4 experiment was repeated including conditions in which the foetal bovine serum (FBS) was replaced by either normal or heat-treated mouse serum. The modified HEL samples which were included were the same as for the first MD4 experiment, however, different positive controls were included. Firstly, there was a HEL + HyHEL9 condition. HyHEL9 is another HEL specific mAb which recognises a different epitope to HyHEL10. For a positive control, a condition was needed in which there was complement dependent enhancement of B cell activation. It was hoped that the Fc region of HyHEL9, which is also an IgG1 (Silverton et al. 1984), would be capable of activating complement

which could in turn activate B cells. However, in hindsight this was a mistake as IgG1 does not induce complement activation (Collins 2016). Also included were HEL + LPS and HEL GA 3 h + LPS to see if enhanced responses were noted to HEL GA 3 h in the presence of a secondary signal.

The first point of note is that the choice of sera had a clear effect on the size and shape of the cells, as is evident from the flow cytometry plots in Figure 3.4.5.1. The percentage of live cells was the same or higher in cultures with mouse serum (Figure 3.4.5.2), however, the percentage of these that were CD45+ was substantially lower. When the number of Ki67+ cells is examined, either taken as a percentage of live cells or CD45+ cells, it can be seen that in both the heated and normal mouse serum there is reduced proliferation compared to FBS cultures. The same effect is seen in the thymidine proliferation assay (Figure 3.4.5.3). Mouse serum has been reported to inhibit proliferation of lymphocytes so this is a probable cause (Nelson and Shneider 1974). Thus it is not possible to assess complement activation with this system.

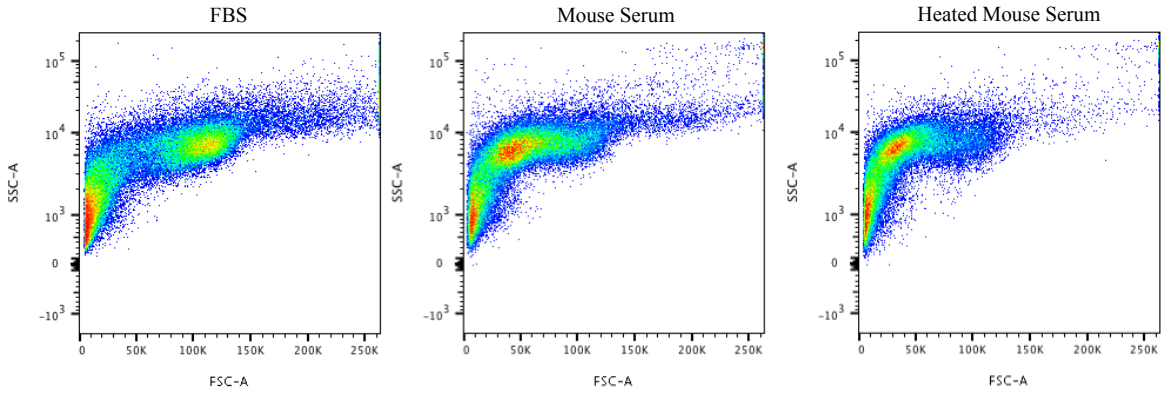

Figure 3.4.5.1: Flow cytometry plots showing the forward scatter (FSC) and side scatter (SSC) of unstimulated cultures of MD4 splenocytes cultured for 4 days in medium containing 10% foetal bovine serum (FBS), 10% mouse serum or 10% heated mouse serum.

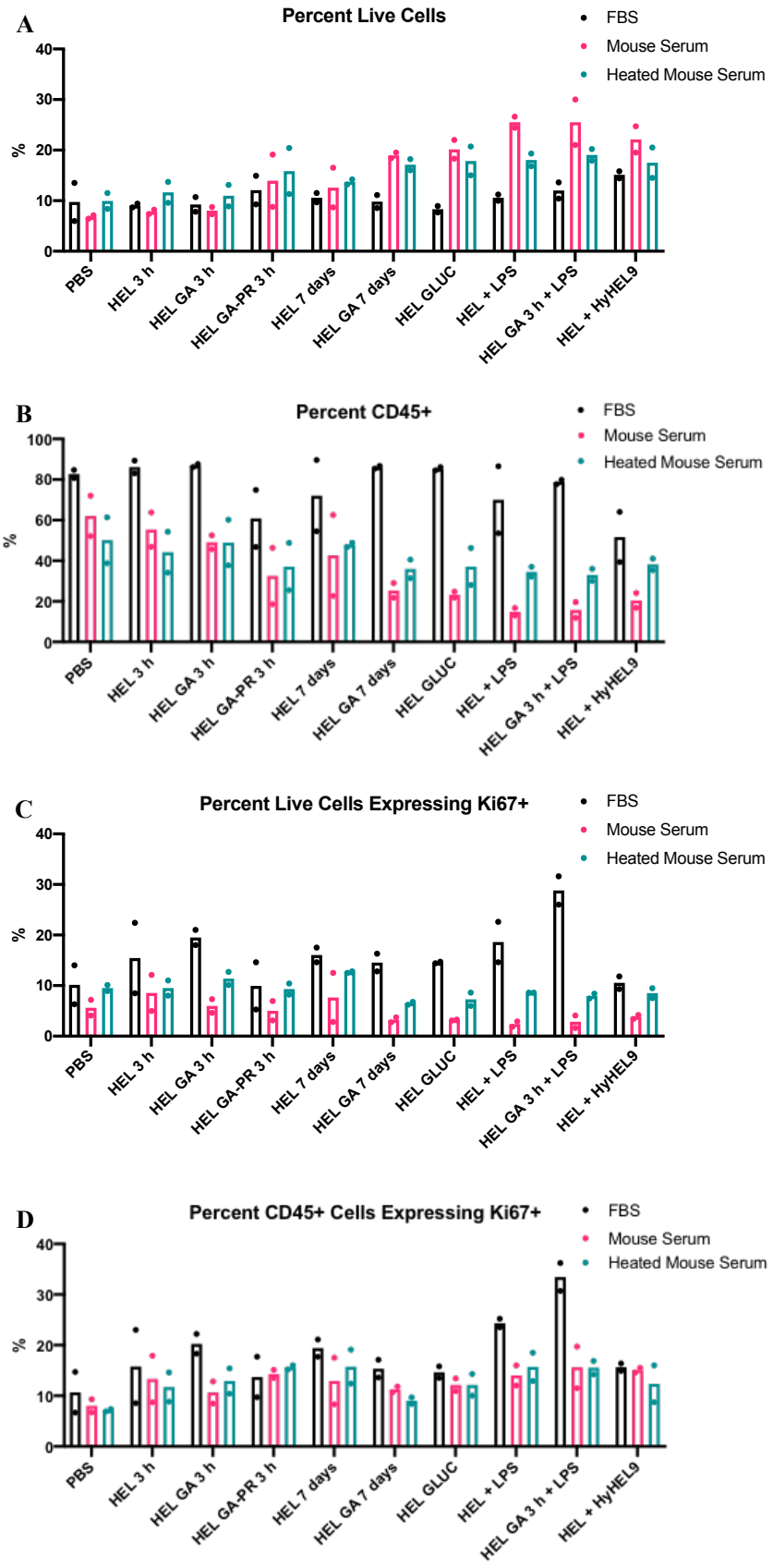

Figure 3.4.5.2: Splenocytes from MD4 mice were cultured in medium containing 10% FBS, 10% mouse serum or 10% heated mouse serum. These cells were pulsed with the indicated stimuli. After 4 days in culture, cells were collected for flow cytometry to assess proliferation by measuring Ki67 expression. Shown in A and B are the percentage of live cells and the percentage of live cells which were CD45+. The percentage of Ki67+ cells, either amongst live cells or live, CD45+ cells, is shown in C and D respectively. Each dot shows the response of one mouse. The bars indicate average.

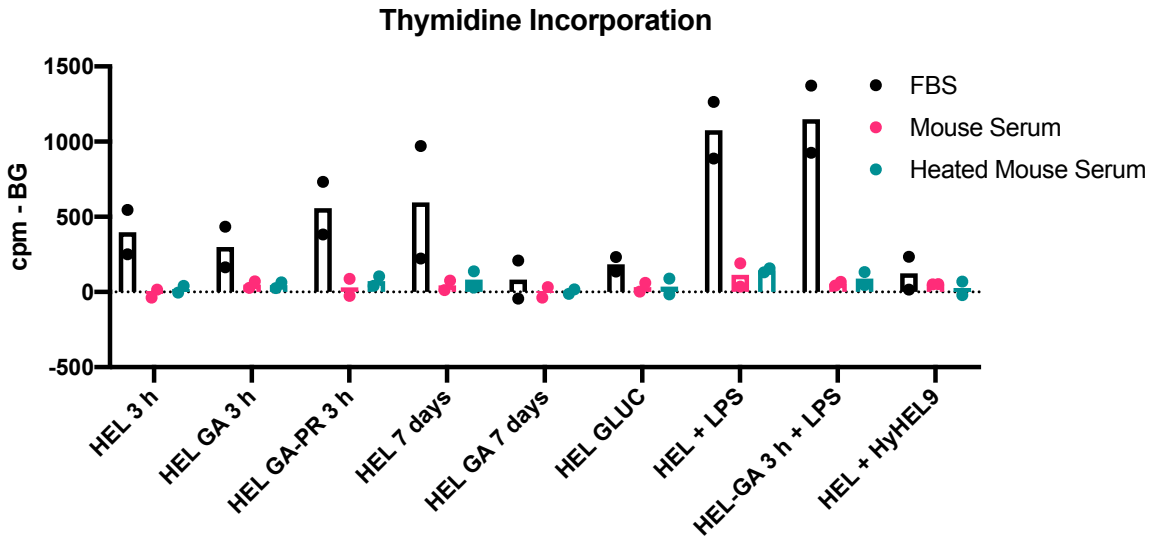

Figure 3.4.5.3: The proliferation of MD4 splenocytes cultured in 10% FBS, 10% mouse serum or 10% heated mouse serum and pulsed with the indicated stimuli was also measured by thymidine incorporation. After 3 days of culture, ^{3}H-thymidine was added to the wells. 18 h later, cell radioactivity was measured. The results on the left show the cpm minus the cpm in unpulsed wells. Each dot shows the response of one mouse. The bars show average.

One point of interest is that the HEL GA 3 h + LPS condition seemed to induce stronger proliferative responses than the HEL + LPS condition. The percentage of Ki67+ cells was approximately 10% higher in the former. Looking at these populations specifically (Figure 3.4.5.4), we can see that in both cases CD19 expressing cells make up the largest group of proliferating cells and there is an increase across all groups for the HEL GA 3 h + LPS condition. This result suggests that in the presence of a secondary signal enhanced responses to HEL GA 3 h can be observed, however further experiments are needed to confirm this as the results are from only 2 mice.

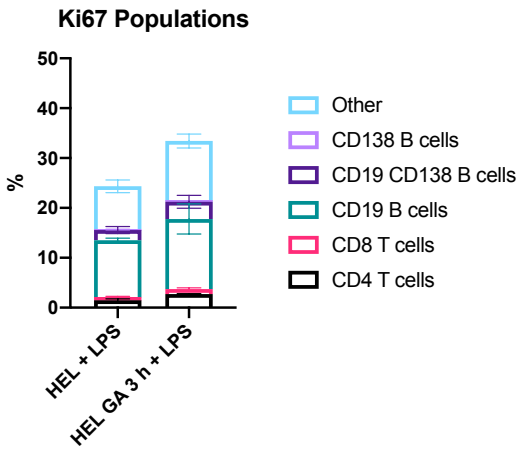

Figure 3.4.5.4: The proliferating (Ki67+) CD45+, live population in the HEL + LPS and HEL GA 3 h + LPS stimulated MD4 splenocytes from the experiment in Figure 3.4.5.2, were assessed for their expression of CD3, CD4, CD8, CD19 and CD138. As in Figure 3.4.4.1, the population was divided into CD8 T cells (CD3+, CD8+), CD4 T cells (CD3+, CD4+), CD19 B cells (CD3-, CD19+, CD138-), CD138 B cells (CD3-, CD19- CD138+) and CD19 CD138 B cells (CD3-, CD19+, CD138+). Cells which did not fit into these categories are referred to as "other". The results are from two mice and the bars show mean whilst the error bars show range.

3.4.6 AGE-modified Protein Do Not Induce DC Maturation when DCs are Cultured in Mouse Serum

The complement system also affects the function of DCs. DCs also possess complement receptors, including CD35 and CD21, and secrete C1q when immature. Complement components bound to antigens act as opsonins and therefore aid DC phagocytosis. Depending on the specific component and context, this can induce maturation of DCs or a tolerogenic phenotype (Killick et al. 2018; Castellano et al. 2004; Merle et al. 2015). It was therefore decided to investigate the possibility that complement activation could also alter DC responses to modified proteins. As before, mBMDCs were pulsed o/n with modified samples. However, in this experiment FBS was replaced with mouse serum or heat-inactivated mouse serum. Whilst the B cell experiments had demonstrated mouse serum could not be included in experiments requiring proliferation, the DC pulsing assay did not require cells to proliferate. Instead the measured outcome was cytokine secretion in the supernatant and expression of maturation markers.

DC activation was initially assess by flow cytometry. Figure 3.4.6.1 shows FSC/SSC plots for cells grown in each of the serum conditions. These show that incubation with normal or heat-inactivated mouse serum resulted in quite dramatic changes in the size and shape of the cells with the DCs becoming smaller and more granular in the mouse serum conditions (Figure 3.4.6.1). One possibility was that the DCs were dying in the presence of mouse

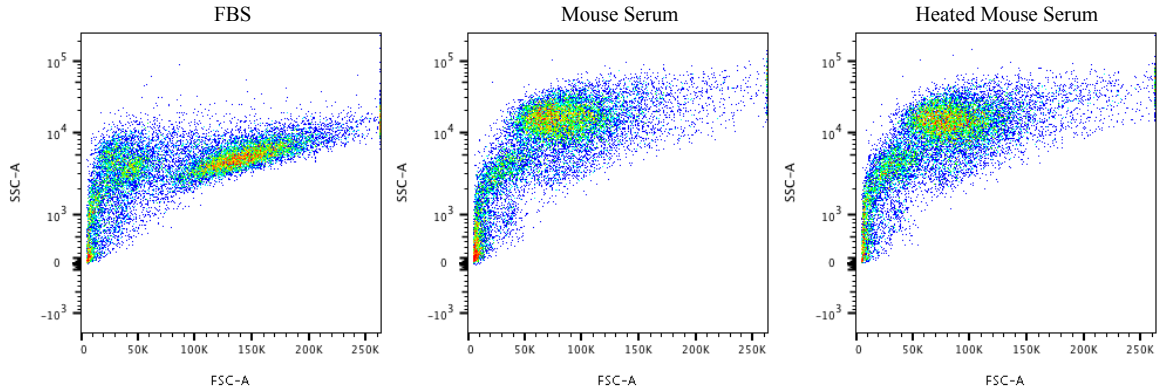

Figure 3.4.6.1: BMDCs were cultured o/n in medium containing 10% FBS, 10% mouse serum or 10% heated mouse serum. The flow cytometry plots show the FSC and SSC of unstained/unstimulated cells.

serum, however this seemed unlikely as the percentage of live cells, as measured by a live/dead stain, was not significantly different between the different conditions. Likewise, the CD11c+ population size was also not significantly altered based on serum exposure (Figure 3.4.6.2).

Next the expression of a panel of different activation markers on DCs exposed to AGE-modified proteins in different serum conditions was examined. The fold change compared to PBS pulsed DCs in the same serum condition is shown in the heatmaps in Figure 3.4.6.2. Starting with the response to LPS, all the different serum conditions show the same pattern of response with regard to which markers are up- or down- regulated. Therefore, the capacity to respond remains similar in DCs exposed to normal or heated mouse serum. As with the previous flow cytometry experiments in Figure 3.4.3.1, the expression of CD40, CD86 and OX40L is not affected by exposure to AGE-modified proteins. Indeed, the protein samples do not seem to induce substantial changes in expression of any of the markers tested. This seen across all the different serum conditions. Therefore, even with intact complement components present, there is no maturation of DCs in response to AGE-modified proteins.

Additionally, changes to the secretion of some of the cytokines of interest identified in section 3.4.3 were examined. The results of the Luminex assay are shown in the heatmaps in Figure 3.4.6.3. The 3 h GA and PR samples produced the same effect as before with inflammatory cytokines such as CCL3 and TNFα being suppressed and a modest increase in HGF. This was broadly the same across all the serum groups indicating that the culture conditions did not have a significant impact on the response to AGEs. Interestingly, the more heavily modified GA 7 day and GA-PR 7 day samples appeared to have opposing effects on the secretion of a number of cytokines. For example, HGF secretion was decreased compared to PBS whilst CXCL2 and CCL3 secretion was unchanged or even slightly increased.

Figure 3.4.6.2: mBMDCs were pulsed for 18 h with AGE-modified proteins in medium containing 10% FBS, 10% mouse serum or 10% heated mouse serum. The following days the cells were collected and stained for a variety of activation markers. The percentage of live cells (A) or CD11c+ cells (B) was not significantly different between different serum conditions (Kruskal-Wallis, each data point represents mBMDCs derived from a different mouse, the bars show mean). The MFI amongst the CD11c+ population for the different activation markers was measured and normalised to the unstimulated (PBS) cells. The log fold change is shown in the heatmaps. The activation marker expression was measured once for each of the protein samples in each sera condition. Included for the first time in this figure is the sample HEL GA-PR days, a HEL GA 7 days which has been reduced with sodium borohydride. ILT3 = immunoglobulin-like transcript 3.

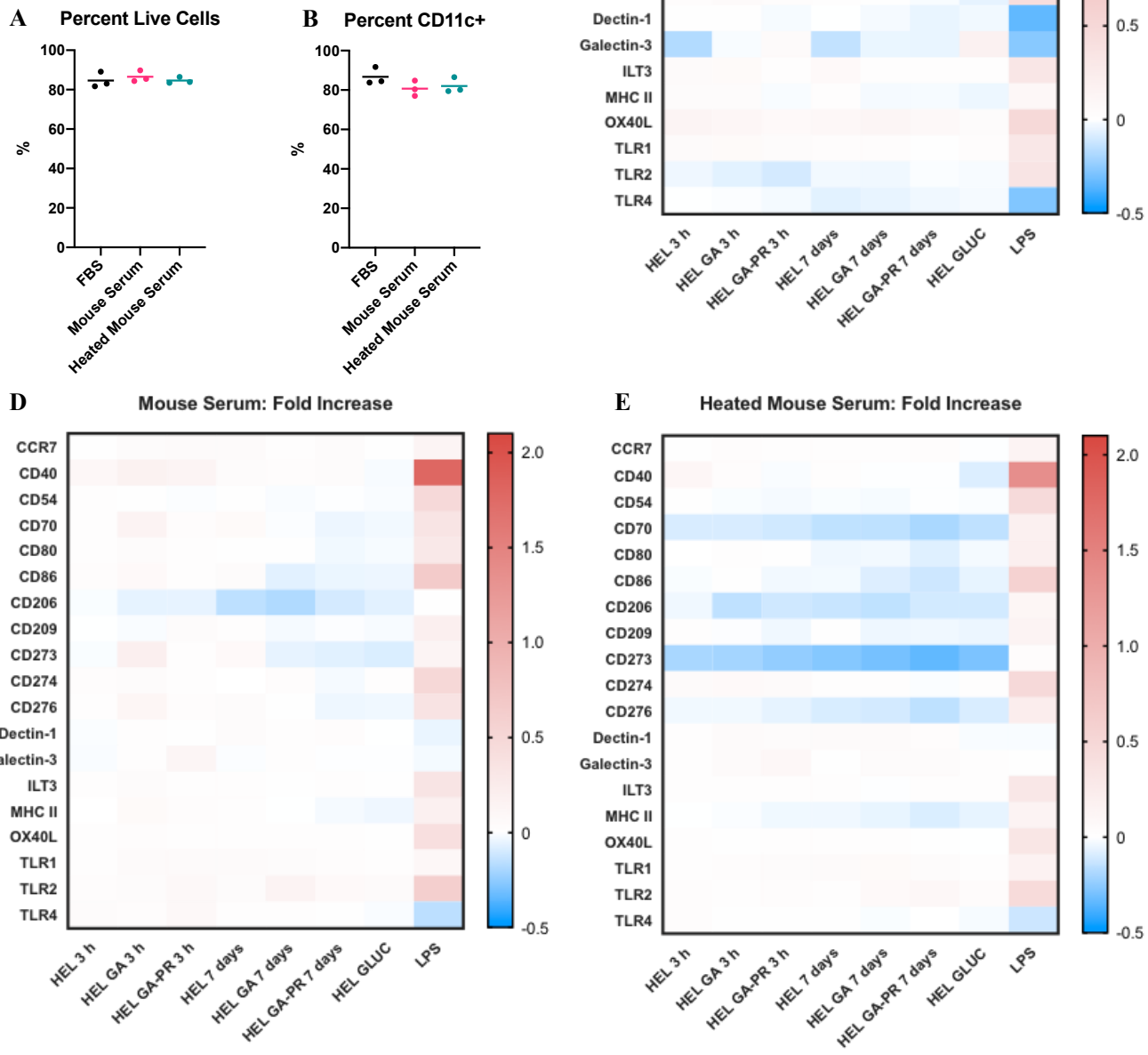

Lastly, in Figure 3.4.6.4 the concentration data for the cytokines from the Luminex assay is shown. As can be the seen, the concentration of cytokines in the DC media varied widely depending on the serum condition. In the presence of heated or normal mouse serum the production of CCL3 and TNFα was decreased. In contrast, IL-16 and HGF concentration was much higher in mouse serum-containing culture media. In particular, HGF secretion in the mouse serum condition appeared to be an exaggerated version of that seen with heated mouse serum or FBS. This suggests that the DCs in mouse serum were more readily able to produce HGF in response to AGE-modified proteins, although the overall fold change was similar.

Also shown in Figure 3.4.6.4 is the production of PGE_2 by DCs in response to AGE-modified proteins. This lipid mediator is known to modulate immune responses, including promoting Th2 responses and suppressing the production of inflammatory cytokines in DCs (Kalinski 2012). Moreover, AGE-modified proteins have been shown to induce production of PGE_2 from human synoviocytes and chondrocytes and can upregulate cyclooxygenase-2 in THP-1 cells (Nah et al. 2008; Shanmugam et al. 2003; Chen et al. 2016). This was therefore an inflammatory mediator of interest which had not yet been measured in this report. However, there was no evidence of PGE_2 production in response to the AGE-modified proteins, although there was enhanced secretion with LPS as has previously been reported (Harizi et al. 2001). No PGE_2 signal could be detected in supernatant from DCs cultured with normal or heated mouse serum.

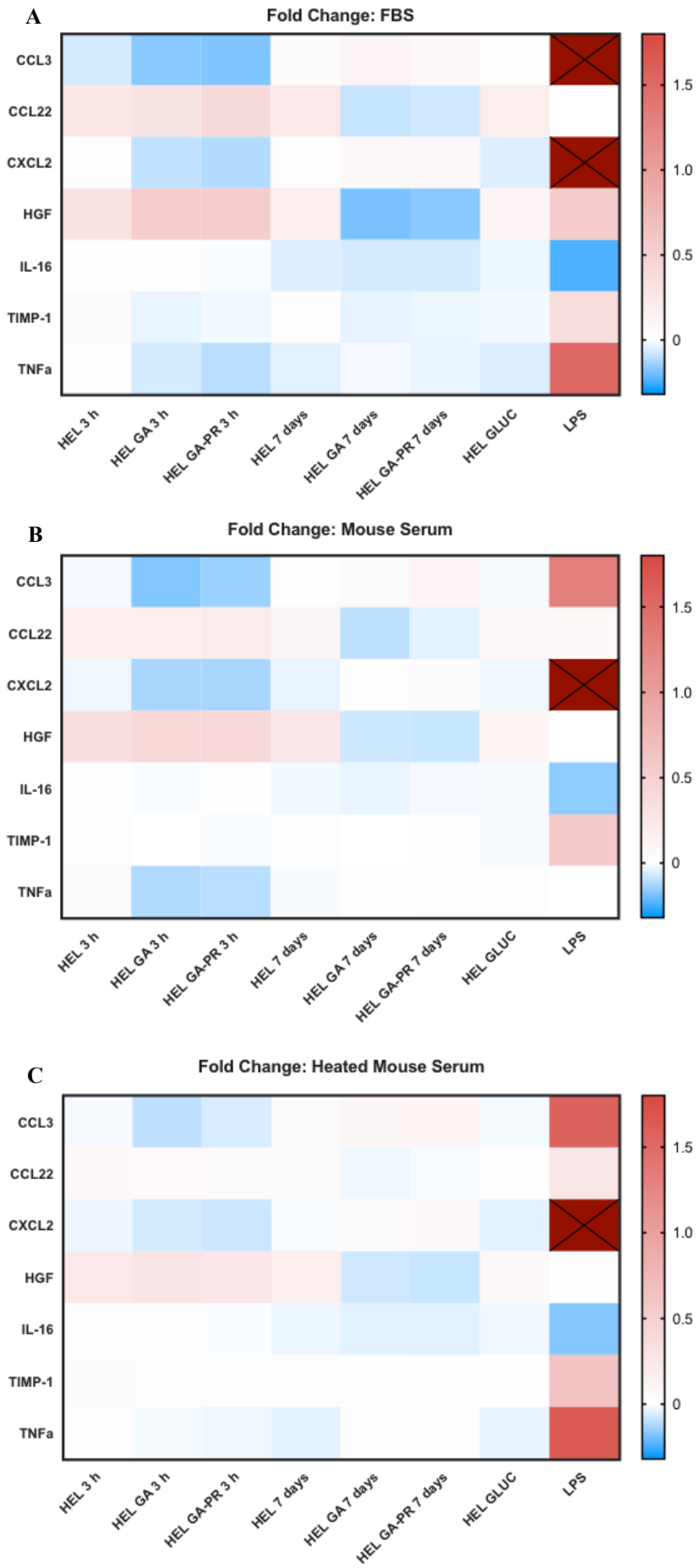

Figure 3.4.6.3: Supernatant from DCs pulsed with different AGE-modified HEL samples in the presence of 10% FBS, 10% mouse serum or 10% heated mouse serum was collected after an 18 h incubation. The secretion of some selected cytokines was assessed by Luminex. The heatmaps show the log fold change compared to PBS. Results show the average response of three mice. Where the cytokine secretion was above the standard curve, this has been marked with an X and coloured dark red.

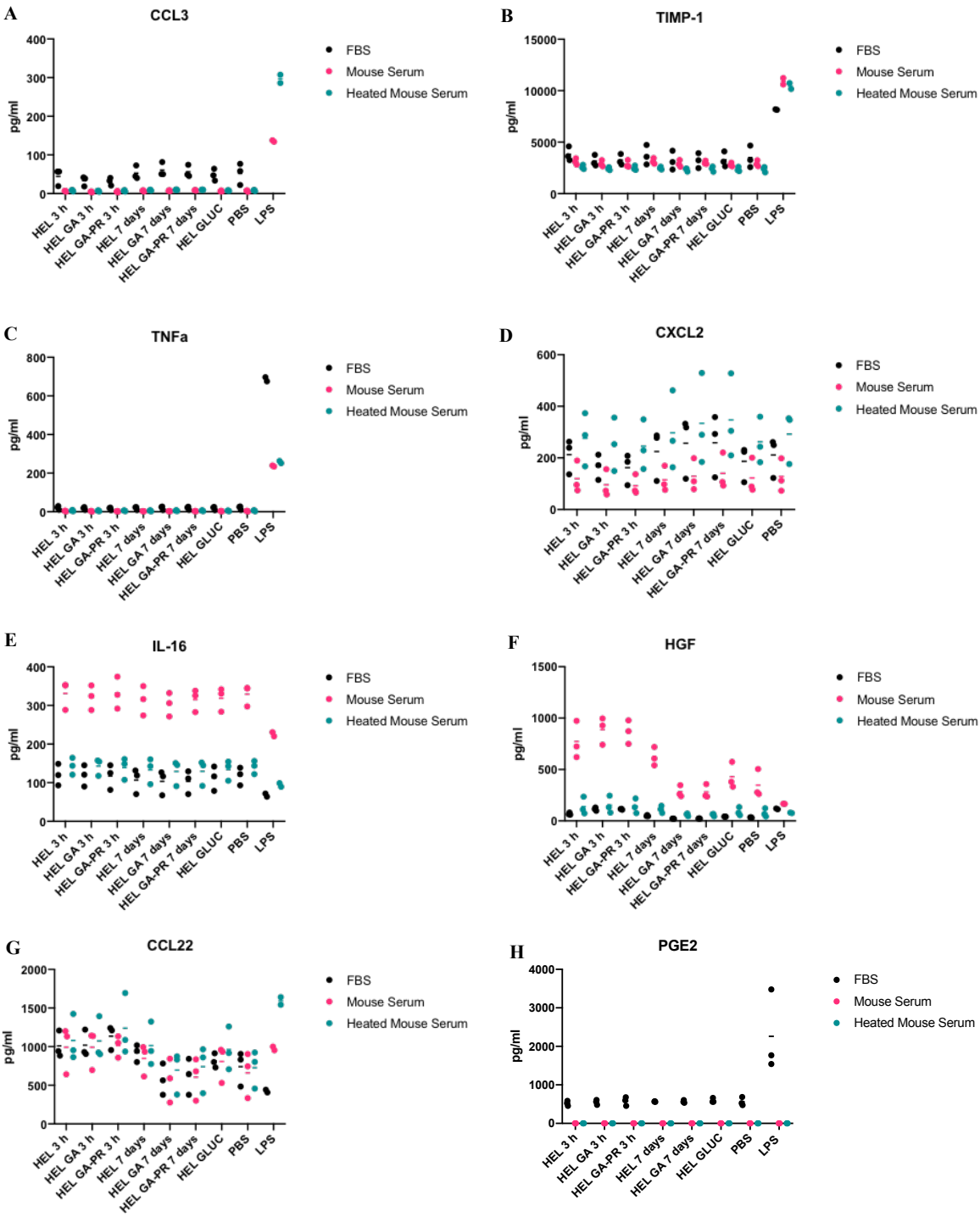

Figure 3.4.6.4: The graphs show the concentration of the indicated cytokine in the supernatant of DCs pulsed with AGE-modified protein for 18 h. A-G were measured by luminex (the log fold change for these cytokines is shown in Figure 3.4.6.3). Each dot represents an individual mouse, except for LPS where, due to a shortage of available tests, the supernatant from DCs derived from three mice was pooled and then tested in duplicate, the bars show mean. For CCL3, the concentration in the supernatant from LPS stimulated FBS DCs was beyond the standard curve and so no points are shown. H shows the results of a PGE_2 ELISA. Again, each dot represents an individual mouse, including LPS. Bars show mean.

3.4.7 AGE-modified Proteins Induce Complement Activation

As the results of the proliferation study in 3.4.5 had indicated that *in vitro* studies could not be utilised to investigate the role of mouse complement on B cell activation, another system to investigate complement activation was required. Different ELISA based assays were therefore designed to examine the binding of complement components to AGE-modified proteins and any resulting activation. Firstly capacity of C1q to bind to different modified protein samples was examined. As discussed in this introduction, this has previously been shown to bind AGE-modified proteins (Chikazawa et al. 2016) and, as this is the first step in the classical complement cascade (Sarma and Ward 2011), seemed to be a logical place to start. The initial attempts to establish an assay capable of showing C1q binding used native human C1q and an anti-C1q antibody. As can be seen from Figure 3.4.7.1.A, using this method there was a dose-dependent binding of C1q to a positive control (the human anti-HIV antibody, 2G12 (Trkola et al. 1996)). However, although there was a higher signal for the HEL GA 3 h sample, there was not a dose-response curve. Further investigation

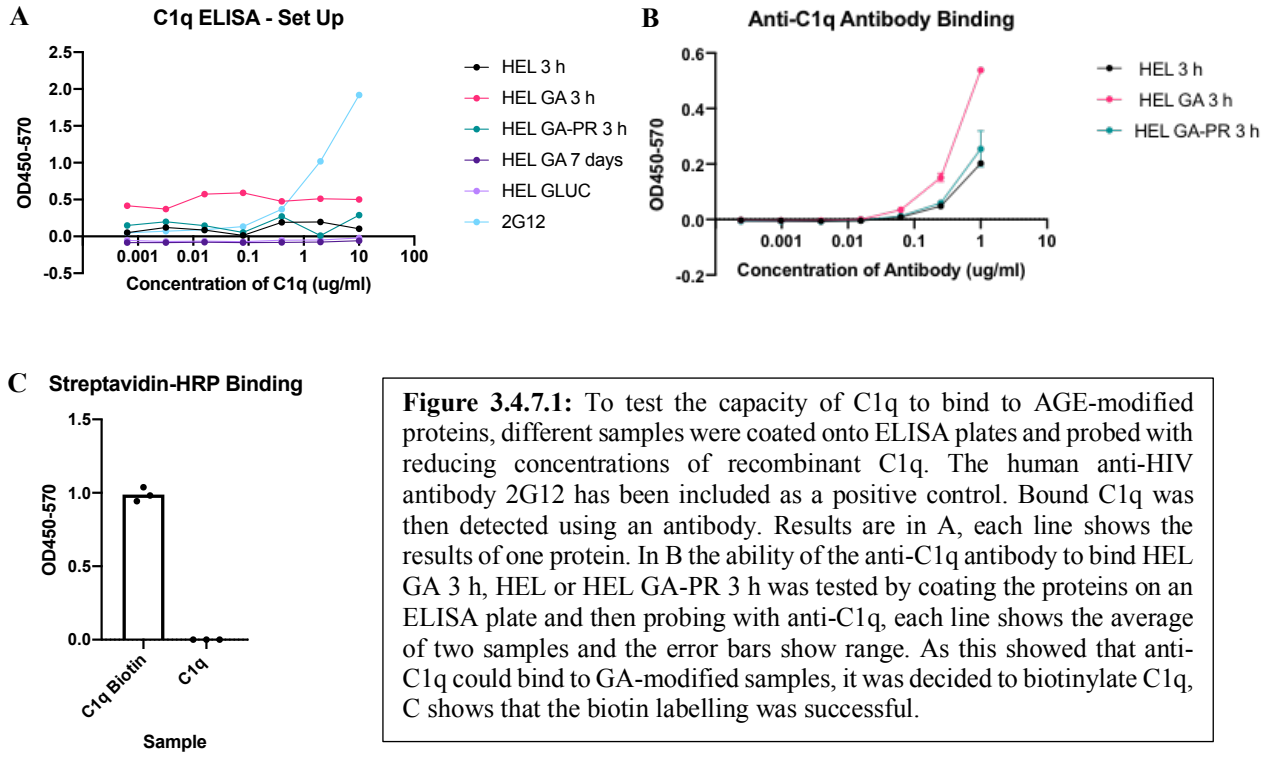

Figure 3.4.7.1: To test the capacity of C1q to bind to AGE-modified proteins, different samples were coated onto ELISA plates and probed with reducing concentrations of recombinant C1q. The human anti-HIV antibody 2G12 has been included as a positive control. Bound C1q was then detected using an antibody. Results are in A, each line shows the results of one protein. In B the ability of the anti-C1q antibody to bind HEL GA 3 h, HEL or HEL GA-PR 3 h was tested by coating the proteins on an ELISA plate and then probing with anti-C1q, each line shows the average of two samples and the error bars show range. As this showed that anti-C1q could bind to GA-modified samples, it was decided to biotinylate C1q, C shows that the biotin labelling was successful.

demonstrated that this signal was the result of the anti-C1q antibody binding to HEL GA 3 h (Figure 3.4.7.1.B). To remove the need for this antibody, a biotinylated version of the C1q was synthesised (Figure 3.4.7.1.C), which would allow for detection using streptavidin-HRP. As this reagent is also used in the carbonyl ELISAs, it was known that streptavidin-HRP did not bind non-specifically to AGE-modified proteins. The results of this updated assay are in Figure 3.4.7.2. Interestingly, C1q binding to HEL GA 3 h was enhanced compared to HEL 3 h. However the removal of RC groups by reduction decreased C1q binding, as indicated by the decreased signal with the HEL GA-PR 3 h sample. Therefore, this effect seemed to be dependent on the RC groups in the samples. Furthermore, GLUC modification appeared to decrease C1q recognition of the HEL sample. These experiments therefore confirmed the previously published results and found a GA 3 h specific signature which could reasonably lead to enhanced antibody responses.

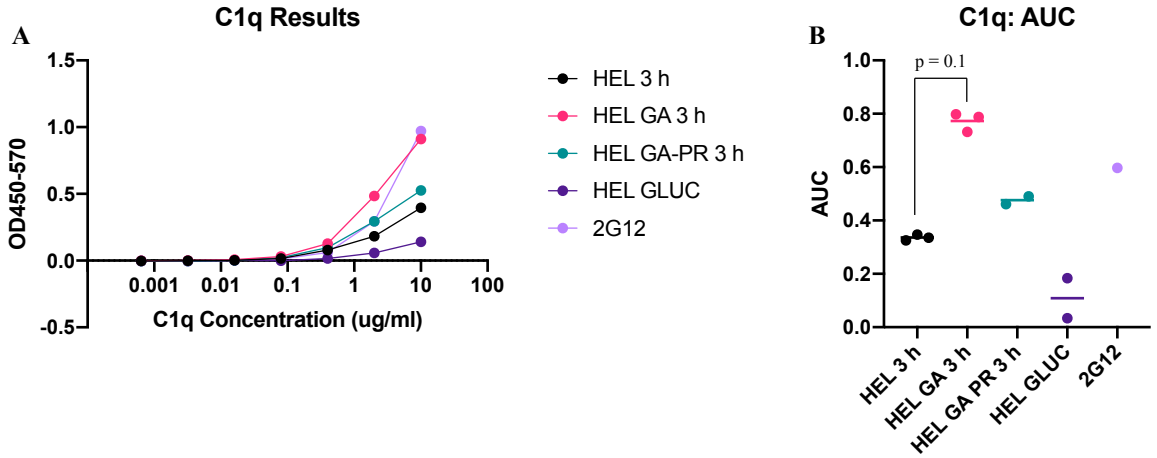

Figure 3.4.7.2: Plates were coated with the indicated protein sample and probed with the biotinylated-C1q, again 2G12 has been included as a positive control. A gives the resultant C1q curve, each line indicates the mean of 3 (3 h and GA 3 h) or 2 (GA-PR 3 h and GLUC) samples. 2G12 was included as a positive control and was run in singlet. The results are representative of two independent experiments. B shows the AUC results, each dot represents an individual sample and the bar indicates average. The difference between the 3 hr and GA 3 h samples was assessed by a two-tailed Mann-Whitney test, the p value is indicated. AUC = area under the curve.

The other complement assays developed were designed to measure the formation of C3 products. As all complement pathways result in the formation of a C3 convertase (Sarma and Ward 2011), this would allow one to assess whether any pathways were initiated in response to AGE-modified proteins. For this, antibodies recognising human C3b and mouse

C3d were obtained. For these experiments, modified proteins were coated onto plates, blocked and then incubated with sera at 37 °C. Formation of the indicated product was then tested using the above antibodies followed by an appropriate secondary. Initial studies using positive control stimuli (oxLDL or 2G12) demonstrated that it was possible to see formation of these products using this method (Figure 3.4.7.3.A and D).

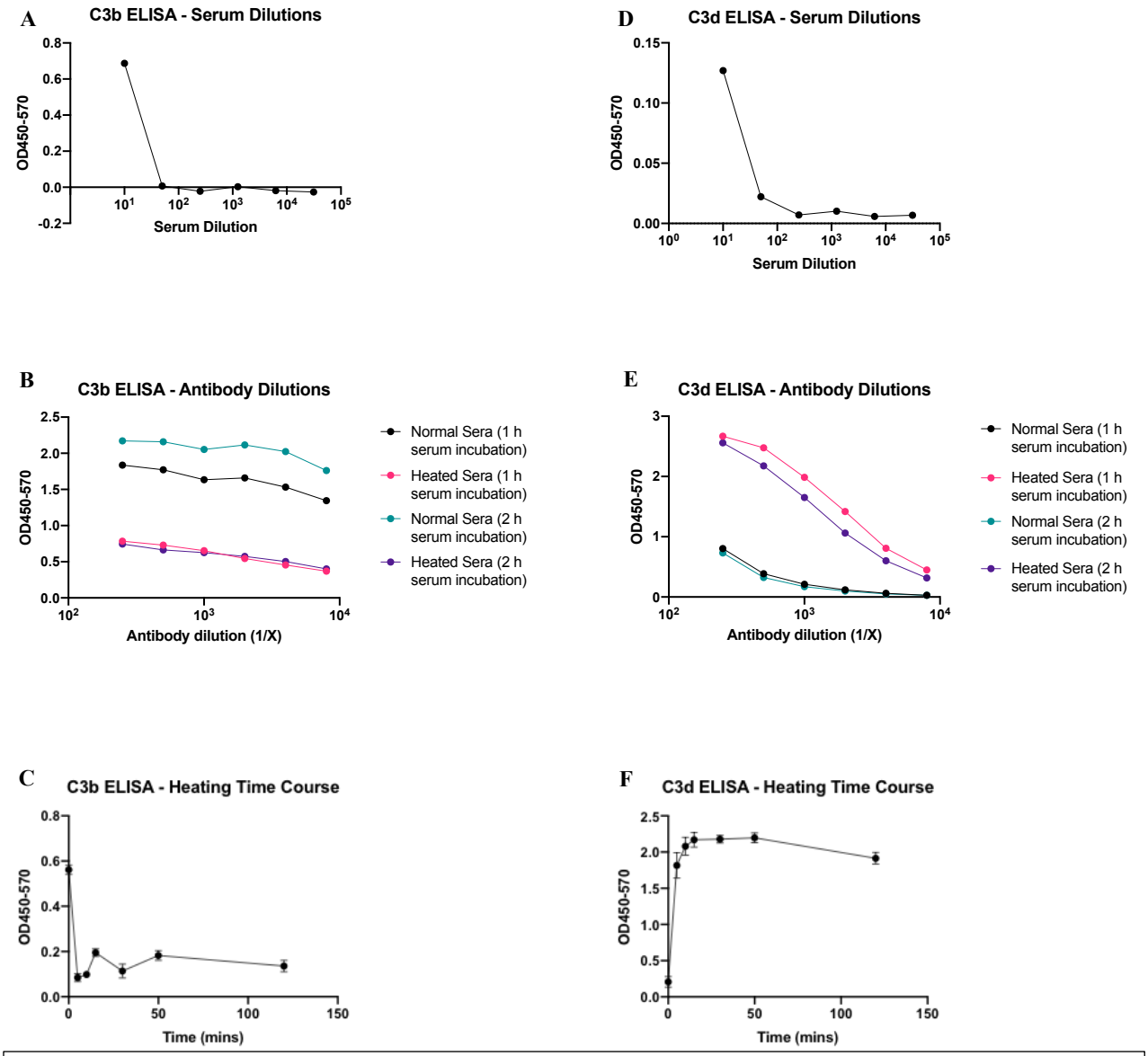

Figure 3.4.7.3: Plates were coated with known activators of the complement system (oxLDL in A-C and 2G12 in D-F) and then incubated at 37 °C with human (A-C) or mouse (D-F) sera for 1-2 hr followed by an anti-human C3b antibody or anti-mouse C3d antibody. A and D show the initial set-up experiment, demonstrating complement activation could be observed with this system. In B and E normal and heated serum were compared. Heating serum is reported to inactivate complement. However for the anti-mouse C3d ELISA (E), heating increased C3d deposition. To examine this further, human (C) or mouse (F) serum samples were heated for the indicated length of time at 56 °C and then complement activation was assessed. For A, B, D and E each line represents one sample run in singlet, whilst for C and F each dot represents the mean of technical triplicates and the error bars show SD.

To prove that this was complement activation, another experiment was performed that included sera which had been heated to 56 °C for 30 mins, a long-established method for inactivating the complement system (Nesargikar, Spiller, and Chavez 2012). For the C3b ELISA, this reduced the signal (Figure 3.4.7.3.B). However, using heat-inactivated sera in the C3d ELISA resulted in a much higher signal. To investigate this further, a time course experiment was performed where human and mouse serum was heated for various time points between 5 mins and 2 h and then assessed the C3b and C3d deposition in response to positive controls. As can be seen from Figure 3.4.7.3.C heating human sera rapidly decreased the C3b signal. However, heating mouse sera had the opposite effect on C3d deposition which had an increasing curve.

Regardless of the C3d result, the time course experimented indicated that the C3b ELISA at least could detect a specific signal. Therefore, the capacity of the modified proteins to induce complement activation and deposition was then tested. The results are in Figure 3.4.7.4. The mouse serum results are shown in panels E-H. As can been seen, there was enhanced C3d deposition in response to GA-modified samples, and whilst the increase in production with "heat inactivation" seen above remained, GA 3 h modified samples still showed enhanced C3d production under these conditions. In contrast, enhanced C3b deposition with GA 3 h modified samples was not seen with normal human serum. However, increased C3b production was noted with HEL GA 3 h, and to a lesser extent HEL GA-PR 3 h, with heat inactivated serum. The heat inactivation procedure did work as the C3b production in response to the positive control, oxLDL, was lost with heated serum. Therefore, these studies provide evidence for enhanced complement activation and deposition in response to GA 3 h modified samples in mouse serum, but the results for human serum require further investigation.

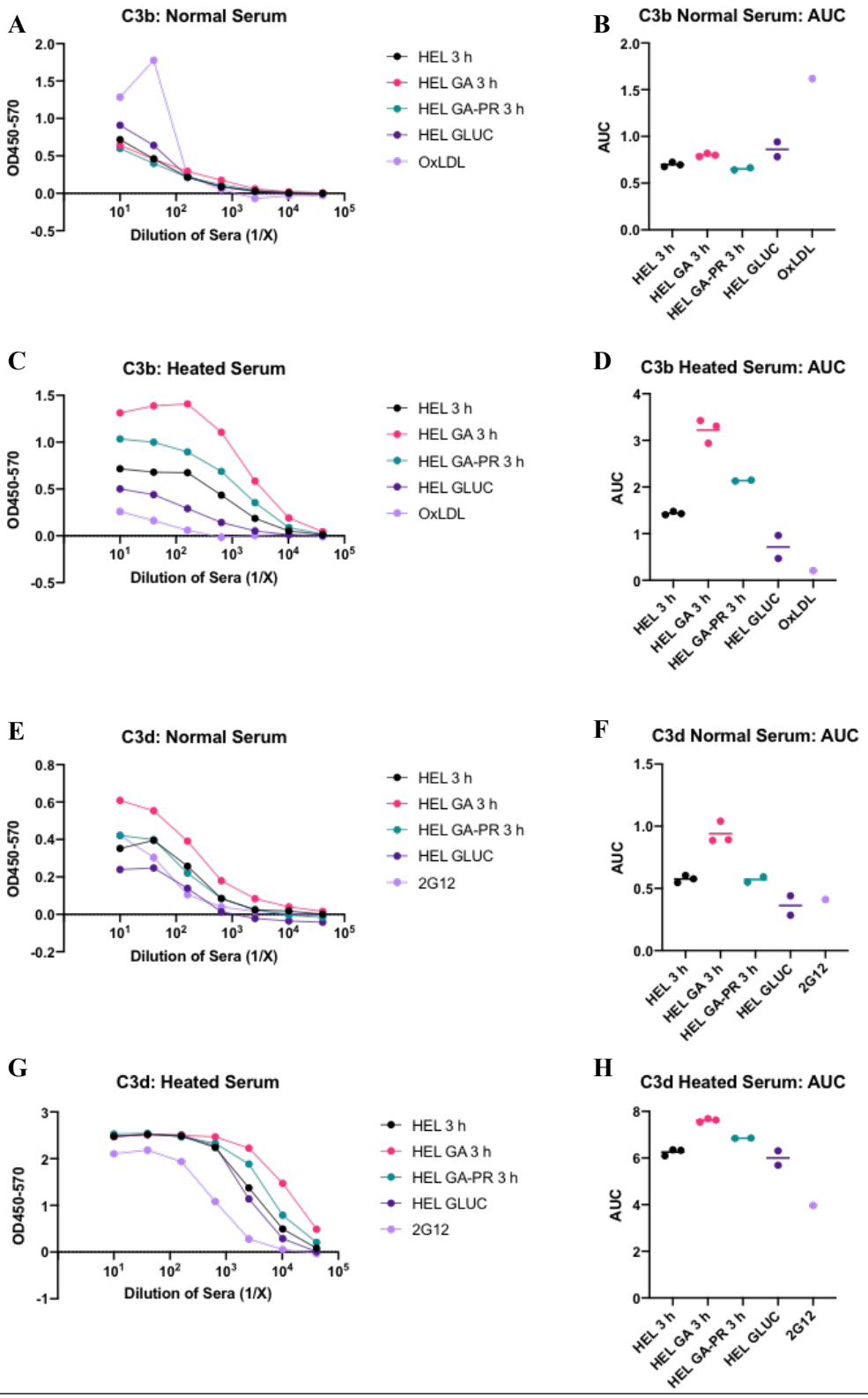

Figure 3.4.7.4: Plates were coated with the indicated protein sample or positive control (oxLDL for human serum, 2G12 for mouse serum) and then incubated with various dilution of normal human (A-D) or naïve mouse serum (E-H) for 2 h at 37 °C, followed by detection with anti-human C3b or anti-mouse C3d antibodies as above. In C, D, G and H heat inactivated serum was used. HEL 3 h and GA 3 h are the results from three separate sample preparations, the GA-PR 3 h and GLUC two separate sample preparations. In B, D, F and H, each dot shows the results of an independent samples with a bar showing the mean. A, C, E and G give dilution curves showing the average response of these samples. The AUC data were analysed by Mann-Whitney test comparing HEL 3 h and HEL GA 3 h, p = 0.1 in all cases. Graphs A and E are representative of two independent experiments.

3.4.8 AGE-modified Proteins Bind Natural Antibodies

Finally, the capacity of mouse and human IgM and IgG to bind to modified proteins was investigated. As mentioned in the introduction, IgM is another activator of complement which has been reported to bind to modified proteins with an electronegative charge (Uchida 2014). To determine whether natural IgM antibodies present in naïve sera could bind to the modified proteins, plates were coated with the different samples, incubated with normal human or naïve mouse serum, then IgM binding was examined with anti-IgM human or mouse antibodies (Figure 3.4.8.1). For both mouse and human IgM the same pattern is seen with the signal increasing from HEL GLUC, HEL 3 h, HEL GA-PR 3 h to HEL GA 3 h. The actual difference in binding between HEL 3 h and HEL GA 3 h is rather modest, but it

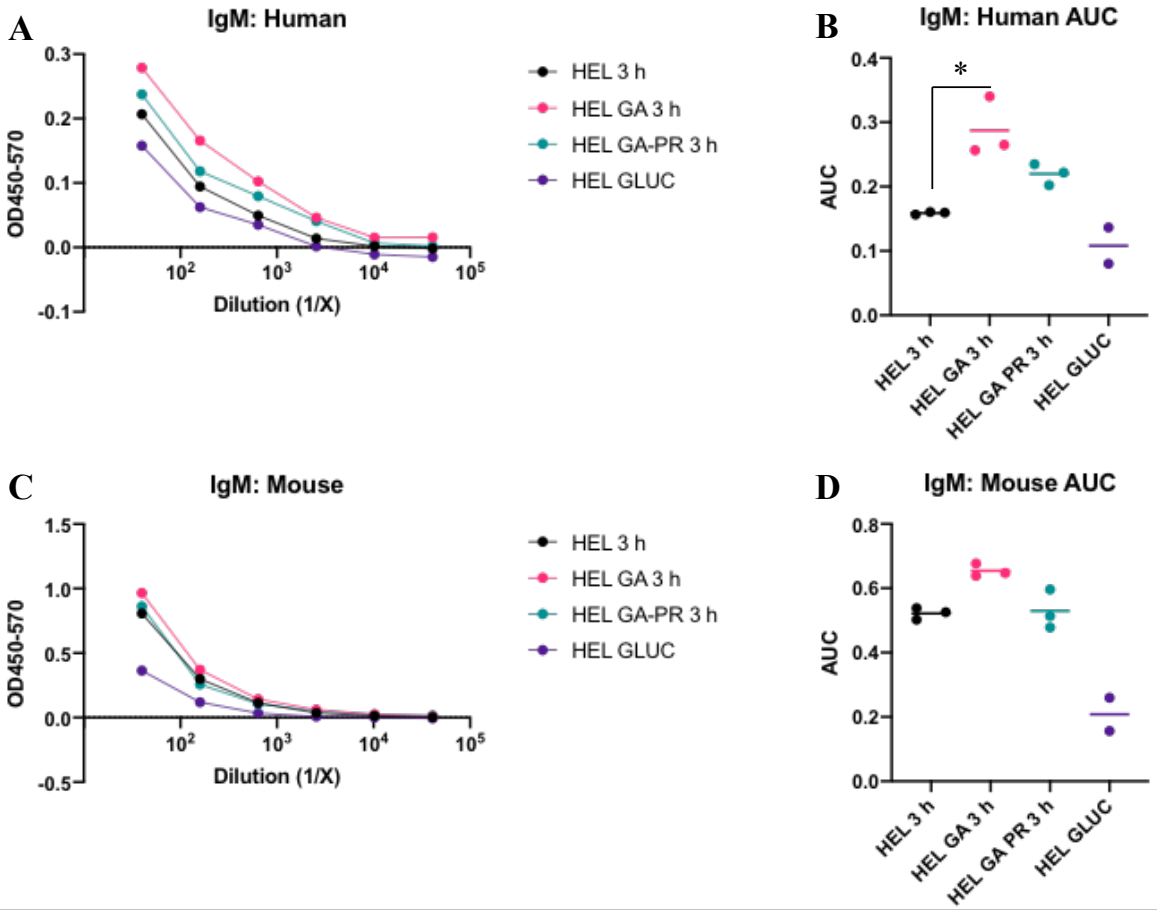

Figure 3.4.8.1: Plates were coated with the indicated protein sample and then incubated with various dilutions of normal human or naïve mouse serum. This was followed by detection with anti-human IgM or anti-mouse IgM to determine if IgM antibodies present in normal sera could recognise the modified proteins. The results of the dilutions is shown in A and C, whilst AUC for individual samples are shown in B and D. For B and D, each dot shows the results of an individual sample, with a bar showing mean. In A to C the average of these samples is shown. The results for HEL 3 h, HEL GA 3 h and HEL GA-PR 3 h were analysed by Kruskal-Wallis followed by Dunn's multiple comparison test, * = $p \leq 0.05$.

is significant for human IgM. This suggests there are natural antibodies present in the sera which bind to GA-modified proteins.

The same procedure was done to examine IgG binding using anti-IgG antibodies (Figure 3.4.8.2). This was investigated as the C1q experiments demonstrated that the anti-C1q mAb (which is a mouse IgG2b) could bind non-specifically to the GA 3 h sample and the author wanted to determine if this might also be true for other IgG antibodies. The results for human IgG are similar to the human and mouse IgM results, with stronger binding seen with HEL GA 3 h. This indicates that there are IgG antibodies present in human sera which bind to GA-modified proteins. These could be natural antibodies which bind to oxidatively modified proteins, or non-specific binding of other IgG antibodies raised against different stimuli.

The results for mouse IgG are slightly different (Figure 3.4.8.2.C and D). As can be seen, the signal increases with decreasing concentrations of sera. Indeed, incubation with no sera gave a strong signal in the ELISA (Figure 3.4.8.1.E). These results indicate recognition of the modified samples by the anti-mouse IgG secondary. The increasing signal seen with decreasing sera concentration likely indicates that non-IgG molecules present in sera compete with the anti-mouse IgG for binding to the modified samples. Once again, this secondary antibody shows preferential binding to the HEL GA 3 h sample, and this is decreased when RCs are removed by reduction.

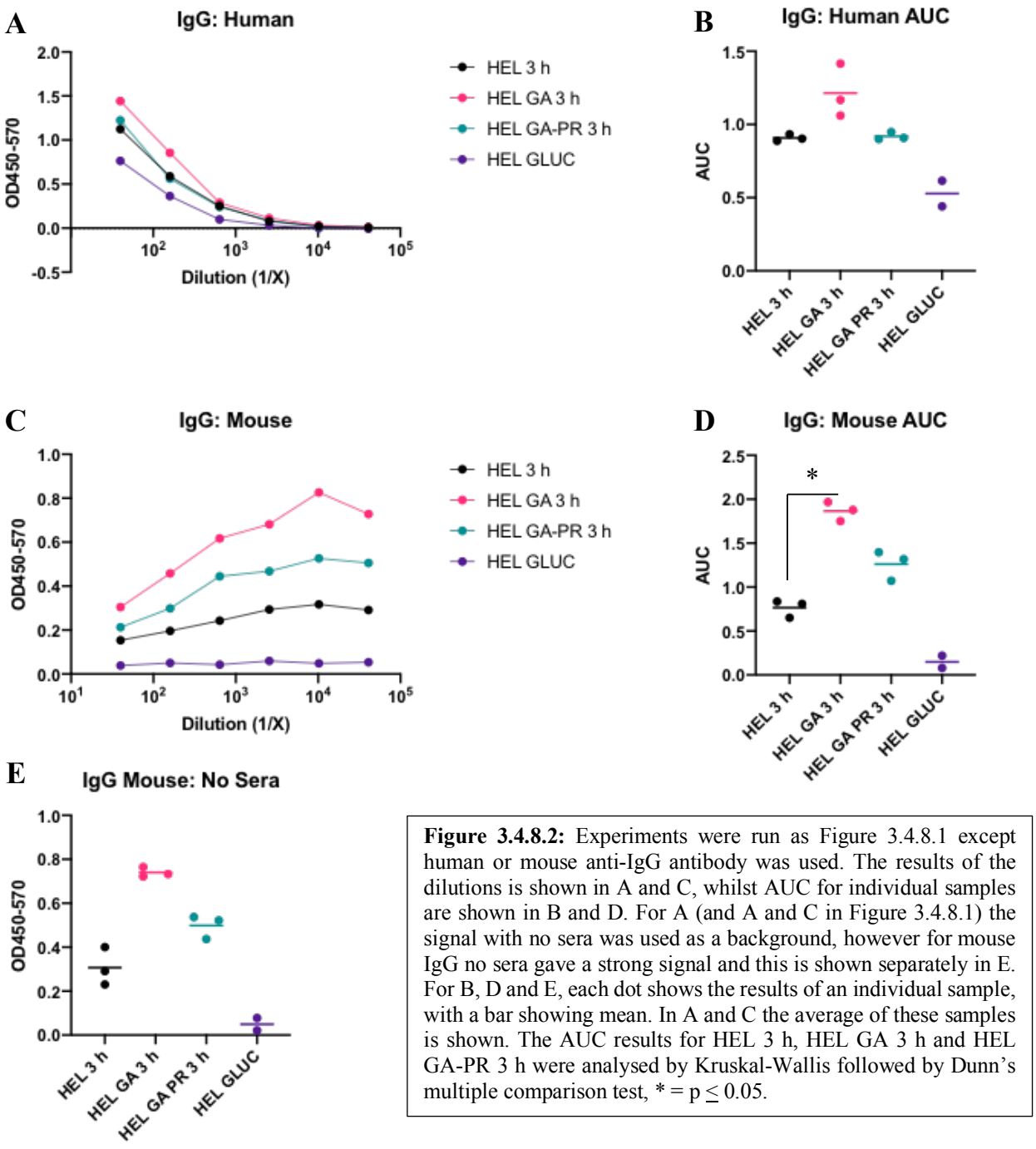

Figure 3.4.8.2: Experiments were run as Figure 3.4.8.1 except human or mouse anti-IgG antibody was used. The results of the dilutions is shown in A and C, whilst AUC for individual samples are shown in B and D. For A (and A and C in Figure 3.4.8.1) the signal with no sera was used as a background, however for mouse IgG no sera gave a strong signal and this is shown separately in E. For B, D and E, each dot shows the results of an individual sample, with a bar showing mean. In A and C the average of these samples is shown. The AUC results for HEL 3 h, HEL GA 3 h and HEL GA-PR 3 h were analysed by Kruskal-Wallis followed by Dunn's multiple comparison test, * = $p \leq 0.05$.

3.5 Discussion and Conclusions

To summarise, the results in this chapter show that, in the absence of exogenous adjuvant, GA-modified samples were the most immunogenic of the AGE-modified proteins tested based on the capacity of these samples to induce anti-HEL antibody responses. After a single s.c. immunisation, strong antigen-specific IgG responses were seen in two-thirds of the BALB/c mice and all of the CBA mice immunised with HEL GA 3 h samples. In contrast, no detectable antigen-specific IgG responses were seen in mice immunised with other modified samples. Moreover, this appeared to be an RC-mediated effect as the capacity to induce these antibody responses was lost when the samples were reduced. This fits with previous research which identified RCs as a Th2 inducing DAMP (Moghaddam et al. 2011). However, using this immunisation protocol, none of the AGE-modified samples induced significant T cell immune responses. Therefore, there seemed to be a disconnect between the T and B cell responses.

One possibility is that the antibody responses may be T cell-independent. As discussed in the introduction, antibody responses can be classified as T cell-independent or T cell-dependent. The former involves specialised B cells found in the peritoneal cavity (B1 cells) or the marginal zone of the spleen (marginal zone B cells) (Hoffman, Lakkis, and Chalasani 2016). T cell-independent responses are rapid, often target carbohydrates and are usually IgM. In contrast, in T cell-dependent responses B cells differentiate into antibody producing plasma cells in the germinal centre reaction. The responses therefore take longer to develop, but result in high affinity antibodies which have undergone isotype switching (Bonilla and Oettgen 2010). The antibodies seen in this study were IgG1 and IgG2a, which would suggest that the responses are T cell-dependent, although this does not provide definitive proof as it is possible for T cell-independent B cell responses to produce isotype switched antibodies (Liao et al. 2017). However, additional immunisation studies performed by Mrs Lu Li

Jovanoska provide further evidence that the antibody response seen to HEL GA 3 h was T cell-dependent as anti-HEL antibodies took more than a week to develop and did not reach a peak until four weeks after the initial immunisation. In contrast, T cell-independent B cell responses would be expected to produce antibody rapidly, within a few days (Hoffman, Lakkis, and Chalasani 2016). However, to confirm that the responses are T cell-dependent, immunisation experiments could be done in TCR KO mice (Liao et al. 2017).

Alternatively, it is possible that a single immunisation was not sufficient to stimulate a T cell response which was detectable using this assay as the number of HEL responsive T cells in the spleen was too low. One option would have been to isolate T cells from spleens to increase the frequency of responsive T cells. However, this is a more labour intensive procedure which, due to the size of these experiments, would have been practically very difficult. Another option would have been to include boosts in the immunisation schedule, this would be expected to increase the frequency of HEL responsive T cells (Schunk and Macallum 2005). However, immunisation experiments from another member of the group (Mrs Lu Li Jovanoska), in which mice received a prime and a boost, also failed to induce significant T cell responses. One possibility, is that the HEL specific T cell responses were located predominantly in the draining lymph node (LN), therefore analysis of splenocytes would not reveal whether T cell responses had developed. This has been reported in another immunisation model were significant B cell proliferation could be detected in both the spleen and LNs, whereas T cell proliferation responses were primarily detected in the LNs (Andersen et al. 2019).

With regard to the mechanism by which GA-modified proteins could induce adaptive immune responses, in this study, there was no evidence of classical DC maturation in response to AGE-modified proteins, either in the presence of mouse serum or FBS. This is in line with other previous studies examining activation of murine DCs by AGE-modified

proteins (Heilmann et al. 2014; Ilchmann et al. 2010; Moghaddam et al. 2011), but contrasts with others which have demonstrated upregulation of costimulatory molecules, secretion of inflammatory cytokines and activation of signalling molecules such as NF-κB (Hilmenyuk et al. 2010; Buttari et al. 2011; Ge et al. 2005). These latter studies were done using DCs derived from human peripheral blood monocytes, therefore one possible explanation is that mice and humans respond differently to AGE-modified proteins. However, other studies using human DCs have reported that AGEs have an inhibitory effect on DC maturation (Price et al. 2004). These DCs were directly isolated from the blood so another possibility is that different DC populations have variable responses.

In this study, GM-CSF/IL-4 BMDCs were used. This is a well-established system that has been used for the last three decades and allows for the rapid generation of high numbers of DCs (Inaba et al. 1992; Lutz et al. 1999; Son et al. 2002) A major drawback is that other cell types, namely macrophages and granulocytes, are also produced in response to GM-CSF (Inaba et al. 1992). To improve purity, these cells have been separated by their adherent properties and expression of CD11c (Lutz et al. 1999; Helft et al. 2015). However, it has been shown that even the CD11c+MHC II+ population in BMDC cultures consists of DC-like and macrophage-like subpopulations (Helft et al. 2015). These cells have similar adherence properties but are derived from different progenitors and have distinct functional properties. Moreover, another major question is how the BMDCs relate to their *in vivo* counterparts. In Helft et al, the authors attempted to determine the equivalent *in vivo* identity of the BMDC cells by comparing RNA expression between their sorted cells and DC isolated from various tissues in the ImmGen database (Helft et al. 2015). The DC-like cells were found to be most closely related to migratory DCs, whilst the macrophage-like cells did not have an *in vivo* equivalent. Overall, when interpreting the results reported here, it is important to acknowledge that they will represent the responses of a variety of cell types

within the BMDC cultures. This does not mean the results are completely irrelevant as within a given tissue AGE-modified proteins will potentially interact with many tissue resident immune cells, including both macrophages and DCs. Whether they will be reflective of the response of a tissue-resident DC is a more challenging question to address. One option would have been to isolate primary DCs, for example from the spleen. These cells may have been more representative of DCs *in vivo* but the isolation process can activate the cells and this may affect the response (Schlecht et al. 2006). Moreover, as the initial studies with the BMDCs had not been very fruitful, it is hard to justify the use of the much higher number of mice that isolation of splenic DCs would require.

Although there was no upregulation in costimulatory molecules or inflammatory cytokines in response to modified proteins, the RNAseq data did indicate that there were some changes to DC biology. There were 24 genes which showed significantly different expression between HEL GLUC and HEL pulsed DCs and pathway analysis showed these clustered into either cell proliferation or cell-adhesions pathways. As these are functions known to be regulated by the AGE-receptor Galectin-3 (Pricci et al. 2000), it is tempting to speculate that these changes might be mediated through this receptor. Moreover, ligands for Galectin-3 are reported not to directly activate BMDCs or modulate their responses to TLR agonists, which would fit with the general lack of activation seen in this study (Breuilh et al. 2007). Nevertheless, DCs lacking this receptor induce stronger T cell responses in *in vitro* priming experiments, indicating Galectin-3 induces other changes in DC behaviour. However, overall the expression changes seen are very minor and it is unclear whether they would be sufficient to produce a biologically significant effect. Certainly in the immunisation studies these did not translate to a significantly increased adaptive immune response in the HEL GLUC immunised mice.

Experiments to examine AGE-induced changes to cytokine secretion indicated that at least HEL GA 3 h and GA-PR 3 h modified proteins could suppress the release of inflammatory cytokines such as CXCL2 and induce secretion, albeit modestly, of some other factors such as HGF and FABP4. However, further experiments showed that these changes were not statistically significant, except for HEL GA-PR 3 h which induced significant secretion of HGF and FABP4. Moreover, these findings are unlikely to be of relevance to the AGE-enhanced immunogenicity HEL GA-PR 3 h which did not induce strong antibody responses in mice However, these findings might be of relevance in other conditions in which AGE-modified/carbonylated proteins are found. For example the HGF-cMET pathway is dysregulated in many types of cancer where it is reported to contribute to metastasis (K.-H. Kim and Kim 2017). Moreover, the metabolism of cancer cells promotes AGE and dicarbonyl formation and these have been suggested to contribute to tumour formation and progression (Lin et al. 2016). A link between these two pathways may therefore be of interest in this context.

The last point of interest with regard to DCs is that there were significant changes to DC responses depending on the sera the cells were cultured in during incubation with AGEs. For example, culturing DCs in normal or heated mouse serum seemed to suppress their response to LPS as the concentration of CCL3 and TNFα was reduced in the supernatant compared to DCs in FBS. Given that there were also changes in the overall cell size and granularity, one possibility is that there are factors in the mouse serum which act directly on DCs and suppress their responses, either in a specific manner or by causing general damage to the DCs. Alternatively, FBS may contain factors which promote the development of inflammatory responses in mouse cells. This has been suggested before in studies where macrophage activation in response to PMA was compared when cells were cultured in mouse serum or FBS (Grace, Guthrie, and Johnston 1988). The authors found that in FBS

the macrophages had higher responses, although this was suggested to be the result of LPS contamination in commercial preparations which appeared to be a significant problem at the time. The FBS used in cell culture medium in this thesis is reported to have endotoxin contamination of ≤ 10 EU/ml (1-2 ng/ml), as LPS can stimulate responses from murine cells at very low (pg/ml) concentrations (Tynan et al. 2012), this may explain the effect. Lastly, it is also possible the mouse serum components may interact with and degrade the inflammatory mediators.

The next mechanism considered was whether GA-modified proteins could directly activate B cells. To investigate this MD4 mice, which are transgenic for a BCR specific for HEL, were used (Goodnow et al. 1988). However, there was no evidence of B cell proliferation in cultures of splenocytes from these mice exposed to different modified HEL samples. As this system uses heat-treated FBS, it does not allow us to assess the effects of complement activation on B cell responses to AGE-modified proteins. In the studies of Chikazawa et al. both C1q and IgM, activators of the classical complement pathway, bound to AGE-modified proteins and in turn these proteins have been shown to activate the complement cascade. Of particular interest, is that in these studies modified proteins were created by incubating proteins with dicarbonyl compounds for 7 days, including GA (Chikazawa et al. 2013, 2016). Therefore, this may be similar to the HEL GA 7 day compound used here, which the ELISA results show have RCs, although to a lesser extent than the 3 h sample. It has long been established that complement activation can act as natural adjuvant for B cells (Dunkelberger and Song 2010). For example, in Dempsey et al. the addition of two to three C3d molecules to HEL in recombinant fusion proteins was found to significantly enhance the development of anti-HEL antibody responses. Indeed three C3d molecules were more effective than the powerful adjuvant Freunds in inducing anti-HEL antibodies (Dempsey et al. 1996). This therefore seemed like a promising lead to follow, however it was not possible

to assess the capacity of complement to activate B cells in the *in vitro* system due to the inhibitory effects of mouse serum on lymphocyte proliferation.

Instead, ELISA-based complement binding and activation studies were designed to investigate previous work showing complement activation in response to AGE-modified protein. Furthermore, the capacity of the more minimally-modified 3 h GA samples to activate complement had not previously been examined and therefore needed investigating. The results demonstrated enhanced C1q binding to HEL GA 3 h and subsequent complement activation, at least with the mouse serum. Of note, the pattern of C1q binding/C3d production mirrored the *in vivo* immunisation results as the GA 3 h samples showed both strong C1q binding and significant antibody responses, whilst post-reduction decreased both the C1q binding and antibody response. These results provide some circumstantial evidence supporting the hypothesis that complement activation is responsible for the enhanced immunogenicity of GA-modified proteins. Unfortunately, limited laboratory access as a result of COVID-19 meant that the author was only able to do a small number of assays examining complement activation. Future experiments with this assay would aim to expand the number and type of samples tested, including HEL GA 7 days for example, allowing for properly powered statistical testing.

An unanswered question is why heating serum resulted in greater C3d deposition with all of the proteins tested so far and greater C3b deposition with the HEL GA 3 h and GA-PR 3 h samples. For well over 100 years, complement has been defined as a heat labile component of serum and the inactivation method used in this chapter is well-established and used in commercial preparations (Nesargikar, Spiller, and Chavez 2012). These results were therefore puzzling. However, there are reports in the literature showing that pre-heating serum enhances the antibody-based detection of most complement components, a phenomenon the authors suggest is due to partial denaturation exposing epitopes or release

of complement components from complexes (Hamsten et al. 2015). Whilst this study examined the presence of specific components rather than activation of the complement cascade, it is possible their findings and the results reported here may have similar causes. Examining the nature of the complement components binding the modified proteins in heated serum with MS may provide answers.

The results of the natural antibody binding ELISAs also demonstrated non-specific binding to HEL GA 3 h samples with two of the antibodies so far used in testing, the anti-C1q and anti-mouse IgG. The anti-mouse IgG results were particularly interesting in this regard as the binding of anti-mouse IgG to HEL GA 3 h could be inhibited by serum. This implies the existence of factors in the serum which compete with anti-mouse IgG for binding to HEL-GA 3 h. These may include C1q, however this could be further probed using co-immunoprecipitation studies to examine whether there are other binding proteins for HEL GA 3 h in serum and if so, whether this may also contribute to the observed enhanced immunogenicity seen with this modification.

To summarise, HEL samples modified with GA can induce the formation of significant antibody responses, whilst other AGE-modified forms of HEL cannot. None of the experiments indicated that GA-modified HEL or other AGE-modified samples could induce maturation of GM-CSF mBMDCs. Moreover, GA-modified samples could not induce activation of HEL specific B cells *in vitro.* However, GA-modified proteins could induce activation of complement and bind to natural antibodies. These results of this chapter therefore support a model in which complement components, specifically C3d, are deposited on the GA-modified HEL. This C3d can then bind CD21 receptors on HEL-specific B cells, resulting in B cell activation and antibody production.

Chapter 4: The Contribution of the Scavenger Receptors SR-A and MARCO to AGE-mediated Immunogenicity

4.0 Abstract

Scavenger receptors (SR) are a broad family of endocytic receptors defined by their capacity to bind and internalise a range of polyanionic ligands including AGEs. DC uptake of AGE-modified proteins via SRs, in particular scavenger receptor A (SR-A), has been suggested to enhance the immunogenicity of proteins due to increased T cell presentation. In this study the uptake of a range of AGE-modified proteins was assessed in murine bone marrow derived DCs (mBMDCs) lacking SR-A and/or MARCO (macrophage receptor with collagenous structure). *In vivo* immunogenicity of hen egg lysozyme (HEL) samples modified with glycolaldehyde (GA) or glucose was then examined in these strains and wildtype (WT) controls. The results show that glucose-modified samples had significantly greater uptake compared to unmodified controls. Uptake of the modified proteins was not affected by loss of either receptor. Moreover, the generation of immune responses in the knockout (KO) mice remained intact, and in fact appeared to be enhanced in mice lacking SR-A. To conclude, SR-A and MARCO are dispensable for DC uptake of AGE-modified proteins and instead may act to inhibit the development of immune responses to these proteins *in vivo.*

4.1 Introduction

4.1.1 The Scavenger Receptor Family

The existence of "scavenger receptors" was first proposed by Goldstein and Brown in 1979 who identified the presence of a binding site on macrophages capable of recognising and internalising modified forms of low density lipoprotein (LDL) and other negatively charged molecules (Goldstein et al. 1979). Approximately 10 years later, the first SRs were identified and were later named SR-AI and SR-AII (Kodama et al. 1990). These are splice variants of the same gene and although slight variations in the binding capacity of the two proteins have been reported (Peiser et al. 2000), their overall ligand binding behaviour is very similar. An additional splice variant can also be produced (SR-AIII), however this is non-functional and remains trapped in the endoplasmic reticulum (Plüddemann, Neyen, and Gordon 2007).

Today, SRs form an ever expanding family with over 20 members spread across 10 different classes (PrabhuDas et al. 2014). At first glance, these receptors show little family resemblance as structure varies widely between the different classes. For example class A family members (which includes SR-AI, SR-AII and MARCO) are defined by their collagenous domains, whilst the lone member of class J belongs to the immunoglobin gene superfamily (Zani et al. 2015). The structures of the SRs relevant to this Chapter, SR-AI/II and MARCO, are shown in Figure 4.1.1. The feature which unifies this mismatched family is the capacity of each member to bind to a broad range of polyanionic ligands (Plüddemann, Neyen, and Gordon 2007). This recognition is then followed by internalisation and degradation of the bound ligand and in some cases the initiation of signalling cascades (PrabhuDas et al. 2014). The majority of SRs are expressed predominantly or exclusively by myeloid cells, particularly macrophages (Plüddemann, Neyen, and Gordon 2007). These receptors allow macrophages to phagocytose both non-self (e.g. gram positive and negative bacteria) and altered-self (e.g. oxidised LDL (oxLDL)) ligands (PrabhuDas et al. 2014).

Thus, SRs are an important class of PRRs used by the immune system to sense and respond to both foreign invaders and tissue damage.

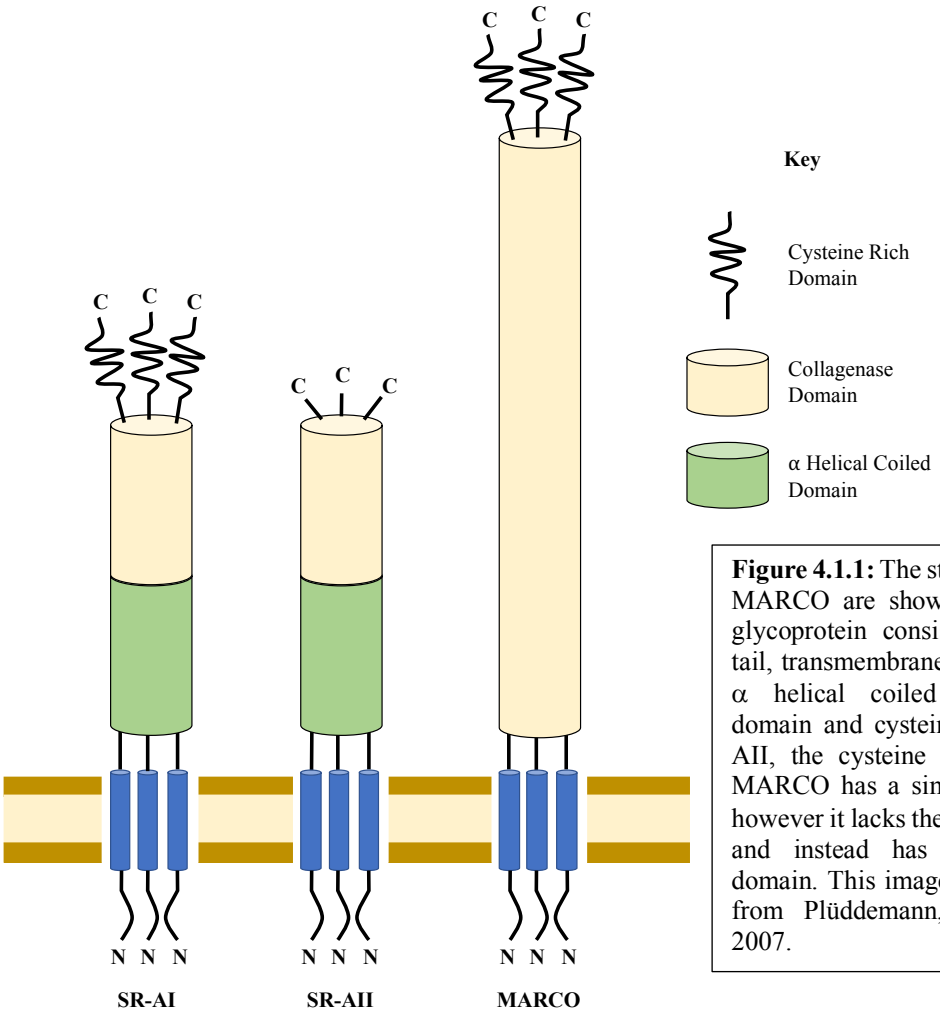

Figure 4.1.1: The structures of SR-AI/II and MARCO are shown. SR-AI is a trimeric glycoprotein consisting of a cytoplasmic tail, transmembrane domain, spacer region, α helical coiled domain, collagenous domain and cysteine rich domain. In SR-AII, the cysteine rich domain is absent. MARCO has a similar structure to SR-A, however it lacks the α helical coiled domain and instead has a longer collagenase domain. This image was based on a figure from Plüddemann, Neyen, and Gordon 2007.

4.1.2 SRs Which Bind AGEs

One form of protein damage recognised by SRs is the addition of AGEs. The capacity of SRs to bind to AGE-modified proteins was initially demonstrated in 1995 in a study from Horiuchi and colleagues (Araki et al. 1995). AGEs are negatively charged and this is a feature shared with other known SR-A ligands such as oxLDL. Thus, this group reasoned that AGEs may also bind to SR-A. To test this hypothesis they took Chinese hamster ovary (CHO) cells overexpressing SR-AII and tested their capacity to internalise AGE-modified bovine serum albumin (BSA). Only the cells expressing SR-A were capable of endocytosing

and degrading AGE-BSA and this uptake could be inhibited by acetylated LDL (acLDL), a model form of modified LDL. Subsequent studies using the same system demonstrated that AGE-modified proteins could also bind to the SRs CD36, SR-BI, LOX-1 and FEEL-1/FEEL-2 ((Tamura et al. 2003; Ohgami et al. 2001; Jono et al. 2002; Ohgami et al. 2003). The generation of mice lacking the gene encoding SR-AI/II allowed for this phenomenon to be investigated in more physiologically relevant systems. AGE/ALE uptake is significantly reduced in both peritoneal macrophages and bone marrow derived macrophages (BMDM) from SR-A KO mice compared to WT controls (Warnecke et al. 2017; Suzuki et al. 1997). However, questions remain as to how all the different AGE-binding SRs co-operate *in vivo* and whether certain members have dominant roles in recognition and clearance of AGE-modified proteins. Certainly, in the past, roles for SRs demonstrated *in vitro* have not always translated *in vivo*. For example, SR-A was the first SR identified to clear apoptotic cells, however, SR-A KO mice do not have a significant defect in their capacity for apoptotic cell clearance (Plüddemann, Neyen, and Gordon 2007). This is likely to be a reflection of the high degree of redundancy in the SR family which makes pinning down precise roles for each receptor very challenging. Nevertheless, AGE-modified protein uptake by SRs remains an important area of research as both SRs and AGEs are linked to many chronic diseases, such as atherosclerosis and Alzheimer's disease (Ramasamy et al. 2005; PrabhuDas et al. 2014). Therefore understanding the relationship between them could help us gain an insight into the pathogenesis of these conditions. This includes whether SRs are involved in the altered immunogenicity of AGE-modified proteins.

4.1.3 DCs and SRs: SR-A

Whilst initial studies focused on the expression and function of SR-A in macrophages, work in the mid-2000s demonstrated that SR-A is expressed by GM-CSF derived BMDCs and

also specific populations of DCs in the spleen (Becker et al. 2006; Amiel et al. 2007). These studies demonstrated that SR-A is involved in endocytosis of *E. coli* and acLDL by DCs (Becker et al. 2006; Amiel et al. 2007) and work from Toda and colleagues has extended this to AGE-modified proteins (Heilmann et al. 2014; Ilchmann et al. 2010; Hilmenyuk et al. 2010). In these studies, mBMDCs derived from WT or SR-A KO mice were incubated with FITC-conjugated native or AGE-modified ovalbumin (OVA). The AGE-OVA had enhanced DC uptake compared to native protein. However, AGE-OVA uptake was reduced in BMDCs lacking SR-A compared to the WT controls, indicating that uptake is mediated by this receptor (Heilmann et al. 2014; Ilchmann et al. 2010). Further work from the same group showed that uptake of AGE-modified proteins was also enhanced in human monocyte-derived DCs and this uptake was decreased when the cells were preincubated with a generic SR blocker. However, as this compound blocks multiple SRs, it is not possible to determine whether this uptake was SR-A mediated (Hilmenyuk et al. 2010; Peiser et al. 2000). The authors of these studies have suggested that uptake of AGE-modified protein through SR-A leads to increased MHC II presentation and consequently enhanced CD4 T cell responses. This has been previously demonstrated in work which showed a nonredundant role for SR-A in uptake and presentation of modified protein to T cells (Nicoletti et al. 1999). Therefore, this is one mechanism by which AGE-modification could enhance protein immunogenicity.

Additionally, SR-A has been shown to regulate the maturation of DCs. Studies using splenic DCs and BMDCs have demonstrated that LPS-stimulated SR-A KO DCs have higher expression of costimulatory molecules and cytokine secretion compared to WT controls (Becker et al. 2006; Yi et al. 2009). In further work examining the development of anti-tumour immune responses, SR-A KO and WT DCs pulsed with dying tumour cells were injected into WT mice. The SR-A KO DCs induced stronger immune responses and

subsequently enhanced protection against tumour growth (Guo et al. 2012). Collectively, these data suggests that SR-A acts as an anti-inflammatory clearance receptor which limits the maturation of DCs and subsequently the development of immune responses. This could be through the removal of stimuli, which would otherwise be recognised by other PRRs that could then initiate inflammation Alternatively, binding of ligands to SR-A could initiate anti-inflammatory signalling. Conversely, studies using human peripheral blood and monocyte-derived DCs have suggested that uptake of *Neisseria Meningitidis* and fucoidan through SR-A drives the production of inflammatory cytokines which in turn promote DC maturation (Villwock et al. 2008; Jin et al. 2009). This may represent differences between human and mouse SR-A, between DCs taken from different sources, or in experimental approaches and choice of ligand. However, the human studies have to be interpreted with a certain degree of caution as they include the use of agonists and inhibitors which can bind to receptors other than SR-A (van Weelden et al. 2019; McKenzie et al. 2006). Regardless, the data discussed here leave open the possibility that uptake of AGE-modified proteins through SR-A in fact produces an anti-inflammatory signal which limits the immunogenicity of the protein.

One important study currently missing from the literature which would determine whether AGE-immunogenicity is dependent on SR-A is an immunisation study using SR-A KO mice. As discussed above, SR dependencies do not always translate from *in vitro* to *in vivo*, thus until we have this piece of evidence we cannot know whether the interaction between SR-A on DCs and AGE is unique to this SR or indeed whether this interaction promotes or inhibits the development of immune responses. Furthermore, the DC uptake studies mentioned above have so far been limited to extensively AGE-modified OVA and BSA. The effect on the rate of uptake and dependency on SR-A have not been investigated for more minimally modified proteins such as HEL GA 3 h. This protein was shown to induce

strong antibody responses in Chapter 3 and as previous studies have demonstrated that SR-A is involved in B cell activation (Haasken et al. 2013; Raycroft et al. 2012), it is possible that SR-A is involved in this phenomenon. Therefore, extending the currently published uptake studies and translating these findings *in vivo* are two key studies which would significantly benefit the field.

4.1.4 DCs and SRs: MARCO

Another class A SR reported to have a key role in DC biology is MARCO (McKenzie et al. 2006). In a steady state, MARCO expression in mice is limited to alveolar macrophages, marginal zone macrophages in the spleen and medullary macrophages in LNs (McKenzie et al. 2006). However, studies examining changes in gene expression during DC maturation have demonstrated that MARCO expression is strongly upregulated after exposure to LPS or tumour lysates (Granucci et al. 2003; Grolleau et al. 2003). This result indicates that this receptor may play a key role during inflammatory processes and currently the evidence suggests this may be through regulation of the cytoskeletal changes necessary for DC maturation. Ectopic expression of MARCO in cell lines such as CHO, HeLa and 293 induces substantial changes in cell shape as a result of actin cytoskeleton rearrangement (Pikkarainen, Brännström, and Tryggvason 1999). Similarly, forced expression of MARCO in DC cell lines was sufficient to induce a "mature" morphology, whilst blockade of MARCO expression impeded the development of this morphology (Granucci et al. 2003). How these *in vitro* findings translate *in vivo* is still a matter for investigation. Perhaps somewhat surprisingly, MARCO KO DCs pulsed with tumour lysate are reported to have increased migratory capacity *in vitro* and *in vivo* and this was associated with stronger anti-tumour immune responses and improved survival during tumour challenge (Komine et al.

2013). This would suggest that MARCO, like SR-A, has an anti-inflammatory role in the development of immune responses.

At the time of writing no studies had demonstrated AGE binding to MARCO. Therefore whether MARCO had any role in the development of immune responses to AGE-modified proteins was completely unknown. However, given its relatedness to SR-A and evidence suggesting an important role in DCs, this seemed to be another receptor worth investigating. Moreover, as with SR-A, MARCO has been shown to interact with B cells (McKenzie et al. 2006). Specifically, MARCO expressed on the marginal zone macrophages of the spleen interacts with B cells in the marginal zone, ensuring proper positioning of marginal zone B cells (A-Gonzalez and Castrillo 2018). Therefore, MARCO might also be of relevance to enhanced antibody responses induced by GA-modified proteins.

4.2 Hypothesis and Aims

Hypothesis: That the SRs SR-A and MARCO modulate the immune responses to AGE-modified proteins.

Aims

1. To generate fluorescently labelled AGE-modified proteins for use in *in vitro* BMDC uptake studies.
2. To examine DC uptake of a variety of AGE-modified proteins to confirm or refute previous findings showing enhanced uptake compared to unmodified proteins, and determine whether this also applies to more minimally modified proteins such as HEL GA 3 h.
3. To determine whether any SR-dependent uptake is observed *in vitro* using DCs derived from KO mice.
4. To perform immunisation studies using SR KO mice to determine the contribution of SR-A and MARCO to the enhanced immunogenicity of AGE-modified proteins

4.3 Materials and Methods

The following methods were used in this chapter, for a full description please refer to the indicated subsection of the Materials and Methods chapter.

- Glucose, GA and CML modification (2.2.2-2.2.4)
- SDS-PAGE (2.2.12)
- Fluorescent Labelling (2.2.16)
- Generation of GM-CSF BMDCs (2.3.3)
- *In Vitro* Uptake Studies (2.3.4)
- Flow Cytometry (2.3.6)
- Mouse Origin and Care (2.4.1)
- Subcutaneous (s.c.) Immunisation Protocols (2.4.3)
- Tissue Harvesting (2.4.6)
- IgG, IgG1, IgG2a and IgG2c ELISAs (2.5.1)
- Splenocyte Harvest, Cytokine ELISAs and Thymidine Pulse (2.6.1-2.6.3)
- Statistical Analysis (2.9)

4.4 Results

4.4.1 Generation of Fluorescently-labelled AGE-modified Proteins

Previous studies examining DC uptake of AGE-modified proteins have often used amine based labelling to add a fluorescent tag to the proteins (Heilmann et al. 2014; Hilmenyuk et al. 2010; Ilchmann et al. 2010). The major limitation of this strategy is that these amines are the same ones which are modified by AGEs and so it is not possible to label heavily modified proteins using this method. Instead maleimide-based labelling was used and various experiments were performed to find the optimal time, concentration and desalting method to get the best labelling intensity whilst minimising protein loss (data not shown). The final method is detailed in Materials and Methods section 2.2.16. Representative gels for HEL, OVA and BSA are shown in Figure 4.4.1.1. The images in A, D and G show the intensity of the fluorescent (A488) signal for each protein, only the labelled samples show a signal with this imaging method. B, E and H show a silver stain of the same gel, revealing that the labelled and unlabelled samples have the same band pattern.

In previous studies examining the uptake of labelled AGE-modified protein, samples were only used if the labelling was "comparable" (Heilmann et al. 2014; Ilchmann et al. 2010), a somewhat ambiguous term. In order to assess the similarity of sample labelling in this study, the intensity of the A488 signal for each protein was measured and normalised to the intensity of the silver stain signal. The results are plotted in C, F and I in Figure 4.4.1.1. Both the OVA and BSA samples passed a normality test, whereas the HEL samples required a log transformation in order to conform to a normal distribution. Samples with a labelling intensity which fell within 1 SD of the mean were considered "comparable", whilst any

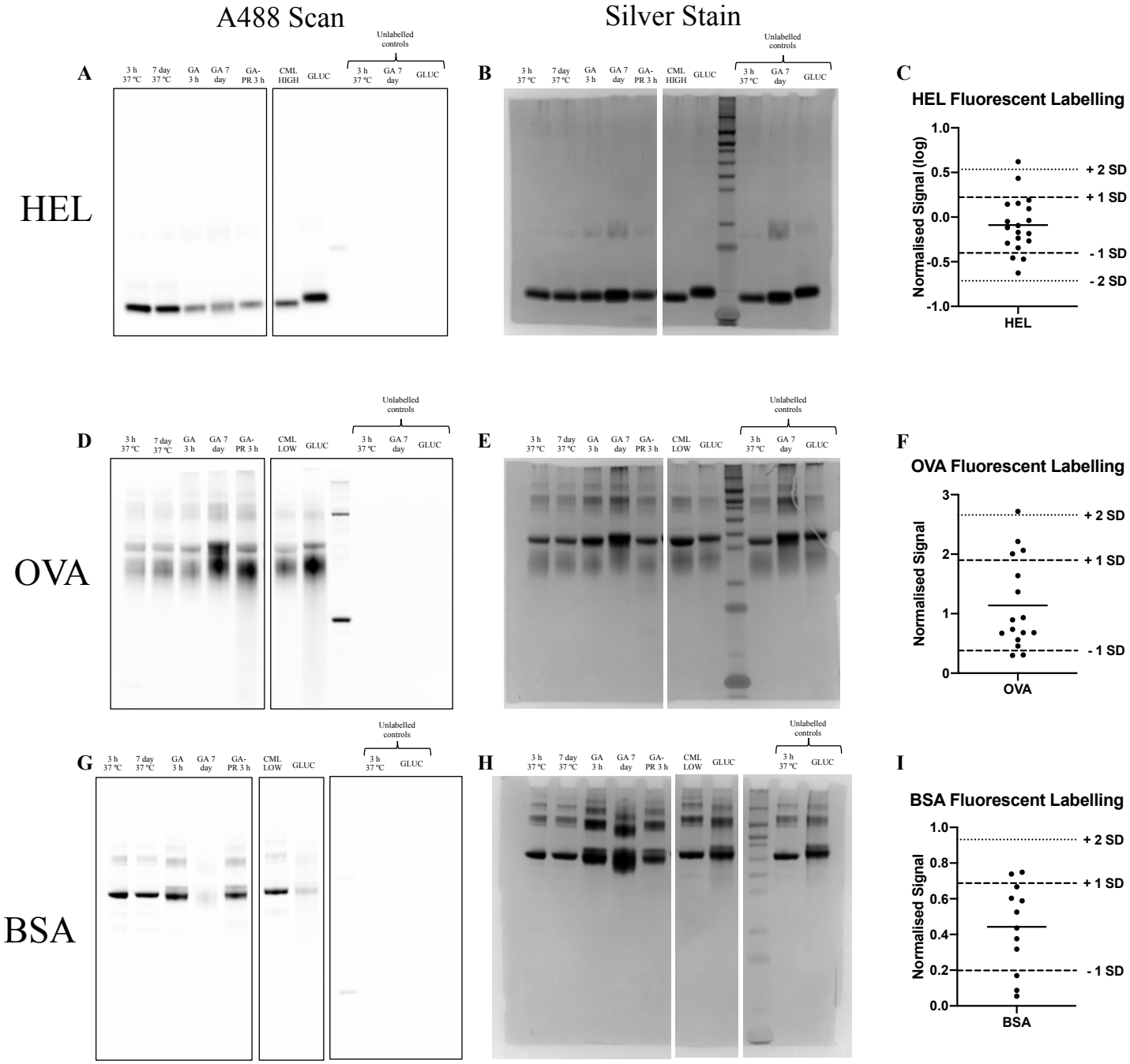

Figure 4.4.1.1: AGE-modified proteins were fluorescently labelled with A488. The fluorescent samples and untagged controls were run on an SDS-PAGE gel. The images in A, D and G were produced using a Bio-Rad Pharos Molecular Imager set to detect A488 and show the intensity of labelling. The gels were then silver stained and the results are shown in D, E and H. The gels also included some samples which were not relevant to this project, in this case the bands have been removed and this is represented by a break in the gel. The A488 scan and the silver stain were used to calculate a normalised fluorescence intensity for each protein (area A488 band/area silver stain band, calculated using ImageJ) and this is plotted in the graphs. To assess whether the labelling was comparable between samples, the mean and standard deviation (SD) of the populations were calculated. Samples with a labelling intensity which was beyond 2 SD were considered incomparable and removed from the analysis. Those with a labelling intensity between 1 SD and 2 SD from the mean have been included but are shown as upward (above) or downward (below) triangles in subsequent graphs. The gels are a representative example of the labelled proteins used whilst the graphs include all samples used in this project. The abbreviations used are: GLUC = glucose modified, GA 3 h/ 7 day = glycolaldehyde modified for 3 h or 7 days, 3 h/ 7 day 37 °C = sample incubated at 37°C for 3 h/ 7 day as a control, GA-PR 3 h = GA 3 h modified sample which has been post-reduced, CML HIGH = modified to add CML for 24 h, CML LOW = modified to add CML for 3 h.

samples which were beyond 2 SDs could not and so these were not used. Samples which fell between 1 and 2 SDs were included in the analysis but as it seemed possible that the intensity of staining could influence the results, these have been signified in subsequent plots. Samples with labelling intensities which are above one SD are labelled with an upwards triangle, whilst those below are labelled with a downturned triangle.

4.4.2 Glucose-modified Samples Have Enhanced DC Uptake

The fluorescently-labelled samples were then used for uptake studies with mBMDCs. The first uptake assay used was a "plate-based" assay in which DCs are first allowed to adhere onto flat-bottomed 96-well plates before the addition of labelled samples for 30 mins. "Uptake" was then assessed by flow cytometry. Since it is not possible to distinguish between surface bound and internalised protein using this method the resultant fluorescent signal will be a product of both. To assess the contribution of SRs to this uptake, DCs were derived from WT, SRMA (SR-A and MARCO DKO) and MARC (MARCO KO) mice. At the time the SRA (SR-A KO) mouse colony was breeding poorly and there was shortage of these mice, hence they were not included in these studies.

The development of DCs seems to have been unaffected by the loss of SR-A or MARCO as the percentage of cells expressing CD11c was very similar across the genotypes (Figure 4.4.2.1.A). All subsequent analysis steps were performed after gating for this CD11c+ population. Loss of SR-A expression was confirmed for the SRMA mice with antibody staining (Figure 4.4.2.1.B). Unfortunately, a reliable anti-MARCO antibody could not be

sourced during this work and so MARCO expression was not examined with flow cytometry in this assay.

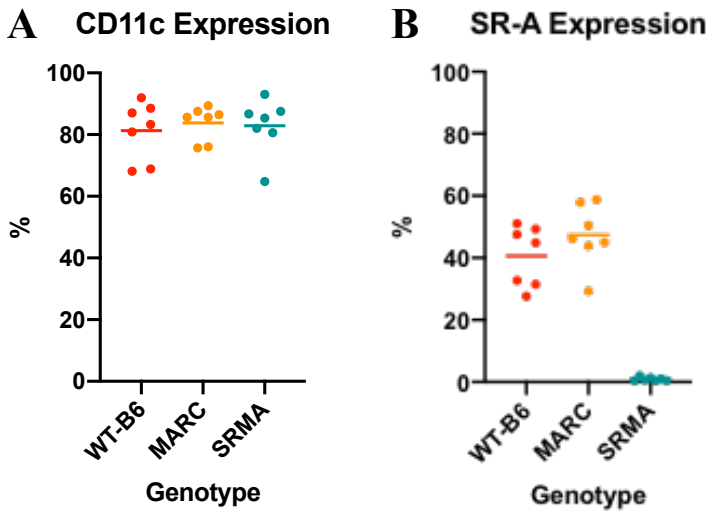

Figure 4.4.2.1: Murine bone marrow derived DCs (mBMDCs) were generated from bone marrow from WT-B6, MARC or SRMA mice. These were examined for expression of CD11c and SRA using flow cytometry. A shows the expression of CD11c. There were no significant differences between genotypes (Kruskal-Wallis test). B shows the percentage of CD11c+ cells which were also positive for SR-A. Each dot shows the expression of BMDCs derived in separate experiments and the bars show mean. Abbreviations: MARC = MARCO KO mice, SRMA = SR-A/MARCO double KO mice, WT-B6 = wild type C57BL/6J control.

Figure 4.4.2.2 shows the results of the uptake assay for HEL, OVA and BSA. As can be seen, the GLUC-modified samples for all 3 proteins have a higher uptake than the unmodified and more minimally modified proteins. As mentioned above, samples which have a labelling intensity which is > 1 SD from the mean intensity of the protein samples are shown as either upwards or downwards triangles. The BSA GLUC and GA 7 days samples had a lower labelling intensity than the other samples, therefore measuring uptake of these samples by fluorescence may underestimate the actual level of uptake. In contrast, the OVA GLUC sample had a labelling intensity > 1 SD, thus, this result must be interpreted with caution. However, overall these results indicate that GLUC modified samples have greater uptake than unmodified controls.

With the exception of BSA GA 7 days, which showed significantly greater uptake than BSA 3 h with WT-B6 and MARC DCs, the uptake of the non-GLUC modified samples was not significantly increased above that of the unmodified controls. This is of particular interest for the GA 3 h modified samples as the previous *in vivo* experiments showed that the HEL version of this induced the strongest antibody responses. Therefore, this result argues against enhanced uptake by DCs being crucial to this phenomenon.

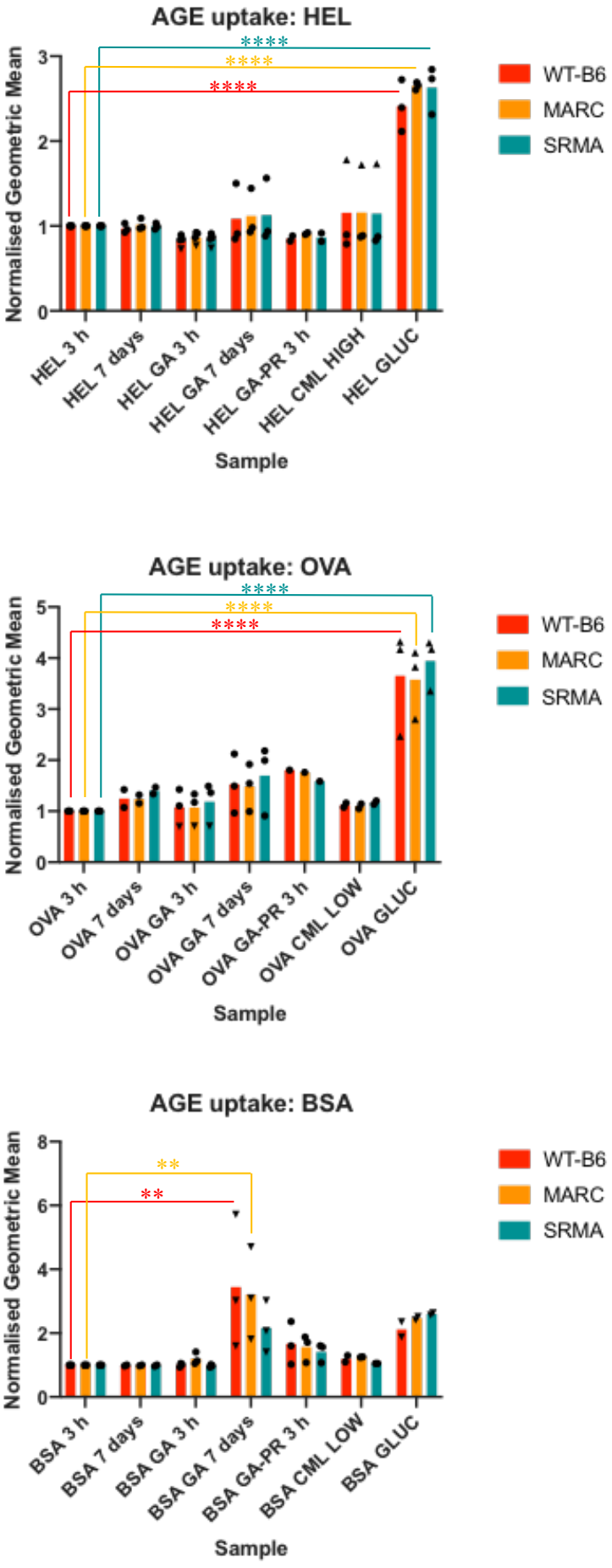

Figure 4.4.2.2: mBMDCs were generated from WT-B6, MARC and SRMA mice. The DCs were collected, allowed to adhere to flat bottomed plates for 3 h, then incubated with fluorescently (A488) labelled AGE-modified proteins for 30 mins. Cells were then collected, stained for CD11c and uptake assessed by flow cytometry. Each figure shows the A488 MFI amongst the CD11c+ population normalised to the A488 MFI of the unmodified control. Each dot represents an independent experiment and the bars show mean. In most experiments, biological triplicates were run except for one experiment where BSA GA 3 h was run in singlet and BSA GA-PR 3 h was run in duplicate due to low sample. Samples with at least three data points were compared using a two-way ANOVA followed by Dunnett's multiple comparison test, ** = $p \leq 0.01$, **** = $p \leq 0.0001$. In all cases, the two-way ANOVA reported no significant differences between genotypes. An FHS student, Luis Avellano-Khan, assisted with some of these studies. MFI = mean fluorescence intensity, measured as geometric mean.

Uptake of the GLUC modified proteins was not significantly lower in SRMA DCs which lack SR-A and MARCO. This finding was consistent for BSA, OVA and HEL over repeated experiments, arguing against SR-A being critical to uptake of modified proteins in this system. To probe this further, the data were assessed to determine whether the GLUC-modified proteins were taken up mainly by the SR-A positive or SR-A negative DCs in the WT-B6 and MARC mice. These results are shown in Figure 4.4.2.3. In WT-B6 and MARC mice, both BSA GLUC and HEL GLUC were preferentially taken up by cells which expressed SR-A. This provides some circumstantial evidence that SRA contributed to the uptake of the GLUC modified samples in these genotypes. In contrast, OVA GLUC was taken up equally by SR-A positive and negative cells, which may be a reflection of the fact that OVA is also internalised by the mannose receptor (Kindberg et al. 1990).

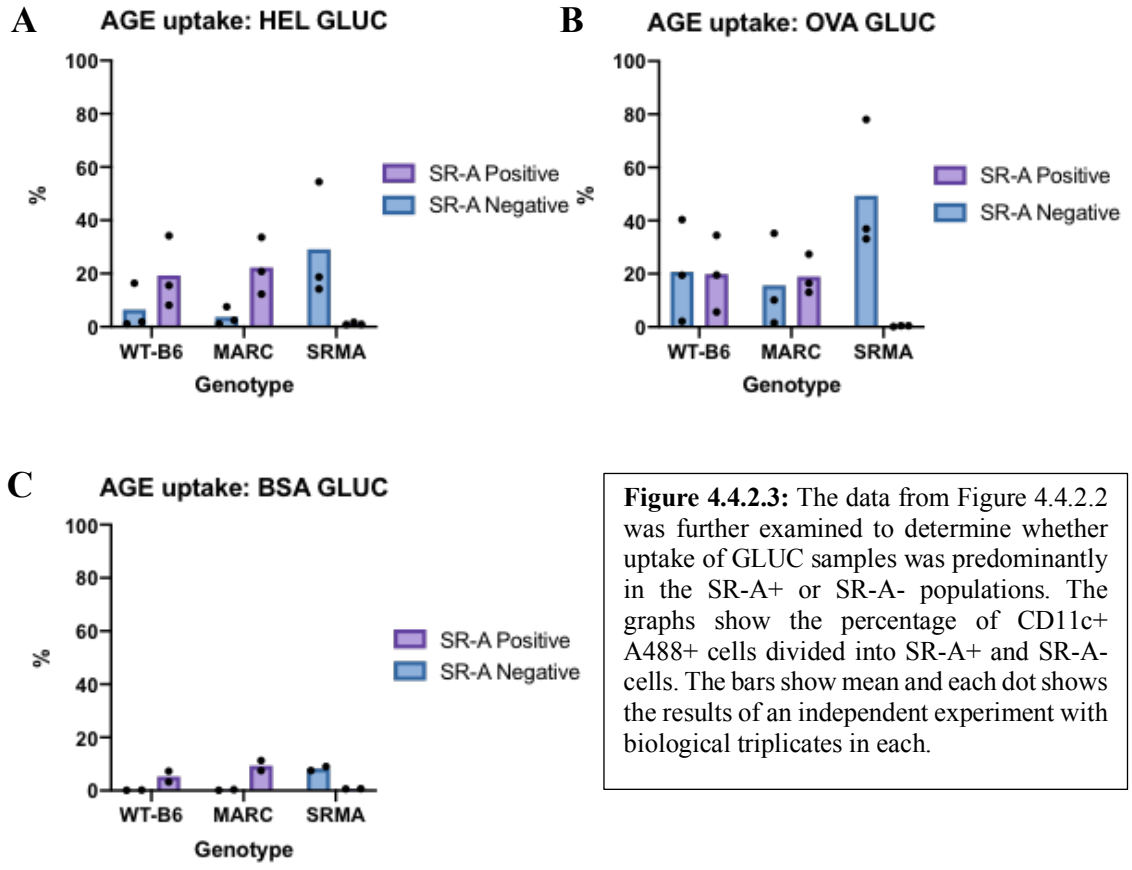

Figure 4.4.2.3: The data from Figure 4.4.2.2 was further examined to determine whether uptake of GLUC samples was predominantly in the SR-A+ or SR-A- populations. The graphs show the percentage of CD11c+ A488+ cells divided into SR-A+ and SR-A- cells. The bars show mean and each dot shows the results of an independent experiment with biological triplicates in each.

When the colony recovered, uptake studies were also performed using DCs derived from SRA mice. These confirmed that the lack of SR-A dependence was unlikely to be the result of MARCO KO in the SRMA mice as the uptake was very similar between DCs derived from SRA and WT-B6 mice (Figure 4.4.2.4).

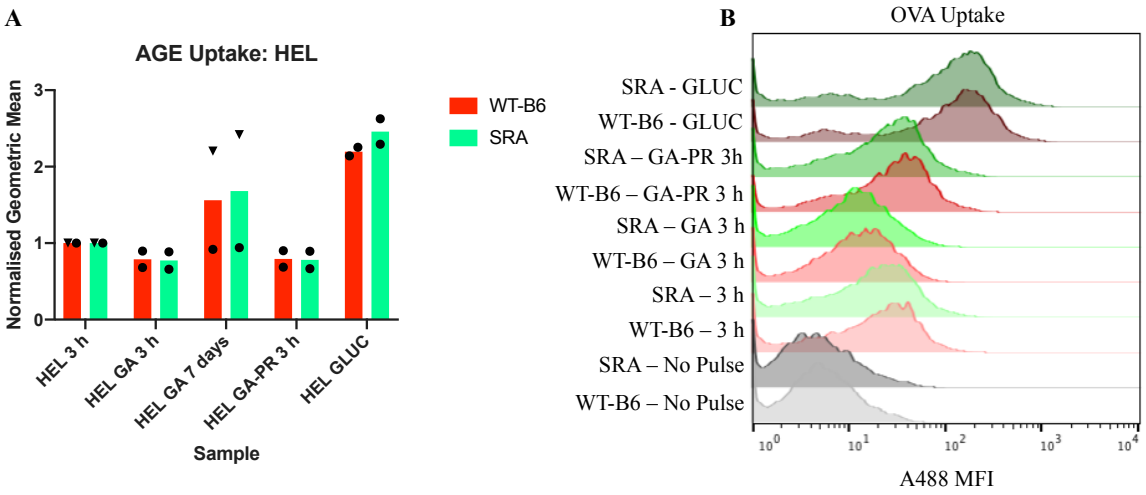

Figure 4.4.2.4: Uptake of AGE-modified proteins by DCs lacking SR-A only. The same protocol was followed as in 4.4.2.2, except using BMDCs from SRA mice. The graph and flow cytometry plot show the fluorescent signal amongst live cells incubated with the indicated proteins. In A this was normalised to the MFI of the HEL 3 h sample. Each dot represents the average of biological triplicates from an independent experiment, whilst the bars show mean. The flow graph shows a representative biological triplicate from a single independent experiment. SRA = SR-A KO mice.

4.4.3 Uptake of Glucose-modified Samples Is Not Dependent on SR-A in In-tube Uptake Studies

It was important to address why the studies reported here contrasted so dramatically with previously published AGE-uptake studies. As SR-A is known to mediate cellular adherence to plastic (Fraser, Hughes, and Gordon 1993), one possibility considered was that in a plate-based uptake system SR-A molecules are engaged in binding to the surface of the plate and so other SRs take over the role of clearing modified protein. Indeed, a previous study examining uptake of modified LDL and *E. coli* in macrophages from WT and SRA mice showed that results were highly dependent on experimental conditions with the difference in uptake between the genotypes disappearing when macrophages were cultured on tissue culture plates as opposed to bacteriological plates (Peiser et al. 2000). To test whether this was also affected the results of the plate-based studies, an assay was established where DCs were lifted and then kept in suspension by keeping them in low-binding flow cytometry tubes with occasional shaking during the incubation with fluorescently-labelled protein. This assay was called the "in-tube" uptake assay. As before, CD11c expression in the derived population was assessed. Again there were no significant differences between the percent CD11c+ between the genotypes. Loss of SR-A expression was again confirmed by antibody staining (Figure 4.4.3.1).

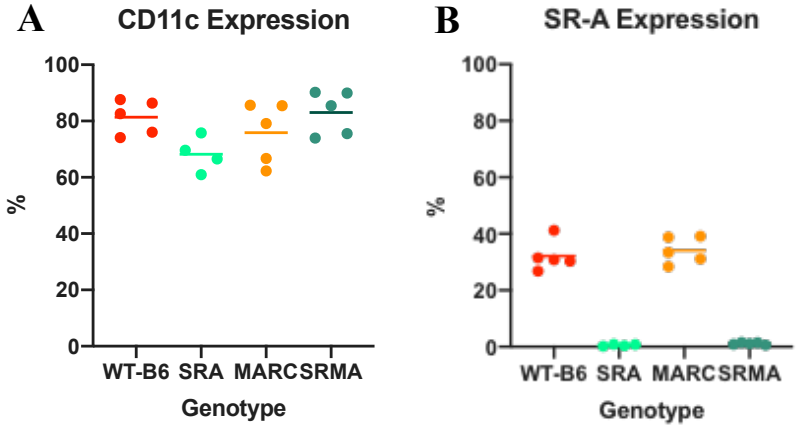

Figure 4.4.3.1: BMDCs were isolated from the SR KO mice. Expression of CD11c was assessed by flow cytometry. The data were analysed using a Kruskal-Wallis test. B shows SR-A expression in the CD11c+ population. Each dot shows the results from one independent experiment and the bars show mean.

To confirm that this approach would work, acLDL was used as a positive control in the uptake experiment. This modified LDL is known to be cleared by SRs on myeloid cells, including SR-A (Horiuchi, Sakamoto, and Sakai 2003). The results for this are shown in Figure 4.4.3.2. This experiment confirmed that uptake was possible in this system. As has previously been reported, this uptake was predominantly mediated through SR-A as the percentage of DCs staining positive for acLDL and the MFI were both significantly decreased for SRA BMDCs. For the SRMA mice uptake of acLDL appeared to show a slight recovery, although this may be the result of a single outlier.

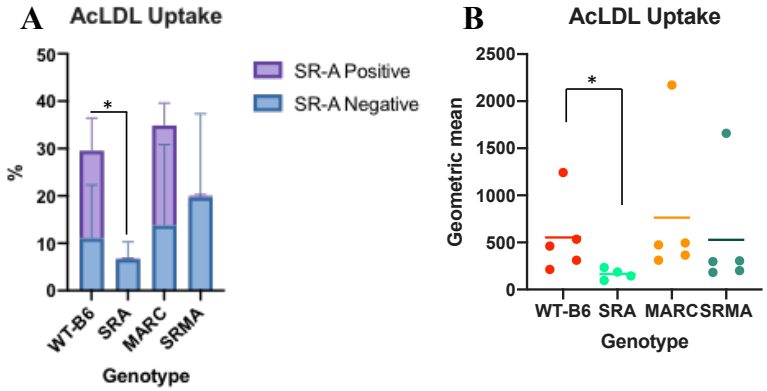

Figure 4.4.3.2: BMDCs were derived from SRA, MARC, SRMA and WT-B6 mice. The cells were collected, immediately transferred to low-bind flow cytometry tubes and incubated with acLDL (fluorescently labelled with DiI) for 30 mins. This protocol is called the "in-tube uptake assay". Cells were then collected, stained for CD11c and SRA and analysed by flow cytometry. The percentage of positive cells and the MFI amongst the CD11c+ population was measured and is shown in A and B respectively. A shows mean with SD, whilst in B each dot represents each independent experiment and the bars show mean. Significance was determined using a Kruskal-Wallis test followed by Dunn's multiple comparison test, * = $p \leq 0.05$.

Uptake results for BSA, OVA and HEL using this assay are in Figure 4.4.3.3. Uptake was reduced in this system compared to the plate-based assay and this is reflected in the reduced geometric means and percentage of positive cells. However, the overall picture is very similar between the two assays. Again GLUC-modified samples show an increased uptake, whilst the other AGE-modified samples do not. As before, uptake in the WT-B6 and MARC DCs of GLUC samples is predominantly or exclusively limited to the SR-A positive population, but there is no significant loss of uptake with DCs lacking SR-A. The overall conclusion from the uptake studies is that AGE-protein uptake is either mediated through

receptors other than SR-A or that this can be compensated by other SRs, at least in these systems.

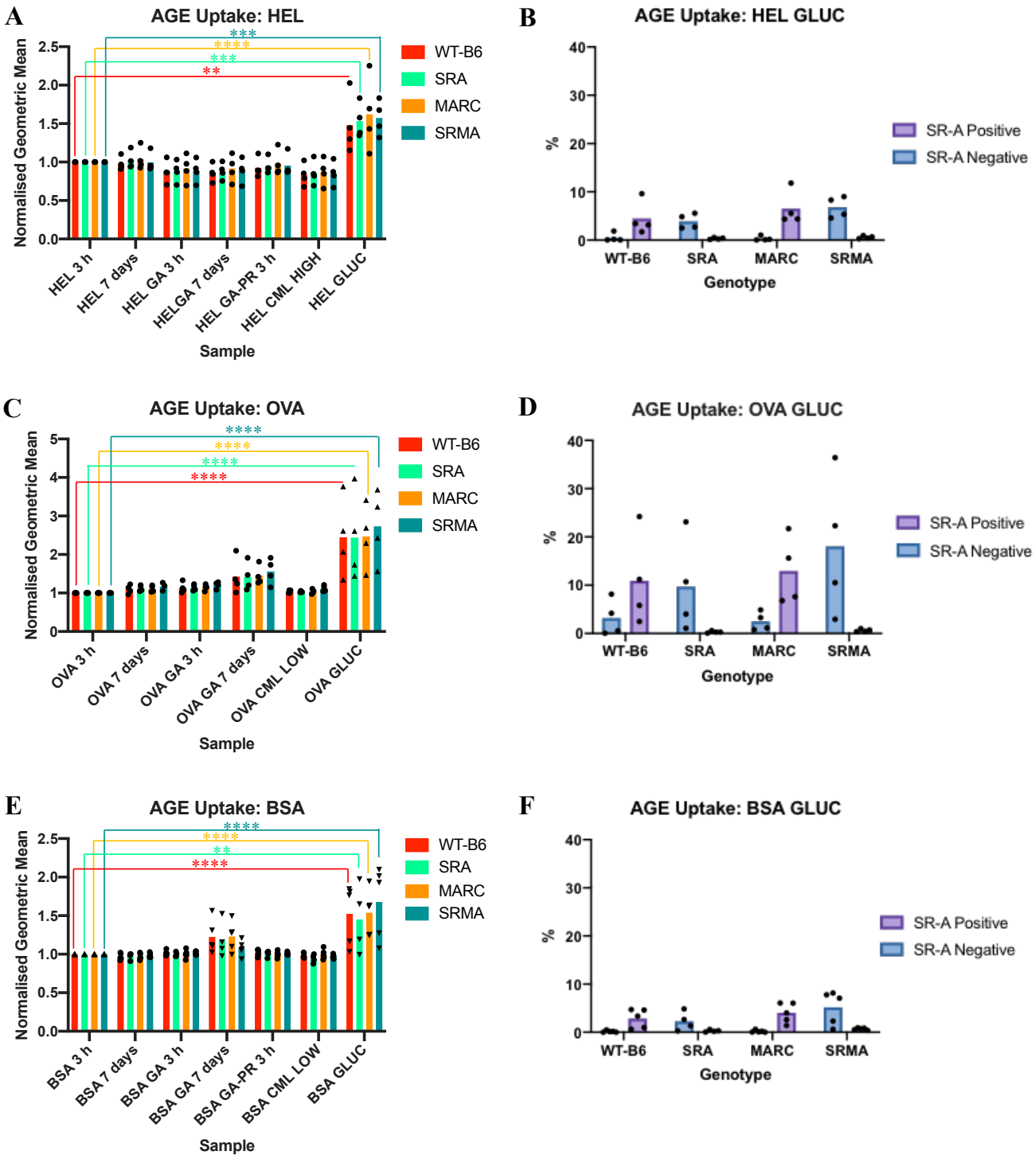

Figure 4.4.3.3: The in-tube uptake assay described in Figure 4.4.3.2 was used to assess DC uptake of AGE-modified proteins. Uptake of A488-labelled AGE-modified proteins in CD11c+ BMDCs was assessed using normalised MFI as for Figure 4.4.2.2. The results were analysed by two-way ANOVA followed by Dunnett's multiple comparison test, ** = $p \leq 0.01$, *** = $p \leq 0.001$, **** = $p \leq 0.0001$. Uptake of GLUC samples was assessed further by examining the percentage of CD11c+ cells which were A488 positive and whether these cells were SRA positive or negative. In all graphs the bars show mean and each dot represents an independent experiment.

4.4.4 Immunisation Studies Using SRA, MARC and SRMA mice

There are many reasons why results reported here may differ from previously published studies. For example previous research has used different methods for BMDC culture and for producing AGE-modified proteins (Ilchmann et al. 2010; Heilmann et al. 2014). Given the large number of variables which could affect these *in vitro* systems, it would be almost impossible to completely address the role of SRs in these systems. It was therefore decided to move to an *in vivo* system which would more completely confirm whether these SRs are involved in AGE immunogenicity.

WT-B6, SRA, MARC and SRMA mice were immunised according to the procedure outlined in the Materials and Methods section 2.4.3. The immunisation protocol is given again in Figure 4.4.4.1. The development of antibody responses throughout the immunisation protocol was followed by ELISA (Figure 4.4.4.2). The results are shown as signal overtime and as area under the curve (AUC). Unlike in previous immunisation experiments with CBA and BALB/c mice (see Chapter 3) in which only one immunisation was given, the development of strong antibody responses took several immunisations. Moreover, there was a large variation in the response with the majority of mice failing to develop antibodies to HEL even after five injections. However, all except one of the mice which did develop an antibody response were in the HEL GA 3 h group. Moreover, this response was predominantly IgG1 with little production of IgG2c. Thus, even in a C57BL/6

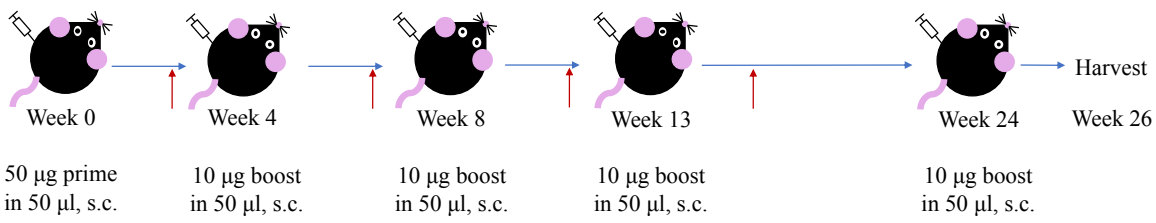

Figure 4.4.4.1: SRA, MARC, SRMA and WT-B6 control mice were immunised with HEL 3 h, HEL GA 3 h or HEL GLUC. The immunisation schedule is shown above. The red arrows indicate when sera was collected.

background which favours Th1 like responses (Sellers et al. 2012), the antibody response was biased towards a Th2 type response.

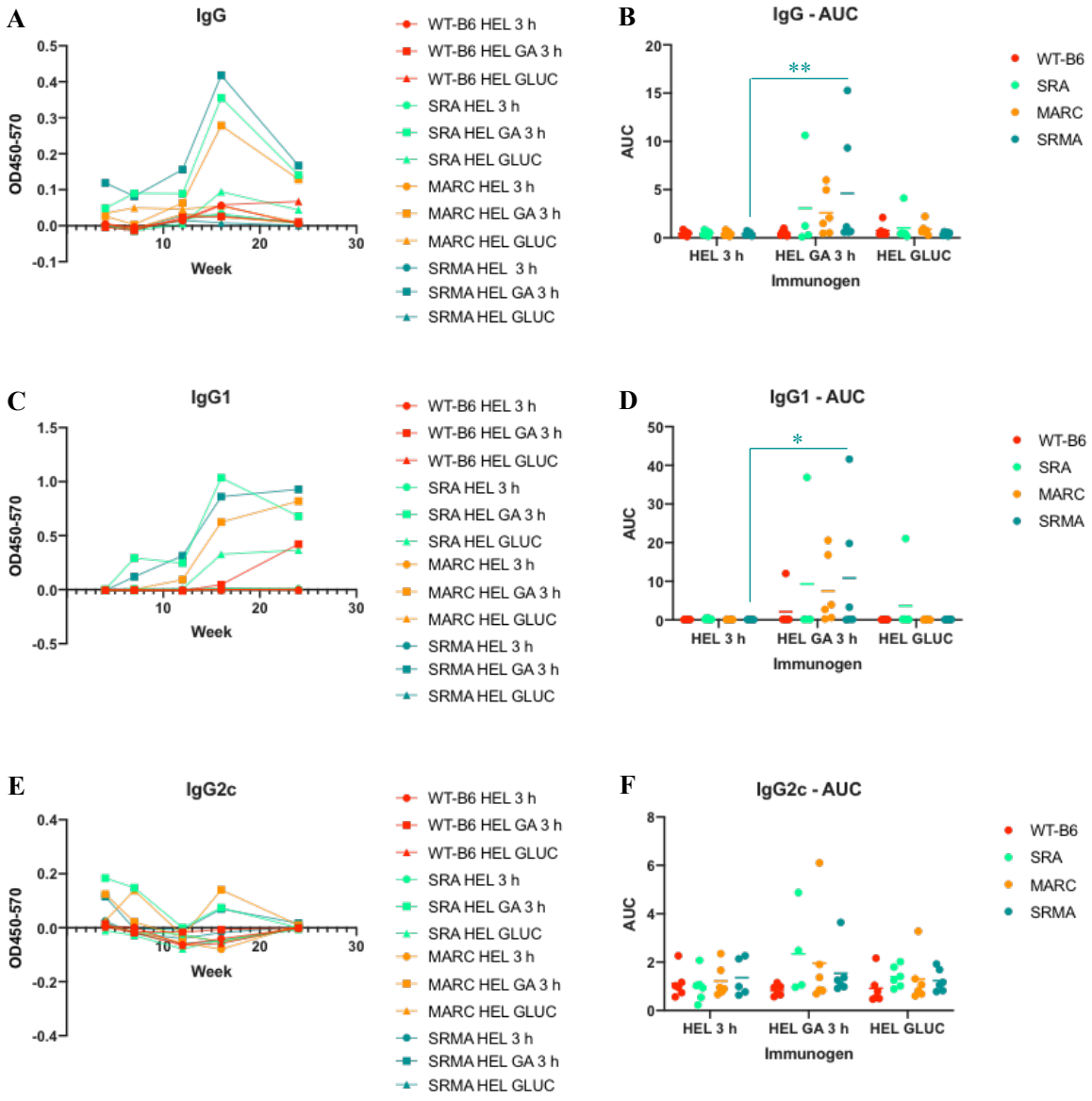

Figure 4.4.4.2: Sera was collected from mice immunised with the indicated proteins throughout the experiment (see Figure 4.4.4.1), and used to assess antibody responses to unmodified HEL. Total IgG, IgG1 and IgG2c were measured by ELISA and used to produce the curves in A, C and E which show the average response in each group. Individual curves for each mouse were used to measure area under the curve (AUC) and these results are shown in B, D and F. In these, each dot shows the response of an individual mouse with a bar showing mean of each group. The data were analysed by two-way ANOVA followed by Dunnett's multiple comparison test, * = $p \leq 0.05$, ** = $p \leq 0.01$. OD = optical density.

With regards to the contribution of SR, the antibody responses in fact appear to be higher in the KO mice, with significant responses only developing in SRMA mice. However, a two-way ANOVA indicated that the differences between genotypes were not significant. Overall, this data suggests inhibitory roles for these receptors in the WT-B6 mouse but further repeats would be required to confirm this.

At the end of the experiment, spleens were harvested from the mice and the splenocyte recall responses assessed by *in vitro* restimulation experiments. The strength of the splenocyte responses was assessed initially by thymidine pulse (Figure 4.4.4.3). As can be seen, HEL GLUC immunised mice had higher proliferation than HEL immunised mice. Importantly, this was not decreased in mice lacking SR-A, in fact significantly increased proliferation was only seen in the SRA and SRMA mice. Although again the two-way ANOVA indicates that there were no significant differences between genotypes.

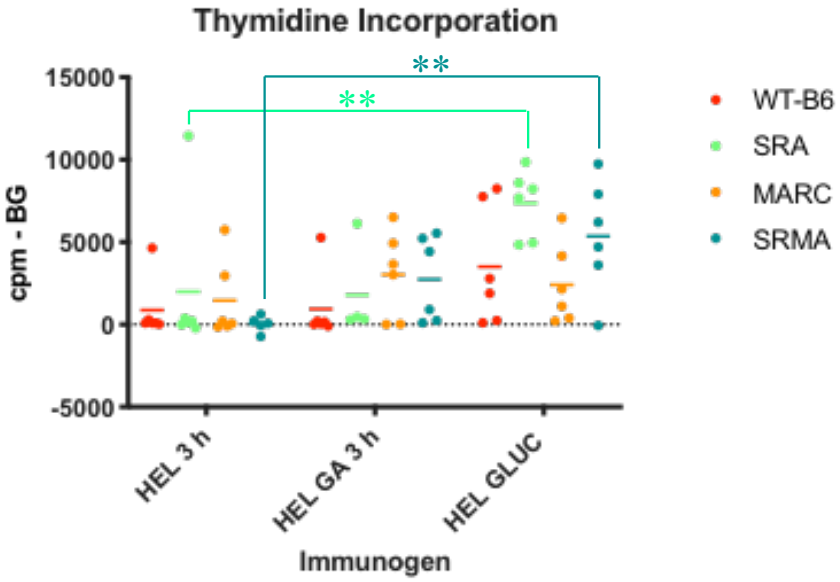

Figure 4.4.4.3: Spleens from mice immunised with the indicated protein were harvested at week 26 (see Figure 4.4.4.1). Isolated splenocytes were pulsed with unmodified HEL or left unpulsed. On day 3 the cell cultures were pulsed with ^{3}H-Thymidine and then radioactivity within the cells was assessed the following day. Specific proliferation in response to HEL was determined by removing the background signal seen in unpulsed wells. Each dot represents an individual mouse and the bars show mean. Results were analysed by two-way ANOVA followed by Dunnett's multiple comparison test, ** = $p \leq 0.01$. Abbreviations used: cpm = counts per minute, BG = background.

Cytokine production by the splenocytes was also measured (Figure 4.4.4.4). Generally these results reflect the thymidine results with increased secretion in HEL GLUC immunised mice. Again, this response appeared enhanced in SRA mice, although the responses in the SRMA mice are more similar to the WT-B6. The two-way ANOVAs generally indicated that the genotype did not have a significant influence on the results. The exception is IL-4, where genotype was a significant factor.

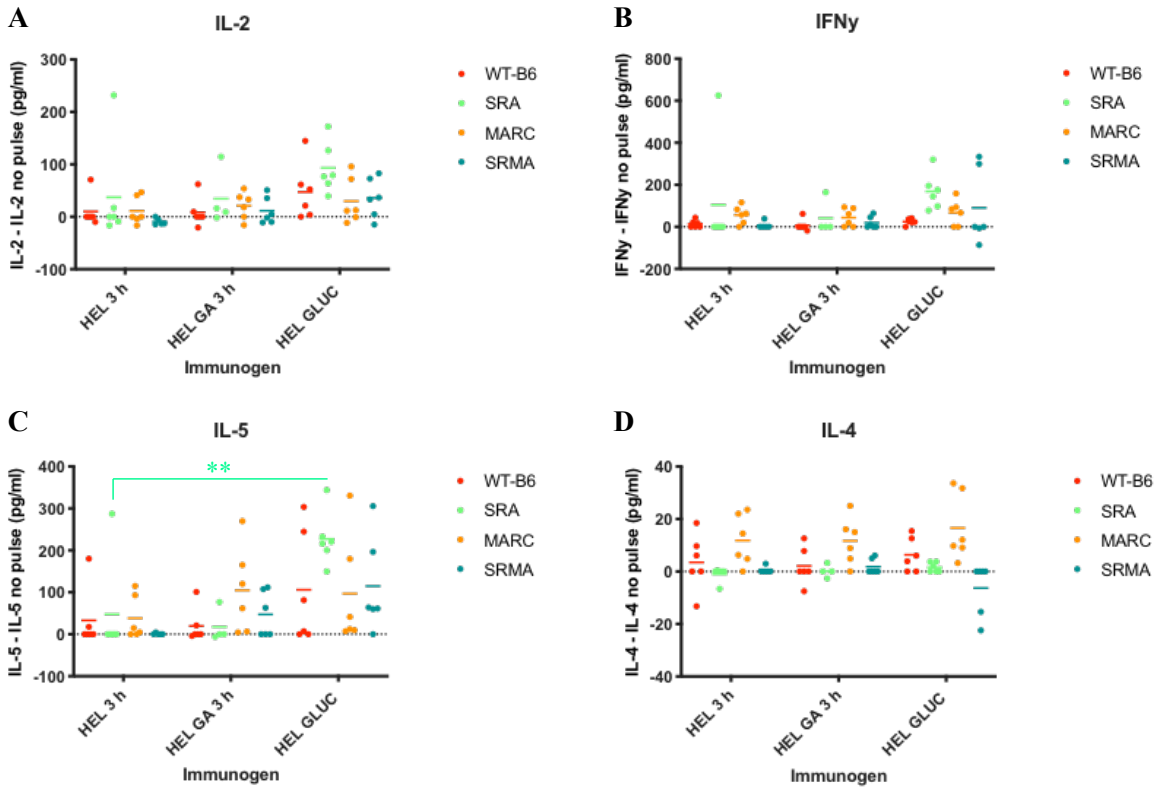

Figure 4.4.4.4: On day 1 (IL-4) and day 3 (IL-2, IL-5 and IFNγ) supernatant was collected from the splenocyte cultures described in Figure 4.4.4.3 and used to assess cytokine secretion. As with the thymidine incorporation, non-specific background production was removed from the production in HEL pulsed wells to give a specific signal. Each dot is an individual mouse and the bars show mean. Data were analysed by two-way ANOVA followed by Dunnett's multiple comparison test, ** = $p \leq 0.01$

Lastly, proliferation was also assessed by flow cytometry (Figure 4.4.4.5). Expression of Ki67 was used to identify cells which were proliferating. As with the thymidine results, there was a higher percentage of Ki67+ cells in mice immunised with HEL GLUC and this increase was significant for the SRA group. This increase in proliferation seems to be largely the result an expansion of the CD19+ B cell population, a somewhat surprising finding given

that strong antibody responses were not seen in these mice. Regardless, these findings demonstrate that SR-A is dispensable for enhanced AGE-immunogenicity *in vivo*. In fact, this evidence suggests that SR-A acts to inhibit the development of adaptive immune responses to AGE-modified proteins.

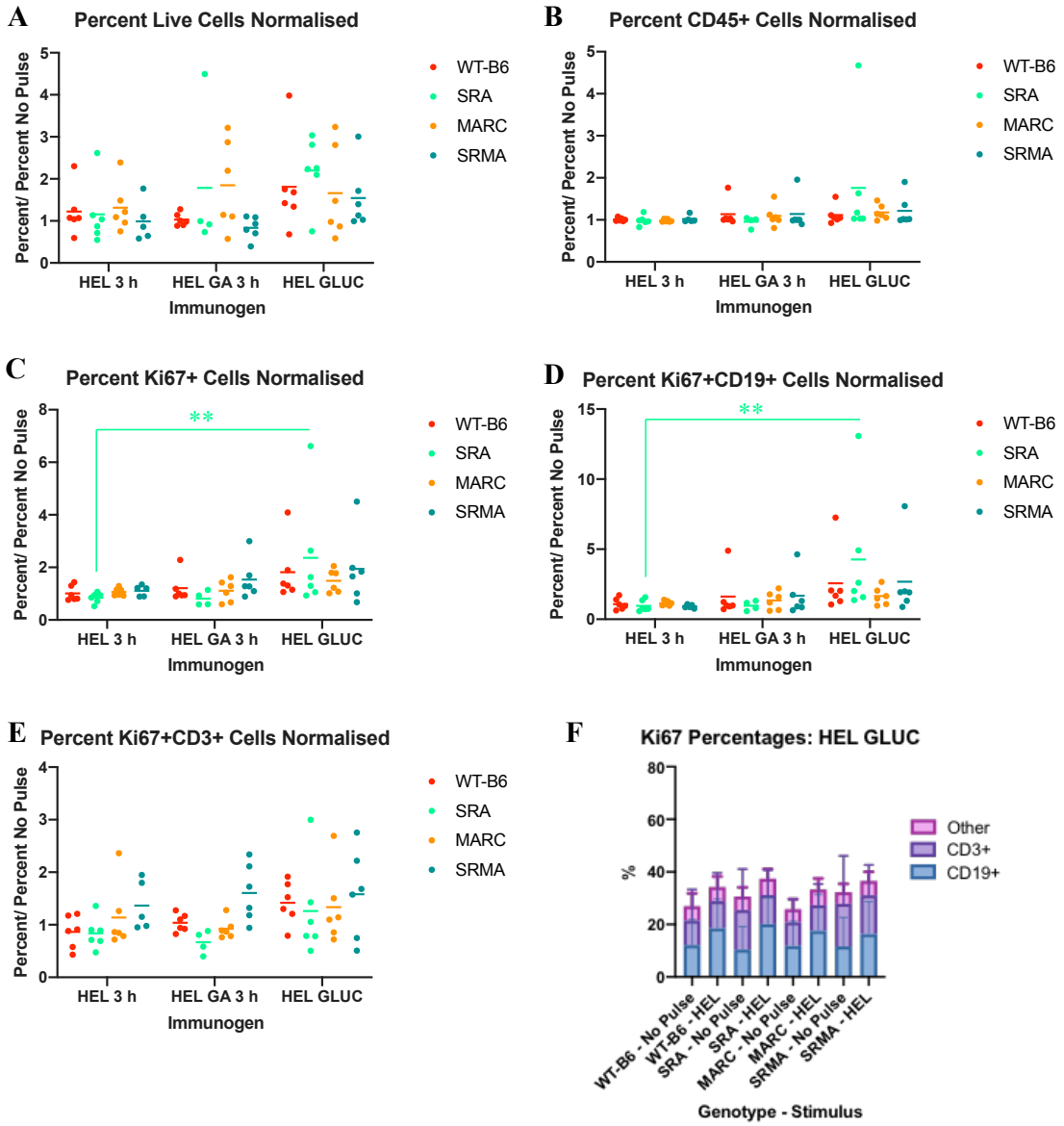

Figure 4.4.4.5: Flow cytometry was used to determine the identity of the proliferating cells in the splenocyte cultures (see Figure 4.4.4.3). Cells were collected on day 4 then stained for CD45 (general leukocyte marker), CD3 (T cell marker), CD19 (B cell marker) and Ki67 (marker of proliferation). In all the graphs the percentage is normalised to the percentage in unpulsed cultures to account for unspecific proliferation. Graph A shows the normalised percentage of live cells within the cultures, whilst graph B shows the proportion of lives cells which are CD45+. The normalised percentage of Ki67+ cells within the CD45+ population is shown in C. In graphs D and E the increase in Ki67+ CD19+ and Ki67+ CD3+ cells compared to unpulsed cultures is shown respectively. The data for HEL GLUC from D and E is summarised in F, in which the CD45+ Ki67+ population is divided by expression of CD3, CD19 or neither marker (other). This is given as a percentage of the live cells. The data were analysed by two-way ANOVA followed by Dunnett's multiple comparison test where appropriate, ** = $p \leq 0.01$. In A – E the responses of individual mice are shown and the bars show mean. In F the bars show the average response from the mice immunised with HEL GLUC and the error bars show SD.

4.5 Discussion and Conclusions

There are two keys findings in this chapter. Firstly, GLUC-modified samples have significantly greater DC uptake than unmodified samples. Thus, the enhanced immune response in GLUC-immunised mice seen in Figures 4.4.4.2 – 4.4.4.4 may be the result of increased DC presentation to T cells. One limitation of the uptake assay used in this thesis is that it cannot discriminate between internalisation of the labelled proteins and binding of the protein to the cell surface. This would influence interpretation as internalisation of the protein would then allow for processing and presentation on MHC. Whereas, cell surface binding would suggest binding to cell surface receptors which may then initiate signalling pathways. To investigate this further, location of the AGE-modified proteins could be examined with confocal microscopy. This technique would discriminate between cell-surface bound and cell-internalised proteins.

The second key finding is that SR-A is not critical for AGE enhanced immunogenicity, in fact the evidence suggests that *in vivo* SR-A may act to inhibit the development of adaptive immune responses to AGE-modified proteins. To the best of the author's knowledge, this is the first study to examine the contribution of SR-A *in vivo* to AGE-mediated immunogenicity and so is an important step for this field, particularly given that many studies have focused on SR-A.

Moreover, the uptake studies included in this chapter demonstrate that AGE-protein uptake is not decreased in BMDCs lacking SR-A. One interpretation of these results is that AGE-protein uptake is not normally mediated by SR-A and instead is predominantly through another unidentified receptor(s). Alternatively, in WT-B6/MARC DCs, SR-A may contribute to uptake. However, due to the lack of SR-A in the SRA/SRMA DCs, AGE uptake is instead mediated through other SRs, possibly with compensatory upregulation of these alternative receptors. It is known that amongst SRs there is a high degree of

redundancy and there are several other receptors which are known to bind to AGEs that could be involved in DC uptake of AGE-modified proteins (Horiuchi, Sakamoto, and Sakai 2003).

Interestingly, the HEL GA 3 h modified samples, which induced the strongest antibody responses in the immunisation experiments in Chapter 3, had an uptake which was similar to the unmodified samples. This finding contrasts with previous work showing that GA is an important intermediate for the generation of AGEs recognised by SR-A. However, this older study used BSA which was incubated with GA for 7 days (Nagai et al. 2000). Therefore, it is possible that the structures which act as ligands for SR-A have either not formed at early time points in the incubation or are required in sufficient number for recognition. There may also be protein specific effects as in this study BSA GA 7 days showed a significantly greater uptake than the control, but the equivalent OVA and HEL samples did not. Overall, the results suggest that the enhanced immunogenicity of HEL GA 3 h was not due to increased uptake by DCs and subsequent enhanced presentation to T or B cells.

One important question which needs to be resolved is why the results included in this chapter differ so significantly from previously published results which have reported that AGE-uptake into DCs is dependent on SR-A (Heilmann et al. 2014; Hilmenyuk et al. 2010; Ilchmann et al. 2010). There are a number of differences between this and previous studies which may help to answer this question. Firstly, as discussed above, in this set of studies cysteine-based labelling was used rather than the amine-based labelling which has been used in many previous studies. A major drawback of utilising amine reactive dyes is that as these target the same sites which are modified by sugars during the Maillard reaction, extensively modified proteins cannot be labelled with this method. Other studies using amine-based tags have instead used a different approach in which the protein is first fluorescently labelled and

then modified (Warnecke et al. 2017). This method has its own limitations, namely that it removes sites of potential modification and may not be appropriate for the long term incubations used in this study which require the protein to be heated for several months. The major advantage of the cysteine-labelling method is that it could label the extensively modified proteins which were of particular interest in this study. However, this does require a harsher labelling procedure than amine-reactive dyes and it is not possible to assess the effect of this labelling on every single possible AGE-modification. Moreover, a major limitation of the studies shown here is that there is variation in the labelling intensity of the protein samples which may have affected the results and their interpretation. Overall, there are significant benefits and drawbacks to both these labelling methods and neither is the perfect solution. An alternative approach may have instead been to have designed a competition assay where the ability of unlabelled proteins to inhibit the uptake of modified LDL was assessed. This would have overcome the problem of variable labelling.

Another key point of variation between different AGE uptake studies is the technique for deriving DCs (Ilchmann et al. 2010). The concentration of cytokines used and the protocol for deriving BMDCs differs widely and this is likely to produce disparate populations with varying levels of SR expression. One option would be to derive DCs using the different reported methods and compare the dependency of uptake through SR-A. However, this is unlikely to provide a definitive answer as to the role of SR-A in DC uptake of AGE modified proteins *in vivo*. Defining GM-CSF derived bone marrow cells has proved challenging, whilst they are considered DC-like it has been shown that even the CD11c+ MHC II+ contains a population of monocyte-derived macrophages which behave differently from the classic DCs (Helft et al. 2015). If one wanted to further study this phenomenon using an *in vitro* system one option would be to isolate primary DCs from mouse tissue. Although this would not be a perfect reflection of DCs *in vivo,* it is a step closer than using derived DCs.

Finally, another major difference between studies is the methods used to produce AGE modified proteins. For the GLUC modification in this study, proteins were incubated with glucose for 6 months at 37 °C. In contrast the studies from the Toda and colleagues, heated protein with glucose to 50 °C for 6 weeks (Hilmenyuk et al. 2010; Ilchmann et al. 2010; Heilmann et al. 2014). Obviously, this could have affected the profile of AGE modifications in the samples and previous work has indicated that not all AGE production protocols result in the formation of SR ligands (Miyazaki, Nakayama, and Horiuchi 2002). In order to address this, the AGE structures formed by the two protocols would need to be compared. However this is very difficult to assess as the only method which could give a complete picture of the modifications is mass spectrometry, which is complex with AGE-modified proteins (Zhang et al. 2009).

To summarise, the data produced in this report demonstrate that uptake through SR-A does not enhance the immunogenicity of AGE modified proteins. Instead, the data seem more in line with a model where SR-A inhibits the development of immune response to AGE-modified proteins. This would fit with the known role of SR-A, which has been suggested to limit the development of immune responses (Yi et al. 2009; Guo et al. 2012), and would explain why the development of immune responses appeared enhanced in the mice lacking SR-A immunised with HEL GLUC. One possibility is that under normal circumstances, SR-A is involved in the uptake of AGE-modified proteins. However, this shuttles proteins into non-immunogenic clearance pathways. In the KO mice, loss of SR-A may result in clearance by alternative receptors which instead target proteins for antigen processing and presentation in DCs. Alternatively, SR-A binding to AGE may induce inhibitory signalling pathways and in the absence of this receptor the balance between activatory and inhibitory signals tips towards the former. Both of these possibilities could be the subject of further studies.

Chapter 5: Weight Gain Phenotype and Immunophenotyping of SR-A and MARCO KO Mice

5.0 Abstract

Obesity is a major public health issue worldwide. In order to tackle this crisis, the factors which contribute to the development of obesity and its associated conditions need to be understood. In this regard, there has been a substantial interest in the role of the immune system in metabolic dysfunction. In this study, the weights of mice lacking scavenger receptor A (SR-A), macrophage receptor with collagenous structure (MARCO), or both receptors were monitored for up to a year. This revealed that MARCO KO mice have a significantly higher body weight and fat pad mass than their wildtype (WT) counterparts and this phenotype is even more pronounced in the double knockout (KO) mice. In contrast, the weight of SR-A KO mice was not significantly different from their WT counterparts. Various experiments were then attempted to further define this phenotype and determine the underlying cause.

5.1 Introduction

5.1.1 The Obesity Crisis

The World Health Organisation (WHO) estimates that 650 million people in the world are obese and that more people now die of diseases linked to obesity and being overweight than die of malnutrition (World Health Organisation 2020). Obesity is not simply a state where the calorie intake exceeds calorie use, many factors can influence the energy intake and expenditure of the individual. For example, genetics, epigenetics, maternal state during pregnancy, endocrine changes, microbiota and sleep patterns have all been shown to contribute to the development or maintenance of the obesity phenotype (González-Muniesa et al. 2017). Obesity is linked to many life-threatening conditions and even in otherwise healthy individuals obesity can have a significant negative impact on quality of life (González-Muniesa et al. 2017). Unfortunately, finding effective and practical treatments for obesity has proved challenging. Changes to diet and exercise often fail to lead to long-term weight reduction (Lean, Astrup, and Roberts 2018). Meanwhile bariatric surgery, whilst effective, is not without significant side effects and is only available to a limited number of patients (Ruban et al. 2019; González-Muniesa et al. 2017).

In order to fulfil this unmet clinical need, we need to increase our understanding of the pathological changes which occur in a person with obesity. Researchers have used various different tools to probe the causes and consequences of obesity, including mouse models of which there are three broad types. Firstly, certain strains of mice, specifically C57BL/6, have a tendency to gain weight on a high fat diet (HFD) and so are used for diet-induced obesity models. Secondly, obesity can be induced surgically in mice, for example by damaging the areas of the brain which are involved in appetite regulation. Lastly, there are genetic models of obesity of which perhaps the most famous examples are the *ob/ob* and *db/db* mice (Lutz and Woods 2012). These genetic models have revealed the fundamental pathways which

regulate weight, including appetite regulation by leptin, a hormone secreted by adipocytes. Various studies using these mouse models have demonstrated that chronic low-grade inflammation is a feature of obesity and this has been confirmed in studies using human tissue.

5.1.2 Inflammation in Obesity

In lean individuals, adipose tissue is in an anti-inflammatory state. Resident macrophages are small, dispersed and are reported to have an "M2" phenotype (Lumeng, Bodzin, and Saltiel 2007). Adipocytes secrete adiponectin, an anti-inflammatory hormone which regulates lipid metabolism by promoting lipid oxidation and suppressing lipogenesis (Ellulu et al. 2017). However, during obesity there is a switch to a pro-inflammatory tissue state. It is thought that the adipocytes become overwhelmed by the excess fats and as a result the cells become hypertrophied and there is an increase in adipocyte death (Strissel et al. 2007; Boutens and Stienstra 2016). Secretion of adiponectin by adipocytes decreases, and instead the adipocytes produce inflammatory cytokines such as IL-6 and CCL2 (Ellulu et al. 2017; Cai et al. 2012). In response to adipocyte cell death and secretion of these and other cytokines, increased numbers of macrophages are recruited to the tissue (Weisberg et al. 2003). These have a very different phenotype to the steady-state adipose tissue macrophages. They are M1 in character, producing pro-inflammatory cytokines, such as TNFα, and instead of being dispersed they cluster into "crown-like structures" which surround dead and dying adipocytes (Lumeng, Bodzin, and Saltiel 2007; Boutens and Stienstra 2016; Weisberg et al. 2003; Cinti et al. 2005). The cytokines released from macrophages result in further adipocyte death and thus, a vicious cycle is formed which will maintain the inflammatory state (Xu et al. 2003). As disordered macrophage function is

clearly important to this process, understanding how macrophages respond to adipocyte dysfunction and excess lipids during obesity is a key area of scientific interest.

5.1.3 SRs and Obesity

Adipose tissue macrophages can bind lipoproteins using SRs, many of which are known to bind and endocytose oxLDL (Greaves and Gordon 2008). Studies using KO mouse models and examining human tissues are beginning to establish roles for these receptors in the pathogenesis of obesity. Some receptors appear to drive inflammation in adipose tissue, contributing to weight gain and the development of metabolic disease. For example, CD36 KO mice fed a HFD gain less weight than their WT counterparts and have lower fasting blood glucose, a phenotype possibly due to the lower inflammation and cell death in the adipose tissue in these mice (Cai et al. 2012). In human studies, this receptor has been shown to be significantly upregulated in obese adipose tissue (Bonen et al. 2006).

Conversely, studies using KO mice have suggested that SR-A plays a protective role in obesity. SR-A KO mice have a similar body weight on a HFD to WT mice, however, they have poorer blood glucose control (Cavallari et al. 2018; Zhu et al. 2014). It has been suggested this is due to SR-A involvement in the development of a "M2" macrophage phenotype. *In vitro* studies using macrophages derived from SR-A KO mice demonstrated that these cells have reduced ability to polarise towards an M2 anti-inflammatory phenotype in response to IL-4 but their expression of M1 markers in response to LPS is enhanced. *In vivo*, this was reflected by an increased proportion of M1:M2 like macrophages in the adipose tissue of obese SR-A KO mice (Zhu et al. 2014). In contrast, in human adipose samples SR-A expression has been shown to inversely correlate with insulin sensitivity. Furthermore, treatment with pioglitazone, an insulin sensitising drug, decreased SR-A expression (Rasouli et al. 2009).

Very few studies have examined the role of MARCO, a SR belonging to the same class as SR-A, in obesity. One study using KO mice fed a HFD found no difference in body weight or blood glucose control compared to WT controls (Cavallari et al. 2018). Another study showed that feeding a HFD induced expression of MARCO in the livers of WT mice. These mice also had significant liver damage and inflammation providing a possible link between this receptor and inflammatory liver disease (Yoshimatsu et al. 2004).

Clearly, there are still large gaps in our understanding of SRs in obesity with the role of some receptors being almost entirely unexplored. This chapter focuses on mice with a genetic deletion of SR-A (SRA), MARCO (MARC) or both receptors (SRMA). Mice lacking MARCO, either singly or in combination with SR-A, have significantly higher weight and body fat compared to SRA or WT-B6 mice. This result indicates that MARCO has a key role in regulating lipid metabolism/storage. Mice were then analysed to assess changes in their microbiome, food intake and immune populations in order to understand which factors may drive this phenotype.

5.2 Hypothesis and Aims

Hypothesis: MARCO and SR-A have key roles in the regulation of lipid metabolism and/or adipose tissue function

Aims

1. To examine weight gain over time in SRA, MARC and SRMA mice.
2. To examine the contribution of the microbiome to the weight gain phenotype in a cohousing study.
3. To examine immune populations in adipose and other relevant tissues.

5.3 Materials and Methods

A list of procedures used in this chapter is given below. For complete descriptions please refer to the indicated section of the Materials and Methods Chapter.

- Flow Cytometry (2.3.6)
- Mouse Origin and Care (2.4.1)
- Fasting Blood Glucose Measurements (2.4.5)
- Tissue Harvesting (2.4.6)
- Cell Isolation from Tissue Samples and Tissue Analysis (2.7)
- Statistical Analysis (2.9)

5.4 Results

5.4.1 SR KO Mice Gain Excess Body Fat

The project began with an *in vivo* experiment examining AGE immunogenicity in SRA, MARC and SRMA mice (see Chapter 4). As part of this experiment, the age-matched mice were weighed at multiple time points. Figure 5.4.1.1 shows the weights of the mice at the end of the experiment (A) and over time (B). As can be seen, MARC mice had a significantly higher weight compared to both WT-B6 and SRA mice. This effect was even more pronounced for the SRMA mice, whose weight is significantly higher than the single KO mice. This is also shown when weight is plotted against mouse age as the excess weight gain in SRMA mice is apparent at an earlier age than the MARC mice.

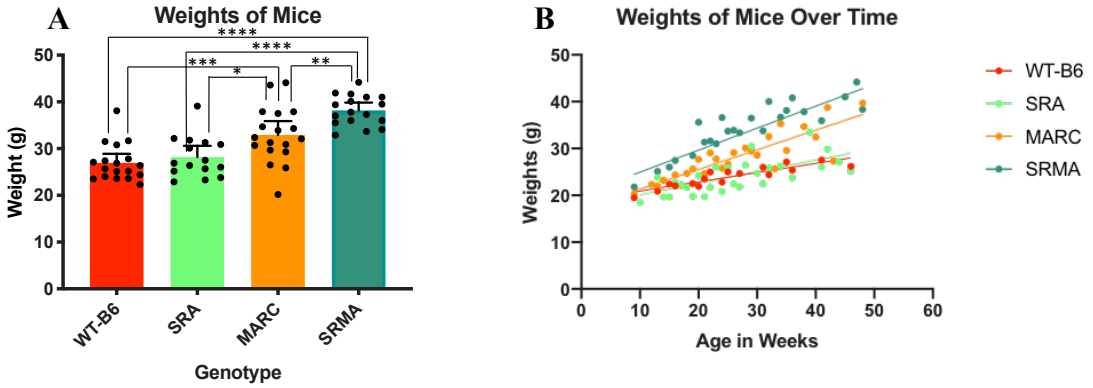

Figure 5.4.1.1: The graphs show the weights of mice in the immunisation experiment described in Chapter 4. The weights are given either at the end of the experiment (A) or plotted against individual age in weeks (B). A shows mean with 95% CI, each dot shows the result from one mouse, n = 16 - 18. Data were analysed using an ordinary one-way ANOVA with Tukey's multiple comparisons test. * = $p \leq 0.05$, ** = $p \leq 0.01$, *** = $p \leq 0.001$, **** = $p \leq 0.0001$. B shows the weight of the mice over time, each dot shows the average weight of mice at the given age. The mice in the experiment were age-matched as closely as possible. The average ages of the mice at the end of the experiment (A) are as follows: WT-B6 41 weeks, SRA = 42 weeks, MARC = 41 weeks, SRMA = 41 weeks. Abbreviations used: WT-B6 = C57BL/6 wildtype control, SRA = SR-A KO mice, MARC = MARCO KO mice, SRMA = SR-A/MARCO DKO mice.

At the end of the experiment, various tissues were harvested including gonadal fat. This fat pad was collected because previous tissue harvests with these mice had revealed that they tended to have particularly high levels of visceral fat, producing "pear-shaped" mice. Figure 5.4.1.2 shows the weights of these fat pads. The changes reflect those seen in body weight with larger fat pads in MARC and especially SRMA mice. These results suggest that the increased weight seen in these mice is due to excessive fat deposition.

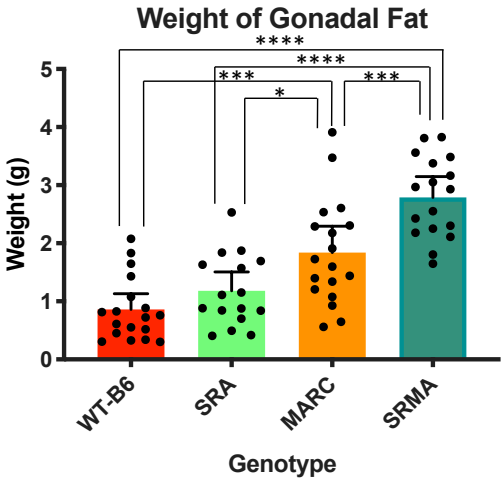

Figure 5.4.1.2: At the end of the immunisation experiment shown in Figure 5.4.1.1, the mice were culled and various tissues collected. One tissue collected were the gonadal fat pads, which were then weighed. The weights of the fat pads are shown in the graph. Data are shown as mean with 95% CI, each dot shows the result of one mouse, n = 16 - 18. Data were analysed using an ordinary one-way ANOVA with Tukey's multiple comparison test. * = $p \leq 0.05$, ** = $p \leq 0.01$, *** = $p \leq 0.001$, **** = $p \leq 0.0001$.

Despite the gain in weight, fasting blood glucose was not significantly higher amongst obese mice and there was no correlation between mouse weight and blood glucose. This is shown in Figure 5.4.1.3. This suggests that the mice did not have impaired insulin sensitivity. Overall, these results indicate that MARCO is required for the regulation of body weight and fat composition in mice. Moreover, it seems that SR-A is also either normally involved in this regulation or is able to at least partially compensate for the loss of MARCO. Hence, loss of both receptors enhances the phenotype.

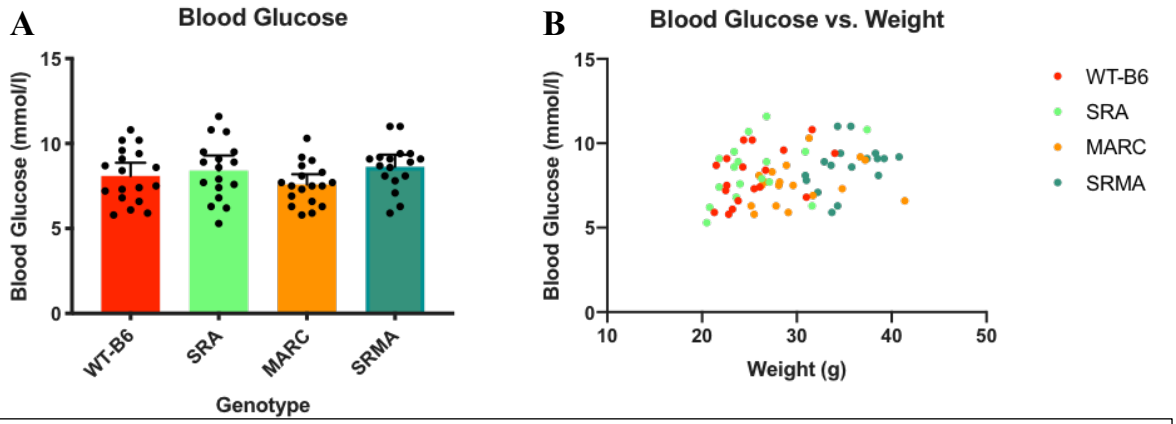

Figure 5.4.1.3: The blood glucose levels of the KO mice described in Figure 5.4.1.1 were also measured to examine whether the excess weight gain was also accompanied by worse blood glucose control. Mice were fasted for 5 – 6 h and then blood glucose levels measured. These are shown in A. The bars give mean with 95% confidence interval, each dot represents an individual mouse, n = 17 - 18. Data were analysed using an ordinary one-way ANOVA, there were no significant differences between groups. The data from A were plotted against the weight of the mice to give graph B. Each data point shows the result of an individual mouse. Data were analysed using Pearson's correlation coefficient, there was no significant correlation between weight and blood glucose for any of the genotypes.

5.4.2 Cohousing KO and WT Mice

Having observed this obesity phenotype, the next stage was to determine the underlying cause. To this end, an experiment was designed in which a young KO mouse was housed with a WT-B6 mouse of the same age. If the obesity phenotype was transferrable to the WT mice, this would suggest that changes in the microbiome may contribute. Whereas, if the WT-B6 mice were able to maintain a normal body weight, this would indicate that there was an intrinsic defect in metabolic regulation within the KO mice (Gérard 2017; Caruso et al. 2019). The grams of food eaten each week was also monitored to determine if the phenotype was simply due to excessive consumption.

Monitoring the weights of these mice confirmed the previous finding that SRMA and MARC are overweight and suggests that the obesity phenotype was unlikely to be due to the changes in the microbiome as the WT mice maintained a normal body weight (Figure 5.4.2.1.A). However, the mice housed with SR-A knockouts, either single or double, appeared to be slightly heavier (approximately 3g higher body weight) than those housed with MARC mice. This may indicate an altered microbiome, but further studies would be

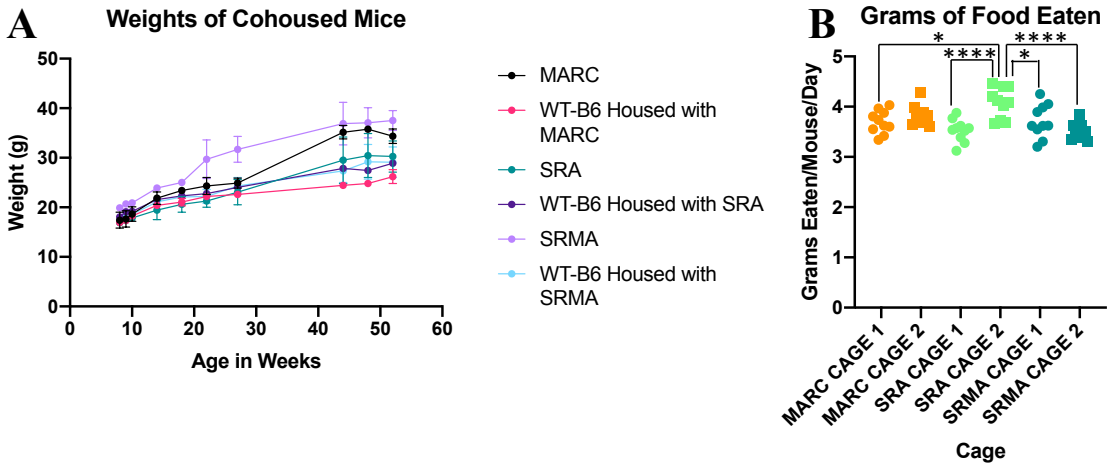

Figure 5.4.2.1: To examine whether the microbiome influenced the obesity phenotype, a KO mouse was paired with a WT-B6 control. The two mice were then cohoused for almost a year. A shows average weight of the cohoused mice over time, n = 2 per group. Each dot shows the mean weight at the given age and the error bars show range. The amount of food eaten by the mice in each of the cages was also measured and the results are shown in B. Each data point shows the average daily food intake per mouse over the course of one month. The data were analysed using an ordinary one-way ANOVA followed by Tukey's multiple comparison test, * = $p \leq 0.05$, **** = $p \leq 0.0001$

needed to confirm the effect and determine whether it was statistically and biologically significant.

As shown in Figure 5.4.2.1.B, the average food consumption by mice in each cage was generally similar between genotypes. The only cage which did have a significantly greater food consumption was the SRA cage 2, which ate a significantly greater amount of food compared to many of the other cages. The experiment suggests excessive food consumption was not a key cause of fat gain in KO mice as cages containing obese MARC or SRMA mice did not have a significantly greater food consumption than those containing non-obese SRA mice. However, it is not possible to determine consumption of individual mice using this method.

At harvest, tissues were collected and weighed as for the previous experiment. These data are shown in Table 5.4.1. This confirms that the SRMA and MARC mice have higher levels of gonadal fat than WT or SRA mice, and there are similar increases in s.c. fat and brown adipose tissue (BAT). Again this phenotype is more pronounced in the DKO SRMA mice. As before, the fasting blood glucose levels of the mice remain normal.

	MARC	WT-B6	SRA	WT-B6	SRMA	WT-B6
Body Weight (g)	34.4	26.2	30.3	28.9	37.5	29.10
Body Length (mm)	91.0	87.0	91.5	89.5	92.0	89.50
BMI (kg/m²)	4.148	3.475	3.623	3.608	4.431	3.638
Weight s.c. Fat (g)	1.121	0.433	1.076	0.630	1.652	0.890
Weight Gonadal Fat (g)	2.115	0.660	1.397	0.994	3.023	1.133
Weight BAT (g)	0.123	0.080	0.119	0.089	0.150	0.091
Weight Kidney (g)	0.196	0.180	0.180	0.199	0.216	0.195
Weight Spleen (g)	0.099	0.112	0.090	0.120	0.106	0.109
Blood Glucose (mmol/l)	6.6	7.1	7.65	6.95	6.45	6.35

Table 5.4.1: At the end of the cohousing experiment described in Figure 5.4.2.1, the mice were culled and various tissues collected. The weights of these tissues are given above. The results are the average of the 2 mice in each group. Results from cages containing a MARC mouse are colour coded orange, SRA mouse cages are green, and SRMA cages are turquoise. BMI = body mass index.

5.4.3 Immune Infiltration and Activation in Adipose Tissue

Having ruled out the microbiome or excessive food consumption as the principal cause of the weight gain in the KO mice, other routes through which SR loss may alter lipid metabolism were then considered. Firstly, as these are receptors of the immune system, one obvious possibility to consider was whether their loss might result in adipose inflammation. As discussed in the introduction, SR-A has been suggested to be critical to the development of "M2" anti-inflammatory macrophages. MARCO has also been reported to have an anti-inflammatory role. In the lungs of mice exposed to ozone, MARCO clearance of oxidised lipids was shown to reduce inflammation (Dahl et al. 2007). Therefore, it seemed possible that loss of SR-A and MARCO may shift the immune balance in the mouse towards pro-inflammatory responses which could alter the function of adipocytes and contribute to obesity. Even if these receptors do not have an overt anti-inflammatory role, it was possible that oxidised lipids and other inflammatory stimuli which might normally be cleared by these receptors in an anti-inflammatory fashion could instead be recognised by receptors which initiate pro-inflammatory responses. Again, this could lead to inflammation in adipose tissue.

To examine this, the stromal vascular fraction (SVF) was isolated from adipose tissue and immune populations within this fraction were examined. The SVF consists of the cell types remaining in tissue digests after adipocytes are removed. It includes immune cells, endothelial cells and preadipocytes (Bora and Majumdar 2017). Of particular interest were the adipose tissue macrophages (ATM), which are considered F4/80+ CD11b+ (Cho, Morris, and Lumeng 2014). ATMs make up the majority of the immune cell population in adipose tissue and, as discussed in this introduction, are involved in adipose tissue inflammation during obesity. The results from this experiment are shown in Figure 5.4.3.1. Overall, the percentage of CD45+ cells and macrophages were approximately the same

across all genotypes, the exception was SRA mice which had an increase in the percentage of ATMs. However, the SRMA and MARC mice do not show as obvious an increase which indicates no excessive recruitment of macrophages into adipose tissue in the mice.

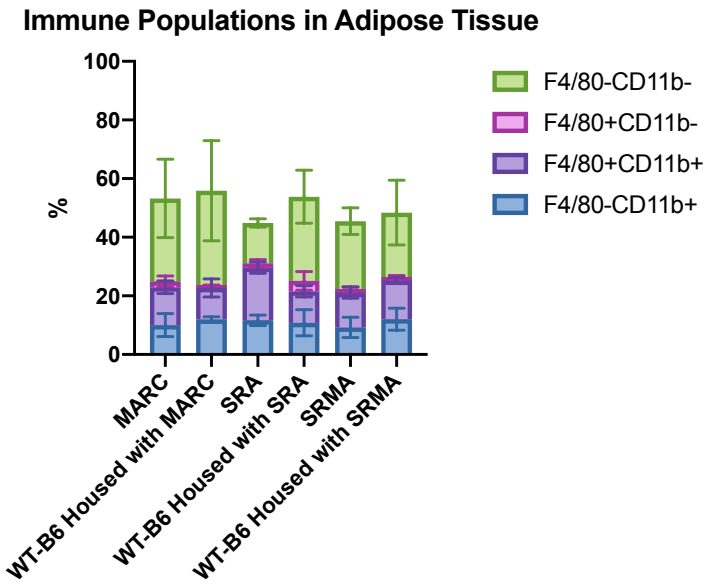

Figure 5.4.3.1: Gonadal adipose tissue from the mice in the cohousing experiment was enzymatically digested and the SVF fraction collected. The SVF cells were then stained for the pan-leukocyte marker CD45, and the macrophage markers CD11b and F4/80. The graph shows the percentage of SVF which expressed CD45+, and this population was further subdivided by expression of CD11b and F4/80. There are 2 mice per group and the bars show mean with error bars giving range. SVF = stromal vascular fraction. The SVF contains a variety of cell types including endothelial cells, preadipocytes and immune cells. It is what remains when adipocytes are removed from the cells isolated from adipose tissue.

The phenotype of the ATMs isolated from the different mice was then examined. The aim was to compare the expression of macrophage activation between WT and KO mice to determine if the obese KO mice had a higher expression of inflammatory macrophage markers than their WT counterparts. Three different markers were used to assess activation status of the ATMs: CCR2, MHC II and CD206. MHC II is a marker for "M1" like macrophages (Biswas and Mantovani 2010), whilst CCR2 is one of the chemokine receptors involved in migration of macrophages into adipose tissue and their polarisation towards an M1 phenotype (Oh et al. 2012; Bolus et al. 2015). The final activation marker in the panel is CD206, a receptor frequently used to define "M2" anti-inflammatory macrophages (Biswas and Mantovani 2010). Figure 5.4.3.2 shows the percentage of ATMs showing each of these markers. For all of the KO mice, the percentage of ATMs expressing CD206 is the same or higher than their WT cage mates. Additionally, mice lacking SR-A, either singly or

in the DKO, have a higher percentage of ATMs expressing CCR2 and MHC II compared to the WT controls. However, as the SRA mice do not generally gain excess weight and these changes are not seen in the MARC mice, these increases are unlikely to be the principal cause of the obesity phenotype.

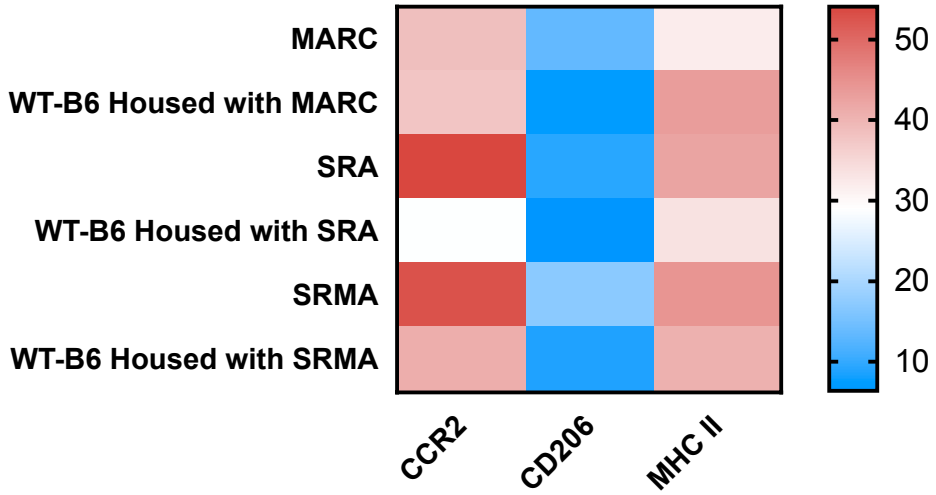

Figure 5.4.3.2: The SVF fraction isolated in Figure 5.4.3.1 were also stained for the macrophage activation markers CCR2, CD206 and MHC II. This was done in order to examine macrophage phenotype in cells isolated from KO mice compared to WT controls. The heatmap shows the average percentage of ATMs expressing markers CCR2, CD206 and MHC II, n = 2. ATMs = adipose tissue macrophages, this cell type was defined as F4/80+, CD11b+.

One final factor considered was whether there were changes in noradrenaline release in the KO mice. Noradrenaline is known to drive lipolysis and the fat content of this neurotransmitter is regulated by macrophages (Pirzgalska et al. 2017). The s.c. fat pads from each of the mice were therefore collected and the noradrenaline content was measured by ELISA. The results are shown, plotted against body weight, in Figure 5.4.3.3. The SRMA and MARC mice had an adipose noradrenaline content within the same range as the WT counterparts. This suggests excess weight gain in the MARC and SRMA mice is not due to loss of noradrenaline.

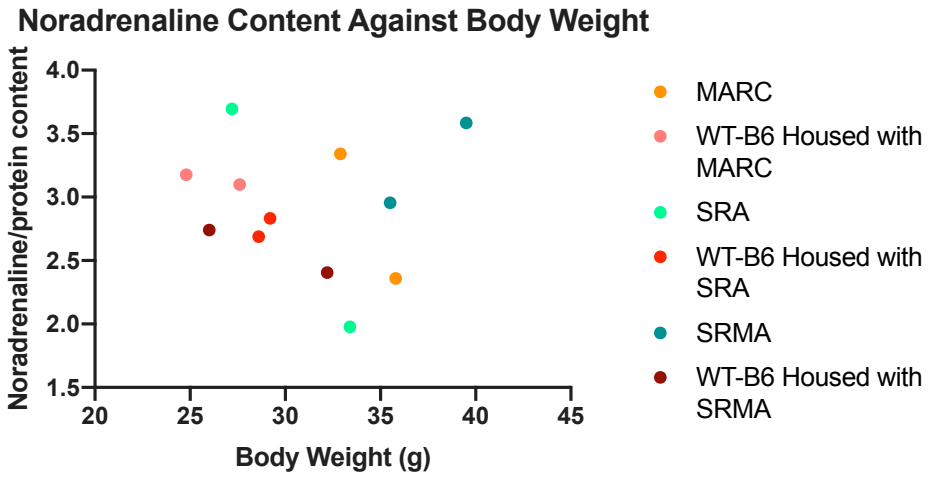

Figure 5.4.3.3: S.c. fat pads from the cohoused mice described in Figure 5.4.2.1 were also collected at harvest. These were homogenised and the noradrenaline content in the resultant supernatants measured by ELISA. The protein concentration in the supernatants were also measured and used to normalise the concentration of noradrenaline measured in the ELISA. The above graph shows the normalised fat pad noradrenaline content plotted against the weight of the mice. Each dot represents the results of one mouse.

5.4.4 Immune Populations and Triglyceride Content of Liver Samples

Another tissue collected at harvest was the liver. This tissue was collected because the liver is a key organ involved in lipid metabolism, with roles including oxidation/conversion of fatty acids and their transport into circulation. Moreover, along with adipose, these two tissues are major sites of fatty acid synthesis (Nguyen et al. 2008) . Changes to liver function could therefore have a significant impact on fat processing in the mice, and, importantly, MARCO is constitutively expressed in the liver. In mice it has been shown to be expressed exclusively on Kupffer cells derived from the yolk sack rather than bone marrow derived monocytes which have differentiated to become "Kupffer" like (Beattie et al. 2016). In humans MARCO expression is reported to define a population of "immune-regulatory" Kupffer cells present in the periportal region of the liver (MacParland et al. 2018). Therefore, it seemed likely that MARCO loss could affect these populations. Additionally, the liver can be a site of inappropriate lipid storage (steatosis), a condition known as non-alcoholic fatty liver disease. This change can results in liver inflammation, with release of pro-

inflammatory cytokines (e.g. TNFα) and chemokines such as CCL2 which recruit circulating monocytes leading to an expansion of the immune cell populations in the liver (Krenkel and Tacke 2017; Kim and Lee 2018). Liver samples were therefore analysed to determine whether there were changes to the proportions of immune populations in the liver. The liver triglyceride content was also measured as changes to this may indicate alterations in metabolism or inappropriate storage.

In the flow cytometry analysis, the liver samples showed a high degree of cell death and so required a different gating strategy. This involved first removing dead cells, followed by doublets and finally cell debris, as outlined in Figure 5.4.4.1. Next, macrophage/monocyte populations in the liver were examined. There are two broad macrophage populations in the liver, resident Kupffer Cells and liver monocyte-derived macrophages (MoMF). There is some controversy in the literature concerning the markers for these populations, with different studies suggesting different levels of CD11b expression in Kupffer cells. However,

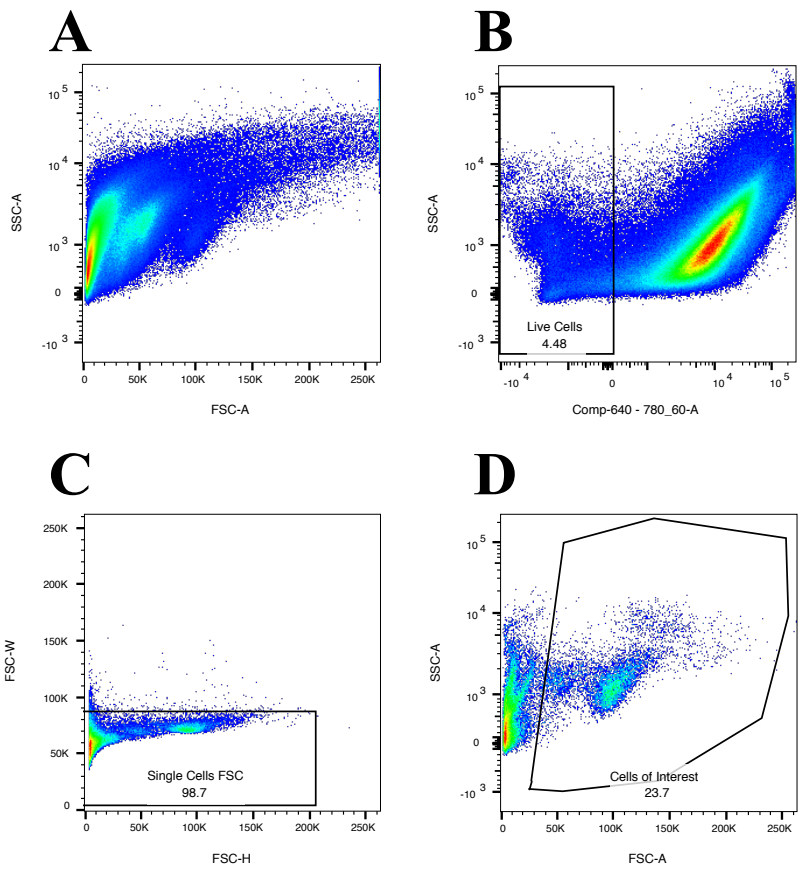

Figure 5.4.4.1: Liver samples were also collected at the end of the cohousing experiment. As for the gonadal fat pads, cells were then isolated from the tissue samples by enzymatic digestion. The cells were then analysed by flow cytometry. A gating method used to remove doublets, cell debris and dead cells throughout the rest of this thesis is described in the Materials and Methods. However, due to high levels of cell death in the liver samples a different gating strategy was adopted for flow cytometry analysis. The starting point is shown in A. This strategy started by removing dead cells using a live/dead stain (B). This made subsequent steps to remove doublets (C) and cell debris (D) easier to gate.

generally it seems that MoMFs are defined as F4/80^{+} CD11b^{hi}, whilst the Kupffer cells are considered to be CD11b$^{-/lo}$ (Elchaninov et al. 2019). Another population worth considering in the liver are infiltrating monocytes, these will be F4/80^{-}, CD11b^{+} and a proportion will be Ly6C+ (Krenkel and Tacke 2017). The results are shown in Figure 5.4.4.2. Overall, the populations are broadly the same between the KO mice and their WT controls, suggesting no overt inflammation, as this is usually accompanied by recruitment of monocyte-derived macrophages, or loss of these populations in the SR KO mice.

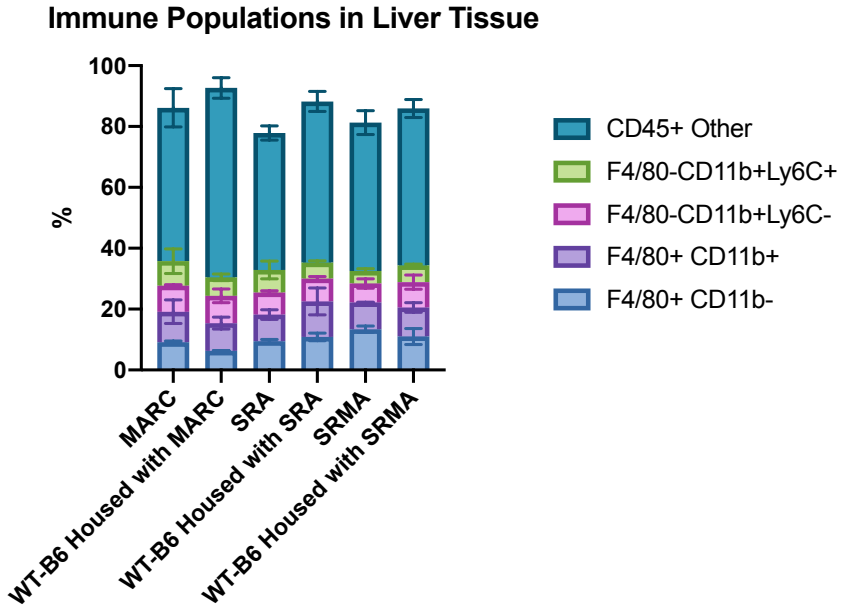

Figure 5.4.4.2: Liver cells were isolated by enzymatic digestion from tissue samples collected from cohoused mice. These were then stained for CD45 and markers of macrophage or monocyte identity (F4/80, CD11b and Ly6C). Expression of these markers was analysed by flow cytometry. Shown in the graph is the percentage of cells which expressed CD45, divided into CD45+, F4/80+, CD11b- cells (most likely Kupffer cells), CD45+ F4/80+ CD11b+ cells (predominantly MoMFs), CD45+ F4/80- CD11b+ cells (monocytes, which can be further subdivided based on expression of Ly6C), and other CD45+ cells. There were 2 mice in each group and the bars show mean with range.

With regard to fat storage, liver triglyceride content in the MARC and SRMA mice was the same or higher than their WT counterparts and across the populations there was a statistically significant correlation between body weight and liver triglyceride content (Figure 5.4.4.3). Overall, the data indicate a moderate increase in fat content in the liver of the obese mice, which may indicate that excess lipid storage is not limited to the adipose tissue.

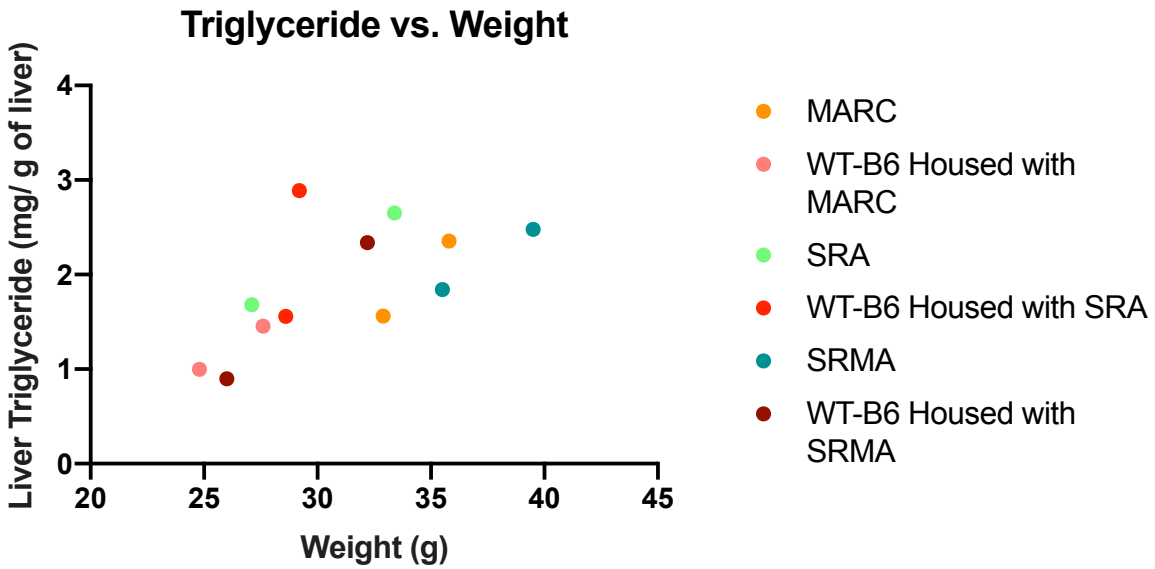

Figure 5.4.4.3: Liver samples were also collected from cohoused mice in order to measure the liver triglyceride content of the SRA, SRMA and MARC mice, and their WT-B6 cage mates. The liver triglyceride content was plotted against weight of the mice in order to produce the above graph. Correlation between liver triglyceride and weight was assessed using Pearson's correlation coefficient, the p value = 0.0252. Each dot shows the result from one mouse.

5.4.5 Immune Populations in the Spleen and Lymph Nodes (LNs)

I also examined immune populations in the spleens of the KO mice. This began as a project to understand the results seen in Chapter 4 in which loss of SR-A seemed to increase the immune responses to AGE-modified proteins. This may be as a result of proteins being shuttled into different processing pathways for presentation, or alternatively changes in the balance of macrophage/DC populations may favour the uptake by DCs and subsequent presentation to T cells. The spleen was examined because it has a variety of macrophage and DC populations and so could give an overview of changes to these populations in the different KO mice (Hey and O'Neill 2012). Moreover, MARCO is strongly expressed in the marginal zone macrophage subset in the spleen (A-Gonzalez and Castrillo 2018). Mice lacking this receptor have defective organisation of the marginal zone, a phenotype even more pronounced in mice also lacking SR-A (Chen et al. 2005). Consequently, there was

already a precedent to suggest changes would be seen here which may be of relevance to the results of the immunisation study.

I designed a flow cytometry panel to examine a variety of myeloid populations within the spleen. The spleen consists of 4 distinct macrophage populations: red pulp macrophages, white pulp macrophages, marginal zone macrophages and marginal zone metallophilic macrophages. Each has a distinct function and can be identified by their distinctive marker expression. Red pulp macrophages are found in the red pulp of the spleen where they remove senescent red blood cells, and can be defined as CD11b+, F4/80+, CD68+ (Hey and O'Neill 2012). White pulp macrophages appear in the spleen post weaning, at the same time as germinal centres. Their main role is to phagocytose apoptotic B cells which die during B cell maturation in germinal centres (A-Gonzalez and Castrillo 2018). These macrophages also express CD68 but can be distinguished from red pulp macrophages by their lack of F4/80. Next, are the macrophages of the marginal zone, marginal zone and marginal zone metallophilic macrophages, which are involved in the recognition and clearance of blood-borne pathogens (A-Gonzalez and Castrillo 2018). In addition to MARCO, the marginal zone macrophages express a variety of other PRRs and CD209b can be used as a marker (Hey and O'Neill 2012). Finally, there are the marginal zone metallophilic macrophages, which can be identified by their expression of CD169. Unfortunately, it was not possible to reliably detect CD169 staining. This lectin can be internalised during cell isolation for flow cytometry so may have been lost before staining (A-Gonzalez and Castrillo 2018). Alternatively, this may indicate a problem with the panel/antibody, or that it was not possible to isolate this cell type using the enzymatic digestion method employed here. The classical DC population in the spleen was also examined. This can be divided based on the expression of CD8a and CD11b into CD8a+CD11b- and CD11b+CD8a- groups.

In order to examine the myeloid populations across the spleen simultaneously, FlowSOM analysis was used (Van Gassen et al. 2015). This is a dimensionality reduction tool which identifies different populations in samples based on marker expression. Changes in the size of populations between genotypes can be identified as changes in the size of the circles. Representative FlowSOM plots are shown in Figures 5.4.4.1 – 5.4.4.3. Overall, there are only minor differences between the plots for KO mice and their WT-B6 controls. For the MARC and SRMA mice this was somewhat surprising as previous reports had shown that these mice have a loss of marginal zone macrophages (Chen et al. 2005). This may indicate that the enzymatic digestion used to isolate cells here cannot be used to isolate this population. Alternatively, it may not be possible to identify this population with flow cytometry. As with CD169, CD209b can be internalised during cell processing for flow cytometry which makes identification of the marginal zone macrophages challenging with this method (A-Gonzalez and Castrillo 2018). A CD209b+ population is identifiable in the FlowSOM plots. However these may represent a DC population as a CD209b+ MHC II+ population in the spleen with DC like properties has been previously reported (Lyszkiewicz et al. 2011).

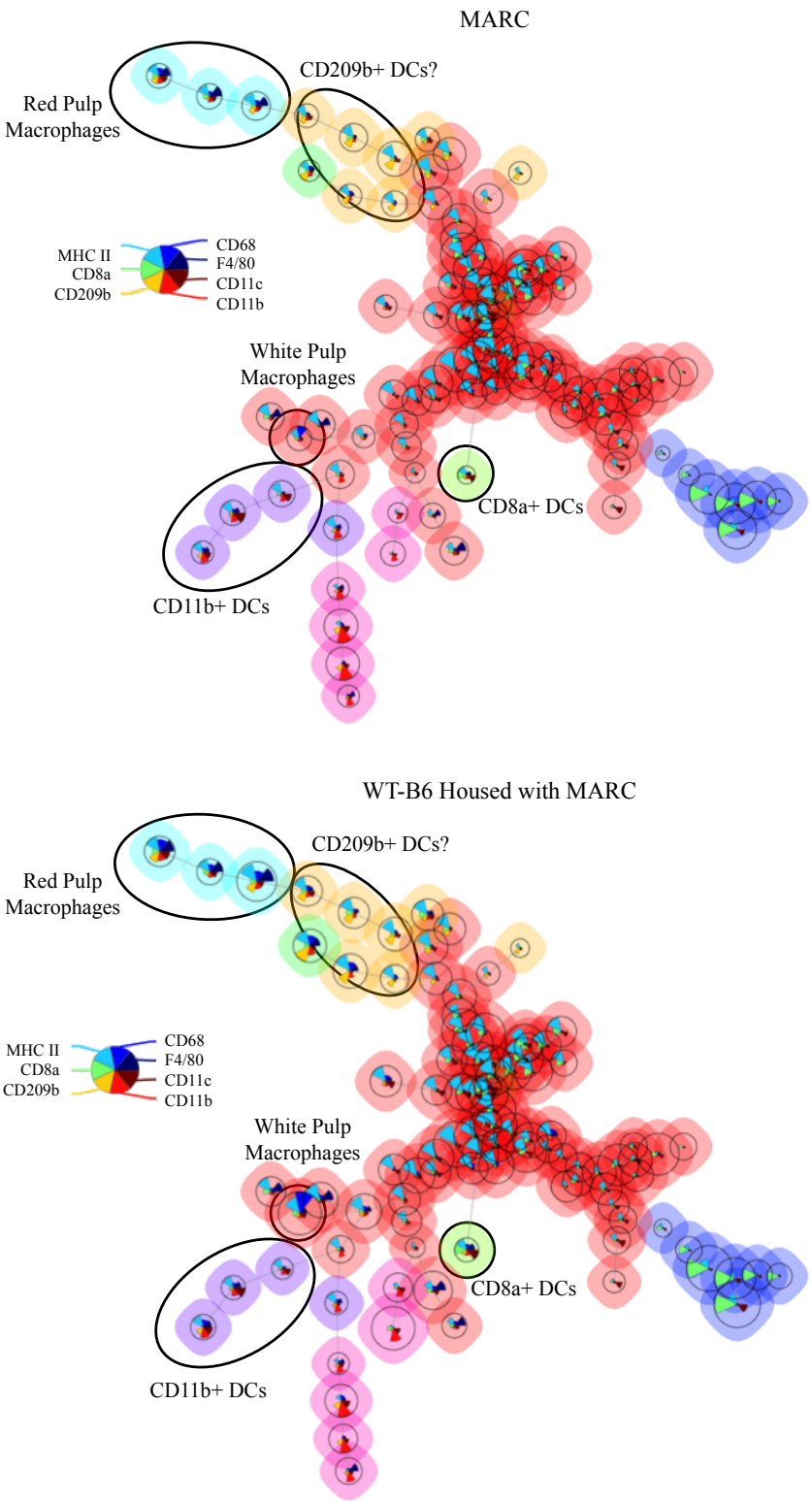

Figure 5.4.5.1: Spleens were also collected from the cohoused mice. These were enzymatically digested, and the resultant cells were stained for macrophage and DC markers then analysed by flow cytometry. The data were used to make FlowSOM plots. This is a dimensionality reduction tool which can be used to assess changes in immune cell populations. Each circle represents a different population which are grouped into clusters by colour. The size of the circle shows the size of the population. Inside the circle is a pie-chart showing which markers are present in each population and level of expression. Shown above are representative plots for MARC mice (top) and WT-B6 Housed with MARC (bottom). Based on marker expression, specific populations of interest have been identified. The plots are representative of data from 4 MARC and 4 WT-B6 mice (2 each from the co-housing experiment and 2 others). SOM = self-organising map

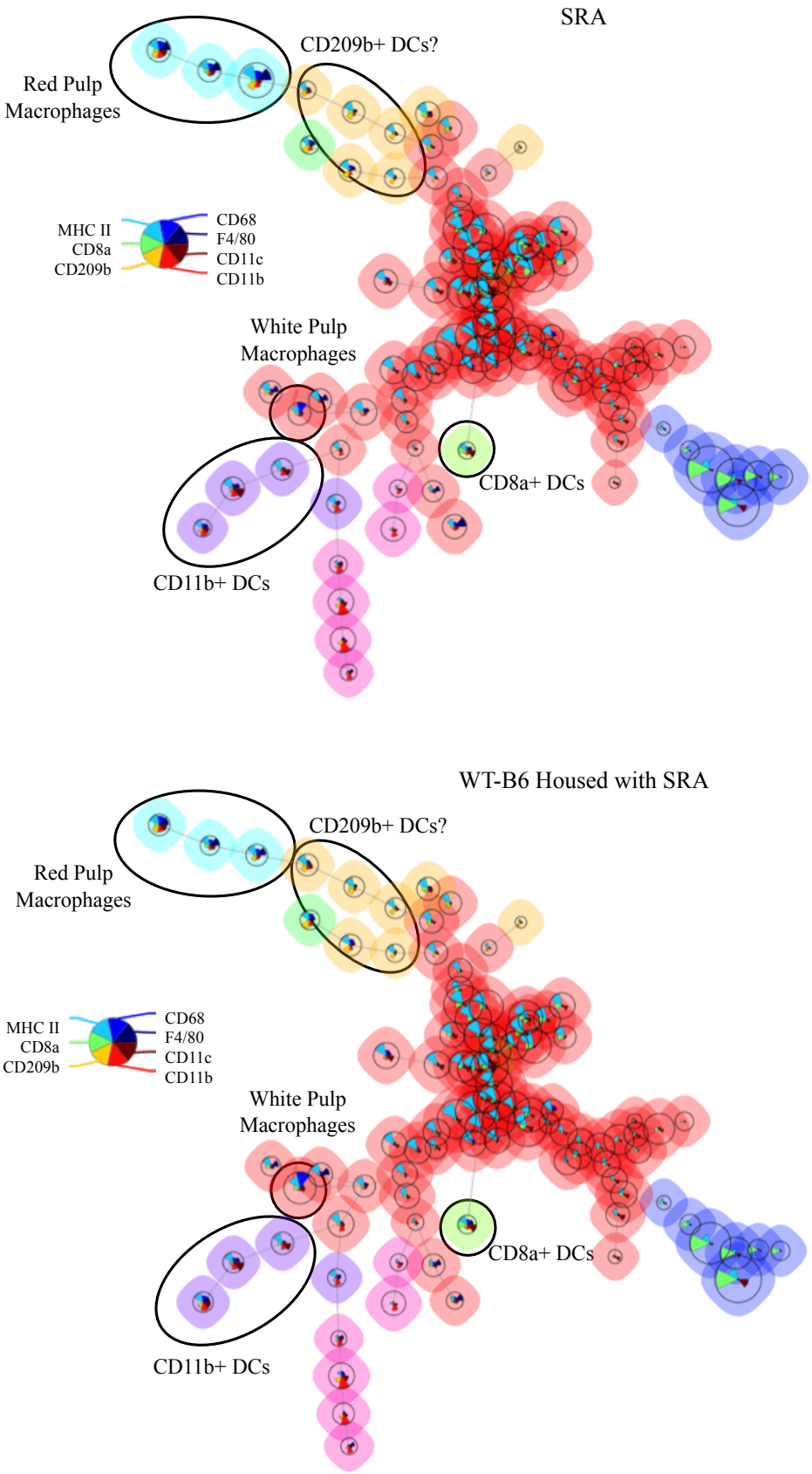

Figure 5.4.5.2: Representative FlowSOM plots for SRA mice (top) and WT-B6 Housed with SRA (bottom). For a description of a FlowSOM plot, see Figure 5.4.5.1. Data are representative of FlowSOM plots from 3 SRA mice (2 from the co-housing experiment and one other) and 2 WT-B6 mice from the co-housing experiment.

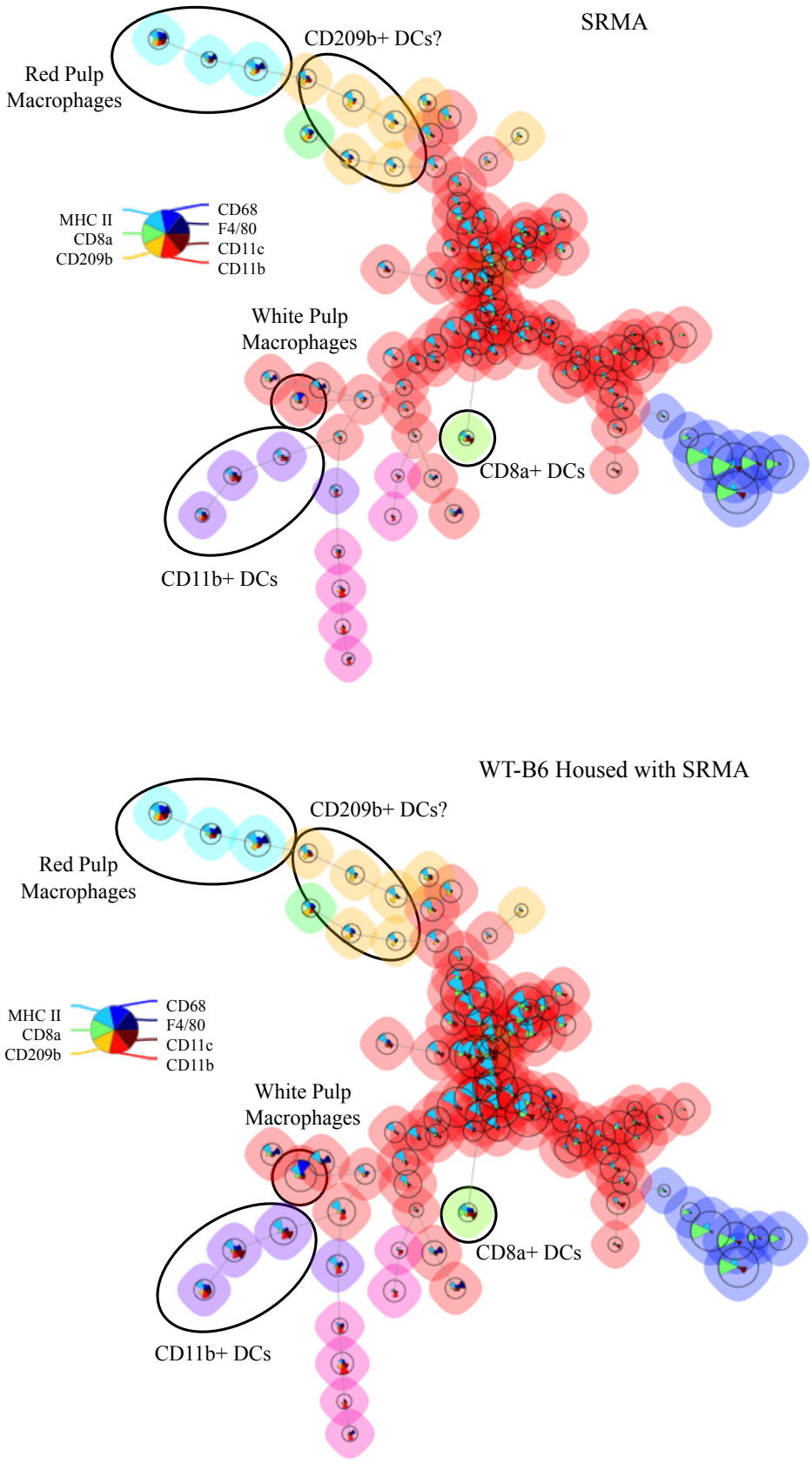

Figure 5.4.5.3: Representative FlowSOM plots for SRMA mice (top) and WT-B6 Housed with SRMA (bottom). For a description of a FlowSOM plot, see Figure 5.4.5.1. Data are representative of FlowSOM plots from 4 SRMA mice (2 from the co-housing experiment and 2 others) and 2 WT-B6 mice from the co-housing experiment.

Another immune tissue examined were the LNs. Auxiliary, inguinal and mesenteric LNs were removed from the mice and a flow cytometry panel was designed to examine changes to T cell populations. The results are shown in Figure 5.4.4.5.A, for most of the genotypes CD3 T cell populations are essentially identical, however, in SRMA mice there is an increased percentage of T cells. This increase is especially apparent in the CD8 T cell population. As SRMA mice have the biggest increase in weight, the increase in the T cell population may also be of relevance to the obesity phenotype. However, if this were the case an increase in the MARC mice would also be expected. In Figure 5.4.4.5.B and C the CD4 and CD8 T cell populations were divided based on the expression of the activation markers CD69 and CD25, these are expressed as a percentage of the total population in the lymph node. The percentage of cells which are positive for CD69 and/or CD25 is not substantially different between the genotypes or their WT controls.

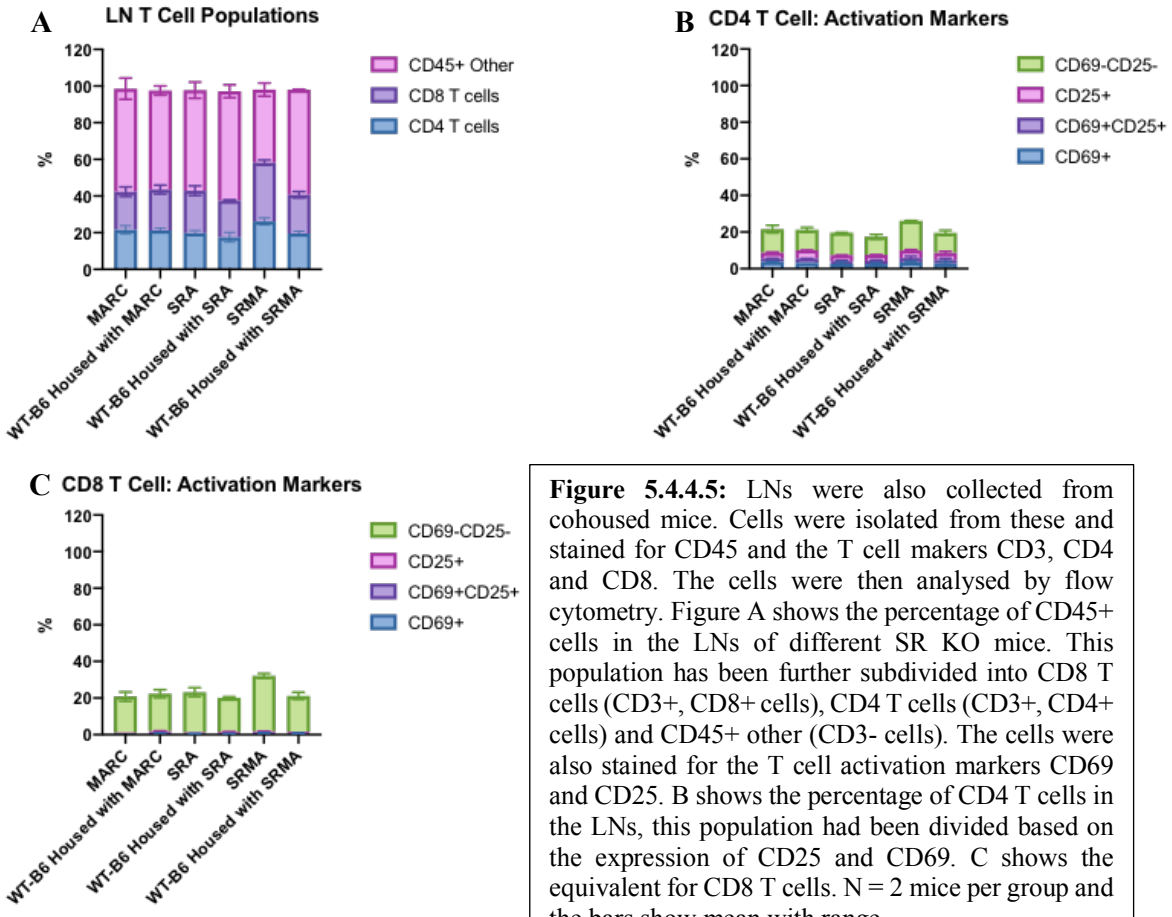

Figure 5.4.4.5: LNs were also collected from cohoused mice. Cells were isolated from these and stained for CD45 and the T cell makers CD3, CD4 and CD8. The cells were then analysed by flow cytometry. Figure A shows the percentage of CD45+ cells in the LNs of different SR KO mice. This population has been further subdivided into CD8 T cells (CD3+, CD8+ cells), CD4 T cells (CD3+, CD4+ cells) and CD45+ other (CD3- cells). The cells were also stained for the T cell activation markers CD69 and CD25. B shows the percentage of CD4 T cells in the LNs, this population had been divided based on the expression of CD25 and CD69. C shows the equivalent for CD8 T cells. N = 2 mice per group and the bars show mean with range.

5.5 Discussion and Conclusions

This project started with the observation that mice lacking MARCO, especially those also lacking SR-A, have a significantly greater body weight than WT or SR-A single KO mice, a phenotype due to excess fat deposition. Whether this excess weight gain is accompanied by any metabolic disease is still a matter of investigation, however, the data collected do not show any evidence of this. The fasting blood glucose levels remained normal, however this is a simple screening test which may not completely reflect the basal steady state in the mice. More advanced tests, such as a glucose or insulin tolerance test, would give a better indication of insulin sensitivity in the mice (Ayala et al. 2010). Similarly, the results from the flow cytometry analysis do not suggest that there is increased immune cell recruitment to the adipose or liver tissue or that there is a switch to a more pro-inflammatory phenotype amongst the ATMs, at least in the MARC mice. Histological analysis of the adipose tissue would allow us to confirm the absence of enhanced macrophage infiltration, to examine the distribution of the cells and whether the adipocyte have become hypertrophied. These are all pathological changes seen in obesity (González-Muniesa et al. 2017).

There were signs of a switch to a proinflammatory phenotype in the SRA and SRMA mice, most notably in the enhanced expression of M1 markers in the ATM population. Moreover, the increases in the T cell populations in the SRMA mice may be of relevance to the obesity phenotype as T cells have also been suggested to contribute to inflammation in obesity (Zhao et al. 2018). As with macrophages, T cells in obese adipose tissue are reported to shift from a Th2 to a Th1 phenotype with secretion of cytokines such as IFNγ. These cytokines enhance macrophage activation and adipocyte dysfunction. HFD-induced obesity has also been reported to result in enlarged visceral LNs in mice and alter the immune populations present, including decreasing Tregs (Magnuson et al. 2017).

Overall, what is most striking is how little deviation there seems to be from the WT controls for the MARC mice. As discussed above, the immune populations remain mostly similar to their WT cage-mates in relation to size and activation status. Moreover, triglyceride content is only mildly increased in the livers of these mice and they maintain an adipose noradrenaline content similar to the WT controls. Therefore, it seems most likely that there is another factor driving fat deposition which is not addressed here, such as changes to lipid metabolism. Given the evidence indicating enhanced inflammation in the SRMA mice, one possibility is that in the SRMA mice, the inbuilt error in the MARC mice is combined with a tendency towards pro-inflammatory responses, and it is this which enhances the obesity phenotype.

This project is still at a very early stage and there is much more which could be done to further define the obesity phenotype and understand why it has developed. Logically, there must be a defect in the MARC and SRMA mice at a minimum of one of three points. Firstly, they may have excessive intake of lipids or other nutrients which result in increased fat storage. This could be at the level of food intake or later in the digestive process where extra fat may be absorbed in the intestine. Secondly, the mice may have reduced energy expenditure, resulting in fat accumulation on the same diet. For example, the mice may be less physically active than their WT counterparts. Finally, food intake and overall energy expenditure may be the same between WT and KO mice, but in the KO mice other metabolic processes are downregulated to favour the storage of lipids in adipose tissue.

There are several experiments which could be performed to address the above hypotheses. Firstly, the food intake monitoring in the cohousing experiment suggests that excessive food consumption is unlikely to be the principal cause of the observed phenotype. However, as these mice were cohoused with WT-B6 it is impossible to determine the exact amount eaten by each mouse and it is possible that the KO mice were consuming excess food whilst

preventing the WT-B6 from eating. This seems unlikely as if this was the case a weight reduction in the WT mice housed with obese mice would also be expected. However, it would be important to address this by monitoring food intake in cages containing a single genotype. An alternative hypothesis is that compensatory upregulation of other SRs in the MARC/SRMA mice may increase lipid absorption in the intestine and in turn lead to excess weight gain. This has been reported before in other mouse models of obesity. Petersen et al. concluded that excessive weight gain in mice with genetic deletion of MyD88 specifically in T cells was due to a microbiome-mediated increase in CD36 expression. This in turn resulted in increased lipid uptake in the gut (Petersen et al. 2019). Attempts were made to investigate this by flow cytometry with staining for SRs, however it was not possible to obtain robust staining with this method which may indicate receptor loss during isolation or poor quality of antibody (data not shown). This factor therefore needs more thorough examination.

Changes to physical activity and energy expenditure can be easily monitored with metabolic cages (Song et al. 2014). Disruption to metabolic processes could be examined at many levels, for example by examining changes to metabolites in plasma to see if triglyceride or other lipid metabolites were altered between genotypes (Kaabia et al. 2018). It is also possible to use a bulk screening technique such as RNAseq to examine whether there are changes to the usage of different metabolic pathways between the different SR KO mice (Temate-Tiagueu et al. 2016).

Chapter 6: The Role of RAGE in AGE Immunogenicity

6.0 Abstract

RAGE is a promiscuous receptor known to bind a diverse range of ligands, including AGEs, and initiate inflammatory signalling. It is particularly associated with chronic inflammation, and some evidence indicates that it is involved in the development of adaptive immune responses. However, whether it is involved in the enhanced immunogenicity of AGE-modified proteins has not been investigated *in vivo.* In this study, RAGE knockout (KO) or wildtype (WT) control mice were immunised with unmodified, glycolaldehyde (GA)-modified, glucose (GLUC)-modified or (carboxymethyl)lysine (CML)-modified hen egg lysozyme (HEL). The development of antibody and splenocyte responses was then assessed. Neither WT or RAGE KO mice developed significant anti-HEL antibodies, however in both genotypes significant splenocyte responses developed in mice immunised with HEL GLUC which did not differ in magnitude. These results demonstrate that RAGE is dispensable for AGE-mediated enhanced immunogenicity. However, these studies did reveal that mice lacking RAGE have significantly lower body fat than WT controls and have cells which are strongly autofluorescent.

6.1 Introduction

6.1.1 The Receptor RAGE and its Ligands

As its name suggests, the receptor for advanced glycation end products (RAGE) was first identified based on its capacity to bind to AGEs. A 1992 study from Schmidt et al. identified a 35 kDa protein in lung tissue which bound specifically to AGE-modified proteins (Schmidt et al. 1992). In a subsequent study, DNA encoding this protein was isolated from bovine and human lung tissue which was found to be a previously unidentified member of the immunoglobulin superfamily (Neeper et al. 1992). Expression of this receptor in 293 cells was shown to give these cells to capacity to bind to AGEs, hence the name RAGE. However, it is now recognised that this is a multi-ligand receptor capable of binding to a wide variety of endogenous and exogenous ligands which share little structural similarity (Hudson and Lippman 2018). The first of the non-AGE ligands to be identified was HMGB1 (high mobility group box 1), a DNA binding protein secreted actively by immune cells and passively by dying cells. Other endogenous ligands include many members of the S100 family, amyloid-β proteins and extracellular DNA. RAGE has also been shown to bind to LPS independently of TLR4 and can bind to synthetic single-stranded DNA which resembles unmethylated microbial DNA. Binding of ligands to RAGE initiates inflammatory signalling cascades resulting in the secretion of inflammatory cytokines, activation of immune cells and their recruitment to affected sites (Kierdorf and Fritz 2013). Thus, RAGE functions as a PRR capable of binding both DAMPs and PAMPs. Unlike other members of the PPR family, such as TLR4, which are evolutionarily ancient, RAGE is a relatively recent addition to the immune repertoire and is found exclusively in mammals (Sessa et al. 2014).

Structural studies have given insights into how RAGE is able to bind such a diverse range of ligands. RAGE is a transmembrane protein consisting of a large extracellular domain,

single transmembrane helix and a short C-terminal cytoplasmic domain. The extracellular domain has three Ig-like subdomains: a V-type at the N-terminus followed by two C-type domains (Neeper et al. 1992). Structural characterisation has demonstrated that the V-type and the first C-type domain form a single structural unit joined to the C2 domain by a short flexible linker (Dattilo et al. 2007). This structural unit is termed VC1 and ligands for RAGE bind almost exclusively to this region (Kierdorf and Fritz 2013). In the V region, highly conserved arginine and lysine residues form positively charged patches and a positively charged patch is also found in the C1 region (Koch et al. 2010). Thus, the VC1 domain contains an electropositive surface, whilst in contrast the C2 domain is negatively charged (Hudson and Lippman 2018). A schematic of this structure is shown in Figure 6.1.1.A. Moreover, RAGE molecules have been shown to preassemble into multimers on the cell surface and this multimerization is required for RAGE signalling (Xue et al. 2016; Xie et al. 2008). These two features, positive charge and multimerization, are thought to be key for ligand specificity as RAGE ligands universally have the capacity to form higher order oligomers and are negatively charged (Hudson and Lippman 2018).

The cytoplasmic domain of RAGE lacks enzymatic activity and so activation of intracellular signalling is mediated by adaptor proteins, most notably mDia1 (Hudson and Lippman 2018). Ligand binding induces structural changes in RAGE which allow this adaptor to bind. Various downstream signalling pathways can then be activated by RAGE including MAPKs (e.g. ERK 1 /2), PI3K/Akt and Rho GTPases (e.g. Cdc42). These in turn activate transcription factors such as NF-κB, Egr-1 and STAT3, which induce expression of proinflammatory genes including cytokines (e.g. IL-6, TNFα and CCL2) and adhesion molecules (e.g. vascular cell adhesion molecule 1) (Kierdorf and Fritz 2013). The exact response depends on a variety of factors including cell type, the identity of the ligand and its concentration.

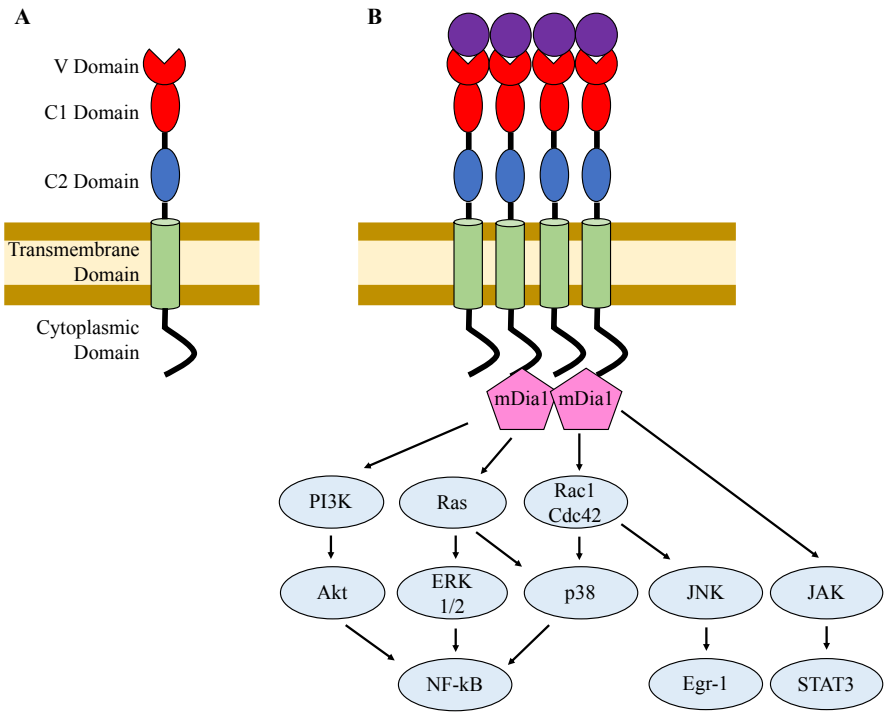

Figure 6.1.1: The structure of the receptor RAGE is shown in A. This receptor has a short cytoplasmic domain which lacks enzymatic activity, a single transmembrane domain and a large extracellular domain. The latter consists of a negatively charged C2 domain and positively charged V and C1 domains which combine to form a single unit. B gives a simplified signalling pathway showing some of the downstream pathways which result in inflammatory signalling. This is based on a figure from Hudson and Lippman 2018 and the KEGG pathway database.

Under normal circumstances expression of RAGE is low, apart from in lung tissue where it is constitutively expressed. However this receptor is strongly upregulated in chronic inflammatory states (Hudson and Lippman 2018). Activation of RAGE not only releases inflammatory signals but also increase the expression of both RAGE and NF-κB. Moreover, the proinflammatory state induced by RAGE promotes the development of its ligands by causing tissue damage and activation of immune cells. Therefore, signalling through RAGE can create a positive feedback loop as high levels of RAGE and NF-κB overcome negative regulation, resulting in further inflammation which creates new RAGE ligands to continue the cycle. Thus RAGE can sustain the inflammatory state resulting in chronic inflammation (Kierdorf and Fritz 2013). *In vivo* signalling can be moderated through the production of alternative splice variants which are non-functional. The most common version lacks the transmembrane and cytoplasmic domains and is secreted into the extracellular space

(esRAGE). A similar product can be produced when full length RAGE is cleaved by the metalloproteases ADAM10 and MMP9, releasing the soluble extracellular domain (sRAGE). These products can act as competitors for RAGE ligands. Moreover, these products and other signalling incompetent RAGE isoforms are thought to participate in RAGE multimerization, inhibiting signalling in a dominant-negative fashion (Kierdorf and Fritz 2013; Hudson and Lippman 2018).

6.1.2 RAGE in Metabolic Disease

Given the role of RAGE in maintaining chronic inflammation, it is not surprising that this receptor is implicated in the pathogenesis of a number of inflammatory conditions including Alzheimer's disease, diabetes and cardiovascular disease (Hudson and Lippman 2018). During diabetes, higher circulating glucose levels promote the formation of AGEs which drive diabetic complications. Diabetic rodent models using RAGE inhibition, either through genetic KO or treatment with sRAGE, have implicated the AGE-RAGE axis in these complications as this treatment is protective against atherosclerosis, nephropathy, peripheral neuropathy and retinal damage (Hudson and Lippman 2018). Moreover, studies in humans have also implicated RAGE in the development of diabetic complications, including atherosclerosis and myocardial infarction (Egaña-Gorroño et al. 2020).

RAGE is also implicated in the pathogenesis of obesity. As discussed in the previous chapter, this is also characterised by chronic inflammation. In human s.c. adipose tissue, obese subjects had significantly higher levels of CML, a specific AGE known to be a ligand for RAGE, compared to healthy controls (Gaens et al. 2014). RAGE protein levels were also increased in the adipose tissue of these individuals. Similarly, mice fed a high fat diet (HFD) have an increased expression of RAGE compared to healthy controls (Song et al. 2014). When the effects of this diet were compared in WT and RAGE KO mice, the RAGE KO

mice gained significantly less weight, were resistant to hyperglycaemia and showed better insulin sensitivity despite having the same food intake. Bone marrow transplant studies indicated that this effect was at least in part mediated by immune cells. However, subsequent studies using adipocyte-specific RAGE KO mice have shown these mice are also protected from HFD-induced obesity (Hurtado Del Pozo et al. 2019). Thus, RAGE may contribute to the development of obesity through multiple mechanisms. It should also be noted that another group has reported the exact opposite finding, with weight gain being increased in RAGE KO mice on HFD compared to WT controls (Leuner et al. 2012).

6.1.3 RAGE and Adaptive Immune Responses

In addition to promoting inflammation, it has also been suggested that RAGE influences the development of adaptive immune responses (Kierdorf and Fritz 2013). With regards to the initiation of T cell responses, RAGE expression is reported to be critical for the migration of DCs to the lymph nodes (LNs) in mice (Manfredi et al. 2008). Moreover, for both mice and humans RAGE blockade, either by genetic loss or antibody inhibition, has been shown to prevent upregulation of costimulatory molecules and cytokine secretion by LPS-matured DCs *in vitro* (Dumitriu et al. 2005). However, in other studies, migration and maturation of RAGE KO DCs was found to be normal (Moser et al. 2007). Instead, this paper concluded that T cells require RAGE for normal function as loss of this receptor inhibited their proliferation in both *in vitro* and *in vivo* stimulation assays. RAGE seems to be particularly important for the development of Th1 responses as the loss of cytokine response was specific for type 1 cytokines. Moreover, expression of RAGE is specifically upregulated during the differentiation of Th1 cells (Chen et al. 2008). Therefore, the exact relationship between RAGE and the adaptive immune system is still controversial.

Regardless, these papers indicate that there are several mechanisms by which RAGE could influence the development of immune responses to AGE-modified proteins. Firstly, RAGE may initiate inflammation in response to AGE-modifications on the protein immunogens. Similarly, AGE-RAGE signalling on DCs may promote their maturation and migration to LNs. Although the evidence in Chapter 3 indicated that DCs do not mature in response to AGE-modified proteins, this work was done *in vitro* using BMDCs which do not fully resemble natural DCs. Alternatively, AGEs may more directly influence the activation of T cells through RAGE receptors expressed on these cells. One simple experiment which can be done would be to immunise RAGE KO mice (referred to as RAGE mice in this thesis) with AGE-modified proteins. This would show whether this receptor is dispensable for the development of immune responses to AGE-modified proteins seen in previous chapters.

6.2 Hypothesis and Aims

Hypothesis: AGE-mediated enhanced immunogenicity is due to inflammatory signalling through RAGE.

Aims

1. To test the immunogenicity of AGE-modified proteins in RAGE mice

6.3 Materials and Methods

A list of methods used in these studies is shown below. For full details please refer to the indicated sections in the Materials and Methods.

- Glucose, GA and CML Modification (2.2.2 - 2.2.4)
- Flow Cytometry (2.3.6)
- Mouse Origin and Care, and Immunisation Protocols (2.4.1, 2.4.3)
- Fasting Blood Glucose Measurements (2.4.5)
- Tissue Harvesting (2.4.6)
- IgG, IgG1, IgG2a and IgG2c ELISAs (2.5.1)
- Splenocyte Harvest, Cytokines ELISAs, Thymidine Pulse (2.6.1-2.6.3)
- Isolation of cells from Spleen, Liver, LNs and Fat (2.7.1-2.7.4)
- Measurement of Liver Triglyceride Content (2.7.5)
- Statistical Analysis (2.9)

6.4 Results

6.4.1 Immunisation Studies Using RAGE Mice

As discussed in the introduction, signalling through RAGE is one possible mechanism by which AGE-modification could enhance the immunogenicity of proteins. It was therefore decided to assess the contribution of this receptor to *in vivo* AGE immunogenicity. To do this, RAGE mice were acquired and used for the same type of immunisation experiment as for the SRA/MARC/SRMA mice (see Chapter 4). The RAGE mice could not be included in this experiment as they were on a different background sub-strain, namely C57BL/6N. Despite both being B6, the C57BL/6J and C57BL/6N differ substantially from each other in a number of different parameters including in their immune responses (Simon et al. 2013). It was therefore important to include the appropriate WT C57BL/6N controls in order to confirm that any differences were due to lack of RAGE and not background stain. Additionally, a HEL CML group was included in this experiment because CML has been identified as a key AGE ligand for RAGE (Kislinger et al. 1999). Therefore, this modification may be more likely to show a dependency on RAGE with regard to immunogenicity. The immunisation schedule is given in Figure 6.4.1.1.

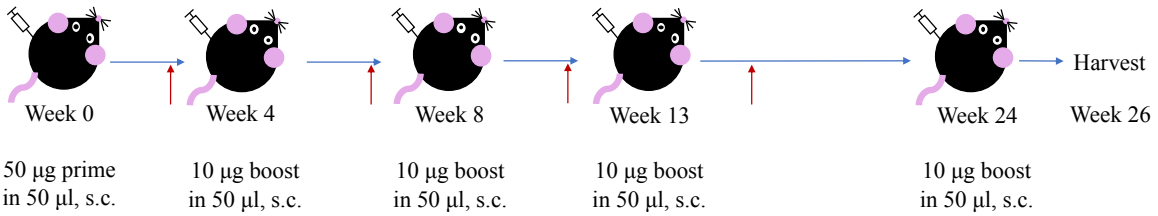

Figure 6.4.1.1: RAGE and WT-B6N mice were acquired. These were then immunised with HEL 3 h, HEL GA 3 h, HEL CML HIGH or HEL GLUC according to the protocol given above. The red arrows indicate when sera was collected. Abbreviations used: RAGE mice = RAGE KO mice, WT-B6N mice = C57BL/6N WT controls, HEL 3 h = HEL incubated at 37 °C for 3 h, HEL GA 3 h = HEL incubated with glycolaldehyde (GA) at 37 °C for 3 h, HEL CML HIGH = HEL modified to add CML for 24 h, HEL GLUC = HEL incubated with glucose at 37 °C for 24 weeks.

The development of anti-HEL antibody responses was followed over the course of the experiment. Figure 6.4.1.2 shows both the average response over time and area under the curve (AUC) measurements. As can be seen, the majority of the mice failed to develop anti-

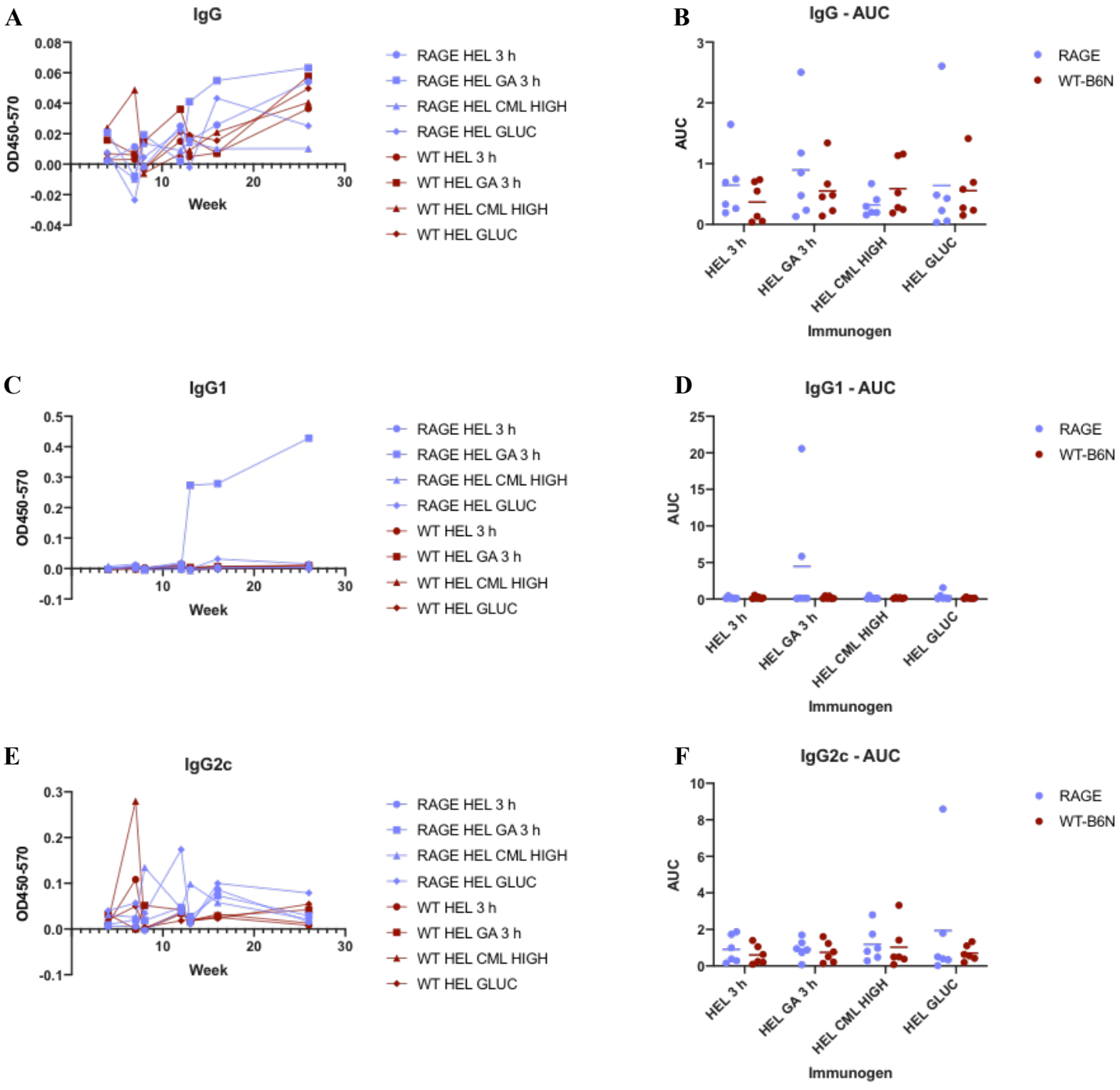

Figure 6.4.1.2: RAGE mice WT-B6N controls were immunised according to the schedule outlined in Figure 6.4.1.1. Sera was collected at the indicated time points and analysed for the development of anti-HEL antibodies (total IgG, IgG1 and IgG2c) over the course of the immunisation. The average results for each group over time are shown in A, C and E, whilst area under the curve (AUC) measurements for individual mice are shown in B, D and F. In B, D and F each dot shows the results of an individual mice whilst the bars show mean. There were no significant differences between groups (two-way ANOVA). OD = optical density.

HEL antibodies even after five immunisations. The only mice which developed anti-HEL antibodies were RAGE mice and 2/3 mice which developed a detectable response were immunised with HEL GA 3 h. However, overall there were no significant differences between groups. In previous pilot experiments using RAGE mice, they had been able to develop strong antibody responses when HEL was injected with adjuvant (complete Freund's adjuvant followed by a boost in incomplete Freund's adjuvant). So whilst these mice can respond with sufficient immune stimulation, they clearly require a stronger innate stimulus than can be provided by the GA 3 h modification alone.

In contrast to the antibody response, significant splenocyte responses did develop (Figure 6.4.1.3). Starting with the thymidine incorporation results, strong proliferation was seen almost exclusively in mice immunised with HEL GLUC. For WT-B6N mice, the difference between the response in the HEL and HEL GLUC groups was significant and there was a strong trend in the RAGE mice. Moving to the cytokine data, significant IL-2 and IL-5 responses were apparent in the HEL GLUC groups compared to the HEL groups for both RAGE and WT-B6N. Interestingly, only the WT-B6N in this group developed a significant IFNγ response. The HEL GLUC immunised mice did not have a significantly greater IL-4 secretion compared to HEL immunised in either genotype.

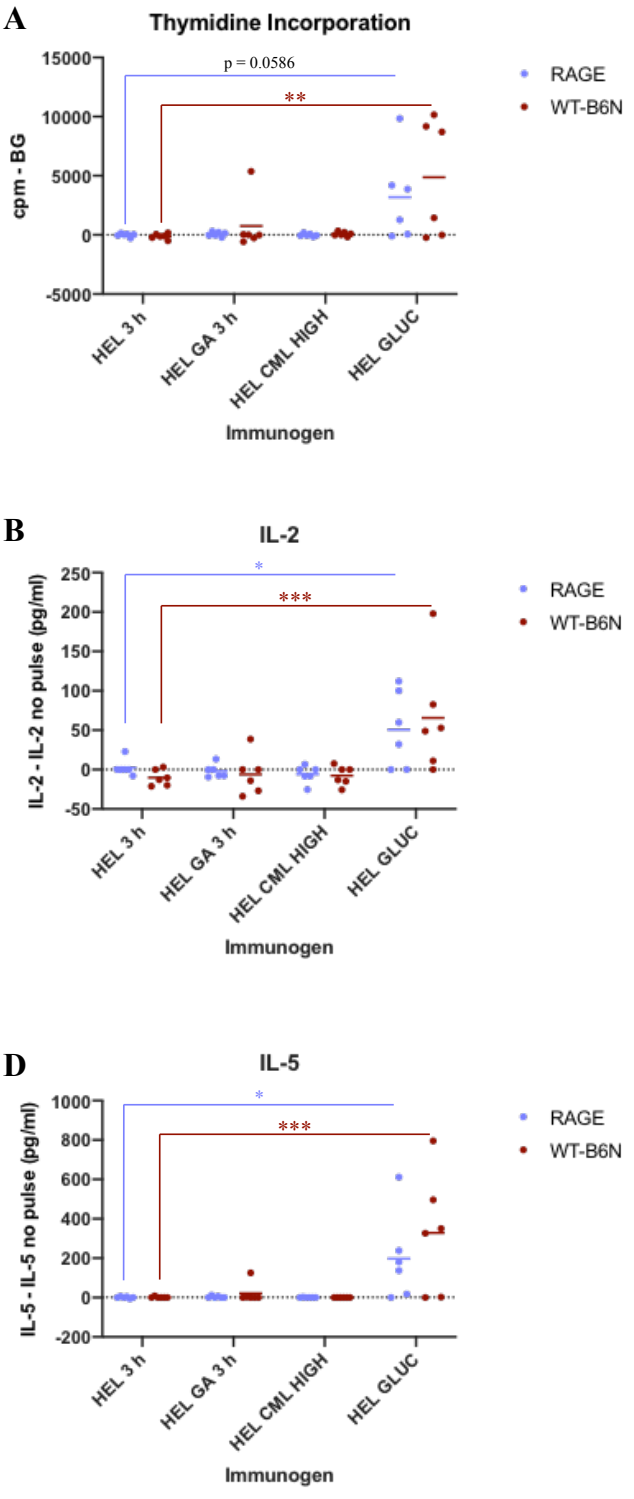

Figure 6.4.1.3: Spleens from RAGE and WT-B6N mice immunised with the indicated protein sample according to the protocol in Figure 6.4.1.1 were harvested at week 26. Isolated splenocytes were pulsed with HEL and proliferation and cytokine secretion assessed by thymidine incorporation (A) and ELISA (B-E) respectively. Unpulsed cultures were used as a background measure in all assays. For thymidine incorporation, splenocytes were pulsed with ^{3}H-thymidine on day 3 and cell radioactivity measured the following day. IL-2, IL-5 and IFNγ secretion was assessed in supernatant collected on day 3, whilst day 1 supernatant was used for IL-4 secretion. Data were analysed using a two-way ANOVA followed by Dunnett's multiple comparison test, * = $p \leq 0.05$, ** = $p \leq 0.01$, *** = ≤ 0.001. Each dot shows the result of an individual mouse and the bars show mean. Abbreviations used: cpm = counts per minute, BG = background.

Proliferation was also assessed by flow cytometry, these results are shown in Figure 6.4.1.4. The results broadly match the thymidine and cytokine data with significantly increased proliferation (and in the case of the RAGE mice, cell survival) in the HEL GLUC immunised group. Looking at the identity of these cells, it can be seen that the majority of this increase is due to expansion of the CD19+ B cell compartment. In contrast, the percentage of proliferating T cells is not significantly different between treatment groups. This is an interesting finding given that the HEL GLUC mice did not develop significant IgG antibody responses.

Examining the splenocyte data collectively, the RAGE HEL GLUC mice had slightly lower responses than the WT-B6N controls for the thymidine and cytokine data. However, for the flow cytometry analyses the two genotypes had very similar percentages of proliferating cells in the HEL GLUC group. Overall, there were no significant differences between the two genotypes for any of the measures. Therefore, it seems RAGE is unlikely to be a key mediator of the enhanced immunogenicity of AGE-modified proteins. Certainly, mice lacking this receptor can develop strong splenocyte responses to GLUC modified proteins. It may be possible that the role of the receptor can be easily compensated for by another receptor(s) or that other receptors are more critical to the development of immune responses to AGE-modified proteins.

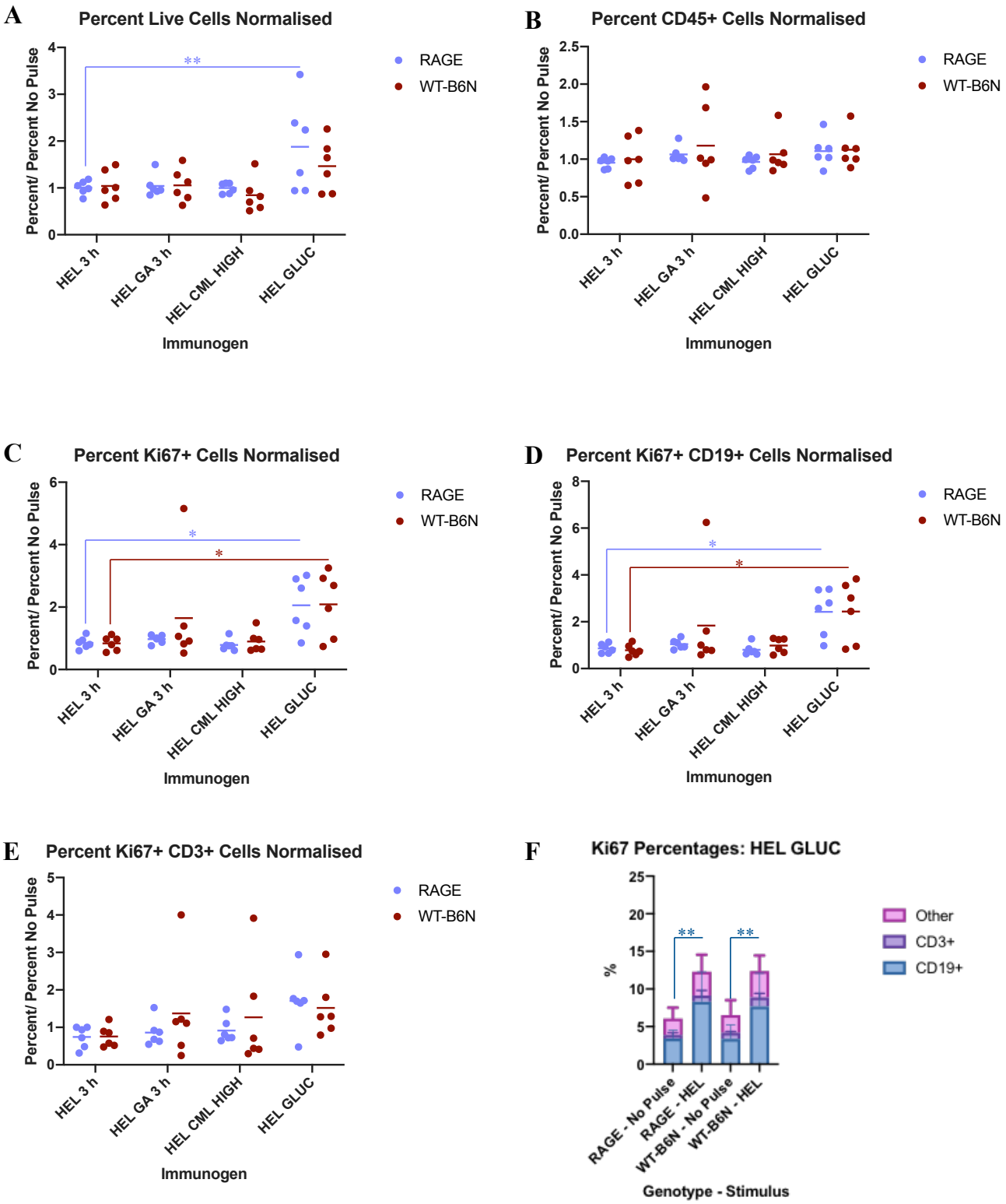

Figure 6.4.1.4: Splenocyte proliferation in the cultures described in 6.4.1.3 was also assessed by flow cytometry. Cells were collected on day 4 then stained for CD45 (general leukocyte marker), CD3 (T cell marker), CD19 (B cell marker) and Ki67 (marker of proliferation). Included are graphs showing the normalised percentage of live cells in the cultures (A) and the percentage of these which are CD45+ (B). Expression of Ki67+ cells amongst CD45+ cells was then assessed (C). This population was further divided into those expressing CD19 (D) and CD3 (E). In all cases, the percentage in the HEL pulsed cultures was divided by the percentage in the unpulsed cultures to account for background proliferation. The raw percentages of Ki67+ cells in splenocyte cultures from HEL GLUC immunised mice are shown in F. The Ki67+ population was divided into cells expressing CD3 (T cells), CD19 (B cells) or neither receptor (other). Data were analysed using a two-way ANOVA followed by Dunnett's or Tukey's multiple comparison test, * = $p \leq 0.05$, ** = $p \leq 0.01$. A-E show the responses of individual mice with the mean, whilst F shows the average response of the 6 mice with standard deviation (SD).

6.4.2 Underweight Phenotype in the RAGE Mice

The weights of the RAGE and WT-B6N mice were followed over the course of the immunisation experiment. Figure 6.4.2.1 shows both the weight at the end of the experiment and the weight change over time. As can be seen, the RAGE mice are significantly lighter than their WT counterparts, although the actual difference in average weight is fairly small (29.4458 g vs 26.15 g). However, when the weight of the adipose tissue is examined, the difference between the two genotypes is much more apparent, with the RAGE mice carrying approximately half the gonadal fat of their WT-B6N controls. Clearly, the mice lacking RAGE have an altered lipid content and this could be the result of different non-mutually exclusive mechanisms. Firstly, they may have problems gaining or producing fats, which could be due to reduced consumption, fat absorption in the intestine, or lipogenesis. Secondly, there may be a problem with lipid storage. Finally, the RAGE mice may have an increased capacity for metabolising fat.

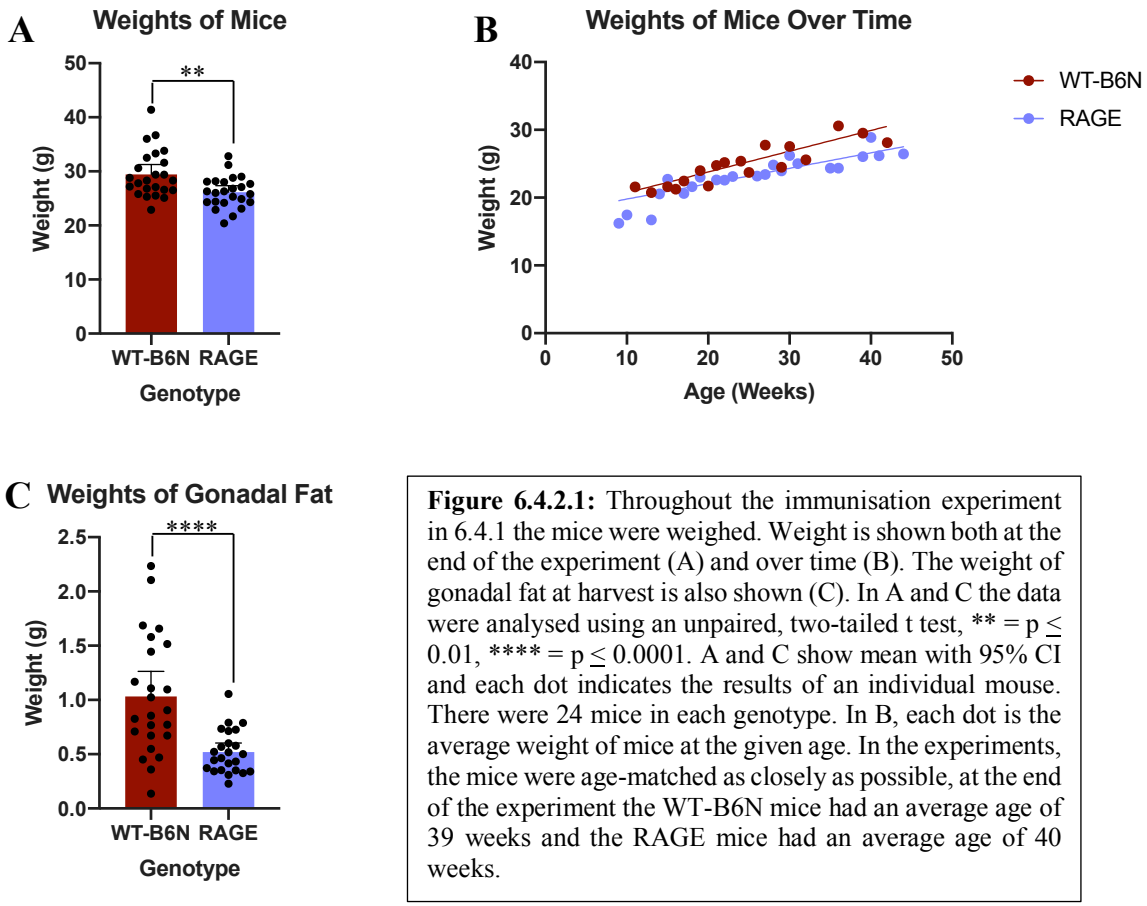

Figure 6.4.2.1: Throughout the immunisation experiment in 6.4.1 the mice were weighed. Weight is shown both at the end of the experiment (A) and over time (B). The weight of gonadal fat at harvest is also shown (C). In A and C the data were analysed using an unpaired, two-tailed t test, ** = $p \leq 0.01$, **** = $p \leq 0.0001$. A and C show mean with 95% CI and each dot indicates the results of an individual mouse. There were 24 mice in each genotype. In B, each dot is the average weight of mice at the given age. In the experiments, the mice were age-matched as closely as possible, at the end of the experiment the WT-B6N mice had an average age of 39 weeks and the RAGE mice had an average age of 40 weeks.

One basic method to examine the metabolic state of the mice is to measure their fasting blood glucose. Impaired control of blood glucose is indicative of problems with insulin regulation and it is known that loss of insulin results in weight loss with a higher blood glucose (Daneman 2006). As shown in Figure 6.4.2.2, the RAGE mice seemed to have a slightly higher fasting blood glucose level, but this was not significant ($p = 0.1241$, unpaired two-tailed t test). There was also no significant correlation between the weight of the mice and the blood glucose level.

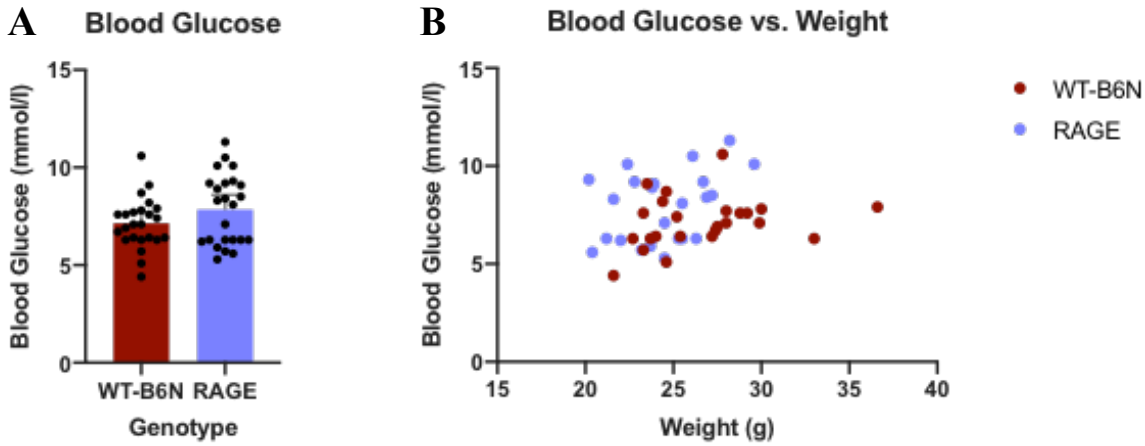

Figure 6.4.2.2: Fasting blood glucose was measured in the RAGE and WT-B6N mice from Figure 6.4.2.1 (A), there was no significant difference between genotypes (unpaired, two-tailed t test). When fasting blood glucose is plotted against weight (B), there is no significant correlation between the two variables for either group (Pearson's correlation coefficient). A shows mean with 95% CI and in both graphs each dot represents an individual mouse. There were 24 mice in each genotype.

Finally, liver samples were assessed to examine whether the RAGE mice also had alterations in their liver triglyceride content. With regards to fat, this is another important organ to consider as it has key roles in lipid metabolism (Nguyen et al. 2008). The results are shown in Figure 6.4.2.3. They demonstrate that the triglyceride content in the livers of WT-B6N and RAGE mice is on average almost identical and there are no significant differences between the genotypes. Overall, the RAGE mice clearly have some metabolic/lipid processing modification but the blood glucose and liver triglyceride content appear normal.

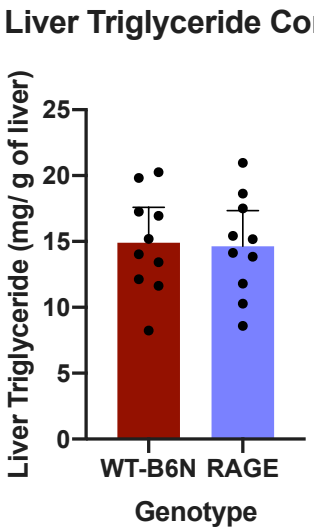

Figure 6.4.2.3: The triglyceride content was measured in liver samples from RAGE and WT-B6N mice. There was no significant difference between the two genotypes (unpaired, two-tailed t test). The bars show mean with 95% CI, each dot shows the result of an individual mouse. There were 10 mice in each group.

6.4.3 RAGE Mice Have Autofluorescent Cells

During flow cytometry experiments, it was noted that cells freshly isolated from immune tissue samples of RAGE mice were highly autofluorescent, most notably in the 488-530/30 channel. This phenomenon is shown in Figure 6.4.3.1 which includes example plots of

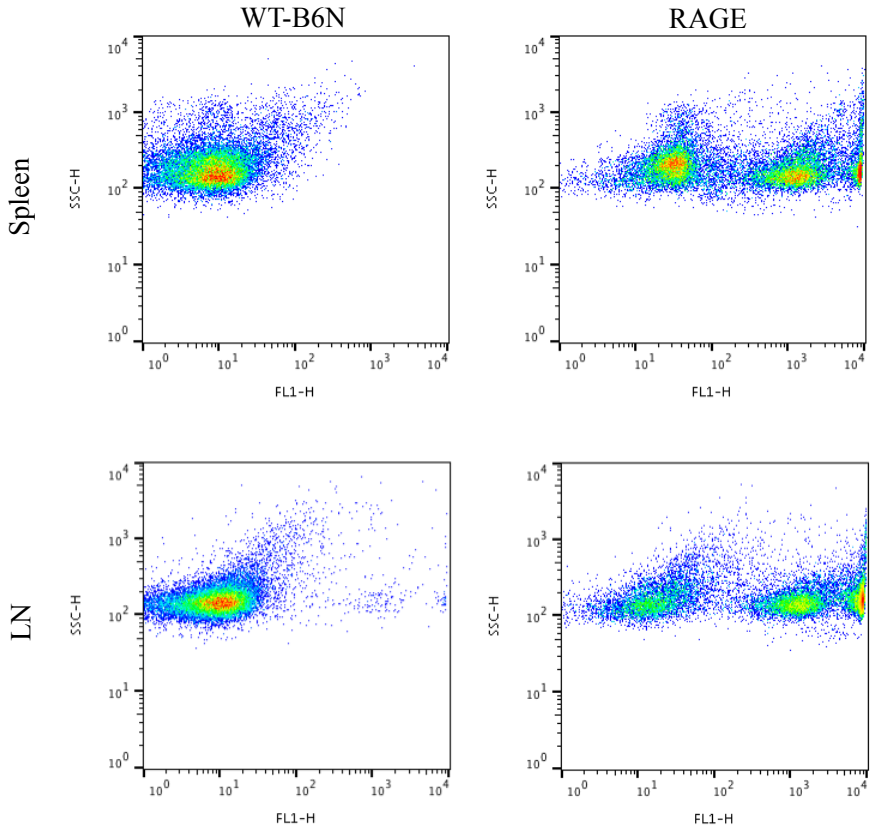

Figure 6.4.3.1: Unstained cells freshly isolated from the spleens and LNs of WT-B6N and RAGE mice were analysed by flow cytometry. The plots show the signal in the FL1/488-530/30 channel. The cells were pooled from three mice. Abbreviations used: LNs = lymph nodes, SSC = side scatter.

unstained cells from the spleens and LNs of WT-B6N and RAGE mice. Whilst the WT-B6N are clearly negative, in both tissues the RAGE mice have three distinct populations of either low, medium or high autofluorescence. In previous experiments with splenocyte cultures from the immunised mice, the RAGE cells did not have this phenotype. This could be due to differences in the staining procedure as the cells were fixed with ethanol to assess proliferation, or this autofluorescence may be lost with time spent in tissue culture as these cells were stained after 4 days.

To further probe this phenomenon the identity of the cells in the different fluorescent populations was examined. The aim was to determine whether the low, medium and high autofluorescence groups contained the same cell types, or whether specific cell types could be segregated by level of autofluorescence. Cells isolated from these tissues were therefore stained for immune cell markers. The results for the spleen are shown above in Figure 6.4.3.2. The majority of cells in this tissue are in the medium autofluorescence category, indeed the proportion of cells showing low autofluorescence is very low. The spleen contains a large number of different immune populations which can require complex panels to differentiate, so the initial characterisation started with a narrow search. It was decided to focus specifically on the F4/80 population as other studies have indicated that this marker is often associated with autofluorescent cells and it can be used to identify red pulp macrophages in the spleen (Mitchell et al. 2010; Hey and O'Neill 2012). Dividing the CD45+ population by F4/80 expression we can see that the majority of the high autofluorescent cells express this macrophage marker. The medium autofluorescence group is made up predominantly of CD45+, F4/80- cells. This group is therefore most likely made up of the other immune cells in the spleen including T and B cells. Also shown in this figure is a comparison between the WT-B6N and RAGE, the proportion of CD45+ cells expressing F4/80 is very similar between the two genotypes.

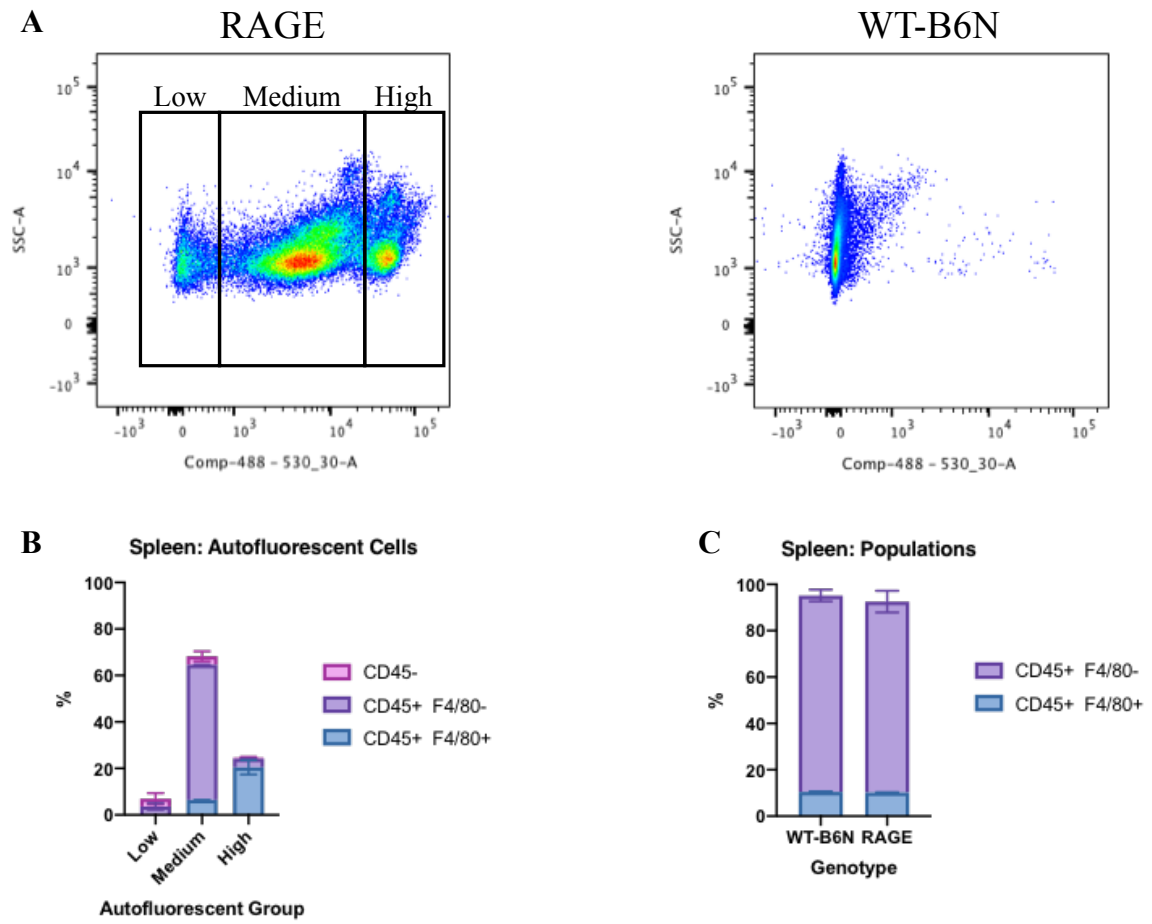

Figure 6.4.3.2: To determine the identity of the autofluorescent cells in the spleen, the population was divided into 3 groups: low, medium and high. These are shown in A. The expression of the pan-leukocyte marker CD45 and macrophage marker F4/80 in these populations was then examined. B shows the percentage of cells in each autofluorescence group expressing these markers. Also shown is a comparison between RAGE mice and WT-B6N (C). All of the fluorescent groups in the RAGE mice were combined for the comparison in C. There are two mice in each group and the bars show mean with range.

The results for the LN are shown in Figure 6.4.3.3. For this tissue, the majority of cells were in the high autofluorescence group. In the LN, the high autofluorescent cells were almost exclusively T cells, both CD4+ and CD4-. The medium autofluorescence groups was made up predominantly of non-T cell leukocytes, identified as CD45+ CD3- cells. Again, this figure includes a comparison between the WT-B6N and RAGE mice. The proportions of the CD4+/- T cell populations are almost identical between the two genotypes. The expression of the activation markers CD25 and CD69 amongst the CD4 T cells was also examined, again there were no substantial differences between genotypes.

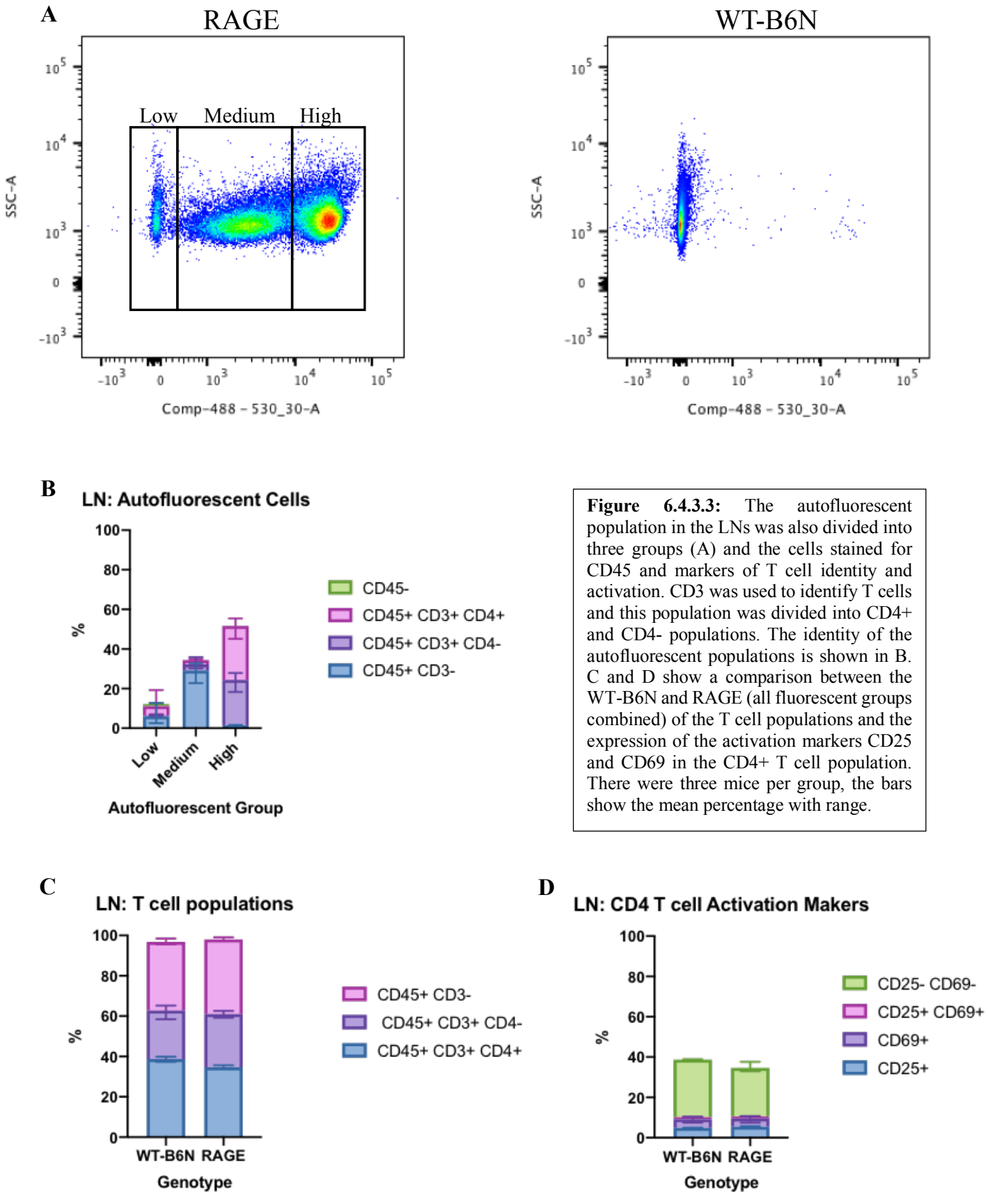

Figure 6.4.3.3: The autofluorescent population in the LNs was also divided into three groups (A) and the cells stained for CD45 and markers of T cell identity and activation. CD3 was used to identify T cells and this population was divided into CD4+ and CD4- populations. The identity of the autofluorescent populations is shown in B. C and D show a comparison between the WT-B6N and RAGE (all fluorescent groups combined) of the T cell populations and the expression of the activation markers CD25 and CD69 in the CD4+ T cell population. There were three mice per group, the bars show the mean percentage with range.

To examine whether this phenomenon was unique to immune tissues, cells isolated from liver and adipose tissue were also examined for the autofluorescence phenotype. These tissues were chosen as the weight data suggested a metabolic defect in these mice, specifically RAGE mice had lower body fat. This suggested there may be alterations to the function of adipose and liver tissue, which are the major organs regulating lipid metabolism. The results from the liver are shown above in Figure 6.4.3.4. Once again, three populations of autofluorescent cells can be identified. The distribution of the cell amongst these groups is similar to that seen in the spleen, with the majority of cells showing medium autofluorescence.

As discussed in the previous chapter, Kupffer cells are the resident macrophages in the liver but monocyte-derived macrophages are also present, the former are F4/80+ but express low levels of CD11b, whereas the latter express F4/80+ and high levels of CD11b (Elchaninov et al. 2019). In this thesis Kupffer cells are therefore considered F4/80+ CD11b-. Another population in this lineage are infiltrating monocytes which have yet to differentiate into resident-like cells, these express CD11b but not F4/80 (Krenkel and Tacke 2017). These two markers were used to examine the different autofluorescent populations. The CD11b- F4/80+ cells were found almost exclusively in the medium autofluorescent groups whereas the double positive and CD11b+ F4/80- cells were spread more evenly across the medium and high autofluorescent compartments. This suggests that Kupffer cells are in the medium autofluorescence group whereas monocyte-derived macrophages are split between low and high. One point of note is that the majority of CD45- cells can be characterised as low autofluorescence, this may indicate that medium/high autofluorescence is specific to the immune compartment. A comparison of these populations between the WT-B6N and RAGE

mice is also included in this figure, once again, there are no dramatic differences between the two genotypes.

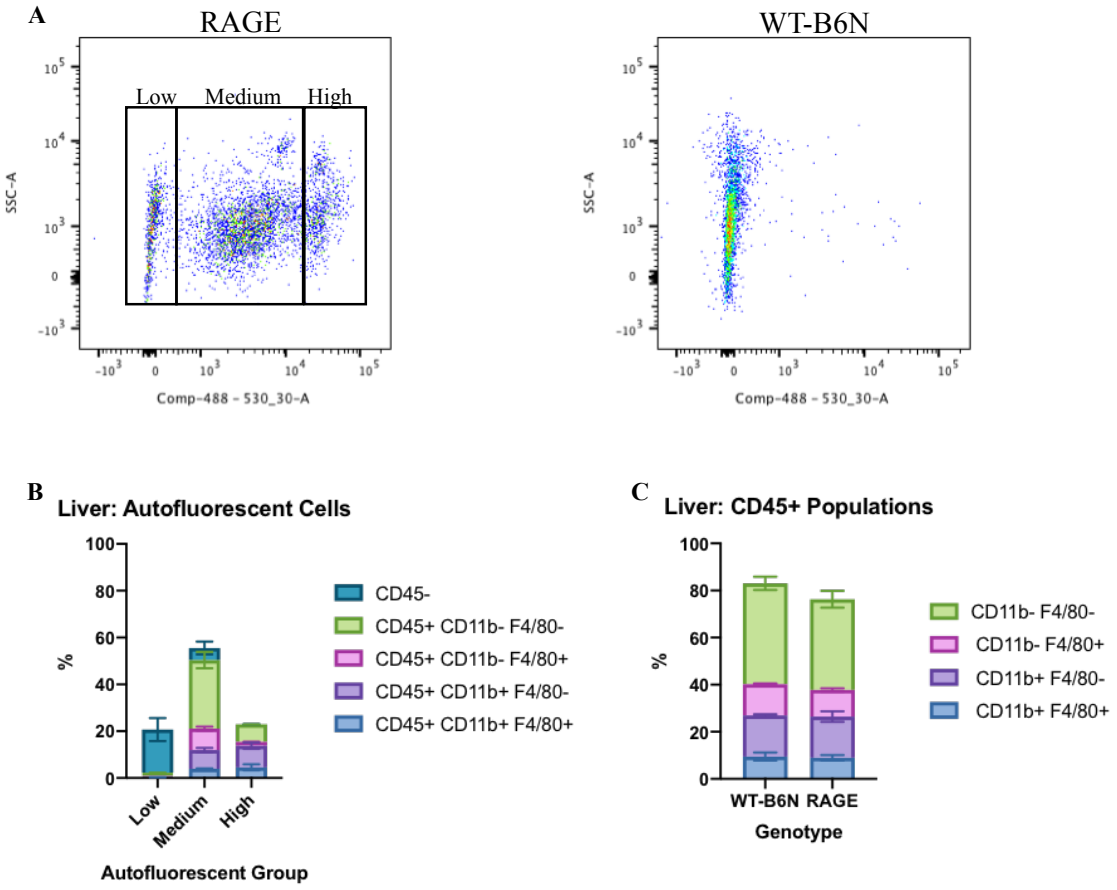

Figure 6.4.3.4: An autofluorescent phenotype was also seen in cells freshly isolated from the livers of RAGE mice (A). The expression of the macrophage markers F4/80 and CD11b was analysed in the different autofluorescent populations and the results shown in B. In this thesis, F4/80+ CD11b- cells are identified as Kupffer cells, F4/80+ CD11b+ cells are monocyte-derived macrophages and F4/80- CD11b+ cells are infiltrating monocytes which have not differentiated into macrophages. CD45+ cells not expressing these markers will be other immune cells. Again, these populations were compared between WT-B6N and RAGE mice, again for RAGE mice all fluorescent groups were combined (C). There are two mice per genotype, the bars show mean with range.

Lastly, the results from the stromal vascular fraction (SVF) of the adipose tissue are shown in Figure 6.4.3.5. Again, the presence of autofluorescent cells is clearly seen in the RAGE mice. As the number of isolated cells is relatively low, the distinction between populations is somewhat less clear and so it is harder to categorise the cells as medium and high autofluorescence. Examining the plots more closely it is easier to divide the autofluorescent RAGE cells into two populations which can be divided both on level of autofluorescence and SSC. As with the liver, the low autofluorescent group is almost exclusively CD45- cells

and in this tissue this group is the largest. Population 2, which consists of cells with generally higher autofluorescence and SSC, is the second biggest and consists mostly of adipose tissue macrophages (CD11b+ F4/80+), which are exclusively found in this group. Also shown in Figure 6.4.3.5 is a comparison between RAGE and WT-B6N mice in terms of adipose immune populations and activation markers. The CD45 population seemed to be slightly lower in the mice lacking RAGE and the percentage of immune cells expressing CCR2 was also noticeably smaller. However, this characterisation has only been done with a small number of mice and so further work is required to determine whether these differences are significant.

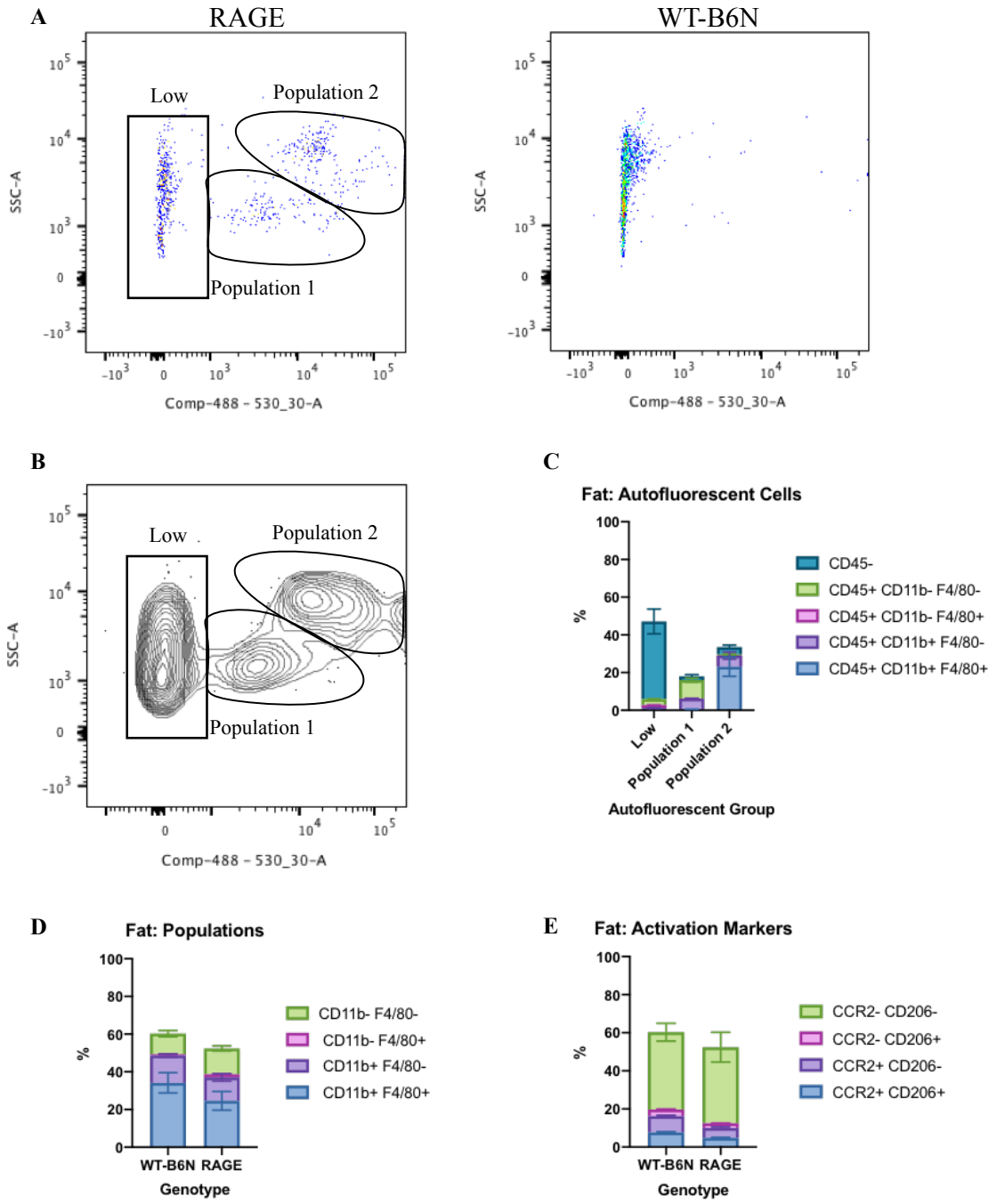

Figure 6.4.3.5: The adipose SVF also contains autofluorescent cells in RAGE mice, this is shown both as a pseudocolour (A) and contour plot (B) to ease identification of the populations. The phenotype of the cells in these populations is shown above in C. Cells were stained for the macrophage markers F4/80 and CD11b. Adipose tissue macrophages can be identified as F4/80+ CD11b+ cells. Finally, the CD45+ populations were examined for their expression of macrophage markers (D), and their expression of the activation markers CD206 and CCR2 (E). These was compared between WT-B6N and RAGE mice. There are two mice in each genotype and the bar graphs show mean with range. SVF = stromal vascular fraction.

6.5 Discussion and Conclusions

The results reported here provide clear evidence that RAGE is not required for the enhanced immunogenicity of AGE-modified proteins as in both genotypes significant cellular immune responses developed in HEL GLUC immunised mice. The magnitude of the response appeared to be slightly smaller in RAGE immunised mice when proliferation was measured by thymidine incorporation, however in the flow cytometry proliferation assay the results were essentially identical between genotypes. Regardless, there were no significant differences between the genotypes for any measure used to assess the response. One point of interest is that significant secretion of IFNγ was only noted in WT-B6N mice. As RAGE is reported to be particularly involved in the development of Th1 responses (Chen et al. 2008), this may indicate a role for this receptor in directing the nature rather than the initiation or scale of the response to AGE-modified proteins. However, testing the data with a two-way ANOVA indicated that the IFNγ response was not significantly different between the genotypes.

Regarding the mechanism underlying AGE-mediated enhanced immunogenicity, one possible interpretation of these results is that there is another receptor which is either predominantly involved in initiating adaptive immune responses to AGEs, or which can easily compensate for its absence. RAGE may still be involved in AGE-induced inflammation as the effects of RAGE KO on the responses of macrophages and other innate immune cells to AGE-modified proteins was not tested here. However, this receptor is not required for the development of adaptive immune responses to AGE-modified proteins. This would fit with the findings of Liliensiek et al who also investigated the development of adaptive immune responses in mice lacking RAGE. In their study, RAGE expression was shown to be dispensable in models of adaptive immunity, namely experimental autoimmune encephalomyelitis and delayed type hypersensitivity (Liliensiek et al. 2004). However, loss

of RAGE was protective in a model of innate immunity, namely sepsis through cecal ligation and puncture. In contrast, genetic or pharmacological RAGE blockade has been demonstrated to prevent transplant rejection in mice and this would fit with data showing a role for RAGE in normal T cell function (Moser et al. 2007; Chen et al. 2008). Overall, it seems likely that the requirement for RAGE in adaptive immune responses will vary depending on the model and AGE-mediated immunogenicity may be another example where this receptor is not required.

Interestingly, neither WT or KO mice developed responses to HEL when immunised with HEL CML. This is a very common AGE product and is present in the HEL GLUC sample. Moreover, this is a specific ligand for RAGE (Kislinger et al. 1999), so it was surprising that even after repeated immunisations no anti-HEL responses developed. One possibility is that this modification induces inflammation but not adaptive immune activation. Instead other modifications in the GLUC sample may mediate T cell activation, or a variety of modifications may be required. Alternatively, the high levels of CML may have destroyed T cell/B cell epitopes in HEL meaning that responses to the native form of this protein never developed. One outcome which was not assessed in this study was whether anti-CML antibody or splenocyte responses developed and this could be examined in subsequent investigations.

An interesting finding in the immunisation study was that the RAGE mice were significantly lighter and had significantly lower body fat than their WT-B6N counterparts. Other studies examining weight in RAGE mice have not reported this phenomenon. There are several reasons this may be the case. Firstly, the mice used in other studies have generally been male and the mice were younger (max 31 weeks). Whereas in this thesis female mice were used and the average age was 40 weeks. Secondly, the relatively small number of mice used in these previous studies may not have been enough to detect a statistically significant

difference in body weight which in this thesis differed on average by a few grams. Instead, in this thesis differences in body fat were more obvious. Regardless, these previous studies have also indicated a role for RAGE in weight gain in HFD induced obesity. Whilst one study did report increased weight gain in RAGE mice (Leuner et al. 2012), others have concluded the opposite with lower body weight and body fat in mice lacking RAGE (Song et al. 2014; Hurtado Del Pozo et al. 2019). The metabolic analysis in these latter studies was also more extensive and included assessment in metabolic cages. Whilst the RAGE mice and their WT counterparts ate a similar amount of food, the energy expenditure in RAGE mice was significantly higher and this could not be explained by increased physical activity. The findings reported here are more in line with these latter studies and may support a model in which loss of RAGE protects against fat gain during aging. The two metabolic analyses have done so far, fasting blood glucose and liver triglyceride content, appeared normal in the KO mice. However, this obviously only gives a very limited picture as to the metabolic state of the mice. Far more extensive analysis could be done, for example examining levels of triglyceride and other metabolites in the blood.

Another finding was that cells isolated from RAGE mice were highly autofluorescent when analysed by flow cytometry. The majority of autofluorescent cells were leukocytes and the exact identity depended on the tissue. For example in the spleen the majority of cells in the high autofluorescence cells were macrophages, whilst in the LN the majority of the high autofluorescence cells were T cells. Autofluorescence is not an uncommon phenomenon, many cells show some degree of autofluorescence which depends on cell type, activation status and tissue. For example, alveolar macrophages are particularly autofluorescent (Misharin et al. 2013; Mitchell et al. 2010). However, the cells from the RAGE mice were clearly substantially more autofluorescent than those from their WT-B6N counterparts. Autofluorescence results from the presence of endogenous fluorophores in cells, these

include NAD(P)H, flavins (e.g. FAD), collagen, fatty acids and lipofuscin (Croce and Bottiroli 2014). The latter consists of aggregates of indigestible materials from phagocytosis and autophagy which accumulate with age. The majority of studies examining autofluorescence in cells have focused on NAD(P)H and FAD. The properties of these depend on their oxidation status and whether they are free or bound, thus autofluorescence can be used to assess the mitochondrial activity and determine the activation status of immune cells (Bartolomé and Abramov 2015; Alfonso-García et al. 2016).

In this study, the autofluorescent signature was seen when the cells were excited with the 488 nm laser and emission measured in the 530/30 channel. The majority of endogenous fluorophores are excited by UV light with excitation and emission ranges not included in this study. However, flavins and lipofuscins can be excited in the 400-500 nm range and emit at 480-540 nm and 480-700 nm respectively (Croce and Bottiroli 2014; Deal et al. 2018). It seems most likely that the autofluorescent signature seen in this case was due to flavins as the autofluorescence was predominantly seen in the 530/30 channel (the peak emission for FAD is 525 nm). Furthermore, lipofuscin typically accumulates in long lived, non-proliferative cells such as neurons and is a sign of aging (Moreno-García et al. 2018). However, the current data cannot completely exclude a contribution from this aggregate. To further define this phenomenon, other excitation wavelengths could be used and the emission measured in a greater number of channels. Using microscopy or ImageStream would also help to identify the location of the autofluorescent molecules within the cell (e.g. whether the endogenous fluorophores are in mitochondria or the cytoplasm). Moreover, one key question worth addressing is whether the autofluorescence phenomenon is exclusive to immune cells. The results from the adipose and liver samples suggest that this is the case as the majority of cells not expressing CD45 were in the low autofluorescence category. However, the procedures used to isolate cells from these tissues mean that not all cells were

samples. For adipose tissue, the SVF fraction was specifically isolated. This includes preadipocytes, immune populations and endothelial cells but not the adipocytes themselves (Bora and Majumdar 2017), whilst in the liver isolation there was a high level of cell death (see Chapter 5). To investigate this further, autofluorescence in other tissues could be investigated, including in histological sections which would not require isolation of cells for analysis.

Based on both the autofluorescence and weight loss data, one hypothesis is that RAGE has a critical role in regulating metabolism and that RAGE loss results in a higher metabolic rate and accumulation of autofluorescent metabolites. Other studies have also postulated that RAGE is key to metabolism as thermogenesis is increased in both brown and white adipose tissue from RAGE mice (Hurtado Del Pozo et al. 2019). Further work is required to further define this role, however this is arguably worth the investment, particularly as RAGE is already a disease target and inhibitors for this receptor are safe and have been used in human trials (Galasko et al. 2014).

Chapter 7: The Impact of Dry Roasting on Immune Responses to Peanut Proteins

7.0 Abstract

Peanut allergy is one of the most severe food allergies and is potentially life threatening. Its prevalence in western countries has been increasing since the 1990s, whereas rates of peanut allergy are disproportionately low in Asian countries. Several studies have indicated that this difference might be due to the different food processing techniques used in these two regions. In the west peanuts are typically consumed dry roasted (DR) whilst in the east boiling or frying is preferred. Furthermore, evidence from our laboratory indicates that DR peanut proteins are more immunogenic than raw peanut proteins in mice. However, the underlying mechanisms which drive this phenomenon are unclear. In this study, peanut protein extract (PPE) and individual allergens were extracted from raw and DR peanuts. These were characterised to examine reactive carbonyl (RC) and AGE formation, and their ability to induce maturation of BMDCs *in vitro,* and to elicit *in vivo* immune responses, were tested. The results indicated that dry roasting added RCs, but not other common AGE adducts such as CML, to peanut proteins. None of the peanut allergens tested could induce classical maturation of DCs. Moreover, DR PPE did not induce greater immune responses than PPE from raw peanuts. In conclusion, dry roasting results in the formation of intermediate glycation/lipid peroxidation products but this did not translate to greater immunogenicity.

7.1 Introduction

7.1.1. The Peanut Allergy Epidemic

Since the 1990s, food allergy rates in the western world have been increasing (Platts-Mills 2015). Why exactly we are seeing this increase is still a matter of debate and probably includes many factors, for example better hygiene, more indoor living and antibiotic use (Platts-Mills 2015; Strachan 2000). Food allergy can have many negative and potentially life-threatening consequences for afflicted individuals. Of these, peanut allergy is particularly severe, being the most common cause of fatal anaphylactic reactions to foods (Bock, Muñoz-Furlong, and Sampson 2001). Individuals allergic to peanuts can respond to doses of peanut protein as low as a few mg, and the ubiquitous nature of peanut products makes accidental ingestion common. Moreover, unlike many other food allergies, it tends to be life-long with only around 1/5 children outgrowing their allergy by school (Sicherer and Sampson 2007; Stiefel et al. 2017).

Treatment options for peanut allergy remain limited. The current practice involves food avoidance, training for peanut recognition and creating a management plan for emergencies including the use of medications such as auto-injected adrenaline. However, patients can find it difficult to determine which foods are safe, particularly when eating out, and the fear of accidental ingestion can have a very significant negative effect on quality of life (Stiefel et al. 2017). As such, a variety of experimental treatment options have been explored with the hope of improving disease burden or providing an effective "cure". One noteworthy example is the use of oral/sublingual immunotherapy in which patients are dosed with increasing amounts of peanut allergens orally in the hope of creating a tolerant state (Sicherer and Sampson 2007). Whilst this has been shown to effectively desensitise patients, meaning they were able to tolerate higher amounts of allergen without developing allergic symptoms, it is still unclear whether this can result in long term tolerance (Stiefel et al.

2017). Moreover this strategy is associated with significant risk. A recent metanalysis of oral immunotherapy trials revealed that rates of anaphylaxis were actually increased in patients receiving treatment (Chu et al. 2019). Therefore, continued research is needed to develop effective and safe treatments for peanut allergy. Understanding why individuals develop peanut allergy is incredibly important because it would inform better strategies for prevention and potentially allow for the development of new therapies.

7.1.2 Key Peanut Allergens

The peanut, *Arachis hypogea*, is a member of the legume family grown and consumed worldwide (Beyer et al. 2001). There are currently 16 peanut allergens recognised by the WHO/International Union of Immunological Societies Allergen Nomenclature subcommittee (Pi et al. 2019). With the exception of Ara h 1 and Ara h 3, they are all small with a molecular weight of less than 20 kDa. The major peanut allergens (those recognised by more than 50% of allergic individuals) are Ara h 1, Ara h 3, Ara h 2 and Ara h 6 (Mueller, Maleki, and Pedersen 2014). The first of these to be discovered was Ara h 1. In 1991 Burks et al used anion exchange chromatography to purify proteins from PPE. They then examined the capacity of the anion exchange fractions to bind to IgE in sera from peanut allergy patients. Using this method they identified a 63.5 kDa glycoprotein with an isoelectric point of 4.55 (A. W. Burks et al. 1991). Further research has revealed Ara h 1 to be a 7S globulin/vicilin seed storage protein which is a member of the cupin superfamily, a group defined by a β-barrel motif. It usually exists in a trimer and it is thought that these trimers form into higher order oligomers (Mueller, Maleki, and Pedersen 2014). Ara h 1 accounts for 12-16% of the total peanut protein, making it the most abundant, and is recognised by 35-95% of peanut allergy patients depending on the population (Shefcheck and Musser 2004; Zhou et al. 2013). Ara h 3 is also a member of the cupin superfamily and another seed

storage protein. Despite sharing only 21% of its sequence with Ara h 1, the two have a similar structure with Ara h 3 consisting of a hexamer composed of two Ara h 1-like trimers (Mueller, Maleki, and Pedersen 2014). The total weight of the hexamer is 360-380 kDa and each monomer has a molecular weight of around 60 kDa, but on SDS-PAGE multiple fragments have been identified including ones of 14 kDa and 37 kDa. Ara h 4 was originally identified as a separate allergen but is now known to be an isoform of Ara h 3 and was renamed to Ara h 3.02 (W. Burks, Sampson, and Bannon 2008; Zhou et al. 2013; Pi et al. 2019).

Using the same method as for the discovery of Ara h 1, Burks et al were also able to identify Ara h 2. This is a 17 kDa protein which appears as two bands in SDS-PAGE which have near identical sequence (A. W. Burks et al. 1992). Later, Ara h 6 was discovered, a 15 kDa protein which is 59% homologous to Ara h 2 (Kleber-Janke et al. 1999; Pi et al. 2019). Both of these are 2S albumins and have structures featuring five α-helices and multiple disulphide bonds, 4 in Ara h 2 and 5 in Ara h 6. It is the latter feature which is thought to give these proteins their heat and protease resistant properties. These two are considered the most potent of the peanut allergens and are recognised by more than 95% of allergic individuals (Sicherer and Sampson 2007; Uotila et al. 2017). In skin prick tests of peanut allergy patients, Ara h 2 and Ara h 6 were found to elicit stronger responses than Ara h 1 and Ara h 3 (Peeters et al. 2007). Similarly, studies which have examined *in vitro* basophil degranulation in response to peanut extract have found that removing Ara h 2 and Ara h 6 reduces the degranulation capacity of the peanut extract by 90%. Interestingly, adding back either allergen individually could restore degranulation capacity to at least 80%, suggesting a high degree of redundancy between the two (Chen et al. 2013). The importance of these allergens in disease has been demonstrated in mouse studies which have shown that removal

of Ara h 2/6 from peanut extract prevents the development of anaphylaxis in challenge studies of mice sensitised to peanut proteins (Kulis et al. 2012).

7.1.3 Food Processing: Dry Roasting

In addition to the increases in allergy prevalence discussed above, epidemiology studies have also indicated that peanut allergy is a predominantly western phenomenon with lower prevalence in eastern countries in spite of similar peanut consumption rates between the two (Sicherer and Sampson 2007). This does not seem to be an extension of the hygiene hypothesis as studies have indicated that the overall rates of allergy are similar between the two regions, but the type of allergy is variable (Lee, Thalayasingam, and Lee 2013). Moreover, this does not seem to be caused by genetic differences as the rates of peanut allergy amongst individuals of an Asian background living in western countries are reported to be similar to those of European origin (Lee, Thalayasingam, and Lee 2013; Beyer et al. 2001). Studies attempting to explain this discrepancy have identified differences in food processing between the two regions as key factors of interest. In the west, peanuts are typically consumed roasted or as processed peanut butter, whilst in Asian cuisine peanuts are generally fried or boiled. Papers comparing these methods have reported reduced extraction of Ara h 1 from peanuts which were fried or boiled with loss of peanut proteins to the boiling water (Beyer et al. 2001; Mondoulet et al. 2005). Moreover, the peanut proteins from these fried/boiled peanuts showed reduced IgE binding compared to roasted or raw peanuts. Conversely, DR peanut samples have been shown to bind more strongly to IgE from peanut allergy patient sera (Maleki et al. 2000; Mondoulet et al. 2005). Therefore, one possibility was that roasting was increasing the allergenicity of the peanut proteins.

During dry roasting, the peanut kernels are exposed to high temperatures (>125 °C) for short periods of time (mins) (Shi et al. 2017). Under these conditions, many processes can alter

the peanut proteins including the Maillard reaction. Amadori products, pyrraline and CML have all been identified in roasted peanut samples from laboratory and commercial sources using chromatographic methods (Wellner, Nußpickel, and Henle 2012). Further mass spectrometry (MS) studies have localised these to Ara h 1 and Ara h 3, with none so far detected on Ara h 2 (Mueller et al. 2013; Hebling et al. 2013). The formation of AGE structures on peanut proteins has been the focus of a variety of studies examining increased allergenicity of DR peanuts. Artificially replicating this process by incubating peanut proteins with reducing sugars has in some studies been shown to increase IgE binding (Maleki et al. 2000; Chung and Champagne 1999), possibly indicating the formation of neoepitopes in the processed samples recognised by patient IgE. This is supported by the finding that anti-AGE antibodies can inhibit anti-peanut IgE from binding to DR PPE (Chung and Champagne 2001). However, other reports have indicated that the IgE binding response is more variable, with the response depending on the patient sample, or that glycation/roasting can actually decrease IgE binding (Vissers, Iwan, et al. 2011; Mueller et al. 2013; Vissers, Blanc, et al. 2011).

A more limited set of papers have examined the altered immunogenicity of DR vs raw peanuts, that is their ability to induce adaptive immune responses. In a 2014 study from Moghaddam et al, mice were immunised s.c. with DR or raw PPE in the absence of adjuvant followed by oral gavage with crude peanut homogenate from DR peanuts. The DR PPE induced significantly greater titres of IgG and IgE, the latter of which was functional in basophil degranulation assays. Moreover, in splenocyte restimulation experiments, splenocytes from mice immunised with DR PPE had greater proliferative responses and secreted significantly higher amounts of the Th2 cytokines IL-5 and IL-13 when pulsed with either raw or DR PPE compared to mice immunised with raw PPE. With both the antibody and cellular responses, the DR-immunised mice showed equal responses to both DR and

raw PPE, indicating that this enhancement was not due to the formation of neoepitopes in the DR samples but an increased intrinsic immunogenicity (Moghaddam et al. 2014). Immunisation with isolated DR or raw Ara h 1 also demonstrated the same effect. Similarly, heat-treated Ara h 2 has been shown to induce stronger IgG and IgE responses in oral immunisation mouse studies compared to native protein in the absence of adjuvant (Starkl et al. 2011). However, in this latter study enhanced splenocyte responses were not apparent. However, other studies using glycation of isolated Ara h 1 to mimic roasting have found that this product is not a superior elicitor of anti-peanut IgG and IgE responses in rats compared to native Ara h 1 (Kroghsbo et al. 2014). Therefore, there are still questions regarding the immunogenic potential of DR peanut proteins and the structures which may drive this.

Overall, alterations of the immunogenicity of peanut proteins by thermal processing is still relatively unexplored compared with roasting-induced changes to IgE binding. In particular, the mechanism underlying the enhanced immunogenicity is still unclear. Current evidence suggests that enhanced immunogenicity of modified peanut proteins is more likely to be due to changes in antigen uptake and processing rather than intrinsic immune activation properties. As with other AGE-modified proteins, dry roasting of Ara h 1 and Ara h 3 has been demonstrated to enhance uptake of modified protein by DCs (Moghaddam et al. 2014; Cabanillas et al. 2018). This could enhance the development of immune responses by increasing the amount of protein presented to T cells. In contrast, DR PPE samples are reported to be unable to induce maturation of DCs, with no increase in costimulatory molecules or cytokine secretion in response to modified proteins (Moghaddam et al. 2014). However, to the best of the author's knowledge, this has been the only study to investigate the capacity of DR peanut samples to modulate the activatory status of DCs. The effects of DR peanut proteins on DCs compared to raw peanut proteins is therefore still relatively unexplored. Understanding how the peanut-immune system relationship is altered by food

processing could provide insights into the development of peanut allergy and is therefore an important area of research.

7.2 Hypothesis and Aims

Hypothesis: DR peanuts have enhanced immunogenicity compared to raw peanuts, which is mediated through their interactions with elements of the innate and/or adaptive immune systems.

Aims

1. To isolate and characterise PPE and individual allergens from raw and DR peanuts
2. To examine whether roasting changes peanut protein uptake by DCs and/or their activation
3. To test *in vivo* immunogenicity of DR and raw PPE and Ara h 1

7.3 Materials and Methods

A list of methods used in this chapter is shown below. For full details please refer to the indicated section in the Materials and Methods chapter.

- Carbonyl, CML, GA-Pyridine and Pyrraline ELISAs (2.2.6-2.2.9)
- Fluorescence Measurements (2.2.11)
- SDS-PAGE, Native PAGE, Western Blotting and Carbonyl Western Blotting (2.2.12-2.2.15)
- Fluorescent Labelling (2.2.16)
- Endotoxin Cleaning (2.2.21)
- Endotoxin Reporter Assay (2.3.2)
- Generation of GM-CSF BMDCs (2.3.3)
- *In Vitro* Uptake and Pulsing Assays (2.3.4, 2.3.5)
- Luminex Assay (2.3.9)
- Immunisation and Tissue Harvesting (2.4.2 - 2.4.3. 2.4.6)
- IgG, IgG1, IgG2a, IgG2c and IgE ELISAs (2.5.1, 2.5.2)
- Splenocyte Harvest, Cytokine ELISAs and Thymidine Proliferation (2.6.1-2.6.3)
- Peanut Protein Manufacture and Isolation (2.8)
- Statistical Analysis (2.9)

7.4 Results

7.4.1 Optimising Conditions for Peanut Protein Extraction

For the peanut project, two main peanut products were needed which could then be used for *in vivo* and *in vitro* studies. The first of these was peanut protein extract (PPE), a mix of peanut proteins. Individual peanut allergens could then be isolated from PPE using fast protein liquid chromatography (FPLC). A scheme for PPE production is shown in Figure 7.4.1.1 (Beyer et al. 2001). The first stage was to find the optimal conditions for this protocol, starting by finding the best buffer for extracting PPE from defatted, peanut powder. Five different buffers were selected based on the literature (Walczyk et al. 2017) and previous experience in the laboratory. Details are given in Table 7.4.1. These were then used to extract proteins from defatted peanut powder from either raw or DR peanuts. This powder had previously been used to extract proteins for *in vivo* experiments (Moghaddam et al. 2014).

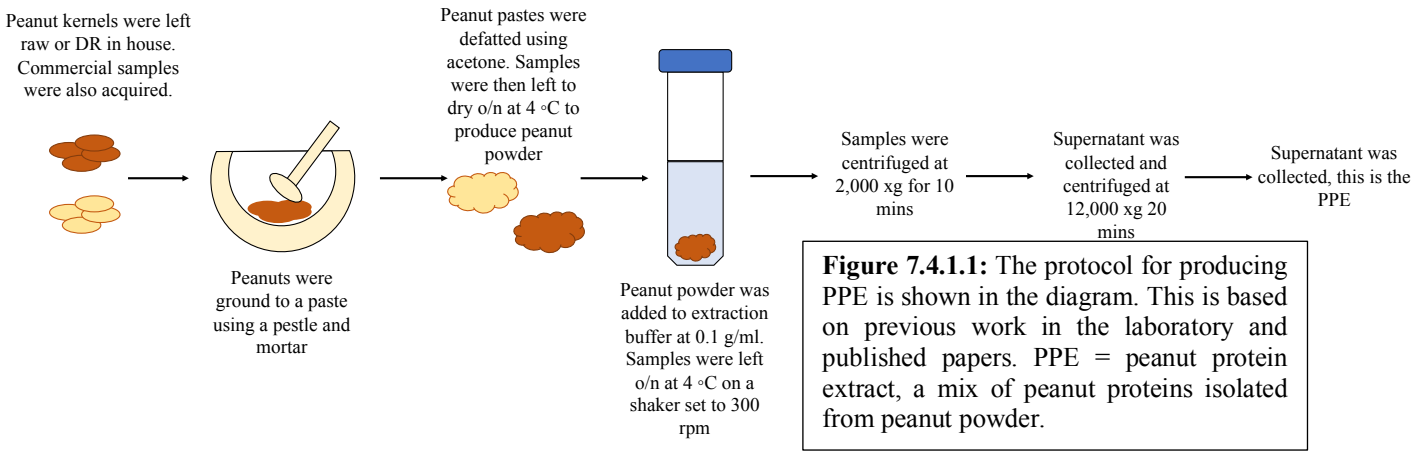

Figure 7.4.1.1: The protocol for producing PPE is shown in the diagram. This is based on previous work in the laboratory and published papers. PPE = peanut protein extract, a mix of peanut proteins isolated from peanut powder.

Buffer	Composition	pH
1	50 mM Sodium Carbonate	pH 11
2	7 mM Sodium Borate	pH 9.2
3	50 mM Tris-HCl with 0.2 M NaCl	pH 8.2
4	6 M Urea	pH 8.7
5	10x PBS	pH 7.4

Table 7.4.1: The different buffers used to examine peanut protein extraction

Extracted samples were then analysed by SDS-PAGE to assess the protein contents, results are shown in Figure 7.4.1.2. As can be seen from the gel, dry roasting significantly alters the extracted protein composition with loss of an approximately 60 kDa band, identified here as Ara h 1, being particularly apparent. This is in keeping with previous studies which have reported loss of solubility of high molecular weight peanut proteins with roasting (Kopper et al. 2005). With regards to buffer choice, Buffer 3 seemed to perform particularly poorly as almost no Ara h 1 was recovered from the DR powder. The other buffers appeared to behave similarly and so moving forward buffer 5 was selected. The decision was based on the need to limit the number of processing steps in order to prevent protein losses. Protein samples would need to be buffer exchanged into PBS in order to be safely injected into mice. As buffer 5 was simply 10x PBS this buffer could simply by diluted to 1x PBS. Use of buffer 1, 2 or 4 would require buffer exchange, which could result in loss of proteins and protein aggregation.

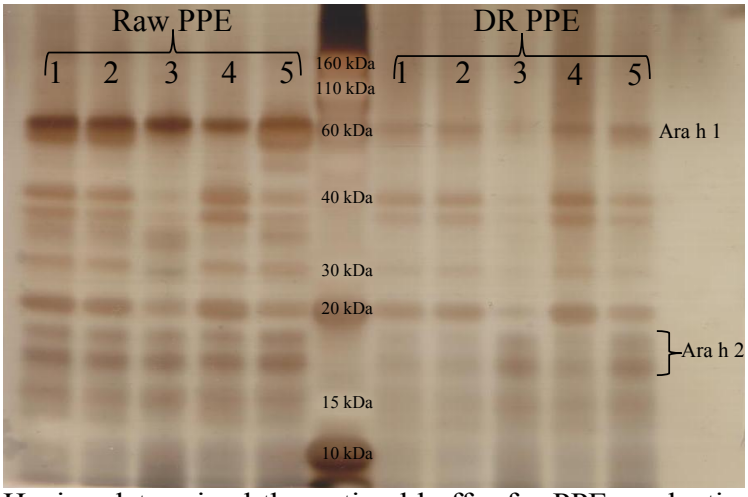

Figure 7.4.1.2: PPE was produced using peanut powder from raw or dry roasted (DR) peanuts and the indicated buffer (see Table 7.4.1). The protein concentration was measured by BCA and 1 µg of each sample was analysed by SDS-PAGE. The gel was then silver stained to assess protein content. The molecular weight of the ladder markers is shown. Based on the molecular weight of the bands, an approximately 60 kDa band was initially identified as Ara h1, whilst a pair of bands around 17 kDa were identified as Ara h 2.

Having determined the optimal buffer for PPE production, the next step was to determine the best conditions for roasting peanuts. Raw peanuts were roasted at either 160 °C or 178 °C for between 5 and 20 mins. These conditions were selected based on previous experiments in our laboratory. PPE was then extracted from the roasted peanuts and examined the formation of RCs by ELISA (Figure 7.4.1.3). This modification was focused

on as previous publications indicated that these were of particular interest with regards to enhanced immunogenicity (Moghaddam et al. 2011). In both cases, newly prepared modified samples were compared to the DR sample extracted from an older peanut powder sample used in previous studies in the laboratory. The two carbonyl ELISAs (BH and DNPH) gave differing results, although the overall pattern was the same. In the BH ELISA, raw and lightly modified samples already have a signal above background and this is increased in the old DR sample and the more extensively roasted samples. In contrast, the DNPH ELISA only showed a large RC signal with DR PPE and the 178 °C 15 and 20 mins samples. Different hydrazine/hydrazide based probes can have different labelling efficiencies and reactivities, so this may be the reason for the difference (Matthews et al. 2016; Ugur, Coffey, and Gronert 2012). Interestingly, there was no evidence of CML formation in any of the roasted peanut samples. Whilst this product has been identified in roasted samples before, analysis of different commercial products has indicated that this is

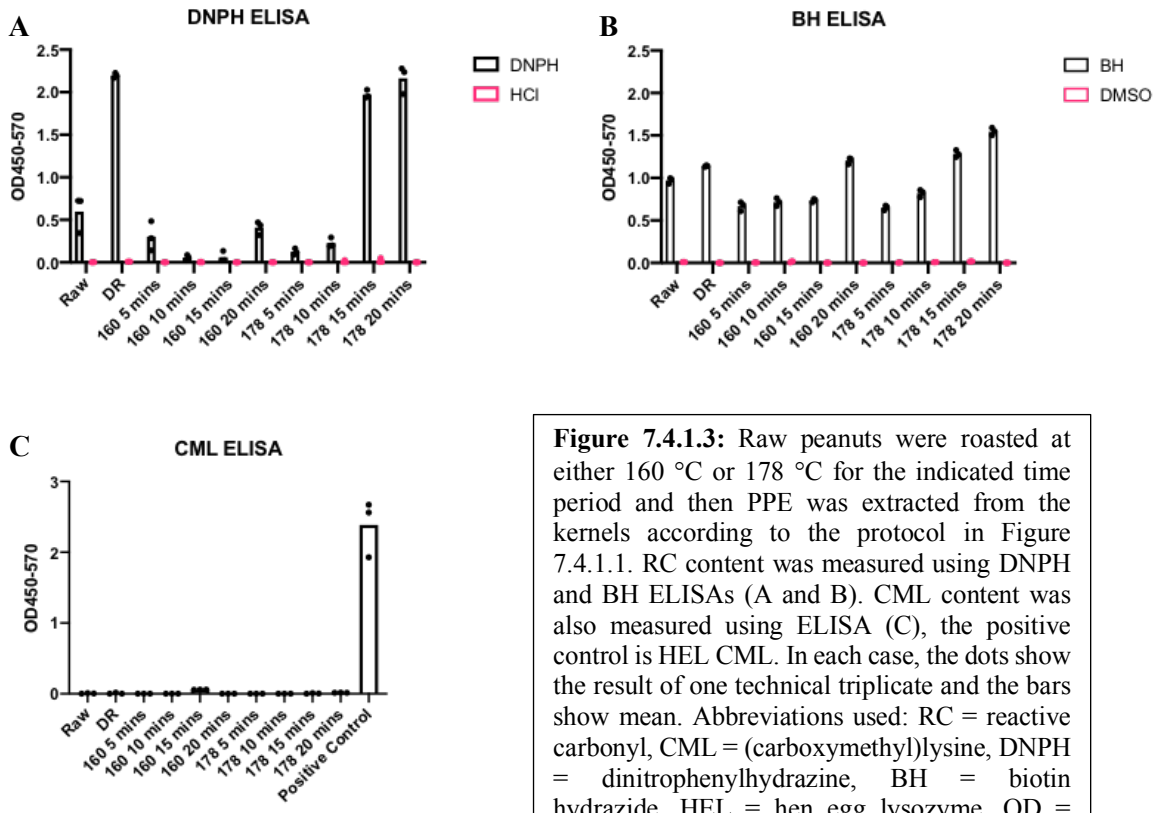

Figure 7.4.1.3: Raw peanuts were roasted at either 160 °C or 178 °C for the indicated time period and then PPE was extracted from the kernels according to the protocol in Figure 7.4.1.1. RC content was measured using DNPH and BH ELISAs (A and B). CML content was also measured using ELISA (C), the positive control is HEL CML. In each case, the dots show the result of one technical triplicate and the bars show mean. Abbreviations used: RC = reactive carbonyl, CML = (carboxymethyl)lysine, DNPH = dinitrophenylhydrazine, BH = biotin hydrazide, HEL = hen egg lysozyme, OD = optical density.

a relatively minor component of the AGE adducts formed during roasting (Wellner, Nußpickel, and Henle 2012).

Next, RC formation was assessed using a carbonyl western blot (Figure 7.4.1.4). The advantage of this technique is that it allows one to determine the distribution of RCs amongst the peanut allergens. Using this method, a substantial RC signal was only seen after longer incubation times (20 mins) and this was comparable to the DR signal. Moreover, the distribution of RCs was the same between these samples, with the higher molecular weight proteins, including Ara h 1, showing the strongest signal. In contrast, the Ara h 2 samples showed no RC signal. Based on all of these results, 20 mins at 178 °C were selected as the roasting conditions as this gave a good RC signal and produced a product which was similar

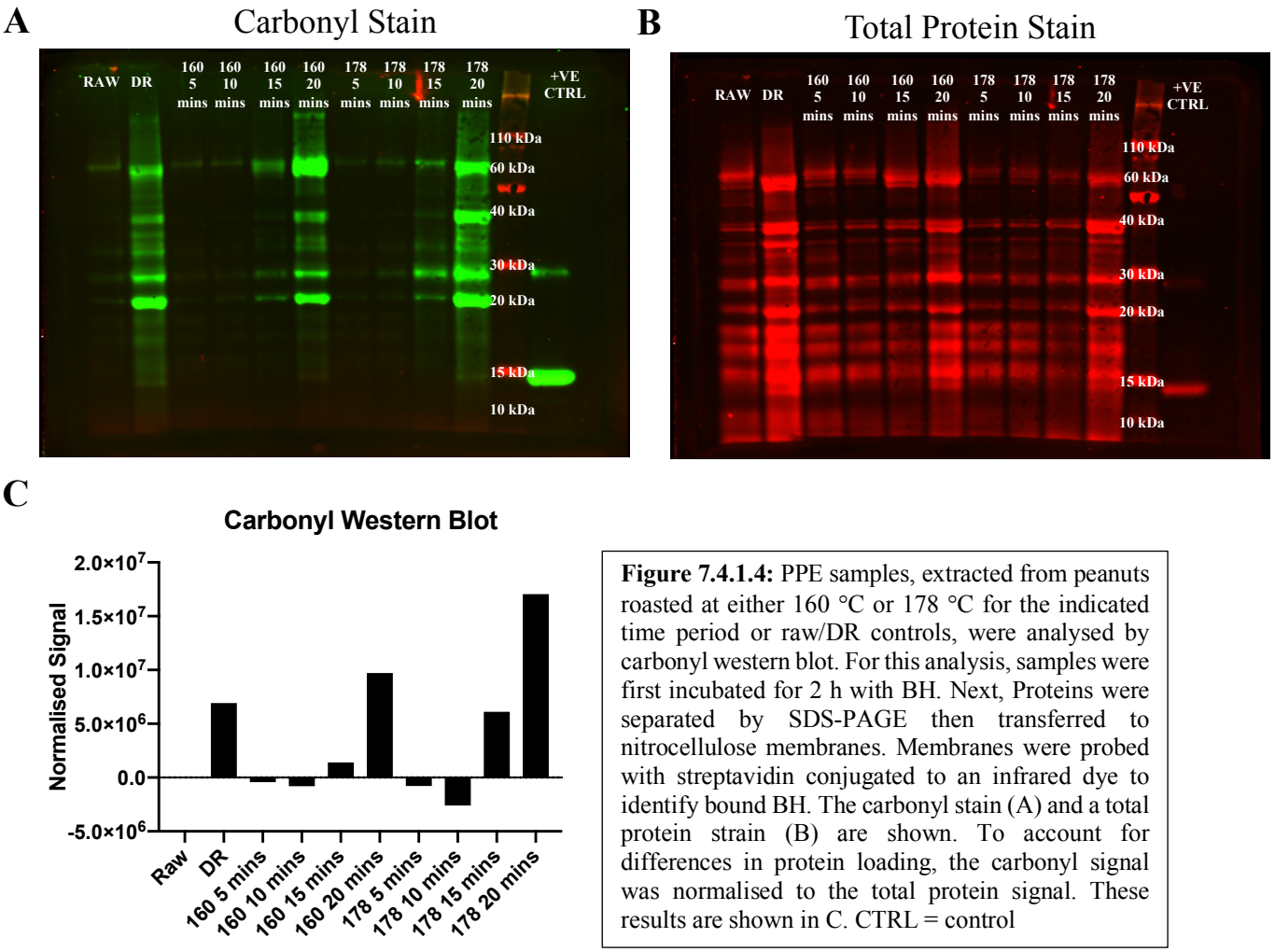

Figure 7.4.1.4: PPE samples, extracted from peanuts roasted at either 160 °C or 178 °C for the indicated time period or raw/DR controls, were analysed by carbonyl western blot. For this analysis, samples were first incubated for 2 h with BH. Next, Proteins were separated by SDS-PAGE then transferred to nitrocellulose membranes. Membranes were probed with streptavidin conjugated to an infrared dye to identify bound BH. The carbonyl stain (A) and a total protein strain (B) are shown. To account for differences in protein loading, the carbonyl signal was normalised to the total protein signal. These results are shown in C. CTRL = control

to that used in previous studies, thereby allowing comparison between current and past experiments.

To confirm this was the right decision, PPE was also isolated from commercial dry roasted (cDR) peanuts and then examined for RC content by ELISA and western blot as before. Obviously, it was important that the laboratory-produced samples be similar to what is commercially available in order to aid translation of any findings here to the real-world scenario. The ELISA results are shown below in Figure 7.4.1.5. DR and cDR samples had a comparable RC content in the two ELISAs. CML, GA-Pyridine and pyrraline content of the PPE preparations was also measured by ELISA and the results are also shown in Figure 7.4.1.5. Again, there was no evidence of CML formation, and this was also the case for GA-pyridine. Pyrraline was detected in the DR and cDR samples, but at a much lower level than the positive control. Likewise, when general AGE formation was assessed by examining fluorescence, a low signal was seen in all samples, which was slightly higher in the DR and cDR samples, but still much lower than that seen in other preparations (BSA GA 7 days is shown as a comparison). The results of the RC ELISAs were supported by the western blot results (Figure 7.4.1.6), which also showed a comparable signal between DR and cDR and also identical RC distribution. Collectively, these data suggests that the roasting conditions produced in the laboratory were comparable to the commercial product.

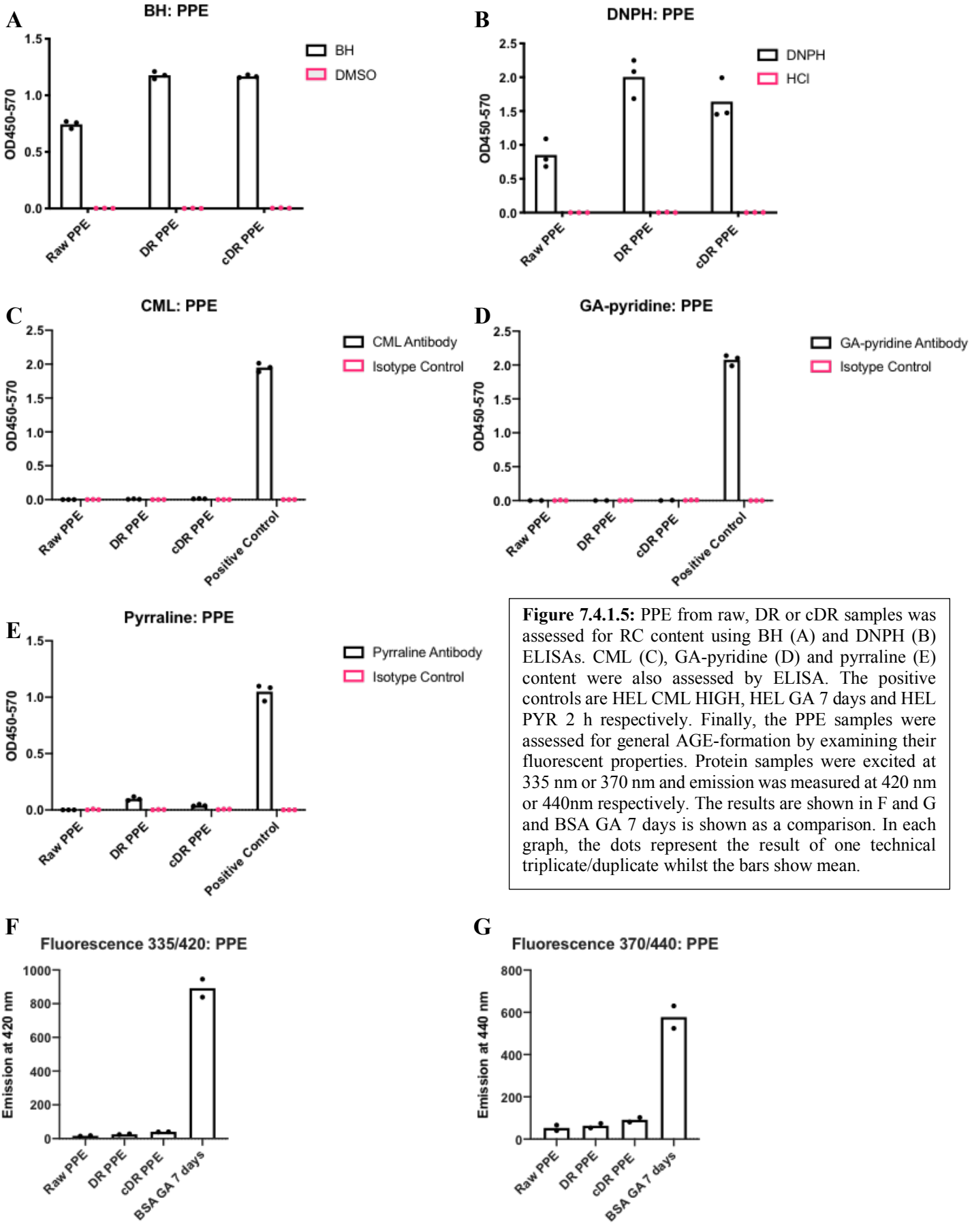

Figure 7.4.1.5: PPE from raw, DR or cDR samples was assessed for RC content using BH (A) and DNPH (B) ELISAs. CML (C), GA-pyridine (D) and pyrraline (E) content were also assessed by ELISA. The positive controls are HEL CML HIGH, HEL GA 7 days and HEL PYR 2 h respectively. Finally, the PPE samples were assessed for general AGE-formation by examining their fluorescent properties. Protein samples were excited at 335 nm or 370 nm and emission was measured at 420 nm or 440nm respectively. The results are shown in F and G and BSA GA 7 days is shown as a comparison. In each graph, the dots represent the result of one technical triplicate/duplicate whilst the bars show mean.

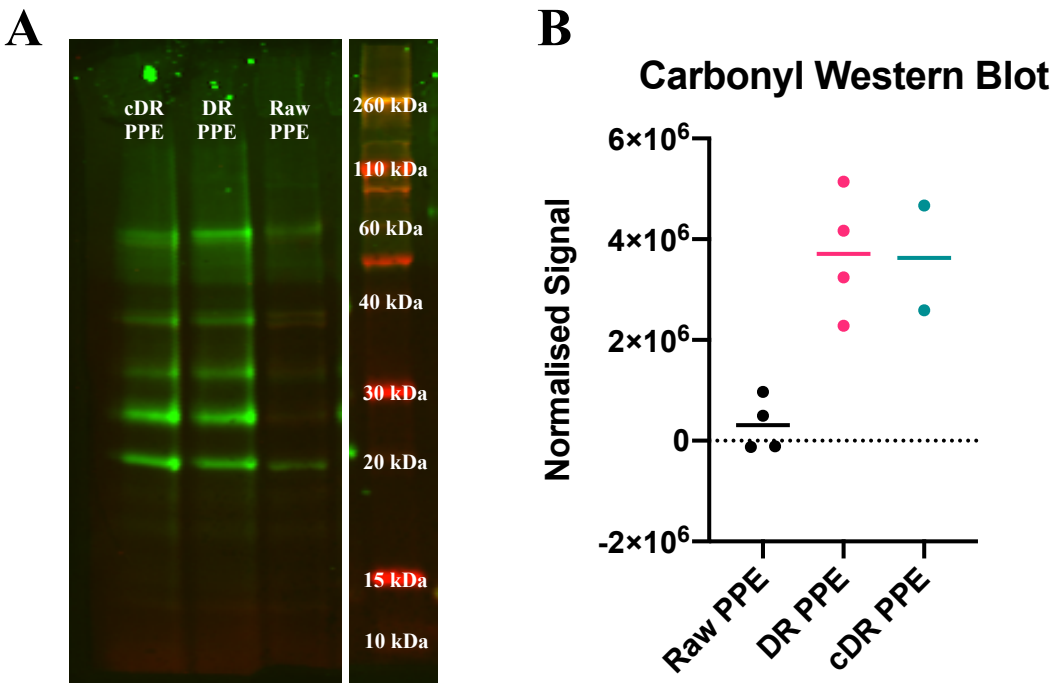

Figure 7.4.1.6: RC content of raw, DR or cDR PPE was also assessed by carbonyl western blot using the protocol outlined in 7.4.1.4. A representative blot is shown above, irrelevant lanes have been removed and this is represented by the break in the blot. The total protein stain for this blot is shown later in 7.4.3.2. As for 7.4.1.4, the carbonyl signal was normalised to the total protein stain and the results are shown in the graph, each dot represents one measurement.

7.4.2 Isolating Individual Peanut Allergens

Having generated PPE samples, the next stage was to generate purified samples of individual allergens. As discussed in the introduction, within the peanut there are 16 currently named allergens and these are of variable importance with regard to allergy. In this study, it was decided to focus on Ara h 1 and Ara h 2. Many previous studies using MS and SDS-PAGE to examine the effects of thermal processing/glycation on peanuts proteins had indicated that Ara h 1 is significantly affected by roasting, with loss of solubility, crosslinking and the addition of AGE structures such as CML (Kopper et al. 2005; Maleki et al. 2000; Hebling et al. 2013). Moreover, the carbonyl western blots indicated that this protein had a high level of RCs in the DR samples which supports these older findings. In contrast, Ara h 2 did not appear to be extensively modified in the western blotting experiments. This is in line with some studies which have been unable to find AGE modifications on Ara h 2 using MS (Mueller et al. 2013), although other studies have indicated that dry roasting can alter the IgE binding properties of Ara h 2 (Mondoulet et al. 2005). Nevertheless, Ara h 2 seems to be more clinically relevant than Ara h 1, being associated with more severe reactions (Kulis et al. 2012), therefore this was still an important protein to investigate.

A variety of different chromatography methods have been used to isolate individual allergens in the literature. In previous experiments in our laboratory, PPE samples were first run through a gravity-driven size exclusion column, followed by anion exchange and finally a further round of size exclusion to remove any additional impurities. This was successful in isolating Ara h 1, however, there were concerns that the initial size exclusion step was introducing LPS contamination into the samples. Moreover, others have managed to use anion exchange alone to isolate Ara h 1 (A. W. Burks et al. 1991). Similarly, the first reported isolation and identification of Ara h 2 only utilised anion exchange (A. W. Burks et al. 1992). It was therefore decided to omit the first size exclusion step from the

previous protocol and start with the anion exchange. The buffer was also changed from Tris-HCl to PBS. Anion exchange works on the principle that at pH above their isoelectric point, proteins will have a negative charge and this allows them to bind to a positively charged matrix. The strength of this interaction will depend on the charge of the protein and so by increasing the concentration of a competitor ion, proteins with different charges can be eluted from the column at different points. The pH for this process needs to be carefully chosen so that all the proteins of interest have a negative charge (above the isoelectric point), but the pH must also be close to the elution point in order to allow easy elution from the column. In this case, the proteins of interest all had acidic isoelectric points (4.55 for Ara h 1 and 5.2 for Ara h 2 (A. W. Burks et al. 1991, 1992)) and so both would be negatively charged in both PBS (pH 7.5) and Tris-HCl (pH 8.2). However, using PBS would remove the need to buffer exchange the samples into and out of Tris-HCl, limiting the number of steps where protein loss may occur.

For the anion exchange raw, DR and cDR PPE samples were run on a MonoQ column using a gradient from 0.1 M to 1M NaCl. The protocol for running the machine had been previously optimised in the laboratory. Examples of elution curves for each protein sample are shown below in Figure 7.4.2.1. Fractions from each of the peaks were selected and 15 µl samples were taken for analysis by SDS-PAGE. Based on these it seemed that the initial peak which eluted from the column contained allergens which were not of interest and this was followed by a peak which, based on molecular weight, was likely predominantly Ara h 2. The main peak which commenced at B13 included a mix of allergens. However, a protein with an approximately 60 kDa protein, most likely Ara h 1, seemed to elute first. This allowed for a relatively pure sample of this protein to be obtained.

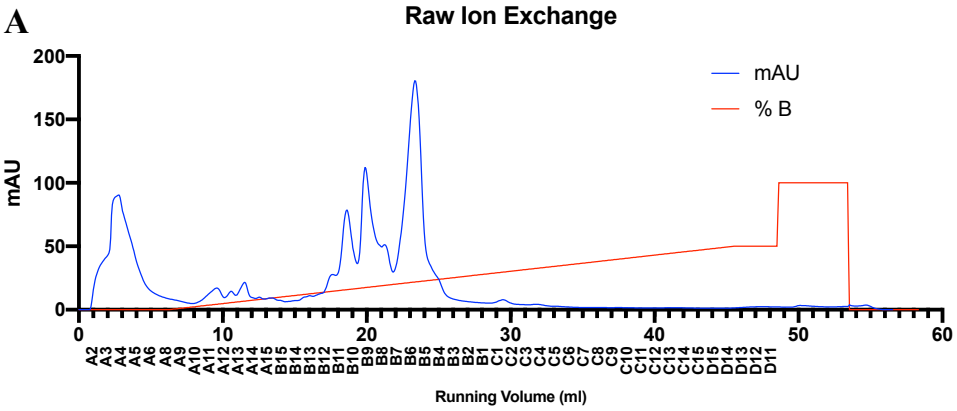
A
Raw Ion Exchange
mAU
% B
mAU
Running Volume (ml)

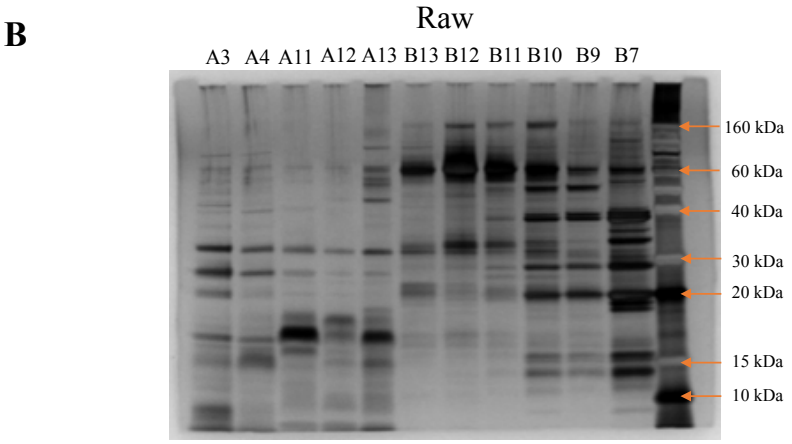
B
Raw
A3 A4 A11 A12 A13 B13 B12 B11 B10 B9 B7
160 kDa
60 kDa
40 kDa
30 kDa
20 kDa
15 kDa
10 kDa

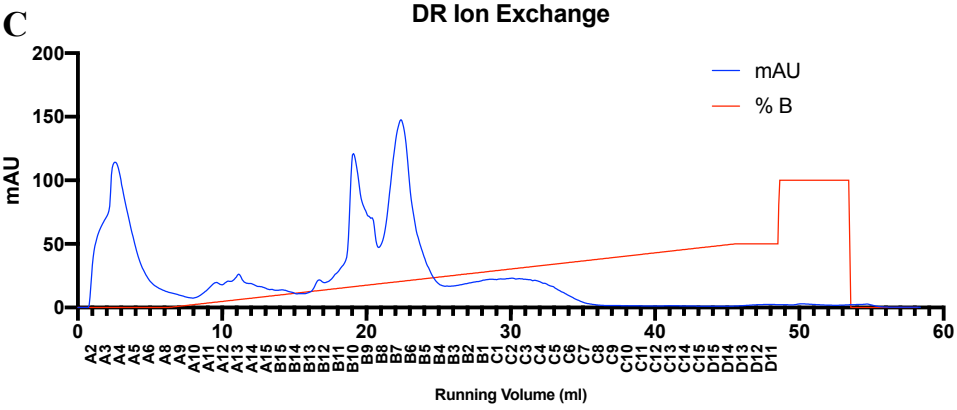
C
DR Ion Exchange
mAU
% B
mAU
Running Volume (ml)

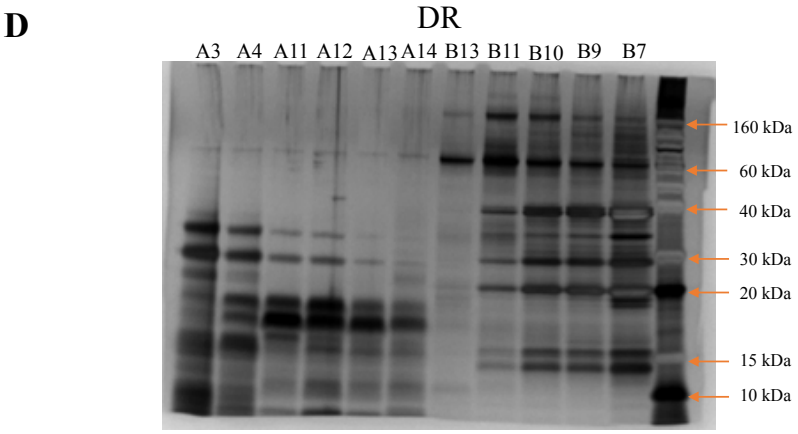
D
DR
A3 A4 A11 A12 A13 A14 B13 B11 B10 B9 B7
160 kDa
60 kDa
40 kDa
30 kDa
20 kDa
15 kDa
10 kDa

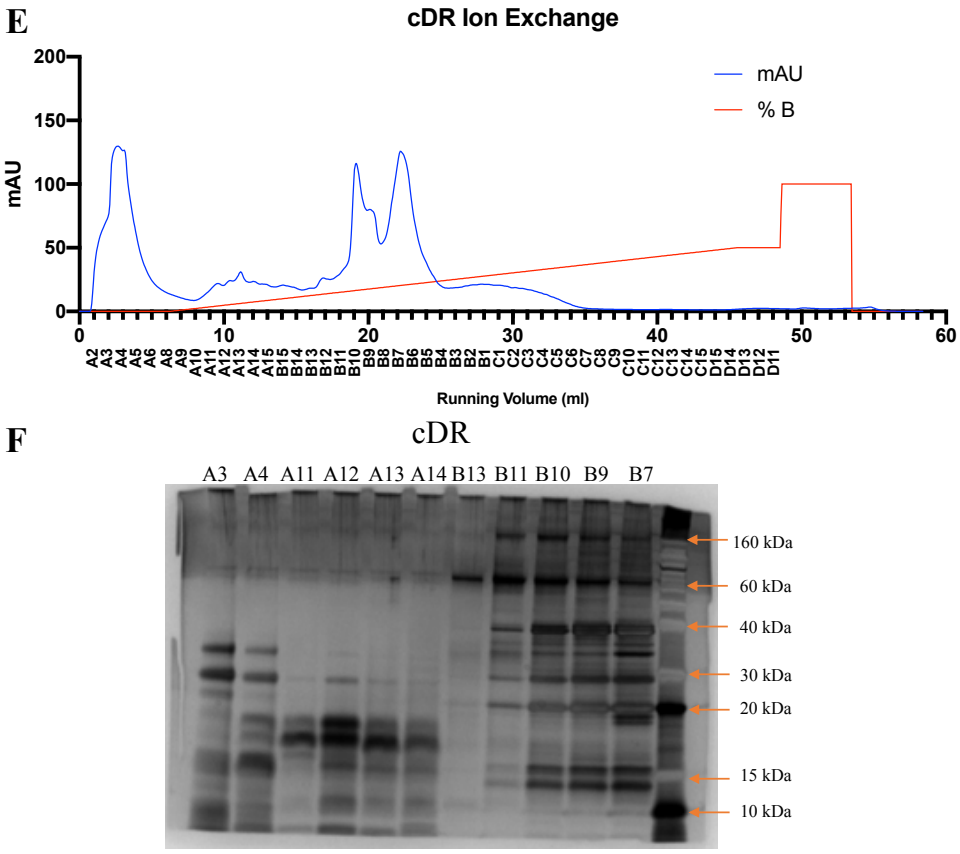

Figure 7.4.2.1: In order to manufacture Ara h 1 and Ara h 2 samples, raw, DR and cDR PPE were subjected to anion exchange using a MonoQ column. Samples were initially loaded onto the column in PBS adjusted to have a NaCl concentration of 0.1 M. The concentration of NaCl in the buffer was slowly increased to 1 M, allowing protein samples to elute from the column. Shown in graphs A, C and E are representative UV traces for each of the samples, which measures proteins eluted from the column, and the NaCl gradient (B is PBS with 2M NaCl). For each sample, fractions were selected to represent each of the peaks and 15µl of each was analysed by SDS-PAGE followed by silver staining (B, D, F). The gels are shown beneath their respective graph.

To confirm the identity of the samples, selected peaks of interest were then analysed by western blot for Ara h 1 and Ara h 2. The results are shown in Figure 7.4.2.2. The Ara h 1 western blot revealed the major band at around 60 kDa does correspond to the Ara h 1 monomer. Also present is a larger molecular weight band, most likely the trimer, and a smaller fragment. A similar banding pattern has been seen by others who have isolated Ara h 1 from PPE (Vissers, Iwan, et al. 2011). The Ara h 1 samples were also analysed using Native PAGE followed by western blot to examine the full trimer and higher order oligomers, the blot is shown in Figure 7.4.2.3. The Coomassie dye used in the Native PAGE is visible in the 700 channel of the LiCor. This turns the whole membrane red and so a total protein stain was not possible. The Native PAGE/blot show the presence of a main band between 146 kDa and 242 kDa, this is likely to be the trimer of Ara h 1 which is reported to have a molecular weight of around 180 kDa (Palladino 2018). Higher order oligomers can also be seen in all samples. Finally, the Ara h 2 western blot also confirmed the presence of the characteristic doublet in the Ara h 2 samples (Figure 7.4.2.2).

Using the data from the western blot and the SDS-PAGE, the purity of the Ara h 1 samples was estimated to be around 75% based on the percentage area of each peak measured in ImageJ. The estimated purity for the Ara h 2 using the same method was lower, around 50%. The major contaminant was the 15 kDa band found just beneath the doublet, most likely Ara h 6 which is highly homologous to Ara h 2. In previous experiments in the laboratory Ara h 2 could not be separated from Ara h 6 and so these were used as a combined fraction. Other reports have shown it is possible to purify these individually (Chen et al. 2013). However, given the reported similarity and redundancy between these two allergens it is possible to justify using the two together, so for the purpose of these experiments, it was decided not to purify them further.

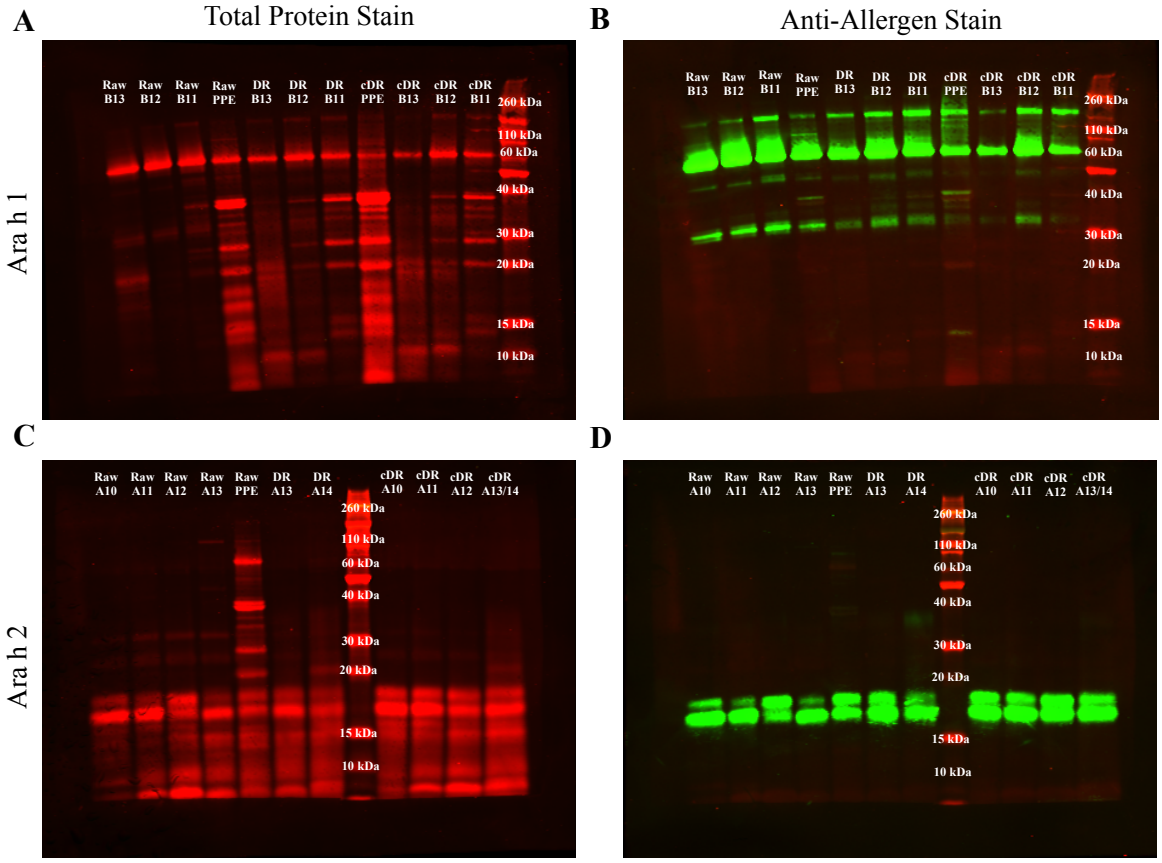

Figure 7.4.2.2: To confirm the identity of the proteins isolated using anion exchange, samples of interest were analysed by western blot. 1 µg of the indicated samples was run on SDS-PAGE, transferred to a nitrocellulose membrane and then probed with anti-Ara h 1 (B) or anti-Ara h 2 (D) antibodies. The blots above show the total protein stain in red (A and C) and the anti-allergen stain in green (B and D).

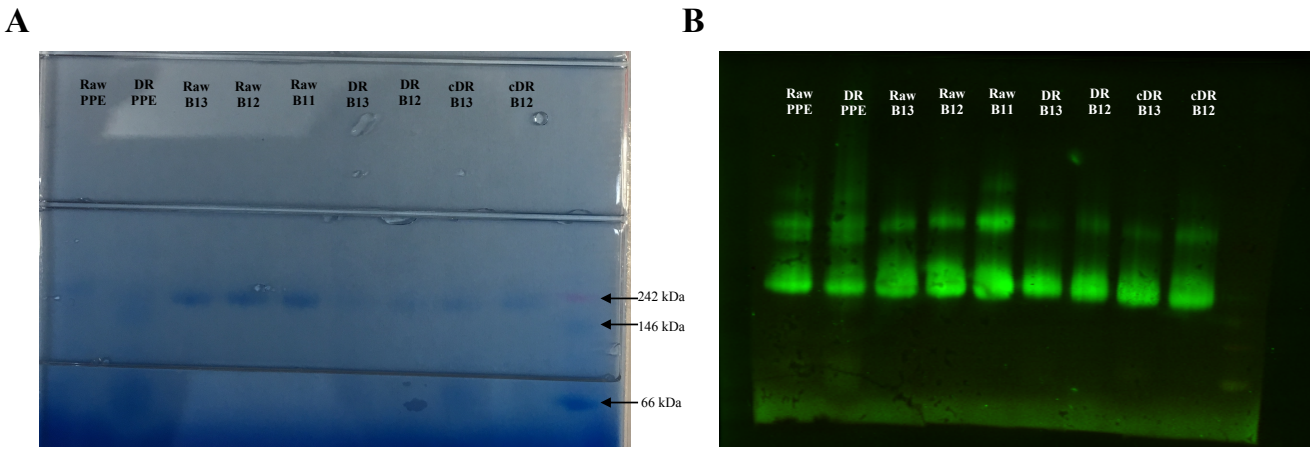

Figure 7.4.2.3: Ara h 1 samples were also analysed by Native PAGE. 1 µg samples were run on Native PAGE gels, transferred to a PVDF membrane and probed with an anti-Ara h 1 antibody as in Figure 7.4.2.2. The western blot is shown in B. The Coomassie stain required for the Native PAGE prevents the use of the total protein stain and so an image of the gel itself is included instead (A).

The enriched protein samples were then examined for their content of RC, CML, GA-pyridine and pyrraline. The results are shown in Figure 7.4.2.4. Interestingly, whilst an increase with roasting in RC content could be noted with Ara h 1 when measured by BH ELISA, there was also a very strong signal with raw, DR and cDR Ara h 2. This contrasts significantly with the carbonyl WB results which showed Ara h 1 to be the major source of carbonyl groups. This phenomenon had been noticed in some previous ELISAs, including using DNPH (data not shown). One possibility is that the different streptavidin detection reagents may be responsible for the different results of the two assays as the ELISAs use HRP-conjugated reagents, whilst the reagent for the western blot is conjugated to an infrared-dye. In this case, the DNPH ELISA gave no signal with the Ara h 2 samples, although the differences between the raw and DR Ara h 1 samples is less apparent. As would be expected from the PPE samples analysed previously, no CML could be detected on the isolated proteins and this was also the case with GA-pyridine and pyrraline. As with the PPE samples, general AGE formation was also assessed by measuring fluorescence. A very low signal is apparent for the DR and cDR samples which is most noticeable for the Ara h 1 samples. This data supports a model in which Ara h 1 is a greater target for modification than Ara h 2.

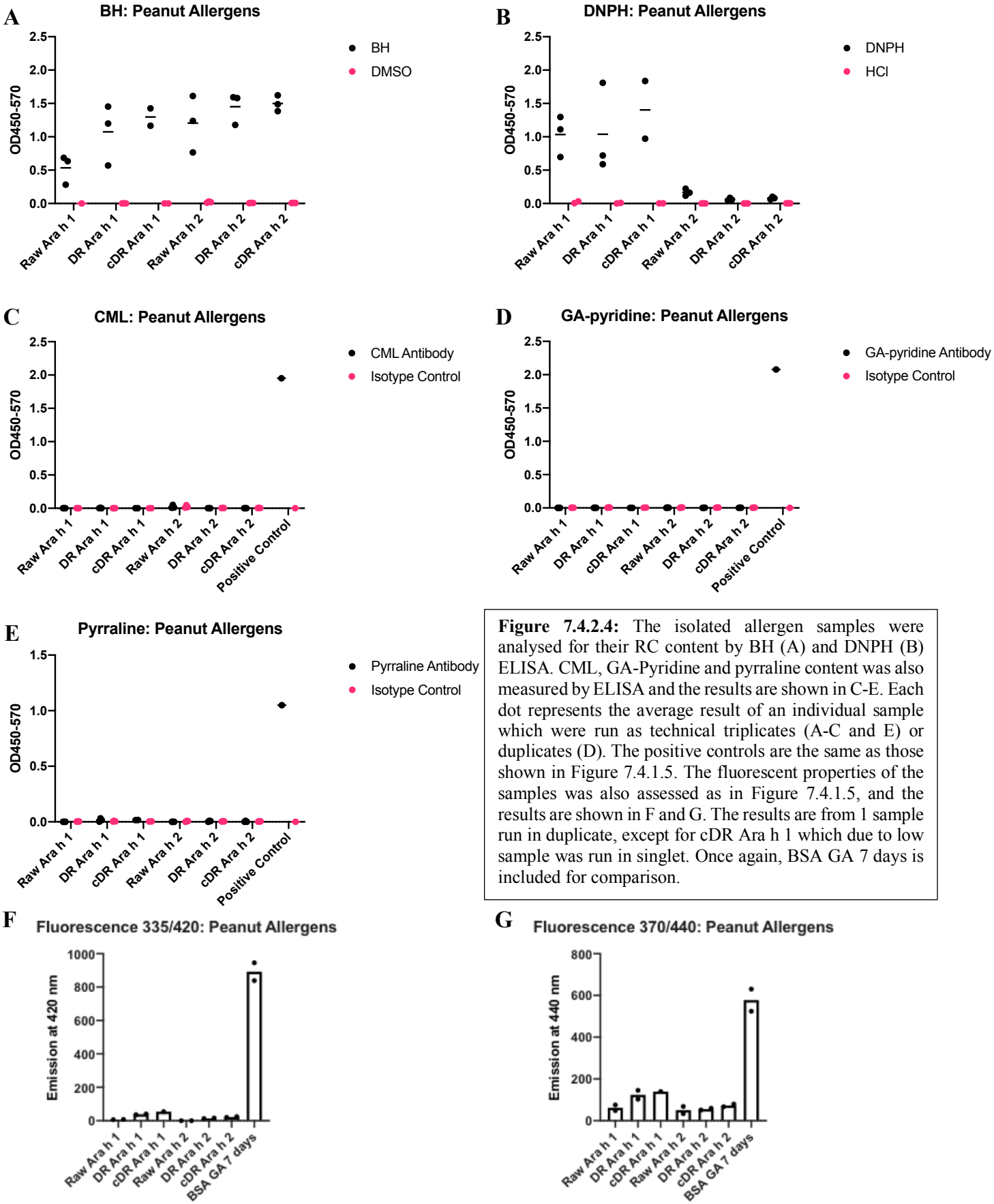

Figure 7.4.2.4: The isolated allergen samples were analysed for their RC content by BH (A) and DNPH (B) ELISA. CML, GA-Pyridine and pyrraline content was also measured by ELISA and the results are shown in C-E. Each dot represents the average result of an individual sample which were run as technical triplicates (A-C and E) or duplicates (D). The positive controls are the same as those shown in Figure 7.4.1.5. The fluorescent properties of the samples was also assessed as in Figure 7.4.1.5, and the results are shown in F and G. The results are from 1 sample run in duplicate, except for cDR Ara h 1 which due to low sample was run in singlet. Once again, BSA GA 7 days is included for comparison.

7.4.3 Testing PPE Samples for Endotoxin Contamination

As the peanut samples were going to be used for immunisation studies and for *in vitro* DC stimulation experiments, it was important to determine whether there was significant endotoxin contamination of the peanut samples. Any endotoxin contamination could alter the results and make interpretation difficult, especially if there was variation in the contamination levels between the samples. TLR4 reporter cells were pulsed with the peanut samples and supernatant assessed for IL-8 secretion to test endotoxin contamination. The results are shown in Figure 7.4.3.1. As can be seen, whilst the raw and DR samples have baseline levels of IL-8 secretion, a small signal can be seen with the cDR PPE and Ara h 1 samples, although not in the cDR Ara h 2.

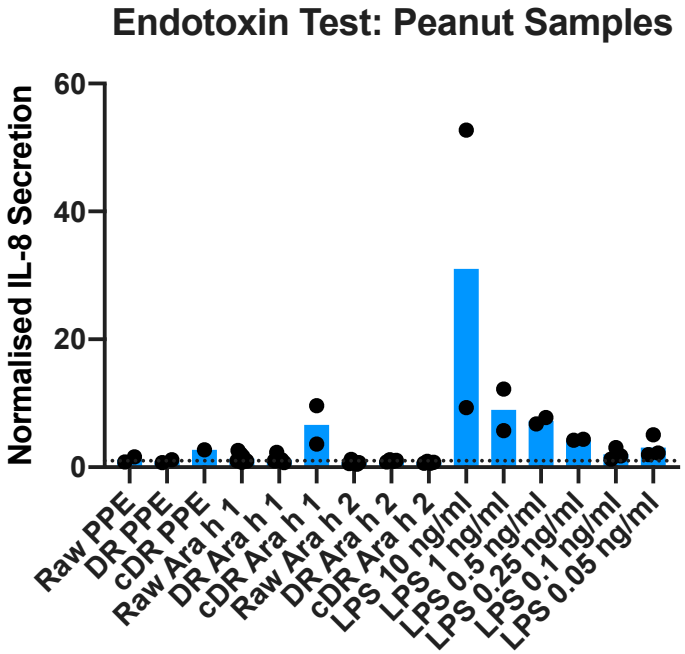

Figure 7.4.3.1: TLR4 reporter cells were pulsed with the indicated protein sample or LPS controls o/n. IL-8 secretion was then measured by ELISA. The IL-8 concentration was normalised to the background secretion by cells pulsed with PBS alone. Each dot represents the results of an independent experiment (LPS) or sample (peanut proteins), whilst the bars show mean. In each experiment each sample was run as two to three biological replicates and the average is shown. The dotted line gives the background IL-8 secretion.

Although the level of contamination was low (approximately 0.1 ng/ml – 0.5 ng/ml), it was still possible the endotoxin could affect the results of future experiments. Therefore, samples were run through an endotoxin removal column. As can be seen in Figure 7.4.3.2, the LPS contamination could be successfully removed using this method. However, examining the proteins by western blot revealed that in the cleaned fractions there was a loss of Ara h 1. Obviously, this sample cannot be used as altering the composition of allergens

within the samples could also substantially impact the results in future experiments, particularly as Ara h 1 seemed to have the majority of the RC groups. One possibility was that the protein sample was incompatible with the endotoxin removal column. The EndoTrap red column was the standard one used in the laboratory. However, it does not always work well with proteins with extreme isoelectric points, such as Ara h 1 which has a pI of 4.55. In contrast, the EndoTrap HD is reported to work over a broader range. Endotoxin removal was therefore attempted with this column. Additional cleaning steps using H_2O and regeneration buffer were also included in the endotoxin removal procedure to ensure to protein remained trapped on the column. However, even with this method there was still loss of Ara h 1 (Figure 7.4.3.2.C).

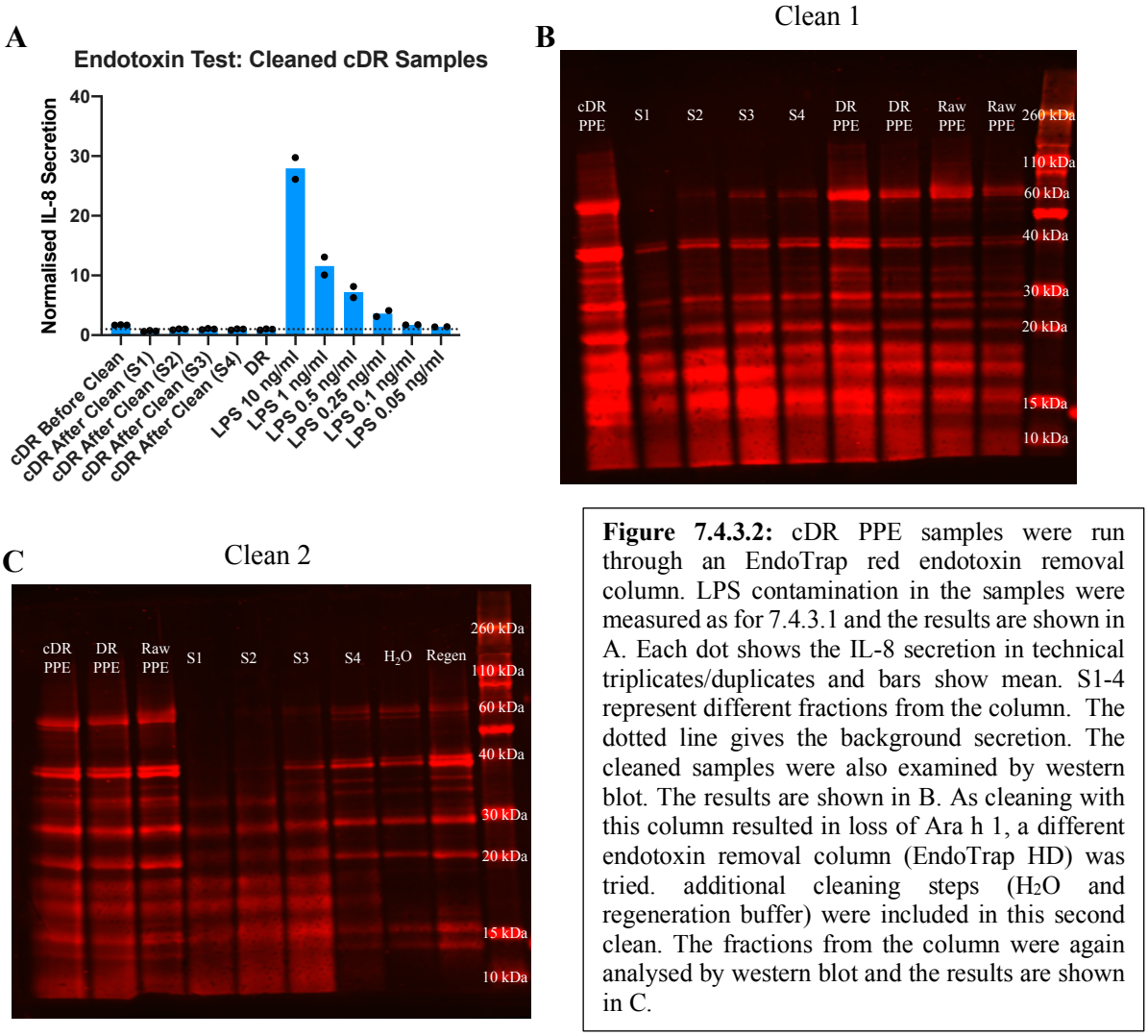

Figure 7.4.3.2: cDR PPE samples were run through an EndoTrap red endotoxin removal column. LPS contamination in the samples were measured as for 7.4.3.1 and the results are shown in A. Each dot shows the IL-8 secretion in technical triplicates/duplicates and bars show mean. S1-4 represent different fractions from the column. The dotted line gives the background secretion. The cleaned samples were also examined by western blot. The results are shown in B. As cleaning with this column resulted in loss of Ara h 1, a different endotoxin removal column (EndoTrap HD) was tried. additional cleaning steps (H_2O and regeneration buffer) were included in this second clean. The fractions from the column were again analysed by western blot and the results are shown in C.

With the methods available, it was not possible to remove the endotoxin contamination from the sample. One possibility considered was that the Ara h 1 in these samples was forming a complex with LPS and it was this that was causing the protein to become trapped on the column. Certainly, the LPS contamination seemed to be specific for Ara h 1 as the Ara h 2 produced from the same sample appeared to be clean. It was therefore decided to investigate whether this was a specific problem with the prepared sample, or whether commercial preparations in general had some level of LPS contamination. If it was the case that there was minor contamination in most commercially available dry roasted peanuts, then the cDR samples produced in the laboratory may actually be more representative of the product that most people would be exposed to. Therefore, it would be worth including the endotoxin contaminated samples in future studies. Any differences between the in-house DR and cDR would just need to be interpreted with regard to the different endotoxin contamination level. Therefore DR peanut samples were purchased from a variety of sources, then cDR PPE was isolated and tested them for LPS contamination. As can be seen below in Figure 7.4.3.3, all the tested samples had some level of endotoxin contamination. For future *in vivo* experiments, brand 1 was selected as it had the lowest endotoxin contamination.

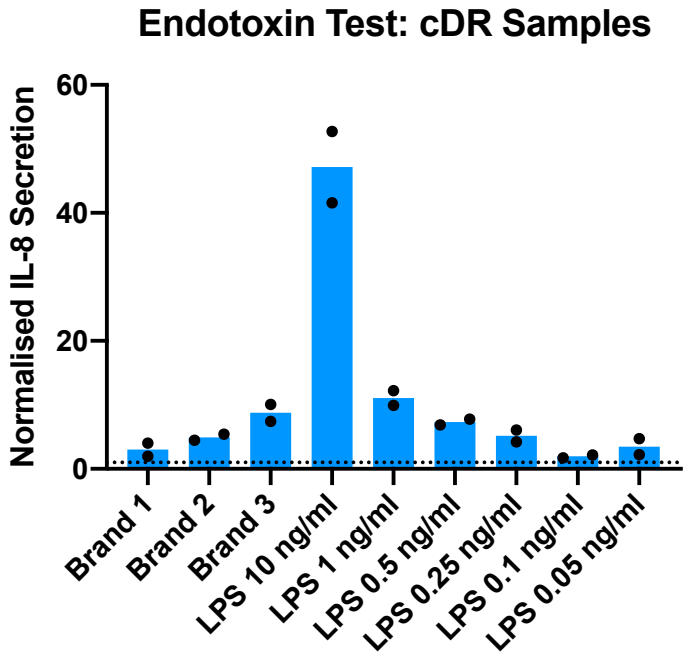

Figure 7.4.3.3: different brands of dry roasted peanuts were acquired and used to produce cDR PPE samples. These were than analysed for LPS contamination as in 7.4.3.1. Each dot show the average from one independent experiments, there were three biological replicates in each experiment. The bars show mean and the dotted line gives the background IL-8 secretion.

7.4.4 DC Uptake and Activation Studies Using Peanut Proteins

Having prepared the peanut samples, the next stage was to assess their *in vitro* and *in vivo* immune-modulating effects. As for the protein samples in Chapter 4, Ara h 1 was fluorescently labelled and uptake by DCs was assessed. In Figure 7.4.4.1.A a gel showing the fluorescent signal and silver stain is shown. This shows successful labelling of samples and that there was no nonspecific background fluorescence. These samples were then used to examine uptake of DR and raw Ara h 1 by bone marrow derived DCs (BMDCs) using either the plate-based or in-tube assay (see Chapter 4). As can be seen, there was no significant increase in protein uptake with DR compared to raw Ara h 1 when the uptake was measured using either assay. As it was only heavily modified samples which showed an increase uptake in previous experiments (see Chapter 4), this may suggest DR Ara h 1 is more minimally modified, an idea supported by the assays in the previous section showing RC formation but no CML or other AGEs.

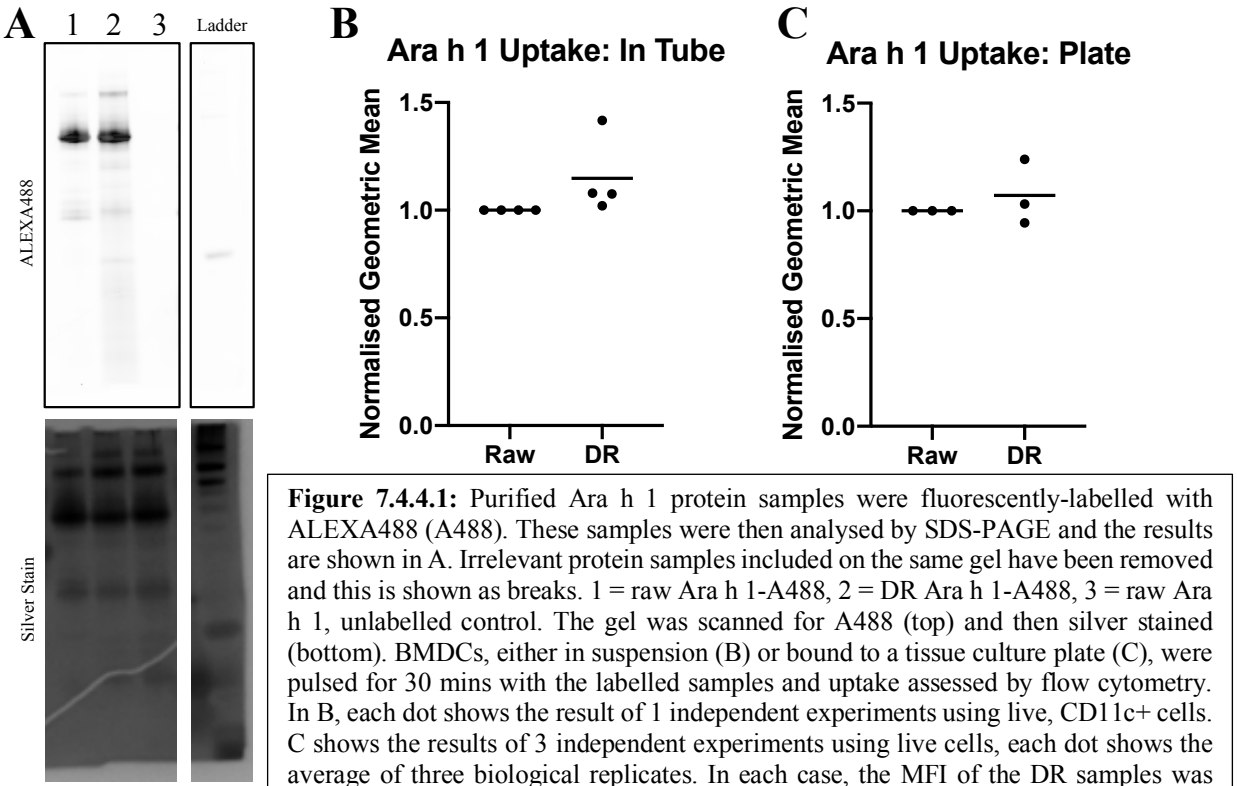

Figure 7.4.4.1: Purified Ara h 1 protein samples were fluorescently-labelled with ALEXA488 (A488). These samples were then analysed by SDS-PAGE and the results are shown in A. Irrelevant protein samples included on the same gel have been removed and this is shown as breaks. 1 = raw Ara h 1-A488, 2 = DR Ara h 1-A488, 3 = raw Ara h 1, unlabelled control. The gel was scanned for A488 (top) and then silver stained (bottom). BMDCs, either in suspension (B) or bound to a tissue culture plate (C), were pulsed for 30 mins with the labelled samples and uptake assessed by flow cytometry. In B, each dot shows the result of 1 independent experiments using live, CD11c+ cells. C shows the results of 3 independent experiments using live cells, each dot shows the average of three biological replicates. In each case, the MFI of the DR samples was normalised to the MFI of the raw samples. Significance was tested using Wilcoxon Signed Rank test. In B and C the bars show mean. MFI = mean fluorescence intensity.

Next, the capacity of the different allergens and mixed protein samples to alter the activation status of DCs was assessed. Previous work from our laboratory had shown that the modified peanut samples could not induce increased expression of costimulatory molecules or secretion of proinflammatory cytokines (Moghaddam et al. 2014). Therefore, to extend these findings, changes in the secretory profile of BMDCs exposed to peanut allergens were examined more broadly. Raw and DR Ara h 1, Ara h 2 or PPE samples were included in the Luminex assay originally shown in Chapter 3. The results for these samples are shown in the heatmap in Figure 7.4.4.2. None of the peanut proteins induced the dramatic changes in cytokine secretion seen with LPS and this data set confirmed that these proteins were not inducers of inflammatory cytokine release. In general, the raw and DR Ara h 2 and PPE samples behaved very similarly to each other. Overall differences between raw and DR Ara h 1 were also relatively minor, however, DR Ara h 1 did seem to suppress the release of inflammatory cytokines such as TNFα and induce the secretion of HGF. In this way, it behaved very similarly to the HEL GA 3 h and HEL GA-PR 3 h samples (see Chapter 3).

These changes were further investigated by including Ara h 1 samples in the time course experiment also discussed in Chapter 3. Examining the results (Figure 7.4.4.3), both raw and DR Ara h 1 could induce the release of HGF from mBMDCs. Secretion was higher for DR than raw, but this difference was not statistically significant. None of the other tested cytokines showed significant differences.

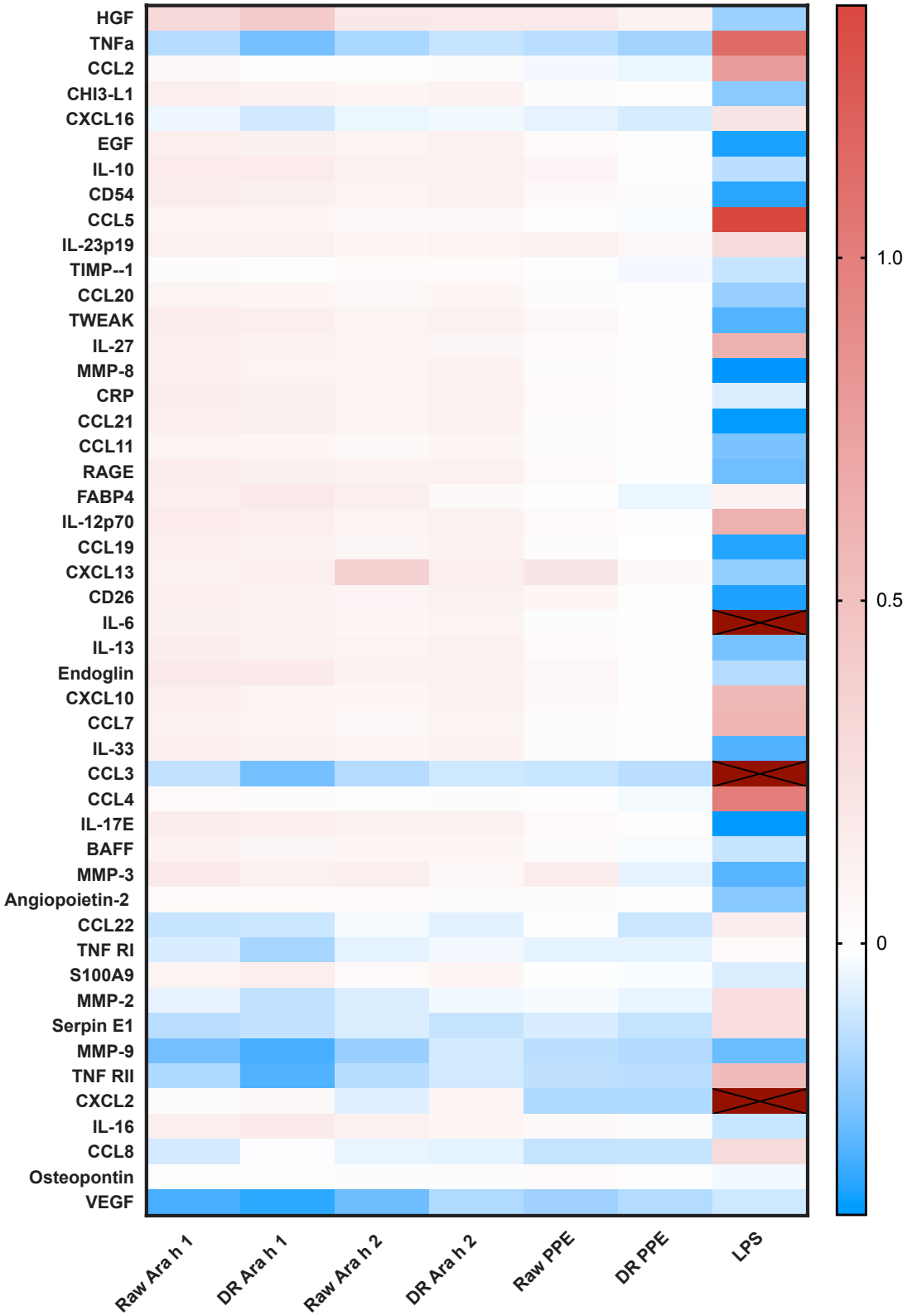

Figure 7.4.4.2: mBMDCs were pulsed with the indicated sample for 18 h. Cytokine release in the supernatant was then assessed by Luminex Assay. The heatmap shows the log fold change in cytokine secretion compared to unpulsed BMDCs. The LPS data is also shown in Chapter 3. The results show the average response from two independent experiments with two biological replicates in each. In the case of LPS, the concentration of three cytokines was above the limits of the standard curve, these are shown as dark red boxes with a cross through them.

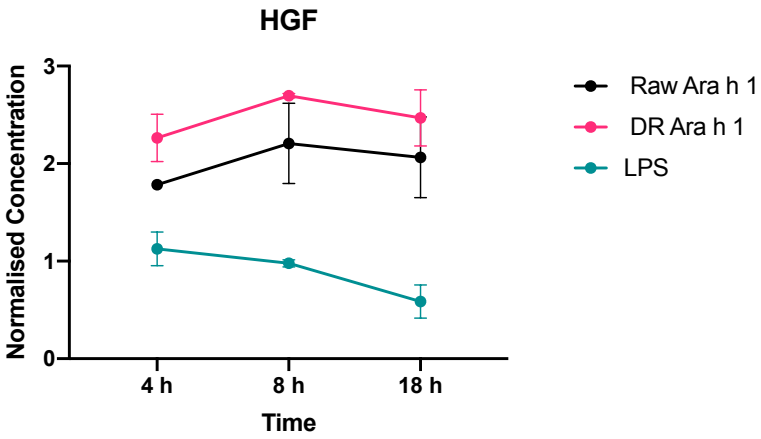

Figure 7.4.4.3: mBMDCs were pulsed with raw Ara h 1, DR Ara h 1 or LPS for 4, 8 or 18 h. Supernatant was collected and cytokine secretion assessed by Luminex assay. The graph shows HGF release normalised to the concentration of HGF in unpulsed BMDCs left for the same amount of time. At 4 h n = 3, 8 h n = 2 and at 18 h n = 4, where n is the result from an independent experiment. The results are shown as mean with standard deviation (SD). Significance was assessed using a Mann Whitney test. The LPS data are also shown in Chapter 3.

7.4.5 Initial Immunisation Studies with PPE

Having generated PPE samples with minimal endotoxin contamination, the next stage was to test *in vivo* immunogenicity. The experiment was performed to confirm or refute previous findings from our laboratory, and to include cDR which had not been used in the previous study. Multiple different antigen administration routes had been included in the previous publication (Moghaddam et al. 2014), including s.c. injection followed by peanut feeding and s.c. injection followed by gavage. In this study, s.c. injection followed by peanut feeding was chosen. It was decided to feed the mice peanuts rather than gavage as this would be less invasive for the mice and more reflective of normal exposure to peanuts. Mice were immunised, bled and fed according to the schedule outlined in Figure 7.4.5.1. In each feed, the mice ate a similar amount of food regardless of immunisation group (Figure 7.4.5.2).

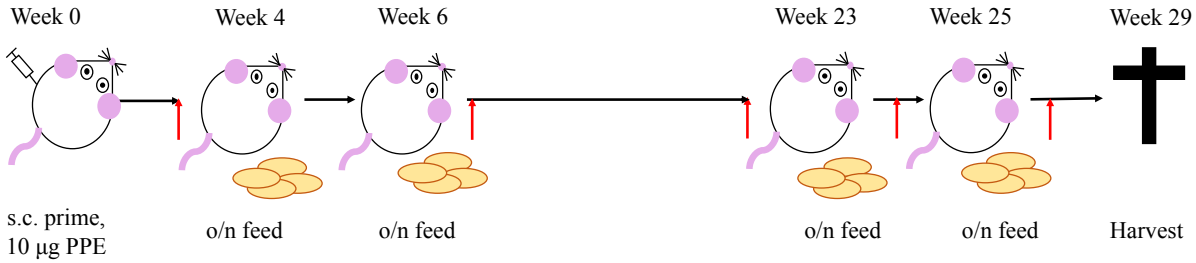

Figure 7.4.5.1: The immunisation and bleed schedule for the first *in vivo* PPE experiment is shown. Bleeds are indicated by the red arrows. BALB/c mice were used for this experiment.

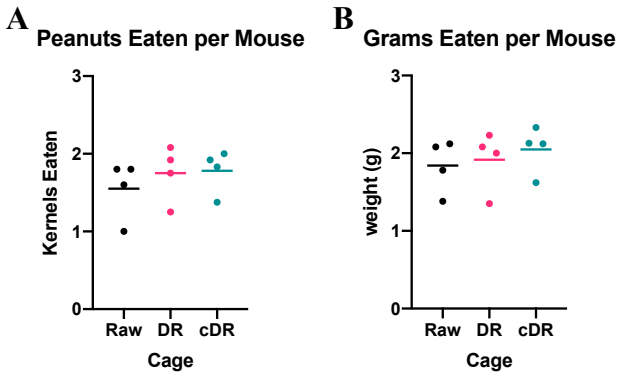

Figure 7.4.5.2: The amount and weight of the peanuts consumed per mouse at each feed is shown in the graphs on the left. There were no statistically significant differences between treatment groups (Kruskal-Wallis test). See Figure 7.4.5.1 for the feeding schedule.

The mice were bled and sera collected at multiple points during the experiment. At each time point, the generation of antibodies to raw, DR or cDR PPE was assessed and the results are shown in Figure 7.4.5.3. Before the first feeding, there was only a very weak signal which increased after the first two feeds. Initially, the DR and cDR seemed to behave very similarly, inducing higher levels of peanut-specific IgG than raw PPE. However, during the period between weeks 7 and 24 the two groups diverged, with the average response in the cDR being similar to that seen in the raw group whilst the DR group remained higher. However, for both the DR groups the response seems to have saturated as a further increase was not seen with more feeds. In contrast, after the fourth feed, the IgG levels in the raw PPE immunised group increased to around those seen in DR PPE immunised mice. Also shown in Figure 7.4.5.3 are the individual mouse results at week 26. As can be seen the mice in the Raw and DR immunised group had tightly clustered responses, whereas the cDR showed more divergent responses. In the latter group, there seem to be two clusters, one containing responders which have similar IgG levels to the DR group, and 2 non-responders which have no or very low responses despite multiple feeds. Based on these results, it was decided to terminate the mice as further feedings did not seem likely to increase the responses.

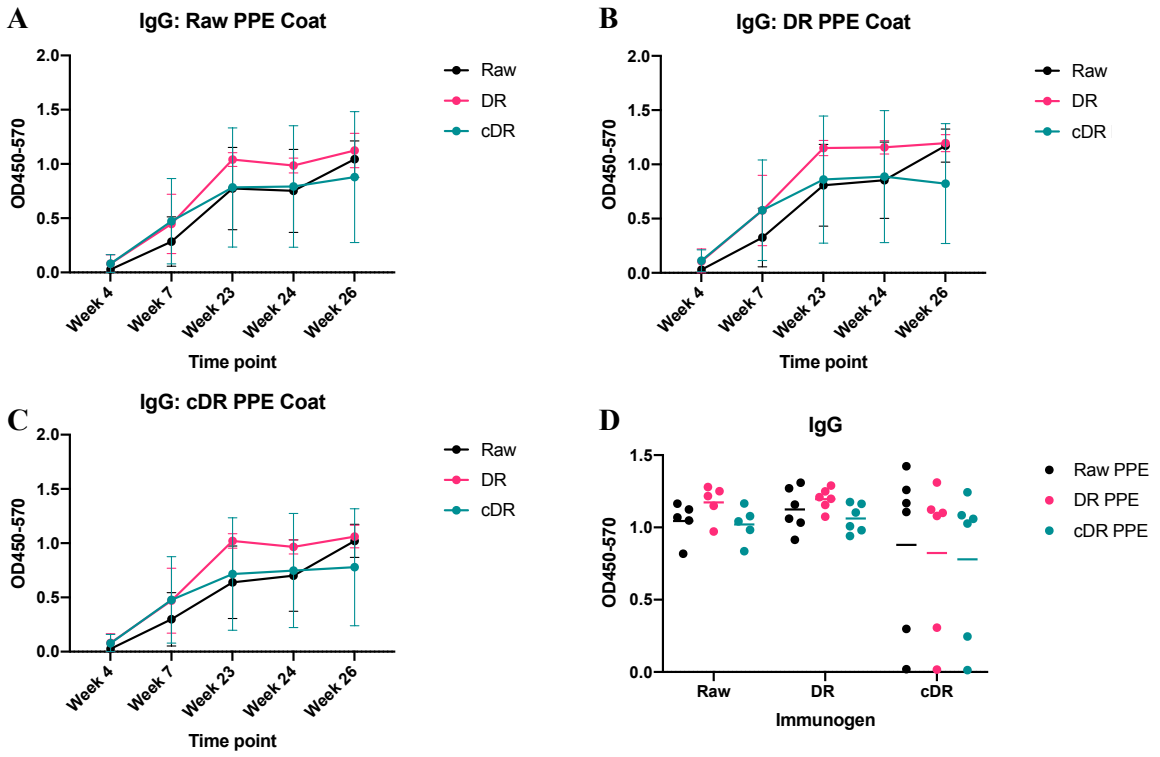

Figure 7.4.5.3: The anti-PPE antibody responses in the mice immunised with raw, DR or cDR PPE were followed over the course of the immunisation experiment. The ELISA plates were coated with raw, DR or cDR PPE to determine if the responses were to native protein or to neo-antigens formed during roasting. The graphs show mean and 95% CI and n = 5 - 6. D shows the responses of individual mice at week 26 (each dot is one individual whilst bars show mean), the protein used for coating is indicated in the legend. There were no significant differences between groups (two-way ANOVA).

Next, the antibody levels in the mice were quantified using end point titres ELISAs using serum samples from selected time points. In Figure 7.4.5.3, the antibody responses to raw, DR and cDR PPE were examined in order to determine whether there were specific responses to DR PPE samples which may have indicated the formation of responses to neoantigen present only in roasted samples. However, the responses were very similar regardless of the antigen used for coating the ELISA plates, which suggested that the majority of responses were against native protein. Therefore for future experiments raw PPE was used in ELISAs. The results of the end point titre ELISA are shown in Figure 7.4.5.4, and they indicate that the response was dominated by IgG1, which is not surprising given

the Th2 bias of BALB/c mice (Sellers et al. 2012). However, there are no significant differences between immunisation groups at any time point, which suggests that dry roasting did not make the peanut samples substantially more immunogenic than raw.

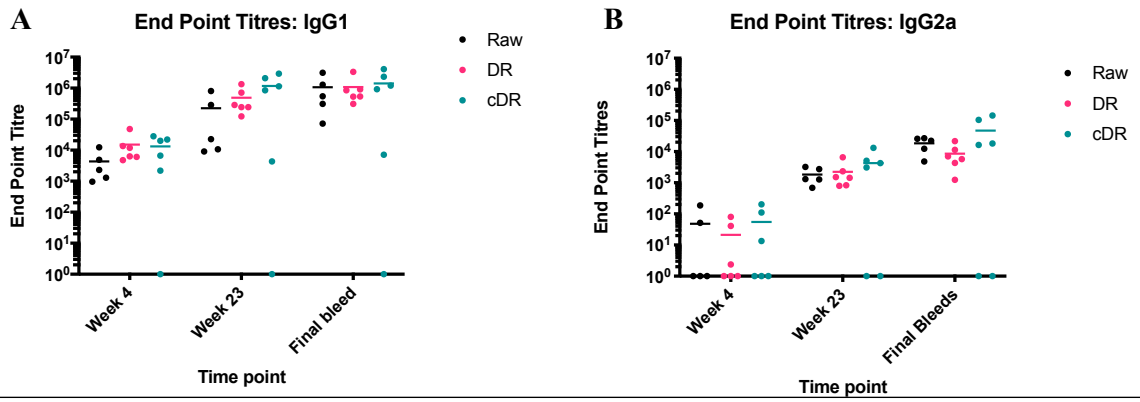

Figure 7.4.5.4: To provide a quantitative measure of antibody production, IgG1 and IgG2a end point titres were determined for the PPE immunised mice at selected time points. Namely week 4 (after immunisation, before feeds 1 and 2), week 23 (before feeds 3 and 4) and at harvest (final bleeds). Each dot shows an individual mouse and bars show mean. Significance was determined using a two-way ANOVA, there were no significant differences between groups at any time point. To allow for a log transformation, 1 was added to all 0 values. The immunisation group is given in the legend.

Lastly, the generation of anti-peanut IgE responses in mice was measured. The IgG results had indicated that the different samples had similar immunogenicity, but the IgE would indicate whether the DR samples had increased allergenicity, that is whether they were better able to induce allergic-type responses. However, this revealed that the raw PPE immunised mice did not have lower IgE levels than DR or cDR immunised, as there were no significant differences between groups. At least with regard to antibody responses, this study had therefore failed to replicate previous findings.

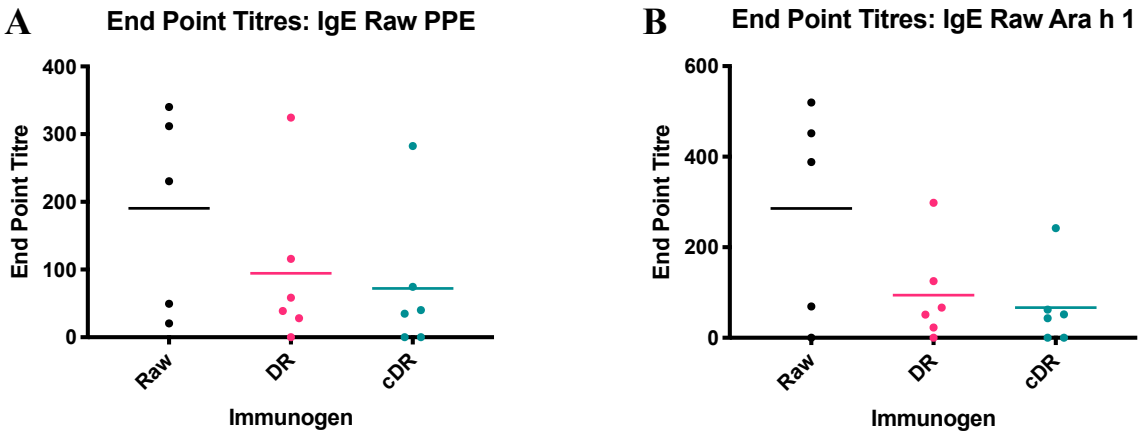

Figure 7.4.5.5: The development of anti-peanut IgE in the mice immunised with PPE was assessed by ELISA. Specifically, levels of anti-raw PPE and anti-raw Ara h1 IgE were assessed by calculating the end point titre using sera collected at harvest. The results are shown in A and B, there were no significant differences (Kruskal-Wallis test). Each dot shows the response of one mouse with bars showing mean.

Finally, the development of cellular responses was assessed by isolating splenocytes from each mouse and pulsing them with PPE samples. After 3 days in culture, rates of proliferation were determined by 18 h incubation with ^{3}H-Thymidine. The results are shown below in Figure 7.4.5.6. Neither immunisation group or pulsing conditions had a significant influence on the outcome with all groups showing similar responses.

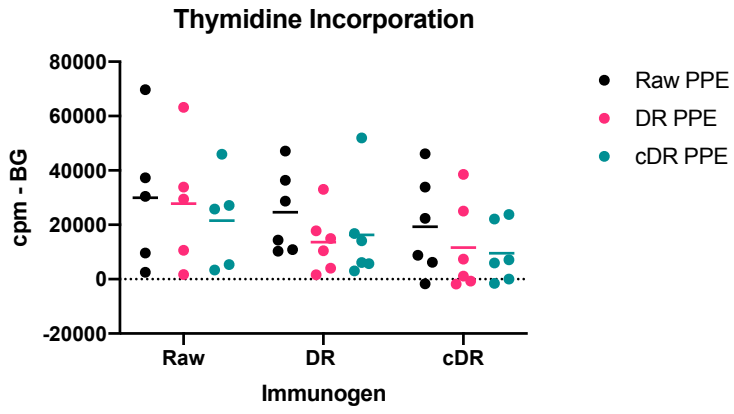

Figure 7.4.5.6: Spleens from the PPE immunised mice were collected at harvested. Isolated splenocytes were then pulsed with raw PPE, DR PPE or cDR PPE. The sample used for pulsing is given in the figure legend. After 3 days in culture, ^{3}H-thymidine was added to the wells and 18 h later the thymidine incorporation was measured. In all cases the signal from unpulsed wells has been used as the background. The data were analysed using a two-way ANOVA, there were no significant differences. Each dot shows an individual mouse and the bars show mean. Abbreviations used: cpm = counts per minute, BG = background

Lastly, the nature of the immune responses were assessed by examining cytokine secretion in the splenocyte cultures by ELISA (IL-4) or Luminex assay (IL-2, IL-5, IL-13, IL-6, IL-17a, TNFα and IFNγ). For the most part, there were no significant differences between the responses of different immunisation groups (Figure 7.4.5.7). Although, there were occasional variations in response to type of PPE within groups, this is most notable for IFNγ, TNFα and IL-17a where secretion is only seen when the splenocytes were pulsed with cDR PPE. The only significant differences between immunisation groups were an increased secretion of TNFα and IFNγ in the raw immunised group over the DR or cDR immunised mice. Notably this was only seen when the splenocytes were pulsed with cDR PPE. This may be a reflection of the minor LPS contamination still in the cDR PPE, however it is surprising that this effect is only seen in the raw PPE immunised group. One possibility is that in the DR and cDR mice, a suppressive response has developed preventing the activation of Th1, PPE-responsive cells. However, overall the data produced in this study do not support the hypothesis that dry roasting peanuts increases their immunogenicity.

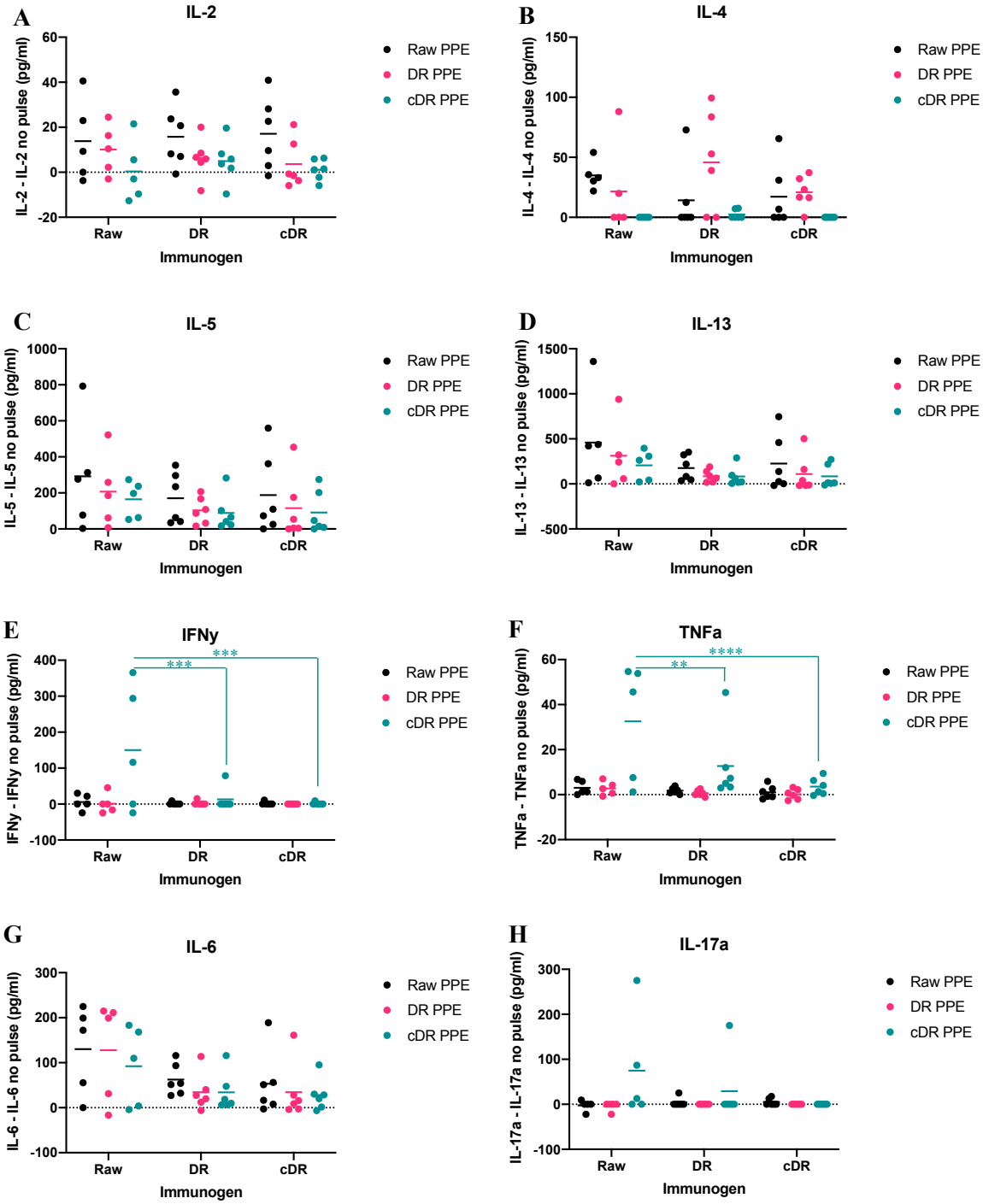

Figure 7.4.5.7: Supernatant from the splenocyte culture in Figure 7.4.5.6 was collected on day 1 (IL-4) and day 3 (all other cytokines). Cytokine secretion was assessed by Luminex assay, except for IL-4 where secretion was analysed by ELISA. In all cases, unpulsed background wells were included and any non-specific signal seen in those wells was removed to find the specific response. All data were assessed by two-way ANOVA followed by Dunnett's multiple comparison test. Each dot is an individual mouse and bars show mean, ** = $p \leq 0.01$, *** = $p \leq 0.001$, **** = $p \leq 0.0001$. Black dots give the results from splenocyte cultures pulsed with raw PPE, pink dots DR PPE and teal dots cDR PPE. This key is given in the legend.

7.4.6 Further Immunisation Studies with PPE and Isolated Ara h 1

Given that the results reported above contrasted with those that had previously been seen in the laboratory, it was important to address factors which may have caused these differences. One possibility considered was that the mice had received too many boosts (feeds) and this had masked differences between the groups. Examining the time course, it did appear that before feeds 3 and 4 the DR immunised mice had a greater response than the raw. To examine whether excess feeds had influenced the results, another immunisation and feeding experiment was performed which included only two feedings, this is outlined in Figure 7.4.6.1.

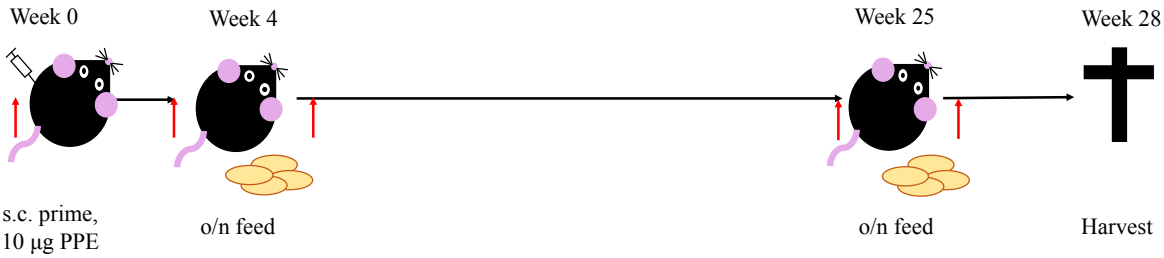

Figure 7.4.6.1: Modified immunisation schedule for the second PPE immunisation. Again, red arrows indicate bleeds. C57BL/6N mice were used for this experiment.

As before, food consumption in each cage was monitored to determine if the mice ate similar amounts. The amount eaten in the two feeds is shown in Figure 7.4.6.2. C57BL/6N mice were also used in this experiment instead of BALB/c. Previous experiments demonstrated these mice require a greater number of immunisations to develop significant immune

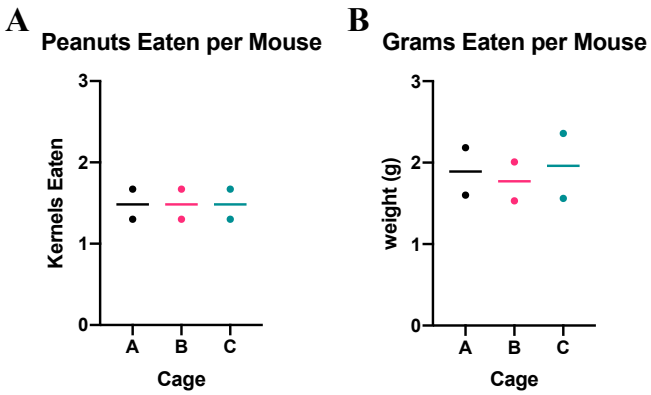

Figure 7.4.6.2: At each feed outlined in Figure 7.4.6.1, the number of kernels and weight eaten in each cage was recorded. Each cage contained three mice, immunised with raw, DR or cDR PPE. The results are shown in A and B.

responses. Therefore "overboosting" resulting in saturation of the immune response seemed less likely. Moreover, using this strain would also confirm whether the type 2 bias seen in the experiment in 7.4.5 was a result of background strain or the immunogens, as C57BL/6 mice have a Th1 biased immune system (Sellers et al. 2012).

The antibody responses are shown in Figure 7.4.6.3. As can be seen, the responses were highly variable within groups with both the raw and cDR groups possessing one high responder in each case. The responses in the DR group were more clustered but generally low. Overall, there were no significant differences between groups. In all cases, the response was dominated by IgG1, indicating that even in a Th1 biased strain the PPE samples induced Th2 responses. Similarly, when the development of anti-peanut IgE responses were assessed (Figure 7.4.6.4), the end point titres in each group were very variable. Only one mouse in each group developed a high IgE titre and there were no statistically significant differences between groups.

Finally, the cellular PPE responses in the spleen were determined as for the previous study, although in this case all cytokines were measured by ELISA. The results are shown below in Figure 7.4.6.5. Interestingly, responses were highly dependent on the PPE sample. In this case, DR PPE seemed to exert a toxic effect on the cells as no proliferation was seen and cytokine responses were suppressed when this was used to pulse the splenocytes. cDR PPE did not have the same effect, but responses were highest when raw PPE was used as the stimulus. Generally, the responses in the mice immunised with raw PPE were higher than for those immunised with DR or cDR PPE, and this reached significance with the IL-5 and IFNγ responses. Thus, this experiment had again been unable to confirm the finding that DR PPE is more immunogenic than raw.

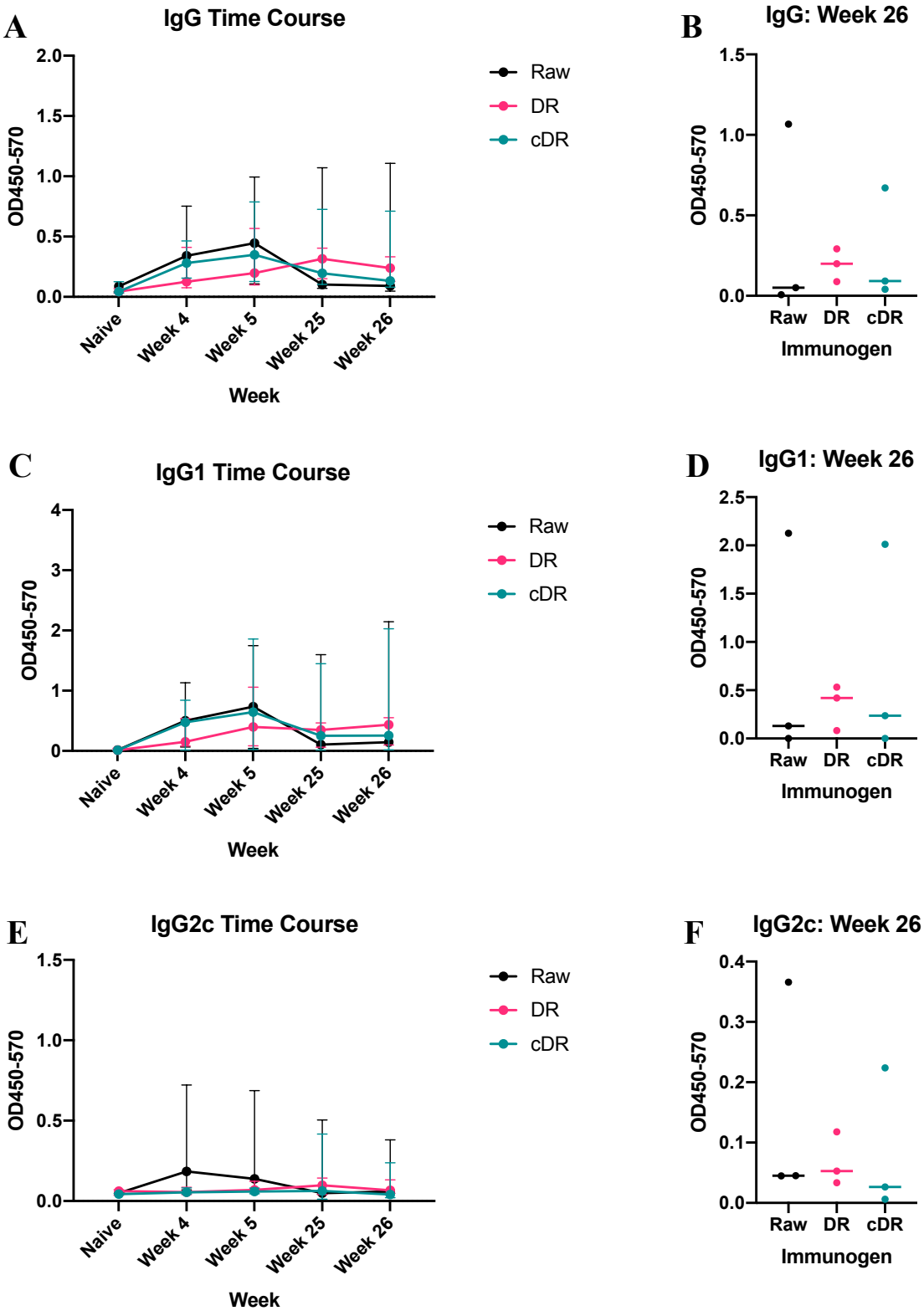

Figure 7.4.6.3: The anti-peanut IgG, IgG1 and IgG2c responses were followed throughout the second PPE immunisation/peanut feeding experiment. In each case the ELISA plates were coated with raw PPE. The time course graphs show median with range. B, D and F show the responses at week 26, each dot represents an individual mouse whilst the bars show median. Significance was tested using a Kruskal-Wallis test, the differences were not significant.

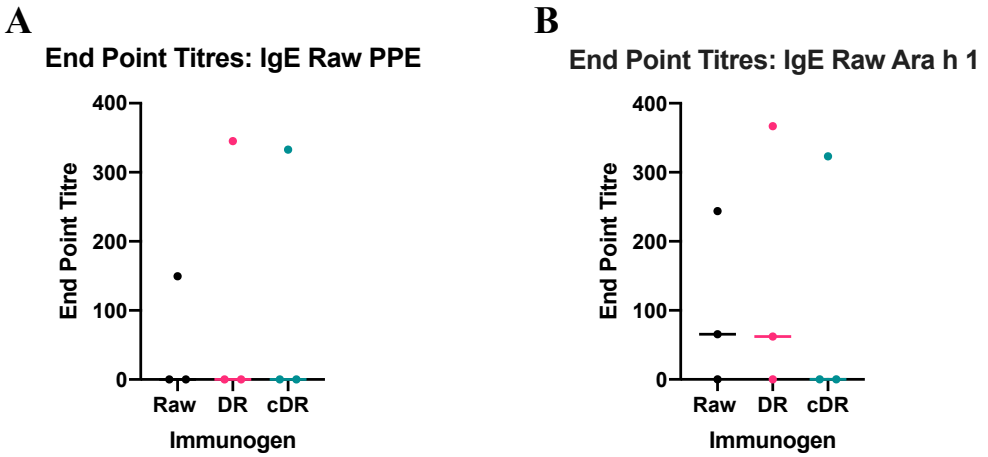

Figure 7.4.6.4: The development of peanut specific IgE responses was examined in mice in the second immunisation study. Again, anti-raw PPE and anti-raw Ara h 1 IgE levels were quantified by end point titres for each mouse. The sera for this experiment was collected at harvest. Each dot represents an individual mouse and the bars show median. Results were analysed by Kruskal-Wallis.

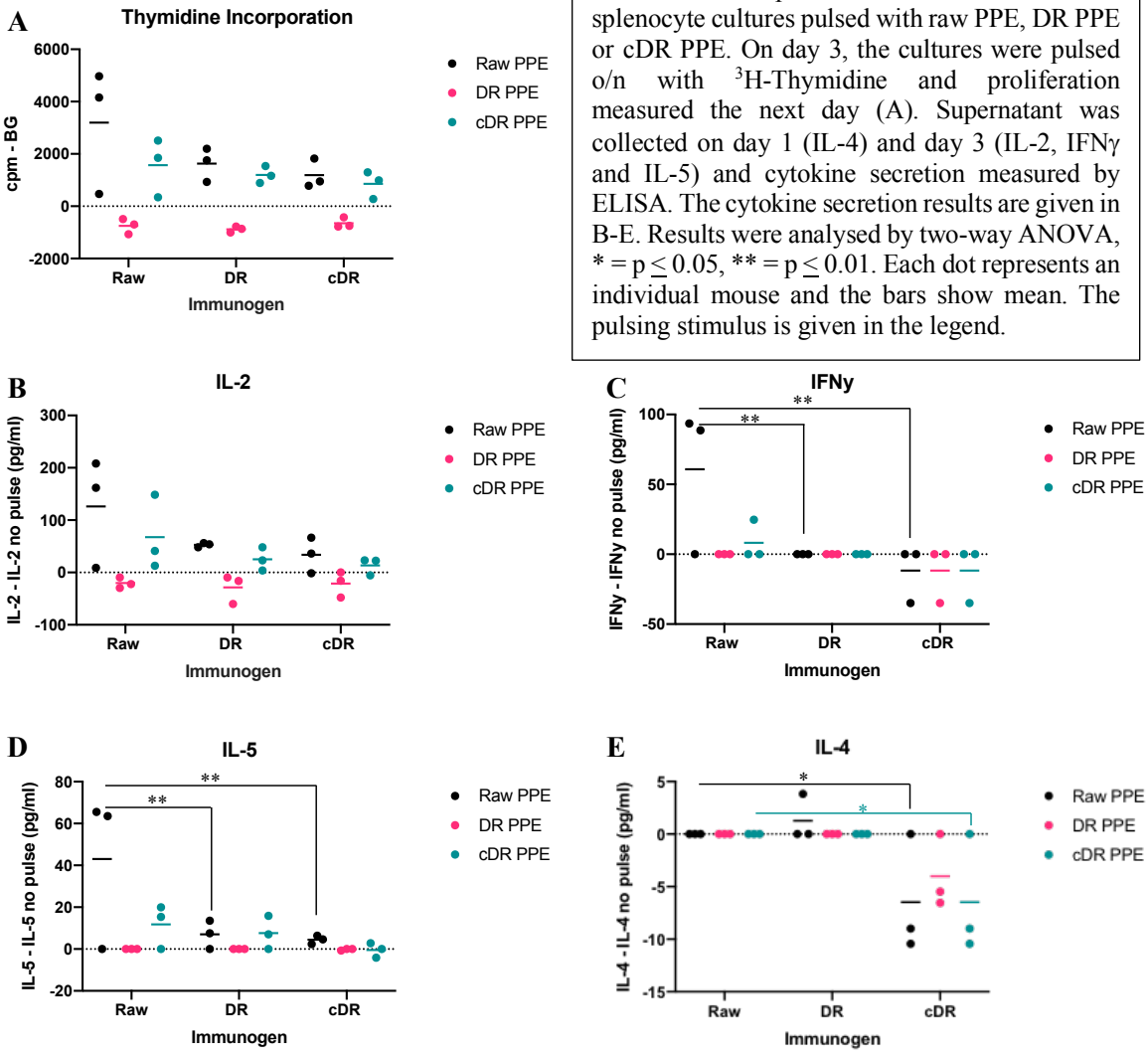

Figure 7.4.6.5: Spleens from the mice in the second PPE experiment were harvested and splenocyte cultures pulsed with raw PPE, DR PPE or cDR PPE. On day 3, the cultures were pulsed o/n with ^{3}H-Thymidine and proliferation measured the next day (A). Supernatant was collected on day 1 (IL-4) and day 3 (IL-2, IFNγ and IL-5) and cytokine secretion measured by ELISA. The cytokine secretion results are given in B-E. Results were analysed by two-way ANOVA, * = $p \leq 0.05$, ** = $p \leq 0.01$. Each dot represents an individual mouse and the bars show mean. The pulsing stimulus is given in the legend.

The last immunisation experiment with peanut samples was a s.c. immunisation using isolated Ara h 1 samples. Obviously, one factor which could have affected the previous results was the balance of allergens in the extracted samples, this can be altered by dry roasting and is hard to control. Using a pure allergen sample would account for this. Moreover, the s.c. immunisation experiment in Chapter 3 had indicated that HEL GA 3 h was a strong inducer of antibody responses and the data on protein characterisation and *in vitro* BMDC experiments had indicated that HEL GA 3 h and the DR Ara h 1 samples behaved similarly. It was therefore of interest whether these samples also behaved similarly *in vivo*. BALB/c mice were immunised s.c. with 5 µg of Raw, DR or cDR Ara h 1 and left for 10 weeks, thereby following the same protocol used in Chapter 3. At weeks 5 and 9 serum samples were collected to measure the antibody responses. The results are shown in Figure 7.4.6.6. All but two of the mice (both in the DR group) developed good antibody responses by week 5. This was an IgG1 dominated response with little IgG2a formed. However, the DR Ara h 1 was not a better inducer of antibody responses than raw, and overall there were no significant differences between groups.

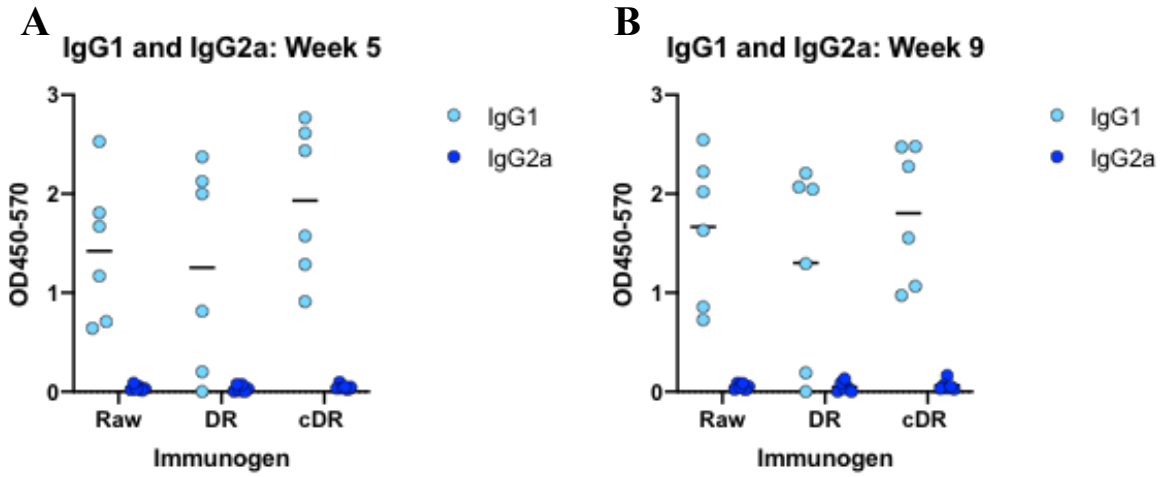

Figure 7.4.6.6: BALB/c mice were immunised s.c. with 5 µg of raw, DR or cDR Ara h 1. Sera were collected and tested for the development of antibody responses to raw PPE at weeks 5 and 9. Specifically, levels of peanut specific IgG1 and IgG2a were measured by ELISA. Each dot shows the response of one mouse and the bars show mean. Data were analysed using a Kruskal-Wallis test, there were no significant differences.

The development of anti-peanut IgE responses was also assessed and the results are shown in Figure 7.4.6.7. The end point titres in this experiment are low in comparison to the peanut feeding experiments, indeed the responses to raw PPE are almost non-existent. This is not surprising as these mice had only had a single immunisation whereas in the previous experiments the mice had multiple exposures over a long period of time. However, only mice immunised with DR or cDR Ara h 1 developed detectable levels of anti-Ara h 1 IgE. Whilst these differences did not quite reach significance when tested with a Kruskal-Wallis test ($p = 0.0504$), this evidence does suggest that the DR and to a lesser extent the cDR Ara h 1 samples may be more allergenic than the raw.

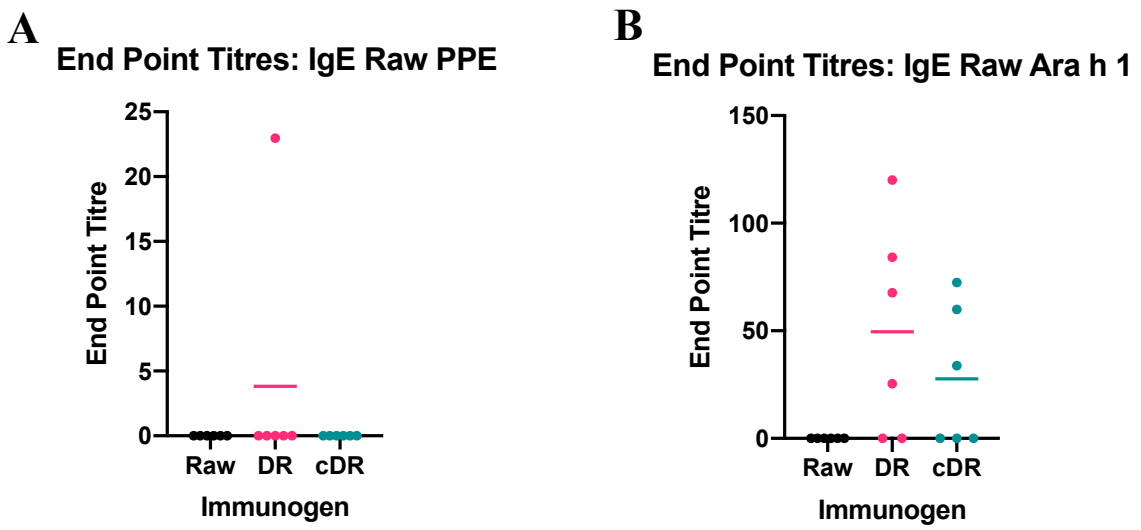

Figure 7.4.6.7: At week 10, the mice immunised with raw, DR or cDR Ara h 1 were culled and sera was collected. This sera was tested for the presence of IgE against raw PPE or raw Ara h 1. As in Figure 7.4.5.5, the IgE levels were quantified by end point titre ELISA. The results are shown in A and B. Each dot shows the response of one mouse and the bars indicate mean. The data were analysed using a Kruskal-Wallis test.

As with the other experiments, the splenocyte responses were then assessed (Figure 7.4.6.8). Similar to the C57BL/6N immunisation experiment, the responses were highly dependent on the stimulus with DR PPE suppressing responses and the strongest responses being seen with raw PPE. In this case, mice immunised with DR Ara h 1 developed significantly stronger cellular responses compared to those immunised with raw Ara h 1 as spleens from

mice immunised with DR Ara h 1 had significantly greater production of IL-2 and IL-5, and higher proliferation. However, this effect was not seen with the cDR samples. Instead for this latter group there are cDR specific IFNγ and IL-4 responses, although a two-way ANOVA indicated that there were no significant differences between immunisation groups for these cytokines. Therefore, whilst the dry roasting procedure may make Ara h 1 more immunogenic with regard to splenocyte responses, this is not necessarily true for commercially available samples.

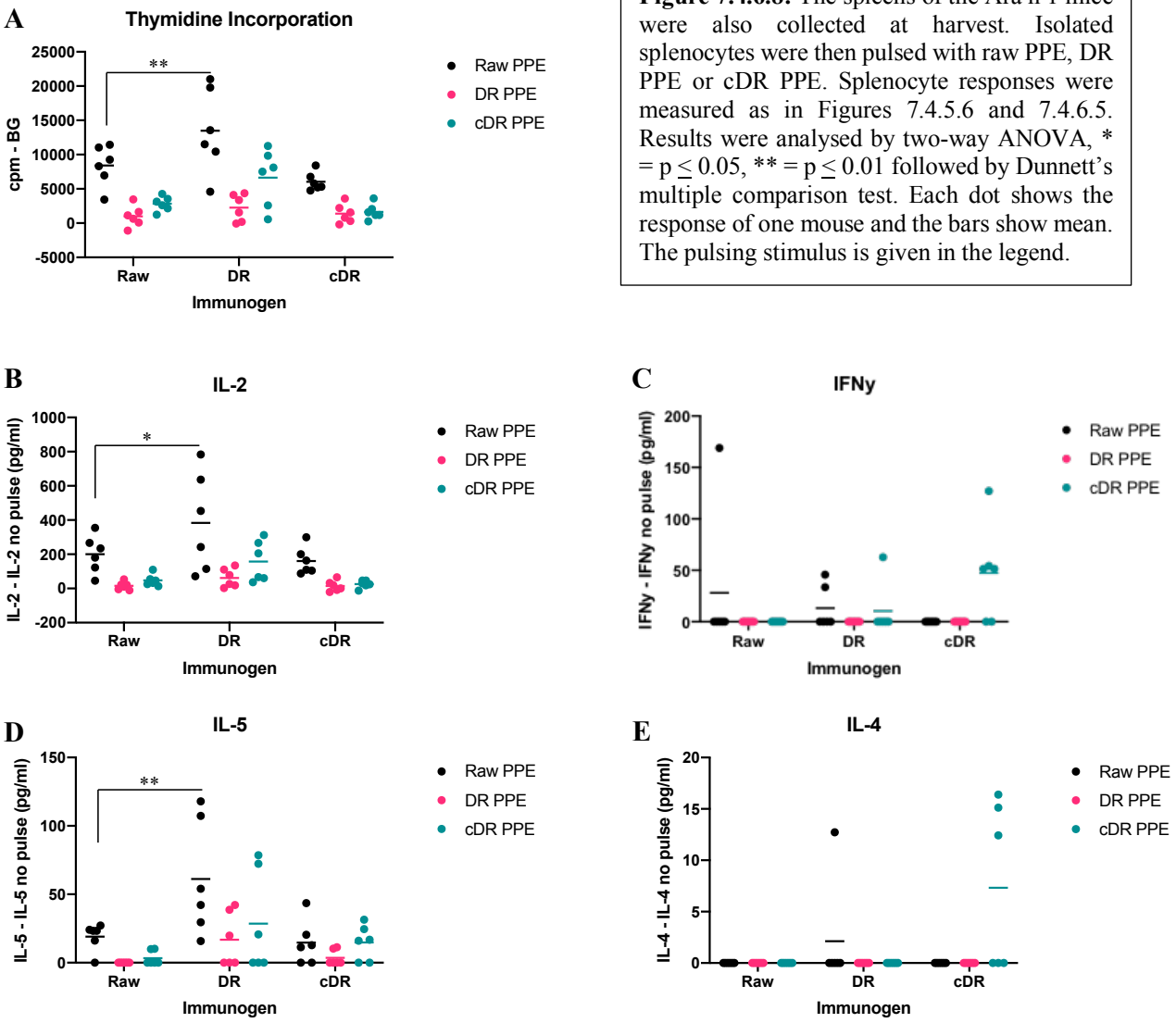

Figure 7.4.6.8: The spleens of the Ara h 1 mice were also collected at harvest. Isolated splenocytes were then pulsed with raw PPE, DR PPE or cDR PPE. Splenocyte responses were measured as in Figures 7.4.5.6 and 7.4.6.5. Results were analysed by two-way ANOVA, * = $p \leq 0.05$, ** = $p \leq 0.01$ followed by Dunnett's multiple comparison test. Each dot shows the response of one mouse and the bars show mean. The pulsing stimulus is given in the legend.

7.5 Discussion and Conclusions

Overall, these studies failed to find convincing and consistent evidence that dry roasting enhances the immunogenicity of peanut proteins thereby contributing to the development of allergic type responses. One major question it is important to address is why the data in this thesis differ so significantly from previously published results. There are several possible answers. Firstly, variations in the samples used between the two studies may have contributed as the raw peanuts used in each study were from different sources (Moghaddam et al. 2014). Different curing processes can add AGE to "raw" peanuts (Chung et al. 2003) and this is reflected in studies examining the formation of end products with thermal processing. Whilst some have identified the presence of AGEs in raw and DR peanut samples, others have identified them only in the latter samples (Hebling et al. 2013; Mueller et al. 2013). Alternatively, the dry roasting procedure may not have been adequately replicated, resulting in a more/less modified product. If raw and DR peanut samples produced in this thesis were more alike in terms of modification profile than in previous studies, this could have reduced the differences in immunogenicity potential. However, the RC ELISA and western blot data indicates that the samples produced here and older samples made in the laboratory by others were comparable in terms of modification. However, without a more complete and quantitative picture of all the modifications in the samples it is difficult to assess how similar they may be.

Another key area of difference is the study design itself. The previous paper did include one study where DR and raw PPE immunised mice were fed raw peanut kernels, however, the mice were only fed once 18 weeks after the initial immunisation (Moghaddam et al. 2014). The decision was made to feed mice with peanuts earlier on in the experiment in the hope that this would replicate the finding in a shorter period of time, reducing the amount of time the mice needed to be kept. However, initial results indicated that whilst DR and cDR PPE

might induce stronger antibody responses, this was not significant. This is in line with previous unpublished results from the laboratory which indicated that differences between groups were only significant at later time points. It was therefore decided to extend the experiment and included additional feeds to produce a final protocol more akin to the s.c. immunisation and gavage studies in the published work (s.c. immunisation followed by gavage with peanut homogenate at weeks 8, 20 and 30). However, there are obviously major differences between this older protocol and the one used here, including exact timings of the feeds and the nature of the boosts. As discussed above, feeding was chosen because it is less invasive for the mice than gavage and is more reflective of what happens when a human eats a peanut. A drawback is that dosing becomes more difficult as it is impossible to prove that each mouse ate the same amount of peanuts. Moreover, whilst mice in the studies reported here were fed raw peanuts, the older experiment used DR homogenate for gavage boosts. It is possible that repeated feeds with raw may have favoured the development of responses in the mice immunised with the equivalent PPE over the DR and cDR preparations.

The results of the Ara h 1 immunisation study were more promising as the DR sample induced significantly higher splenocyte responses and both the cDR and DR samples were capable of inducing detectable IgE responses whilst the raw sample was not. However, the antibody responses were not significantly different so this result again fails to replicate the previously published result. One explanation may be that although the previous study also used a single immunisation, antibody response were measured at a much earlier time point (2 weeks as compared to 5 and 9 weeks here).

A more significant issue is that although the DR Ara h 1 was more immunogenic with regard to cellular responses, this was not the case with cDR. There are many reasons this may be the case. Firstly, although the DR and cDR samples look similar in terms of modification with the methods included here, complete modification profiles of the Ara h 1 samples were

not attempted. Therefore, the cDR could be lacking the right balance of modifications needed for the enhanced immunogenicity. Alternatively, the higher LPS contamination in the cDR samples could be influencing the results. Regardless, none of the *in vivo* experiments indicated the cDR samples were significantly more immunogenic than raw. As this is the product that individuals are exposed to in the real-world situation, failure to find an altered immune relationship with this is a serious setback to the hypothesis that dry roasting enhances immunogenicity.

Altogether, the results provided here do not provide a clear answer as to the effects of dry roasting on the allergenic properties or peanuts. Studies in this field have frequently produced conflicting results and how their findings relate to their real-world scenario is often unclear. For example, the IgE binding to thermally-processed peanut products using sera from peanut allergy patients has been shown to be increased, decreased or unchanged depending on the study (Maleki et al. 2000; Mondoulet et al. 2005; Vissers, Iwan, et al. 2011). Even if one accepts that IgE binding is increased with DR, what this actually means is uncertain. It could be that dry roasting exposes IgE epitopes or creates neo-epitopes thereby enhancing the allergenicity of the protein, however it is equally possible that individuals respond more strongly to DR simply because that is what they were sensitised to originally. Given that the majority of peanuts consumed worldwide have been thermally processed, it seems probable that the majority of people in western countries will have first been exposed to DR peanut (Mueller et al. 2013; Shi et al. 2017). Likewise, the *in vivo* studies of this thesis and previously published immunisation studies also conflict with each other (Moghaddam et al. 2014; Kroghsbo et al. 2014). Collectively, it is very hard to draw firm conclusions from the data and despite more than 20 years of research, we do not seem to be any closer to a complete answer. Discussed below are a couple of key issues which need to be resolved before the field can make substantial progress.

Firstly, dry roasting and the modifications it induces in peanuts needs to be better defined. Initial studies focused on the importance of the Maillard reaction products in dry roasting (Maleki et al. 2000). Clearly, this process does occur as AGEs have been found in roasted peanut samples. However, studies have indicated that these may form only a small fraction of all the lysine modifications formed during roasting (Wellner, Nußpickel, and Henle 2012). Given the composition of the peanut this is perhaps not surprising. Reducing sugars make up less than 1% of the peanut whilst protein accounts for about 25%. Notably, the fat content in peanuts is about 50% and this raises the possibility that lipid peroxidation and its products may be far more important in thermal processing of peanuts. Lipid peroxidation products can also add RCs to proteins and so this would be in line with the biochemical characterisation studies which showed high RC content with low AGE formation (Fedorova, Bollineni, and Hoffmann 2014). Moreover, lipid peroxidation products have been identified in roasted peanut samples (Chung and Champagne 2001).

Very little research has been done in this area and so further work is required, but the potentially premature focus on one reaction may limit the value of studies which have used glycation to model roasting. In particular, many studies have used thermal processing, with or without glucose, of individual isolated allergens to model dry roasting (Vissers, Blanc, et al. 2011; Vissers, Iwan, et al. 2011). However, structural studies have demonstrated that these heated samples do not resemble those isolated from DR peanuts. For example in the study of Kroghsbo et al, glycated Ara h 1 was not found to be a superior elicitor of antibody responses in rats (Kroghsbo et al. 2014). To generate their glycated Ara h 1, they heated isolated protein with glucose for 15 mins at 100°C. However previous work had demonstrated that this protocol does not produce a protein which resembles Ara h 1 isolated from DR peanuts (Blanc et al. 2011). Therefore, model proteins produced with this method cannot be used to determine the effects of DR peanut proteins on the development of

immune responses. There are advantages to using proteins modified artificially rather than purifying proteins from the processed peanuts themselves. For example, processing can change the solubility of peanut proteins meaning that it may not be possible to isolate more extensively modified proteins from peanuts (Kopper et al. 2005). However, more care needs to be taken to ensure that these products resemble the DR proteins. This includes modelling the key reactions of interest and more extensive testing to confirm presence of AGE/ALE adducts.

Secondly, improvements could be made in the experimental design of murine studies. In this report s.c. immunisation followed by feeding were used to induce allergic-like responses in the mice. Current evidence suggest that peanut allergic individuals become sensitised to peanuts through their skin. For example, eczema is a risk factor for peanut allergy, particularly in households where there are high amounts of peanut dust in the environment (Stiefel et al. 2017). This would also fit with clinical history as typically individuals have an allergic response on their first known ingestion of peanuts. Epicutaneous sensitisation may therefore be a better model to study the development of peanut allergy and previous studies have demonstrated that DR PPE is more immunogenic using this protocol (Moghaddam et al. 2014). It can also be argued that in order to be considered a major contributor to peanut allergy, the enhanced immunogenicity of DR peanuts needs to be consistently demonstrated across studies with different conditions. There are multiple factors which contribute to the development of peanut allergy and the exact combinations are likely to be unique for each individual. If in the laboratory, the enhanced immunogenicity of DR peanut proteins is only noted under very specific and artificial conditions, then dry roasting is unlikely to be a significant factor in the development of peanut allergy as those exact conditions are unlikely to be replicated in the real world.

To summarise samples of PPE, Ara h 1 and Ara h 2 were produced from DR and raw peanuts. Biochemical characterisation was used to confirmed the presence of RC and absence of other AGE adducts such as CML. Whilst it was possible to replicate previous findings showing that the DR samples do not induce classical maturation of DCs, it was not possible to repeat experiments showing enhanced DC uptake of DR Ara h 1 compared to raw. Similarly, overall the *in vivo* studies reported here do not support the hypothesis that dry roasting enhances the immunogenicity of PPE. If these studies were continued, it would be important to more extensively characterise the peanut allergens, particularly focusing on the development of lipid peroxidation products, and refine the *in vivo* studies by moving to a epicutaneous immunisation model.

Chapter 8: Discussion and Conclusions

8.0 Outline of Discussion

In this thesis various aspects of the AGE-immune system relationship have been investigated, and the results have been discussed in detail in the previous chapters. This discussion focuses on the main findings, draws together data from the different chapters, and considers future directions.

8.1 Glycolaldehyde (GA) Modification: An Antibody Inducer

One of the key outcomes of this thesis was that it confirmed the previously reported enhanced immunogenicity of GA-modified proteins (Moghaddam et al. 2011; Allison and Fearon 2000). Specifically, this thesis showed that this modification promoted the development of an antibody responses against the native antigen. The first point of discussion is whether this should be regarded as an AGE-mediated phenomenon. Certainly there were AGE-structures present, as indicated by the GA-pyridine ELISA and fluorescence spectra. However, GA-enhanced immunogenicity was dependent on the presence of reactive carbonyls (RCs), as indicated by the loss of antibody response when these were removed by chemical reduction. In previous studies, the main source of RCs in GA-modified HEL was aldoamine, an early-stage product (Moghaddam et al. 2011). As such, the enhanced antibody responses seen in HEL GA immunised mice may be better categorised as an effect mediated by RC-containing early/intermediate glycation products. This idea is further supported by the data obtained with the HEL GLUC samples which produced remarkably different responses compared to the GA-modified samples.

The main aim of this thesis was to uncover the mechanisms underlying the enhanced immunogenicity phenomenon, and whilst it is not possible at this stage to provide a complete answer, the results in this thesis represent a significant step forward. The mechanism had to

meet a number of criteria. Firstly and most obviously, it had to apply to GA-modified proteins. Enhanced DC uptake is therefore unlikely to be the main underlying cause, as the GA-modified proteins were not taken up to a greater extent than their unmodified controls. Secondly, the mechanism had to be RC specific, meaning any effect was lost with the GA-PR sample. This makes DC activation an unlikely contributor as although there was some evidence of GA-modified protein-induced changes in the DC secretory profile, these also applied to PR samples. In contrast, the analysis of complement and natural antibody binding to modified proteins did yield results that correlated with *in vivo* immunogenicity. C1q binding and C3d deposition were enhanced by GA-modification, and importantly this was lost when the samples were reduced. Therefore, the data in this thesis would support a model in which enhanced antibody responses result from complement activation induced by RC groups in the GA-modified protein. The resulting C3d deposition could then signal via the CD21-CD19-CD81 co-receptor complex on B cells and act as the secondary signal needed for full B cell activation (Fearon 1998; Dunkelberger and Song 2010).

The complement activation studies in this thesis are still at an early stage and much further work needs to be done to confirm a role for complement as the principal factor stimulating antibody responses against GA-modified samples. Importantly, one would need to show a dependency on this system for GA-induced antibodies *in vivo.* One option would be to immunise mice in the presence of inhibitors of the complement cascade, for example by depleting complement factors with cobra venom factor (Vogel and Fritzinger 2017). Alternatively, mice lacking components of the complement system could be used. For example, CD21 KO mice are commercially available, which would allow for experiments examining the contribution of this receptor specifically (Molina et al. 1996). It would also be important to examine the activation of B cells *in vitro,* however in Chapter 3 this proved challenging due to the inhibitory effects of mouse serum on lymphocyte proliferation. One

can imagine experiments in which the proteins are first bound to beads or plates and incubated with serum, allowing excess serum components to be washed away before cells are introduced. *In vitro* assays would allow for examination of the signalling pathways involved and would also be required if the effects of GA-modification on human B cell activation are to be investigated. Currently, the evidence indicates that human C1q binds to the HEL GA 3 h but it was not possible to find evidence of enhanced C3b activation with this sample using normal human serum. Obviously, if one wanted to use these findings to understand human pathology or design vaccines, we would need to confirm that this mechanism also holds true for human immune responses.

It is interesting to speculate why the immune system might respond to RCs specifically. As GA is formed *in vivo* through the actions of ROS produced during respiratory burst (Anderson et al. 1999, 1997), one hypothesis is that the body has learned to respond to pathogen products "tagged" by GA to add RCs (Allison and Fearon 2000). This would allow the body to respond to normally non-immunogenic microbial components whilst also maintaining native epitopes. As RCs are an indicator of oxidative protein damage (Fedorova, Bollineni, and Hoffmann 2014), an alternative explanation would be that they are recognised by complement in order to allow clearance of damaged proteins. Certainly, the complement system is known to assist in the clearance of apoptotic cells in a non-inflammatory manner (Castellano et al. 2004; Killick et al. 2018), and has been suggested to also aid in the clearance of damaged plasma proteins (Ramadass, Ghebrehiwet, and Kew 2015).

Regardless of mechanism and type of adaptive immune response, the fact that RC-adduction acts as an 'intrinsic adjuvant' to promote B cell responses makes this of particular interest for two reasons. Firstly, because this might be a mechanism for enhancing vaccine-elicited antibody responses against specifically RC-tagged antigens without the use of exogenous

adjuvants. Secondly, because unwanted RC adduction to self-proteins might trigger autoimmune antibody responses. Further investigation will reveal whether these two concepts might yield outcomes helpful to biomedical research

However, it is worth noting that the immunisation studies using PPE and Ara h 1 isolated from raw and DR peanuts, did not show that DR peanut proteins induced greater antibody responses than raw peanut proteins. This is despite biochemical characterisation showing increased RC levels in the DR samples. There are many reasons that GA modification of HEL enhances antibody responses whilst dry roasting of peanuts does not. Firstly, the immune system may respond differently to RCs present on HEL than it does to RCs present on peanut proteins. Secondly, whilst unmodified HEL did not have RC groups, the raw peanut protein samples did, albeit to a lower level than the DR samples. It may be that immune responses induced by RC groups are "all or nothing". That is, once a threshold level of RC modification is reached an antibody response is induced, and further RC addition does not enhance this response. However, this seems unlikely as previous research indicated that level of RC addition on OVA correlated with the strength of the antibody response induced (Moghaddam et al. 2011). Finally, the modifying agent and the specific identity of the RC containing adduct may also determine whether RC adduction induced antibody responses. As discussed in Chapter 7, the RCs formed during dry roasting of peanuts may be the result of lipid peroxidation. Whilst GA can be formed during lipid peroxidation (Chikazawa et al. 2020), so are many products which can also add RCs to proteins (Vistoli et al. 2013). It is possible that the RC containing structures induced by these other products cannot stimulate antibody responses in the same way as GA-induced RC adducts.

8.2 Glucose Modification: Cellular Responses

Another important finding was the demonstration of enhanced cellular immune responses to HEL GLUC in the absence of adjuvant or significant endotoxin contamination. In Chapter 3, immunising BALB/c or CBA mice with a single s.c. injection of HEL GLUC was not sufficient to induce significant antibody or splenocyte responses. However, in chapters using immunisation regimes with boosts (Chapters 4 and 6), significant splenocyte recall results were seen. These results also show that GLUC modification can enhance responses to native protein, although in a contrasting manner to GA modification as GLUC-modified proteins did not elicit obvious antibody responses.

One general criticism of the immunisation studies is that only responses to native protein were examined. As discussed in the introduction, the focus of this study was whether AGE modifications could activate elements of the immune system, thereby inducing responses to native epitopes remaining in the protein. As such only unmodified proteins were included in the splenocyte recall studies and ELISAs measuring antibody production. Modified proteins could have been included in these experiments. However, this was not done as, due the size and number of immunisation groups, including all modified proteins would have resulted in very large recall studies that would have been difficult to manage. Moreover, in some cases only limited amounts of the modified sample were available and so recall studies requiring large amounts of protein were not possible. However, it is possible that AGE-specific immune responses developed and this could be the subject of future investigations. For example, it is possible that in the mice immunised with HEL GLUC, antibodies targeting epitopes specific to the immunogen developed and these were missed in ELISAs only measuring anti-native HEL antibodies.

A key question is what is the mechanism underlying the enhanced immunogenicity of glucose-modified proteins. Previous studies have concluded that enhanced T cell responses

to AGE-modified proteins are the result of increased DC uptake (Heilmann et al. 2014; Hilmenyuk et al. 2010; Ilchmann et al. 2010), and the results in this thesis offer some support to this hypothesis as increased uptake was seen with all the GLUC modified samples tested. In contrast, there was no evidence for DC maturation in response to GLUC modified proteins, providing evidence against this being a dominant mechanism.

Importantly the roles of the SRs SR-A, MARCO and RAGE in AGE-mediated immunogenicity have not previously been investigated *in vivo* so the results in this thesis are an important advance for the field. The immunogenicity studies clearly indicate that none of these receptors is required for the development of immune responses to AGE-modified proteins. In both the SRA/MARC/SRMA/C57BL/6J and RAGE/C57BL/6N experiments the majority of proliferating cells in splenocyte cultures from HEL GLUC immunised mice were B cells. This is despite of the fact that these mice failed to develop antibody responses to HEL. This was true for all the s.c. immunisation studies, indeed the results of the immunisation of CBA mice suggest that GLUC modification may block the development of antibody responses to native protein. One possibility would be that GLUC modification destroys B cell epitopes, however, in the DC transfer studies mice immunised with DCs pulsed with HEL GLUC did develop stronger antibody responses than those immunised with DCs pulsed with HEL alone. This indicates that HEL GLUC can be an antibody inducer given the right circumstances. One possibility is that in standard immunisation studies the GLUC modified proteins are cleared and degraded by non-APCs before they can reach DCs. The results using HEL GLUC may be of relevance to diseases which feature high levels of AGE accumulation and where enhanced activation and proliferation of T cells may contribute to pathogenesis, such as diabetes and atherosclerosis.

There has been much discussion in the literature on the relationship between the AGE-RAGE axis and these diseases (Ramasamy et al. 2005), so it was perhaps surprising to find

no involvement of RAGE in the enhanced immunogenicity of HEL GLUC. However, when one examines the literature more closely it would seem that the relationship between RAGE and AGE is still contentious. Whilst this receptor was discovered on the basis of its AGE binding ability and can initiate inflammatory signalling, there is some evidence to question whether AGEs are indeed true ligands for this receptor - that is, whether they can bind and initiate intracellular signalling (Valencia et al. 2004; Neeper et al. 1992). Moreover, many studies investigating the role of AGE/RAGE in disease models have relied on sRAGE to inhibit RAGE signalling (Ramasamy et al. 2005; Hudson and Lippman 2018). However, RAGE has a large range of endogenous and exogenous ligands and so this treatment could have affected any of these ligand-RAGE axes. In that sense, RAGE may be a misnomer and the results here suggest it is not involved in AGE-mediated enhanced immunogenicity.

8.3 SRs and Adipose Tissue: Key Roles in Metabolism?

Another general theme in this thesis is the role of scavenger receptors in controlling weight and adiposity. In the past two decades, there has been increasing interest in role of the immune system in the pathogenesis of obesity (Eagle and Chawla 2010). Much of this research has focused on ATMs, which are recruited to adipose tissue in obesity and whose inflammatory phenotype is thought to contribute to adipocyte dysfunction and obesity complications (Boutens and Stienstra 2016; González-Muniesa et al. 2017). However, more recent studies are beginning to question this narrative. Large scale single-cell RNAseq studies of visceral adipose tissue from obese humans and mice have demonstrated the presence of multiple macrophage subsets, one of which is defined by its expression of Trem2, a lipid receptor. Genetic deletion of this receptor resulted in increased weight gain, impaired glucose tolerance and higher circulating cholesterol levels in mice fed HFD (Jaitin et al. 2019). This indicates that, far from having detrimental effects, at least one macrophage

subset has beneficial effects on lipid processing during obesity. Furthermore, acute weight loss is also associated with recruitment of macrophages to adipose tissue and these regulate lipolysis (Eagle and Chawla 2010). The roles of macrophages in lipid metabolism and weight regulation are therefore more complex than previously thought.

One area of research which is relatively unexplored is the roles of macrophages in regulating adipocyte function and lipid metabolism under normal conditions. It is known that yolk sac-derived macrophages are present in adipose tissue and are required for normal adipocyte development (Cox 2020), indicating key roles for macrophages in organising lipid storage. The results in this thesis provide further evidence for a role of the innate immune system in regulating overall lipid metabolism and storage in the body as all three SRs examined clearly influenced adiposity. Loss of MARCO resulted in excess body fat, a phenotype which could be further enhanced by additional loss of SR-A, whilst loss of RAGE resulted in lower body fat. Furthermore, it has been proposed that macrophages act as metabolic sensors, sampling their environment and responding accordingly to regulate the metabolic response. Nuclear receptors such as PPARγ are thought to act as metabolic detectors for macrophages (Cox 2020). One possibility is that the SRs investigated in this thesis are also able to act as nutrient sensors. As discussed in Chapter 6, RAGE has previously been shown to regulate thermogenesis (Hurtado Del Pozo et al. 2019), and the high autofluorescent signature in the immune cells of RAGE mice may indicate that this receptor also has roles in regulating metabolism in non-adipocyte cells. This evidence coupled with the lower body weight seen in the RAGE mice may suggest that this receptor acts as a "metabolic brake", reducing energy expenditure in the organism. The role of MARCO in metabolism is relatively unexplored and this thesis did not examine changes in metabolic pathways in the MARC and SRMA KO mice. However, given the excess weight gain seen in these mice, one can speculate that MARCO, and possibly SR-A, have some role in regulating lipid metabolism.

For example, they may act as a sensor of lipid stores in adipocytes. When this sensor is lost in the KO, the macrophages may lose a signal to indicate sufficient lipid storage and so instead promote the further fat deposition seen in these mice. Further work and experiments, including those discussed in the relevant chapters, will hopefully shed light onto the precise nature of metabolic control by these receptors and whether it may be possible to target these pathways therapeutically.

Bibliography

A-Gonzalez, Noelia, and Antonio Castrillo. 2018. “Origin and Specialization of Splenic Macrophages.” *Cellular Immunology* 330 (August): 151–58. https://doi.org/10.1016/J.CELLIMM.2018.05.005.

Acharya, A S, and J M Manning. 1983. “Reaction of Glycolaldehyde with Proteins: Latent Crosslinking Potential of Alpha-Hydroxyaldehydes.” *Proceedings of the National Academy of Sciences of the United States of America* 80 (12): 3590–94. http://www.ncbi.nlm.nih.gov/pubmed/6574500.

Akhter, Firoz, M Salman Khan, and Saheem Ahmad. 2015. “Acquired Immunogenicity of Calf Thymus DNA and LDL Modified by D-Ribose: A Comparative Study.” *International Journal of Biological Macromolecules* 72 (January): 1222–27. https://doi.org/10.1016/j.ijbiomac.2014.10.034.

Akkaya, Munir, Javier Traba, Alexander S. Roesler, Pietro Miozzo, Billur Akkaya, Brandon P. Theall, Haewon Sohn, et al. 2018. “Second Signals Rescue B Cells from Activation-Induced Mitochondrial Dysfunction and Death.” *Nature Immunology* 19 (8): 871–84. https://doi.org/10.1038/s41590-018-0156-5.

Alfonso-García, Alba, Tim D. Smith, Rupsa Datta, Thuy U. Luu, Enrico Gratton, Eric O. Potma, and Wendy F. Liu. 2016. “Label-Free Identification of Macrophage Phenotype by Fluorescence Lifetime Imaging Microscopy.” *Journal of Biomedical Optics* 21 (4): 046005. https://doi.org/10.1117/1.JBO.21.4.046005.

Allison, Michael E. D., and Douglas T. Fearon. 2000. “Enhanced Immunogenicity of Aldehyde-Bearing Antigens: A Possible Link between Innate and Adaptive Immunity.” *European Journal of Immunology* 30 (10): 2881–87. https://doi.org/10.1002/1521-4141(200010)30:10<2881::AID-IMMU2881>3.0.CO;2-9.

Ames, Jennifer M. 2007. “Evidence against Dietary Advanced Glycation Endproducts Being a Risk to Human Health.” *Molecular Nutrition & Food Research* 51 (9): 1085–90. https://doi.org/10.1002/mnfr.200600304.

Amiel, Eyal, Susan Nicholson-Dykstra, Julie Jo Walters, Henry Higgs, and Brent Berwin. 2007. “Scavenger Receptor-A Functions in Phagocytosis of E. Coli by Bone Marrow Dendritic Cells.” *Experimental Cell Research* 313 (7): 1438–48. https://doi.org/10.1016/J.YEXCR.2007.02.011.

Andersen, Tor Kristian, Peter C. Huszthy, Ramakrishna P. Gopalakrishnan, Johanne T. Jacobsen, Marte Fauskanger, Anders A. Tveita, Gunnveig Grødeland, and Bjarne Bogen. 2019. “Enhanced Germinal Center Reaction by Targeting Vaccine Antigen to Major Histocompatibility Complex Class II Molecules.” *Npj Vaccines* 4 (1): 9. https://doi.org/10.1038/s41541-019-0101-0.

Anderson, M M, S L Hazen, F F Hsu, and J W Heinecke. 1997. “Human Neutrophils Employ the Myeloperoxidase-Hydrogen Peroxide-Chloride System to Convert Hydroxy-Amino Acids into Glycolaldehyde, 2-Hydroxypropanal, and Acrolein. A Mechanism for the Generation of Highly Reactive Alpha-Hydroxy and Alpha,Beta-Unsaturated Aldehydes by Phagocytes at Sites of Inflammation.” *Journal of Clinical Investigation* 99 (3): 424–32. https://doi.org/10.1172/JCI119176.

Anderson, M M, Jesús R. Requena, Jan R. Crowley, Suzanne R. Thorpe, and Jay W. Heinecke. 1999. “The Myeloperoxidase System of Human Phagocytes Generates Nε-(Carboxymethyl)Lysine on Proteins: A Mechanism for Producing Advanced Glycation End Products at Sites of Inflammation.” *The Journal of Clinical Investigation* 104 (1): 103–13. https://doi.org/10.1172/JCI3042.

Ansari, Nadeem A., Moinuddin, Khursheed Alam, and Asif Ali. 2009. “Preferential Recognition of Amadori-Rich Lysine Residues by Serum Antibodies in Diabetes Mellitus: Role of Protein Glycation in the Disease Process.” *Human Immunology* 70 (6): 417–24. https://doi.org/10.1016/J.HUMIMM.2009.03.015.

Araki, Norie, Takayuki Higashi, Takashi Mori, Rie Shibayama, Yoshiki Kawabe, Tatsuhiko Kodama, Kiyoshi Takahashi, Motoaki Shichiri, and Seikoh Horiuchi. 1995. “Macrophage Scavenger Receptor Mediates the Endocytic Uptake and Degradation of Advanced Glycation End Products of the Maillard Reaction.” *European Journal of Biochemistry* 230 (2): 408–15. https://doi.org/10.1111/j.1432-1033.1995.0408h.x.

Arif, Binish, Jalaluddin M Ashraf, Moinuddin Moinuddin, Jamal Ahmad, Zarina Arif, and Khursheed Alam. 2012. “Structural and Immunological Characterization of Amadori-Rich Human Serum Albumin: Role in Diabetes Mellitus.” *Archives of Biochemistry and Biophysics* 522 (1): 17–25. https://doi.org/10.1016/j.abb.2012.04.005.

Ayala, Antonio, Mario F. Muñoz, and Sandro Argüelles. 2014. “Lipid Peroxidation: Production, Metabolism, and Signaling Mechanisms of Malondialdehyde and 4-Hydroxy-2-Nonenal.” *Oxidative Medicine and Cellular Longevity* 2014: 1–31. https://doi.org/10.1155/2014/360438.

Ayala, Julio E, Varman T Samuel, Gregory J Morton, Silvana Obici, Colleen M Croniger, Gerald I Shulman, David H Wasserman, Owen P McGuinness, and NIH Mouse Metabolic Phenotyping Center Consortium. 2010. “Standard Operating Procedures for Describing and Performing Metabolic Tests of Glucose Homeostasis in Mice.” *Disease Models & Mechanisms* 3 (9–10): 525–34. https://doi.org/10.1242/dmm.006239.

Baek, Jea-Hyun, Carmen Birchmeier, Martin Zenke, and Thomas Hieronymus. 2012. “The HGF Receptor/Met Tyrosine Kinase Is a Key Regulator of Dendritic Cell Migration in Skin Immunity.” *The Journal of Immunology* 189 (4): 1699–1707. https://doi.org/10.4049/JIMMUNOL.1200729.

Bartolomé, Fernando, and Andrey Y. Abramov. 2015. “Measurement of Mitochondrial NADH and FAD Autofluorescence in Live Cells.” In , 263–70. Humana Press, New York, NY. https://doi.org/10.1007/978-1-4939-2257-4_23.

Beattie, Lynette, Amy Sawtell, Jason Mann, Teija C M Frame, Bianca Teal, Fabian de Labastida Rivera, Najmeeyah Brown, et al. 2016. “Bone Marrow-Derived and Resident Liver Macrophages Display Unique Transcriptomic Signatures but Similar Biological Functions.” *Journal of Hepatology* 65 (4): 758–68. https://doi.org/10.1016/j.jhep.2016.05.037.

Becker, Mike, Alessia Cotena, Siamon Gordon, and Nick Platt. 2006. “Expression of the Class A Macrophage Scavenger Receptor on Specific Subpopulations of Murine Dendritic Cells Limits Their Endotoxin Response.” *European Journal of Immunology* 36 (4): 950–60. https://doi.org/10.1002/eji.200535660.

Berin, M. C. 2015. “Pathogenesis of IgE-Mediated Food Allergy.” *Clinical and Experimental Allergy*. https://doi.org/10.1111/cea.12598.

Beyer, Kirsten, Ellen Morrowa, Xiu-Min Li, Ludmilla Bardina, Gary A. Bannon, A.Wesley Burks, and Hugh A. Sampson. 2001. “Effects of Cooking Methods on Peanut Allergenicity.” *Journal of Allergy and Clinical Immunology* 107 (6): 1077–81. https://doi.org/10.1067/mai.2001.115480.

Biswas, Subhra K, and Alberto Mantovani. 2010. “Macrophage Plasticity and Interaction with Lymphocyte Subsets: Cancer as a Paradigm.” *Nature Immunology* 11 (10): 889–96. https://doi.org/10.1038/ni.1937.

Bizzozero, O. A. 2009. “Protein Carbonylation in Neurodegenerative and Demyelinating CNS Diseases.” In *Handbook of Neurochemistry and Molecular Neurobiology*, 543–62. Boston, MA: Springer US. https://doi.org/10.1007/978-0-387-30375-8_23.

Blanc, Fany, Yvonne M. Vissers, Karine Adel-Patient, Neil M. Rigby, Alan R. Mackie, A. Patrick Gunning, Nikolaus K. Wellner, et al. 2011. “Boiling Peanut Ara h 1 Results in the Formation of Aggregates with Reduced Allergenicity.” *Molecular Nutrition and Food Research*. https://doi.org/10.1002/mnfr.201100251.

Bock, S.Allan, Anne Muñoz-Furlong, and Hugh A. Sampson. 2001. “Fatalities Due to Anaphylactic Reactions to Foods.” *Journal of Allergy and Clinical Immunology* 107 (1): 191–93. https://doi.org/10.1067/MAI.2001.112031.

Boekel, M.A.J.S. van. 2006. “Formation of Flavour Compounds in the Maillard Reaction.” *Biotechnology Advances* 24 (2): 230–33. https://doi.org/10.1016/j.biotechadv.2005.11.004.

Bolus, W Reid, Dario A Gutierrez, Arion J Kennedy, Emily K Anderson-Baucum, and Alyssa H Hasty. 2015. “CCR2 Deficiency Leads to Increased Eosinophils, Alternative Macrophage Activation, and Type 2 Cytokine Expression in Adipose Tissue.” *Journal of Leukocyte Biology* 98 (4): 467–77. https://doi.org/10.1189/jlb.3HI0115-018R.

Bonen, A, N N Tandon, J F C Glatz, J J F P Luiken, and G J F Heigenhauser. 2006. “The Fatty Acid Transporter FAT/CD36 Is Upregulated in Subcutaneous and Visceral Adipose Tissues in Human Obesity and Type 2 Diabetes.” *International Journal of Obesity* 30 (6): 877–83. https://doi.org/10.1038/sj.ijo.0803212.

Bonilla, Francisco A, and Hans C Oettgen. 2010. “Adaptive Immunity.” *Journal of Allergy and Clinical Immunology* 125: S33–40. https://doi.org/10.1016/j.jaci.2009.09.017.

Bora, Pablo, and Anish S Majumdar. 2017. “Adipose Tissue-Derived Stromal Vascular Fraction in Regenerative Medicine: A Brief Review on Biology and Translation.” *Stem Cell Research & Therapy* 8 (1): 145. https://doi.org/10.1186/s13287-017-0598-y.

Boutens, Lily, and Rinke Stienstra. 2016. “Adipose Tissue Macrophages: Going off Track during Obesity.” *Diabetologia* 59 (5): 879–94. https://doi.org/10.1007/s00125-016-3904-9.

Breuilh, Laetitia, François Vanhoutte, Josette Fontaine, Caroline M. W. van Stijn, Isabelle Tillie-Leblond, Monique Capron, Christelle Faveeuw, et al. 2007. “Galectin-3 Modulates Immune and Inflammatory Responses during Helminthic Infection: Impact of Galectin-3 Deficiency on the Functions of Dendritic Cells.” *Infection and Immunity* 75 (11): 5148–57. https://doi.org/10.1128/IAI.02006-06.

Burks, A W, L W Williams, R M Helm, C Connaughton, G Cockrell, and T O’Brien. 1991. “Identification of a Major Peanut Allergen, Ara h I, in Patients with Atopic Dermatitis and Positive Peanut Challenges.” *The Journal of Allergy and Clinical Immunology* 88 (2): 172–79. http://www.ncbi.nlm.nih.gov/pubmed/1880317.

Burks, A W, Larry W Williams, Cathie Connaughton, Gael Cockrell, Timothy J O’brien, and Ricki M Helm. 1992. “Identification and Characterization of a Second Major Peanut Allergen, Ara h II, with Use of the Sera of Patients with Atopic Dermatitis and Positive Peanut Challenge.” *Journal of Allergy and Clinical Immunology*. https://www.jacionline.org/article/0091-6749(92)90469-I/pdf.

Burks, W., H. A. Sampson, and G.A. Bannon. 2008. “Peanut Allergens.” *Allergy* 53 (8): 725–30. https://doi.org/10.1111/j.1398-9995.1998.tb03967.x.

Buttari, Brigitta, Elisabetta Profumo, Antonella Capozzi, Francesco Facchiano, Luciano Saso, Maurizio Sorice, and Rachele Riganò. 2011. “Advanced Glycation End Products of Human B2 Glycoprotein I Modulate

the Maturation and Function of DCs." *Blood* 117 (23). http://www.bloodjournal.org/content/117/23/6152.long?sso-checked=true.
Cabanillas, Beatriz, Soheila J. Maleki, Hsiaopo Cheng, and Natalija Novak. 2018. "Differences in the Uptake of Ara h 3 from Raw and Roasted Peanut by Monocyte-Derived Dendritic Cells." *International Archives of Allergy and Immunology* 177 (1): 35–39. https://doi.org/10.1159/000489277.
Cabiscol, Elisa, Jordi Tamarit, and Joaquim Ros. 2014. "Protein Carbonylation: Proteomics, Specificity and Relevance to Aging." *Mass Spectrometry Reviews* 33 (1): 21–48. https://doi.org/10.1002/mas.21375.
Cai, Lei, Zhen Wang, Ailing Ji, Jason M. Meyer, and Deneys R. van der Westhuyzen. 2012. "Scavenger Receptor CD36 Expression Contributes to Adipose Tissue Inflammation and Cell Death in Diet-Induced Obesity." Edited by Patricia T. Bozza. *PLoS ONE* 7 (5): e36785. https://doi.org/10.1371/journal.pone.0036785.
Caruso, Roberta, Masashi Ono, Marie E. Bunker, Gabriel Núñez, and Naohiro Inohara. 2019. "Dynamic and Asymmetric Changes of the Microbial Communities after Cohousing in Laboratory Mice." *Cell Reports* 27 (11): 3401-3412.e3. https://doi.org/10.1016/J.CELREP.2019.05.042.
Castellano, Giuseppe, Andrea M Woltman, Francesco Paolo Schena, Anja Roos, Mohamed R Daha, and Cees van Kooten. 2004. "Dendritic Cells and Complement: At the Cross Road of Innate and Adaptive Immunity." *Molecular Immunology* 41 (2–3): 133–40. https://doi.org/10.1016/J.MOLIMM.2004.03.018.
Cavallari, Joseph F., Fernando F. Anhê, Kevin P. Foley, Emmanuel Denou, Rebecca W. Chan, Dawn M. E. Bowdish, and Jonathan D. Schertzer. 2018. "Targeting Macrophage Scavenger Receptor 1 Promotes Insulin Resistance in Obese Male Mice." *Physiological Reports* 6 (22): e13930. https://doi.org/10.14814/phy2.13930.
Caza, Tiffany, and Steve Landas. 2015. "Functional and Phenotypic Plasticity of CD4(+) T Cell Subsets." *BioMed Research International* 2015: 521957. https://doi.org/10.1155/2015/521957.
Chan, Po-Chao, Shu-Yi Chen, Chun-Hwa Chen, and Hong-Chen Chen. 2006. "Crosstalk between Hepatocyte Growth Factor and Integrin Signaling Pathways." *Journal of Biomedical Science* 13 (2): 215–23. https://doi.org/10.1007/s11373-005-9061-7.
Charles A Janeway, Jr, Paul Travers, Mark Walport, and Mark J Shlomchik. 2001a. "Immunological Memory." https://www.ncbi.nlm.nih.gov/books/NBK27158/.
———. 2001b. "The Complement System and Innate Immunity." https://www.ncbi.nlm.nih.gov/books/NBK27100/.
———. 2001c. "The Distribution and Functions of Immunoglobulin Isotypes." https://www.ncbi.nlm.nih.gov/books/NBK27162/.
———. 2001d. "The Production of Armed Effector T Cells." https://www.ncbi.nlm.nih.gov/books/NBK27118/.
Chen, Kang, and Andrea Cerutti. 2011. "The Function and Regulation of Immunoglobulin D." *Current Opinion in Immunology* 23 (3): 345–52. https://doi.org/10.1016/j.coi.2011.01.006.
Chen, Xueni, Qian Wang, Rabab El-Mezayen, Yonghua Zhuang, and Stephen C. Dreskin. 2013. "Ara h 2 and Ara h 6 Have Similar Allergenic Activity and Are Substantially Redundant." *International Archives of Allergy and Immunology* 160 (3): 251–58. https://doi.org/10.1159/000341642.
Chen, Yali, Eitan M Akirav, Wei Chen, Octavian Henegariu, Bernhard Moser, Dharmesh Desai, Jane M Shen, et al. 2008. "RAGE Ligation Affects T Cell Activation and Controls T Cell Differentiation." *Journal of Immunology (Baltimore, Md. : 1950)* 181 (6): 4272–78. https://doi.org/10.4049/jimmunol.181.6.4272.
Chen, Ying-Ju, Ding-Cheng Chan, Chih-Kang Chiang, Ching-Chia Wang, Ting-Hua Yang, Kuo-Cheng Lan, Sung-Chuan Chao, Keh-Sung Tsai, Rong-Sen Yang, and Shing-Hwa Liu. 2016. "Advanced Glycation End-Products Induced VEGF Production and Inflammatory Responses in Human Synoviocytes via RAGE-NF-KB Pathway Activation." *Journal of Orthopaedic Research* 34 (5): 791–800. https://doi.org/10.1002/jor.23083.
Chen, Yunying, Timo Pikkarainen, Outi Elomaa, Raija Soininen, Tatsuhiko Kodama, Georg Kraal, and Karl Tryggvason. 2005. "Defective Microarchitecture of the Spleen Marginal Zone and Impaired Response to a Thymus-Independent Type 2 Antigen in Mice Lacking Scavenger Receptors MARCO and SR-A." *Journal of Immunology (Baltimore, Md. : 1950)* 175 (12): 8173–80. https://doi.org/10.4049/jimmunol.175.12.8173.
Chikazawa, Miho, Natsuki Otaki, Takahiro Shibata, Hiroaki Miyashita, Yoshichika Kawai, Shoichi Maruyama, Shinya Toyokuni, Yasuyuki Kitaura, Tsukasa Matsuda, and Koji Uchida. 2013. "Multispecificity of Immunoglobulin M Antibodies Raised against Advanced Glycation End Products: Involvement of Electronegative Potential of Antigens." *The Journal of Biological Chemistry* 288 (19): 13204–14. https://doi.org/10.1074/jbc.M113.452177.
Chikazawa, Miho, Takahiro Shibata, Yukinori Hatasa, Sayumi Hirose, Natsuki Otaki, Fumie Nakashima, Mika Ito, Sachiko Machida, Shoichi Maruyama, and Koji Uchida. 2016. "Identification of C1q as a Binding Protein for Advanced Glycation End Products." *Biochemistry* 55 (3): 435–46. https://doi.org/10.1021/acs.biochem.5b00777.

Chikazawa, Miho, Jun Yoshitake, Sei-Young Lim, Shiori Iwata, Lumi Negishi, Takahiro Shibata, and Koji Uchida. 2020. “Glycolaldehyde Is an Endogenous Source of Lysine N-Pyrrolation.” *The Journal of Biological Chemistry* 295 (22): 7697–7709. https://doi.org/10.1074/jbc.RA120.013179.

Cho, Kae Won, David L Morris, and Carey N Lumeng. 2014. “Flow Cytometry Analyses of Adipose Tissue Macrophages.” *Methods in Enzymology* 537: 297–314. https://doi.org/10.1016/B978-0-12-411619-1.00016-1.

Chu, Derek K, Robert A Wood, Shannon French, Alessandro Fiocchi, Manel Jordana, Susan Waserman, Jan L Brożek, and Holger J Schünemann. 2019. “Oral Immunotherapy for Peanut Allergy (PACE): A Systematic Review and Meta-Analysis of Efficacy and Safety.” *The Lancet* 393 (10187): 2222–32. https://doi.org/10.1016/S0140-6736(19)30420-9.

Chung, Si-Yin, Christopher L. Butts, Soheila J. Maleki, and Elaine T. Champagne. 2003. “Linking Peanut Allergenicity to the Processes of Maturation, Curing, and Roasting.” *Journal of Agricultural and Food Chemistry* 51 (15): 4273–77. https://doi.org/10.1021/jf021212d.

Chung, Si-Yin, and Elaine T. Champagne. 1999. “Allergenicity of Maillard Reaction Products from Peanut Proteins.” *Journal of Agricultural and Food Chemistry* 47 (12): 5227–31. https://doi.org/10.1021/jf9904416.

———. 2001. “Association of End-Product Adducts with Increased IgE Binding of Roasted Peanuts.” *Journal of Agricultural and Food Chemistry* 49 (8): 3911–16. https://doi.org/10.1021/jf001186o.

Cinti, Saverio, Grant Mitchell, Giorgio Barbatelli, Incoronata Murano, Enzo Ceresi, Emanuela Faloia, Shupei Wang, Melanie Fortier, Andrew S Greenberg, and Martin S Obin. 2005. “Adipocyte Death Defines Macrophage Localization and Function in Adipose Tissue of Obese Mice and Humans.” *Journal of Lipid Research* 46 (11): 2347–55. https://doi.org/10.1194/jlr.M500294-JLR200.

Clem, Angela S. 2011. “Fundamentals of Vaccine Immunology.” *Journal of Global Infectious Diseases* 3 (1): 73–78. https://doi.org/10.4103/0974-777X.77299.

Collins, Andrew M. 2016. “IgG Subclass Co-expression Brings Harmony to the Quartet Model of Murine IgG Function.” *Immunology & Cell Biology* 94 (10): 949–54. https://doi.org/10.1038/icb.2016.65.

Cox, Nehemiah. 2020. “Macrophage Ontogeny in the Control of Adipose Tissue Biology.” *Current Opinion in Immunology* 62 (February): 1–8. https://doi.org/10.1016/J.COI.2019.08.002.

Croce, A.C., and G. Bottiroli. 2014. “Autofluorescence Spectroscopy and Imaging: A Tool for Biomedical Research and Diagnosis.” *European Journal of Histochemistry : EJH* 58 (4). https://doi.org/10.4081/EJH.2014.2461.

Dahl, Morten, Alison K Bauer, Mohamed Arredouani, Raija Soininen, Karl Tryggvason, Steven R Kleeberger, and Lester Kobzik. 2007. “Protection against Inhaled Oxidants through Scavenging of Oxidized Lipids by Macrophage Receptors MARCO and SR-AI/II.” *The Journal of Clinical Investigation* 117 (3): 757–64. https://doi.org/10.1172/JCI29968.

Daneman, Denis. 2006. “Type 1 Diabetes.” *The Lancet* 367 (9513): 847–58. https://doi.org/10.1016/S0140-6736(06)68341-4.

Dattilo, Brian M, Günter Fritz, Estelle Leclerc, Craig W Vander Kooi, Claus W Heizmann, and Walter J Chazin. 2007. “The Extracellular Region of the Receptor for Advanced Glycation End Products Is Composed of Two Independent Structural Units.” *Biochemistry* 46 (23): 6957–70. https://doi.org/10.1021/bi7003735.

Deal, Joshua, Sam Mayes, Craig Browning, Shante Hill, Paul Rider, Carole Boudreaux, Thomas C. Rich, and Silas J. Leavesley. 2018. “Identifying Molecular Contributors to Autofluorescence of Neoplastic and Normal Colon Sections Using Excitation-Scanning Hyperspectral Imaging.” *Journal of Biomedical Optics* 24 (02): 1. https://doi.org/10.1117/1.JBO.24.2.021207.

DeGroot, Jeroen, Nicole Verzijl, Marion J. G. Wenting-Van Wijk, Ruud A. Bank, Floris P. J. G. Lafeber, Johannes W. J. Bijlsma, and Johan M. TeKoppele. 2001. “Age-Related Decrease in Susceptibility of Human Articular Cartilage to Matrix Metalloproteinase-Mediated Degradation: The Role of Advanced Glycation End Products.” *Arthritis & Rheumatism* 44 (11): 2562–71. https://doi.org/10.1002/1529-0131(200111)44:11<2562::AID-ART437>3.0.CO;2-1.

Delgado-Andrade, C. 2016. “Carboxymethyl-Lysine: Thirty Years of Investigation in the Field of AGE Formation.” *Food & Function* 7 (1). https://doi.org/10.1039/C5FO00918A.

Dempsey, Paul W., Michael E. D. Allison, Srinivas Akkaraju, Christopher C. Goodnow, and Douglas T. Fearon. 1996. “C3d of Complement as a Molecular Adjuvant: Bridging Innate and Acquired Immunity.” *Science* 271 (5247): 348–50. https://doi.org/10.1126/SCIENCE.271.5247.348.

Dumitriu, Ingrid E, Paramita Baruah, Barbara Valentinis, Reinhard E Voll, Martin Herrmann, Peter P Nawroth, Bernd Arnold, Marco E Bianchi, Angelo A Manfredi, and Patrizia Rovere-Querini. 2005. “Release of High Mobility Group Box 1 by Dendritic Cells Controls T Cell Activation via the Receptor for Advanced Glycation End Products.” *Journal of Immunology (Baltimore, Md. : 1950)* 174 (12): 7506–15. https://doi.org/10.4049/jimmunol.174.12.7506.

Dunkelberger, Jason R, and Wen-Chao Song. 2010. “Complement and Its Role in Innate and Adaptive Immune

Responses." *Cell Research* 20 (1): 34–50. https://doi.org/10.1038/cr.2009.139.
Eagle, Alex Red, and Ajay Chawla. 2010. "In Obesity and Weight Loss, All Roads Lead to the Mighty Macrophage." *The Journal of Clinical Investigation* 120 (10): 3437. https://doi.org/10.1172/JCI44721.
Egaña-Gorroño, Lander, Raquel López-Díez, Gautham Yepuri, Lisa S Ramirez, Sergey Reverdatto, Paul F Gugger, Alexander Shekhtman, Ravichandran Ramasamy, and Ann Marie Schmidt. 2020. "Receptor for Advanced Glycation End Products (RAGE) and Mechanisms and Therapeutic Opportunities in Diabetes and Cardiovascular Disease: Insights From Human Subjects and Animal Models." *Frontiers in Cardiovascular Medicine* 7: 37. https://doi.org/10.3389/fcvm.2020.00037.
Elchaninov, Andrey V, Timur Kh Fatkhudinov, Polina A Vishnyakova, Anastasia V Lokhonina, and Gennady T Sukhikh. 2019. "Phenotypical and Functional Polymorphism of Liver Resident Macrophages." *Cells* 8 (9). https://doi.org/10.3390/cells8091032.
Ellis, E.M. 2007. "Reactive Carbonyls and Oxidative Stress: Potential for Therapeutic Intervention." *Pharmacology & Therapeutics* 115 (1). https://doi.org/10.1016/J.PHARMTHERA.2007.03.015.
Ellulu, Mohammed S, Ismail Patimah, Huzwah Khaza'ai, Asmah Rahmat, and Yehia Abed. 2017. "Obesity and Inflammation: The Linking Mechanism and the Complications." *Archives of Medical Science : AMS* 13 (4): 851–63. https://doi.org/10.5114/aoms.2016.58928.
Fearon, Douglas T. 1998. "The Complement System and Adaptive Immunity." *Seminars in Immunology* 10 (5): 355–61. https://doi.org/10.1006/SMIM.1998.0137.
Fedorova, Maria. 2017. "Diversity of Protein Carbonylation Pathways." In *Protein Carbonylation*, 48–82. Hoboken, NJ, USA: John Wiley & Sons, Inc. https://doi.org/10.1002/9781119374947.ch3.
Fedorova, Maria, Ravi Chand Bollineni, and Ralf Hoffmann. 2014. "Protein Carbonylation as a Major Hallmark of Oxidative Damage: Update of Analytical Strategies." *Mass Spectrometry Reviews* 33 (2): 79–97. https://doi.org/10.1002/mas.21381.
Fraser, Iain, Derralynn Hughes, and Siamon Gordon. 1993. "Divalent Cation-Independent Macrophage Adhesion Inhibited by Monoclonal Antibody to Murine Scavenger Receptor." *Nature* 364 (6435): 343–46. https://doi.org/10.1038/364343a0.
Gaens, Katrien H J, Gijs H Goossens, Petra M Niessen, Marleen M van Greevenbroek, Carla J H van der Kallen, Hans W Niessen, Sander S Rensen, et al. 2014. "Nε-(Carboxymethyl)Lysine-Receptor for Advanced Glycation End Product Axis Is a Key Modulator of Obesity-Induced Dysregulation of Adipokine Expression and Insulin Resistance." *Arteriosclerosis, Thrombosis, and Vascular Biology* 34 (6): 1199–1208. https://doi.org/10.1161/ATVBAHA.113.302281.
Galasko, Douglas, Joanne Bell, Jessica Y Mancuso, James W Kupiec, Marwan N Sabbagh, Christopher van Dyck, Ronald G Thomas, Paul S Aisen, and For the Alzheimer's Disease Cooperative Alzheimer's Disease Cooperative Study. 2014. "Clinical Trial of an Inhibitor of RAGE-Aβ Interactions in Alzheimer Disease." *Neurology* 82 (17): 1536–42. https://doi.org/10.1212/WNL.0000000000000364.
Gassen, Sofie Van, Britt Callebaut, Mary J. Van Helden, Bart N. Lambrecht, Piet Demeester, Tom Dhaene, and Yvan Saeys. 2015. "FlowSOM: Using Self-Organizing Maps for Visualization and Interpretation of Cytometry Data." *Cytometry Part A* 87 (7): 636–45. https://doi.org/10.1002/cyto.a.22625.
Ge, Junbo, Qingzhe Jia, Chun Liang, Yukun Luo, Dong Huang, Aijun Sun, Keqiang Wang, Yunzeng Zou, and Haozhu Chen. 2005. "Advanced Glycosylation End Products Might Promote Atherosclerosis through Inducing the Immune Maturation of Dendritic Cells." *Arteriosclerosis, Thrombosis, and Vascular Biology* 25 (10): 2157–63. https://doi.org/10.1161/01.ATV.0000181744.58265.63.
Gérard, Philippe. 2017. "Gut Microbiome and Obesity. How to Prove Causality?" *Annals of the American Thoracic Society* 14 (Supplement_5): S354–56. https://doi.org/10.1513/AnnalsATS.201702-117AW.
Glomb, MA, and VM Monnier. 1995. "Mechanism of Protein Modification by Glyoxal and Glycolaldehyde, Reactive Intermediates of the Maillard Reaction." *The Journal of Biological Chemistry* 270 (17). https://doi.org/10.1074/JBC.270.17.10017.
Goldstein, J L, Y K Ho, S K Basu, and M S Brown. 1979. "Binding Site on Macrophages That Mediates Uptake and Degradation of Acetylated Low Density Lipoprotein, Producing Massive Cholesterol Deposition." *Proceedings of the National Academy of Sciences of the United States of America* 76 (1): 333–37. https://doi.org/10.1073/pnas.76.1.333.
González-Muniesa, Pedro, Miguel-Angel Mártinez-González, Frank B. Hu, Jean-Pierre Després, Yuji Matsuzawa, Ruth J. F. Loos, Luis A. Moreno, George A. Bray, and J. Alfredo Martinez. 2017. "Obesity." *Nature Reviews Disease Primers* 3 (1): 17034. https://doi.org/10.1038/nrdp.2017.34.
Goodnow, Christopher C., Jeffrey Crosbie, Stephen Adelstein, Thomas B. Lavoie, Sandra J. Smith-Gill, Robert A. Brink, Helen Pritchard-Briscoe, et al. 1988. "Altered Immunoglobulin Expression and Functional Silencing of Self-Reactive B Lymphocytes in Transgenic Mice." *Nature* 334 (6184): 676–82. https://doi.org/10.1038/334676a0.
Gordon, Siamon, and Annette Plüddemann. 2017. "Tissue Macrophages: Heterogeneity and Functions." *BMC Biology* 15 (1): 53. https://doi.org/10.1186/s12915-017-0392-4.

Grace, S., L.A. Guthrie, and R.B. Johnston. 1988. “The Use of Mouse Serum and the Presence of Non-Adherent Cells for the Culture of Mouse Macrophages.” *Journal of Immunological Methods* 114 (1–2): 21–26. https://doi.org/10.1016/0022-1759(88)90148-2.

Granucci, Francesca, Filippo Petralia, Matteo Urbano, Stefania Citterio, Francesco Di Tota, Laura Santambrogio, and Paola Ricciardi-Castagnoli. 2003. “The Scavenger Receptor MARCO Mediates Cytoskeleton Rearrangements in Dendritic Cells and Microglia.” *Blood* 102 (8): 2940–47. https://doi.org/10.1182/blood-2002-12-3651.

Greaves, David R, and Siamon Gordon. 2008. “The Macrophage Scavenger Receptor at 30 Years of Age: Current Knowledge and Future Challenges.” *Journal of Lipid Research*. https://doi.org/10.1194/jlr.R800066-JLR200.

Grimsrud, Paul A., Hongwei Xie, Timothy J. Griffin, and David A. Bernlohr. 2008. “Oxidative Stress and Covalent Modification of Protein with Bioactive Aldehydes.” *The Journal of Biological Chemistry* 283 (32): 21837. https://doi.org/10.1074/JBC.R700019200.

Grolleau, Annabelle, David E Misek, Rork Kuick, Samir Hanash, and James J Mulé. 2003. “Inducible Expression of Macrophage Receptor Marco by Dendritic Cells Following Phagocytic Uptake of Dead Cells Uncovered by Oligonucleotide Arrays.” *Journal of Immunology (Baltimore, Md. : 1950)* 171 (6): 2879–88. https://doi.org/10.4049/jimmunol.171.6.2879.

Guo, Chunqing, Huanfa Yi, Xiaofei Yu, Fanlei Hu, Daming Zuo, John R Subjeck, and Xiang-Yang Wang. 2012. “Absence of Scavenger Receptor A Promotes Dendritic Cell-Mediated Cross-Presentation of Cell-Associated Antigen and Antitumor Immune Response.” *Immunology and Cell Biology* 90 (1): 101–8. https://doi.org/10.1038/icb.2011.10.

Haasken, Stefanie, Jennifer L. Auger, Justin J. Taylor, Patricia M. Hobday, Brian D. Goudy, Philip J. Titcombe, Daniel L. Mueller, and Bryce A. Binstadt. 2013. “Macrophage Scavenger Receptor 1 (Msr1, SR-A) Influences B Cell Autoimmunity by Regulating Soluble Autoantigen Concentration.” *The Journal of Immunology* 191 (3): 1055–62. https://doi.org/10.4049/jimmunol.1201680.

Hamada, Yoji, Norie Araki, Naoki Koh, Jiro Nakamura, Seikoh Horiuchi, and Nigishi Hotta. 1996. “Rapid Formation of Advanced Glycation End Products by Intermediate Metabolites of Glycolytic Pathway and Polyol Pathway.” *Biochemical and Biophysical Research Communications* 228 (2): 539–43. https://doi.org/10.1006/BBRC.1996.1695.

Hamsten, Carl, Lillemor Skattum, Lennart Truedsson, Ulrika von Döbeln, Mathias Uhlén, Jochen M. Schwenk, Lennart Hammarström, Peter Nilsson, and Maja Neiman. 2015. “Heat Differentiated Complement Factor Profiling.” *Journal of Proteomics* 126 (August): 155–62. https://doi.org/10.1016/J.JPROT.2015.05.027.

Han, Xiao-qun, Zuo-jiong Gong, San-qing Xu, Xun Li, Li-kun Wang, Shi-min Wu, Jian-hong Wu, and Hua-fen Yang. 2014. “Advanced Glycation End Products Promote Differentiation of CD4+ T Helper Cells toward Pro-Inflammatory Response.” *Journal of Huazhong University of Science and Technology [Medical Sciences]* 34 (1): 10–17. https://doi.org/10.1007/s11596-014-1224-1.

Harizi, H., M. Juzan, C. Grosset, M. Rashedi, and N. Gualde. 2001. “Dendritic Cells Issued in Vitro from Bone Marrow Produce PGE2 That Contributes to the Immunomodulation Induced by Antigen-Presenting Cells.” *Cellular Immunology* 209 (1): 19–28. https://doi.org/10.1006/CIMM.2001.1785.

Hebling, Christine M., Melinda A. McFarland, John H. Callahan, and Mark M. Ross. 2013. “Global Proteomic Screening of Protein Allergens and Advanced Glycation Endproducts in Thermally Processed Peanuts.” *Journal of Agricultural and Food Chemistry* 61 (24): 5638–48. https://doi.org/10.1021/jf303554t.

Heilmann, Monika, Anne Wellner, Gabriele Gadermaier, Anne Ilchmann, Peter Briza, Maren Krause, Ryoji Nagai, et al. 2014. “Ovalbumin Modified with Pyrraline, a Maillard Reaction Product, Shows Enhanced T-Cell Immunogenicity.” *Journal of Biological Chemistry* 289 (11): 7919–28. https://doi.org/10.1074/jbc.M113.523621.

Helft, Julie, Jan Böttcher, Probir Chakravarty, Santiago Zelenay, Jatta Huotari, Barbara U. Schraml, Delphine Goubau, and Caetano Reis e Sousa. 2015. “GM-CSF Mouse Bone Marrow Cultures Comprise a Heterogeneous Population of CD11c+MHCII+ Macrophages and Dendritic Cells.” *Immunity* 42 (6): 1197–1211. https://doi.org/10.1016/j.immuni.2015.05.018.

Henle, Thomas, and Anja Bachmann. 1996. “Synthesis of Pyrraline Reference Material.” *Zeitschrift F*[illegible]*r Lebensmittel-Untersuchung Und -Forschung* 202 (1): 72–74. https://doi.org/10.1007/BF01229689.

Hensley, Kenneth. 2015. “Detection of Protein Carbonyls by Means of Biotin Hydrazide–Streptavidin Affinity Methods.” In *Methods in Molecular Biology (Clifton, N.J.)*, 1314:95–100. https://doi.org/10.1007/978-1-4939-2718-0_11.

Hermanson, Greg T. 2013. *Bioconjugate Techniques*.

Herwig, Ralf, Christopher Hardt, Matthias Lienhard, and Atanas Kamburov. 2016. “Analyzing and Interpreting Genome Data at the Network Level with ConsensusPathDB.” *Nature Protocols* 11 (10): 1889–1907. https://doi.org/10.1038/nprot.2016.117.

Hey, Ying Y, and Helen C O’Neill. 2012. “Murine Spleen Contains a Diversity of Myeloid and Dendritic Cells

Distinct in Antigen Presenting Function." *Journal of Cellular and Molecular Medicine* 16 (11): 2611–19. https://doi.org/10.1111/j.1582-4934.2012.01608.x.
Hiemstra, Pieter S., and Mohamed R. Daha. 1998. "Opsonization." *Encyclopedia of Immunology*, January, 1885–88. https://doi.org/10.1006/RWEI.1999.0475.
Hilmenyuk, Tamara, Iris Bellinghausen, Bärbel Heydenreich, Anne Ilchmann, Masako Toda, Stephan Grabbe, and Joachim Saloga. 2010. "Effects of Glycation of the Model Food Allergen Ovalbumin on Antigen Uptake and Presentation by Human Dendritic Cells." *Immunology* 129 (3): 437–45. https://doi.org/10.1111/j.1365-2567.2009.03199.x.
Hoffman, William, Fadi G Lakkis, and Geetha Chalasani. 2016. "B Cells, Antibodies, and More." *Clinical Journal of the American Society of Nephrology : CJASN* 11 (1): 137–54. https://doi.org/10.2215/CJN.09430915.
Holodick, Nichol E, Nely Rodríguez-Zhurbenko, and Ana María Hernández. 2017. "Defining Natural Antibodies." *Frontiers in Immunology* 8: 872. https://doi.org/10.3389/fimmu.2017.00872.
Horiuchi, S., Y. Sakamoto, and M. Sakai. 2003. "Scavenger Receptors for Oxidized and Glycated Proteins." *Amino Acids* 25 (3–4): 283–92. https://doi.org/10.1007/s00726-003-0029-5.
Hubo, Mario, Bettina Trinschek, Fanny Kryczanowsky, Andrea Tuettenberg, Kerstin Steinbrink, and Helmut Jonuleit. 2013. "Costimulatory Molecules on Immunogenic versus Tolerogenic Human Dendritic Cells." *Frontiers in Immunology* 4: 82. https://doi.org/10.3389/fimmu.2013.00082.
Hudson, Barry I., and Marc E. Lippman. 2018. "Targeting RAGE Signaling in Inflammatory Disease." *Annual Review of Medicine* 69 (1): 349–64. https://doi.org/10.1146/annurev-med-041316-085215.
Hurtado Del Pozo, Carmen, Henry H Ruiz, Lakshmi Arivazhagan, Juan Francisco Aranda, Cynthia Shim, Peter Daya, Julia Derk, et al. 2019. "A Receptor of the Immunoglobulin Superfamily Regulates Adaptive Thermogenesis." *Cell Reports* 28 (3): 773-791.e7. https://doi.org/10.1016/j.celrep.2019.06.061.
Ibrahim, Zaridatul Aini, Carol L Armour, Simon Phipps, and Maria B Sukkar. 2013. "RAGE and TLRs: Relatives, Friends or Neighbours?" *Molecular Immunology* 56: 739–44. https://doi.org/10.1016/j.molimm.2013.07.008.
Ikeda, Kazuyoshi, Takayuki Higashi, Hiroyuki§ Sano, Yoshiteru Jinnouchi, Masaki Yoshida, Tomohir Araki, Shoichi Ueda, and Seikoh Horiuchi. 1996. "Nε-(Carboxymethyl)Lysine Protein Adduct Is a Major Immunological Epitope in Proteins Modified with Advanced Glycation End Products of the Maillard Reaction†." https://doi.org/10.1021/BI9530550.
Ilangumaran, Subburaj, Alberto Villalobos-Hernandez, Diwakar Bobbala, and Sheela Ramanathan. 2016. "The Hepatocyte Growth Factor (HGF)–MET Receptor Tyrosine Kinase Signaling Pathway: Diverse Roles in Modulating Immune Cell Functions." *Cytokine* 82 (June): 125–39. https://doi.org/10.1016/J.CYTO.2015.12.013.
Ilchmann, Anne, Sven Burgdorf, Stephan Scheurer, Zoe Waibler, Ryoji Nagai, Anne Wellner, Yasuhiko Yamamoto, et al. 2010. "Glycation of a Food Allergen by the Maillard Reaction Enhances Its T-Cell Immunogenicity: Role of Macrophage Scavenger Receptor Class A Type I and II." *Journal of Allergy and Clinical Immunology* 125 (1): 175-183.e11. https://doi.org/10.1016/j.jaci.2009.08.013.
Inaba, Kayo, Muneo Inaba, Nikolaus Romani, Hideki Aya, Masashi Deguchi, Susumu Ikehara, Shigeru Muramatsu, and Ralph M. Steinman. 1992. "Generation of Large Numbers of Dendritic Cells from Mouse Bone Marrow Cultures Supplemented with Granulocyte/Macrophage Colony-Stimulating Factor." *The Journal of Experimental Medicine* 176 (6): 1693. https://doi.org/10.1084/JEM.176.6.1693.
Iwamoto, Keiko, Keishi Kanno, Hideyuki Hyogo, Sho-Ichi Yamagishi, Masayoshi Takeuchi, Susumu Tazuma, and Kazuaki Chayama. 2008. "Advanced Glycation End Products Enhance the Proliferation and Activation of Hepatic Stellate Cells." *Journal of Gastroenterology* 43 (4): 298–304. https://doi.org/10.1007/s00535-007-2152-7.
Jaitin, Diego Adhemar, Lorenz Adlung, Christoph A. Thaiss, Assaf Weiner, Baoguo Li, Hélène Descamps, Patrick Lundgren, et al. 2019. "Lipid-Associated Macrophages Control Metabolic Homeostasis in a Trem2-Dependent Manner." *Cell* 178 (3): 686-698.e14. https://doi.org/10.1016/J.CELL.2019.05.054.
Jin, Jun-O, Hae-Young Park, Qi Xu, Joo-In Park, Tatyana Zvyagintseva, Valentin A. Stonik, and Jong-Young Kwak. 2009. "Ligand of Scavenger Receptor Class A Indirectly Induces Maturation of Human Blood Dendritic Cells via Production of Tumor Necrosis Factor-α." *Blood* 113 (23): 5839–47. https://doi.org/10.1182/blood-2008-10-184796.
Johnson, Katina L., Jason G. Williams, Soheila J. Maleki, Barry K. Hurlburt, Robert E. London, and Geoffrey A. Mueller. 2016. "Enhanced Approaches for Identifying Amadori Products: Application to Peanut Allergens." *Journal of Agricultural and Food Chemistry* 64 (6): 1406–13. https://doi.org/10.1021/acs.jafc.5b05492.
Jono, Tadashi, Akira Miyazaki, Ryoji Nagai, Tatsuya Sawamura, Toshinori Kitamura, and Seikoh Horiuchi. 2002. "Lectin-like Oxidized Low Density Lipoprotein Receptor-1 (LOX-1) Serves as an Endothelial Receptor for Advanced Glycation End Products (AGE)." *FEBS Letters* 511 (1–3): 170–74.

https://doi.org/10.1016/S0014-5793(01)03325-7.
Josefowicz, Steven Z, Li-Fan Lu, and Alexander Y Rudensky. 2012. “Regulatory T Cells: Mechanisms of Differentiation and Function.” *Annual Review of Immunology* 30 (January): 531–64. https://doi.org/10.1146/annurev.immunol.25.022106.141623.
Jouihan, Hani. 2012. “Measurement of Liver Triglyceride Content.” *BIO-PROTOCOL* 2 (13). https://doi.org/10.21769/BioProtoc.223.
Kaabia, Zied, Julie Poirier, Michelle Moughaizel, Audrey Aguesse, Stéphanie Billon-Crossouard, Fanta Fall, Manon Durand, Elie Dagher, Michel Krempf, and Mikaël Croyal. 2018. “Plasma Lipidomic Analysis Reveals Strong Similarities between Lipid Fingerprints in Human, Hamster and Mouse Compared to Other Animal Species.” *Scientific Reports* 8 (1): 15893. https://doi.org/10.1038/s41598-018-34329-3.
Kalinski, Pawel. 2012. “Regulation of Immune Responses by Prostaglandin E2.” *Journal of Immunology (Baltimore, Md. : 1950)* 188 (1): 21–28. https://doi.org/10.4049/jimmunol.1101029.
Kierdorf, Katrin, and Günter Fritz. 2013. “RAGE Regulation and Signaling in Inflammation and Beyond.” *Journal of Leukocyte Biology* 94 (1): 55–68. https://doi.org/10.1189/jlb.1012519.
Killick, Justin, Gregoire Morisse, Dirk Sieger, and Anne L Astier. 2018. “Complement as a Regulator of Adaptive Immunity.” *Seminars in Immunopathology* 40 (1): 37–48. https://doi.org/10.1007/s00281-017-0644-y.
Kim, Kang Ho, and Joel M Sederstrom. 2015. “Assaying Cell Cycle Status Using Flow Cytometry.” *Current Protocols in Molecular Biology* 111 (July): 28.6.1-28.6.11. https://doi.org/10.1002/0471142727.mb2806s111.
Kim, Ki-Hyun, and Hyori Kim. 2017. “Progress of Antibody-Based Inhibitors of the HGF–CMET Axis in Cancer Therapy.” *Experimental & Molecular Medicine* 49 (3): e307–e307. https://doi.org/10.1038/emm.2017.17.
Kim, Kook Hwan, and Myung-Shik Lee. 2018. “Pathogenesis of Nonalcoholic Steatohepatitis and Hormone-Based Therapeutic Approaches.” *Frontiers in Endocrinology* 9 (August): 485. https://doi.org/10.3389/fendo.2018.00485.
Kindberg, G M, S Magnusson, T Berg, and B Smedsrød. 1990. “Receptor-Mediated Endocytosis of Ovalbumin by Two Carbohydrate-Specific Receptors in Rat Liver Cells. The Intracellular Transport of Ovalbumin to Lysosomes Is Faster in Liver Endothelial Cells than in Parenchymal Cells.” *Biochemical Journal* 270 (1): 197–203. https://doi.org/10.1042/bj2700197.
Kislinger, T, C Fu, B Huber, W Qu, A Taguchi, S Du Yan, M Hofmann, et al. 1999. “N(Epsilon)-(Carboxymethyl)Lysine Adducts of Proteins Are Ligands for Receptor for Advanced Glycation End Products That Activate Cell Signaling Pathways and Modulate Gene Expression.” *The Journal of Biological Chemistry* 274 (44): 31740–49. https://doi.org/10.1074/jbc.274.44.31740.
Klaus, Gerry G. B., Anne O’Garra, Martin K. Bijsterbosch, and Mary Holman. 1986. “Activation and Proliferation Signals in Mouse B Cells VIII. Induction of DNA Synthesis in B Cells by a Combination of Calcium Ionophores and Phorbol Myristate Acetate.” *European Journal of Immunology* 16 (1): 92–97. https://doi.org/10.1002/eji.1830160118.
Kleber-Janke, Tamara, Reto Crameri, Ulrich Appenzeller, Max Schlaak, and Wolf-Meinhard Becker. 1999. “Selective Cloning of Peanut Allergens, Including Profilin and 2S Albumins, by Phage Display Technology.” *International Archives of Allergy and Immunology* 119 (4): 265–74. https://doi.org/10.1159/000024203.
Koch, Michael, Seth Chitayat, Brian M. Dattilo, Andre Schiefner, Joachim Diez, Walter J. Chazin, and Günter Fritz. 2010. “Structural Basis for Ligand Recognition and Activation of RAGE.” *Structure* 18 (10): 1342–52. https://doi.org/10.1016/J.STR.2010.05.017.
Kodama, Tatsuhiko, Mason Freeman, Lucia Rohrer, James Zabrecky, Paul Matsudaira, and Monty Krieger. 1990. “Type I Macrophage Scavenger Receptor Contains α-Helical and Collagen-like Coiled Coils.” *Nature* 343 (6258): 531–35. https://doi.org/10.1038/343531a0.
Komine, Hiroshi, Lisa Kuhn, Norimasa Matsushita, James J. Mulé, and Shari Pilon-Thomas. 2013. “Examination of MARCO Activity on Dendritic Cell Phenotype and Function Using a Gene Knockout Mouse.” *PLoS ONE* 8 (7). https://doi.org/10.1371/JOURNAL.PONE.0067795.
Kopper, Randall A., N. Joey Odum, Moon Sen, Ricki M. Helm, J. Steve Stanley, and A. Wesley Burks. 2005. “Peanut Protein Allergens: The Effect of Roasting on Solubility and Allergenicity.” *International Archives of Allergy and Immunology* 136 (1): 16–22. https://doi.org/10.1159/000082580.
Krenkel, Oliver, and Frank Tacke. 2017. “Liver Macrophages in Tissue Homeostasis and Disease.” *Nature Reviews Immunology* 17 (5): 306–21. https://doi.org/10.1038/nri.2017.11.
Kretz-Rommel, Anke. 2005. “Tolerance.” In *Encyclopedic Reference of Immunotoxicology*, 646–50. Berlin/Heidelberg: Springer-Verlag. https://doi.org/10.1007/3-540-27806-0_1483.
Kroghsbo, Stine, Neil M. Rigby, Philip E. Johnson, Karine Adel-Patient, Katrine L. Bøgh, Louise J. Salt, E. N. Clare Mills, and Charlotte B. Madsen. 2014. “Assessment of the Sensitizing Potential of Processed Peanut

Proteins in Brown Norway Rats: Roasting Does Not Enhance Allergenicity." Edited by Kottarappat N. Dileepan. *PLoS ONE* 9 (5): e96475. https://doi.org/10.1371/journal.pone.0096475.
Kulis, M, X Chen, J Lew, Q Wang, O P Patel, Y Zhuang, K S Murray, et al. 2012. "The 2S Albumin Allergens of Arachis Hypogaea, Ara h 2 and Ara h 6, Are the Major Elicitors of Anaphylaxis and Can Effectively Desensitize Peanut-Allergic Mice." *Clinical and Experimental Allergy : Journal of the British Society for Allergy and Clinical Immunology* 42 (2): 326–36. https://doi.org/10.1111/j.1365-2222.2011.03934.x.
Lean, Michael E J, Arne Astrup, and Susan B Roberts. 2018. "Making Progress on the Global Crisis of Obesity and Weight Management." *BMJ (Clinical Research Ed.)* 361 (June): k2538. https://doi.org/10.1136/bmj.k2538.
Lederer, Markus O, and Ralph G Klaiber. 1999. "Cross-Linking of Proteins by Maillard Processes: Characterization and Detection of Lysine–Arginine Cross-Links Derived from Glyoxal and Methylglyoxal." *Bioorganic & Medicinal Chemistry* 7 (11): 2499–2507. https://doi.org/10.1016/S0968-0896(99)00212-6.
Lee, Alison Joanne, Meera Thalayasingam, and Bee Wah Lee. 2013. "Food Allergy in Asia: How Does It Compare?" *Asia Pacific Allergy* 3 (1): 3–14. https://doi.org/10.5415/apallergy.2013.3.1.3.
Leuner, B., M. Max, K. Thamm, C. Kausler, Y. Yakobus, A. Bierhaus, S. Sel, et al. 2012. "RAGE Influences Obesity in Mice." *Zeitschrift Für Gerontologie Und Geriatrie* 45 (2): 102–8. https://doi.org/10.1007/s00391-011-0279-x.
Li, Cunshu, Ye Chang, Yuan Li, Shuang Chen, Yintao Chen, Ning Ye, Dongxue Dai, and Yingxian Sun. 2017. "Advanced Glycation End Products Promote the Proliferation and Migration of Primary Rat Vascular Smooth Muscle Cells via the Upregulation of BAG3." *International Journal of Molecular Medicine* 39 (5): 1242. https://doi.org/10.3892/IJMM.2017.2938.
Li, He, and Shu-Juan Yu. 2018. "Review of Pentosidine and Pyrraline in Food and Chemical Models: Formation, Potential Risks and Determination." *Journal of the Science of Food and Agriculture* 98 (9): 3225–33. https://doi.org/10.1002/jsfa.8853.
Li, Yuan, Ye Chang, Ning Ye, Dongxue Dai, Yintao Chen, Naijin Zhang, Guozhe Sun, and Yingxian Sun. 2017. "Advanced Glycation End Products Inhibit the Proliferation of Human Umbilical Vein Endothelial Cells by Inhibiting Cathepsin D." *International Journal of Molecular Sciences* 18 (2): 436. https://doi.org/10.3390/ijms18020436.
Liang, T.Chyau. 1998. "Epitopes." *Encyclopedia of Immunology*, January, 825–27. https://doi.org/10.1006/RWEI.1999.0219.
Liang, Zhili, Lin Li, Quanyi Fu, Xia Zhang, Zhenbo Xu, and Bing Li. 2016. "Formation and Elimination of Pyrraline in the Maillard Reaction in a Saccharide-Lysine Model System." *Journal of the Science of Food and Agriculture* 96 (7): 2555–64. https://doi.org/10.1002/jsfa.7376.
Liao, Wenhua, Zhaolin Hua, Can Liu, Lin Lin, Rui Chen, and Baidong Hou. 2017. "Characterization of T-Dependent and T-Independent B Cell Responses to a Virus-like Particle." *Journal of Immunology (Baltimore, Md. : 1950)* 198 (10): 3846–56. https://doi.org/10.4049/jimmunol.1601852.
Liggins, Jason, and Anna J. Furth. 1997. "Role of Protein-Bound Carbonyl Groups in the Formation of Advanced Glycation Endproducts." *Biochimica et Biophysica Acta (BBA) - Molecular Basis of Disease* 1361 (2): 123–30. https://doi.org/10.1016/S0925-4439(97)00023-9.
Liliensiek, Birgit, Markus A. Weigand, Angelika Bierhaus, Werner Nicklas, Michael Kasper, Stefan Hofer, Jens Plachky, et al. 2004. "Receptor for Advanced Glycation End Products (RAGE) Regulates Sepsis but Not the Adaptive Immune Response." *The Journal of Clinical Investigation* 113 (11): 1641–50. https://doi.org/10.1172/JCI18704.
Lim, Jun Feng, Heidi Berger, and I-Hsin Su. 2016. "Isolation and Activation of Murine Lymphocytes." *Journal of Visualized Experiments : JoVE*, no. 116. https://doi.org/10.3791/54596.
Lin, Jer An, Chi Hao Wu, Chi Cheng Lu, Shih Min Hsia, and Gow Chin Yen. 2016. "Glycative Stress from Advanced Glycation End Products (AGEs) and Dicarbonyls: An Emerging Biological Factor in Cancer Onset and Progression." *Molecular Nutrition and Food Research*. https://doi.org/10.1002/mnfr.201500759.
Litman, Gary W, Jonathan P Rast, and Sebastian D Fugmann. 2010. "The Origins of Vertebrate Adaptive Immunity." *Nature Reviews. Immunology* 10 (8): 543–53. https://doi.org/10.1038/nri2807.
Liu, Ting, Lingyun Zhang, Donghyun Joo, and Shao-Cong Sun. 2017. "NF-KB Signaling in Inflammation." *Signal Transduction and Targeted Therapy* 2 (1): 17023. https://doi.org/10.1038/sigtrans.2017.23.
Lorenzi, Mara. 2007. "The Polyol Pathway as a Mechanism for Diabetic Retinopathy: Attractive, Elusive, and Resilient." *Experimental Diabetes Research* 2007: 1–10. https://doi.org/10.1155/2007/61038.
Luckheeram, Rishi Vishal, Rui Zhou, Asha Devi Verma, and Bing Xia. 2012. "CD4 $^{+}$ T Cells: Differentiation and Functions." *Clinical and Developmental Immunology* 2012: 1–12. https://doi.org/10.1155/2012/925135.
Luevano-Contreras, Claudia, and Karen Chapman-Novakofski. 2010. "Dietary Advanced Glycation End

Products and Aging." *Nutrients* 2 (12): 1247–65. https://doi.org/10.3390/nu2121247.
Lumeng, Carey N, Jennifer L Bodzin, and Alan R Saltiel. 2007. "Obesity Induces a Phenotypic Switch in Adipose Tissue Macrophage Polarization." *The Journal of Clinical Investigation* 117 (1): 175–84. https://doi.org/10.1172/JCI29881.
Lutz, Manfred B, Nicole Kukutsch, Alexandra L.J Ogilvie, Susanne Rößner, Franz Koch, Nikolaus Romani, and Gerold Schuler. 1999. "An Advanced Culture Method for Generating Large Quantities of Highly Pure Dendritic Cells from Mouse Bone Marrow." *Journal of Immunological Methods* 223 (1): 77–92. https://doi.org/10.1016/S0022-1759(98)00204-X.
Lutz, Thomas A, and Stephen C Woods. 2012. "Overview of Animal Models of Obesity." *Current Protocols in Pharmacology* Chapter 5 (September): Unit5.61. https://doi.org/10.1002/0471141755.ph0561s58.
Lyszkiewicz, M., N. Zietara, M. Rohde, N. O. Gekara, J. Jablonska, K. E. Dittmar, and S. Weiss. 2011. "SIGN-R1+MHC II+ Cells of the Splenic Marginal Zone--a Novel Type of Resident Dendritic Cells." *Journal of Leukocyte Biology* 89 (4): 607–15. https://doi.org/10.1189/jlb.0610368.
MacParland, Sonya A., Jeff C. Liu, Xue-Zhong Ma, Brendan T. Innes, Agata M. Bartczak, Blair K. Gage, Justin Manuel, et al. 2018. "Single Cell RNA Sequencing of Human Liver Reveals Distinct Intrahepatic Macrophage Populations." *Nature Communications* 9. https://doi.org/10.1038/S41467-018-06318-7.
MacPherson, Gordon, and Jonathan M. Austyn. 2012. *Exploring Immunology : Concepts and Evidence*. Wiley-Blackwell. https://www.wiley.com/en-gb/Exploring+Immunology%3A+Concepts+and+Evidence-p-9783527324125.
Magnuson, A. M., D. P. Regan, J. K. Fouts, A. D. Booth, S. W. Dow, and M. T. Foster. 2017. "Diet-Induced Obesity Causes Visceral, but Not Subcutaneous, Lymph Node Hyperplasia *via* Increases in Specific Immune Cell Populations." *Cell Proliferation* 50 (5): e12365. https://doi.org/10.1111/cpr.12365.
Maleki, Soheila J., Si-Yin Chung, Elaine T. Champagne, and Jean-Pierre Raufman. 2000. "The Effects of Roasting on the Allergenic Properties of Peanut Proteins." *Journal of Allergy and Clinical Immunology* 106 (4): 763–68. https://doi.org/10.1067/mai.2000.109620.
Manfredi, Angelo A, Annalisa Capobianco, Antonio Esposito, Francesco De Cobelli, Tamara Canu, Antonella Monno, Angela Raucci, et al. 2008. "Maturing Dendritic Cells Depend on RAGE for in Vivo Homing to Lymph Nodes." *Journal of Immunology (Baltimore, Md. : 1950)* 180 (4): 2270–75. https://doi.org/10.4049/jimmunol.180.4.2270.
Martins, Raquel Rua, Pam S. Ellis, Ryan B. MacDonald, Rebecca J. Richardson, and Catarina Martins Henriques. 2019. "Resident Immunity in Tissue Repair and Maintenance: The Zebrafish Model Coming of Age." *Frontiers in Cell and Developmental Biology* 7 (February): 12. https://doi.org/10.3389/fcell.2019.00012.
Matthews, Megan L., Lin He, Benjamin D. Horning, Erika J. Olson, Bruno E. Correia, John R. Yates, Philip E. Dawson, and Benjamin F. Cravatt. 2016. "Chemoproteomic Profiling and Discovery of Protein Electrophiles in Human Cells." *Nature Chemistry*, October. https://doi.org/10.1038/nchem.2645.
McKenzie, Emma J., Subhankar Mukhopadhyay, Siamon Gordon, and Luisa Martinez-Pomares. 2006. "Scavenger Receptors on Dendritic Cells." In *Handbook of Dendritic Cells*, 141–63. Weinheim, Germany: Wiley-VCH Verlag GmbH. https://doi.org/10.1002/9783527619696.ch9.
Merle, Nicolas S., Sarah Elizabeth Church, Veronique Fremeaux-Bacchi, and Lubka T. Roumenina. 2015. "Complement System Part I: Molecular Mechanisms of Activation and Regulation." *Frontiers in Immunology* 6 (June): 262. https://doi.org/10.3389/fimmu.2015.00262.
Merle, Nicolas S., Remi Noe, Lise Halbwachs-Mecarelli, Veronique Fremeaux-Bacchi, and Lubka T. Roumenina. 2015. "Complement System Part II: Role in Immunity." *Frontiers in Immunology* 6 (May): 257. https://doi.org/10.3389/fimmu.2015.00257.
Mir, Abdul Rouf, Moinuddin, Safia Habib, Farzana Khan, Khursheed Alam, and Asif Ali. 2016. "Structural Changes in Histone H2A by Methylglyoxal Generate Highly Immunogenic Amorphous Aggregates with Implications in Auto-Immune Response in Cancer." *Glycobiology* 26 (2): 129–41. https://doi.org/10.1093/glycob/cwv082.
Misharin, Alexander V., Luisa Morales-Nebreda, Gökhan M. Mutlu, G. R. Scott Budinger, and Harris Perlman. 2013. "Flow Cytometric Analysis of Macrophages and Dendritic Cell Subsets in the Mouse Lung." *American Journal of Respiratory Cell and Molecular Biology* 49 (4): 503–10. https://doi.org/10.1165/rcmb.2013-0086MA.
Mitchell, Andrew J., Lydie C. Pradel, Lionel Chasson, Nico Van Rooijen, Georges E. Grau, Nicholas H. Hunt, and Giovanna Chimini. 2010. "Technical Advance: Autofluorescence as a Tool for Myeloid Cell Analysis." *Journal of Leukocyte Biology* 88 (3): 597–603. https://doi.org/10.1189/jlb.0310184.
Miyata, S, V Monnier, Satoshi Miyata, and Vincent Monnier. 1992. "Immunohistochemical Detection of Advanced Glycosylation End Products in Diabetic Tissues Using Monoclonal Antibody to Pyrraline." *J Clin Invest* 89 (4): 1102. https://doi.org/10.1172/JCI115690.
Miyazaki, Akira, Hitoshi Nakayama, and Seikoh Horiuchi. 2002. "Scavenger Receptors That Recognize

Advanced Glycation End Products." *Trends in Cardiovascular Medicine* 12 (6): 258–62. http://www.ncbi.nlm.nih.gov/pubmed/12242049.
Mogensen, Trine H. 2009. "Pathogen Recognition and Inflammatory Signaling in Innate Immune Defenses." *Clinical Microbiology Reviews* 22 (2): 240–73, Table of Contents. https://doi.org/10.1128/CMR.00046-08.
Moghaddam, A. E., K. H. Gartlan, L. Kong, and Q. J. Sattentau. 2011. "Reactive Carbonyls Are a Major Th2-Inducing Damage-Associated Molecular Pattern Generated by Oxidative Stress." *The Journal of Immunology* 187 (4): 1626–33. https://doi.org/10.4049/jimmunol.1003906.
Moghaddam, A. E., W. R. Hillson, M. Noti, K. H. Gartlan, S. Johnson, B. Thomas, D. Artis, and Q. J. Sattentau. 2014. "Dry Roasting Enhances Peanut-Induced Allergic Sensitization across Mucosal and Cutaneous Routes in Mice." *The Journal of Allergy and Clinical Immunology* 134 (6): 1453–56. https://doi.org/10.1016/j.jaci.2014.07.032.
Moldogazieva, Nurbubu T., Innokenty M. Mokhosoev, Tatiana I. Mel'nikova, Yuri B. Porozov, and Alexander A. Terentiev. 2019. "Oxidative Stress and Advanced Lipoxidation and Glycation End Products (ALEs and AGEs) in Aging and Age-Related Diseases." *Oxidative Medicine and Cellular Longevity* 2019 (August): 1–14. https://doi.org/10.1155/2019/3085756.
Molina, H, V M Holers, B Li, Y Fung, S Mariathasan, J Goellner, J Strauss-Schoenberger, R W Karr, and D D Chaplin. 1996. "Markedly Impaired Humoral Immune Response in Mice Deficient in Complement Receptors 1 and 2." *Proceedings of the National Academy of Sciences of the United States of America* 93 (8): 3357–61. https://doi.org/10.1073/pnas.93.8.3357.
Mondoulet, L., E. Paty, M. F. Drumare, S. Ah-Leung, P. Scheinmann, R. M. Willemot, J. M. Wal, and H. Bernard. 2005. "Influence of Thermal Processing on the Allergenicity of Peanut Proteins." *Journal of Agricultural and Food Chemistry* 53 (11): 4547–53. https://doi.org/10.1021/jf050091p.
Monnier, VM, and A Cerami. 1981. "Nonenzymatic Browning in Vivo: Possible Process for Aging of Long-Lived Proteins." *Science (New York, N.Y.)* 211 (4481). https://doi.org/10.1126/SCIENCE.6779377.
Moreno-García, Alexandra, Alejandra Kun, Olga Calero, Miguel Medina, and Miguel Calero. 2018. "An Overview of the Role of Lipofuscin in Age-Related Neurodegeneration." *Frontiers in Neuroscience* 12 (July): 464. https://doi.org/10.3389/fnins.2018.00464.
Morimoto, Keiko, and Kazunori Nakajima. 2019. "Role of the Immune System in the Development of the Central Nervous System." *Frontiers in Neuroscience* 13: 916. https://doi.org/10.3389/fnins.2019.00916.
Moser, Bernhard, Dharmesh D Desai, Matthew P Downie, Yali Chen, Shi Fang Yan, Kevan Herold, Ann Marie Schmidt, and Raphael Clynes. 2007. "Receptor for Advanced Glycation End Products Expression on T Cells Contributes to Antigen-Specific Cellular Expansion in Vivo." *Journal of Immunology (Baltimore, Md. : 1950)* 179 (12): 8051–58. https://doi.org/10.4049/jimmunol.179.12.8051.
Mountford, A. P., A. Fisher, and R. A. Wilson. 1994. "The Profile of IgG1 and IgG2a Antibody Responses in Mice Exposed to Schistosoma Mansoni." *Parasite Immunology* 16 (10): 521–27. https://doi.org/10.1111/j.1365-3024.1994.tb00306.x.
Mueller, G. A., S. J. Maleki, K. Johnson, B. K. Hurlburt, H. Cheng, S. Ruan, J. B. Nesbit, et al. 2013. "Identification of Maillard Reaction Products on Peanut Allergens That Influence Binding to the Receptor for Advanced Glycation End Products." *Allergy* 68 (12): 1546–54. https://doi.org/10.1111/all.12261.
Mueller, G. A., S. J. Maleki, and L. C. Pedersen. 2014. "The Molecular Basis of Peanut Allergy." *Current Allergy and Asthma Reports*. https://doi.org/10.1007/s11882-014-0429-5.
Murdock, Jessica L, and Gabriel Núñez. 2016. "TLR4: The Winding Road to the Discovery of the LPS Receptor." *Journal of Immunology (Baltimore, Md. : 1950)* 197 (7): 2561–62. https://doi.org/10.4049/jimmunol.1601400.
Nagai, R., K. Matsumoto, X. Ling, H. Suzuki, T. Araki, and S. Horiuchi. 2000. "Glycolaldehyde, a Reactive Intermediate for Advanced Glycation End Products, Plays an Important Role in the Generation of an Active Ligand for the Macrophage Scavenger Receptor." *Diabetes* 49 (10): 1714–23. https://doi.org/10.2337/diabetes.49.10.1714.
Nagai, Ryoji, Cristina Miki Hayashi, Ling Xia, Motohiro Takeya, and Seikoh Horiuchi. 2002. "Identification in Human Atherosclerotic Lesions of GA-Pyridine, a Novel Structure Derived from Glycolaldehyde-Modified Proteins." *Journal of Biological Chemistry* 277 (50): 48905–12. https://doi.org/10.1074/JBC.M205688200.
Nah, S.-S., I.-Y. Choi, C. K. Lee, J. S. Oh, Y. G. Kim, H.-B. Moon, and B. Yoo. 2008. "Effects of Advanced Glycation End Products on the Expression of COX-2, PGE2 and NO in Human Osteoarthritic Chondrocytes." *Rheumatology* 47 (4): 425–31. https://doi.org/10.1093/rheumatology/kem376.
Nathan, D. M., H. Turgeon, and S. Regan. 2007. "Relationship between Glycated Haemoglobin Levels and Mean Glucose Levels over Time." *Diabetologia* 50 (11): 2239–44. https://doi.org/10.1007/s00125-007-0803-0.
Ndrepepa, Gjin. 2019. "Myeloperoxidase – A Bridge Linking Inflammation and Oxidative Stress with

Cardiovascular Disease." *Clinica Chimica Acta* 493 (June): 36–51. https://doi.org/10.1016/J.CCA.2019.02.022.
Neeper, Michael P., Ann Marie Schmidt, Jerold Brett, Shi Du Yan, Fei Wang, Yi Chen Pan, K. O. Elliston, David Stern, and Anthony A. Shaw. 1992. "Cloning and Expression of a Cell Surface Receptor for Advanced Glycosylation End Products of Proteins." *The Journal of Biological Chemistry*. https://www.semanticscholar.org/paper/Cloning-and-expression-of-a-cell-surface-receptor-Neeper-Schmidt/495873b7fd634bedda55271e375a6b9568cad479.
Nelson, D. S., and Cynthia N. Shneider. 1974. "Effect of Normal Mouse Serum on Mouse Lymphocyte Transformationin Vitro." *European Journal of Immunology* 4 (2): 79–86. https://doi.org/10.1002/eji.1830040205.
Nesargikar, P N, B Spiller, and R Chavez. 2012. "The Complement System: History, Pathways, Cascade and Inhibitors." *European Journal of Microbiology & Immunology* 2 (2): 103–11. https://doi.org/10.1556/EuJMI.2.2012.2.2.
Nguyen, P., V. Leray, M. Diez, S. Serisier, J. Le Bloc'h, B. Siliart, and H. Dumon. 2008. "Liver Lipid Metabolism." *Journal of Animal Physiology and Animal Nutrition* 92 (3): 272–83. https://doi.org/10.1111/j.1439-0396.2007.00752.x.
Nicoletti, Antonino, Giuseppina Caligiuri, Ingrid Törnberg, Tatsuhiko Kodama, Sten Stemme, and Göran K. Hansson. 1999. "The Macrophage Scavenger Receptor Type A Directs Modified Proteins to Antigen Presentation." *European Journal of Immunology* 29 (2): 512–21. https://doi.org/10.1002/(SICI)1521-4141(199902)29:02<512::AID-IMMU512>3.0.CO;2-Y.
Oh, Da Young, Hidetaka Morinaga, Saswata Talukdar, Eun Ju Bae, and Jerrold M Olefsky. 2012. "Increased Macrophage Migration into Adipose Tissue in Obese Mice." *Diabetes* 61 (2): 346–54. https://doi.org/10.2337/db11-0860.
Ohgami, Nobutaka, Akira Miyazaki, Masakazu Sakai, Akihiko Kuniyasu, Hitoshi Nakayama, and Seikoh Horiuchi. 2003. "Advanced Glycation End Products (AGE) Inhibit Scavenger Receptor Class B Type I-Mediated Reverse Cholesterol Transport: A New Crossroad of AGE to Cholesterol Metabolism." *Journal of Atherosclerosis and Thrombosis* 10 (1): 1–6. http://www.ncbi.nlm.nih.gov/pubmed/12621157.
Ohgami, Nobutaka, Ryoji Nagai, Mamoru Ikemoto, Hiroyuki Arai, Akihiko Kuniyasu, Seikoh Horiuchi, and Hitoshi Nakayama. 2001. "CD36, a Member of the Class B Scavenger Receptor Family, as a Receptor for Advanced Glycation End Products." *Journal of Biological Chemistry* 276 (5): 3195–3202. https://doi.org/10.1074/JBC.M006545200.
Ott, Christiane, Kathleen Jacobs, Elisa Haucke, Anne Navarrete Santos, Tilman Grune, and Andreas Simm. 2014. "Role of Advanced Glycation End Products in Cellular Signaling." *Redox Biology* 2: 411–29. https://doi.org/10.1016/j.redox.2013.12.016.
Palladino, Chiara. 2018. "Peanut Allergens." *Molecular Immunology* 100 (August): 58–70. https://doi.org/10.1016/J.MOLIMM.2018.04.005.
Palma, Joanna, Beata Tokarz-Deptuła, Jakub Deptuła, and Wiesław Deptuła. 2018. "Natural Antibodies – Facts Known and Unknown." *Central-European Journal of Immunology* 43 (4): 466. https://doi.org/10.5114/CEJI.2018.81354.
Parkin, Jacqueline, and Bryony Cohen. 2001. "An Overview of the Immune System." *The Lancet* 357 (9270): 1777–89. https://doi.org/10.1016/S0140-6736(00)04904-7.
Pasquale, Alberta Di, Scott Preiss, Fernanda Tavares Da Silva, and Nathalie Garçon. 2015. "Vaccine Adjuvants: From 1920 to 2015 and Beyond." *Vaccines* 3 (2): 320–43. https://doi.org/10.3390/vaccines3020320.
Peeters, K. A. B. M., S. J. Koppelman, E. van Hoffen, C. W. H. van der Tas, C. F. den Hartog Jager, A. H. Penninks, S. L. Hefle, C. A. F. M. Bruijnzeel-Koomen, E. F. Knol, and A. C. Knulst. 2007. "Does Skin Prick Test Reactivity to Purified Allergens Correlate with Clinical Severity of Peanut Allergy?" *Clinical & Experimental Allergy* 37 (1): 108–15. https://doi.org/10.1111/j.1365-2222.2006.02628.x.
Peiser, L, P J Gough, T Kodama, and S Gordon. 2000. "Macrophage Class A Scavenger Receptor-Mediated Phagocytosis of Escherichia Coli: Role of Cell Heterogeneity, Microbial Strain, and Culture Conditions in Vitro." *Infection and Immunity* 68 (4): 1953–63. https://doi.org/10.1128/iai.68.4.1953-1963.2000.
Pertyńska-Marczewska, Magdalena, Serafim Kiriakidis, Robin Wait, Jonathan Beech, Marc Feldmann, and Ewa M. Paleolog. 2004. "Advanced Glycation End Products Upregulate Angiogenic and Pro-Inflammatory Cytokine Production in Human Monocyte/Macrophages." *Cytokine* 28 (1): 35–47. https://doi.org/10.1016/J.CYTO.2004.06.006.
Petersen, Charisse, Rickesha Bell, Kendra A Klag, Soh-Hyun Lee, Raymond Soto, Arevik Ghazaryan, Kaitlin Buhrke, et al. 2019. "T Cell-Mediated Regulation of the Microbiota Protects against Obesity." *Science (New York, N.Y.)* 365 (6451). https://doi.org/10.1126/science.aat9351.
Pi, Xiaowen, Yin Wan, Yili Yang, Ruyi Li, Xiaojiang Wu, Mingyong Xie, Xin Li, and Guiming Fu. 2019. "Research Progress in Peanut Allergens and Their Allergenicity Reduction." *Trends in Food Science & Technology* 93 (November): 212–20. https://doi.org/10.1016/J.TIFS.2019.09.014.

Pikkarainen, T, A Brännström, and K Tryggvason. 1999. “Expression of Macrophage MARCO Receptor Induces Formation of Dendritic Plasma Membrane Processes.” *The Journal of Biological Chemistry* 274 (16): 10975–82. https://doi.org/10.1074/jbc.274.16.10975.

Pirzgalska, Roksana M, Elsa Seixas, Jason S Seidman, Verena M Link, Noelia Martínez Sánchez, Inês Mahú, Raquel Mendes, et al. 2017. “Sympathetic Neuron–Associated Macrophages Contribute to Obesity by Importing and Metabolizing Norepinephrine.” *Nature Medicine* 23 (11): 1309–18. https://doi.org/10.1038/nm.4422.

Platts-Mills, Thomas A.E. 2015. “The Allergy Epidemics: 1870-2010.” *Journal of Allergy and Clinical Immunology* 136 (1): 3–13. https://doi.org/10.1016/j.jaci.2015.03.048.

Plüddemann, Annette, Claudine Neyen, and Siamon Gordon. 2007. “Macrophage Scavenger Receptors and Host-Derived Ligands.” *Methods* 43 (3): 207–17. https://doi.org/10.1016/J.YMETH.2007.06.004.

PrabhuDas, Mercy, Dawn Bowdish, Kurt Drickamer, Maris Febbraio, Joachim Herz, Lester Kobzik, Monty Krieger, et al. 2014. “Standardizing Scavenger Receptor Nomenclature.” https://doi.org/10.4049/jimmunol.1490003.

Pricci, Flavia, Gaetano Leto, Lorena Amadio, Carla Iacobini, Giulio Romeo, Samantha Cordone, Roberto Gradini, et al. 2000. “Role of Galectin-3 as a Receptor for Advanced Glycosylation End Products.” *Kidney International*. Vol. 58. https://doi.org/10.1046/j.1523-1755.2000.07706.x.

Price, C. L., P. S. Sharp, M. E. North, S. J. Rainbow, and S. C. Knight. 2004. “Advanced Glycation End Products Modulate the Maturation and Function of Peripheral Blood Dendritic Cells.” *Diabetes* 53 (6): 1452–58. https://doi.org/10.2337/diabetes.53.6.1452.

Pugliese, G., C. Iacobini, C. M. Pesce, and S. Menini. 2015. “Galectin-3: An Emerging All-out Player in Metabolic Disorders and Their Complications.” *Glycobiology* 25 (2): 136–50. https://doi.org/10.1093/glycob/cwu111.

Puyvelde, Katrien Van, Tony Mets, Rose Njemini, Ingo Beyer, and Ivan Bautmans. 2014. “Effect of Advanced Glycation End Product Intake on Inflammation and Aging: A Systematic Review.” *Nutrition Reviews* 72 (10). https://doi.org/10.1111/nure.12141.

Ramadass, Mahalakshmi, Berhane Ghebrehiwet, and Richard R Kew. 2015. “Enhanced Recognition of Plasma Proteins in a Non-Native State by Complement C3b. A Possible Clearance Mechanism for Damaged Proteins in Blood.” *Molecular Immunology* 64 (1): 55–62. https://doi.org/10.1016/j.molimm.2014.10.022.

Ramasamy, Ravichandran, Susan J Vannucci, Shirley Shi Du Yan, Kevan Herold, Shi Fang Yan, and Ann Marie Schmidt. 2005. “Advanced Glycation End Products and RAGE: A Common Thread in Aging, Diabetes, Neurodegeneration, and Inflammation.” *Glycobiology* 15 (7): 16R-28R. https://doi.org/10.1093/glycob/cwi053.

Rasheed, Zafar, Lokendra kumar, Sajid, Ishwari Prasad, Nadeem A. Ansari, and Rizwan Ahmad. 2009. “Advanced Glycation End Products (AGEs) Damaged IgG, a Target for Circulating Autoantibodies in Patients with Type 1 Diabetes Mellitus.” *Open Glycoscience* 2 (1): 1–8. https://doi.org/10.2174/1875398100902010001.

Rasouli, Neda, Aiwei Yao-Borengasser, Vijayalakshmi Varma, Horace J Spencer, Robert E McGehee, Charlotte A Peterson, Jawahar L Mehta, Philip A Kern, and Philip A. Kern. 2009. “Association of Scavenger Receptors in Adipose Tissue with Insulin Resistance in Nondiabetic Humans.” *Arteriosclerosis, Thrombosis, and Vascular Biology* 29 (9): 1328–35. https://doi.org/10.1161/ATVBAHA.109.186957.

Raycroft, Maurice T., Bohdan P. Harvey, Matthew J. Bruck, and Mark J. Mamula. 2012. “Inhibition of Antigen Trafficking through Scavenger Receptor A.” *Journal of Biological Chemistry* 287 (8): 5310–16. https://doi.org/10.1074/jbc.M111.316356.

Reber, Laurent L, Joseph D Hernandez, and Stephen J Galli. 2017. “The Pathophysiology of Anaphylaxis.” *The Journal of Allergy and Clinical Immunology* 140 (2): 335–48. https://doi.org/10.1016/j.jaci.2017.06.003.

Renzone, Giovanni, Simona Arena, and Andrea Scaloni. 2015. “Proteomic Characterization of Intermediate and Advanced Glycation End-Products in Commercial Milk Samples.” *Journal of Proteomics* 117 (March): 12–23. https://doi.org/10.1016/j.jprot.2014.12.021.

Rolph, Michael S, Timothy R Young, Bennett O V Shum, Cem Z Gorgun, Carsten Schmitz-Peiffer, Ian A Ramshaw, Gökhan S Hotamisligil, and Charles R Mackay. 2006. “Regulation of Dendritic Cell Function and T Cell Priming by the Fatty Acid-Binding Protein AP2.” *Journal of Immunology (Baltimore, Md. : 1950)* 177 (11): 7794–7801. https://doi.org/10.4049/JIMMUNOL.177.11.7794.

Ross, Michael H., and Wojciech. Pawlina. 2006. *Histology : A Text and Atlas with Correlated Cell and Molecular Biology*. Lippincott Williams & Wilkins. https://books.google.co.uk/books/about/Histology.html?id=FoSiGTXn6BUC.

Ruban, Aruchuna, Kostadin Stoenchev, Hutan Ashrafian, and Julian Teare. 2019. “Current Treatments for Obesity.” *Clinical Medicine (London, England)* 19 (3): 205–12. https://doi.org/10.7861/clinmedicine.19-3-205.

Ryan, Brent J., Ahuva Nissim, and Paul G. Winyard. 2014. “Oxidative Post-Translational Modifications and

Their Involvement in the Pathogenesis of Autoimmune Diseases." *Redox Biology* 2 (January): 715–24. https://doi.org/10.1016/J.REDOX.2014.05.004.
Sarma, J Vidya, and Peter A Ward. 2011. "The Complement System." *Cell and Tissue Research* 343 (1): 227–35. https://doi.org/10.1007/s00441-010-1034-0.
Schlecht, Géraldine, Juliette Mouriès, Maud Poitrasson-Rivière, Claude Leclerc, and Gilles Dadaglio. 2006. "Purification of Splenic Dendritic Cells Induces Maturation and Capacity to Stimulate Th1 Response in Vivo." *International Immunology* 18 (3): 445–52. https://doi.org/10.1093/intimm/dxh384.
Schmidt, A M, M Vianna, M Gerlach, J Brett, J Ryan, J Kao, C Esposito, H Hegarty, W Hurley, and M Clauss. 1992. "Isolation and Characterization of Two Binding Proteins for Advanced Glycosylation End Products from Bovine Lung Which Are Present on the Endothelial Cell Surface." *The Journal of Biological Chemistry* 267 (21): 14987–97. http://www.ncbi.nlm.nih.gov/pubmed/1321822.
Schmitt, Annett, Johannes Schmitt, Gerald Münch, and Jovana Gasic-Milencovic. 2005. "Characterization of Advanced Glycation End Products for Biochemical Studies: Side Chain Modifications and Fluorescence Characteristics." *Analytical Biochemistry* 338 (2): 201–15. https://doi.org/10.1016/j.ab.2004.12.003.
Schunk, M. K., and G. E. Macallum. 2005. "Applications and Optimization of Immunization Procedures." *ILAR Journal* 46 (3): 241–57. https://doi.org/10.1093/ilar.46.3.241.
Sela, Michael. 1998. "Antigens." *Encyclopedia of Immunology*, January, 201–7. https://doi.org/10.1006/RWEI.1999.0055.
Sellers, R S, C B Clifford, P M Treuting, and C Brayton. 2012. "Immunological Variation between Inbred Laboratory Mouse Strains: Points to Consider in Phenotyping Genetically Immunomodified Mice." *Veterinary Pathology* 49 (1): 32–43. https://doi.org/10.1177/0300985811429314.
Sessa, Luca, Elena Gatti, Filippo Zeni, Antonella Antonelli, Alessandro Catucci, Michael Koch, Giulio Pompilio, Günter Fritz, Angela Raucci, and Marco E. Bianchi. 2014. "The Receptor for Advanced Glycation End-Products (RAGE) Is Only Present in Mammals, and Belongs to a Family of Cell Adhesion Molecules (CAMs)." Edited by Barry I. Hudson. *PLoS ONE* 9 (1): e86903. https://doi.org/10.1371/journal.pone.0086903.
Shanmugam, Narkunaraja, Young Sook Kim, Linda Lanting, and Rama Natarajan. 2003. "Regulation of Cyclooxygenase-2 Expression in Monocytes by Ligation of the Receptor for Advanced Glycation End Products." *Journal of Biological Chemistry* 278 (37): 34834–44. https://doi.org/10.1074/jbc.M302828200.
Shefcheck, Kevin J., and Steven M. Musser. 2004. "Confirmation of the Allergenic Peanut Protein, Ara h 1, in a Model Food Matrix Using Liquid Chromatography/Tandem Mass Spectrometry (LC/MS/MS)." *Journal of Agricultural and Food Chemistry* 52 (10): 2785–90. https://doi.org/10.1021/jf035129h.
Shi, Xiaolei, Jack P. Davis, Zhoutong Xia, K.P. Sandeep, Timothy H. Sanders, and Lisa O. Dean. 2017. "Characterization of Peanuts after Dry Roasting, Oil Roasting, and Blister Frying." *LWT* 75 (January): 520–28. https://doi.org/10.1016/J.LWT.2016.09.030.
Sicherer, Scott H., and Hugh A. Sampson. 2007. "Peanut Allergy: Emerging Concepts and Approaches for an Apparent Epidemic." *Journal of Allergy and Clinical Immunology* 120 (3): 491–503. https://doi.org/10.1016/j.jaci.2007.07.015.
Silván, José Manuel, Jürgen van de Lagemaat, Agustín Olano, and Maria Dolores del Castillo. 2006. "Analysis and Biological Properties of Amino Acid Derivates Formed by Maillard Reaction in Foods." *Journal of Pharmaceutical and Biomedical Analysis*. https://doi.org/10.1016/j.jpba.2006.04.004.
Silverton, Enid W., Eduardo A. Padlan, David R. Davies, Sandra Smith-Gill, and Michael Potter. 1984. "Crystalline Monoclonal Antibody Fabs Complexed to Hen Egg White Lysozyme." *Journal of Molecular Biology* 180 (3): 761–65. https://doi.org/10.1016/0022-2836(84)90037-8.
Simon, Michelle M, Simon Greenaway, Jacqueline K White, Helmut Fuchs, Valérie Gailus-Durner, Sara Wells, Tania Sorg, et al. 2013. "A Comparative Phenotypic and Genomic Analysis of C57BL/6J and C57BL/6N Mouse Strains." *Genome Biology* 14 (7): R82. https://doi.org/10.1186/gb-2013-14-7-r82.
Smith-Gill, S J, T B Lavoie, and C R Mainhart. 1984. "Antigenic Regions Defined by Monoclonal Antibodies Correspond to Structural Domains of Avian Lysozyme." *Journal of Immunology (Baltimore, Md. : 1950)* 133 (1): 384–93. http://www.ncbi.nlm.nih.gov/pubmed/6202787.
Smith, D A, and D R Germolec. 1999. "Introduction to Immunology and Autoimmunity." *Environmental Health Perspectives* 107 Suppl 5 (Suppl 5): 661–65. https://doi.org/10.1289/ehp.99107s5661.
Soares, Andreia, Lerisa Govender, Jane Hughes, Wendy Mavakla, Marwou de Kock, Charlene Barnard, Bernadette Pienaar, et al. 2010. "Novel Application of Ki67 to Quantify Antigen-Specific in Vitro Lymphoproliferation." *Journal of Immunological Methods* 362 (1–2): 43–50. https://doi.org/10.1016/J.JIM.2010.08.007.
Son, Seunghwan, Inhwa Hwang, Seung Hyeok Han, Jeon-Soo Shin, Ok Sarah Shin, and Je-Wook Yu. 2017. "Advanced Glycation End Products Impair NLRP3 Inflammasome-Mediated Innate Immune Responses in Macrophages." *Journal of Biological Chemistry*, October, jbc.M117.806307. https://doi.org/10.1074/JBC.M117.806307.

Son, Young-Ik, Shin-ichi Egawa, Tomohide Tatsumi, Richard E. Redlinger, Pawel Kalinski, and Tatsuya Kanto. 2002. “A Novel Bulk-Culture Method for Generating Mature Dendritic Cells from Mouse Bone Marrow Cells.” *Journal of Immunological Methods* 262 (1–2): 145–57. https://doi.org/10.1016/S0022-1759(02)00013-3.

Song, Fei, Carmen Hurtado del Pozo, Rosa Rosario, Yu Shan Zou, Radha Ananthakrishnan, Xiaoyuan Xu, Payal R Patel, et al. 2014. “RAGE Regulates the Metabolic and Inflammatory Response to High-Fat Feeding in Mice.” *Diabetes* 63 (6): 1948–65. https://doi.org/10.2337/db13-1636.

Stagg, Andrew J., Fiona Burke, Suzanne Hill, and Stella C. Knight. 2001. “Isolation of Mouse Spleen Dendritic Cells.” In *Dendritic Cell Protocols*, 9–22. New Jersey: Humana Press. https://doi.org/10.1385/1-59259-150-7:9.

Starkl, Philipp, Durga Krishnamurthy, Krisztina Szalai, Ferdinand Felix, Anna Lukschal, Dominik Oberthuer, Hugh A. Sampson, et al. 2011. “Heating Affects Structure, Enterocyte Adsorption and Signalling, As Well as Immunogenicity of the Peanut Allergen Ara h 2.” *The Open Allergy Journal* 4 (1): 24–34. https://doi.org/10.2174/1874838401104010024.

Steinman, Ralph M. 2012. “Decisions About Dendritic Cells: Past, Present, and Future.” *Annual Review of Immunology* 30 (1): 1–22. https://doi.org/10.1146/annurev-immunol-100311-102839.

Stiefel, G., K. Anagnostou, R. J. Boyle, N. Brathwaite, P. Ewan, A. T. Fox, P. Huber, et al. 2017. “BSACI Guideline for the Diagnosis and Management of Peanut and Tree Nut Allergy.” *Clinical & Experimental Allergy* 47 (6): 719–39. https://doi.org/10.1111/cea.12957.

Stijlemans, Benoit, Amanda Sparkes, Chlo Abels, Jiri Keirsse, Lea Brys, Yvon Elkrim, Patrick Baetselier, Alain Beschin, and Jo Ginderachter. 2015. “Murine Liver Myeloid Cell Isolation Protocol.” *BIO-PROTOCOL* 5 (10). https://doi.org/10.21769/BioProtoc.1471.

Stowell, Sean R., Anne M. Winkler, Cheryl L. Maier, C. Maridith Arthur, Nicole H. Smith, Kathryn R. Girard-Pierce, Richard D. Cummings, James C. Zimring, and Jeanne E. Hendrickson. 2012. “Initiation and Regulation of Complement during Hemolytic Transfusion Reactions.” *Clinical and Developmental Immunology* 2012: 1–12. https://doi.org/10.1155/2012/307093.

Strachan, D P. 2000. “Family Size, Infection and Atopy: The First Decade of the ‘Hygiene Hypothesis’.” *Thorax* 55 Suppl 1 (Suppl 1): S2-10. https://doi.org/10.1136/thorax.55.suppl_1.s2.

Strissel, Katherine J, Zlatina Stancheva, Hideaki Miyoshi, James W Perfield, Jason DeFuria, Zoe Jick, Andrew S Greenberg, and Martin S Obin. 2007. “Adipocyte Death, Adipose Tissue Remodeling, and Obesity Complications.” *Diabetes* 56 (12): 2910–18. https://doi.org/10.2337/db07-0767.

Suzuki, Hiroshi, Yukiko Kurihara, Motohiro Takeya, Nobuo Kamada, Motoyukl Kataoka, Kouichi Jishage, Otoya Ueda, et al. 1997. “A Role for Macrophage Scavenger Receptors in Atherosclerosis and Susceptibility to Infection.” *Nature* 386 (6622): 292–96. https://doi.org/10.1038/386292a0.

Tamura, Yoshiaki, Hideki Adachi, Jun-ichi Osuga, Ken Ohashi, Naoya Yahagi, Motohiro Sekiya, Hiroaki Okazaki, et al. 2003. “FEEL-1 and FEEL-2 Are Endocytic Receptors for Advanced Glycation End Products.” *Journal of Biological Chemistry* 278 (15): 12613–17. https://doi.org/10.1074/jbc.M210211200.

Temate-Tiagueu, Yvette, Sahar Al Seesi, Meril Mathew, Igor Mandric, Alex Rodriguez, Kayla Bean, Qiong Cheng, et al. 2016. “Inferring Metabolic Pathway Activity Levels from RNA-Seq Data.” *BMC Genomics* 17 (S5): 542. https://doi.org/10.1186/s12864-016-2823-y.

Thornalley, Paul J. 2005. “Dicarbonyl Intermediates in the Maillard Reaction.” *Annals of the New York Academy of Sciences* 1043 (1): 111–17. https://doi.org/10.1196/annals.1333.014.

Trkola, A, M Purtscher, T Muster, C Ballaun, A Buchacher, N Sullivan, K Srinivasan, J Sodroski, J P Moore, and H Katinger. 1996. “Human Monoclonal Antibody 2G12 Defines a Distinctive Neutralization Epitope on the Gp120 Glycoprotein of Human Immunodeficiency Virus Type 1.” *Journal of Virology* 70 (2): 1100–1108. https://doi.org/10.1128/JVI.70.2.1100-1108.1996.

Tsekovska, Rositsa, Angelina Sredovska-Bozhinov, Toshimitsu Niwa, Ivan Ivanov, and Roumyana Mironova. 2016. “Maillard Reaction and Immunogenicity of Protein Therapeutics.” *World Journal of Immunology* 6 (1): 19. https://doi.org/10.5411/wji.v6.i1.19.

Turk, Z, S Ljubic, N Turk, and B Benko. 2001. “Detection of Autoantibodies Against Advanced Glycation Endproducts and AGE-Immune Complexes in Serum of Patients With Diabetes Mellitus.” *Clinica Chimica Acta; International Journal of Clinical Chemistry* 303 (1–2). https://doi.org/10.1016/S0009-8981(00)00389-2.

Tynan, Graham A., Anne McNaughton, Andrew Jarnicki, Takao Tsuji, and Ed C. Lavelle. 2012. “Polymyxin B Inadequately Quenches the Effects of Contaminating Lipopolysaccharide on Murine Dendritic Cells.” Edited by Laurel L. Lenz. *PLoS ONE* 7 (5): e37261. https://doi.org/10.1371/journal.pone.0037261.

Uchida, Koji. 2014. “Natural Antibodies as a Sensor of Electronegative Damage-Associated Molecular Patterns (DAMPs).” *Free Radical Biology and Medicine* 72 (July): 156–61. https://doi.org/10.1016/J.FREERADBIOMED.2014.03.016.

Ugur, Zafer, Chelsea M Coffey, and Scott Gronert. 2012. “Comparing the Efficiencies of Hydrazide Labels in

the Study of Protein Carbonylation in Human Serum Albumin." *Analytical and Bioanalytical Chemistry* 404 (5): 1399–1411. https://doi.org/10.1007/s00216-012-6235-9.
Ulrich, P. 2001. "Protein Glycation, Diabetes, and Aging." *Recent Progress in Hormone Research* 56 (1): 1–22. https://doi.org/10.1210/rp.56.1.1.
Uotila, Riikka, Anna Kaarina Kukkonen, Dario Greco, Anna Susanna Pelkonen, and Mika Juhani Mäkelä. 2017. "Peanut Oral Immunotherapy Decreases IgE to Ara h 2 and Ara h 6 but Does Not Enhance Sensitization to Cross-Reactive Allergens." *Journal of Allergy and Clinical Immunology* 139 (4): 1393-1396.e6. https://doi.org/10.1016/J.JACI.2016.09.054.
Uribarri, Jaime, Sandra Woodruff, Susan Goodman, Weijing Cai, Xue Chen, Renata Pyzik, Angie Yong, Gary E Striker, and Helen Vlassara. 2010. "Advanced Glycation End Products in Foods and a Practical Guide to Their Reduction in the Diet." *Journal of the American Dietetic Association* 110 (6): 911-16.e12. https://doi.org/10.1016/j.jada.2010.03.018.
Valencia, J. V., M. Mone, C. Koehne, J. Rediske, and T. E. Hughes. 2004. "Binding of Receptor for Advanced Glycation End Products (RAGE) Ligands Is Not Sufficient to Induce Inflammatory Signals: Lack of Activity of Endotoxin-Free Albumin-Derived Advanced Glycation End Products." *Diabetologia* 47 (5): 844–52. https://doi.org/10.1007/s00125-004-1392-9.
Valencia, J. V., S. C. Weldon, D. Quinn, G. H. Kiers, J. DeGroot, J. M. TeKoppele, and T. E. Hughes. 2004. "Advanced Glycation End Product Ligands for the Receptor for Advanced Glycation End Products: Biochemical Characterization and Formation Kinetics." *Analytical Biochemistry* 324 (1): 68–78. https://doi.org/10.1016/J.AB.2003.09.013.
Valentinis, Barbara, Alessandro Bianchi, Dan Zhou, Arcadi Cipponi, Federica Catalanotti, Vincenzo Russo, and Catia Traversari. 2005. "Direct Effects of Polymyxin B on Human Dendritic Cells Maturation." *Journal of Biological Chemistry* 280 (14): 14264–71. https://doi.org/10.1074/jbc.M410791200.
Vénéreau, Emilie, Chiara Ceriotti, and Marco Emilio Bianchi. 2015. "DAMPs from Cell Death to New Life." *Frontiers in Immunology* 6 (August): 422. https://doi.org/10.3389/fimmu.2015.00422.
Villwock, Andrea, Corinna Schmitt, Stephanie Schielke, Matthias Frosch, and Oliver Kurzai. 2008. "Recognition via the Class A Scavenger Receptor Modulates Cytokine Secretion by Human Dendritic Cells after Contact with Neisseria Meningitidis." *Microbes and Infection* 10 (10–11): 1158–65. https://doi.org/10.1016/J.MICINF.2008.06.009.
Vissers, Y. M., F. Blanc, P. S. Skov, P. E. Johnson, N. M. Rigby, L. Przybylski-Nicaise, H. Bernard, et al. 2011. "Effect of Heating and Glycation on the Allergenicity of 2S Albumins (Ara h 2/6) from Peanut." Edited by Jan-Hendrik Niess. *PLoS ONE* 6 (8): e23998. https://doi.org/10.1371/journal.pone.0023998.
Vissers, Y. M., M. Iwan, K. Adel-Patient, P. Stahl Skov, N. M. Rigby, P. E. Johnson, P. Mandrup Müller, et al. 2011. "Effect of Roasting on the Allergenicity of Major Peanut Allergens Ara h 1 and Ara h 2/6: The Necessity of Degranulation Assays." *Clinical & Experimental Allergy* 41 (11): 1631–42. https://doi.org/10.1111/j.1365-2222.2011.03830.x.
Vistoli, G., D. De Maddis, A. Cipak, N. Zarkovic, M. Carini, and G. Aldini. 2013. "Advanced Glycoxidation and Lipoxidation End Products (AGEs and ALEs): An Overview of Their Mechanisms of Formation." *Free Radical Research* 47 (sup1): 3–27. https://doi.org/10.3109/10715762.2013.815348.
Vlassara, Helen, Yong Ming Li, Farhad Imani, Donald Wojciechowicz, Zhi Yang, Fu-Tong Liu, and Anthony Cerami. 1995. "Identification of Galectin-3 As a High-Affinity Binding Protein for Advanced Glycation End Products (AGE): A New Member of the AGE-Receptor Complex." *Molecular Medicine* 1 (6): 634–46. https://doi.org/10.1007/BF03401604.
Vogel, Carl-Wilhelm, and David C. Fritzinger. 2017. "Cobra Venom Factor: The Unique Component of Cobra Venom That Activates the Complement System." In *Snake Venoms*, 345–404. Dordrecht: Springer Netherlands. https://doi.org/10.1007/978-94-007-6410-1_4.
Vooght, Vanessa De, Jeroen A. J. Vanoirbeek, Katrien Luyts, Steven Haenen, Benoit Nemery, and Peter H. M. Hoet. 2010. "Choice of Mouse Strain Influences the Outcome in a Mouse Model of Chemical-Induced Asthma." Edited by Dominik Hartl. *PLoS ONE* 5 (9): e12581. https://doi.org/10.1371/journal.pone.0012581.
Vray, B., Isabelle Camby, Vincent Vercruysse, Tatjana Mijatovic, Nicolai V. Bovin, Paola Ricciardi-Castagnoli, Herbert Kaltner, Isabelle Salmon, Hans-Joachim Gabius, and Robert Kiss. 2004. "Up-Regulation of Galectin-3 and Its Ligands by Trypanosoma Cruzi Infection with Modulation of Adhesion and Migration of Murine Dendritic Cells." *Glycobiology* 14 (7): 647–57. https://doi.org/10.1093/glycob/cwh068.
Walczyk, Nicole E., Penelope M.C. Smith, Euan R. Tovey, and Thomas H. Roberts. 2017. "Peanut Protein Extraction Conditions Strongly Influence Yield of Allergens Ara h 1 and 2 and Sensitivity of Immunoassays." *Food Chemistry* 221 (April): 335–44. https://doi.org/10.1016/j.foodchem.2016.10.063.
Wang, Xiao Qun, Ke Yang, Yu Song He, Lin Lu, and Wei Feng Shen. 2011. "Receptor Mediated Elevation in FABP4 Levels by Advanced Glycation End Products Induces Cholesterol and Triacylglycerol Accumulation in THP-1 Macrophages." *Lipids* 46 (6): 479–86. https://doi.org/10.1007/s11745-011-3542-

4.
Warnecke, Andreas, Sonja Abele, Sravani Musunuri, Jonas Bergquist, and Robert A. Harris. 2017. “Scavenger Receptor A Mediates the Clearance and Immunological Screening of MDA-Modified Antigen by M2-Type Macrophages.” *NeuroMolecular Medicine* 19 (4): 463–79. https://doi.org/10.1007/s12017-017-8461-y.
Weelden, Geert van, Marcin Bobiński, Karolina Okła, Willem Jan van Weelden, Andrea Romano, and Johanna M A Pijnenborg. 2019. “Fucoidan Structure and Activity in Relation to Anti-Cancer Mechanisms.” *Marine Drugs* 17 (1). https://doi.org/10.3390/md17010032.
Weisberg, Stuart P, Daniel McCann, Manisha Desai, Michael Rosenbaum, Rudolph L Leibel, Anthony W Ferrante, and Jr. 2003. “Obesity Is Associated with Macrophage Accumulation in Adipose Tissue.” *The Journal of Clinical Investigation* 112 (12): 1796–1808. https://doi.org/10.1172/JCI19246.
Wellner, Anne, Lena Nußpickel, and Thomas Henle. 2012. “Glycation Compounds in Peanuts.” *European Food Research and Technology* 234 (3): 423–29. https://doi.org/10.1007/s00217-011-1649-8.
Westwood, Marie E., and Paul J. Thornalley. 1995. “Molecular Characteristics of Methylglyoxal-Modified Bovine and Human Serum Albumins. Comparison with Glucose-Derived Advanced Glycation Endproduct-Modified Serum Albumins.” *Journal of Protein Chemistry* 14 (5): 359–72. https://doi.org/10.1007/BF01886793.
Witztum, J L, U P Steinbrecher, M Fisher, and A Kesaniemi. 1983. “Nonenzymatic Glucosylation of Homologous Low Density Lipoprotein and Albumin Renders Them Immunogenic in the Guinea Pig.” *Proceedings of the National Academy of Sciences of the United States of America* 80 (9): 2757. https://doi.org/10.1073/PNAS.80.9.2757.
Worbs, Tim, Swantje I. Hammerschmidt, and Reinhold Förster. 2017. “Dendritic Cell Migration in Health and Disease.” *Nature Reviews Immunology* 17 (1): 30–48. https://doi.org/10.1038/nri.2016.116.
World Health Organisation. 2020. “Obesity and Overweight.” WHO. 2020. https://www.who.int/news-room/fact-sheets/detail/obesity-and-overweight.
Xie, Jingjing, Sergey Reverdatto, Andrej Frolov, Ralf Hoffmann, David S. Burz, and Alexander Shekhtman. 2008. “Structural Basis for Pattern Recognition by the Receptor for Advanced Glycation End Products (RAGE).” *Journal of Biological Chemistry* 283 (40): 27255–69. https://doi.org/10.1074/JBC.M801622200.
Xu, Haiyan, Glenn T Barnes, Qing Yang, Guo Tan, Daseng Yang, Chieh J Chou, Jason Sole, et al. 2003. “Chronic Inflammation in Fat Plays a Crucial Role in the Development of Obesity-Related Insulin Resistance.” *The Journal of Clinical Investigation* 112 (12): 1821–30. https://doi.org/10.1172/JCI19451.
Xue, Jing, Michaele Manigrasso, Matteo Scalabrin, Vivek Rai, Sergey Reverdatto, David S. Burz, Daniele Fabris, Ann Marie Schmidt, and Alexander Shekhtman. 2016. “Change in the Molecular Dimension of a RAGE-Ligand Complex Triggers RAGE Signaling.” *Structure (London, England : 1993)* 24 (9): 1509. https://doi.org/10.1016/J.STR.2016.06.021.
Yan, Liang Jun, and Michael J. Forster. 2011. “Chemical Probes for Analysis of Carbonylated Proteins: A Review.” *Journal of Chromatography B: Analytical Technologies in the Biomedical and Life Sciences*. https://doi.org/10.1016/j.jchromb.2010.08.004.
Yang, Ke, Xiao Wang, Yu He, Lin Lu, Qiu Chen, Jing Liu, and Wei Shen. 2010. “Advanced Glycation End Products Induce Chemokine/Cytokine Production via Activation of P38 Pathway and Inhibit Proliferation and Migration of Bone Marrow Mesenchymal Stem Cells.” *Cardiovascular Diabetology* 9 (1): 66. https://doi.org/10.1186/1475-2840-9-66.
Yi, Huanfa, Xiaofei Yu, Ping Gao, Yanping Wang, Sun-Hee Baek, Xing Chen, Hyung L Kim, John R Subjeck, and Xiang-Yang Wang. 2009. “Pattern Recognition Scavenger Receptor SRA/CD204 down-Regulates Toll-like Receptor 4 Signaling-Dependent CD8 T-Cell Activation.” *Blood* 113 (23): 5819–28. https://doi.org/10.1182/blood-2008-11-190033.
Yoshimatsu, Mika, Yasuhiro Terasaki, Naomi Sakashita, Emi Kiyota, Hiroo Sato, Luc J. W. Van Der Laan, and Motohiro Takeya. 2004. “Induction of Macrophage Scavenger Receptor MARCO in Nonalcoholic Steatohepatitis Indicates Possible Involvement of Endotoxin in Its Pathogenic Process.” *International Journal of Experimental Pathology* 85 (6): 335–43. https://doi.org/10.1111/j.0959-9673.2004.00401.x.
Yu, Wong, Deborah M. Hussey Freeland, and Kari C. Nadeau. 2016. “Food Allergy: Immune Mechanisms, Diagnosis and Immunotherapy.” *Nature Reviews Immunology* 16 (12): 751–65. https://doi.org/10.1038/nri.2016.111.
Yu, Yen-Rei A., Emily G. O’Koren, Danielle F. Hotten, Matthew J. Kan, David Kopin, Erik R. Nelson, Loretta Que, and Michael D. Gunn. 2016. “A Protocol for the Comprehensive Flow Cytometric Analysis of Immune Cells in Normal and Inflamed Murine Non-Lymphoid Tissues.” Edited by Scott N Mueller. *PLOS ONE* 11 (3): e0150606. https://doi.org/10.1371/journal.pone.0150606.
Zani, Izma Abdul, Sam L Stephen, Nadeem A Mughal, David Russell, Shervanthi Homer-Vanniasinkam, Stephen B Wheatcroft, and Sreenivasan Ponnambalam. 2015. “Scavenger Receptor Structure and

Function in Health and Disease." *Cells* 4 (2): 178–201. https://doi.org/10.3390/cells4020178.
Zhang, Fan, Greg Banker, Xiaodong Liu, Pasithorn A. Suwanabol, Justin Lengfeld, Dai Yamanouchi, K. Craig Kent, and Bo Liu. 2011. "The Novel Function of Advanced Glycation End Products in Regulation of MMP-9 Production." *The Journal of Surgical Research* 171 (2): 871. https://doi.org/10.1016/J.JSS.2010.04.027.
Zhang, Qibin, Jennifer M. Ames, Richard D. Smith, John W. Baynes, and Thomas O. Metz. 2009. "A Perspective on the Maillard Reaction and the Analysis of Protein Glycation by Mass Spectrometry: Probing the Pathogenesis of Chronic Disease." *Journal of Proteome Research* 8 (2): 754–69. https://doi.org/10.1021/pr800858h.
Zhao, Yueshui, Ling Lin, Jing Li, Zhangang Xiao, Bo Chen, Lin Wan, Mingxing Li, Xu Wu, Chi Hin Cho, and Jing Shen. 2018. "CD4+ T Cells in Obesity and Obesity-Associated Diseases." *Cellular Immunology* 332 (October): 1–6. https://doi.org/10.1016/J.CELLIMM.2018.08.013.
Zhou, Yang, Jin Shui Wang, Xiao Jia Yang, Dan Hua Lin, Yun Fang Gao, Yin Jie Su, Sen Yang, Yan Jie Zhang, and Jing Jing Zheng. 2013. "Peanut Allergy, Allergen Composition, and Methods of Reducing Allergenicity: A Review." *International Journal of Food Science*. https://doi.org/10.1155/2013/909140.
Zhu, Jinfang, Hidehiro Yamane, and William E Paul. 2010. "Differentiation of Effector CD4 T Cell Populations." *Annual Review of Immunology* 28: 445–89. https://doi.org/10.1146/annurev-immunol-030409-101212.
Zhu, Xudong, Guijuan Zong, Liu Zhu, Yuchen Jiang, Ke Ma, Hanwen Zhang, Yan Zhang, et al. 2014. "Deletion of Class A Scavenger Receptor Deteriorates Obesity-Induced Insulin Resistance in Adipose Tissue." *Diabetes* 63 (2): 562–77. https://doi.org/10.2337/db13-0815.

Appendix

Given below are the complete results of the enrichment analysis of the RNAseq data. These were not included in Chapter 3 itself due to their large size.

Pathway Name	P value	P adj
Ribosome - Mus musculus (mouse)	3.89E-19	6.87E-16
SRP-dependent cotranslational protein targeting to membrane	2.87E-18	2.53E-15
Translation	5.70E-18	3.36E-15
Metabolism	1.10E-17	4.85E-15
Eukaryotic Translation Elongation	8.07E-17	2.80E-14
Metabolism of proteins	9.53E-17	2.80E-14
Formation of a pool of free 40S subunits	2.22E-16	5.59E-14
Peptide chain elongation	2.79E-16	6.15E-14
L13a-mediated translational silencing of Ceruloplasmin expression	7.21E-16	1.27E-13
3, -UTR-mediated translational regulation	7.21E-16	1.27E-13
Eukaryotic Translation Termination	1.10E-15	1.76E-13
The citric acid (TCA) cycle and respiratory electron transport	3.35E-15	4.92E-13
Nonsense Mediated Decay Independent of the Exon Junction Complex	8.77E-15	1.07E-12
Cap-dependent Translation Initiation	9.08E-15	1.07E-12
Eukaryotic Translation Initiation	9.08E-15	1.07E-12
Parkinson's disease - Mus musculus (mouse)	2.48E-14	2.72E-12
GTP hydrolysis and joining of the 60S ribosomal subunit	2.62E-14	2.72E-12
Nonsense Mediated Decay Enhanced by the Exon Junction Complex	2.01E-13	1.86E-11
Nonsense-Mediated Decay	2.01E-13	1.86E-11
Respiratory electron transport, ATP synthesis by chemiosmotic coupling, and heat production by uncoupling proteins.	1.79E-12	1.58E-10
Electron Transport Chain	2.55E-12	2.14E-10
Cytoplasmic Ribosomal Proteins	2.99E-12	2.40E-10
Oxidative phosphorylation - Mus musculus (mouse)	3.51E-11	2.69E-09
Metabolism of mRNA	8.47E-11	6.23E-09
Respiratory electron transport	1.61E-10	1.14E-08
aerobic respiration -- electron donor II	3.04E-10	2.06E-08
Oxidative phosphorylation	3.19E-09	2.09E-07
Formation of the ternary complex, and subsequently, the 43S complex	1.10E-08	6.93E-07
Metabolism of RNA	1.69E-08	1.03E-06
Translation initiation complex formation	7.23E-08	4.25E-06
Activation of the mRNA upon binding of the cap-binding complex and eIFs, and subsequent binding to 43S	8.19E-08	4.66E-06
Alzheimer's disease - Mus musculus (mouse)	2.05E-07	1.13E-05
NADH to cytochrome *bo* oxidase electron transfer	3.25E-07	1.69E-05
NADH to cytochrome *bd* oxidase electron transfer	3.25E-07	1.69E-05
Ribosomal scanning and start codon recognition	4.89E-07	2.46E-05

Metabolism of lipids and lipoproteins	8.11E-07	3.97E-05
Huntington's disease - Mus musculus (mouse)	9.67E-07	4.61E-05
Antigen processing and presentation - Mus musculus (mouse)	1.34E-06	6.22E-05
Proteasome Degradation	1.94E-06	8.78E-05
PluriNetWork	2.49E-06	0.00011
Valine, leucine and isoleucine degradation - Mus musculus (mouse)	2.09E-05	0.000864
Pyruvate metabolism and Citric Acid (TCA) cycle	2.12E-05	0.000864
Phagosome - Mus musculus (mouse)	2.14E-05	0.000864
Glycolysis / Gluconeogenesis - Mus musculus (mouse)	2.15E-05	0.000864
Proteasome - Mus musculus (mouse)	3.38E-05	0.00133
Peroxisome - Mus musculus (mouse)	3.76E-05	0.00144
Legionellosis - Mus musculus (mouse)	6.97E-05	0.00262
glycolysis I	8.20E-05	0.00298
Glucose metabolism	8.28E-05	0.00298
Citrate cycle (TCA cycle) - Mus musculus (mouse)	9.09E-05	0.00321
Antigen processing-Cross presentation	0.000106	0.00368
Non-alcoholic fatty liver disease (NAFLD) - Mus musculus (mouse)	0.000108	0.00368
glycolysis V (Pyrococcus)	0.000122	0.00407
glycolysis III	0.000126	0.00411
Metapathway biotransformation	0.00013	0.00417
Glycolysis and Gluconeogenesis	0.000139	0.00437
Citric acid cycle (TCA cycle)	0.00021	0.0065
TCA Cycle	0.000232	0.00705
Glycolysis	0.000236	0.00707
TCA cycle variation III (eukaryotic)	0.000305	0.00895
Pyruvate metabolism - Mus musculus (mouse)	0.000309	0.00895
Cell cycle	0.000324	0.00922
gluconeogenesis I	0.00042	0.0118
Gluconeogenesis	0.000473	0.0131
Autoimmune thyroid disease - Mus musculus (mouse)	0.000523	0.0142
Allograft rejection - Mus musculus (mouse)	0.000558	0.0149
Protein processing in endoplasmic reticulum - Mus musculus (mouse)	0.000615	0.0162
Fatty acid degradation - Mus musculus (mouse)	0.000629	0.0163
Cooperation of Prefoldin and TriC/CCT in actin and tubulin folding	0.000808	0.0207
Cell Cycle	0.000861	0.0217
Resolution of Sister Chromatid Cohesion	0.000887	0.0221
alpha-Linolenic acid metabolism - Mus musculus (mouse)	0.00107	0.0262
Gene Expression	0.0011	0.0265
Graft-versus-host disease - Mus musculus (mouse)	0.00128	0.0304
Biological oxidations	0.00151	0.0356
Targeted protein degradation	0.00154	0.0358
Cell Cycle, Mitotic	0.00162	0.0372
CD28 dependent PI3K/Akt signaling	0.00168	0.038
Mitotic Telophase/Cytokinesis	0.00171	0.0382
MicroRNAs in cancer - Mus musculus (mouse)	0.00195	0.0424

XPodNet - protein-protein interactions in the podocyte expanded by STRING	0.00195	0.0424
Peroxisomal lipid metabolism	0.00199	0.0424
Mitotic Prometaphase	0.002	0.0424
GAB1 signalosome	0.00214	0.0449
superpathway of cholesterol biosynthesis	0.00219	0.0456
Transport of the SLBP independent Mature mRNA	0.00223	0.0458
Endochondral Ossification	0.00237	0.0481
Prefoldin mediated transfer of substrate to CCT/TriC	0.00242	0.0484
Formation of ATP by chemiosmotic coupling	0.00244	0.0484
Cytokine-cytokine receptor interaction - Mus musculus (mouse)	0.00272	0.0529
Pentose phosphate pathway - Mus musculus (mouse)	0.00273	0.0529
Lysosome - Mus musculus (mouse)	0.00297	0.0541
Prostaglandin Synthesis and Regulation	0.00301	0.0541
PIP3 activates AKT signaling	0.00302	0.0541
PI-3K cascade	0.00302	0.0541
PI3K/AKT Signaling in Cancer	0.00302	0.0541
PI3K events in ERBB2 signaling	0.00302	0.0541
PI3K events in ERBB4 signaling	0.00302	0.0541
Drug metabolism - cytochrome P450 - Mus musculus (mouse)	0.00303	0.0541
Protein folding	0.00329	0.0581
Glycosaminoglycan biosynthesis - heparan sulfate / heparin - Mus musculus (mouse)	0.00338	0.0586
SNARE interactions in vesicular transport - Mus musculus (mouse)	0.00339	0.0586
TCA cycle	0.00342	0.0586
Metabolism of xenobiotics by cytochrome P450 - Mus musculus (mouse)	0.00366	0.0612
Role of LAT2/NTAL/LAB on calcium mobilization	0.00367	0.0612
Amyotrophic lateral sclerosis (ALS) - Mus musculus (mouse)	0.00367	0.0612
Transport of the SLBP Dependant Mature mRNA	0.00384	0.0633
Fatty Acid Beta Oxidation	0.00441	0.0721
Glucose transport	0.0046	0.0733
Hexose transport	0.0046	0.0733
Regulation of Glucokinase by Glucokinase Regulatory Protein	0.00461	0.0733
miRNA regulation of DNA Damage Response	0.00472	0.0744
Chemical carcinogenesis - Mus musculus (mouse)	0.00503	0.0786
Regulation of KIT signaling	0.00516	0.0799
Transport of Mature mRNA Derived from an Intronless Transcript	0.00569	0.0874
Downstream Signaling Events Of B Cell Receptor (BCR)	0.0058	0.0876
PI3K/AKT activation	0.00581	0.0876
Establishment of Sister Chromatid Cohesion	0.00586	0.0876
PPAR signaling pathway - Mus musculus (mouse)	0.00598	0.0879
PPAR signaling pathway	0.00598	0.0879
Nuclear Pore Complex (NPC) Disassembly	0.00608	0.0883
Cholesterol Biosynthesis	0.0061	0.0883
Purine metabolism	0.00619	0.0886

Propanoate metabolism - Mus musculus (mouse)	0.00623	0.0886
Amino sugar and nucleotide sugar metabolism - Mus musculus (mouse)	0.00637	0.09
Purine salvage	0.00671	0.094
ECM proteoglycans	0.00691	0.096
Sulfur amino acid metabolism	0.00705	0.0972
Cholesterol biosynthesis	0.0073	0.0998
Chaperonin-mediated protein folding	0.0076	0.103
Folding of actin by CCT/TriC	0.00781	0.104
Initiation of Nuclear Envelope Reformation	0.00781	0.104
Nuclear Envelope Reassembly	0.00781	0.104
G2/M Checkpoints	0.00799	0.105
Developmental Biology	0.008	0.105
glutathione-mediated detoxification	0.00822	0.106
Antigen Presentation: Folding, assembly and peptide loading of class I MHC	0.00822	0.106
isoleucine degradation	0.00836	0.107
Constitutive PI3K/AKT Signaling in Cancer	0.00849	0.108
Transport of Mature mRNAs Derived from Intronless Transcripts	0.00874	0.11
Endosomal/Vacuolar pathway	0.00919	0.115
alpha-linolenic acid (ALA) metabolism	0.00928	0.115
alpha-linolenic (omega3) and linoleic (omega6) acid metabolism	0.00928	0.115
Phototransduction - Mus musculus (mouse)	0.00945	0.116
DARPP-32 events	0.00958	0.117
Unwinding of DNA	0.00977	0.118
Supplementary Table 1: Enrichment analysis comparing gene expression in HEL 3 h and HEL GA 3 h pulsed BMDCs. A pathway was considered significantly affected when p = < 0.01.		

Pathway Name	**P value**	**P adj**
Metabolism	1.21E-11	2.14E-08
Oxidative phosphorylation - Mus musculus (mouse)	1.41E-10	1.25E-07
The citric acid (TCA) cycle and respiratory electron transport	5.72E-10	3.36E-07
Parkinson's disease - Mus musculus (mouse)	2.83E-09	1.25E-06
Respiratory electron transport, ATP synthesis by chemiosmotic coupling, and heat production by uncoupling proteins.	7.19E-09	2.54E-06
Electron Transport Chain	5.59E-07	0.000164
Metabolism of lipids and lipoproteins	6.80E-07	0.000172
Respiratory electron transport	1.88E-06	0.000416
aerobic respiration -- electron donor II	6.42E-06	0.00126
Proteasome Degradation	2.45E-05	0.00433
PluriNetWork	4.96E-05	0.00796
Oxidative phosphorylation	5.43E-05	0.00799
Generic Transcription Pathway	8.11E-05	0.0103
Cholesterol biosynthesis	8.20E-05	0.0103
Eukaryotic Translation Elongation	9.79E-05	0.0115
Peptide chain elongation	0.000114	0.0124

Glycerophospholipid biosynthesis	0.000134	0.0124
Proteasome - Mus musculus (mouse)	0.000138	0.0124
Nonsense Mediated Decay Enhanced by the Exon Junction Complex	0.00014	0.0124
Nonsense-Mediated Decay	0.00014	0.0124
Cell Cycle, Mitotic	0.00017	0.0141
Peroxisome - Mus musculus (mouse)	0.000176	0.0141
Antigen processing and presentation - Mus musculus (mouse)	0.000187	0.0143
Kinesins	0.000204	0.015
Cell Cycle	0.000212	0.015
Targeted protein degradation	0.000235	0.016
Transmembrane transport of small molecules	0.000276	0.018
Eukaryotic Translation Termination	0.000297	0.0185
superpathway of cholesterol biosynthesis	0.000305	0.0185
Homologous recombination - Mus musculus (mouse)	0.000321	0.0189
Alzheimer's disease - Mus musculus (mouse)	0.000362	0.0206
Transferrin endocytosis and recycling	0.000408	0.0225
Metabolism of RNA	0.000429	0.023
Lysosome - Mus musculus (mouse)	0.000459	0.0238
Formation of ATP by chemiosmotic coupling	0.000488	0.0239
Cholesterol Biosynthesis	0.000488	0.0239
Nonsense Mediated Decay Independent of the Exon Junction Complex	0.000537	0.0256
Signalling to RAS	0.000622	0.0289
L13a-mediated translational silencing of Ceruloplasmin expression	0.000661	0.0292
3, -UTR-mediated translational regulation	0.000661	0.0292
Metabolism of mRNA	0.000746	0.0319
Mitotic Prometaphase	0.000759	0.0319
Cytoplasmic Ribosomal Proteins	0.000832	0.0341
Phagosomal maturation (early endosomal stage)	0.000875	0.0343
Latent infection of Homo sapiens with Mycobacterium tuberculosis	0.000875	0.0343
GTP hydrolysis and joining of the 60S ribosomal subunit	0.00101	0.0388
Regulation of Lipid Metabolism by Peroxisome proliferator-activated receptor alpha (PPARalpha)	0.00105	0.0388
NOTCH1 Intracellular Domain Regulates Transcription	0.00106	0.0388
miRNA regulation of DNA Damage Response	0.00116	0.0408
Cap-dependent Translation Initiation	0.00119	0.0408
Eukaryotic Translation Initiation	0.00119	0.0408
Formation of a pool of free 40S subunits	0.0012	0.0408
Transcriptional Regulation of Adipocyte Differentiation in 3T3-L1 Pre-adipocytes	0.00125	0.041
Transcriptional Regulation of White Adipocyte Differentiation	0.00125	0.041
Citric acid cycle (TCA cycle)	0.00143	0.046
Resolution of Sister Chromatid Cohesion	0.00152	0.0478
Peroxisomal lipid metabolism	0.00169	0.0523
Receptor-ligand binding initiates the second proteolytic cleavage of Notch receptor	0.00195	0.0575
cholesterol biosynthesis I	0.00195	0.0575

p38MAPK events	0.00195	0.0575
TCA cycle variation III (eukaryotic)	0.00201	0.0583
XPodNet - protein-protein interactions in the podocyte expanded by STRING	0.0021	0.0585
Signalling to ERKs	0.0021	0.0585
Transport of glucose and other sugars, bile salts and organic acids, metal ions and amine compounds	0.00212	0.0585
MicroRNAs in cancer - Mus musculus (mouse)	0.00223	0.0605
Double-Strand Break Repair	0.00248	0.0664
Citrate cycle (TCA cycle) - Mus musculus (mouse)	0.00265	0.0698
Post-translational protein modification	0.00287	0.0745
Protein processing in endoplasmic reticulum - Mus musculus (mouse)	0.00292	0.0747
Pyruvate metabolism and Citric Acid (TCA) cycle	0.003	0.0751
Spliceosome - Mus musculus (mouse)	0.00302	0.0751
Laminin interactions	0.00328	0.0804
ECM-receptor interaction - Mus musculus (mouse)	0.00346	0.0837
Cooperation of Prefoldin and TriC/CCT in actin and tubulin folding	0.00378	0.0902
Gap junction trafficking	0.00391	0.0907
cholesterol biosynthesis III (via desmosterol)	0.00391	0.0907
Translation	0.00403	0.0923
Arrhythmogenic right ventricular cardiomyopathy (ARVC) - Mus musculus (mouse)	0.00412	0.0932
Homologous recombination repair of replication-independent double-strand breaks	0.00427	0.0941
Homologous Recombination Repair	0.00427	0.0941
Huntington’s disease - Mus musculus (mouse)	0.00434	0.0941
S Phase	0.00437	0.0941
TCA Cycle	0.00466	0.0979
tRNA Aminoacylation	0.00472	0.0979
tRNA charging pathway	0.00472	0.0979
Cytosolic tRNA aminoacylation	0.00485	0.0988
Hedgehog Signaling Pathway	0.00487	0.0988
Ribosome - Mus musculus (mouse)	0.00526	0.105
Amyotrophic lateral sclerosis (ALS) - Mus musculus (mouse)	0.00534	0.106
Mismatch repair - Mus musculus (mouse)	0.00603	0.118
Insulin receptor recycling	0.00628	0.121
SRP-dependent cotranslational protein targeting to membrane	0.00629	0.121
Hypertrophic cardiomyopathy (HCM) - Mus musculus (mouse)	0.00661	0.123
Amino acid synthesis and interconversion (transamination)	0.00665	0.123
Nuclear Receptor transcription pathway	0.00669	0.123
Steroid biosynthesis - Mus musculus (mouse)	0.00671	0.123
Tetrahydrobiopterin (BH4) synthesis, recycling, salvage and regulation	0.00684	0.124
Cardiac muscle contraction - Mus musculus (mouse)	0.00729	0.131
NADH to cytochrome *bo* oxidase electron transfer	0.00768	0.134
NADH to cytochrome *bd* oxidase electron transfer	0.00768	0.134
heme biosynthesis II	0.00781	0.134

Heme Biosynthesis	0.00781	0.134
Gap junction degradation	0.00781	0.134
Alcoholism - Mus musculus (mouse)	0.00869	0.147
Collecting duct acid secretion - Mus musculus (mouse)	0.00927	0.155
Cell cycle	0.0093	0.155
Mitotic M-M/G1 phases	0.00957	0.158
Aminoacyl-tRNA biosynthesis - Mus musculus (mouse)	0.00966	0.158

Supplementary Table 2: Enrichment analysis comparing gene expression in HEL 3 h and HEL GLUC pulsed BMDCs. A pathway was considered significantly affected when $p = < 0.01$.